IMPERIAL AGRICULTURAL
RESEARCH INSTITUTE, NEW DELHI

MGIPC-84 III 191-27-8-47-5000

JOURNAL OF COLLOID SCIENCE

Editor-in-Chief

VICTOR K. LAMER, Columbia University, New York

Editors:

F. E. BARTELL
T. R. BOLAM
E. F. BURTON
R. M. FUOSS
H. R. KRUYT
J. W. MCBAIN
E. K. RIDEAL
WILLIAM SEIFRIZ
A. W. THOMAS
ARNE TISELIUS
ROBERT D. VOLD

Consulting Committee:

W. T. ASTBURY
J. J. BIKERMAN
W. CLAYTON
P. DEBYE
W. FEITKNECHT
ALEXANDER FRUMKIN
WILLIAM D. HARKINS
ERNST A. HAUSER
WILFRIED HELLER
HANS JENNY
S. S. KISTLER
HERMAN MARK
J. N. MUKHERJEE
F. F. NORD
R. RUYSSEN
ROBERT SIMHA
THE SVEDBERG

VOLUME 2

1947

ACADEMIC PRESS INC. PUBLISHERS
NEW YORK, N. Y.

Copyright 1948, by Academic Press, Inc.
Made in United States of America

CONTENTS OF VOLUME 2

No. 1, FEBRUARY, 1947

A. NADAI. Eugene Cook Bingham 1
W. H. FULWEILER. E. C. Bingham and the ASTM—An Appreciation.. 5
P. W. BRIDGMAN. The Rheological Properties of Matter Under High Pressure 7
HENRY EYRING AND GEORGE HALSEY. Some Recent Advances in Non-Newtonian Viscosity 17
G. W. SCOTT BLAIR. The Role of Psychophysics in Rheology 21
J. W. ROMBERG AND R. N. TRAXLER. Rheology of Asphalt 33
R. N. TRAXLER. A Review of the Rheology of Bituminous Materials 49
M. MOONEY. The Rheology of Processing Quality of Raw Rubbers 69
R. B. DOW. The Rheology of Lubricants 81
HENRY GREEN. Rheological Properties of Paints, Varnishes, Lacquers, and Printing Inks 93
TURNER ALFREY. The Influence of Solvent Composition on the Specific Viscosities of Polymer Solutions 99
W. O. BAKER. Rheological Properties of Polymers and Plastics 115
R. S. SPENCER AND J. L. WILLIAMS. Concentrated Solution Viscosity of Polystyrene 117
G. J. DIENES. Viscoelastic Properties of Thermoplastics at Elevated Temperatures 131
J. J. BIKERMAN. The Fundamentals of Tackiness and Adhesion 163
JAMES F. SWINDELLS. The Bingham Viscometer and Viscosity Standards. 177
NELSON W. TAYLOR. Mechanism of Brittle Fracture 185
M. C. THRODAHL. Statistical Analysis of Plasticity Measurements of Natural and Synthetic Rubber 187
JULIUS MIKLOWITZ. The Initiation and Propagation of the Plastic Zone Along a Tension Specimen of Nylon 193
JULIUS MIKLOWITZ. The Stress-Strain Relationship of Nylon under Biaxial Stress Conditions 217

No. 2, APRIL, 1947

JOHN R. VAN WAZER. Some Rheological Measurements on the Surface of Saponin in Water 223
OTTO TREITEL. The Submicroscopic Structure of Plant Cell Walls 237
J. N. MUKHERJEE, B. CHATTERJEE AND B. M. BANERJEE. Liberation of H^+, Al^{+++}, and Fe^{+++} Ions from Hydrogen Clays by Neutral Salts.. 247
VICTOR K. LAMER AND ALLEN S. KENYON. Kinetics of the Formation of Monodispersed Sulfur Sols from Thiosulfate and Acid 257
SULLIVAN S. MARSDEN, JR., KAROL J. MYSELS AND GEROULD H. SMITH. Gels and Jellies of Aluminum Dilaurate in Cyclohexane and Benzene Examined by X-ray Diffraction 265
IRWIN B. WILSON. The Deposition of Charged Particles in Tubes, with Reference to the Retention of Therapeutic Aerosols in the Human Lung 271
L. O. BROCKWAY AND J. KARLE. Electron Diffraction Study of Oleophobic Films on Copper, Iron and Aluminum 277
TOMINOSUKE KATSURAI AND MITSUOKI NAKAHIRA. Note on a New Mode of Sol-Gel Transformation 289
GERALD OSTER. Light Scattering from Polymerizing and Coagulating Systems 291
Letters to the Editor:
H. B. KLEVENS. Effect of Temperature on Micelle Formation as Determined by Refraction 301
S. G. WEISSBERG AND ROBERT SIMHA. Viscosities of Solutions of Cellulose Acetate in Solvent-Precipitant Mixtures 305

No. 3, JUNE, 1947

SAUL HORMATS, B. M. ZEFFERT AND F. E. DOLIAN. Heat of Wetting of Charcoal and its Retentivity of Ethyl Chloride 307
E. REED LANG, QUENTIN VAN WINKLE AND WESLEY G. FRANCE. Electrophoresis in an Ultracentrifugal Field 315
WOLFGANG PAULI. The Structure and Properties of Colloidal Sulfur 333
MARION D. BARNES, A. S. KENYON, E. M. ZAISER AND V. K. LAMER. Monodispersed Sulfur Sols. IV. Comparison of the Particle Radius Determined by Transmittance and by the Angular Position of Higher Order Tyndall Spectra from the Mie Theory 349
VICTOR K. LAMER AND MARION D. BARNES. A Note on the Symbols and Definitions Involved in Light Scattering Equations 361
H. B. KLEVENS. Latex Particle Sizes as Determined by Soap Titration and Light Scattering 365
Erratum 374

No. 4, AUGUST, 1947

KAROL J. MYSELS. Study of Aluminum Soap-Hydrocarbon Systems: "Calotropy" and True Stability of the Jelly Phase 375
R. B. DEAN AND JAMES W. MCBAIN. The Sorption of Organic Vapors by Monolayers of Soap 383
J. J. HERMANS. Diffusion with Discontinuous Boundary 387
C. J. PLANK AND L. C. DRAKE. Differences between Silica and Silica-Alumina Gels I. Factors Affecting the Porous Structure of these Gels. 399
C. J. PLANK. Differences between Silica and Silica-Alumina Gels II. A Proposed Mechanism for the Gelation and Syneresis of these Gels . . . 413
R. RUYSSEN AND R. LOOS. Properties of Saponins. Surface Activity and Degree of Dispersion 429
OTTO TREITEL. The Thermoelastic Behavior of Cylindrical Plant Tissues. 453
FRANK LANNI. Higher Order Tyndall Spectra with Mixtures of Antigen and Antiserum (A Note to the Editors of the *Journal of Colloid Science*) 463

No. 5, NOVEMBER, 1947

MATA PRASAD, G. S. HATTIANGDI AND B. K. WAGLE. Behavior of Some Alkali Soap Systems in Organic Solvents 467
JOSEPH M. LAMBERT. Volumetric Analysis of Colloidal Electrolytes by Turbidity Titration 479
S. BAXTER. Membrane Potentials for Keratin 495
RONLAD P. GRAHAM AND DONALD J. CRAWFORD. The Sorption of Oxalate by Hydrous Alumina 509
ROBERT GINELL, A. MARGOT GINELL AND PAUL E. SPOERRI. Association Phenomena. I. The Growth of Particles of Silver Chloride and the Higher-Order Tyndall Effect 521
RYOGO KUBO. Statistical Theory of Rubber-Like Substances 527
BOOK REVIEWS 537

No. 6, DECEMBER, 1947

VICTOR K. LAMER, SEYMORE HOCHBERG, KENNETH HODGES, IRWIN WILSON, JOHN A. FALES AND RANDALL LATTA. The Influence of the Particle Size of Homogeneous Insecticidal Aerosols on the Mortality of Mosquitoes in Confined Atmospheres 539
G. KING. The Effect of Strongly Hydrogen Bonding Agents on Some Polar Polymers 551
W. C. BIGELOW, E. GLASS AND W. A. ZISMAN. Oleophobic Monolayers. II. Temperature Effects and Energy of Adsorption 563
HIDEO AKAMATU AND KAZUO NAGAMATSU. A New Suggestion for a Model Representing the Structure of Carbon Black 593
BOOK REVIEWS 599
INDEXES 603

The Society of Rheology

The function of the Society is the investigation, development, and dissemination of knowledge pertaining to the deformation and flow of matter. It seeks to determine and explain the causes and effects of such phenomena. The reaction to stress of minerals, metals, plastics, liquids, and gases is its range.

The Society was formed in 1929, and one of the most inexhaustible of its founders and servants was Professor E. C. Bingham of Lafayette College. Other well-known founders were W. P. Davey, H. Freundlich, E. A. Hauser, W. H. Herschel, J. Kendall, E. O. Kraemer, W. Ostwald, L. Prandtl and J. Timmermans. The Society has members in many countries throughout the world.

The 1946 annual meeting was the first since Professor Bingham's death and was known as the "Bingham Memorial Symposium on Rheology." Held in New York City, November 1 and 2, it covered a broad field of the applications of rheology. At this meeting the Society established a "Bingham Memorial Award" to be given annually to the scientist making the greatest contribution to rheology.

Past proceedings of the Society have been presented in its own publications and those of the American Institute of Physics. This number of the Journal of Colloid Science marks the beginning of a journalistic alliance with the Academic Press which has graciously offered the Society one issue of this Journal each year for publication of the proceedings of its annual meetings. The Society expresses its appreciation to Mr. Kurt Jacoby of the Academic Press and Professor Victor K. LaMer, Editor, Journal of Colloid Science, for their valued cooperation and assistance.

W. H. MARKWOOD, JR.
Editor, Society of Rheology

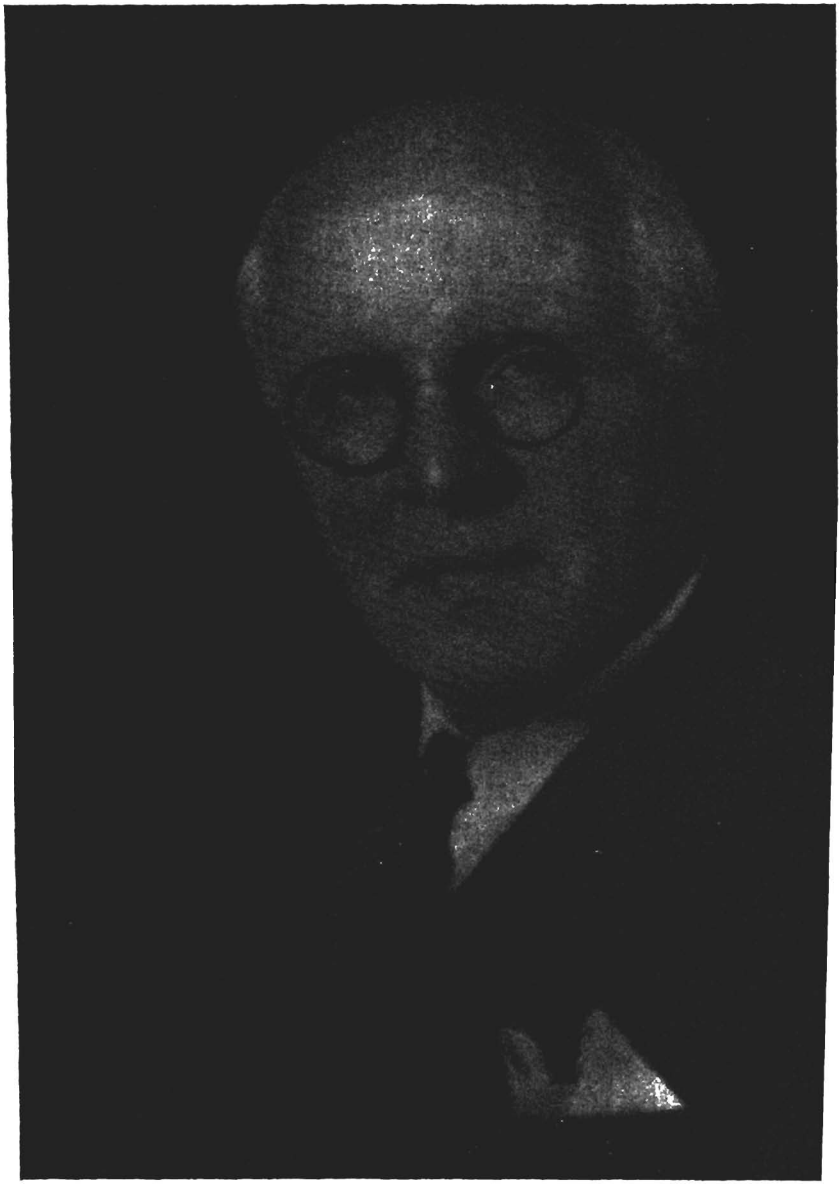

Eugene C. Bingham

EUGENE COOK BINGHAM

A. Nadai

Eugene Cook Bingham was born at Cornwall, Vermont, on December 8, 1878. He studied physical chemistry at Middlebury College, Vermont, from which he graduated in 1899, receiving his Ph.D degree at Johns Hopkins University in 1905. In this year he went to Europe. At the University of Leipzig he came in contact with Wilhelm Ostwald, that great "romanticist" among the natural scientists, publisher of "Ostwald's Klassiker" and author of the book "Great Men" in which the life stories of a few founders of the natural sciences of the nineteenth century were presented. The biographical studies of W. Ostwald, which let him believe that the great founders in the sciences of physics, mathematics, chemistry, biology and medicine could be characterized either as the genial, fast-working, impressive "romanticists," or as the tenacious, assidous, frequently slower-reacting "classicists," must have deeply impressed Bingham, as evidenced in many of his published notes, and also inspired him to devote his later attention to similar efforts. In letters from Berlin Bingham gives very interesting glimpses of his contacts with Nernst and with the great physical chemist van't Hoff, academy professor there. From Berlin Bingham went to Cambridge, England, where he worked for a couple of months under Sir J. J. Thompson whom he admired tremendously.

It is surmised that these men, and perhaps Ostwald most, inspired Bingham's interest in the viscosity of fluids and in collecting later the life stories of the founders of the science of flow of materials. After the death of Ostwald in 1932, Bingham devoted an editorial note to him in the *Journal of Rheology*.

The writer learned from Mrs. Bingham that there were also many discouragements in Bingham's first contacts with these men, difficulties due to the language, peculiarities of the German temperament, his inability to get his ideas across—the many attempts to call on Nernst, who was always out—but none of these difficulties dampened his ardor.

Bingham became professor of chemistry in Richmond, Virginia, in 1906. In 1915 he became assistant physicist at the Bureau of Standards in Washington. From 1916 until 1939 he was head of the Department of Chemistry at Lafayette College, Easton, Pa., from which position he resigned to become Research Professor at the same university and the last six years offered him some of the leisure he was striving for to carry

on his research until a prolonged heart ailment caused his death on November 6, 1945. One of his life-long neighbors and colleagues, Professor B. W. Kunkel, writes in "The Octagon," a publication of the Lehigh Valley Section of the American Chemical Society, for January, 1946, that when Bingham was under an oxygen tent in the hospital, he remarked to his wife (on the day of his death) that it was 170 years ago that Priestley discovered the element oxygen.

On October 17, 1924, a "Plasticity Symposium" was held at Lafayette College, which was sponsored by the American Chemical Society. The four page "Introduction" to it, written by Bingham,* is of considerable interest. In it he wrote as follows:

> Our discussion of plasticity therefore concerns itself with the flow of solids, . . ., for the Greek philosopher Heraklitus was literally correct when he said that "everything flows." It is therefore necessary to limit our discussion by excluding the flow of those things which we are accustomed to refer to as fluids, the pure liquids and gases. But the circle of our lives is not concerned principally with the fluids, even air and water, but with plastic materials. Our very bodies, the foods we eat, and the materials which we fashion in our industries are largely plastic solids. Investigation leads us to the belief that plasticity is made up of two fundamental properties which have been named *yield value* and *mobility*, the former being dependent upon the shearing stress required to start the deformation and the mobility being proportional to the rate of deformation after the yield value has been exceeded.

These last sentences disclose ideas, which he already had developed in his book "Plasticity and Fluidity," published a few years earlier (1922). When dealing with certain fluids he made the observation that they would not start to flow until the pressure head reached a certain finite value. The corresponding shearing stress τ_0 he called the "yield value."

It seemed natural to him as a physical chemist to associate the term "plasticity" with a viscous type of flow which would follow in certain substances after the "yield value" was exceeded, and to introduce *the rate of shear*, $d\gamma/dt$, as the independent variable rather than the shearing strain γ itself. The developments concerned with the slow deformation of other types of solids, such as ductile metals at low temperatures, went in another direction. The mechanical technologists define the limits of plasticity (the "yield point" or "yield stress") similarly, but they call those bodies "plastic" in which the stresses remain practically constant after flow starts or in which they increase with the permanent strains, as in the strain-hardening metals, without much reference to the rates with which these solids deform permanently.

Among the contributors of papers to this "First Plasticity Symposium" appear Wheeler P. Davey, Winslow H. Herschel and S. E. Sheppard, all of whom later became prominently active in the Society of

* J. Phys. Chem. **29**, 1201 (1925).

Rheology. Two plasticity symposia followed. At the third such assembly a committee of 21 men was nominated, including eleven foreign scientists, to form an organizing body. On April 29, 1929, on the initiative of Bingham, 12 men met at the Deschler Wallick Hotel in Columbus, Ohio. At this meeting Bingham proposed the plan for creating an organization for discussing the problems of the flow of non-Newtonian fluids and of solids. In introducing the first issue of a new journal which appeared in October, 1929, he writes:

> Briefly, it was agreed that the organization be known as *The Society of Rheology* and that its official publication be known as the *Journal of Rheology* to be published quarterly. Therefore, it is only fair to all to state our hope for justification, our apologia. It is assumed that the deformation and flow of matter form the material for a science as truly as the flow of electrons, which just about one hundred years ago gave rise to the science of electricity. The deformation and flow of matter were carefully investigated by Sir Robert Hooke as long as two hundred and fifty years ago, and by Sir Isaac Newton two hundred years ago, so that this science may be said to date its beginning well before our scientific era. Perhaps, in fact, this progress was premature, because complications developed in applying the theories to hydraulic flow.
>
> The term "deformation and flow of matter" is a rather cumbersome one to cover the subjects of elasticity, viscosity, and plasticity. There is no single word to cover the field so the only resource has been to invent one. The Greek roots to flow (*rheo*) and science (*logos*) already familiar in numerous words such as rheostat and geology, made the term *rheology* appear to be the best to indicate the *Science of Flow*. No other name has been suggested which would be at the same time distinctive and self-explanatory.*

It is also interesting to note that Bingham proposed the terms *poise* and *rhe* as names for the units of viscosity and fluidity.

The first meeting of the Society, held on December 19 and 20, 1929, in Washington, elected Wheeler P. Davey, Professor at the Pennsylvania State College, for its president, Drs. E. O. Kraemer and W. H. Herschel for vice presidents, Dr. A. S. Hunter, of the DuPont Works in Buffalo, for secretary, Dr. Bingham as editor of the *Journal of Rheology*, and Dr. S. E. Sheppard of the Eastman Kodak Co. in Rochester as assistant editor. On this occasion it is fitting to mention the generous financial support the Journal received during its first years of operation through the whole-hearted help of the Chemical Foundation, represented by W. W. Buffum, who became treasurer of the Society of Rheology. The writer vividly recalls the pleasant discussions at the Daschler-Wallick Hotel in Columbus during the spring, 1929, which preceded this first meeting. Regretfully we note that of those who were present, beside the founder himself, the youthful Dr. Kraemer, who later left for Sweden, and W. H. Herschel of the Bureau of Standards are no longer living. The latter two became active contributors to the new Journal with their work on flow and on lubrication questions, respectively. During these first developmental

* *J. Rheology*, **1**, 92 (1929).

years of the Society, Dr. Bingham established new contacts with various foreign scientists and succeeded in attracting prominent representatives among them as his collaborators at Lafayette College in Easton, Pa. Among the former must be mentioned the names of Dr. G. W. Scott-Blair in England, with whom Bingham for many years enjoyed personal friendship, various Dutch scientists, Wolfgang Ostwald, T. Erk and others, whose papers from abroad on viscosity, plasticity, on international standards, *etc.*, he published. As teacher and head of the Department of Chemistry at Lafayette College he associated himself with many young men who were his pupils, and with whom he published the long series of his joint investigations. Among his foreign associates in research was Dr. M. Reiner, at present scientific advisor to the Public Works in Palestine, Tel Aviv, who spent considerable time with Bingham (1931–1933) in pursuing experimental and theoretical investigations. Later H. Hencky, specialist on the flow of metals, became a research associate of Bingham, working on the theory of finite strains related to the elasticity of rubber.

While a major portion of Bingham's own experimental work was devoted to viscosity, beginning with the time during which he was associated with the National Bureau of Standards, after his attention turned toward the precise absolute determination of the viscosity of water at 20°C. (which he improved himself), and covered broad information on the characteristics of flow of the most diversified types of substances, beginning with water and ending with the plasma of the human blood, he disclosed a continuous interest in many physical problems. He frequently emphasized the fact that seemingly physically or chemically different substances mechanically behave similarly when they deform. The writer recalls many occasions on which the conversation with him during the annual meetings of the Society of Rheology turned to this subject, and to the cases of flow in different types of substances for which the same mathematical functions were valid. In his great enthusiasm he thought that the science of Rheology, true to its motto that "all things flow," should embrace as many materials as were investigated. In the early issues of the *Journal of Rheology* one will find papers dealing with the deformation of such widely different solids or fluids as natural rocks, the ductile metals, concrete, asphalts, rubber, lubricating oils, mixtures of chemical compounds, clay, suspensions of solid particles in viscous fluids, colloids, gels, *etc.*

As already mentioned, Bingham had a keen interest in the life stories of the early founders of the mathematical theory of the flow of viscous fluids. One can imagine how pleased he was, after having obtained a daguerreotype of Poisseuille from Marcel Brillouin, of the College of France, whose biographical sketch, in a translation prepared by Mrs.

Edith I. Bingham, he published in the Journal* with this portrait of Poisseuille as frontispiece. It gave further satisfaction to Bingham that, in 1939, he could publish an English translation in "Rheological Memoirs" of Poisseuille's classic paper on the flow of water through capillaries, which originally was published in 1846 in "Mémoires des Savants étrangers" in Paris. It is perhaps becoming to point to this date on the occasion of this symposium which thus coincides with the centenary of the publication of Poisseuille's paper.

His devotion to his field was instrumental in inspiring him to create the *Rheological Abstracts* which became a major portion of the content of the Rheology Leaflets,† which were continued after the Society of Rheology, in 1931, joined the American Institute of Physics. The *Journal of Applied Physics* became since then the principal outlet for scientific papers which were presented at the meetings of the Society.

All those who knew Bingham during the years in which he succeeded in his attempts at inspiring a large group of researchers to develop the field of the flow of materials on an international basis, must think of him with deep gratitude. He unreservedly and whole-heartedly devoted his efforts toward a goal he himself conceived. This Rheology Symposium of 1946 proves that Bingham has indeed succeeded fully in conveying his enthusiasm for this field to many others.‡

E. C. BINGHAM AND THE ASTM—AN APPRECIATION§

W. H. Fulweiler

Philadelphia, Pa.

Dr. Bingham was a member of the American Society of Testing Materials for 28 years. Dr. Bingham's early work for the Society was in connection with the standardization of the Saybolt viscosimeter in 1922. In 1927 he was made Chairman of Technical Committee II of Committee E-1 on Consistency, Plasticity, and Related Properties. As Chairman of this Committee, Dr. Bingham made many contributions to the work of the Society. Among these may be mentioned

The adoption of definitions of consistency and plasticity;
Cooperation with the Bureau of Standards in the re-determination of the viscosity of water;

* *J. Rheology* **1**, No. 4, 345 (1930).

† At present the *Rheology Bulletin*.

‡ The writer wishes to express his gratitude to Mrs. Edith I. Bingham for having kindly supplied him with personal details which otherwise would have remained unknown.

§ An abstract of a paper read at the meeting concerning Dr. Bingham's activities in the American Society for Testing Materials.

The study and development of new methods for the determination of softening point;
The symposium in 1937 on consistency.

Dr. Bingham served as ASTM representative on the Study Committee on Viscosity of the International Society of Testing Materials. In addition to his committee work, he contributed some 6 papers, 7 discussions, and many committee reports to the proceedings of the Society.

THE RHEOLOGICAL PROPERTIES OF MATTER UNDER HIGH PRESSURE

P. W. Bridgman

Harvard University, Cambridge, Mass.

Received Nov. 21, 1946

Introduction

By the "rheological" properties of matter I shall understand those properties which play a role when a body receives a permanent alteration of geometrical configuration without fracture. Such permanent alterations of shape follow the application of shearing stresses. In the case of liquids, even the feeblest shearing stresses produce flow and the relevant property of the liquid is its viscosity. In the case of solids, permanent deformation or set does not occur until the shearing stress rises above some threshold value, and the relevant property of the solid may be designated by the generic name plasticity. Both viscosity and plasticity are affected by hydrostatic pressure. The effects of pressure are in many cases large—larger than for other ordinary phenomena—and we may accordingly expect a knowledge of the pressure effects to be of considerable significance in its suggestions as to the underlying mechanisms. In the following I shall be mainly concerned with either my own work or with work with which I have had more or less close contact. This will omit phenomena of undoubted significance, such, for example, as the splashing of a steel projectile on impact against an armor plate or the plastic distortion of the plate itself. My reason for not treating such topics is both my own lack of familiarity with them and the poorly defined nature of the stress systems accompanying such phenomena.

Liquids

This discussion of the effects in liquids will be rather academic in character, because I shall omit the effects which are perhaps most interesting from a practical point of view and from the point of view of industry, namely, the effect of pressure on oils and other lubricants, and leave these to the discussion of Dr. Dow, who has experimented extensively in this field.

My own work in this field was done some years ago; discussion will be found in my book, "The Physics of High Pressure," as well as in the original references. Some 45 different liquids were examined, usually over

a pressure range of 12,000 kg./cm.^{2} and at two temperatures, 30° and 75°C. The method was, in most cases, a falling weight method. The time of fall of a weight through the liquid in question was determined electrically, and the apparatus was so mounted that it could be inverted and the measurement repeated a sufficient number of times to give the requisite accuracy. The liquids measured embraced the ordinary organic liquids whose other properties are commonly listed in tables, and included water. The only liquid metal was mercury. In every case, except for a temporary episode in water to be referred to later, viscosity increases with rising pressure at constant temperature. Furthermore, the increase is, in practically every case, at an accelerated rate with increasing pressure, so that the curve of viscosity against pressure is concave upward. In the case of a number of liquids sensible upward curvature does not begin until pressures of 2,000 or 3,000 kg./cm.^{2} are reached, so that the initial part of the curve is straight, as had been found by several early experimenters whose measurements were confined to this range. If the logarithm of viscosity is plotted against pressure, the curve obtained is, in the majority of cases, concave toward the pressure axis. The curvature is much the greatest at low pressures; above 2,000 or 3,000 kg./cm.^{2} the curve approximates to a straight line in a little more than half the cases, while in the remaining cases it gently reverses curvature. This means that above 3,000 kg./cm.^{2} viscosity either increases geometrically or else, even more rapidly as pressure increases, arithmetically. The range in numerical values for the effect of pressure is extreme; the effect of 12,000 kg./cm.^{2} varies from an increase of 30% for mercury, to a two-fold increase for water, a ten-fold increase for methyl alcohol, a 100-fold increase for propyl alcohol, a thousand-fold increase for amyl alcohol, and an increase by 10^7-fold for eugenol. Contrasted with these figures are decreases in compressibility of not more than fifteen-fold brought about by 12,000 kg./cm.^{2}, and decreases of thermal expansion by the same pressure of not more than two- or three-fold. There is a rather close correlation between the magnitude of the effect of pressure on viscosity and the complication of the molecule, the effect being least for monatomic mercury, and greatest for the complicated organic compound, eugenol. The effect of complication of the molecule is very plainly shown, for example, by the series of the alcohols above, or by the various compounds derived from benzene; the relative pressure effect is greater the more complicated the group substituted for hydrogen. There are also very marked constitutive effects, the iso- compounds, for example, having a larger pressure coefficient than normal compounds. Or a heavier atom substituted into a molecule produces, in general, a larger pressure effect, as shown by various series of halogen compounds.

The effect of temperature combined with pressure is abnormal. Most

temperature coefficients become less at high pressures, but the temperature coefficient of viscosity becomes markedly greater with increasing pressure; for some substances the temperature coefficient at 12,000 kg./cm.^{2} is four-fold greater than at atmospheric pressure. The temperature coefficient of viscosity under pressure, when combined with the compressibility, gives important theoretical implications. Several of the earlier theories of the viscosity of liquids agreed in predicting that viscosity at constant volume should be constant. That is, if temperature is raised, decreasing the viscosity and increasing the volume, and if simultaneously the pressure is increased sufficiently to bring the volume back to the initial value, then the expectation was that the increase of viscosity brought about by the increase of pressure would exactly cancel the decrease brought about by the increase of temperature. This is approximately true for the first few thousand kg./cm.^{2}, but above that there may be significant and large departures. The variation is in such a direction that at constant volume the viscosity is less at the higher temperature. That is, the increased molecular agitation due to increasing temperature has a specific effect in decreasing viscosity apart from the effect on volume.

The effects of pressure on the viscosity of water are abnormal, as are so many of its other properties. At low temperatures, between 0° and approximately 25°C., the initial effect of increasing pressure is to decrease viscosity instead of to increase it. At the low temperatures the curves pass through a minimum in the neighborhood of 1000 kg./cm.^{2} and above this rise with upward concavity. Even at higher temperatures the total increase is abnormally low compared with other liquids. The effects can be qualitatively explained in water by well known considerations of the changing proportions of mono- and trihydrol.

Within the last few years there has been considerable theoretical activity in accounting for the viscosity of liquids in general and the pressure effects in particular, improving on the earlier theories which demanded that viscosity be constant at constant volume. In general comment on any theory of the viscosity of liquids it is obvious that the fundamental mechanism must be different from that of gases. This is shown, for example, by the fact that in a gas the reciprocal of viscosity and thermal conductivity change together with pressure, whereas in a liquid thermal conductivity increases with pressure but reciprocal viscosity may decrease enormously.

The most important of the theoretical work has been done by the Princeton school of physical chemists (1). The basic idea of this work is that there is a similarity between the molecular process by which momentum is transferred from one layer to another in a liquid flowing viscously and the molecular processes in ordinary chemical reactions. The molecule which moves along the velocity gradient in viscous flow receives

or delivers energy. When it passes from a position in one layer to one in the next it is thought of as passing over a potential barrier before it can settle down into its new position, just as a molecule taking part in a chemical reaction has to pass over a potential barrier before it finds its new position of greater stability. The same sort of exponential formula governs the velocity of both processes, and there is an activation energy. The activation energy for viscous flow can be calculated from the kinetics of the liquid, and, in general, is considerably smaller than the energy of vaporization. Ewell and Eyring, and also Ewell, develop this point of view, and obtain, among other things, expressions for the effect of pressure on viscosity which agree with my data up to 2,000 kg./cm.^{2} in the early paper, and which were later improved to give agreement up to 7,000. This was followed by papers by Eyring and by Frisch, Kincaid and Stearn, in which the concept of a maneuver space was introduced, which had to be available to the molecule if it is to be able to slip past its neighbor into a position of greater stability with respect to the viscous motion. This maneuver space is connected with various thermodynamic parameters. With a theory of this kind it is possible to reproduce my measurements on viscosity up to 10,000 kg./cm.^{2} with only small error. Qualitatively the concept of maneuver space has points of resemblance to the concept of an interlocking between the molecules which I used to explain qualitatively some of the pressure effects, such as the strong dependence on complexity of the molecule. If the maneuver space is recognized to involve the shapes of the molecules, the connection between the two concepts becomes quite close.

Solids

There is a much richer variety of phenomena for solids than for liquids, corresponding to the much greater range of kinds of deformation to which a solid may be subjected. On the theoretical side our understanding of the nature of the phenomena is, however, in a much more rudimentary state than in the case of liquids. There is practically no theoretical work on plasticity of solids which goes beyond pure description, and even this description is confined to the simplest aspects of the phenomena. For purposes of illustration we may take the simple description of the most elementary facts, as given by the von Mises theory. According to this theory the substance is in the plastic state if a certain function of the stresses, namely,

$$(X_x - Y_y)^2 + (Y_y - Z_z)^2 + (Z_z - X_x)^2, \tag{1}$$

exceeds a critical value. If the stresses do not exceed this value, the substance is in the elastic range. In the plastic range there is a connection between the stresses and the rate at which the strain varies with the time,

that is, the rate of flow, as follows:

$$\frac{\dot{\epsilon}_x}{X_x - \frac{1}{2}(Y_y + Z_z)} = \frac{\dot{\epsilon}_y}{Y_y - \frac{1}{2}(Z_z + X_x)} = \frac{\dot{\epsilon}_z}{Z_z - \frac{1}{2}(X_x + Y_y)}. \quad (2)$$

The symbols in this equation denote the principal components of stress and of strain velocity, which are assumed to be along the same directions. It is usual to integrate these equations, and write an exactly similar set in which the dots in the strains above are omitted, that is, a set of equations connecting the strains instead of the strain rates with the stresses. These equations are recognized to be valid in only a narrow range just above the point of initial flow. They leave out of consideration a great variety of complicated effects, which are of the greatest practical importance, such as strain-hardening and various time effects. The beginning of an attempt has been made to include these other effects within the theory, but the mathematical difficulties are extreme and comparatively little success has been achieved.

The effects of pressure on plastic flow which I have investigated (2) are included only very roughly within the scope of the simple equations given above, because in the pressure effects we are usually concerned with large deformations, whereas the equations are expressly restricted to small plastic deformations. Perhaps the simplest of the pressure effects has to do with the variation of behavior in simple tension. In order to study these effects a miniature testing laboratory was set up within the pressure chamber, and tensile tests conducted exactly as at atmospheric pressure, with measurements of tensile load and elongation. According to the elementary equations given above, the addition of a hydrostatic pressure to a given stress system should be without effect on the plastic behavior, either on the plastic limit as specified in Eq. (1) or on the rates of flow or the strains as specified in Eq. (2). Actually, a tensile test conducted under pressure may be dramatically different from one conducted at atmospheric pressure. The greatest difference for a substance like mild steel is the enormous increase of ductility produced by pressure. In one of my experiments a mild steel when pulled under a surrounding hydrostatic pressure of 25,000 kg./cm.^{2} permitted an elongation of 300-fold at the neck without fracture, whereas at atmospheric pressure it broke with an elongation at the neck of approximately two-fold.

A convenient way of measuring the ductility is in terms of the "natural" strain at fracture, that is, as $\log_e A_0/A$, where A_0 and A are the initial and final cross section at the neck. The natural strain at fracture for mild steel was found to be a linear function of pressure up to the limit of my experiments, 30,000 kg./cm^2. Another effect which is very prominent under pressure is strain-hardening, the existence of which is not even recognized in the elementary equations. It is known that at atmospheric pressure the strain-hardening curve, that is, the curve of "true stress"

against the equilibrium strain, which is the strain reached asymptotically after flow has ceased, starts out by rising with concave curvature toward the axis of strain, but after passing the point of maximum load where "necking" starts becomes straight and continues straight until the fracture point is reached at a strain of the general order of magnitude of unity. If the tension specimen is pulled under pressure a similar strain hardening curve is found, except that now the linear portion of the curve is much prolonged, out to natural strains of four or five, corresponding to the enhanced ductility imparted by the pressure. Furthermore, within the range of strain common to atmospheric and higher pressures, the strain-hardening curve at high pressure coincides with that at atmospheric. To a second approximation, however, strain-hardening at a higher pressure is greater than at a lower pressure. That is, for a given strain the true stress for the pulling under higher pressure is somewhat greater than for the pulling at lower pressure.

At the lower end of the strain-hardening curve, before the curve becomes linear, it is possible to establish an effect of pressure. At high pressure a somewhat greater tensile stress is required to exceed the elastic limit and enter the plastic range than at lower pressures. That is, the "constant" to which the stress function in expression (1) is equal is an increasing function of pressure. This effect of pressure is not large compared with its effect on ductility, the general order of magnitude of the effect being a raising of the elastic limit by from 5 to 10% for a pressure of 10,000 kg./cm.^{2}.

If a tension specimen is pulled under pressure to an elongation greater than the elongation at fracture at atmospheric pressure, but not to the fracture point under pressure, and the pressure is then released and the specimen pulled again at atmospheric pressure, it will be found that fracture does not occur at once, but further elongation is permitted, so that the strain at which a tensile fracture occurs is a function of the previous history and, in particular, a function of the pressure at which it was previously pulled. Theoretically this has most important implications, because it shows that the properties of a substance are not functions only of the state of stress and strain, but involve also the history. It is difficult to formulate this sort of thing in mathematical terms. It is obvious that a complete mathematical theory, even a purely descriptive theory, must be of a very considerable degree of complexity.

The stress at fracture of a specimen previously pulled under high pressure and then broken at atmospheric pressure may be considerably higher than that of a virgin specimen broken at atmospheric pressure. In this way an enhancement of properties may be produced which may be of some practical interest.

The numerical parameters which determine the effect of pressure on the plastic properties of steel are a strong function of the condition of the

steel as determined by the heat treatment. If the steel is heat treated so as to become harder, the slope of the line of strain at fracture as a function of hydrostatic pressure increases markedly, so that the ductility imparted by a given hydrostatic pressure becomes less the harder the steel. Even with the hardest steels a perceptible amount of ductility was imparted by the highest pressures (30,000 kg./cm.^{2}), as contrasted with a completely brittle fracture at atmospheric pressure. The slope of the strain hardening line also increases markedly as the hardness of the steel is increased by heat treatment.

Certain substances which are normally completely brittle to tensile stresses at atmospheric pressure may have a measurable degree of ductility imparted to them by high pressure. Thus Balsley (3), working with apparatus of Griggs, has produced a tensile elongation of 40% in limestone pulled under 10,000 kg./cm.^{2}. In work as yet unpublished, I have found that ordinary glass tolerates no measureable permanent tensile stretch even up to 30,000 kg./cm.^{2}, but does exhibit a great increase of tensile strength. Thus under a hydrostatic pressure of 27,000 kg./cm.^{2} pyrex glass supported up to 24,500 kg./cm.^{2} superposed tensile stress, whereas the tensile strength under normal conditions at atmospheric pressure is of the order of 500 kg./cm.^{2}.

Hydrostatic pressure has an effect on flow under simple compressive stresses as well as under tensile stresses. On mild steel these effects are not as dramatic as the tensile effects, because even at atmospheric pressure very large compressive strains may be supported without fracture if the strain is kept homogeneous. There is an effect of hydrostatic pressure on the stress at initial yield under simple compressive stress; this effect is similar to the corresponding tensile effect. The initial flow stress is raised by something of the order of 5 to 10% for 10,000 kg./cm.^{2}. Other substances, normally brittle for simple compression, may show much larger effects than steel. Thus carboloy, which is normally as brittle as glass, will support plastic shortening up to at least 10% when exposed to simple compressive stress superposed on a pressure of 30,000 kg./cm.^{2}. Glass may become enormously strong in compression. I have measured a compressive strength of 45,000 kg./cm.^{2} in pyrex glass when immersed in a liquid carrying 25,000 kg./cm.^{2}, against a normal compressive strength of not more than 2,000 kg./cm.^{2}. The most striking effect was obtained with single crystal sapphire, made by the Linde Air Products Company by their new technique for producing long single crystal rods. Normally these single crystals break brittlely like glass under simple compressive stresses. One crystal was observed in which failure under simple compression took the form of slip without fracture along the basal plane of the crystal, exactly as in single crystals of a ductile metal. The conditions in this experiment were not altogether simple or well defined, there probably being microscopic internal imperfections in the crystal, but there would

seem to be no reason for doubting the qualitative results that a degree of plasticity has been imparted by pressure to a crystal normally brittle.

Other effects of hydrostatic pressure under somewhat more complicated conditions are qualitatively not different from what might be expected from the simple tension and compression experiments. Thus the Brinell hardness of steel, as measured by the penetration of a ball driven by a known load, increases under pressure by something between 5 and 10% for a pressure increment of 10,000 kg./cm.^{2}. Or, if a plate of mild steel is penetrated by a punch, the ductility may be enormously increased by the pressure. Thus, in one experiment the punch broke completely through the plate after a penetration of perhaps 20% of the thickness at atmospheric pressure, whereas under 25,000 kg./cm.^{2} the punch was driven 95% through the plate with no loss of cohesion and with a degree of strain-hardening that allowed the support of a greater load than a piece of virgin metal of the same geometrical configuration.

Another type of experiment under conditions which are not quite as well defined as in those just mentioned duplicates more nearly the conditions of pure laminar flow obtaining in liquids during viscous flow and permits examination of a wide range of materials. In these experiments (4) the material is in the form of a thin wafer a few thousandths of an inch thick pressed between a very short flat faced boss on a heavy block of steel and a plane steel block. Pressure is applied between boss and plate, forcing out the material of the wafer until an equilibrium thickness is reached corresponding to the pressure. Except at the very edges the material of the wafer is in a state of approximate hydrostatic pressure. The block and boss are then rotated relatively to each other, subjecting the material of the wafer to a shearing force at its faces. At low pressures, there is surface slip between material and steel, but when the pressure has reached a value so high that the friction at the interface equals the internal flow stress, surface slip ceases, and at higher pressures the material yields by internal laminar motion, exactly as in a liquid. By measuring the turning force as a function of pressure, it is possible to determine the stress for plastic flow as a function of hydrostatic pressure. These measurements can be carried up to pressures of 50,000 kg./cm.^{2} with apparatus constructed of steel, and with carboloy apparatus have been carried to 100,000 kg./cm.^{2}. These high stresses are made possible by the geometrical design, in which the highly stressed region is highly localized, and surrounded and supported by much larger regions comparatively free from stress. A very wide variety of materials may be studied with this simple apparatus.

Under these conditions there is no substance which does not differ very markedly from the idealized von Mises plastic solid to which Eq. (1) applies. In all cases the shearing stress at which plastic flow occurs is a rising function of pressure. In the pressure range up to 50,000 kg./cm.^{2}

the rise may be by a factor no more than two in the case of some of the metals or may be thousands of fold in the case of substances like paraffine. Very large deformations may be required to reach a steady state, that is, a constant invariable ratio between shearing stress and pressure; shearing deformations of as much as 100 radians sometimes were necessary. Under these very large deformations the original crystal structure of many of the materials is so highly broken down that very little remnant of structure is detectable by X-ray analysis, and, in fact, the material in some cases appears to be reduced to a true glass (5). It is evident from these results that ordinary materials are capable of existing in an almost infinite number of states of aggregation intermediate between fully crystalline and amorphous, and that, accordingly, a great variety of physical properties is to be expected, depending on the degree of work hardening.

The conditions of these shearing experiments are different in an important respect from those of ordinary testing, in that, when fracture occurs, the fractured surfaces are not separated but are maintained in close contact by the pressure. Fracture under these conditions is not a run-away phenomenon, but self-healing often occurs. A very common pattern of fracture is for the material to suddenly let go, after a critical amount of shearing distortion, with catastrophic decrease of shearing stress. The material then self heals, and as shearing distortion continues, the shearing stress builds up again to its former value, and the cycle of fracture and recovery may be repeated indefinitely. There are sometimes other patterns of fracture. Thus, beyond a certain degree of distortion fracture and self healing may be a practically continuous process, the shearing stress remaining at a constant value while the shearing process is accompanied by chattering or by grinding noises.

Internal fracture is confined almost exclusively to non-metallic substances and among them to those which do not crystallize in the cubic system. Cubic systems are in general richer in cleavage or shear planes than other systems, so that there is more opportunity for slip on one plane or another even after extreme distortion.

Not only is there self healing after internal fracture, but there is often cold welding between the substance and the steel parts. Thus borax glass is as tightly welded to the steel parts after shearing in this way as if it had been fused to the steel.

This type of shearing experiment shows well what is perhaps the most important difference between the viscous flow of a liquid and the plastic flow of a solid. The shearing force required to maintain a liquid in laminar shearing motion is proportional to the velocity of shear, whereas in the case of a plastic solid the shearing stress varies little with the velocity of shear. Different solids vary in this respect over a wide range. Thus, in the cases of tin and lead, the two metals which show the greatest de-

pendence of force on speed, a ten-fold increase in force produced a thousand-fold increase in speed. With mica, on the other hand, an increase in speed of ten-thousand-fold was produced by an increase in force too small to measure. With a substance like mica, the apparatus would obviously be unstable if one attempted to impose a constant force during the shearing process. Measurements on such substances must be made by imposing a constant velocity and then allowing the force to come automatically to its equilibrium value.

It is the first task of a physical theory of the process of plastic flow, as distinguished from the purely descriptive theory, which is all we have at present, to account for this striking lack of dependence of velocity on stress. It would appear that in broad outline the forces which are active during the plastic flow of a solid are configurational in character, depending on the relative locations of atoms and molecules, as contrasted with forces which are dynamic in origin, arising from transfer of momentum on a macroscopic scale, which are primarily concerned in the viscous motion of a liquid. I have made a suggestion along these lines (6), which may express the germs of the essential situation. In an idealized lattice structure a steady "state of slip" is a possibility, in which one part of the crystal moves relatively to another by slip along one of the lattice planes. Once this motion is established it would persist with no force to maintain it, since, on the average, the net work done by the atomic forces during a relative motion by one atomic step would vanish. In actuality, of course, lattices are not perfect, and furthermore are disarranged by relative slip, but in any actual lattice there must be a very appreciable idealized component which may well be the determining factor in the relative independence of velocity of force. A somewhat similar consideration applies also to amorphous substances, for even in a noncrystalline substance such as glass, there is evidence in the details of the shearing experiments that some sort of structure is imposed by the process of shearing itself, and this structure may well function on the average sufficiently like the perfect lattice to account for the small effect of velocity on force.

References

1. Ewell, R. H., and Eyring, H., *J. Phys. Chem.* **5**, 571, 726 (1937); Ewell, R. H., *J. Applied Phys.* **9**, 257 (1938); Frisch, D., Eyring, H., and Kincaid, J. F., *J. Applied Phys.* **11**, 75 (1940); Kincaid, J. F., Eyring, H., and Stearn, A. E., *Chem. Rev.* **28**, 301 (1941).
2. Bridgman, P. W., *Rev. Modern Phys.* **17**, 3 (1945); *J. Applied Phys.* **17**, 201, 225, 692 (1946).
3. Balsley, J. R., *Trans. Am. Geophys. Union* **1941**, Part II, 519.
4. Bridgman, P. W., *Proc. Am. Acad. Arts Sci.* **71**, 387 (1937).
5. Larsen, E. S., and Bridgman, P. W., *Am. J. Sci.* **36**, 81 (1938).
6. Bridgman, P. W., *J. Applied Phys.* **8**, 332 (1937).

SOME RECENT ADVANCES IN NON-NEWTONIAN VISCOSITY*

Henry Eyring

Dean of the Graduate School, University of Utah, Salt Lake City

and

George Halsey

Fellow of the Textile Research Institute, Princeton University, Princeton, N. J.

Received Nov. 21, 1946

In 1936, Henry Eyring (1) developed expressions relating the viscosity of a liquid to parameters of the theory of absolute reaction rates. In the range of small shearing forces, the approximation of a linear viscosity law was shown to be suitable. Using this approximation, a large amount of material concerning the effect of temperature, pressure and degree of polymerization on viscosity was interpreted. This work has been summarized in "The Theory of Rate Processes," Chapter IX (2).

Only a short section of this book was devoted to "non-Newtonian viscosity." The viscosity of milled rubber was treated (3) and it was found that the non-Newtonian law developed was adequate.

This law was derived for polymeric material in (4).

One must turn to flow in solid materials to encounter forces in the range likely to make this non-Newtonian law applicable.

Tobolsky and Eyring (5) applied this law to a number of solids in relaxation and creep. They were successful in fitting the curves, except that the constants were not independent of the initial force or elongation.

However, the theory of the distribution of Newtonian relaxation times (6) also is capable of fitting these relaxation and creep curves with equal success. In addition, this theory predicts the variation of constants when the results are expressed in terms of the non-Newtonian theory.

Therefore, the agreement of the sine-hyperbolic law with relaxation experiments is not particularly convincing. The necessity of the non-Newtonian law first becomes apparent when experiments conducted at a constant rate of elongation are considered (4, 7).

The relaxation curves observed with rayon cover many decades of time, and, if this is to be explained on the basis of the Wiechert model, then the curves at a constant rate of elongation must yield very gradually in a very rounded "yield point." Experimentally, the yield point is sharp,

* Presented at the Meeting of the Society of Rheology, New York City, November 1, 1946.

sharper when the slope of the creep curve is shallow, pointing directly to non-linear viscous elements. When experiments of differing rates are considered, the proof of non-linear elements becomes stronger. Experiments on rayons show that in changing the rate over factors as high as thirty-six, the yield force of the dashpots changes only by a small factor of the rate ratio, proving non-linearity.

The elucidation of the laws governing this non-linear flow is quite another thing, however. There is a criterion that simplifies this task a great deal, if it is satisfied. That is the restriction to the simple system, the three-element model (8).

It is defined as a system in which the available energy is given by a single internal parameter.

In spring-dashpot language, this means that the model contains only two springs and one dashpot, however complicated the laws governing the elements may be.

The experimental criterion for the existence of this system is the single valuedness of the point of no relaxation. The point of no relaxation is found by bracketing its value on both sides by finding relaxation at a high force, going to a lower force to find backward relaxation (increasing force) and narrowing the distance between these forces until the accuracy of the machine limits the process.

It is important that, in order to satisfy this criterion of single valuedness, the spring that is not in series with the dashpot must be a true spring, that is, the force on this spring (the force at the point of no relaxation) must be a function of elongation alone.

This criterion will not detect any irregularity in the remaining two elements, however.

First, the simple case was considered, where the remaining spring follows Hooke's law and the dashpot follows the law discussed above. This case was treated at length in (7, 9 and 10).

The failure of these simple laws is often observed. If the spring in series with the dashpot is not a true spring, there will be a change of the angle at which the stress-strain curve intersects the line joining the point of no relaxation. The constancy of this angle implies an absence of flow-softening of a certain kind which will be called spring-softening for reference (11). Looking at the remaining element, the dashpot, several types of deviation can be formulated. The simple unsymmetrical potential barrier was considered in (10).

Other deviations can be considered. Among them is a flow-softening of a second kind, flow thixotropy (11), which is particularly apparent in a chicken feather keratin fiber, given us by Harold P. Lundgren of the Western Regional Research Laboratories of the U. S. Dept. Agr. (12).

The force at a constant rate of elongation actually reaches a maximum, and then decays to a stable constant value.

Whenever the viscosity of the dashpot ceases to be solely a function of the force on it, it is necessary to formulate a model in terms of multiple equilibrium positions available at one value of the flow coordinate. If the potential energy configuration at the bottoms of the positions are the same, and only the activation free energy differs for the various possible flow steps, then the flow-softening alone must be considered. If spring-softening is found, then these potential valleys are different, and to find the instantaneous spring constant, the populations of the different positions must be known.

Another type of deviation is encountered when the flow coordinate is imperfect, that is, when the actual conditions of flow depend on the elongation of the dashpot, and the dashpot criterion of simple reduplication of equilibrium positions along the flow coordinate fails (11). When the three element criterion fails, then the elucidation of the laws governing flow is very complex. A set of rules has to be set up (13) for dealing with this more general case, but a discussion of this situation (the "distribution of relaxation times") is beyond the scope of this presentation.

References

1. Eyring, H., *J. Chem. Phys.* **4**, 283 (1936).
2. Glasstone, S., Laidler, K. J., and Eyring, H., The Theory of Rate Processes. McGraw-Hill Book Co., New York, 1941.
3. Mooney, M., *Physics* **7**, 413 (1936), concerning raw milled rubber, treated by Smallwood, H. M., *J. Applied Phys.* **8**, 505 (1937).
4. Halsey, G., White, H. J., and Eyring, H., *Textile Research Journal* **15**, 295 (1945).
5. Tobolsky, A., and Eyring, H., *J. Chem. Phys.* **11**, 125 (1943).
6. Wiechert, E., *Ann. Physik* **50**, 335, 546 (1893).
7. Eyring, H., and Halsey, G., *Textile Research Journal* **16**, 13 (1946); **16**, 284 (1946).
8. Eyring, H., and Halsey, G., *Textile Research Journal* **16**, 335 (1946).
9. Stein, R., Halsey, G., and Eyring, H., *Textile Research Journal* **16**, 53 (1946).
10. Eyring, H., and Halsey, G., *Textile Research Journal* **16**, 124 (1946).
11. Halsey, G., In preparation.
12. Lundgren, H. P., *Textile Research Journal* **15**, 335 (1945).
13. Halsey, G., In preparation.

THE ROLE OF PSYCHOPHYSICS IN RHEOLOGY

G. W. Scott Blair

From the National Institute for Research in Dairying, University of Reading, England

Received Nov. 11, 1946

Introduction

It was Professor Bingham who chose the name "Rheology" for our Science and it is his definition—"The Science of the Deformation and Flow of Matter"—which is now universally accepted.

The observables in rheology are deformations or strains, and the changes of strain with time. Changes of strain with time, if permanent, constitute flow and, even if recoverable (primary creep), are generally assumed to be associated with internal flow of some kind.

States of stress are inferred either from the comparative strain behavior of complex and simple (prototype) systems in interaction (as when the stress on a strained test-piece is derived from the deformations of a Hookean spring* attached to it), or, dynamically, from the behavior of a known mass in the gravitational field, or occasionallly by more indirect methods. Times cannot be directly compared but are normally taken as equal when free Newtonian bodies traverse superposable distances in them.

In physical testing, stresses (S), strains (σ)* or their differentials with respect to time ($\dot{S}$, $\dot{\sigma}$) are normally held constant, leaving either a length to be measured, or a time (t) which is recorded as a length on a clock-face or occasionally as a number (*e.g.*, fractional number of rotations of the earth, *etc.*).

The states of strain, from direct observation, and the inferred states of stress can be expressed by resolving the individual displacements and tractions on each of the x, y and z planes (when Cartesian co-ordinates are used) in the x, y and z directions for a unit cube, thus forming ninefold tensors: but, since these are symmetrical, there are six independent components of strain and six of stress. Under elastic conditions, the rheological constants of a homogeneous material consist of the ratios of these components, but again, due to symmetry, the number of independent constants is reduced from 36 to 21.

For some anisotropic materials, such as wood (Barkas, 1940–42; 1945), all, or at least many, of these constants have to be considered;

* Throughout this paper large strains are defined by the Hencky expression $\log_e(l/l_0)$ (see Reiner, 1943).

but for isotropic elastic systems, there are only two independent constants, the tensile or Young's modulus (E) and the shear or rigidity modulus (n).

That these ratios are constant (*i.e.*, independent of strain) for many materials depends (except in the special case of high-elasticity) on the approximate cancellation of the opposite effects of the power laws governing interatomic attraction and repulsion over the narrow range of the ordinary elastic region.

For such small deformations and for isotropic conditions only, it is simply proved that $E = 2(1 + \Pi)n$, where Π is Poisson's ratio. In the very special case of pure fluid flow, it is assumed that the ratio of S_s*/$\dot{\sigma}_s = \eta$ is independent of previous straining, and when $\Pi = \frac{1}{2}$ this equation can be simply differentiated to give: $\tau = 3\eta$, where τ is called the "coefficient of viscous traction" (Trouton, 1906).

Maxwell's "relaxation time" (Maxwell, 1868) may be defined as $\left(\frac{\partial(\log S_s)}{\partial t}\right)_\sigma$ and Alexandrov and Lazurkin's (1940) "orientation time" as the time taken for strain to reach $1 - \frac{1}{e}$ of its equilibrium value for constant stress. It is not clear whether this strain is a tensile or a shear strain.

As already pointed out (Scott Blair, 1944a) the calculation of Maxwellian relaxation times from data obtained in tensile experiments is only valid under very restricted conditions. Much of the recent theoretical work on high elasticity is vitiated, or at best subject to incalculable inaccuracy, on account of the implicit or explicit use of the $2(1 + \Pi)$ formula under conditions of large strains, anisotropy or both, for which it is not valid. Rubber is rather a special case, since even for very large strains $\Pi = \frac{1}{2}$ and, further, Mooney (1940) claims that the elastic properties can be adequately described by only one constant other than E or n, even though the strain axes do not lie at 45° with the direction of shear ("Condition of Superelasticity"). But it must be insisted that a Poisson ratio of $\frac{1}{2}$ does not in itself justify us in calculating shear constants from tensile data or *vice versa*.

Consideration of these facts so tightly condensed into this introductory section leads to the conclusion that the classical methods of rheology, though serving admirably for the study of approximately Hookean or Newtonian systems, are quite inadequate to deal with many complex industrial materials, especially when deformations are relatively large. The division of strains into alleged Hookean and Newtonian additive components, though natural and often useful at an earlier stage in the development of rheology, becomes, as time goes on, increasingly suspect.

* The suffix s indicates shear stresses and strains.

It should also be stressed that just as Hooke's law is no more than an approximation, so also liquids are only Newtonian over a limited range of shear-rate (Grunberg and Nissan, 1945) and that the perfect elastomer (Meyer and Ferri, 1935) is an ideal only approximated to by real materials for a limited range of strain.

In fact, the complex and commercially important rheological "properties" of many industrial materials are still assessed subjectively by handling in the factory and are expressed in terms of "body," "firmness," "spring," "deadness," "shortness," "nerve," *etc.*—concepts which cannot be interpreted, in most cases, in terms of the simple rheological properties at all.

In view of this fact, however much it may be deplored, it is clearly advisable to know something of the accuracy with which these handling judgments can be made and, by bulking sufficiently large numbers of data together so that reproducibility is ensured, to attempt to correlate the entities so derived with manageable functions of $S:\sigma:t$.

A start has been made in this direction and not only have a number of reproducible regularities been observed, but the information obtained has laid the foundations of a theory of "Quasi-properties" which it is hoped will facilitate the study of the purely "physical" rheology of complex materials. Since the psychophysical experiments have been held up by the war and are only now being restarted, this is perhaps a good time at which to review the progress which has already been made.

Thresholds of Viscosity and Shear Modulus

In view of various statements which have been made about the very fine discrimination which is possible in assessing thickness of paper, softness of wool, *etc.*, and also the failure of objective methods to substantiate many of the specific claims of the craftsman (*e.g.*, Binns, 1938), it seemed desirable first to establish the thresholds (just noticeable differences) in judging the viscosity of Newtonian system ($\eta \sim 10^6$–10^7 poises) and of the shear modulus of approximately Hookean systems ($n \sim 10^6$–10^7 dynes/cm.^{2}). The details of experimentation, temperature control, selection of subjects, control of left- or right-handedness, *etc.*, are described in the original paper—Scott Blair and Coppen, 1939.

In Fig. 1 are reproduced (by permission of the Royal Society) threshold curves showing percentage correct answers *vs.* $\log \Delta$ where Δ is the objective percentage difference in viscosity of a series of very nearly Newtonian Californian bitumen samples and in shear modulus for a series of vulcanized rubber cylinders regarded as Hookean. The samples were presented to the subjects in pairs and squeezed simultaneously between thumb and fingers with as steady a pressure as possible, the subject being asked to decide which of each pair was the softer. The curves shown are

composite data from many subjects and show that the viscosities of the bitumens can be correctly distinguished in 80% of the tests when Δ is about 30%, whereas differences of only about $\frac{1}{3}$ of this order could be distinguished at the same level of correctness for the rubbers having different moduli. The linearity of the log Δ plot is probably connected with Weber's Law.

Among the subjects were included expert cheese-makers, used to assessing the "body" of cheese and curd by handling, but they did not show a superior acuity. There was no marked improvement with practice, suggesting that the undoubted skill of the craftsman in assessing such

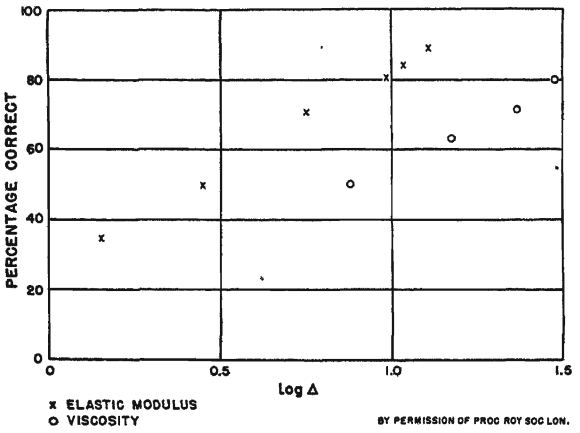

FIG. 1

× Elastic modulus; ⊙ Viscosity.

By permission from *Proc. Roy. Soc.* (*London*) **128 B**, 123 (1939).

factors as "body" is associated rather with a capacity to recognize and appreciate complex rheological conditions than in any acquired increase in sensitivity to small changes of strain in relation to applied pressure.

COMPARISON OF ELASTIC WITH VISCOUS SYSTEMS

An interesting problem arises when subjects are asked to compare directly for firmness-softness, a Newtonian fluid and a Hookean solid simultaneously. Physically, it is not permissible to describe the viscosity of a bitumen as greater or less than the shear modulus of a rubber, since the properties concerned have dimensions which differ by a time unit. In practice, however, very few subjects have any difficulty in making such a comparison provided it is made spontaneously; and, as might be expected, the decision depends on the time allowed for the squeezing (t_c). If t_c is controlled by a metronome it is found that in comparing four rubbers of different modulus (n) for four squeezing times against a single

bitumen the values of n and of t_c are equally important in judging "firmness." A plot of percentage "bitumen softer" answers (p) *vs.* nt_c gives a unique curve independent of n and t_c. This is shown in Fig. 2 (reproduced by courtesy of the *Am. J. Psychol.*) where nt_c is plotted logarithmically since this gives a conveniently linear plot over the greater part of the field. This is but one of many curves of this kind, the conclusions being derived from more than 5,000 squeezings (*vide* Scott Blair and Coppen, 1942).

Since the curve is unique, we may confine our discussion to any convenient time, say 1 sec. After 1 sec., under identical pressures (which can be statistically assumed) the same strain would have been reached

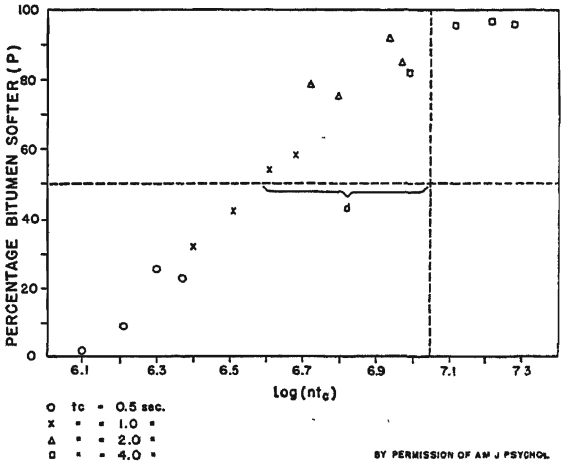

FIG. 2

From *Am. J. Psychol.* **55**, 220 (1942).

by bitumens and rubbers if the viscosities and moduli had been numerically equal.

Had the subjects judged softness-firmness by the total strains produced at the end of the 1 sec. squeezing time, we should have expected the $p = 50$ horizontal line to cross the experimental curve at the value of log (nt_c) corresponding numerically to the viscosity of the bitumen and shown by the vertical dotted line in the figure. Were the subjects to judge by the relative amounts of strain at some period during the squeezing, thus attempting to allow for the fact that the rubber reached its final strain immediately whereas the bitumen did not, there would have been a lateral shift in the curve but in the opposite direction from that actually obtained (d). The explanation of these interesting facts will be dealt with when complex materials are considered.

Although there were individual differences between the curves of single subjects, the pressures actually used (measured subsequently from the deformations of the bitumen samples), although differing widely, were in no way correlated with the position of the curve for the individual. This was found to be the case not only for Hookean *vs.* Newtonian experiments but for complex materials so long as $S \propto \sigma$ for any given time.

Comparison of Complex Materials

In the first place, the complex materials used were selected to ensure a fairly close proportionality between S and σ. They consisted of a mixture of modeling clay, vaseline and rubber, or of lightly vulcanized filled rubbers or of soft "plastics."

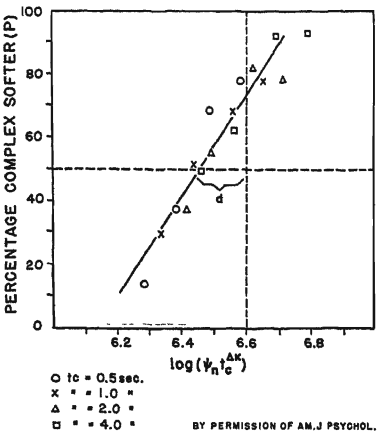

Fig. 3

From *Am. J. Psychol.* **56**, 236 (1943).

The results of one of the many experiments done are shown in Fig. 3 (courtesy of *Am. J. Psychol. vide* Scott Blair and Coppen, 1943).

In this experiment a clay-vaseline-rubber mixture was compared for the usual four t_c's with four vulcanized rubbers of differing modulus (n). It was found that a unique curve could be obtained by plotting p *vs.* $\log (nt_c^{\Delta k})$ where Δk is a fractional number (0.22) chosen to give a unique curve independent of n and t_c. Had the complex material been compared with bitumens of different viscosity, an exponent of $1 - \Delta k$ would have been required. It is therefore assumed that for rubber, $k = 0$; for bitumen, $k = 1$; and for this particular complex material $k = 0.22$. Hence Δk is the difference between k_{complex} and k_{standard}. The same principle is found to hold in all cases tested.

It will be noticed that there is again a discrepancy (d) between the 50% level on the experimental curve and the point where the dotted

lines cross, which is the point where the 50% level would fall if softness-firmness were judged by the total strains produced in the times allowed for squeezing. The slope of the curve gives a measure of the "Range of uncertainty"—*i.e.*, the range of values of $nt_c^{\Delta k}$ over which both "rubber softer" and "rubber firmer" answers were sometimes given. Many curves like Fig. 3 were obtained and it must again be stressed that each such experiment involves a large number of judgments pooled from a panel of subjects.

It was already known from work in these laboratories and elsewhere (Scott Blair, 1940; Scott Blair and Coppen, 1941; and later Scott Blair and Veinoglou, 1944) that many complex materials of the kind used for these experiments closely obey the Nutting equation (Nutting, 1921) which, for the case where $S \propto \sigma$, was independently proposed by Scott Blair and Coppen (1939),

$$\psi = S^{\beta}\sigma^{-1}t^{k}, \tag{1}$$

where ψ* and β are constants. This equation can be derived from the Principle of Intermediacy, regarding complex materials as being intermediate between the four prototypes

$$\sigma \propto S^0t^0,\ S^1t^1,\ S^0t^1 \text{ and } S^1t^0 \text{ (\textit{vide} Scott Blair and Caffyn, 1942).}$$

The usefulness of this idea was greatly strengthened when it was found experimentally that ***k** determined by massed psychophysical experiments such as that shown in Fig. 3 and **k** determined by simple compression tests at constant stress, agreed within the quite narrow limits of experimental error.*

Experiments of this type have so far been confined to materials for which $\beta = 1$ and for which the Nutting equation holds tolerably well. Other experiments which cannot be described here in detail were done on still more complex materials and it was found that when $\beta \neq 1$, materials showing varying degrees of work-hardening, structural viscosity, elasticity, *etc.* were judged relatively firmer or softer by individual subjects depending in a logical way on the magnitude of the pressure used (*vide* Scott Blair and Coppen, 1940). Owing to the war, these very encouraging experiments were discontinued and are only now being resumed.

The following psychological conclusions taken from the results of individual subjects may be of interest:

* In order to keep ψ analogous to η and n it is usual to divide the experimental tensile stresses by 3. It would have been better to have kept to tensile conditions throughout, defining ψ as analogous to τ and E, since the $2(1 + \Pi)$ equation is not valid. This was not clearly understood when many of the earlier data were published and many authors, including the present writer, have now used ψ as a shear constant. So long as it is remembered that the division by 3 is purely formal, no harm is done and it is thought to be simpler to keep to this convention. Fortunately no theoretical use has ever been made of this conversion factor.

The skilled craftsman (cheese-maker) has no better acuity than other subjects, though he sometimes has a better capacity for reproducing his judgments on the same set of materials from day to day. The most important single factor in defining self-consistency and low thresholds is mental set ("frame of mind"). Routine analysts, who are used to carrying out rather dull operations with care and without worrying about the results or purpose of the experiment, were far and away the best category of subject. Younger and less educated subjects were slightly superior to older and more educated people but it was not possible to distinguish the effect of age from that of education. There was no significant difference between men and women.

By What is "Firmness" Judged?

It is clear from the above that, except in the case of a single rubber-rubber comparison, when firmness is judged by the amount of strain produced in the allowed time; and a bitumen-bitumen test when it is judged by rate, in complex experiments it is judged by other factors, the lateral distance d in Figs. 2 and 3 being a measure of the discrepancy from a pure strain judgment. It is not possible here to follow the rather complex argument in detail but it has been suggested (Scott Blair and Coppen, 1943) that in such cases comparative firmness is judged neither by σ, nor by $\dot{\sigma}$, nor by any mixture of these two but by some intermediate entity $\left|\frac{\partial^{\nu}\sigma}{\partial t^{\nu}}\right|$ where $\left|\text{—}\right|$ indicates a fractional differentiation. This suggestion is now known to be somewhat of an over-simplification but the general concept has so far stood the test of time.

Scott Blair (1944b) had already suggested, on purely physical grounds, that the principle of intermediacy might be applied in another way to give:

$$\text{For a fluid: } S \div \frac{d\sigma}{dt} = \eta, \quad \text{a constant,}$$

$$\text{For a solid: } S \div \sigma = n, \quad \text{a constant.}$$

For an intermediate body:

$$S \div \left|\frac{d^{\mu}\sigma}{dt^{\mu}}\right| = \chi_1, \quad \text{a constant.} \tag{2}$$

If we fractionally differentiate the Nutting equation for constant stress conditions, μ times with respect to t, we get

$$\left|\frac{\partial^{\mu}\sigma}{\partial t^{\mu}}\right| = \frac{\Gamma(k+1)}{\Gamma(k-\mu+1)} \cdot t^{k-\mu} \psi^{-1} S. \tag{3}$$

Caffyn and Scott Blair (1945) point out that under conditions when we can equate μ and k, this reduces to

$$\left|\frac{\partial^k \sigma}{\partial t^k}\right| = \Gamma(k+1)\psi^{-1}S,$$

and, since $\Gamma(k+1)$ is a pure number, this means that *under these conditions*, ψ and χ_1 are measures of the same entity. It makes no difference which equation we use so long as Eq. (1) holds with $\beta = 1$, and so long as the pressures exerted are substantially constant.

In a paper now in process of publication (Scott Blair, Veinoglou and Caffyn, *Proc. Roy. Soc.* (*London*)) it is suggested that these complex dimensional "properties" which are not properties in the usual sense, since the exponents of M, L and T differ from one material or group of materials to another, but which are nevertheless of great importance in industry; and which can be assessed reproducibly by handling, and measured, as is shown above, by purely physical means, should be called "quasi-properties." Quasi-properties are of different kinds—some differ but little from true physical properties and can be reproducibly measured by quite independent physical processes; others are less well defined and a strictly laid down procedure must be followed if results are to be reproduced. Quasi-properties are described by an intensity factor, such as ψ or χ_1 above, and one or more exponents (such as k and β) which indicate the (fractional) dimensions of the intensity factor.

The whole entity forms a pattern whose properties are "other than could be derived from the parts in summation" (Koffka) and is called a "Gestalt," though Gestalt psychologists tend to confine the word to groupings which are innate and not formed by training, though they may be modified by it.

Acquired "masses of organized experience" are sometimes called "Schemata" but there seems little point in drawing hard-and-fast lines and we are prepared to speak of "secondary Gestalten" for entities of a Gestalt nature which are largely developed by experience. We have also shown that the complexity of these Gestalten is reduced in any given case to the simplest terms consistent with the dimensional situation. This is a verification of what one of the founders of Gestalt psychology, Wertheimer, calls the "Law of Prägnanz," or "fitness" (*vide* Ellis, 1938). (For further information see Scott Blair, 1943.)

Extension of the Nutting Equation

In cases where the Nutting equation cannot be assumed to hold, Eq. (2) can be integrated to give:

$$\sigma = S^{\beta}(At^{k'} + Bt^{k'-1} + Ct^{k'-2} + \cdots \tag{4}$$

where A, B and C are constants ("intensity factors").

In the paper quoted above (Scott Blair, Veinoglou and Caffyn) it is shown, from an analysis of over 800 curves from 38 different materials tested under constant stress and also constant strain (relaxation) conditions, that in almost all those cases where the simple Nutting equation does not fit the data within the limits of experimental error, the introduction of a second or very rarely also a third term from Eq. (4) gives a satisfactory fit. The Nutting equation is thus regarded as a very useful special case of this more general equation. For materials for which $\beta \neq 1$, the situation is more complex and will be referred to again below.

The Meaning of Fractional Differential Expressions

The use of fractional differentials is not new to rheology. Gemant (1936, 1938) has used half-differentials but, in his later paper, he says that the fractional differential "only occurs as a useful mathematical symbol, whereas the underlying elementary process, whatever it may be, will probably contain differential quotients of an integral order."

We view our use of the Γ function very differently. The theory, which though still incomplete, is developed by Scott Blair, Veinoglou and Caffyn, may be very briefly summarized as follows:—

It has already been pointed out that times are normally defined as equal when "free" Newtonian bodies (or alternatively light) traverse equal (superposable) distances in them. This leads to a definition of velocity as the first differential of length with respect to time which, because of this definition of time equality, is constant for Newtonian bodies; and to the second differential, called acceleration.

When bodies are not uninfluenced by other bodies, and their velocities change with time, a force is postulated and defined as the rate of change of (velocity $\times$ mass). It has long been realized that the Newtonian* time scale is arbitrary (*vide* Poincaré, 1904) and, in the case of a complex plastic being strained, the rheologically active units are certainly not independent Newtonian bodies. It would, therefore, be easy to choose a non-Newtonian time equality definition which would reduce the entities by which firmness is judged to simple whole-number differential expressions.

The use of separate time scales for different materials is not convenient, however, so Newtonian time is used, but, as a result of this arbitrary procedure, the derived constants cannot be expected to be built up entirely from whole-number differentials. It is thus apparent that the fractional differential is an essential feature of our whole mode of approach.

For materials for which $\beta = 1$, the use of a suitable non-Newtonian time scale could be made to give simple linear tensor relations. However,

* It is not implied that this time scale was invented by Newton but it became part of the system of physics which he developed.

a non-Newtonian time scale does not help for materials which obey, for example, Bach's law (Bach, 1888) where stress bears a power relation to strain but equilibrium is immediately established. The whole point of the theory of quasi-properties so far is that the quasi-property describes a process and not a state and that the systems studied are non-equilibrium systems. They are approaching equilibrium (though sometimes exceedingly slowly) in an orderly way and are therefore said to be in a state of "quasi-equilibrium." In the case of Bach systems, the situation is quite different. A hopeful line of approach is being pursued but is not yet sufficiently developed for discussion.

Conclusions and Summary

The observables in the "Science of Deformation and Flow" are strains. For simple elastic bodies, a state of stress is inferred proportional to the observed strain or is related to the behavior of the "causal agent" under subsequent dynamic conditions. For example, a weight hung on the end of a Hookean spring will, when released, show an acceleration *in vacuo* proportional to the strain it had previously produced in the spring. The "potential" state of stress in a complex body is generally inferred from its strain in relation to that of a simple body attached to it.

In our psychophysical experiments, we have so far been mainly concerned with constant stress conditions under which σ/t changes are observed. For convenience a "Newtonian" time definition is used, but in the straining of complex bodies this does not lead to a whole-number differential equation.

In judging σ/t changes subjectively by handling, spontaneous judgments do not depend on any Newtonian time analysis—indeed subjective ("psychological") time is certainly non-Newtonian. It is encouraging that, in spite of these complications, if enough data are massed so as to eliminate purely individual differences, excellent agreement is reached between the values of material constants calculated from purely psychophysical experiments and those derived from the integrated Γ-function equation. Nutting's empirical law is a useful first approximation to the general series equation.

The presence of time in the dimensional units of stress ($ML^{-1}T^{-2}$) is due to the fact that stress has to be *measured* dynamically. Changes in the time-equality definition thus cannot account for non-linear stress-strain conditions such as those described by Bach, and other explanations are being sought.

Complex entities useful for comparing the rheological properties of industrial materials are to be regarded psychologically as Gestalten (though not necessarily "primary" Gestalten). Physically, they may be described as quasi-properties or associated groups of quasi-properties.

The quasi-property describes a process and not an equilibrium state and, if the Newtonian time-scale is used, is defined by an intensity or quantity factor and one or more fractional numerical exponents which are quality factors.

Alternatively, it is possible to explain the purely physical rheological behavior of complex materials on classical lines in terms of dimensionally orthodox "constants." But these constants are apt to be very numerous and bear no relation to the psychophysical facts. Many explanations of this kind have also been marred by the unjustifiable use of equations derived from simple S and σ tensors and based on assumptions only justified for isotropic materials and small strains.

References

Alexandrov, A. P., and Lazurkin, J. S., *Acta Physicochim. U. R. S. S.* **12**, 647 (1940).

Bach, C., *Z. Ver. deut. Ing.* **32**, 192 (1888).

Barkas, W. W., *Trans. Faraday Soc.* **36**, 824 (1940); **37**, 535 (1941); **38**, 194, 447 (1942).

Barkas, W. W., *Forest Prods. Res. Lab. Spec. Rep.* (*D.S.I.R.*) *No.* **6**, (1945).

Binns, H., *J. Textile Inst.* **29** T, 117 (1938).

Caffyn, J. E., and Scott Blair, G. W., *Nature* **155**, 171 (1945).

Ellis, W. D., A Source Book of Gestalt Psychology. Kegan Paul, London, 1938.

Gemant, A., *Physics* **7**, 311 (1936).

Gemant, A., *Phil. Mag.* **25**, 540 (1938).

Grünberg, L., and Nissan, A. H., *Nature* **156**, 241 (1945).

Maxwell, J. C., *Phil. Mag.* **35**, 129 (1868).

Meyer, H. K., and Ferri, C., *Helv. Chim. Acta* **18**, 570 (1935).

Mooney, M., *J. Applied Phys.* **11**, 582 (1940).

Nutting, P. G., *J. Franklin Inst.* **191**, 679 (1921); *Proc. Am. Soc. Testing Materials* **21**, 1162 (1921).

Poincaré, H., La Valeur de la Science, p. 44. Flammarion, Paris, 1904.

Reiner, M., Ten Lectures on Theoretical Rheology. Rubin Mass, Jerusalem, Palestine, 1943.

Scott Blair, G. W., and Coppen, F. M. V., *Proc. Roy. Soc.* (*London*) **128 B**, 109 (1939).

Scott Blair, G. W., *J. Sci. Instruments* **17**, 169 (1940).

Scott Blair, G. W., and Coppen, F. M. V., *Brit. J. Psychol.* **31**, 61 (1940).

Scott Blair, G. W., and Coppen, F. M. V., *J. Soc. Chem. Ind.* **60**, 190 (1941).

Scott Blair, G. W., and Caffyn, J. E., *J. Sci. Instruments* **19**, 88 (1942).

Scott Blair, G. W., and Coppen, F. M. V., *Am. J. Psychol.* **55**, 215 (1942); **56**, 234 (1943).

Scott Blair, G. W., A Survey of General and Applied Rheology. Pitman, London and New York, 1943.

Scott Blair, G. W., *Nature* **154**, 213 (1944a).

Scott Blair, G. W., *J. Sci. Instruments* **21**, 80 (1944b).

Scott Blair, G. W., and Veinoglou, B. C., *J. Sci. Instruments* **21**, 149 (1944).

Trouton, F. T., *Proc. Roy. Soc.* (*London*) **77 A**, 426 (1906).

RHEOLOGY OF ASPHALT

J. W. Romberg and R. N. Traxler

From The Texas Company, Port Neches, Texas

Received Nov. 11, 1946

Introduction

The flow properties of asphalts vary widely. Values of viscosity at 25°C. (77°F.) range from about 10^3 poises for the fluid petroleum residua to 10^9 poises and higher for hard asphalts. The type of flow varies from that of an essentially simple liquid (Newtonian flow) to highly complex (non-Newtonian) flow. Most asphalts are deformed continuously even by the smallest applied shearing stresses and thus do not exhibit measurable yield values. Exceptions to this are certain asphalts very high in wax content. When subjected to stress many asphalts undergo an elastic deformation in addition to the usually more predominate permanent flow. An accurate, complete and rapid evaluation of these different flow properties is the goal of rheological measurements of asphalts.

Viscosity

Viscosity, η, is defined as the ratio of shearing stress, F, to rate of shear, S:

$$\eta = F/S, \text{ poises}, \tag{1}$$

where F = shearing stress, dynes/sq. cm., S = rate of shear, reciprocal seconds.

The energy, W, expended in one second for unit volume (6) is related to viscosity, η, as follows:

$$W = \eta S^2 = FS. \tag{2}$$

A complex material is one for which the viscosity varies with the rate of shear. Another way of saying this is that the plot of rate of shear, S, *vs.* shearing stress, F, is not linear. However, it has been shown (21) that, for many asphalts, in the range of rate of shear and shearing stress employed in the rotary viscometer (20), the plot of log S *vs.* log F is essentially a straight line.

One of the purposes of using absolute viscosity units is to make possible the comparison of all materials on the same basis. In order to compare the viscosities of two complex materials, it is necessary to select arbitrarily some standard conditions under which the viscosities are

obtained. The methods which have been used are discussed in the following pages.

Using the rotary viscometer (20) the viscosities of complex materials have been compared at a particular rate of shear. Since it is impossible to measure both hard and fluid materials under the same conditions, it is necessary to select some intermediate rate of shear. A value of 0.1 reciprocal second has been used in most of the work done at this laboratory. Since neither the very hard nor the very fluid materials can be measured at this rate, all asphalts are measured at two or more convenient rates of shear and a plot of log shearing stress *vs.* log rate of shear is extrapolated to 0.1 reciprocal second. However, this method has several disadvantages. Extrapolation in itself tends to magnify any errors in measurement. In addition, a more serious obstacle to the success of this method has become apparent which is best illustrated by the following example. On Fig. 1, are plotted log rate of shear *vs.* log shearing stress for a series of air-blown Gulf Coast II asphalts. On the log-log plot essentially straight lines are obtained in the region in which the determinations are made. It has been the practice to extend these lines when necessary until they cross the ordinate representing 0.1 reciprocal second (10^{-1} sec.$^{-1}$). From the value of shearing stress at this line the viscosity is calculated.

As asphalts are air blown and become harder, the degree of complex flow becomes greater and the plot of log S against log F becomes steeper. It will be noted from Fig. 1 that, if a rate of shear of 100 reciprocal seconds had been selected instead of 0.1, the calculated viscosity ($\eta = F/S$) of Asphalt 1C (146°F., ring and ball) would have been lower than that for Asphalt 1B (125°F., ring and ball). Although, in the several series of asphalts listed in this paper, no such reversal in magnitude of viscosity has been obtained at 0.1 reciprocal seconds, the effect is apparent in the disproportionately low values of viscosity for the highly complex, hard materials.

The explanation of this reversal in magnitude of calculated viscosity for two succeeding samples in a series and for the unexpectedly low values of viscosity for the hard, complex asphalts probably lies in the fact that the extrapolated lines do not represent the actual behavior of the materials since the plot of log S against log F may be curved over a long distance. For hard asphalts this curvature may be accentuated by slippage, or by a rise in the temperature of the sample caused by the excessive amount of energy that must be dissipated in shearing at high rates. This latter subject is discussed in greater detail below.

With the falling coaxial cylinder viscometer (19) asphalts are compared at a particular shearing stress. For certain purposes, such as evaluating age hardening, where the same shearing stress (same load) can be used

on each sample, this method is useful. However, the same shearing stress cannot be used for materials of widely different viscosities. To make measurements at several different shearing stresses and extrapolate to some common value would be subject to the same disadvantages discussed above.for the use of a particular rate of shear.

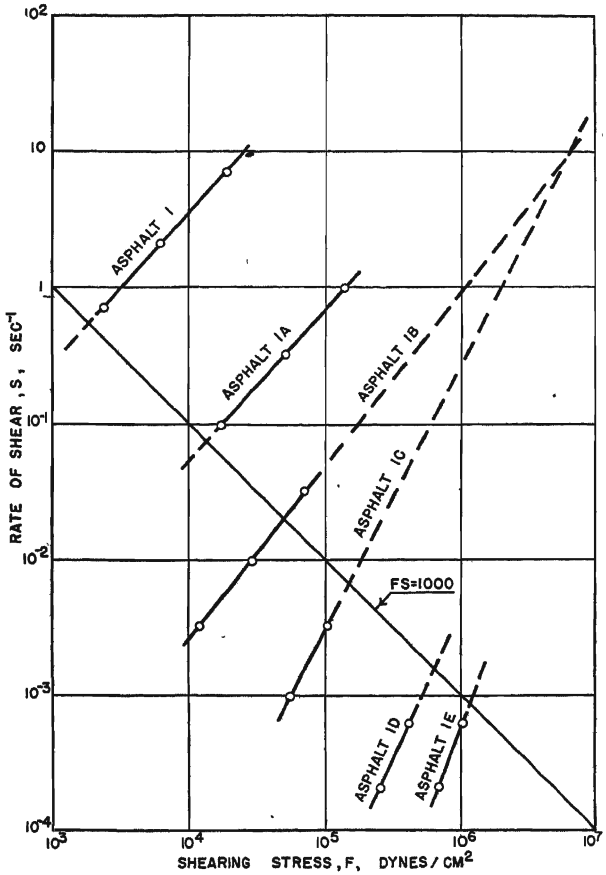

FIG. 1

Variation of the Rate of Shear of Asphalts with the Applied Shearing Stress at 25°C.

These difficulties in comparing viscosities of complex materials apparently can be overcome by making the comparison at a particular power input per unit volume of sample. This requires calculation of the viscosity at a constant value of the product of the shearing stress times the rate of shear, $F \times S$ (6). The product FS is the power input at the mean radius at which F and S are calculated. In a rotary viscometer this is not

TABLE 1

Rheological Data on Various Asphalts

Asphalt	Process	Residuum Source	Softening Point Ring and Ball		Ductility at 25°C. (77°F.) 5 cm./min., cm.	Penetration at 25°C. (77°F.) 100 g., 5 sec.	Rheological Evaluation					
							Temp. of Measurement		Viscosity, Megapoises		Degree of Complex Flow, c	Relaxation One-Half Time, sec.
			°C.	(°F.)			°C.	(°F.)	$S=0.1$ sec.$^{-1}$	$FS=1000$ Ergs, sec.$^{-1}$ cm.$^{-3}$		
1	—	Gulf Coast II Residuum[a]	—		—	—	5	(41)	0.34	0.41	0.80	1—
							25	(77)	0.0045	0.0036	0.90	1—
1A	Air Blown	Gulf Coast II	40.0	(104)	126	220	25	(77)	0.18	0.18	0.90	1—
1B	Air Blown	Gulf Coast II	51.7	(125)	105	102	25	(77)	1.7	2.5	0.80—	3.5
1C	Air Blown	Gulf Coast II	63.3	(146)	7	58	5	(41)	53	480	0.45	—
							25	(77)	6.0	23	0.50	18
							50	(122)	0.24	0.29	0.70	1.6
1D	Air Blown	Gulf Coast II	103.3	(218)	2	27	25	(77)	52	490	0.45	—
1E	Air Blown	Gulf Coast II	138.9	(282)	0	18	25	(77)	74	1360	0.40—	—
2	—	East Texas Residuum	—	—	—	—	5	(41)	0.37	0.47	0.75	1—
							25	(77)	0.0055	0.0046	0.90	1—
2A	Steam	East Texas	38.3	(101)	112	239	25	(77)	0.15	0.15	0.90	1—
2B	Air Blown	East Texas	46.7	(116)	200+	105	25	(77)	0.72	0.82	0.90	1±
2C	Air Blown	East Texas	54.4	(130)	158	55	5	(41)	280	860	0.75	—
							25	(77)	3.2	4.4	0.80	3.5
							50	(122)	0.029	0.028	0.90	1—
2D	Air Blown	East Texas	77.2	(171)	4.5	18	25	(77)	68	310	0.60	—
3	—	Gulf Coast III Residuum[b]	—	—	—	—	5	(41)	1.7	1.7	1.00	1—
							25	(77)	0.010	0.0098	1.00	1—
3A	Steam	Gulf Coast III	38.9	(102)	135	203	25	(77)	0.14	0.14	0.95	1±
3B	Steam	Gulf Coast III	45.6	(114)	200+	100	25	(77)	0.54	0.55	0.95	1±
3C	Steam	Gulf Coast III	50.0	(122)	200+	52	5	(41)	2300	4800	0.85	—
							25	(77)	23	2.4	0.95+	1±
							50	(122)	0.011	0.011	1.00	1—
3D	Steam	Gulf Coast III	63.9	(147)	200+	15	25	(77)	32	33	1.00—	—

[a] From upper Texas Gulf Coast. [b] From lower Texas Gulf Coast.

TABLE I—*Continued*

Asphalt	Process	Residuum Source	Softening Point Ring and Ball		Ductility at 25°C. (77°F.) 5 cm./ min., cm.	Penetration at 25°C. (77°F.) 100 g., 5 sec.	Rheological Evaluation					
							Temp. of Measurement		Viscosity, Megapoises		Degree of Complex Flow, c	Relaxation One-Half Time, sec.
			°C.	(°F.)			°C.	(°F.)	$S=0.1$ sec.$^{-1}$	$FS=1000$ Ergs, sec.$^{-1}$ cm.$^{-3}$		
4		San Joaquin Valley Resid.	—	—	—	—	5	(41)	5.2	5.3	1.00	1—
							25	(77)	0.029	0.029	1.00	1—
4A	Air Blown	San Joaquin Valley	36.7	(98)	132	176	25	(77)	0.18	0.18	0.95+	1—
4B	Air Blown	San Joaquin Valley	43.3	(110)	179	100	25	(77)	0.62	0.62	1.00—	1—
4C	Air Blown	San Joaquin Valley	50.0	(122)	200+	50	5	(41)	650	820	0.95	—
							25	(77)	2.9	3.2	0.95	1.6
	Air Blown	San Joaquin Valley					50	(122)	0.012	0.012	1.00	1—
4D	Air Blown	San Joaquin Valley	58.9	(138)	200+	25	25	(77)	22	24	0.95	—
4E	Air Blown	San Joaquin Valley	77.8	(172)	0	10	25	(77)	230	980	0.70	—
5	Steam	Northeast Texas	56.1	(133)	146	49	5	(41)	110	1130	0.50	—
							25	(77)	6.1	9.1	0.80	3
							50	(122)	0.061	0.059	0.85	1—
6	Air Blown	Northeast Texas	61.7	(143)	30	55	5	(41)	46	640	0.40	—
							25	(77)	8.8	15	0.75	20
							50	(122)	0.11	0.11	0.80	1—
7	Air Blown	Mexican	57.2	(135)	114	55	5	(41)	190	600	0.75	—
							25	(77)	4.0	5.8	0.80	4.5
							50	(122)	0.056	0.053	0.85	1—
8	Steam	East Texas	52.2	(126)	200+	53	5	(41)	370	1060	0.90	—
							25	(77)	2.5	3.0	0.90	2
							50	(122)	0.017	0.017	1.00	1—

quite equal to the total power input divided by the total volume of sample. Since the values of both F and S within the sample vary, the total power input must be obtained by integration.

A power input of 1000 ergs (one kiloerg)/sec./cc. has been selected as a convenient value at which to evaluate the viscosities of asphalts.

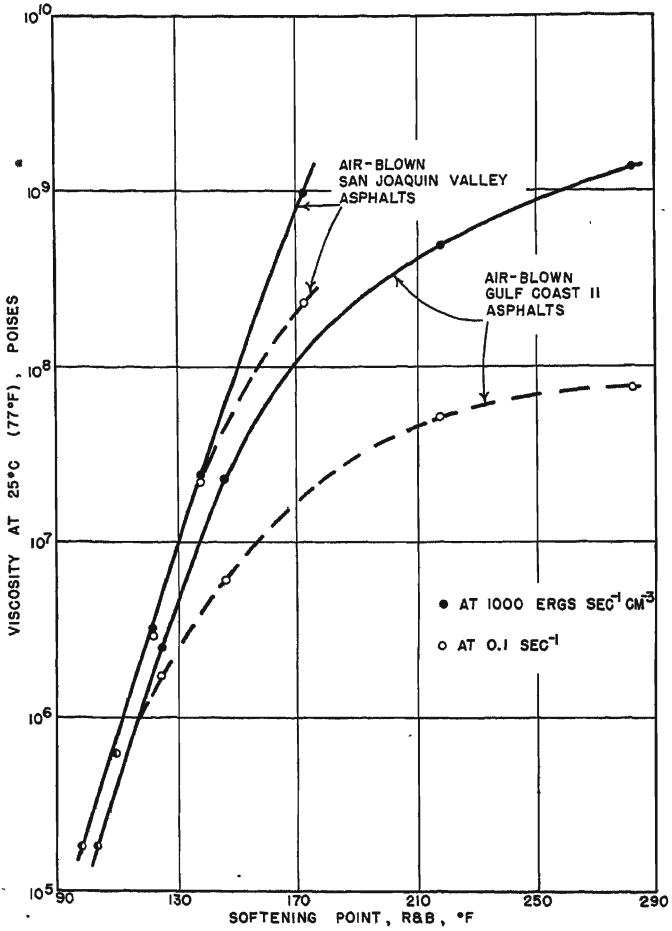

FIG. 2

Ring and Ball Softening Point-Viscosity Relation for Two Series of Asphalts

This power input is represented on Fig. 1 by the diagonal line marked $FS = 1000$. Very little extrapolation is required to reach this line from any of the rheological data normally obtained on asphalts. The rheological data are obtained at two or more rates of shear and log S *vs.* log F plotted. A straight line is drawn through the plotted points and, if

necessary, extrapolated until the line $FS = 1000$ is crossed. The viscosity is equal to F divided by S at $FS = 1000$.

In Table I, viscosities calculated at both 0.1 reciprocal second and at 1000 ergs sec.$^{-1}$ cm.$^{-3}$ are listed for several different asphalts. The values

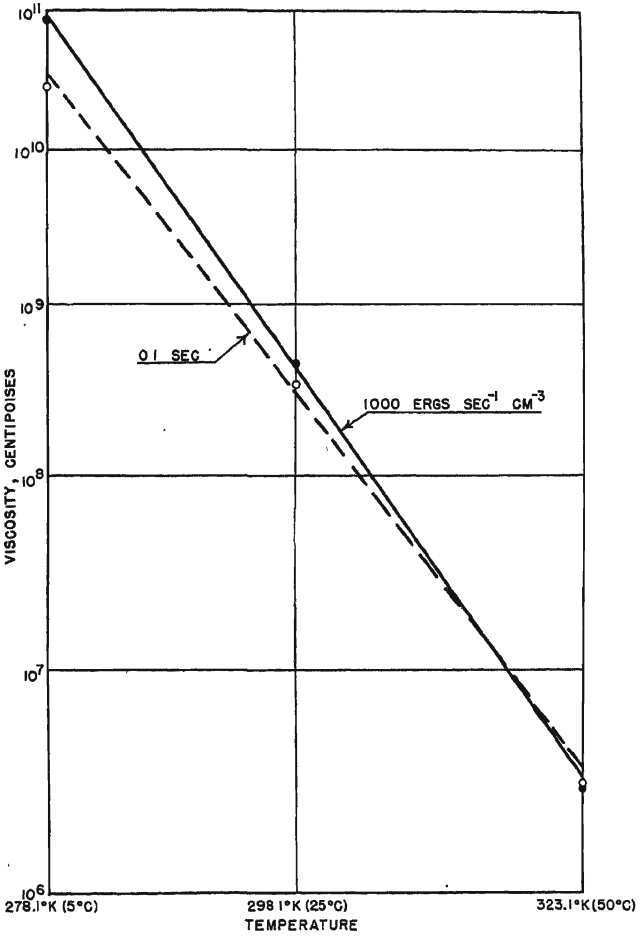

FIG. 3

Log Absolute Temperature—Log-Log Viscosity Relation for Air-Blown East Texas Asphalt, 2C

of viscosity calculated at 1000 ergs sec.$^{-1}$ cm.$^{-3}$ appear to give a better indication of the consistency of the hard, complex materials. The difference in the results obtained by the two methods is illustrated in Fig. 2, in which log viscosity at 25°C. is plotted against softening point, ring and

ball, for two series of asphalts. All except the hardest of the air-blown San Joaquin Valley asphalts are essentially simple liquids, and viscosities obtained by the two methods differ but little. However, for the air-blown Gulf Coast II asphalts which show considerable complex flow, the viscosities calculated by the two methods differ considerably.

Since most air-blown asphalts show increased complex flow as the temperature is lowered, somewhat different values of susceptibility will be obtained depending on whether viscosities are calculated at $S = 0.1$ sec.$^{-1}$ or $FS = 1000$ ergs sec.$^{-1}$ cm.$^{-3}$. This is illustrated in Fig. 3, in which the log-log viscosity (calculated by each of the two methods) is plotted against the log of absolute temperature for air-blown East Texas Asphalt 2C. The line drawn through the points at $FS = 1000$ is somewhat steeper (more susceptible) and fits the data better than the line drawn through the values at $S = 0.1$ sec.$^{-1}$.

Thermodynamic Considerations

The energy required to produce any deformation of matter appears in three forms which are (1) kinetic energy, (2) potential energy, and (3) thermal energy. In the evaluation of the rheological properties of asphalts, kinetic energy effects are usually negligible. The potential energy is that required to overcome the elastic resistance of the material and appears in the early part of the measurement. When equilibrium conditions are reached, essentially all of the energy is being converted to thermal energy (heat).

If the power input and the size of sample are such that the energy dissipated as heat in shearing cannot be conducted away quickly, an appreciable rise in temperature of the sample will occur. For a material as susceptible to temperature as asphalt, even a slight change in temperature will affect the viscosity determination.

Calculations have been made of the power input required to cause a maximum temperature rise of 0.056°C. (0.1°F.) in the sample. It was found that a power input of about 20,000 ergs sec.$^{-1}$ cm.$^{-3}$ would be required to give this temperature rise for an instrument having a rotor length of 2.54 cm., rotor diameter of 3.81 cm. and stator diameter of 2.54 cm. On the basis of these calculations a power input of 1000 ergs sec.$^{-1}$ cm.$^{-3}$ appears to be a safe value at which to compare the viscosities of complex materials.

Complex Flow

An equation for the evaluation of complex flow has been described elsewhere (21). This relation may be written:

$$M = F/S^c, \tag{3}$$

where F = shearing stress, dynes/sq. cm., S = rate of shear, reciprocal sec., c = slope of log F *vs.* log S plot, M = value of F when $S = 1$.

For a simple liquid, the constant c is unity, M is the viscosity in poises and Eq. (3) is the same as Eq. (1). For complex materials, the value of c is a measure of the deviation from simple flow. For materials, such as certain asphalts, which have lower viscosities for increasing values of rate of shear, c is less than one.

Values of the degree of complex flow, c, at 25°C. (77°F.) for various residua and asphalts are given in Table I. The complex flow of the residua at 5°C. (41°F.) and of the 50 penetration (25°C., 100 g., 5 sec.) asphalts at 5°C. (41°F.) and 50°C. (122°F.) are also given in Table I. These values of c vary from 0.40 to 1.00.

Elasticity

Elasticity has been defined (1) as "that property of a body by virtue of which it tends to recover its original size and shape after deformation". Many of the uses of asphalt depend upon its ability to be deformed without rupture and to recover from small deformations. Following deformation of some solids, such as steel and vulcanized rubber, elastic recovery is practically complete and instantaneous (under certain conditions). However, for viscoelastic materials, such as most asphalts, recovery is only partial and takes place over a period of time. Because permanent and continuous deformation occurs in asphalts under stress, it is usually impossible to evaluate the elastic modulus by direct tensile or torsion measurements. Several other methods discussed below have been used for evaluating the elasticity of viscoelastic materials.

Vibrational (Dynamic) Methods

If a viscoelastic material is subjected to alternating stresses, the deformation is essentially elastic if the frequency is high compared with the relaxation time (7). Other vibrational methods involve measurements of the fundamental frequency of a rod or sheet of the material from which the elastic modulus can be calculated (5, 9).

The velocity of sound waves in a liquid is a function of its density and compressibility (reciprocal of bulk modulus of elasticity). From the bulk modulus and Poisson's ratio the shear modulus of elasticity has been calculated (15).

Thermodynamical Methods

The work required to produce an elastic deformation is stored as potential energy and is expended on recovery. In viscous flow, work is dissipated as heat. Thus, if the relative amounts of work which go to heat

and to potential energy are measured, the relative amounts of viscous and elastic deformation are known. The losses of energy to heat have been measured by the damping effect upon a torsional vibration (8).

Elastic Fore- and After-Effects

In viscosity measurements, an increasing ratio of shearing stress to rate of shear at the start of the determination is said to be caused by an elastic fore-effect. Nutting's equation (13, 14), which is discussed below, might be considered a method of evaluating this elastic fore-effect.

Elastic after-effect (recoil) has been measured (2, 4, 11, 16), but quantitative analyses by this method are complicated by the fact that recovery and relaxation are both occuring at the same time. In addition, for such materials as asphalt, recovery may take place over a long period of time.

Relaxation of stress after deformation offers another means of measuring elasticity. Maxwell (12) in his classical treatment was perhaps the first to offer an equation for deformation of materials intermediate between viscous fluids and elastic solids. When such a material is sheared, it tends to recover part of the deformation. If after deformation the material is not allowed to recover (recoil), the stress required to maintain the initial deformation decreases because of relaxation or creep. By making certain assumptions Maxwell obtained the equation:

$$F = GDe^{-t/T} \tag{4}$$

where F = shearing stress, dynes/sq. cm., G = modulus of elasticity in shear, dynes/sq. cm., D = strain in shear, t = time, seconds, e = Naperian base, 2.718. . . ., T = an integration constant with the dimensions of time in seconds, called the "relaxation time". The relaxation time, T, is numerically equal to t when the shearing stress has fallen to $1/e$ of its original value.

Relaxation One-Half Time

After a study of the methods which have been employed for evaluating elastic properties of viscoelastic materials, the simplest procedure appeared to be the evaluation of relaxation. To measure relaxation it is necessary to follow the decrease in shearing stress with time after shearing is stopped. This was made possible with the rotary viscometer (20) in which viscosity and complex flow are evaluated, by employing an indicating balance to measure the torque.

It was found that asphalts, like many other materials (10, 17), do not follow Maxwell's equation. This is illustrated in Fig. 4. It was also

found that the observed values for relaxation time not only varied widely with temperature, but were dependent upon the shearing stress and size of sample. In view of the fact that the relaxation time is not an absolute value and for expediency in routine measurements, a simpler term for relaxation has been used, *i.e.*, the time required for the shearing stress to decrease to one-half its original value. This is called the relaxation one-

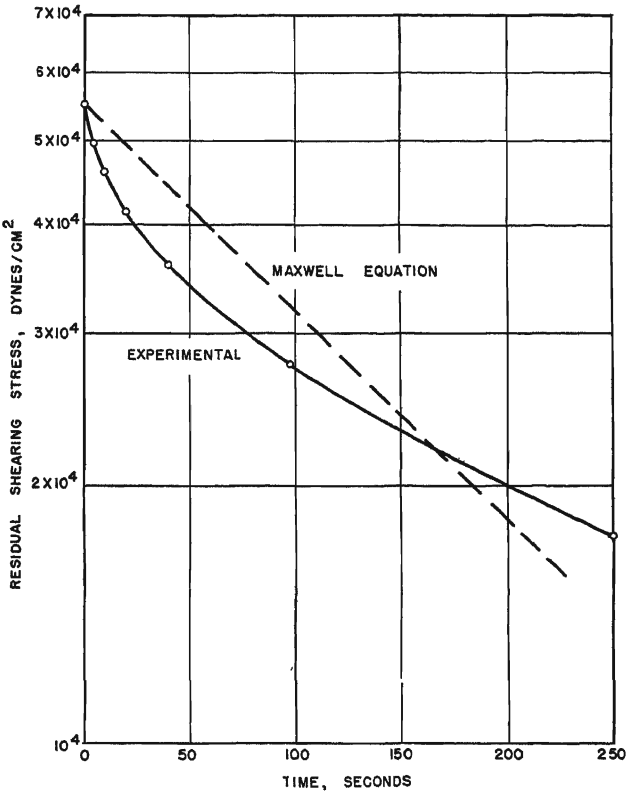

FIG. 4

Relaxation Curve for Air-Blown Gulf Coast II Asphalt 1C at 25°C.

half time and like the Maxwell relaxation time may be used to evaluate relative elasticity of asphalts for certain specified conditions of temperature, shearing stress, and size of sample.

For comparison of elastic effects of different asphalts the relaxation one-half time is evaluated at a power input of 1000 ergs/sec./cc. using the same procedure as for determining viscosity. Values of the relaxation one-half time for several different asphalts are given in Table I.

Stress-Strain-Time Relation

It would simplify the rheological evaluation of viscoelastic materials such as asphalts if the deformation could be represented by a single equation. Nutting (13, 14) has proposed such a law of deformation for semi-solid materials relating stress, strain, and time. Several investigators (3, 18), notably Scott Blair, have used this relation for a wide variety of materials. A few experiments have been made by the authors in order to investigate the possibility of using this equation for evaluating the rheological properties of asphalts.

Nutting's proposed relation represents strain as a function of time and stress as expressed by the following equation:

$$D = at^n F^m, \tag{5}$$

where D = strain in shear, t = time, seconds, F = stress, dynes/sq. cm., a, n, m = constants.

If this relation is valid, the constants a, n, and m should evaluate the deformation properties of a material. The constant a is a measure of intensity while n and m are measures of degree. Thus, for a perfectly elastic deformation $n = 0$, $m = 1$, and a is the reciprocal of the elastic modulus. For a perfectly viscous deformation, $n = 1$, $m = 1$, and a is the fluidity. For intermediate materials a may be considered a measure of softness; however, its dimensions depend on the values of n and m.

There is some difficulty in visualizing which properties n and m measure. The constant, n, being the exponent of time, is a measure of how strain changes with time for a particular stress. The constant n is equal to 1 if the rate of strain is constant; n is greater than 1 if the rate of strain is increasing with time; and n is less than 1 if the rate of strain is decreasing with time. Changes in rate of strain are caused by elasticity as well as by thixotropy, work hardening, *etc.* Without making other measurements, there appears to be no way of telling whether a value of n of less than 1 indicates elasticity, work hardening, or a combination of the two. The constant m, since it is the exponent of stress, is a measure of how strain at a particular time is affected by the stress.

Theoretically, Nutting's equation could be used to analyze data obtained in the constant rate of shear rotary viscometer. However, from available data it is apparent that, even at best, Nutting's equation can hold only for the initial deformation in the constant rate of shear viscometer. Over a period of years, results obtained with the rotary viscometer have shown that F becomes constant (equilibrium is attained), or may go through a maximum for very complex materials. Under such conditions Nutting's equation cannot hold. For this reason a constant shearing stress apparatus was constructed.

In this apparatus the rotor and stator of the regular rotary viscometer were used. The outer cylinder was held stationary in a chuck, and thus became the stator instead of rotor. The inner cylinder was driven by weights suspended on a thread which ran over a pulley and around a drum attached to the vertical shaft. The angular deflection of the inner cylinder was indicated on a graduated scale.

Three asphalts were studied at 25°C. in the constant shearing stress viscometer using three different weights. Each determination was made on a freshly prepared sample, and each measurement was started one hour after pouring. Most determinations were made in duplicate or triplicate.

TABLE II

Stress-Strain-Time Relation

Asphalt Process Residuum Source	9 Steam Gulf Coast III	10 Air Blown Gulf Coast II	11 Air Blown Gulf Coast II*
Physical Tests			
Softening Point, Ring & Ball, °C.	50.0	65.6	81.7
°F.	(122)	(150)	(179)
Ductility at 25°C., 5 cm./min., cm.	200+	8	2
Penetration at 25°C., 100 g., 5 sec.	53	53	48
Rheological Data at 25°C.			
Viscosity, Megapoises, $S=0.1$	3.0	5.7	9.4
Viscosity, Megapoises, $FS=1000$	3.1	22	94
Complex Flow, c	1.00−	0.50	0.35−
Relaxation One-Half Time, sec.	1±	20	66
Value of Parameters in Stress-Strain-Time Equation			
a'	1.49×10^{-5}	2.9×10^{-6}	1.85×10^{-6}
n	0.926	0.566	0.408
m	0.970	1.100	1.059
Standard Error of Estimate, %	10	16	20

* Asphalt 11 was prepared from a lower viscosity residuum than Asphalt 10.

The parameters a', n, and m of Eq. (5) were evaluated* for each asphalt by the method of least squares. For this purpose the angular deformation in degrees,* D', was used instead of strain, D, inasmuch as the rotation is proportional to strain, and hence, only the numerical value of the constant a in the Nutting equation is affected. The calculated values of the parameters are summarized in Table II. Also included are the values for the standard error of estimate.

From these data, it will be noted that values of m vary only slightly

* When angular deformation in degrees, D', is used in place of strain, constant a will be designated as a'.

from 1.00. This means that at any particular time the deformation is essentially proportional to the shearing stress.

Assuming that variations in values of n are caused by differences in elasticity alone, asphalt 9 shows the least elasticity, asphalt 10 is intermediate and asphalt 11 shows the most elasticity. This lists the three asphalts in the same order as the relaxation one-half times given in Table II.

Values of a' would indicate that asphalt 9 is the softest of the three asphalts with asphalt 10 slightly softer than asphalt 11. Other rheological data as well as physical tests given in Table II classify asphalt 10 as being considerably softer than asphalt 11.

Considering the reproducibility of check data, the standard error of estimate of 10% for asphalt 9 is not considered excessively high. However, standard errors of 16% for asphalt 10 and 20% for asphalt 11 appear somewhat high and indicate that the form of Nutting's equation does not satisfactorily fit the data for these two asphalts.

TABLE III

Standard Error of Estimate for Constant Shearing Stress

Asphalt	Process and Residuum Source	Mean Shearing Stress	n	Standard Error of Estimate
		dynes/sq.cm.		*Per cent*
9	Steam Refined Gulf Coast III	5,700	0.940	3
		11,400	0.914	12
		22,800	0.954	2
10	Air Blown Gulf Coast II	11,400	0.576	17
		22,800	0.551	12
		57,000	0.567	18
11	Air Blown Gulf Coast II	22,800	0.378	23
		57,000	0.405	15
		114,000	0.464	13

To study further the difference between observed values of strain and values obtained by Nutting's equation, independent calculations were made at each shearing stress. Under the conditions of constant shearing stress, Nutting's equation becomes:

$$D = Kt^n, \tag{6}$$

where D, t, and n have the same meanings as in Eq. (5), K (a constant) $= a'F^m$.

By the method of least squares the parameter n was calculated for each shearing stress. These values are given in Table III, together with

the values for the standard error of estimate. The percentage errors by this method of computation are of the same order of magnitude as the corresponding results for the same samples given in Table II, calculated using all the available data. This would indicate that the error is largely in the strain-time relation rather than the strain-stress relation.

In addition to viscosity, complex flow, and elasticity, there are other phenomena involving the flow of asphalts. These include the manner in which the rheological properties vary with temperature, age, prior deformation (thixotropy, work hardening, *etc.*) and pressure. With the exception of the latter, these phenomena have been discussed in earlier papers.

Acknowledgment is made to H. E. Schweyer for advice and counsel during the experimental work and in the preparation of the manuscript.

References

1. *Am. Soc. Testing Materials*, Definition of Terms Relating to Rheological Properties of Matter (E–24–42), *Part III*, p. 1072 (1944).
2. Broome, D. C., *J. Inst. Petroleum Tech.* **25**, 509 (1939).
3. Broome, D. C., *Petroleum* **5**, 122 (1942).
4. Coombs, C. E., and Traxler, R. N., *J. Applied Physics* **8**, 291 (1937).
5. Frolick, K., *Kunststoffe* **30**, 10 (1940).
6. Gemant, A., *J. Applied Physics* **12**, 530 (1941).
7. *Ibid.* **13**, 210 (1942).
8. *Ibid.* **14**, 204 (1943).
9. Gemant, A., and Jackson, W., *Phil. Mag.* **23**, 960 (1937).
10. Hatschek, E., and Jane, R. S., *Kolloid-Z.* **39**, 300 (1926).
11. Lee, A. R., Warren, J. B., and Waters, D. B., *J. Inst. Petroleum Tech.* **26**, 101 (1940).
12. Maxwell, J. C., *Phil. Mag.* **35**, 133 (1868).
13. Nutting, P. G., *J. Franklin Inst.* **191**, 679 (1921).
14. Nutting, P. G., *Proc. Am. Soc. Testing Materials* **21**, 1162 (1921).
15. Pochettino, A., *Nuovo cimento* **8**, 77 (1914).
16. Saal, R. N. J., and Labout, J. W. A., *J. Phys. Chem.* **44**, 149 (1940).
17. Schwedoff, T., *J. phys.* **8**, 341 (1889).
18. Scott Blair, G. W., A Survey of General and Applied Rheology. Pitman Publishing Company, New York, 1944.
19. Traxler, R. N., and Schweyer, H. E., *Proc. Am. Soc. Testing Materials* **36**, 518 (1936).
20. Traxler, R. N., Romberg, J. W., and Schweyer, H. E., *Ind. Eng. Chem., Anal. Ed.* **14**, 340 (1942).
21. Traxler, R. N., Schweyer, H. E., and Romberg, J. W., *Ind. Eng. Chem.* **36**, 823 (1944).

A REVIEW OF THE RHEOLOGY OF BITUMINOUS MATERIALS

R. N. Traxler

From The Texas Company, Port Neches, Texas

Received Nov. 21, 1946

Introduction

Asphalt is a generic term covering a wide variety of materials varying in viscosity from about 100 to one billion or more poises. The major source of asphalt is petroleum, from which it is obtained as a residue from crude oils after removal of the more volatile components by distillation; some asphaltic materials are also obtained from the solvent refining of lubricating oils. Other sources are the natural deposits such as the Trinidad Native Lake, the asphalt impregnated sands and limestones found throughout the world and the gilsonites and similar naturally occurring hard bitumens. Tars are obtained by the distillation of coal.

The importance of rheological studies of bitumens resides in the fact that their utilization requires a knowledge of, or is determined by, their flow properties. All customer specifications rely first on some one or more empirical flow tests established to insure a uniformity of product and to determine the suitability of the bitumen for the particular use involved Other specific tests are also applied where the material is to be used for a particular purpose such as for paving, roofing, waterproofing, paper plying, etc. Because of their complex natures, bitumens cannot be described on the basis of their chemical composition. Thus, it is necessary to resort to physical tests among which the flow (rheological) tests are most widely used, in order to describe these materials.

Methods for Evaluating the Consistency of Bituminous Materials in Absolute Units

Excellent reviews of the rheological methods of test applicable to asphalts have been written by Saal and Koens (48) and by Broome (11). The subject is also adequately discussed and many of the more important literature references are given by Scott Blair in his recent book (53). The applicability of certain viscometers to asphaltic materials as investigated in our laboratories is outlined in Table I. It is evident that at least two different viscometers are required for the measurement of the wide range of consistencies encountered in asphalt technology. However, each instrument listed offers some advantage in connection with the solution of specific problems and the evaluation of certain kinds of materials.

TABLE I

Applicability of Certain Viscometers to Bituminous Materials

Approximate visc. range centipoises	Bituminous materials consistency at 77°F.	Viscometer						
		Brookfield	Höppler	Koppers	Saybolt Universal	Furol	Coaxial cylinder	Rotary
1 and lower	—	x	x	x	x			
10	Cutbacks	x	x	x	x	x		
10^2	Road Oils	x	x	x	x	x		
10^3	Road Oils	x	x	x		x		
10^4	Road Oils	x	x	x				
10^5	Road Oils		x	x				x
10^6	Residua		x	x			x	x
10^7	Residua						x	x
10^8	Residua						x	x
10^9	Paving Asph.						x	x
10^{10}	Sat. Asph.						x	x
10^{11}	Roof. Asph.							x
10^{12} and higher	Roof. Asph.							x
Reproducibility (*Per cent* of result)		±2	±0.3	±0.5	±0.5	±0.5	±3	±3
Practical Upper Temp. Limit-°F.		250	300	250	450	450	250	300

Measurement of Low Viscosities

The measurement of viscosities of bituminous materials in the lower range of viscosity offers no serious problem and several different types of instrument may be used. The falling sphere viscometer has been developed and used in the measurement of viscous materials (19), in the evaluation of yield value (73), and has been applied in the study of tars, pitches and related materials (12). The inclined tube and rolling ball viscometer, which is a modification of the falling sphere type, has been investigated recently by Hubbard and Brown (24). The Höppler Viscometer (22), a form of the inclined tube viscometer, has proved satisfactory for measuring consistencies up to about 10,000 poises if the material under test possesses no marked complex flow characteristics.

The Saybolt-Furol efflux type of instrument has proved satisfactory for rapidly measuring absolute viscosities up to about 10 poises. This apparatus is especially useful in evaluating materials at high temperatures. Time of efflux (seconds) may be converted to poises by the following formula (25):

$$\frac{\eta}{d} = 0.0216\,F, \qquad (1)$$

where η = viscosity in poises, d = density, g./cm.^{3}, and F = Saybolt-Furol seconds.

The rheological properties of bituminous emulsions and asphalt cutbacks have been investigated in the writer's laboratory by means of the Brookfield viscometer. This instrument is composed of a spindle rotating at definite, constant speed while immersed in the liquid under test. Measurement of the drag produced on the spindle is indicated on a rotating dial by a pointer which is attached to the spindle shaft. Spindles are furnished which cover the range from zero to 100,000 centipoises. Four different rates of shear can be obtained with each spindle which makes possible the study of materials possessing non-Newtonian flow characteristics.

The Koppers capillary tube viscometer (44) and a simple modification (63) of the Bingham-Murray capillary tube (10) have been found to be well adapted to the measurement of viscosities up to about 10,000 poises. A modified Ostwald viscometer has been designed (6) for measuring the commercial range of asphaltic liquid road materials (cutback asphalts) at a single temperature. Opaque liquids can be measured in the Zeitsfuchs capillary viscometer (74) which is especially useful in the range 1,000 to 75,000 centistokes.

Measurement of High Viscosities

Most bitumens of the consistency used commercially and at service temperatures possess very high viscosities and frequently show marked non-Newtonian flow properties. This situation has made the evaluation of their rheological properties at service temperatures a rather difficult problem.

Over 30 years ago, Pochettino (42) studied the viscosity of pitches using the falling coaxial cylinder viscometer conceived by Segel (54). In this apparatus the coaxial cylinders are separated by an annulus of the material under test and the viscosity at a particular temperature is calculated from the rate of fall of the inner cylinder under a known load. An intensive study of this type of viscometer (63) led to the development of an instrument smaller in size and more convenient to operate than that proposed by Pochettino. The following dimensions and ratio of annulus width to length were found to be satisfactory and convenient:

R = Internal radius of outer cylinder = 1.905 cm. ($\frac{3}{4}$ in.),
r = Radius of inner cylinder = 1.270 cm. ($\frac{1}{2}$ in.),
L = Length of cylinders = 2.540 cm. (1 in.),

$$\frac{R - r}{L} = 0.25. \tag{2}$$

This viscometer requires about 25 ml. of sample for a determination, and is inexpensive to build and operate. For these reasons it has been found convenient for measurement of the age hardening of asphalts (64) wherein six or eight viscometers must be filled at the same time with each asphalt to be tested. Starting one hour after pouring the samples, viscosity determinations are made at selected intervals up to 1,000 hours. Fair and Volkmann (16) used the falling coaxial cylinder type viscometer to study the flow of coal-tar pitches that were viscous liquids at 25°C.

Since studies of bitumens possessing non-Newtonian flow necessitate that the samples be sheared in one direction for a considerable period of time, the falling coaxial cylinder viscometer is not satisfactory for such

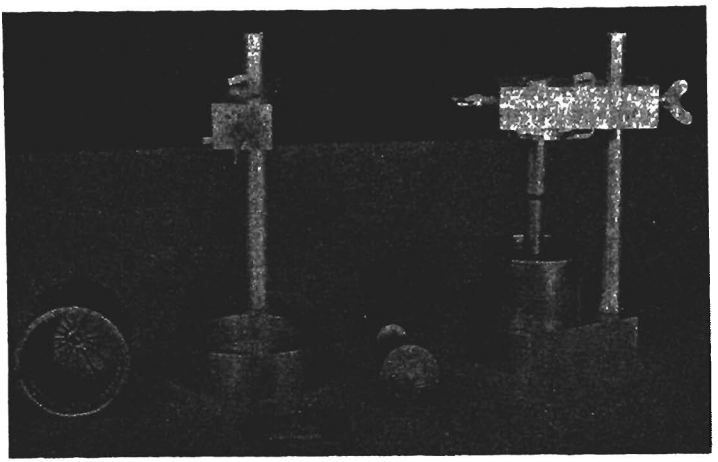

FIG. 1
Rotor and Stator for Rotary Coaxial Cylinder Viscometer Showing Arrangement for Filling Viscometer

investigations. However, a rotating cylinder instrument is entirely suitable for such studies because it can be constructed so as to make possible measurements at either constant rate of shear or constant shearing stress, and the sample can be sheared in the same direction until equilibrium conditions have been established. Also, the same sample can be subjected to successively different amounts of shear. The rotary viscometer has been used by a number of investigators (48, 49, 18) for the study of asphalts. An instrument, the design of which was based on considerable experimental experience and which is applicable to asphalts at service temperatures, is shown in Figs. 1 and 2. The design, operation and calculation of results for this apparatus are discussed fully elsewhere (70) and will not be repeated here.

Deformation by compression of a cylinder of the material has been used by Vokac (72) and Endersby (15) to evaluate the flow properties of asphaltic paving mixtures. Valuable data have been obtained by the triaxial test method (Mohr diagram), although the apparatus required is expensive, the technique exacting, and the calculation of results somewhat involved. The compression of a cylinder or disc of asphalt between

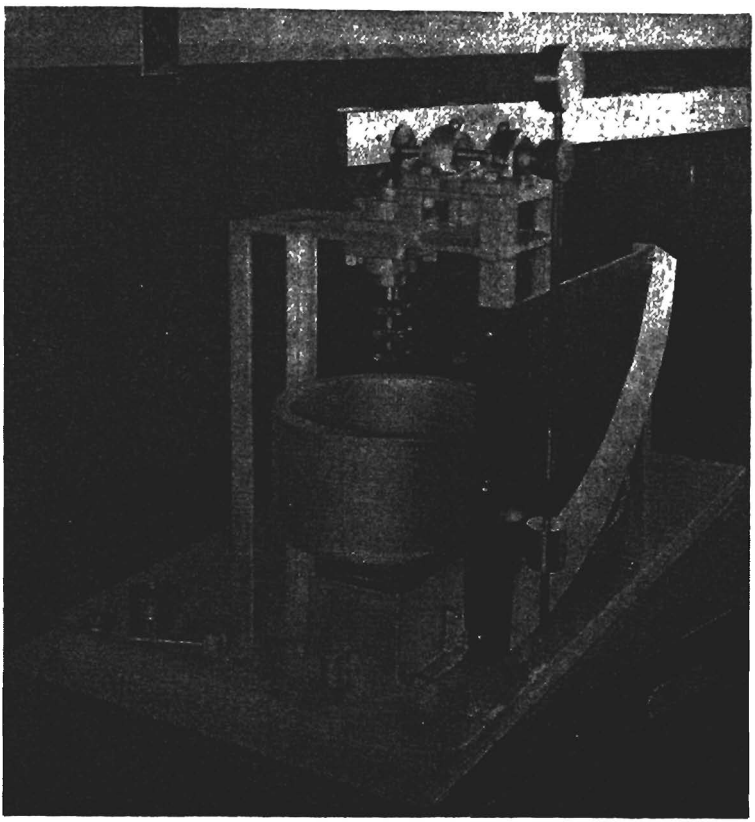

FIG. 2
Rotary Coaxial Cylinder Viscometer

parallel plates has been studied by the writer and his associates with fair success for materials possessing simple flow. However, for complex liquids the method appears to be entirely empirical. It should be noted that Manning (32) used the parallel plate viscometer successfully for measureing the consistency of an essentially viscous pitch but encountered difficulties when he attempted to evaluate an asphalt which was a complex liquid.

The extension of long cylinders of asphalt, supported on mercury, has been used by Lethersich (29) to evaluate viscosity and Young's modulus as affected by different stress and strain conditions. Broome and Bilmes (13) stretched strips of highly filled asphalt under known constant stresses for known times in an effort to evaluate the rheological characteristics.

The indentation made by a sphere acting under a fixed load for a definite period of time has been used (33) in an attempt to evaluate the flow properties of asphalt tile. Work is now in progress on the application of the indentation process to hard unfilled asphalts. Although difficulties are being encountered in the case of highly complex liquids, more extensive investigations may prove that the method has some merit for the study of very hard asphalts.

Extrusion methods may offer a means of evaluating the rheological properties of hard asphalts. Horsfield (23) applied this method to filled asphalts and the extrusion process has been developed and improved in connection with the study of greases (7, 75) and synthetic resins (36). A properly designed extrusion type viscometer utilizing extremely high stresses may provide the means of investigating at service temperatures the flow characteristics of bitumens as hard as gilsonite.

The penetrometer (3) is the oldest and most widely used instrument for measuring the consistency of asphalt. Because of its simplicity, rapidity of operation and widespread use much effort has been expended in studies of the method and attempts to justify its use as a tool for determining the absolute viscosities of asphalts at service temperatures. Bencowitz and Boe (9) investigated 13 asphalts and developed an equation which expresses the variation of penetration with temperature. Pfeiffer and van Doormal (40) found that nearly straight lines were obtained for certain asphalts when the log of the penetration was plotted against the temperature (°C). For the particular asphalts used they found that, if the lines were extrapolated to penetration values of 800, the temperature at that point was the so-called Ring and Ball softening point.

Saal and Koens (48) established the relationship:

$$\eta = (5.13 \times 10^9)/P^{1.93}, \tag{3}$$

where η = viscosity in poises and P = penetration in decimillimeters at 100 g./5 secs. This equation was found by Fair and Volkmann (17) to be applicable to pitches having penetrations above 60 decimillimeters, but below this value considerable deviations were apparent.

Traxler, Pittman and Burns (58), after an extensive experimental investigation, concluded that an accurate correlation would require a much more complicated equation than that proposed by Saal and Koens and that such an equation would be of doubtful value. Later, Mack (31)

established an equation in which depth of penetration was a function of time. He claimed that the constant in his equation expressed numerically the flow properties of asphaltic bitumens. In a discussion of this paper Mill and Harrison (34) pointed out the limitations of the penetrometer test and stated that, although the instrument is simple to operate, it requires a most complicated mathematical treatment.

A procedure for evaluating the surface consistency of asphalts has been developed by Knowles and McCoy (27) using a modification of the A.S.T.M. Penetration method.

Traxler and Moffatt (68) investigated the method of successive penetrations proposed by Thelen (56) and modified by Rhodes and Volkmann (45), but found that the flow was not laminar and that only a portion of the penetrated length of the needle was wetted by the liquid. It was concluded that the method of successive penetrations is not a sound rheological procedure. A theoretical discussion of the penetrometer method for determining the flow properties of high viscosity fluids has been given recently by Pendleton (39). The large amount of research done during the past decade points to the conclusion that the penetrometer is an inadequate and unsatisfactory instrument for the rheological investigation of materials (*e.g.*, asphalts) possessing complex flow and elasticity.

The Rheological Characteristics of Bitumen

Rheology Diagrams

Since bituminous materials may be either simple or complex liquids, it is always necessary to develop a rheology diagram to obtain information concerning the rheological properties of a particular product. Such a diagram is obtained by plotting shearing stress in dynes/cm.^{2} as abscissa and rate of shear in reciprocal seconds as ordinate. In the construction of a rheological diagram 3 or more experimental points at different shearing stresses are established. The diagram may be drawn using arithmetical coordinates by which procedure a simple liquid plots as a straight line and complex liquids as curved lines of various degrees of curvature depending on the deviation from simple flow. If log-log coordinates are used, straight lines are obtained for both simple and complex liquids with a slope of one for the former and less than one usually for the complex liquids. Fig. 3 is a rheology diagram made with log-log coordinates. Asphalt 3C is an essentially simple liquid; Asphalts 5 and 1C are complex materials.

As a general rule pressure still residues, coal tars and steam- or vacuum-refined asphalts exhibit essentially viscous flow up to high viscosities (10^7 poises or above). However, certain residual asphaltic stocks high in wax content may exhibit complex flow characteristics at viscosities of 55,000 poises or less (71).

Simple and Complex Flow

For a simple liquid the viscosity can be calculated by the expression

$$\eta = F/S, \text{ dynes-sec./cm.}^2 = \text{poises}, \tag{4}$$

where F = force, dynes/cm.^{2} and S = rate of shear, sec.$^{-1}$.

For complex liquids

$$M = F/S^c, \tag{5}$$

where M = value of F when $S = 1$ and c = slope of log S *vs.* log F plot. M cannot be used to evaluate the consistency of complex liquids in absolute units because of dimensional considerations resulting from taking S to the c power.

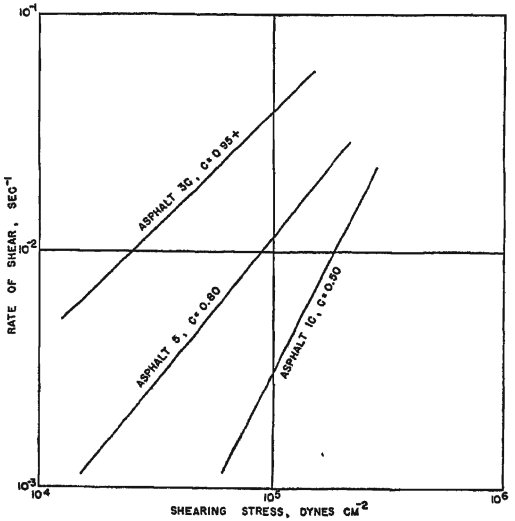

FIG. 3

Rheology Diagrams at 25°C. (77°F.) of Typical Asphalts—Log-log Coordinates

The value of c for simple liquids is 1 and for materials showing complex flow can be greater or less than 1. However, the complex flow of most bituminous materials results in values of c which are less than 1.

It must be recognized that the calculated viscosity for a complex liquid will depend upon the rate of shear used for measurement. For such materials, measurements are generally made at three rates of shear, the data are plotted and the viscosity calculated at some arbitrarily selected rate (*e.g.*, 0.1 reciprocal second) for comparative purposes. It has been established (71) that Eq. 5 is valid over a 30-fold range in rate of shear and that the consistencies and values of c are independent (within certain limits) of the dimensions of the viscometer used.

The viscosity may also be calculated at any arbitrarily selected shearing stress. However, evaluation of the flow characteristics at some selected power input (*e.g.*, 1000 ergs/cm.^{3}) appears to be the most satisfactory procedure. The power input method (47) appears to have considerable merit from a practical standpoint for the study of the rheological properties of asphalts having complex flow. Based on work done on asphalts having Ring and Ball softening points of 100 to 275°F., the viscosities calculated at a particular power input appear to give a better indication of the consistency of the hard, complex materials than is obtained by calculating the viscosity at a constant rate of shear or shearing stress.

The value of c (Eq. 5) and the viscosity in poises calculated at some selected rate of shear, shearing stress or power input, together with a measurement of elasticity (discussed below), establishes the rheological characteristics of any bituminous material possessing complex flow characteristics.

Causes for Variation in Complex Flow

Experienced rheologists recognize that the difficulties so frequently encountered in evaluating the flow properties of bituminous materials are caused by the variations in complex flow that may be encountered. These facts are frequently overlooked or ignored and general conclusions have been drawn from meager data on an insufficient number of materials. Many of the variations in flow properties which will be mentioned below are closely related to the colloidal nature of the bitumen. The chemical nature of the hydrocarbons in the petroleum from which an asphalt is prepared affects the colloidal nature, and consequently the flow characteristics, of the finished asphalt. Method of processing and, of courses the degree of processing, have a marked effect on the rheological propertie, of the material. Air blowing, in general, results in more complex flow than either vacuum or steam distillation or solvent refining. As the temperature of a bitumen is raised any complex flow characteristics diminish and may disappear entirely if the temperature of measurement is increased sufficiently. This effect may be attributed to a gradual change from a gel to a sol structure. Illustrations of the effects of source, method of processing, degree of processing, and temperature on asphalts have been given by Traxler, Schweyer and Romberg (71).

Age-Hardening

All asphalts show an increase in consistency with time that is not caused by loss of volatile components. It has been established (61, 64, 14, 65) that age hardening is dependent on the source of the asphalt, the method and degree of processing, and the temperature of test. The

phenomenon of age-hardening is a manifestation of the colloidal nature (sol-gel structure) of the asphalt or bitumen, since the increased consistency occurring with time may be wholly or partially destroyed by heat or mechanical working.

It appears that increased rates of age-hardening are usually associated with higher degrees of complex flow (lower values of the constant c in Eq. 5). Thus, any effect that decreases the degree of complex flow also decreases the age hardening. This relationship is shown in Table II.

TABLE II

Correlation of Age-Hardening and Degree of Complex Flow

Asphalt	C	P	Q	I
AAI[a]	0.017	0.023	0.073	0.183
c	1.00	0.95	0.85	0.50

[a] Asphalt Aging Index (64) is the slope (*i.e.*, percentage rate of change of viscosity with time) at 100 hours of a log-log plot of viscosity *vs.* time in hours.

The presence of the phenomenon of age-hardening makes it essential that evaluations of consistency and complex flow of bitumens be made at the same sample age for values to be comparable. It has been found satisfactory to determine the consistencies one hour after the viscometer is filled with molten asphalt because during that time the sample can be brought to the desired temperature for testing in an instrument of proper design.

Temperature Susceptibility

The susceptibility of bitumens to changes in temperature has been the subject of considerable study and experimental investigation. Much of the work done prior to 1936 was reviewed (62) and an index proposed which was based on the percentage change in viscosity (in poises) of bituminous materials for a 1°C. rise in temperature. The subject is also discussed fully by Broome (11). Temperature susceptibilities of asphalts from different sources and of mixtures of certain asphalts with varying amounts of mineral filler (slate, trap rock, silica and limestone) have been recorded (52).

Nevitt and Krchma (38) and Stanfield (55) have compared various methods of evaluating temperature susceptibility. The former advocate the use of kinematic viscosities at absolute temperatures to establish the viscosity-temperature susceptibility coefficient, which is applicable over a wide range of consistencies and temperatures. Pfeiffer and van Doormal (40) pointed out that the temperature susceptibility of asphaltic bitumen can be expressed by a single number known as the Pene-

tration Index. The index figure is the slope of the log penetration *vs.* temperature curve in the temperature interval between 15° or 25°C. and the temperature of the softening point of the material.

The effect of temperature susceptibility is complicated and confused by the presence of complex flow. The high degree of complex flow of most air-blown asphalts has engendered the concept that their viscosities change much less with temperature than do steam-refined asphalts. Because of the unrecognized effect of complex flow much of the published data concerning temperature susceptibility gives entirely erroneous ideas concerning the true properties of the material.

Thixotropy

Considerable experimental work has been done (11, 61) and theoretical consideration given to (49) the presence of a thixotropic structure in certain bitumens. This property is closely related to the complex flow and age-hardening characteristics discussed above because of the structural causes for all 3 phenomena. Although he did not work with bitumens, J. Pryce-Jones (43) has given an excellent discussion of the flow properties of thixotropic systems.

Elasticity

Many of the uses of bitumen and bituminous mixtures depend upon their ability to deform without rupture and to recover elastically from small deformations. Some materials, such as steel and rubber, show practically complete and instantaneous elastic recovery, but for visco-elastic materials, such as most bitumens, the recovery is partial, and frequently takes place over a considerable period of time. Because viscous deformation occurs in asphalts under stress, it is almost impossible to evaluate the elastic modulus by direct tensile or torison measurements.

Pochettino (42) used the velocity of sound waves in pitch to measure its compressibility (the reciprocal of the bulk modulus of elasticity). From the bulk modulus and Poisson's ratio he calculated the shear modulus of elasticity.

Elastic after-effect has been measured on asphalts by several investigators (11, 14, 28, 49), but quantitative evaluations are complicated since recovery and relaxation are occurring at the same time.

Relaxation of stress after deformation has been investigated recently (47) as a means of evaluating elasticity. In order to measure relaxation, it was necessary to follow the decrease in shearing stress with time after shearing was stopped. This determination was made in the rotary viscometer (70) by using an indicating balance to measure the torque. The time required for the shearing stress to decrease to one-half of its original value (called the relaxation one-half time) was taken as an evaluation of

the elasticity under specified conditions of temperature, shearing stress, consistency range, and sample size. A high relaxation time indicates high elasticity. The data given in Table III show that a high degree of complex flow (low value for c) is associated with high elasticity. This is logical because both phenomena probably have their origin in the same colloidal structures.

TABLE III

Relation of Complex Flow and Elasticity

Asphalt Process	1-C, Air Blown	2-C, Air Blown	8, Steam Refined
Softening Point, R & B °F.	146	130	126
Penetration, 100 g./5 sec./77°F.	58	55	53
Viscosity, megapoises at 0.1 sec.$^{-1}$	6.0	3.2	2.5
Degree of complex flow c	0.50	0.80	0.90
Relaxation one-half time, sec.	18	3.5	2

Filled Asphalts

Mineral powders are frequently added to a bitumen to increase its resistance to deformation. Utilizing absolute viscosities determined at 77°F. (25°C.) an index was developed (59) for evaluating the capacity of a mineral powder to increase the viscosity when mixed with a bitumen. The primary properties of a pulverulent solid are (51):

1—Particle size,
2—Particle shape,
3—Surface structure, and
4—Particle Size Distribution.

These primary properties regulate the secondary effects of void content and void size of the compacted powder. The average diameter of the voids in the powder *as present in the bituminous mixture* must be considered in the evaluation of the stabilizing effect of a filler. Methods for determining the average void diameter of a powder have been described (60).

In a later paper (66), it was concluded that the viscosity of a mixture of a particular filler and liquid (asphalt) is inversely proportional to the average void diameter of the dispersed powder at the percentage of voids represented by the vol.-% of liquid (asphalt) present in the mixture. This may be expressed by the following relationships:

$$\eta_m = C/d, \tag{6}$$

where η_m = viscosity of the mixture at 25°C., poises; d = average void diameter of the powder as present in the mixture, μ; and C = a constant for a particular liquid and a particular pulverulent solid.

Mitchell and Lee (35) investigated the effect of the addition of filler on the viscosity of tar. When the bulk volume of the filler added to 100 ml. of tar was plotted against the log viscosity at 25°C. (in poises) a straight line relationship was obtained. Data are given for a number of different fillers.

By the use of a tension apparatus Broome and Bilmes (13) investigated the rheological characteristics of highly filled asphalts.

Rheological Aspects of Commonly Used Tests

It has been pointed out above that frequently the selection of a material suitable for a particular purpose depends upon some combination of properties which cannot be evaluated satisfactorily except by rheological methods. The empirical flow tests commonly used at present are inadequate because they do not evaluate quantitatively the many types of anomalous flow possessed by bituminous materials.

In addition to the A.S.T.M. penetration test which has been mentioned above, the more important of these empirical methods are the Ring and Ball softening point and the ductility test. The common weakness of these three tests is that they measure combinations of other properties in addition to consistency. Thus, any correlation between the test results and consistency in absolute units holds only for materials having the same combination of properties as those used to establish the correlation. It is well to consider the rheological aspects of these procedures in order to realize the inadequacies of the empirical tests in providing fundamental data.

Penetration Test

As has been indicated above, the penetrometer (3) has been proposed at recurring intervals as an apparatus for measuring consistency in absolute units. The most serious criticism of the method can be directed at assumptions concerning the method of shearing which provides the basis for the theoretical equations offered by various investigators (31, 39). Movement of the penetrometer needle displaces a relatively small volume of fluid. The flow under the conditions of the test is not the same as in a coaxial cylinder viscometer where the displacement of the moving cylinder results in no movement of the material at the wall unless slippage occurs. In addition, the theoretical equations make no correction for the conical depression around the needle. This depression was recognized by Rhodes and Volkmann (45) and is shown in the photographs in Fig. 4. The end effect of the needle passing through the material is another fault of the penetrometer. Use of an equivalent cylindrical surface for the surface of the needle may be a satisfactory assumption for calculating surface area, but it does not correct for end effect. As pointed out above the needle point

effects were indicated by Fair and Volkmann (17) to be of sufficient magnitude to limit the applicability of Saal and Koens relation (48). It has been concluded (71) from a study of asphalts of widely different flow properties that "the penetrometer must be considered as measuring a combination of consistency and adhesiveness of asphalt to steel." It appears that little hope can be entertained for the development of the penetrometer into a satisfactory rheometer.

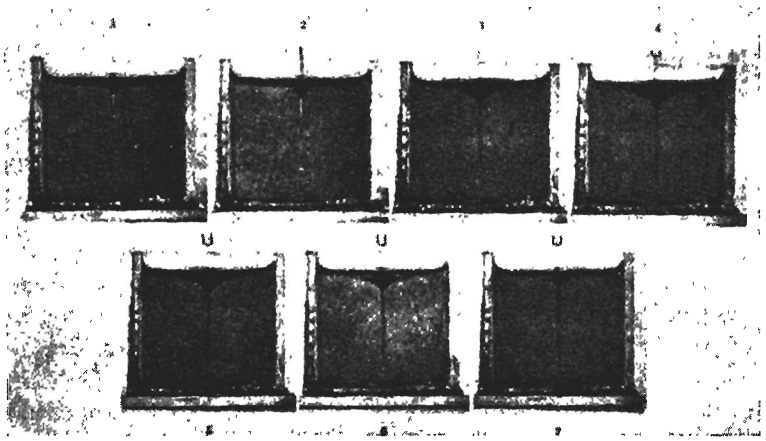

FIG. 4

Penetrometer Needle Entering a Bakelite Resin Possessing Viscosity of 69,000 Poises at 25°C.

1, 2, 3—Entering
4—Completion of penetration
5, 6—Receding cone
7—Receding cone, 5 minutes after 4
5, 6, and 7 show flow of resin into conical depression caused by penetration of needle.

RING AND BALL SOFTENING POINT

Since bitumens do not possess a true melting point, an arbitrary test, such as the A.S.T.M. Ring and Ball softening point (4), has been widely used. The concept has been proposed (2) that all bitumens at their Ring and Ball softening points are simple liquids having the same viscosity. This statement has been refuted by investigators (46, 57) who have shown that the consistency at the softening point varies from 8,000 to 30,000 poises, and by Traxler, Schweyer and Romberg (71) who found that certain asphalts are complex liquids even at their softening points. The latter investigators pointed out that "by judicious selection of the shearing stresses used in the measurement, it is possible to alter the consistency values of the complex liquids to a value similar to that for asphalts showing Newtonian flow."

It should be understood that the softening point test measures a combination of consistency, density, thermal conductivity, and heat capacity and that all of these factors vary with the temperature (50) and the degree of complex flow possessed by the material.

Ductility Test

The work of several investigators (8, 11, 69) has shown that the A.S.T.M. ductility test (5) does not evaluate consistency because the shearing stress and rate of shear vary with the flow characteristics of the material under test. A more recent paper (71) includes the statements quoted below concerning the rheological aspects of the ductility test.

"The ductility test result is actually the length at which a thread of the material breaks because the shearing stress at the area of the break exceeds the cohesive strength of the material. For many soft materials at 25°C., this breaking point is not attained under the conditions of the test and high ductility values result; for very hard materials at 25°C., the break point is attained soon after the start of the test because the cohesive strength is exceeded before the material can flow appreciably, with the result that zero ductility values are obtained. Between these two extremes there is a range of ductility where the results vary with different asphalts and the degrees of complex flow exhibited by them." These conditions are illustrated by the data given in Table IV. "In the

TABLE IV

Relation of Complex Flow and Ductility

Asphalt	H	V	Y	O
Softening Point, R & B °F.	137	143	135	139
Penetration, 100 g./5 sec./77°F.	64	32	64	17
Viscosity, megapoises at 0.1 sec.$^{-1}$	6.8	36.0	5.0	38.0
Ductility, 77°F./5 cm./min., cm.	31	38	125	200+
Degree of complex flow, c	0.75	0.85	0.85	1.00

case of asphalts Y and H, with the same penetration and softening point, the decrease in ductility is in direct agreement with the decrease in the value of c. The importance of the degree of complex flow on ductility is also illustrated by the data for asphalts V and O which have the same consistency in megapoises and about the same softening point."

These results may be explained by the fact that the consistency of materials having the greater degree of complex flow (smaller values of c) decrease more with an increase in shearing stress. Since the cross section of the thread decreases as the ductility test proceeds the shearing stress in the thread increases rapidly and induces a more rapid flow of

the complex liquid. For complex materials such as asphalts H and V, "the region of lowest viscosity is localized at the point of highest shearing stress with the result that 'necking' occurs. This rapid reduction in cross-sectional area produces low ductility values because the shearing stress exceeds the cohesive strength of the material in a short time after the test is started. Where the material is a simple liquid, such as asphalt O, the nature of the flow is independent of the shearing stress and 'necking' does not occur. Such materials will deform readily into a long thread, under the conditions of the test, before the cohesive strength of the material is exceeded." Fig. 5 illustrates the effect of flow characteristics on

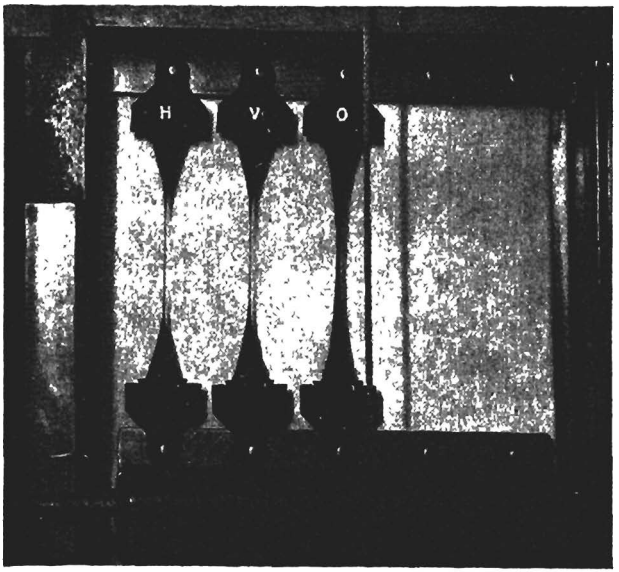

FIG. 5

A.S.T.M. Ductility Tests on Typical Asphalts

the ductility test. The reader is referred to the original paper (71) for a further discussion and illustrations of the effect of complex flow on the ductility of hard asphalts.

Tensile strength tests were made by Abraham (1) and by Grant and Pullar (20) with apparatus of special design. It appears that such measurements, if made with apparatus of high sensitivity, might give fundamental information. However, data so obtained might be no more informative than rheological measurements made employing a suitable range of shearing stresses in a properly designed viscometer.

The Colloidal Properties of Asphalts as Affecting their Rheological Characteristics

The complex rheological properties possessed by bitumens offer strong evidence for the concept that such materials are colloidal systems. Consideration of asphalts as colloids probably dates from the work of Nellensteyn (37) who proposed that such substances were composed of micelles held in dispersion in an oily medium by means of protective bodies. He conceived of the micelles as being made up of a nucleus of carbon surrounded by layers of adsorbed asphaltenes, each successive layer being composed of hydrocarbons of higher hydrogen to carbon ratio and lower molecular weight. Mack (30) precipitated the asphaltenes from various asphalts by means of 86° Be. naphtha and ultrafiltered the remaining solution of petrolenes in naphtha. Ten and fifteen *per cent* of asphaltenes from each of the asphalts were blended with the different petrolenes. Some of the "synthetic" asphalts thus prepared were found to be essentially Newtonian liquids, whereas others showed definite complex flow characteristics. He concluded that ". . . it is evident that the type of the oily constituents brings about the degree of dispersion of the asphaltenes. It seems that asphalts containing oily constituents which are solvents for asphaltenes are liquids of high viscosity." In continuation of his discussion Mack wrote, "In asphalts of low susceptibility the oily constituents are a poor solvent for asphaltenes and the asphaltenes are in a lower degree of dispersion. This relatively low dispersion of the asphaltenes causes structure in the asphalt. This is concluded from the fact that the viscosities of these asphalts are dependent on the pressure (shearing stress). These asphalts form a truly colloidal system of the lyophilic type. With increased asphaltene content the plasticity or resistance to flow is increased. The asphalts resemble gels, and it is evident that they possess elasticity, *viz.*, the ability to store energy." From molecular weight determinations Mack concluded further that the asphaltenes became associated to various degrees in the different petrolenes.

Saal and Koens (48) also argued that the "plasticity" of asphalts is governed by the nature of the oily constituents present. More recently Pfeiffer and Saal (41) concurred with this statement, but emphasized the importance of the nature of the asphaltenes present. The complex rheological behavior of asphalts is ascribed to their colloidal properties. These investigators also believe that compounds with the greatest molecular weight and aromatic character are located near the nucleus of the micelle. Presumably, no clear boundary exists between the oily constituents (malthenes or petrolenes) and resins, or between the resins and asphaltenes. Hillman and Barnett (21) investigated the effects of the chemical nature of the dispersing phase on the colloidal and rheological properties of asphalts.

The relationship between the colloidal characteristics of asphalts and their rheological properties have been discussed (61). Some direct evidence, based on the treatment of asphalt surfaces with selected solvents, has been obtained (67) which indicates the presence of structure in certain asphalts. The microscopic surface patterns appeared only on asphalts possessing complex flow; no surface pattern was developed on asphalts that were essentially Newtonian liquids.

Katz and Beu (26) examined several asphaltic residua and asphalts by means of the electron microscope and concluded that any particles present must be less than 65 Å. in diameter. The results of this work might be interpreted as refuting the concept of the colloidal nature of asphalts.

The effects of mechanical working and changes in temperature on the rheological properties of bitumens strongly support the concept of a reversible sol-gel structure of these materials. Whether the sol-gel condition is caused by variable degrees of association of the micelles present, or is a manifestation of different degrees of solution-solvation of the higher molecular weight hydrocarbons by those of lower molecular weight, awaits clarification by experimental data. Possibly the structure present is, in some ways, analogous to the phenomenon of liquid crystals.

It must be realized that the asphaltenes, resins, and oils separated from asphalts are not in the same physical condition as they are when combined together. Although the study of the separated constituents has given valuable information, the colloidal system which comprises the bitumens is the material which, in the final analysis, must be considered in the clarification of this problem. Now that apparatus and methods are available for the study of the rheological characteristics of bitumens, the most urgent need is for the application of the various techniques of colloid chemistry to these materials. The correlation of the results of such studies with fundamental flow characteristics should result in a clearer understanding of the basic constitution of bituminous materials and of the properties which are of interest to the bituminous technologist.

References

1. Abraham, H., Asphalt and Allied Substances, 5th ed., 1016. D. Van Nostrand Co., New York. 1945.
2. Acad. Sci. (Amsterdam), First Report on Viscosity and Plasticity Prepared by the Committee for the Study of Viscosity, 148. Uitgave van de N. V. Noord Hollandische Uitgevers—Maatschappi, Amsterdam. 1935.
3. Am. Soc. Testing Materials, Standard Method of Test for Penetration of Bituminous Materials (D5–25), **Part II**, 483 (1942).
4. Am. Soc. Testing Materials, Standard Method of Test for Softening Point of Bituminous Materials (Ring and Ball Method) (D36–26), **Part II**, 488 (1942).
5. Am. Soc. Testing Materials, Standard Method of Test for Ductility of Bituminous Materials (D113–39), **Part II**, 466 (1942).

6. ANDERSON, A. P., WRIGHT, K. A., AND GRIFFIN, R. L., *Ind. Eng. Chem., Anal. Ed.* **12**, 466 (1940).
7. ARVESON, M. H., *Ind. Eng. Chem.* **24**, 71 (1932); **26**, 628 (1934).
8. BASKIN, C. M., *Proc. Assoc. Asphalt Tech.* **1932**, 88.
9. BENCOWITZ, I., AND BOE, E. S., *Ind. Eng. Chem., Anal. Ed.* **8**, 157 (1936).
10. BINGHAM, E. C., AND MURRAY, H. A., JR., *Proc. Am. Soc. Testing Materials* **23**, II, 655 (1923).
11. BROOME, D. C., *J. Inst. Petroleum Tech.* **25**, 509 (1939).
12. BROOME, D. C., AND THOMAS, A. R., *J. Soc. Chem. Ind.* **50**, 424T (1931).
13. BROOME, D. C., AND BILMES, L., *J. Soc. Chem. Ind.* **60**, 184 (1941).
14. COOMBS, C. E., AND TRAXLER, R. N., *J. Applied Phys.* **8**, 291 (1937).
15. ENDERSBY, V. A., *Proc. Am. Soc. Testing Materials* **40**, 1154 (1940).
16. FAIR, W. F., JR., AND VOLKMANN, E. W., *Ind. Eng. Chem., Anal. Ed.* **15**, 235 (1943).
17. FAIR, W. F., JR., AND VOLKMANN, E. W., *Ind. Eng. Chem., Anal. Ed.* **15**, 240 (1943).
18. FORD, T. F., AND ARABIAN, K. G., *Proc. Am. Soc. Testing Materials* **40**, 1174 (1940).
19. FULMER, E. I., AND WILLIAMS, J. C., *J. Phys. Chemistry* **40**, 143 (1936).
20. GRANT, F. R., AND PULLAR, H. B., *Proc. Assoc. Asphalt Paving Tech.* Jan. **1936**, 124.
21. HILLMAN, E. S., AND BARNETT, B., *Proc. Am. Soc. Testing Materials* **37**, II, 558 (1937).
22. HÖPPLER, F., *World Petroleum Congress* **2**, 503 (1933).
23. HORSFIELD, H. T., *J. Soc. Chem. Ind.* **53**, 107T (1934).
24. HUBBARD, R. M., AND BROWN, G. G., *Ind. Eng. Chem., Anal. Ed.* **15**, 212 (1943).
25. International Critical Tables, Vol. **1**, 32. McGraw-Hill Book Co., Inc., New York. 1926.
26. KATZ, D. L., AND BEU, K. E., *Ind. Eng. Chem.* **37**, 195 (1945).
27. KNOWLES, E. C., AND MCCOY, F. C., *Ind. Eng. Chem.* **35**, 1118 (1943).
28. LEE, A. R., WARREN, J. B., AND WATER, D. B., *J. Inst. Petroleum* **26**, 101 (1940).
29. LETHERSICH, W., *J. Soc. Chem. Ind.* **61**, 101 (1942).
30. MACK, C., *Proc. Assoc. Asphalt Paving Tech.* December, **1933**, 40.
31. MACK, C., *J. Soc. Chem. Ind.* **58**, 306 (1939).
32. MANNING, A. B., *Dept. Sci. Ind. Research (England) Tech. Paper No.* **39**. (1933).
33. MCBURNEY, J. W., *Proc. Am. Soc. Testing Materials* **34**, II, 591 (1934).
34. MILL, C. C., AND HARRISON, V. G. W., *J. Soc. Chem. Ind.* **59**, 66 (1940).
35. MITCHELL, J. G., AND LEE, A. R., *J. Soc. Chem. Ind.* **58**, 299 (1939).
36. NASON, H. K., *J. Applied Phys.* **16**, 338 (1945).
37. NELLENSTEYN, F. J., *J. Inst. Petroleum Tech.* **10**, 311 (1924).
38. NEVITT, H. G., AND KRCHMA, L. C., *Ind. Eng. Chem., Anal. Ed.* **9**, 119 (1937).
39. PENDLETON, W. W., *J. Applied Phys.* **14**, 170 (1943).
40. PFEIFFER, J. P., AND VAN DOORMAL, M., *J. Inst. Petroleum Tech.* **22**, 414 (1936).
41. PFEIFFER, J. P., AND SAAL, R. N. J., *J. Phys. Chem.* **44**, 139 (1940).
42. POCHETTINO, A., *Nuovo cimento* **8**, 77 (1914).
43. PRYCE-JONES, J., *J. Sci. Instruments* **18**, 39 (1941).
44. RHODES, E. O., VOLKMANN, E. W., AND BARKER, C. T., *Eng. News Record* **115**, 714 (1935).
45. RHODES, E. O. AND VOLKMANN, E. W., *J. Applied Phys.* **8**, 492 (1937).
46. RHODES, E. O., VOLKMANN, E. W., AND BARKER, C. T., Symposium on Consistency—Critical Discussion on Present-Day Practices in Consistency Measurements, p. 30. *Am. Soc. Testing Materials*, June 29, 1937. (Symposium available as separate publication.)
47. ROMBERG, J. W., AND TRAXLER, R. N., Rheology of Asphalt. Presented 1946 Annual Meeting Society of Rheology.

48. SAAL, R. N. J., AND KOENS, G., *J. Inst. Petroleum Tech.* **19**, 176 (1933).
49. SAAL, R. N. J., AND LABOUT, J. W. A., *J. Phys. Chem.* **44**, 149 (1940).
50. SAAL, R. N. J., HEUKELN, W., AND BLOKKER, P. C., *J. Inst. Petroleum Tech.* **26**, 29 (1940).
51. SCHWEYER, H. E., *Chem. Rev.* **31**, 295 (1942).
52. SCHWEYER, H. E., COOMBS, C. E., AND TRAXLER, R. N., *Proc. Am. Soc. Testing Materials* **36**, II, 531 (1936).
53. SCOTT BLAIR, G. W., A Survey of General and Applied Rheology. Pitman Pub. Corp., New York. 1944.
54. SEGEL, M., *Phys. Z.* **4**, 493 (1903).
55. STANFIELD, K. E., Asphalts From Some Wyoming and Other Asphalt-bearing Crude Oils. *Bureau of Mines, Report of Investigations* **3568**, May, 1941.
56. THELEN, E., *J. Applied Phys.* **8**, 135 (1937).
57. TRAXLER, R. N., Symposium on Consistency—Critical Discussion on Present-Day Practices in Consistency Measurements, p. 23. *Am. Soc. Testing Materials*, June 29, 1937. (Symposium available as separate publication.)
58. TRAXLER, R. N., PITTMAN, C. U., AND BURNS, F. B., *Physics* **6**, 58 (1935).
59. TRAXLER, R. N., AND MILLER, J. S., JR., *Proc. Assoc. Asphalt Paving Tech.* January **1936**, 112.
60. TRAXLER, R. N., AND BAUM, L. A. H., *Physics* **7**, 9 (1936).
61. TRAXLER, R. N., AND COOMBS, C. E., *J. Phys. Chem.* **40**, 1133 (1936).
62. TRAXLER, R. N., AND SCHWEYER, H. E., *Physics* **7**, 67 (1936).
63. TRAXLER, R. N., AND SCHWEYER, H. E., *Proc. Am. Soc. Testing Materials* **36**, II, 518 (1936).
64. TRAXLER, R. N., AND SCHWEYER, H. E., *Proc. Am. Soc. Testing Materials* **36**, II, 544 (1936).
65. TRAXLER, R. N., AND COOMBS, C. E., *Proc. Am. Soc. Testing Materials* **37**, II, 549 (1937).
66. TRAXLER, R. N., SCHWEYER, H. E., AND MOFFATT, L. R., *Ind. Eng. Chem.* **29**, 489 (1937).
67. TRAXLER, R. N., AND COOMBS, C. E., *Ind. Eng. Chem.* **30**, 440 (1938).
68. TRAXLER, R. N., AND MOFFATT, L. R., *Ind. Eng. Chem., Anal. Ed.* **10**, 188 (1938).
69. TRAXLER, R. N., SCHWEYER, H. E., AND ROMBERG, J. W., *Proc. Am. Soc. Testing Materials* **40**, 1182 (1940).
70. TRAXLER, R. N., ROMBERG, J. W., AND SCHWEYER, H. E., *Ind. Eng. Chem., Anal. Ed.* **14**, 340 (1942).
71. TRAXLER, R. N., SCHWEYER, H. E., AND ROMBERG, J. W., *Ind. Eng. Chem.* **36**, 823 (1944).
72. VOKAC, R., *Proc. Am. Soc. Testing Materials* **37**, II, 509 (1937).
73. WILLIAMS, J. C., AND FULMER, E. I., *J. Applied Phys.* **9**, 760 (1938).
74. ZEITFUCHS, E. H., *Oil Gas J.* January, **1946**, 99.
75. ZIMMER, J. C., AND PATBERG, J. B., *Inst. Spokesman* **9**, Nos. 4 and 5, July and Aug. (1945).

THE RHEOLOGY OF PROCESSING QUALITY OF RAW RUBBERS

M. Mooney

From United States Rubber Company General Laboratories, Passaic, N. J.
Received Nov. 21, 1946

Introduction

After a crude rubber, such as Hevea or GR-S, has been compounded with the ingredients necessary for vulcanizing, or curing, the raw mix must be formed in some way before it is cured. This forming operation is nearly always either calendering or extruding. Naturally, it is important that the stock should take the desired form as closely as possible; but in practice it is found that the elastomers are in general difficult to form. It seems to be inevitable that those materials which exhibit long-range elasticity after curing will also exhibit considerable elasticity before curing and will, therefore, refuse to hold shape after a forming operation.

This and other processing troubles were handled in the early history of the rubber industry simply by trial and error methods in the factories. Later, particularly during the last 10 years, further progress in processing problems was made by introducing various plastometers and other devices for testing specific properties of the raw stock. These test methods replaced simple tests by hand and by visual inspection, and made it possible to set up specifications for some of the stock properties empirically found necessary for acceptable processing.

As a final step in processing control, there are now being developed in the industry methods for making quantitative measurements of particular processing defects. Such methods involve a small or full-scale processing operation under standardized conditions, and a standardized procedure for quantitative evaluation of the results in terms of departures from perfection.

In the present discussion of processing quality of raw stocks in the rubber industry, various specific processing defects will be described, various rheological methods used for testing raw stocks will be mentioned, and finally, a few experimental results will be reported which show correlations between some of the rheological tests and quantitative measurements of certain processing properties.

Processing Defects

The most striking, and perhaps the most troublesome, defect is caused by elastic recovery, which produces a shrinkage in the length of the extruded or calendered material, accompanied by an increase in thickness and width. As suggested above, this defect is apparently an essential characteristic of any material showing long range elasticity in its final or cured state. Consequently, all that the rubber technologist can hope to do is to limit the recovery as much as possible without damage to the quality of the finished product, and he must allow for some shrinkage in all cases.

If shrinkage is not uniform throughout the mass of the formed stock, surface irregularities necessarily develop. If the stock is subsequently cured in a mold, moderate roughness of the surface in the raw state is of no consequence. On the other hand, if the material is to be cured in open steam, as is the practice, for example, in manufacturing rubber footwear, surface irregularities constitute a serious defect. Furthermore, a stock which calenders rough where it should be smooth will also develop blemishes in any pattern embossed in the sheet.

Aside from irregularities in elastic recovery, there are other possible sources of surface roughness. One of these, encountered in calendering operations, arises apparently from the failure of the stock to form completely as it passes between the calender rolls. The calendered stock then has small valleys or pockets scattered over the surface. A defect encountered in extruding operations consists of saw-toothed tears in the surface. These develop as a result of friction of the stock against the extruder die, especially at any narrow peripheral section where the flow is retarded and the faster moving stock in the center pulls on the slower edges.

Occasionally, a compounded stock is encountered which fails to pass through an extruder, or goes so slowly as to result in incipient curing, or scorching of the stock. Surface roughness then develops because of broken lumps of the scorched stock, or the extruder may be stopped up completely. Scorching frequently occurs in a stock which extrudes at a normal speed but which overheats because of its high viscosity.

Rheological Tests

Before attempting to analyze in rheological terms the various properties of the stock which lead to the above processing defects, we shall discuss briefly the various rheological measurements which have been developed in the rubber industry. Of these, the one most frequently used is a viscosity measurement. Tests of this type are generally referred to in the industry as plasticity tests, but in many cases this term is a misnomer, since the measurement usually made yields only a stress-rate of

strain relationship under some particular set of test conditions. Any relationship between such a single viscosity figure and true plasticity, in any reasonable sense of the latter word, is purely coincidental.

The earliest and simplest instrument for measuring the viscosity of rubbers is the Williams Plastometer (1), which consists essentially of a 5 kg. weight which rests on and compresses the sample, initially in the form of a pellet or short cylinder. The figure usually reported in the test is the thickness of the sample after three minutes' compression at a standard temperature. Theoretical formulas (2, 3, 4) have been developed for calculating viscosity from such measurements. If applied to rubbers, none of these formulae can be accepted as accurate, since they ignore the thixotropy of the material, which is quite pronounced in all commercial rubbers. Nevertheless, the Williams and similar instruments (5, 6, 7) have found considerable useful application as empirical tests.

In viscometers of the extrusion type, first used extensively by Marzetti (8), the sample, contained in a cylinder, is forced by compressed air or by a moving piston to extrude through a small orifice. The rate of extrusion under various pressures is measurable. The most elaborate but most rapid and convenient extrusion viscometer is that developed by Dillon (9). An auxiliary preheater for the sample saves considerable time and makes it possible to attain an operating cycle of 1.5 minutes per sample. The most obvious formula for calculating viscosity from such a test is that expressed in Poiseuille's Law. However, even if the orifice consists of a tube of considerable length in comparison with its diameter, this law cannot be applied to this test with any reliance. This is true also of a more sophisticated formula (10) which is obtained by allowing both for departure from the Newtonian law of flow and for slippage along the surface of the capillary. The reason for the failure of such formulas to give correct values for viscosity again lies in the high thixotropy of the material. In a series of measurements of extrusion through circular dies of various diameters and lengths, it was found that the energy required to deform the sample within the cylinder and get it started into the die was from one-third to one-half of the total energy required for the extrusion. Thus, for example, the pressure required to maintain a given rate of extrusion through a $\frac{1}{8}''$ capillary 0.6″ long was only twice that required to maintain the same rate of extrusion through a hole of the same diameter but 0.06″ long. Such results clearly indicate that it is unsafe to calculate viscosity from extrusion measurements which do not permit a quantitative separation of preorifice and interorifice work of extrusion. These remarks of course do not question the value of an extrusion plastometer as an empirical factory control instrument.

A third type of rubber viscometer subjects the sample to a continuous shearing deformation. Such instruments have been developed in two

forms, the first being a rotating cylinder viscometer (11) particularly adapted to the measuring of true viscosity as well as elastic recovery, the second one being a rotating disk viscometer (12) with a single speed of rotation and designed particularly for factory control work. In both instruments the metal parts in contact with the sample are fluted or cross-hatched to prevent slipping. In the first instrument, which we may call a rubber rheometer, the precision attainable is somewhat reduced by the friction of auxiliary devices required to keep the sample from working out of the space between the cylinders. Nevertheless, the precision is quite adequate for many purposes. True viscosities over a wide range of rates of shear can be reliably determined, also elastic recovery, and, in addition, the modulus and damping factor in free vibrations at frequencies of the order of 10 cycles per second. While this rheometer is quite effective in scientific investigations, it is much too slow for factory control work. The shearing disk viscometer, developed for the latter purpose, consists essentially of a disk rotating within a shallow, cup-shaped cavity. The torque required to maintain a given speed of rotation is measured. When multiplied by a numerical factor, the reading of the instrument is converted to an effective viscosity as averaged over a range of shear extending from zero at the center of the rotating disk to the maximum at the periphery. The standard commercial instrument of this type operates at a single speed of 2 r.p.m.; but one experimental instrument has been fitted with a three-speed drive of 2, 4 and 8 r.p.m.

In a recent modification of the disk viscometer, developed by G. H. Piper and J. R. Scott (13), a wide range of speeds is available; and, furthermore, the disk rotor is replaced with a conical rotor, which has the advantage that the rate of shear is essentially uniform throughout the sample, as in the cylindrical viscometer.

In addition to viscosity, the elastic recovery of a stock is frequently measured. In a compression test, this is the recovery in height of the sample after a few minutes release from the compressing load. In an extrusion test, it is the ratio of the section dimensions of the extruded stock, after recovery is complete, to the dimensions of the extruder die. In the shearing test, it is the reverse rotation of the rotor after being released from the driving mechanism. The three-speed shearing disk viscometer mentioned above also has a clutch release and indicating mechanism which permit a measurement of elastic recovery.

Tack, or the ability of raw stock to adhere to itself or to other materials, is of considerable importance in building operations, such as the assembly of the rubber and fabric parts of a tire. In spite of its importance, tack has usually been estimated only by crude hand tests; but apparatus and methods for quantitative measurements have recently been described (14). Such measurements, aside from their direct application to

building operations, can probably be of considerable value in studying the rheology of rubbers, because tack is undoubtedly closely related to the ability of the molecules within a rubber sample to form quickly new attachments of full strength when, in the continuous deformation of the sample, they are forced into new configurations. Thus, we should expect high tack to be correlated with low thixotropy, thixotropy being dependent on the difference in the strength of an old in comparison with a newly established intermolecular attachment.

Another property of rubbers of practical importance, and perhaps related to tack, is friction against hot metal. In the process of extrusion, the rubber must move over the metal surfaces of the extrusion barrel, the screw, and the die. If the friction is too high, slippage of the rubber over the metal will be retarded, and those processing troubles associated with slow extrusion, referred to above, will develop. Nevertheless, in spite of the importance of friction of raw rubber on hot metal, there is no published method for measuring it. Various attempts made by the present writer to develop such a method have been unsuccessful. In the extrusion experiments referred to above, the slip velocity was too small in comparison with the mean velocity of the extrusion to be measurable with the apparatus employed. A more critical test, employing the shearing disk plastometer, likewise indicated a zero velocity of slip within the precision of the measurements. In this test a special rotor with a smooth surface was compared with a standard rotor with a knurled surface, the theory being that the rubber would slip on the surface of the smooth rotor and yield a lower reading with a given stock. The very surprising results were that the smooth rotor gave slightly higher readings. The smooth rotor had the same dimensions as the outside of the knurled rotor; and apparently any slippage that took place on the smooth rotor was so small that it was not even sufficient to compensate for the slight difference in mean dimensions of the two rotors.

The discussion of all the above measurements has been on the tacit assumption that the material in the test was homogeneous. This assumption, of course, cannot be strictly valid and, as a matter of fact, there is good reason to suspect that some processing defects, particularly roughness, are partly due to inhomogeneity. Aside from incomplete mixing of compounding ingredient, one possible source of inhomogeneity lies in nonuniformity of the rubber itself. Such lack of uniformity could result from incomplete and nonuniform breakdown of the crude rubber or from local variations in the degree or type of polymerization in synthetic rubbers. It would seem, therefore, that some direct measurement of nonuniformity of viscosity or hardness in a raw mixed stock would be useful, but, so far as the writer knows, no one has yet attempted to develop such a measurement.

Correlation between Rheological Tests and Processing Properties

We shall now consider the extent to which the above rheological measurements can be used to predict processing quality. The ideal situation would be one in which quantitative tests were available for all processing defects, and the values obtained in such measurements on any particular stock could be predicted from a proper selection of rheological measurements made on the stock before processing. We are far from reaching this goal, but at least some progress can be reported.

The most obvious and direct application of a viscosity measurement would be in predicting the power consumption in the calender or extruder. Such a check with regard to calendering has not yet been made, to the author's knowledge; but, in extruding operations, it has been found by

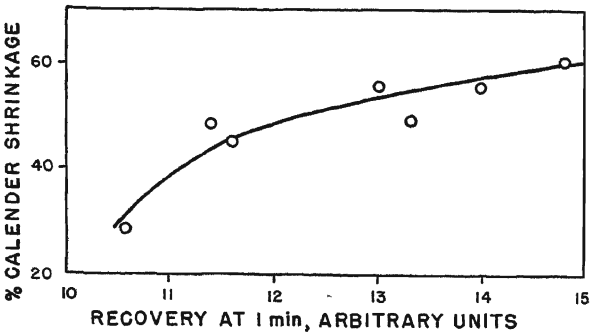

Fig. 1

Calender Shrinkage *vs.* Elastic Recovery in the Disk Viscometer.

G. R. Vila (15) that the power consumed increases linearly with the mean viscosity as measured with the shearing disk viscometer. The power consumption is usually not of primary importance in itself, but, since the power is mostly converted into heat in the rubber, the high power necessarily consumed in a stock of high viscosity results in scorching.

Another processing property obviously and closely related to a simple rheological measurement is shrinkage. Calender shrinkage is the lengthwise shrinkage of a calendered sheet compared with the length of the sheet while on the calender roll. Shrinkage may be permitted to take place while the sample is immersed or floating in hot water or while it is resting on a talced table top. Fig. 1 shows the correlation that was obtained in one experiment between calender shrinkage of a group of commercial stocks and the elastic recovery as measured in the disk viscometer. The correlation in this case is fairly good. On the other hand, in several other calendering programs carried out by L. M. White of the

General Laboratories of the U. S. Rubber Company, involving a narrower range in type of stock, no correlation was found between shrinkage and measured elastic recovery*. The data showed definitely that the trouble could not be attributed simply to experimental error. It may be pointed out that in the calendering operation the stock before shrinkage is subjected to a momentary, very high rate of deformation in passing through the nip, followed by a period of fixed strain while on the calender roll. If the viscometer rotor could be given a momentary high rate of rotation, the subsequent elastic recovery might be found to correlate better with calender shrinkage.

Shrinkage after an extruding operation has been measured by R. L. Zapp and A. M. Gessler (16) and compared with rheological measure-

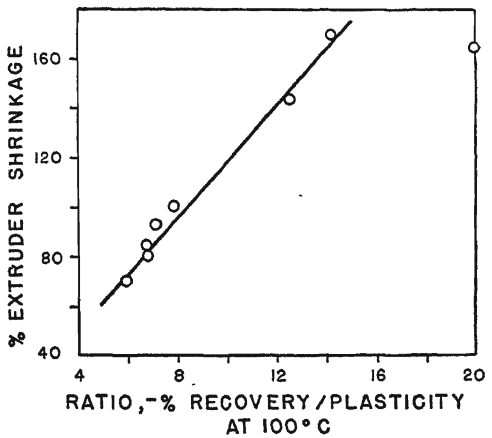

FIG. 2

Extruder Shrinkage *vs.* Recovery/Plasticity, on Series of Butyl Rubber Stocks of Different Mol. Wts., 100 Parts by Weight, Compounded with 50 Parts Easy Processing Channel Black. From Zapp and Gessler.

ments obtained with a compression type of instrument. The rheological function found to give good correlation with shrinkage, or lateral swell, was R/P, where P, the "plasticity," is the load required to compress the test cylinder to half its original height in 10 seconds, and R is the subsequent *per cent* elastic recovery. The stocks tested were butyl rubbers of different molecular weights and molecular weight distributions, all compounded with 50 parts of channel black. Fig. 2 shows the correlation obtained, which is good except for one point badly off.

Some efforts made by the author to correlate recovery with the extruder shrinkage failed completely, and the correlation could not be im-

* Private communication.

proved by combining recovery with viscosity data as was done by Zapp and Gessler. Apparently shrinkage after calendering or extruding is a more complex phenomenon than might be assumed, and more work will be required before it can be well understood.

Mention has been made of the fact that stocks are sometimes encountered which give trouble in the factory because of low rates of extrusion. So far as simple, or Newtonian, viscosity is concerned, there is no reason to anticipate that the rate of extrusion would be reduced by high viscosity. Velocity of rotation of the screw can usually be maintained in spite of the increased power consumption, and, while high viscosity necessarily increases the pressure required to push the stock through the die, the stresses developed within the stock by the forced movements within the barrel would also be increased, and presumably in the same proportion. Obviously, to find any solution to the problem of rate of extrusion, we must cease thinking in terms of simple viscosity and consider the rheological diagram, or the stress-rate of shear relationship over the rates of shear developed in the extrusion process. With this idea in mind, the rates of extrusion of some experimental stocks in a No. ½ Royle extruder were compared with a measure of the relative increase in viscosity reading with rate of shear obtained with the three-speed shearing disk viscometer. Only the two extreme speeds, 2 and 8 r.p.m., were employed; and the function calculated for comparison with rate of extrusion was the relative stress increment

$$I_s = \frac{V_8 - V_2}{V_2},$$

in which V_2 and V_8 are respectively the shearing disk readings at 2 and 8 r.p.m. The temperature of the viscometer was adjusted to the observed temperature of the stocks as they came out of the extruder.

The degree of correlation found is shown in Fig. 3. In connection with this figure, it should be mentioned that four of the stocks, in pairs, were the same except for the addition of a commercial softener—pine tar in one case, stearic acid in the other. These softeners are generally considered to have a lubricating effect which reduces the friction of the stocks on the interior extruder surfaces. While such an effect on ease of slippage may possibly occur, the data show that the stress increment also is increased by the softeners. The correlation shown in Fig. 3, therefore, suggests strongly that in this connection it is the effect on the stress increment which is of major importance. The stocks represented by the data were of a wide variety, involving hard and soft carbon blacks, gum stocks, and some commercial stocks of high shrinkage and low shrinkage, and it is very unlikely that the close correlation shown would have been obtained unless the stress increment were the primary factor determining rate of extrusion.

The fact that the rate of extrusion increases with the stress increment can be understood if we assume that in the barrel, where the extruding pressure is developed, the effective rate of shear is higher than in the throat and die, where the opposing force is developed.

The defect of surface roughness results undoubtedly in a very complex way from a considerable number of different rheological properties. While roughness can be and has been approximately rated by visual inspection, such a method is obviously inadequate for any precise analysis of the problem. A recently developed apparatus for measuring the roughness of calendered sheet, called a rugosimeter, has been described in the literature (17). The test depends essentially upon the resistance to air

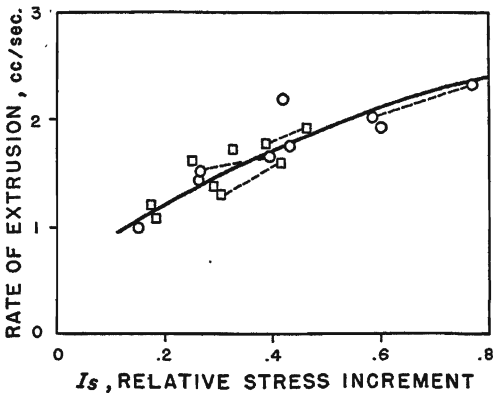

FIG. 3

Rate of Extrusion *vs.* Relative Stress Increment, $(V_8 - V_2)/V_2$, where V_8 and V_2 Are the Disk Viscosity Readings at 8 and 2 r.p.m., Respectively.

Points connected by dotted lines are similar stocks with and without softener, the one with softener having the larger I_s in all cases. Circles indicate a circular die; squares indicate a rectangular die.

flow between the rough surface of the sample and a circular test plate resting upon it. The rougher the surface, the lower the resistance to flow. On the assumption that the surface irregularities are sinusoidal in profile, the flow resistance can be converted to the mean effective height of the irregularities. This effective height is called the rugosity.

The stock properties of conceivable importance in rugosity would include elastic recovery, inhomogeneity, thixotropy, tack, and the rheological diagram or stress-rate of strain curve.

Elastic recovery will produce roughness if the recovery is not uniform. Inhomogeneity of the stock will cause nonuniformity in recovery. The same effect will result also from thixotropy, for in this case local variations in immediate past history of shearing action within the rolling bank

will cause temporary, local variations in viscosity. Variations in viscosity, or local hard spots, may also cause failure of the sheet to form completely, aside from irregularity in elastic recovery. Low tack probably means high thixotropy and, hence, rough calendering. Low tack probably has also a direct effect in causing pockets, because of failure of rubber surfaces to adhere even when forced into contact within the bite. Large curvature in the rheological diagram, or large departure from Newtonian viscosity, probably means high thixotropy and, hence, rough calendering. The shape of the rheological diagram probably influences also the perfection of forming within the bite, but the precise nature of this influence is not easily predicted.

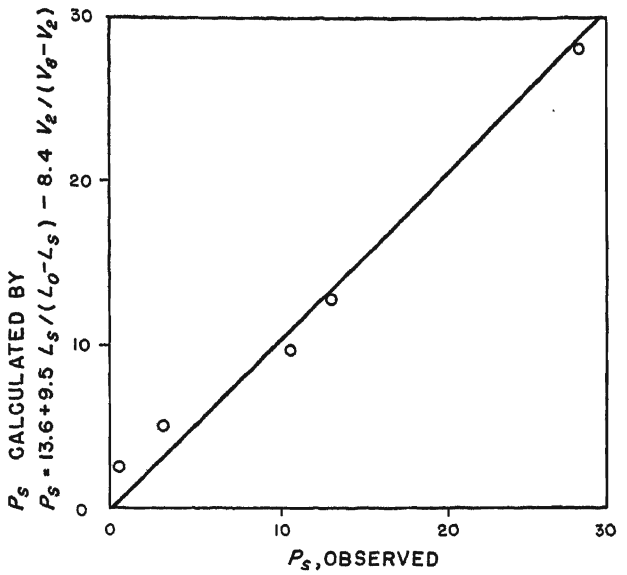

FIG. 4

Calculated and Observed P_s.

P_s is a measure of smoothness. $L_s/(L_0 - L_s)$ is calender shrinkage. V_8 and V_2 are the disk viscosity readings at 8 and 2 r.p.m.

This discussion indicates what sort of rheological measurements we may expect to find correlated with rugosity measurements. It indicates also, however, that some of the rheological properties mentioned are interrelated. Hence, in order to find close multiple correlation between rugosity and the rheological properties, it may not be necessary to include all of the rheological properties that have been mentioned.

Fig. 4 shows the correlation found in one experiment between rugosity and certain rheological properties. This experiment was made before the

rugosimeter was developed to its present stage, but the fundamental principle of the roughness measurement was, nevertheless, the same. As is evident from the figure, the range in roughness exhibited by the selected stocks is wide. The rheological function found to correlate with rugosity, or, in this case, an inverse measure of rugosity, or smoothness, is indicated by the equation:

$$P_s = 13.6 + 9.50\,\frac{L_s}{L_0 - L_s} - 8.40\,\frac{V_2}{V_8 - V_2},$$

where P_s is the smoothness, $(L_0 - L_s)/L_s$ is the *per cent* calender shrinkage, and V_2 and V_8 are the viscosity readings at 2 and 8 r.p.m., respectively, as previously defined. For the first rheological factor in the equation, elastic recovery would be preferred, but the accessory of the disk viscometer for measuring elastic recovery had not at this time been satisfactorily developed. Consequently, instead of elastic recovery, shrinkage as measured on the calendered sheet was used. The second factor is the reciprocal of the relative stress increment previously defined. According to generally accepted ideas, the larger the stress increment, the lower is the "structure viscosity" and likewise the thixotropy of the material.

This equation tells us that the smoothness of the calendered sheet increases as the shrinkage decreases and as the stress increment increases. This was to be expected on the basis of the preceding discussion of the effects of thixotropy and nonuniform elastic recovery.

A later attempt to repeat these results with another group of stocks was not successful when the same rheological function was tried; but fair correlation with roughness was obtained by including an additional factor in the rheological function. This factor was the ratio of the breaking tensile force to the force at 100% elongation in a dumbbell test piece of the raw stock when pulled at a temperature of 70°C. This ratio may conceivably be a measure of the ratio of highest to the average elastic stress within the rubber as it comes through the calender rolls.

A different approach to the problem of processing quality has led to the development, by B. S. Garvey, M. H. Whitlock, and J. A. Freese, Jr. (18), of a special small-scale extrusion test. The die used has an orifice which is essentially trapezoidal in form, with a sharp angle of approximately 20° at one corner. The processing quality of a stock is taken as the average of visual ratings for the four properties, (1) section contour of the extruded stock, (2) tearing at the sharp corner, (3) surface roughness, (4) corner sharpness. The test is reported to be reliable in predicting processing behavior in large-scale extruders. It has the obvious disadvantage of depending upon visual ratings, but it would probably be possible to develop instrumental measurements for at least some of these ratings.

With regard to the way in which the four ratings obtained in this test are used together in an arbitrary averaging procedure, it can only be stated that, from either a scientific or a practical point of view, such a procedure is, in this writer's opinion, to be deplored. Since we recognize and have independent measurements of different processing defects, we should cease thinking of processing quality as a single, one-dimensional property.

From the various experimental results that have been reviewed here, it is obvious that our present understanding of the rheology of processing quality is very incomplete, but that a substantial beginning has been made. Doubtless, our limited understanding will improve as more and better tests are developed and more attempts are made to establish empirical relationships between rheological properties and measurable processing qualities. Eventually, on the basis of such empirical knowledge theoretical treatments of calendering and extruding quality will doubtless be developed.

References

1. Williams, J., *Ind. Eng. Chem.* **16**, 362 (1924).
2. Griffiths, R. W., *Trans. Inst. Rubber Ind.* **1**, 308 (1926).
3. Scott, J. R., *Trans. Inst. Rubber Ind.* **7**, 169 (1931).
4. Peek, R. L., Jr., *J. Rheology* **3**, 345 (1932).
5. J. Hoekstra, *Proc. Rubber Technology Conference* **1938**, 362; *Rubber Chem. Tech.* **12**, 434 (1939).
6. Höppler, F., *Kautschuk* **17**, 17 (1941).
7. Karrer, E., and Dietrich, E. O., *India Rubber World*, October 1, **70** (1928); *Ind. Eng. Chem.* **21**, 770 (1929).
8. Marzetti, B., *India Rubber World* **68**, 776 (1923).
9. Dillon, J. H., *Physics* **7**, 73 (1936); *Rubber Chem. Tech.* **9**, 496 (1936).
10. Mooney, M., *J. Rheology* **2**, 210 (1931).
11. Mooney, M., *Physics* **7**, 413 (1936).
12. Mooney, M., *Ind. Eng. Chem., Anal. Ed.* **6**, 147 (1934).
13. Piper, G. H., and Scott, J. R., *Rubber Chem. Tech.* **19**, 822 (1946); *J. Sci. Instruments* **22**, 206 (1945).
14. Busse, W. F., Lambert, J. M., and Verdery, R. B., *J. Applied Phys.* **17**, 376 (1946).
15. Vila, G. R., *Ind. Eng. Chem.* **36**, 1113 (1944).
16. Zapp, R. L., and Gessler, A. M., *Rubber Chem. Tech.* **17**, 882 (1944).
17. Mooney, M., *Ind. Eng. Chem., Anal. Ed.* **17**, 514 (1945).
18. Garvey, B. S., Whitlock, M. H., and Freese, J. A., Jr., *Ind. Eng. Chem.* **34**, 1309 (1942).

THE RHEOLOGY OF LUBRICANTS

R. B. Dow

From the Bureau of Ordnance, Navy Dept., Washington, D. C.

Received Nov. 11, 1946

Two significant developments in the field of liquid lubricants appeared during the period of the last war, the new heat-stable, organo-silicon oxide polymers which are characterized by their serviceability over a wide temperature range, and the fluorinated hydrocarbons which exhibit great thermal stability and inertness toward the most reactive chemical agents. Some of the silicone liquids, for example, remain fluid at temperatures as low as −70°F., have a good oxidation resistance and waterproofness, and their viscosity-temperature slopes are rather flat as compared to those of common petroleum oils. Fluorocarbons range from the gases through the liquid and solid ϕ-paraffins, C_nF_{2n+2}, ϕ-olefins, C_nF_{2n}, the isomeric ϕ-naphthenes boiling in the range of gasoline through oils (C_{16} to C_{21}) and greases to the waxes. It is evident that a new field of hydrocarbon chemistry is just opening up.

Fig. 1 illustrates the viscosity-temperature relations of a light silicone lubricant, DC 500–50 of Dow-Corning, and a fluorinated, highly naphthenic lubricating oil, the data of which are contributed by W. S. Struve of du Pont. In contrast to the silicone it will be noted that the viscosity-temperature slope of a common petroleum oil, hydraulic oil "A" which will be discussed later in more detail, is considerably greater. Comparing the fluorinated product with the base naphthenic oil, it is seen that the slope of the former greatly exceeds that of the latter. In terms of Viscosity Index (V.I.), the +65.5 of the base oil decreased to −674 through the fluorination process. It appears to be a general result that the substitution of F for H bonds increases the temperature coefficient of viscosity of the hydrocarbon.

The chemistry of additives to lubricants has been greatly broadened during the last five years by the impetus coming from the study of additives in improving the "oiliness" of liquid lubricants. Additives serve a variety of purposes: to increase the lubricating quality, *e.g.*, reducing friction; to reduce wear characteristics; to inhibit corrosion or oxidation; and to tailor an oil for a particular application. Their mode of action may be physical or chemical, or both, as illustrated by such substances as graphite, powdered metals, asbestos, or the more complicated chemical compounds such as benzotrichloride and tricresyl phosphate. Boundary

film studies have brought forth the great value of high molecular weight, oxygen-containing additives (1) in reducing friction. Sulfur, phosphorus and chlorine compounds have also been used extensively in this respect.

Davey (2) has assessed the extreme pressure lubricating properties of some chlorinated compounds using 10% blends in Pennsylvania neutral oil. Benzotrichloride exhibited marked superiority over trichloromethylene and carbon tetrachloride as extreme pressure lubricants in reducing wear as measured by the four-ball wear machine. The extreme pressure properties are due apparently to the liberation of atomic Cl which forms

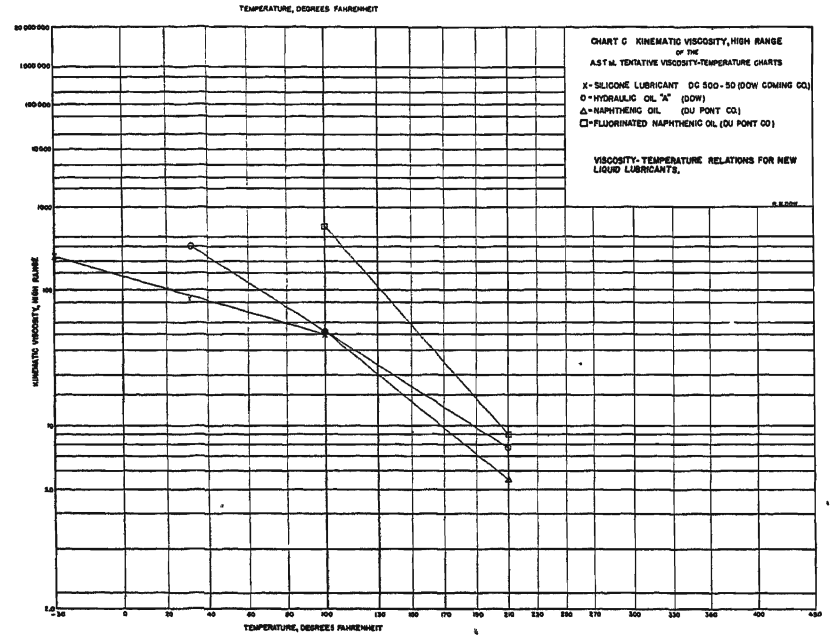

FIG. 1

an additive compound with the metal surfaces to exhibit low wear qualities. If HCl forms, due to combination of Cl with the H atoms of the aliphatic chain, the release of ionic Cl causes corrosion and high wear. A compound having Cl attached to an aromatic nucleus has only slight E. P. properties.

Tricresyl phosphate has proven to be a most beneficial antiwear agent when 1% is incorporated in a mineral oil suitable for aircraft and hydraulic use. This compound and others, such as the alkyl sebacates, phthalates, citrates, *etc.*, commonly increase the wear characteristics of an oil by an amount comparable to a two- or three-fold increase in viscosity. The viscosity-temperature slopes of such compounded oils are usually greater than those of the oils alone.

Webber (3) has recently reviewed similar improvements achieved with lubricating greases containing additives.

The causes of oxidation of motor oils in service have been extensively investigated by Larsen, Thorpe and Armfield (4), and Von Fuchs and Diamond (5). Sludge and lacquer-like substances, possessing moderately high contents of O_2, result from oxidation in an engine and have a deleterious effect on performance. The former authors confirm the reactivity of the saturated hydrocarbons, paraffinic or cycloparaffinic, and that aromatics containing a benzene ring attached to a saturated chain or hydroaromatic ring are still more reactive. By contrast, the naphthenic and other polynuclear aromatics are very stable, apparently as a result of the formation of effective inhibitors upon oxidation. They synthesized an oil by condensing cetene with naphthalene to obtain a product with almost the identical physical properties of a Pennsylvania and extracted mid-continent oils. The alkylated naphthalene was as resistant to oxidation as the other two oils at 150°C., although it contained a high aromatic content as shown by a high specific dispersion. Von Fuchs and Diamond give data on the oxidation rate of two oils of the same viscosity at 210°F. and of about the same V.I. when exposed to iron at 313°F. A blended oil of 80% light neutral and 20% bright stock showed considerably less absorption of O_2 than the unblended, medium-heavy neutral. It is well established that greater stability is not attained in practice by using an oil of higher viscosity.

The subject of viscosity characteristics of lubricating oils containing gases at high pressures has been further investigated by Swearingen and Redding (6) who employed a capillary viscometer enclosed in a bomb with glass windows, the bomb being charged with oil and natural gas to a pressure as high as 3500 ψ. By rotation of the bomb, the viscometer was filled and the flow time past a mark observed through the glass windows. Both petroleum and castor oils showed a marked decrease in viscosity as the pressure was raised, the order being about 70% at 120°F. for a pressure increase of 3000 ψ. Castor oil was unique in that the curves showed breaks, at which points the oil became opaque. Typical viscosity ratios at several temperatures are illustrated below:

Oil	Density (60° F.)	Vis. (S.U.S.)		$\frac{\text{Vis (15 }\psi)}{\text{Vis (3000 }\psi)}$			
		100°	210°	85°	120°	154°	186°
SAE 30	0.881	519	67	11.6	5.1	3.5	2.8
B.S.	0.912	2975	165		8.7	4.1	3.9
B.S.+Kerosene	0.900	507	67	8.7	4.1	2.8	2.4
Castor oil	0.963	1370	105		2.4	2.0	1.8

High pressure effects in rheology continue to be of current interest, both experimentally and theoretically. The comprehensive review of Bridgman (7) on recent work in the field of high pressures, between 1930 and 1945, lists 40 papers on the viscosity of fluids, 20 of which are concerned with lubricants. Hersey and Hopkins (8) have summarized the 10 principal investigations on viscosity of lubricants at high pressures, between the years 1916–41. Some 106 fatty and petroleum oils were subjected to pressures ranging from 4000 to 170,000 ψ at temperatures from 68° to 313°F. Hersey and Hopkins also computed the film thickness for a 2″ pinion gear at a pressure of 13,200 ψ for a typical fatty and a typical petroleum oil, both having the same viscosity at atmospheric pressure but whose pressure coefficients at that pressure were 7.05 and 15.10×10^{-5} in.^{2}/lb., respectively. The film thicknesses were computed to be 7.2 and 12.0×10^{-6} in. respectively.

The rolling-ball viscometer which has been extensively used by Dow and associates at high pressures has been further investigated at atmospheric pressure by Hubbard and Brown (9) who used 4 glass tubes ranging from about 0.6 to 1.0″ in diameter, 17 steel and aluminum balls and 16 calibrating fluids. The roll times were accurately observed by the interruption of a light beam which activated a photoelectric cell. They were able to evaluate Reynolds number in terms of the resistance factor and the diameter of tube to diameter of ball ratio. Of special interest is the effect of temperature on the calibration, and their correction factor which permits the computation of the viscosity in the turbulent region.

The previously reported use of the ASTM chart (10) to represent viscosity-temperature-pressure data has been extended by Dow to represent the data of other investigators. Fig. 2 shows data taken from the papers of Hersey and Shore (15), Suge (16), and unpublished data of Dow and of Fenske. Fig. 3 consists of similar data of Thomas, Ham and Dow (12), Dow, McCartney and Fink (14), and Dibert, Dow and Fink (13). The data were picked at random pressures to give illustrations of typical results. In each case the subject oils exhibited a linear relationship at atmospheric pressure, with the exception of Suge's data at 221° and 255°F. which are badly out of line. His data show the same behavior under pressure at these two temperatures. Since his oils were normal types, it is to be concluded that his temperatures were incorrect in these two cases.

The ASTM chart is essentially an expression of the well-known Walther formula with the constant ω placed equal to 0.8, *i.e.*,

$$\nu + \omega = k \exp. b/T$$

Fundamentally, the equation appears to have no greater accuracy than the equally well-known Vogel equation

$$\eta = k \exp. b/t + \theta$$

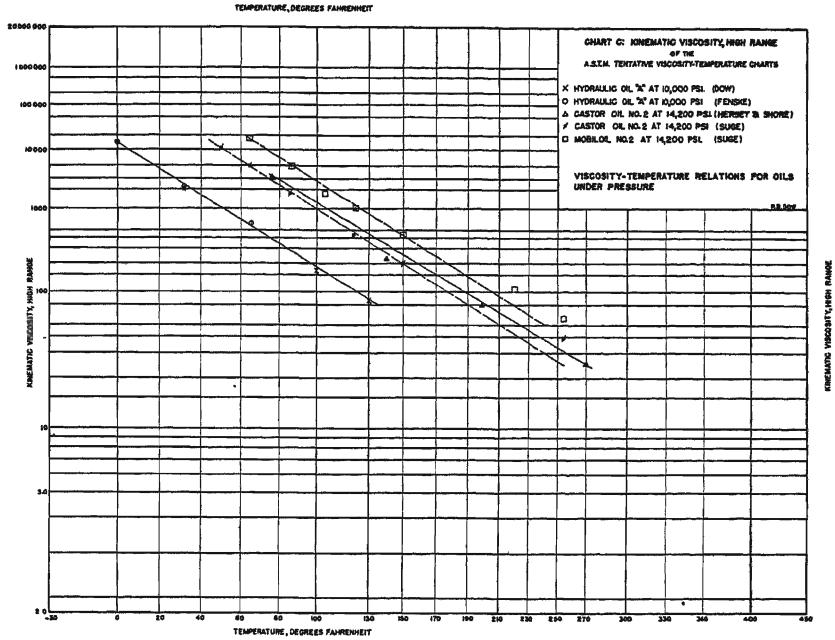
TEMPERATURE, DEGREES FAHRENHEIT
CHART C: KINEMATIC VISCOSITY, HIGH RANGE
OF THE
A.S.T.M. TENTATIVE VISCOSITY-TEMPERATURE CHARTS
X HYDRAULIC OIL "A" AT 10,000 PSI. (DOW)
O HYDRAULIC OIL "A" AT 10,000 PSI (FENSKE)
Δ CASTOR OIL NO. 2 AT 14,200 PSI (HERSEY & SHORE)
✓ CASTOR OIL NO. 2 AT 14,200 PSI (SUGE)
□ MOBILOIL NO. 2 AT 14,200 PSI. (SUGE)
VISCOSITY-TEMPERATURE RELATIONS FOR OILS
UNDER PRESSURE
R.R.DOW
KINEMATIC VISCOSITY, HIGH RANGE
TEMPERATURE, DEGREES FAHRENHEIT

FIG. 2

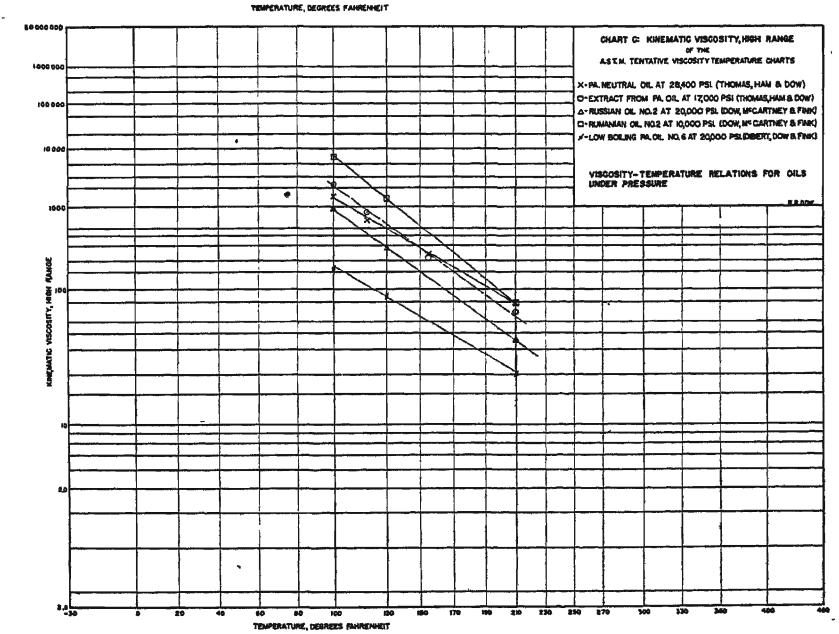
TEMPERATURE, DEGREES FAHRENHEIT
CHART C: KINEMATIC VISCOSITY, HIGH RANGE
OF THE
A.S.T.M. TENTATIVE VISCOSITY-TEMPERATURE CHARTS
X - PA. NEUTRAL OIL AT 28,400 PSI. (THOMAS, HAM & DOW)
O - EXTRACT FROM PA. OIL AT 17,000 PSI (THOMAS, HAM & DOW)
Δ - RUSSIAN OIL NO. 2 AT 20,000 PSI. (DOW, McCARTNEY & FINK)
□ - RUMANIAN OIL, NO. 2 AT 10,000 PSI. (DOW, McCARTNEY & FINK)
✓ - LOW BOILING PA. OIL NO. 6 AT 20,000 PSI. (DEBERT, DOW & FINK)
VISCOSITY-TEMPERATURE RELATIONS FOR OILS
UNDER PRESSURE
R.R.DOW
KINEMATIC VISCOSITY, HIGH RANGE
TEMPERATURE, DEGREES FAHRENHEIT

FIG. 3

In either equation, two constants are at least necessary to relate the viscosity of an oil to temperature. Pressure adds another constant, so theoretically the ASTM chart offers no new possibilities,* but does offer a simplification in mapping the viscosity-temperature-pressure relationships inasmuch as only two temperatures at any pressure are required to define a viscosity isobar.

The problem of these relationships has been discussed recently by Cameron (18) who attempts to combine pressure and temperature effects in the equation

$$\eta = k \exp. b + AP/t + \theta$$

where

$$A = \phi(t + \theta)$$

This results from a combination of Eyring's equation for the pressure effect and Vogel's equation for the temperature effect. Cameron finds, that for good accuracy, a single θ does not suffice for both effects and that $\theta_t = 95$ and $\theta_p = 52$. These represent mean values for all the oils examined. Over limited ranges, a mean $\theta = 73$ can be used without serious error. The data for the fatty oils did not permit close correlation of the constants b and A, but for mineral oils the following relationships were found

$$[1/A]_{\theta p=52} = 9.00 - 4.20 \times 10^{-3}[b]_{\theta t=95}$$

and

$$\text{Mol. Wt.} = 0.546(b^{1.47} \cdot k^{0.473})_{\theta t=95}$$

There obviously remains room for more careful study of the viscosity of lubricating oils under pressure at various temperatures, particularly at the lower temperatures. It is to be hoped that many new data of this type will be forthcoming soon from the new program recently undertaken at Harvard University under the auspices of the Special Research Committee on Lubrication of the ASME.

Table II summarizes new data by Dow on the viscosity of four hydraulic oils at four temperatures over a moderate pressure range. These were all high V.I. oils of similar characteristics, and the data are of interest chiefly to illustrate the effect of temperature on viscosity. The results for oil "A" are typical, and some of them were represented on the ASTM chart of Fig. 2.

The program of study of the viscosity of foreign oils under pressure which was undertaken by Dow and associates before the war, and with the cooperation of the Institute of Petroleum (British) is completed by the present data of Dow and Veith for three Burma oils. The results are

* It should be recalled in this connection that the method of Cragoe (17) offers possibilities which have not been fully exploited with the additional data which are now available.

given in Table I. They do not show marked differences from the Russian and Rumanian oils investigated previously.

On searching for some readily measured characteristic which might show a reasonably close correlation with the pressure effect on the vis-

TABLE I

Viscosity-Pressure Data of Dow & Veith for Oils at 100° and 130°F.

	BURMA NO.1		BURMA NO 2		BURMA NO.3	
	100°	130°	100°	130°	100°	130°
DENSITY (GM/CM³)	895	885	925	.915	.938	.927
PRESSURE (PSI)	COEFFICIENT OF VISCOSITY (CENTIPOISES)					
15	174	100	112.0	42.5	310.0	104.0
2000	233	130	172.0	66.5	502.0	163.0
4000	312	165	264.0	94.5	798.0	242.0
6000	40.8	20.6	388.0	124.0	1300.0	351.0
8000	55.4	26.0	584.0	178.0	2080.0	510.0
10000	73.0	33.3	867.0	257.0	3360.0	760.0
12000	95.5	42.3	1300.0	359.0	5530.0	1145.0
14000	125.0	52.3		499.0		1720.0
16000	162.0	65.9		712.0		
18000	208.0	84.1		1000.0		
20000		105.0		1420.0		
VISCOSITY INDEX	79.0		14.0		-9.0	
ANILINE POINT °C	73.0		75.8		78.9	
MOL. WGT.	319.0		367.0		412.0	
% PARAFFINS	66.8		61.9		60.9	
% NAPHTHENES	12.8		16.3		16.3	
% AROMATICS	20.4		21.8		22.8	

TABLE II

Viscosity-Pressure Data of Dow for Four Hydraulic Oils

V.I.	OIL A-142				OIL B-135				OIL C-120				OIL D-126			
TEMPERATURE °F	10	32	100	130	10	32	100	130	10	32	100	130	10	32	100	130
DENSITY (GM/CM³)	.881	.873	.850	.839	.896	.889	.865	.854	.910	.903	.879	.869	.890	.882	.858	.848
PRESSURE (PSI)	COEFFICIENT OF VISCOSITY (CENTIPOISES)															
15	705.0	264.0	35.4	19.8	887.0	329.0	38.1	20.6	1202.0	264.0	35.4	20.7	906.0	291.0	35.5	19.3
2000	1130	404	48	26	1456	502	50	27	2052	612	55	27	1448	430	48	25
4000	1718	590	65	35	2360	755	69	35	3218	945	73	36	2260	640	63	32
6000	2602	860	85	45	3790	1140	94	47	—	1507	103	48	3425	965	83	41
8000	3990	1267	113	57	—	1733	128	62	—	2305	144	63	—	1408	109	53
10000	—	1817	148	71	—	2575	171	80	—	3456	194	82	—	2036	144	68
15000	—	—	285	126	—	—	347	148	—	—	392	157	—	—	273	120
20000	—	—	541	223	—	—	689	270	—	—	814	296	—	—	511	208
30000	—	—	—	651	—	—	—	869	—	—	—	1017	—	—	1670	593
40000	—	—	—	1825	—	—	—	—	—	—	—	—	—	—	—	1603

cosity of a lubricating oil, Dow and Fink found that the aniline point bears a close relationship to the pressure coefficient of viscosity. Fig. 4 shows a plot of the data summarized in Table III which contains the results of 24 mineral oils from widely distributed sources. The pressure coefficient is taken at 100°F. and is defined by

$$a = 1/P[(\log \eta - \log \eta_0)/\log \eta_0]$$

which in many cases has been found to better represent the data than

$$a = 1/P[\log \eta/\eta_0]$$

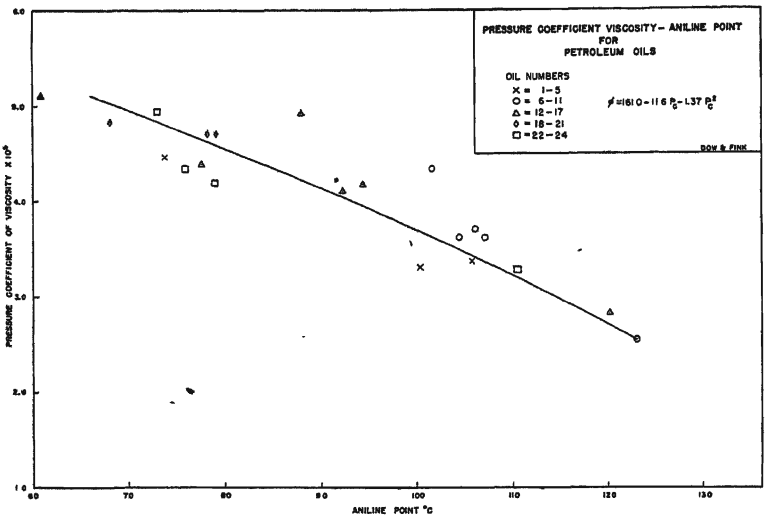

FIG. 4

The empirical relation between aniline point in °C., ϕ, and the pressure coefficient of viscosity in in.²/lb., P', is

$$\phi = 161.0 - 11.6\,P' - 1.37\,P'^2$$

The authors have sought other relationships of more fundamental significance, *e.g.*, molecular weight, paraffinic content, aromatic content, index of refraction, rings per molecule, H/C content, V.I., density, *etc.*, with little success.

The extremely high thrust-shear technique which has been developed and extensively applied by Bridgman, and summarized by him in another paper of this Symposium, has been used by Boyd and Robertson (19) to measure the friction of various lubricants under pressure. Twenty-four materials were studied, 16 of which can be classified as either fixed or mineral oils and greases. The double-anvil test surfaces were compressed

TABLE III

Pressure Coefficient of Viscosity-Aniline Point Data of Dow & Fink for Hydrocarbon Oils

OIL NUMBER	SOURCE	REFERENCE	P.C.V. (P_C) AT 100°F	ANILINE PT (ϕ)°F	OIL NUMBER	SOURCE	REFERENCE	P.C.V. (P_C) AT 100°F	ANILINE PT (ϕ)°F
1	PENN	11	3.28×10^{-5}	110 3	13	RUSSIAN #1	14	4.17×10^{-5}	94 3
2	OKLAHOMA	11	3.56×10^{-5}	98.4	14	RUSSIAN #2	14	4.92×10^{-5}	88.0
3	CALIF	11	4.46×10^{-5}	73.8	15	RUSSIAN B S	14	2.81×10^{-5}	120 1
4	PENN.	12	3.30×10^{-5}	100 3	16	RUMANIAN #1	14	5.11×10^{-5}	60.8
5	PENN. RAFF	12	3.36×10^{-5}	105.7	17	RUMANIAN #2	14	4.38×10^{-5}	77.8
6	PENN.	13	2.53×10^{-5}	122.9	18	U.S. NAPHTHENIC	DATA OF FINK	4.70×10^{-5}	78.2
7	PENN	13	3.54×10^{-5}	99.1	19	U.S. NAPHTHENIC	DATA OF FINK	4.70×10^{-5}	79 1
8	PENN.	13	3.61×10^{-5}	107 1	20	U.S. NAPHTHENIC	DATA OF FINK	4.83×10^{-5}	68.1
9	PENN.	13	3.70×10^{-5}	106.1	21	U.S. NAPHTHENIC	DATA OF FINK	5.11×10^{-5}	60 9
10	PENN	13	3.61×10^{-5}	104.4	22	BURMA #1	DOW & VEITH TABLE 1	4.93×10^{-5}	73.0
11	PENN.	13	4.33×10^{-5}	101.7	23	BURMA #2	DOW & VEITH TABLE 1	4.33×10^{-5}	75 8
12	RUSSIAN #00	14	4.10×10^{-5}	92.2	24	BURMA #3	DOW & VEITH TABLE 1	4.18×10^{-5}	78 9

between the platens of a 400,000 lb. hydraulic press. The torque required for twisting the anvils under a given thrust was measured for each sample. The coefficient of friction as a function of pressure was computed, as well as the shearing stress against angle of shear, both over a pressure range of 400,000 ψ.

It was found, generally speaking, that the shearing stress increased slowly with angle of shear up to 50°, after a sharp initial rise, and the effect did not seem to increase materially over a 10-fold pressure rise. Stearic acid, $CH_3(CH_2)_{16}COOH$, was outstanding as the oil showing the lowest shearing stress for a given compressive pressure. Capric acid, $CH_3(CH_2)_8COOH$, on the other hand, exhibited the greatest shearing stress. Is the difference due to CH_2 groups alone? The coefficient of friction-pressure results were quite different in nature. The curves appear to be a series of broken straight lines which may show regions where there is an increase or decrease of friction with pressure. Here again stearic and capric acids showed the greatest differences, both in magnitude and behavior. It is interesting to note that stearic acid had a coefficient of friction between 0.01 and 0.04 over a range of 400,000 ψ. Mineral oils had coefficients considerably larger (0.10) than the fixed or fatty oils. Some tests were also made with 1% additives, such as graphite, mica, MoS_2 and stearic acid, added to a mineral oil.

High rates of shear remain a most intriguing problem for rheologists, especially those concerned with lubricants. Grunberg and Nissan (20) suggest Newtonian viscosity may be expected to become a function of the rate of shear at high rates, but there is a paucity of experimental data on this important matter. Considerable work on shear has been done during the war and it is to be hoped that some of the results can be released at an early date for publication. Two techniques should be mentioned which offer the greatest promise in studying high rates of shear, both developed at the University of Virginia: the method of Beams in developing high rotational speeds far in excess of those required for shear measurements, and the spark photography of Snoddy which would permit examination of turbulence when the critical Reynold's number is exceeded. While these two techniques have not been applied together to the study of viscosity of fluids at high rates of shear, it would appear to be a most worth-while investigation and one which could be done relatively simply.

Another rheological phenomenon of interest at high pressures is the solidification of lubricants. Hersey and Shore (15), and Kleinschmidt (21) reported apparent solidification pressures which were quite low at temperatures near room temperature. Hersey and Shore, using a rolling-ball viscometer, found that for lard oil the viscosity became infinite at 24,000 ψ. For Veedol mineral oil the pressure was about 20,400 ψ. Klein-

schmidt, using a falling-weight viscometer, at somewhat higher temperatures, found the pressures to be 38,000 and 24,000 ψ for the same oils, lard and mineral, respectively. At 104°F. the pressures were 59,000 ψ for lard oil and 42,000 ψ for the mineral oil. Dow (22) examined several oils over a pressure range of 140,000 ψ by means of a piston displacement method (compression) and concluded that the oils did not freeze, in a thermodynamic sense, at those pressures. Apparent solidification, as found by viscosity measurements, is undoubtedly some stage of the process, depending on the history of the process, where the formation of a labile, vaseline-like substance prevents relative motion of the lubricant. Poulter and associates (23) have shown that in a very short capillary some mineral oils possess flow properties at pressures as high as 250,000 ψ at room temperatures. While the work was initially a study of viscosity (24) at this order of pressure, recent emphasis has been placed on the solidification characteristics (25) of mineral oils from various crudes. It is obviously unsafe to attribute any absolute significance to apparent solidification when it is determined by a viscosity measurement, as judged by the great differences of results obtained by the different methods of measurement. However, Poulter's measurement, because it permits very little disturbance due to flow, probably approaches the thermodynamic freezing point, if one exists, closer than the other methods of viscosity measurement. In these regions of partial solidification, it should be emphasized that Newtonian viscosity is not measured by any of the methods cited.

Turning to some of the theoretical contributions to the rheology of lubricants, Bondi (26) has considered flow orientation in highly viscous materials of high molecular weight, with particular reference to the Eyring theory of flow and, more recently (27), has computed the volume increase of the activated molecules over the ordinary molecules for viscous flow for several lube oils. For large spherical molecules, like pentachlorodiphenyl, he finds ΔV is about 55% larger than for a paraffinic lube oil and 200% larger than for decane, the latter two possessing long, chain-type molecules. Alfrey (28) has pointed out the necessity of considering rotational jumps in the activation process in order to obtain a velocity gradient which is required by hydrodynamics for viscous flow.

The foregoing survey on lubricants would be incomplete without brief mention of the joint meeting (29) of the British Rheologists' Club and the Institute of Petroleum (British) held in the Summer of 1945. The paper of Hardiman and Nissan on "A Rational Basis for the Viscosity Index System. Part I" is worthy of special mention since it applies to high V.I. oils (greater than 140) where anomalous values are obtained by the original Dean and Davis viscosity index system. The authors propose the equation

$$\text{V.I.} = (60.0 - \text{antilog } n) \times 3.63$$

where $n = \log \nu - 0.4336/\log$ visc. at 210°F. and ν is the viscosity in centistokes at 100°F. One cannot help but hope that the time will come when the concept of a viscosity index will be discarded by popular agreement. It certainly is a more complicated and less fundamental concept than temperature coefficient of viscosity, which also, it should be mentioned, applies equally well when pressure effects are considered.

In conclusion, Scott Blair (30) has reviewed briefly the Russian Conference on viscosity of liquids and colloidal solutions which was held in Moscow in 1944. Several papers were devoted to viscosity effects in oils, including the effects of pressure, temperature, static electric fields and electromagnetic radiation.

The thoughts expressed in the above paper are those of the writer and do not represent the views of the Navy Dept.

References

1. Oiliness, 3rd Ed. Alox Corp., New York, N. Y. (1942).
2. Davey, W., *J. Inst. Petroleum Tech.* **31**, 73 (1945).
3. Webber, M. W., *J. Inst. Petroleum Tech.* **31**, 89 (1945).
4. Larsen, R. G., Thorpe, R. E., and Armfield, F. A., *Ind. Eng. Chem.* **34**, 183 (1942).
5. Von Fuchs, G. H., and Diamond, H., *Ind. Eng. Chem.* **34**, 927 (1942).
6. Swearingen, J. S., and Redding, E. D., *Ind. Eng. Chem.* **34**, 1497 (1942).
7. Bridgman, P. W., *Rev. Modern Phys.* **18**, 44 (1946).
8. Hersey, M. D., and Hopkins, R. F., *Mech. Eng.* **67**, 820 (1945).
9. Hubbard, R. M., and Brown, C. G., *Ind. Eng. Chem.* **15**, 212 (1943).
10. Dow, R. B., *Rheol. Bull.* **13**, 8 (1942).
11. Dow, R. B., *J. Applied Phys.* **8**, 367 (1937).
12. Thomas, B. W., Ham, W. R., and Dow, R. B., *Ind. Eng. Chem.* **31**, 1267 (1939).
13. Dibert, R. M., Dow, R. B., and Fink, C. E., *J. Applied Phys.* **10**, 113 (1939).
14. Dow, R. B., McCartney, J. S., and Fink, C. E., *J. Inst. Petroleum Tech.* **27**, 301 (1941).
15. Hersey, M. D., and Shore, H., *Mech. Eng.* **50**, 221 (1928).
16. Suge, Y., *Inst. Phys. Chem. Research (Tokyo)* **34**, 2, 1244 (1938).
17. Cragoe, C. S., *Proc. World Petroleum Cong. (London)* **II**, 529 (1933).
18. Cameron, A., *J. Inst. Petroleum Tech.* **31**, 401 (1945).
19. Boyd, J., and Robertson. B. P., *Trans. Am. Soc. Mech. Engrs.* **67**, 51 (1945).
20. Grunberg, L., and Nissan, A. N., *Nature* **156**, 335 (1945).
21. Kleinschmidt, R. V., *Trans. Am. Soc. Mech. Engrs.* **50**, APM–50–4 (1928).
22. Dow, R. B., *Rheol. Bull.* **13**, 7 (1942).
23. Poulter, T. C., *J. Applied Phys.* **9**, 307 (1938).
24. Larson, C. M., *Mech. Eng.* **68**, 580 (1946).
25. Poulter, T. C., Am. Chem. Soc. 110 Meeting, Chicago, Sept. 9–13, Abstracts 131 (1946).
26. Bondi, A., *J. Applied Phys.* **16**, 539 (1945).
27. Bondi, A., *Mech. Eng.* **68**, 577 (1946).
28. Alfrey, T., *Rheol. Bull.* **16**, 3 (1945).
29. *Nature* **155**, 734 (1945).
30. Scott Blair, G. W., *Nature* **156**, 147 (1945).

RHEOLOGICAL PROPERTIES OF PAINTS, VARNISHES, LACQUERS, AND PRINTING INKS

Henry Green

From Interchemical Corporation, New York City

Received Nov. 21, 1946

In recent years rheology, as a science, has taken an increasingly important position in industry, particularly in industries that manufacture products of the pigment-vehicle types. Unfortunately our colleges have not always kept pace with the trend, and the number of such institutions that possess the necessary personnel and equipment for teaching a practical scientific rheology is still regrettably small. There are, of course, well-known and outstanding exceptions to this generalization; but in the main, one must turn toward our industrial laboratories to discover the *status quo* of what might be called "pigment-vehicle rheology."

The paint and printing ink industries have always felt the necessity for consistency control. Prior to 1916, when the Bingham (1) concept of plastic flow was first given to the world, no type of control existed that was based on a recognized difference between liquid and plastic flow. Consequently existing tests were of questionable value. Such methods, however, became thoroughly intrenched, due to their long usage, and their subsequent dislodgement has been an almost impossible task.

Undoubtedly one of the greatest difficulties in introducing modern rheological methods into industrial laboratories, where the products of manufacture are non-Newtonian, arises from the necessity of replacing the single-point viscosity measurement with a multiple-point consistency curve. Resistance has resulted from three basic causes—time, money, and the necessity for an increased personnel. It requires more time to produce a consistency curve; it requires more money to secure the necessary equipment; and it takes a larger staff to make the necessary number of measurements per day.

It would hardly be true to say that the consistency curve method resulted from Dr. Bingham's pioneering work in plastics, for the record shows that consistency curves were employed many years prior to 1916. It might not be far from the mark, however, to state that, as a result of Bingham's work, the paint and related industries, for the first time in their history, became aware of the fact that plastics and liquids are not members of the same rheological class, and that, for plastics at least, the consistency curve method of measurement must eventually be

adopted. One of Bingham's greatest achievements, undoubtedly, has been to make industry fully conscious of the importance of that fact.

That was in 1916. In the meantime what has industry done toward the development of an industrial rheology based on the Bingham concept of plastic flow? As early as 1918, the paint and rubber industries were both in a frame of mind that indicated eagerness and not hesitancy toward the acceptance of a scientific rheology for control work. Yet, it is well known that no general acceptance ever occurred. A survey of the literature indicates this fact only too clearly by the paucity of papers dealing exclusively with the Bingham method of measuring plastic materials. It is not the purpose of this article to delve into the history of rheology. Nevertheless, what happened between the Bingham era (1916) and the one that subsequently followed—the Reiner era (1927)—is of such importance in its bearing on today's methods that it cannot be passed by totally without comment.

The Bingham concept of plastic flow is the same as Newton's flow for liquids, except that the idea of yield value is introduced. Unfortunately, the Bingham formula was originally inserted directly into the Poiseuille equation. The results indicated that a linear relationship should exist between the shearing stress and the ensuing rate of flow. Neither Bingham nor other investigators were able to obtain experimental verification of such an ideal relationship. It was on this rock that the ship of industrial rheology temporarily foundered.

In 1921 Buckingham (2) and later, independently, Reiner deduced the equation of capillary flow for a Bingham plastic, *i.e.*, one where there is a constant yield value. Their equation is non-linear and shows conclusively that as long as the yield value is finite and constant, the consistency curve cannot be linear. Their curve coincides to a certain extent with laboratory measurement, but the lower end of the curve differs radically from experiment and so their equation cannot be solved satisfactorily either for yield value or for plastic viscosity. Industrial rheology was in no better position than it was prior to 1916.

The time was now ripe for the advocates of empirical formulae. These formulae, as a rule, are power equations like

$$P = A\sigma^B,$$

where A and B are the parameters. A corresponds to the viscosity coefficient, but its dimensions vary according to the value of B. Unfortunately, laboratory data occasionally give curves corresponding to this equation, and this coincidence is considered sufficient evidence that the equation is correct. As a matter of fact, the equation is not deduced from rheological concepts and its parameters are quite meaningless. It constitutes, therefore, a serious impediment to the development of industrial rheology.

In 1927 Reiner and Riwlin (3) developed their equation of flow for Bingham-bodies in rotational viscometers. Their equation predicted a linear relationship over that part of the curve where complete laminar flow ensues. In the capillary viscometer no such region can exist, except at infinitely high rates of shear. In the rotational viscometer shear takes place between two substantial walls; and so complete laminar flow is easily attained at finite shearing rates. In the capillary viscometer, shear occurs between a single wall and a mathematical line—the axis of the tube. This line offers no resistance to flow and consequently the shearing stress must be infinitely high in order to secure laminar flow in the center of the tube.

A number of investigators examined the Reiner equation and found that it agreed substantially with laboratory data. Industry had, therefore, been presented with a simple method for determining yield value and plastic viscosity. What effect did this have on industrial rheology? The answer is, it had none. The reason lay in the fact that the instrument makers were not ready. They had no rotational viscometers built for producing suitable consistency curves, and industry evidently had no urgent desire to build them.

Briefly, the causes for delay in adopting the Bingham concept of plastic flow in the development of industrial rheology are:

(*a*) The attempt to introduce yield value directly into the Poiseuille equation. The result predicted a linear relation between shearing stress and rate of shear. Such a prediction could not be fulfilled.

(*b*) Solution of the Buckingham and Reiner equation for flow of plastics in a capillary tube was found impractical.

(*c*) The introduction of empirical equations of flow prevented the use of the Bingham concept.

(*d*) The purchasing of suitable rotational viscometers giving continuous consistency curves was not possible.

The above situation prevailed in the 1920's. In addition, there existed an inherited desire to treat materials such as paints, printing inks, varnishes, and lacquers as though they all belonged in the same rheological category. Hence, a single-point method was employed in measuring them. A distinction, however, was made. In the case of varnishes and lacquers, the measurement was called the "viscosity"; in the case of paints and printing inks, it was called the "apparent viscosity." Probably this concession was made as a safeguard against possible criticism by the advocates of the Bingham concept.

After the Reiner and Riwlin equation received recognition, it was applied to commercial viscometers like the MacMichael and Stormer. It was found that the prediction of a linear equation in the region of laminar flow is correct. In 1935, one of our largest printing ink companies

commenced constructing a rotational viscometer that was especially designed for producing consistency curves. This was accomplished by making possible a rapid change in r.p.m. over a suitably wide range. Both up- and down-curves could be produced with equal facility. When plotted together, these curves coincide, except when thixotropy exists. In such cases, they form a loop (4). The downcurve of the loop is solvable by means of the Reiner equation, which gives both yield value and plastic viscosity. From the area of the loop, the amount of thixotropic breakdown can be calculated. This viscometer has been described in detail elsewhere and will not be discussed here (5).

If the time arrives when instrument makers place upon the market a reasonably priced rotational viscometer, so constructed that a smooth continuous change in r.p.m. is possible, and the instrument is temperature controlled, there will then be no further necessity for single point measurements of plastic materials. This event should constitute a great stimulus for industrial rheology. Investigators will then be able to produce consistency curves subject to interpretation by the Reiner equation. However, there will always be some investigator who will not accept the Reiner formula because the concept of yield value, to them, seems false. That is beside the point at present. Let investigators first learn to make *comparable consistency curves* and to eliminate the practically meaningless term "apparent viscosity." The interpretation of the curve will follow naturally, particularly as additional knowledge is gained in regard to the mechanism of plastic flow.

Consider for a moment a dilute suspension of a resin in a solvent. The molecules are elongated. As soon as a shearing force is applied, the molecules, being disconnected, begin to orient in the direction of flow. Under the circumstances, it is impossible to visualize the existence of a yield value. Such a model of flow, however, should not be applied to Bingham-bodies (like paints and printing inks). Microscopical examination of flow in capillaries shows that Bingham-bodies hold together until the shearing stress attains a definite finite value. In such cases yield value is easily visualized. The argument against this conclusion is, that the investigator did not wait long enough to detect a perceptible amount of flow.

From the academic point of view, a truly rigid body might never exist above absolute zero. In actual practice, however, the manufacturer can not wait an infinite number of years to see whether his product has a yield value. If the surface of his material does not flatten out in a reasonable length of time after stirring, it possesses a property that substantially affects the nature of his product. That property has been called "yield value." The manufacturer would like to have a measurement of it, indicating its magnitude. He is not interested in whether the academician considers yield value to be a myth or not.

Yield value is one of the two parameters in the Reiner equation; the one imparting plasticity to the material possessing it. That is the simplest way to look at the subject, and it should not be objectionable to the most conscientious opponent of the yield value concept. It is not necessary to visualize the cause of yield value, or what happens to it in an infinite period of time. Yield value should be accepted as a measurement that is definitely associated with the quality of the manufactured product. The investigator needs speculate no further, if that is his deisre.

Paints and printing inks are non-Newtonian suspensions that have been termed "Bingham-bodies" by Reiner. As a rule they are thixotropic. The rheologist of today now has sufficient means for measuring their yield value, plastic viscosity, and thixotropic breakdown at a known rate of shear.

It is quite conceivable that the paint industry will never require a high degree of rheological control over its products. Naturally this is a guess, but when the rheological requirements for the printing ink industry are examined, a different degree of precision will be found there. In process printing, the inks must trap in their order of printing. Their ability to do this depends on the correct adjustment of their plastic viscosities. At high printing speeds thixotropic inks break down, and, unless full consideration is given to this possibility, their order of trapping might readily change. This is a case where considerable rheological control is demanded. So far no similar situation exists in the paint industry.

Product control is not the only type of problem to which the paint and printing ink rheologist has devoted his time. Rheology plays an important part in pure research. The development of new products and the matching of old ones is almost an everyday occurrence. In the past, the rheological matching of two materials consisted mainly in watching them flow, side by side, down an inclined plane. If their rate of flow was the same, and each flowed the same distance, the materials were considered to be rheologically alike. Most plant rheologists know, today, that such "matching" is fortuitous and that these same materials might have quite different yield values and plastic viscosities, in which case they could behave differently under different circumstances.

The viscometer, especially in connection with the microscope, is being employed for the study of emulsions, paints and printing inks. So far this work has not been extensive. Its possibilities, however, are far reaching, especially for investigating structural differences. Structure produces such manifestation as yield value and thixotropy; it also affects the magnitude of the plastic viscosity.

Structure forms an interesting and important part of industrial rheology. A structure need not always be composed of particles held together by a binding or connecting force. Resins, or other soluble materials com-

posed of long molecules, can form, in a way, a type of structure when subjected to flow orientation. Such a structure is a "loose" one, and has very little right to the title of "structure." Its only justification, perhaps, is the fact that such a formation is an oriented mass and urgently in need of a name.

Lately rheologists who have been exploring the field composed of materials like oils, varnishes, and lacquers are beginning to realize that such products might not only be non-Newtonian but thixotropic also. Evidence of such appears when the materials are subjected to high rates of shear. An accumulation of heat could cause both effects and, at present, considerable argument exists as to what actually happens. Both sides have their advocates. Both sides admit, however, that non-Newtonian and thixotropic behaviors under high shearing rates are quite possible. The question is, have such high shearing rates ever been attained? The final answer will be of considerable importance to the investigators of lubricating oils, especially in connection with subjects like aviation.

If asked what the position of rheology is with respect to the paint and printing ink industries of today, the answer can be but a personal opinion. No comprehensive survey of the field has ever been made. Any conclusion, naturally, will depend on the number of published papers that have appeared, and on the contacts the investigator has made with individual paint and printing ink companies. The printing ink industry has an urgent need for rheological control. At present this industry is in a transition stage. It is reaching for new rheological ideas while trying to retain as long as possible single point methods of measurement. However, it will probably be one of the first of the pigment industries to let go of the past. When it has taken this step, and has found that it has not been a dangerous one, other companies in related fields will undoubtedly follow suit.

In comparison with the amount of rheological work that has been done with pseudoplastics, the rheological study of Bingham-bodies is almost negligible. However, the situation is far from discouraging. All the evidence in the last few years indicates that a change is taking place. The requirements in regard to instruments, methods, and theories are better understood. When these requirements are fully attained, the motivating force that will set them in operation will come from the rheologist himself. He must prove that the application of scientific rheology in the control laboratories of his company produces an improvement in his company's products.

References

1. Bingham, E. C., *Natl. Bur. Standards, Sci. Papers No.* **278** (1916).
2. Buckingham, E., *Proc. Am. Soc. Testing Materials* **21**, 1154 (1921).
3. Reiner, M., and Riwlin, R., *Kolloid-Z.* **43**, 1 (1927).
4. Green, H., and Weltmann, R. N., *Ind. Eng. Chem.* **15**, 201 (1943).
5. Green, H., *Ind. Eng. Chem.* **14**, 576 (1942).

THE INFLUENCE OF SOLVENT COMPOSITION ON THE SPECIFIC VISCOSITIES OF POLYMER SOLUTIONS

Turner Alfrey

From the Polymer Research Institute, Brooklyn Polytechnic Institute
Received Nov. 25, 1946

Introduction

At sufficiently low concentrations, the specific viscosity, η_{sp}, of a polymer solution can be satisfactorily related to the concentration by the first two terms of a power series:

$$\eta_{sp} = a_1 \cdot c + a_2 \cdot c^2.$$

The first coefficient, a_1, is ordinarily called the "intrinsic viscosity" and represented by the symbol $[\eta]$. Unless permanent intermolecular association effects are present, the intrinsic viscosity is clearly a measure of the hydrodynamic interference provided by the individual solute molecules at infinite dilution. The second coefficient, a_2, reflects the *interaction* among solute molecules. Such interaction can be purely hydrodynamic in character (interpenetration of the flow patterns around neighboring polymer molecules) or it can include a tendency toward intermolecular agglomeration at finite concentrations. In many cases it has been found that the second coefficient is related to the first by the equation:

$$a_2 = k'[\eta]^2,$$

where k' is constant for a given chemical species of polymer in a given solvent, and is independent of the molecular weight of the polymer.

Both $[\eta]$ and k' are observed to vary from one solvent to another, and the purpose of this paper is to review the probable reasons for such variations (6, 7, 10, 11). It must be recognized at the outset that there are marked differences among different polymers as far as sensitivity to solvent composition is concerned. Polystyrene, for example, follows a distinctly different pattern of behavior from cellulose acetate. An attempt will be made to correlate the type of behavior of a polymer with the degree of flexibility of the chain, and the uniformity of groups along the chain.

Behavior of Polystyrene

Polystyrene behaves in a particularly simple fashion. Briefly stated: (1) the intrinsic viscosity is high in "good" solvents and low in "poor"

solvents; (2) the k' value is higher in poor solvents than in good solvents; and (3) in a poor solvent, an increase in temperature results in an increase of the intrinsic viscosity, whereas in an energetically indifferent solvent the intrinsic viscosity is practically independent of temperature.

The author believes that the above pattern of behavior is characteristic of polymer molecules which (a) are fairly uniform in their structure (specifically, do not have groups distributed along the chain which are much more polar than the bulk of the chain) and (b) are fairly flexible in solution. Such behavior for this type of molecule has been explained as follows (1):

A long chain hydrocarbon molecule in solution takes on a somewhat kinked or curled shape, intermediate between a tightly rolled up mass and the rigid linear configuration assumed by Staudinger. Presumably all possible degrees of curling are represented, owing to the internal Brownian movement of the flexible chains, but the configurations of intermediate extension predominate statistically. The average or effective value of any shape-dependent molecular property (such as hydrodynamical influences) may be obtained by summing this property over all configurational states, after each state has been given a proper weight factor. If the long chain molecule is surrounded by a continuous, energetically indifferent solvent, then the weight factor for a particular configuration is determined only by internal parameters—potential energy function for restricted rotation, prohibition of segment interpenetration, *etc.* The mean value of any molecular property in such an indifferent (and perhaps hypothetical) solvent might be called the 'unbiased' statistical mean for the property.

If the solvent is energetically unfavorable, so that the dissolving of the high polymer is an endothermic process, then the polymer segments will attract each other in solution and squeeze out the solvent between them. Those molecular configurations which involve many contacts of the molecule with itself will be weighted more heavily than in an indifferent solvent, and the mean value of any molecular property will represent a more curled and contracted shape than the unbiased mean. On the other hand, if a solvent is energetically more favorable than the indifferent solvent as previously defined, then in solution the long chain molecule will be surrounded by a solvated hull which tends to prevent polymer-polymer contacts. Uncurled configurations will be favored, and the mean value of any property will represent a more extended shape than the unbiased mean. Since an extended or uncurled configuration is associated with a high intrinsic viscosity, and *vice versa*, the first prediction as to effect of solvent type upon viscosity is the following: Other conditions being equal, a given high polymeric material made up of flexible molecules will exhibit a high intrinsic viscosity in an energetically favorable solvent, and a low intrinsic viscosity in an energetically unfavorable solvent. If a good solvent is mixed with a precipitating agent, the resulting mixture can be expected to be energetically less favorable to a long chain molecule than is the pure solvent. A dilute solution of high polymer in a solvent-non-solvent mixture should, therefore, exhibit a lower intrinsic viscosity than a solution of the same polymer in the pure solvent.

The effect of temperature upon intrinsic viscosity should depend strongly upon the nature of the solvent. In a poor solvent, the effective molecular shape is more compact and curled than the unbiased statistical mean. An increase of temperature should increase the relative importance of entropy factors over energetic factors, and result in an uncurling of the molecule. In such a solvent, a temperature increase should result in an increase of intrinsic viscosity. In a very good solvent, the energetic weighting factors favor the more extended configurations; here a temperature increase should result in a

downward approach to the unbiased statistical mean shape. In a very good solvent, therefore, a temperature increase should cause a decrease in intrinsic viscosity. There should be an intermediate case in which the intrinsic viscosity is independent of temperature over a limited range.

As one proceeds to a finite concentration, it is clear that intermolecular agglomeration will be more pronounced in a poor solvent than in a good solvent. This leads to the expectation that k', the interaction constant, should increase as one goes to poorer and poorer solvents. This is indeed observed. A more specific statement involving such intermolecular association effects follows (1). Reported data on polystyrene solutions are consistent with this conjecture, but can hardly be said to prove it:

We have interpreted variations in the intrinsic viscosity of a given high polymeric material as being due to changes in the degree of *intramolecular* agglomeration. If this interpretation is correct, there should be also a close connection between the intrinsic viscosity of a high polymer solution and the degree of *intermolecular* agglomeration. Exactly the same solvent characteristics which determine the mean geometrical properties of an isolated long chain molecule should also determine the amount of association of different solute molecules into aggregates. When a non-solvent is added to a high polymer solution, the point at which precipitation begins represents a certain definite agglomeration tendency for chain segments of different molecules. To a first approximation, therefore, it should represent a certain definite mean value for any shape-dependent *internal* property. That solvent composition which is critical from the standpoint of solubility should correspond to a certain intrinsic viscosity, no matter what the solvent and what the non-solvent. One would therefore conclude the following: The intrinsic viscosities of a series of solutions of a given polymer in solvent-non-solvent mixtures of increasing non-solvent content, should decrease to a final value at the limit of solubility. This final value should be in first approximation the same in all solvent-non-solvent systems.

Another factor of importance is the molecular weight of the polymer. Huggins (12) has demonstrated theoretically that in the equation $[\eta] = KM^a$, the exponent a reflects the shape of the polymer molecule, varying from 0 for a tightly balled up sphere to 2 for a rigidly extended rod. It follows that one should expect a, as well as $[\eta]$ itself, to decrease upon going to poor solvents.

There is not a great deal of experimental evidence available on this point, but experiments by Goldberg indicate that the above expectation based on Huggins's theory is actually fulfilled in the case of solutions of emulsion polymerized polystyrene. Goldberg determined the K and a values for emulsion polymerized polystyrene in toluene and methyl ethyl ketone and reported the following results:

(in toluene) $K = 3.7_3 \times 10^{-4}$, $a = 0.62_3$;
(in methyl ethyl ketone) $K = 7.0_3 \times 10^{-4}$, $a = 0.53_0$.

Typical experimental results on polystyrene solutions are shown in Figs. 1 to 5.

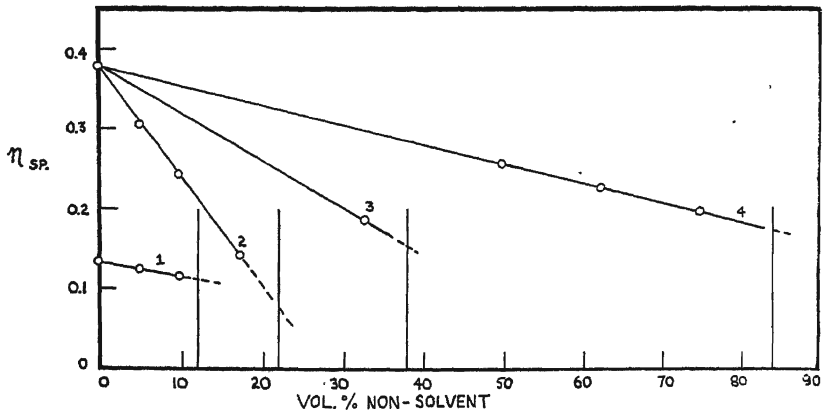

FIG. 1

Variation of Specific Viscosity of 0.2% Polystyrene Solutions with Non-Solvent Content. (1) methyl ethyl ketone-methanol; (2) toluene-methanol; (3) toluene-isoamyl alcohol; (4) toluene-acetone. (Ref. 1).

Fig. 1 shows how η_{sp} of a 0.2% polystyrene solution varies with solvent composition. Unfortunately, these results were on unfractionated polystyrene, and the results were not extrapolated to infinite dilution. However, the general pattern of behavior described above seems to hold moderately well. We now quote from reference (2):

Fig. 2 shows the variation of intrinsic viscosity of a polystyrene *fraction* with temperature and with the composition of mixed solvent in the case of the system toluene-butanol (2). Increasing amounts of butanol in the solvent mixture results in a regular decrease in the intrinsic viscosity at 20°, 40°, and 60°C. When corrected for concentra-

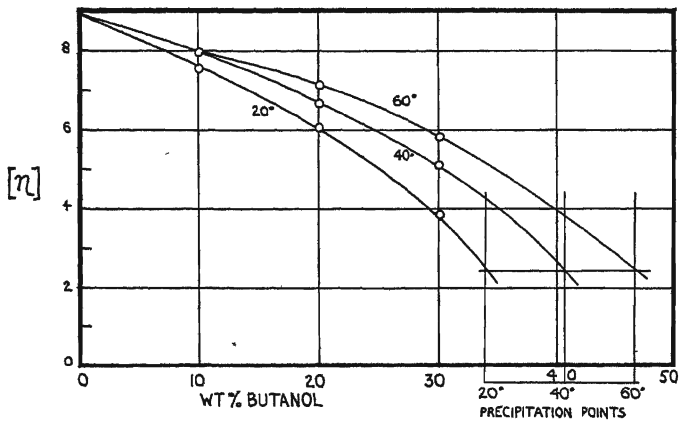

FIG. 2

Intrinsic Viscosity of Polystyrene Fraction JNZ–2 in Toluene-Butanol. (Ref. 2)

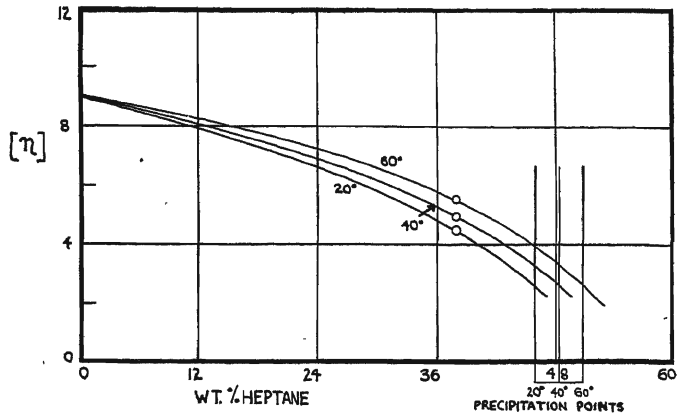

FIG. 3

Intrinsic Viscosity of Polystyrene Fraction JNZ–2 in Toluene-Heptane. (Ref. 2)

tion changes, the intrinsic viscosity in pure toluene is, within experimental error, independent of temperature. In the more unfavorable mixtures, however, the intrinsic viscosity increases markedly with an increase in temperature, as is to be expected. The curves extrapolate to an intrinsic viscosity of slightly over 2.0 at the precipitation points. In this case, the extrapolations are rather dubious. The data are consistent with the observation that a definite intrinsic viscosity characterizes the precipitation point, but are not sufficient to prove this observation. In Fig. 3 are shown similar curves for the system toluene-heptane. The results are qualitatively similar and it is significant that the curves again extrapolate to an intrinsic viscosity slightly greater than 2.0 at the pre-

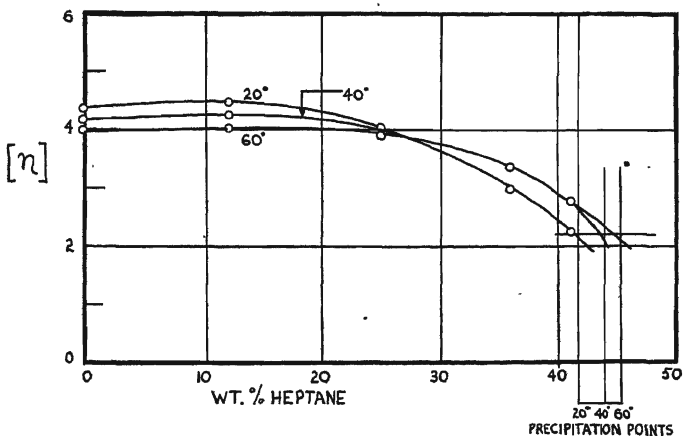

FIG. 4

Intrinsic Viscosity of Polystyrene Fraction JNZ–2 in Methyl Ethyl Ketone-Heptane. (Ref. 2)

cipitation point. In Fig. 4 are shown similar data for the system methyl ethyl ketone-heptane. Three significant features of these latter curves may be pointed out:

(1) Again the curves extrapolate to a specific viscosity of slightly greater than 2 at the precipitation points.

(2) Although pure methyl ethyl ketone is a poor solvent as indicated by the low value of intrinsic viscosity, the intrinsic viscosity *decreases* with an increase in temperature. This rather anomalous behavior is presumably due to the fact that as the temperature rises, the calculated cohesion energy density of methyl ethyl ketone becomes increasingly different from the favorable values as represented by toluene. Thus, methyl ethyl ketone becomes an increasingly unfavorable solvent as the temperature rises, and the intrinsic viscosity therefore decreases.

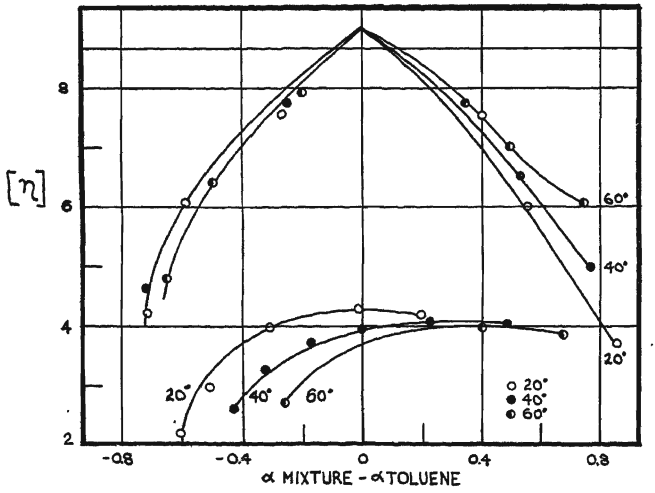

FIG. 5

Intrinsic Viscosity of Polystyrene Fraction JNZ-2 as a Function of Cohesive Energy Density of Mixed Solvents. (Ref. 2)

(3) In the two preceding cases, the intrinsic viscosity began to decrease with the first addition of non-solvent. The first 20% of heptane, however, causes no decrease in the intrinsic viscosity of a polystyrene solution in methyl ethyl ketone. In fact, there is some indication of a small *increase* in intrinsic viscosity upon addition of a small quantity of heptane. This difference in behavior is almost certainly connected with the fact that methyl ethyl ketone has a higher cohesive energy density than polystyrene while heptane has a lower cohesive energy density. Indeed, a naive application of the concept of cohesive energy density would actually predict a much *larger* deviation in this direction. One would expect some intermediate solvent mixture, possessing an average cohesive energy density close to that of polystyrene, to give an intrinsic viscosity equivalent to that observed in toluene. The fact that such a pronounced maximum does not occur in Fig. 4 is an indication of the (quantitative) failure of the cohesive energy density concept in the case of methyl ethyl ketone.

In Fig. 5 the data of Figs. 2, 3, and 4 are plotted against the interaction constant α (square root of cohesive energy density), rather than against the mixed solvent com-

position. Curves for the systems toluene-hexane and toluene-butanol fit moderately well the predictions based on cohesive energy densities. Solutions containing methyl ethyl ketone, however, fall completely out of line. Increasing deviations also are observed in the butanol system with increasing amounts of butanol. When asymmetric polar solvents are concerned, therefore, it must be concluded that the intrinsic viscosity is not determined simply by the difference in cohesive energy density between solvent and polymer. Furthermore, in such cases precipitation does not occur at a definite value of average cohesive energy density.

Other Polymers Exhibiting Behavior Similar to that of Polystyrene

Less complete studies have been made on a number of other polymers the molecules of which can be expected to be flexible and uniform. Rubber, for example, has been reported to behave in the same general fashion as polystyrene, although on the basis of less definite evidence (1). Table I shows how the specific viscosity of polyisobutylene depends upon the character of the solvent.

TABLE I (Ref. 5)

Variation of Viscosity of Polyisobutylene Solutions with Solvent Power

Solvent	η_{sp}/c	Alcohol number
Isoamyl butyrate	0.057	0.0
Isoamyl caproate	0.150	1.8
Benzene	0.221	14.6
Toluene	0.429	20.3
Xylene	0.678	21.7
n-Propylbenzene	0.690	21.7
Mesitylene	0.690	21.8
Cymene	0.714	21.9
Amylbenzene	0.784	22.0
n-Hexane	0.530	22.9
n-Heptane	0.855	26.4
n-Octane	0.923	26.5
Varsol No. 2	1.018	31.8

The alcohol numbers, as listed in Table I, are expressed in numbers of cc. of 2-ethylbutyl alcohol required to produce 400% relative turbidity in 25 cc. of polymer solution.

It is true that the data on polyisobutylene reported above is insufficient to justify all of the conclusions which have been drawn in the case of polystyrene, but it is probably a "fair guess" that polyisobutylene will exhibit a low intrinsic viscosity and a high k' value in a poor solvent. Further experiments on this point would be very interesting. Furthermore, the very wide range of intrinsic viscosities exhibited by polyisobutylene would make it a favorable polymer to use in rigorously testing the hypothesis that the precipitation point in all solvent-non-solvent

systems corresponds to a fairly definite intrinsic viscosity value. It is, of course, impossible to decide whether this hypothesis will hold at all well for polyisobutylene or not.

Experiments by Janssen and Caldwell (13) on polyvinyl chloride dissolved in cyclohexanone and methyl ethyl ketone indicate that in these two solvents, at least, polyvinyl chloride roughly follows the behavior characteristic of polystyrene. Methyl ethyl ketone is known to be a poorer solvent for polyvinyl chloride than cyclohexanone. It was observed that the intrinsic viscosity of polyvinyl chloride was lower in methyl ethyl ketone than in cyclohexanone but that the specific viscosity increased more rapidly with concentration in the case of methyl ethyl ketone. In fact, in this case an actual cross-over was observed; at high concentrations polyvinyl chloride solutions in methyl ethyl ketone showed a higher specific viscosity than solutions of the same concentration in cyclohexanone. This was closely correlated with the fact that actual *gelation* occurs at a lower concentration in methyl ethyl ketone than in cyclohexanone; the rapid increase in specific viscosity at high concentrations in the poor solvent presumably reflects the beginnings of intermolecular association which at somewhat higher concentrations result in gel formation. On the other hand, experiments by Frith (8, 9) indicate that this simple behavior of polyvinyl chloride does not occur in all solvents and there is other evidence to show that intermolecular association in polyvinyl chloride solutions is a very complicated phenomenon.

Polymers Exhibiting "Anomalous" Viscosity Behavior in Dilute Solution

The behavior of polystyrene, which we believe to be characteristic of all flexible, chemically uniform high polymers, is by no means universal. It is, perhaps, unfair to characterize any deviations from this behavior as "anomalous," since this implies that polystyrene and similar polymers represent a unique starting point or "normal" behavior. However, for the purpose of convenience, this definition will be made in this paper.

In some cases, the molecular structures of polymers involved provide fairly reasonable explanations of the reasons for their not exhibiting the behavior which we have chosen to consider "normal." Examples are polymers whose molecules are rigid, or which possess different kinds of chemical groups distributed along the chain, or which possess ionizable groups. In other cases, however, either our knowledge of the molecular structures involved or our ability to predict the effect of these structures is so incomplete that no truly satisfactory explanation of the viscosity data can be made.

Let us consider the effect which arises from chain rigidity alone. If the individual polymer molecules are rigidly extended due to internal restriction of free rotation, then change of the solvent environment cannot be expected to cause marked changes in the molecular configuration. In such a case the intrinsic viscosity would not be expected to vary markedly from good to poor solvents. Small variations might, of course, result from changes in the degree of solvation. On the other hand, change in solvent type would, even in the case of a rigid molecule, result in changes in the amount of intermolecular agglomeration and thus affect the *slope* of the η_{sp}/c *vs.* c curve—*i.e.*, the k' value. Both Spurlin and Frith, who have worked with cellulose derivatives, among other polymers, have expressed the opinion that for such polymers the slope of the η_{sp}/c *vs.* c curve provides a better indication of the solvent power of the solvent than does the intrinsic viscosity. There is, however, some difference of opinion as to whether the good solvents correspond to the highest or to the lowest slopes. Spurlin concludes that, in the systems which he studied, the steepest slope represents the poorest solvent. On the other hand, Frith concludes that, in the systems she studied, the steepest slope represents the best solvent. If the only factor involved were the one of rigidity, the logic which we have used up to the present point would tend to favor the point of view of Spurlin, since we would expect association to be greater in the poor solvent, and we would also expect association to increase the specific viscosity. However, many of the systems concerned differ from polystyrene in chemical uniformity as well as in flexibility and results on polyvinyl chloride indicate that intermolecular association does not necessarily result in increases in specific viscosities in a nonuniform polymer. This point will be dealt with at greater length a little later.

Returning to the importance of the slope of the specific viscosity-concentration curve, we quote Spurlin, Martin, and Tennent (14):

> Fig. 6 shows the magnitude of association effects on solution viscosity in the case of high-viscosity ethylcellulose. The viscosity of a 1% solution in the poor solvent benzene is more than 300% higher than that of a similar solution in the good solvents (benzene-alcohol mixtures and technical methyl acetate). Fig. 7 is a similar graph for medium- and low-viscosity ethylcellulose. The logarithm of specific viscosity divided by concentration was plotted against concentration in this work because the relationship is linear up to concentrations of about 5% if precautions are taken to avoid orientation effects during the viscosity measurement. The slope of these lines divided by the intercept is a well-characterized property of the polymer-plasticizer system, and it is a measure of solvent power, the steepest slope representing the poorest solvent.
>
> A proof of the last statement is illustrated by the inverse relation between the slopes of the curves just described and the slopes of the reduced osmotic pressure-concentration curves given in Fig. 8 for the same systems. Dobry (3) and others have shown that good solvents give a steep osmotic pressure curve, whereas a horizontal line corresponds to a borderline solvent. It follows from Fig. 8 that methyl acetate is a good solvent for

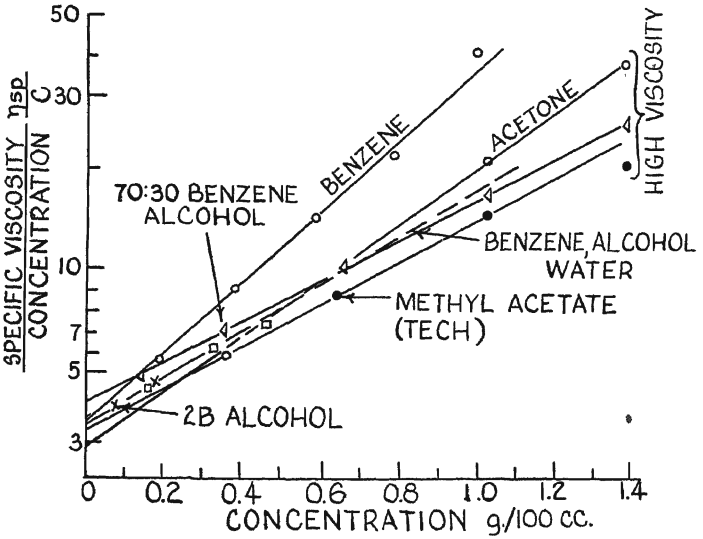

FIG. 6

Effect of Solvent on Slope and Intercept of Viscosity-Concentration Curves of High-Viscosity Ethylcellulose. (Ref. 14)

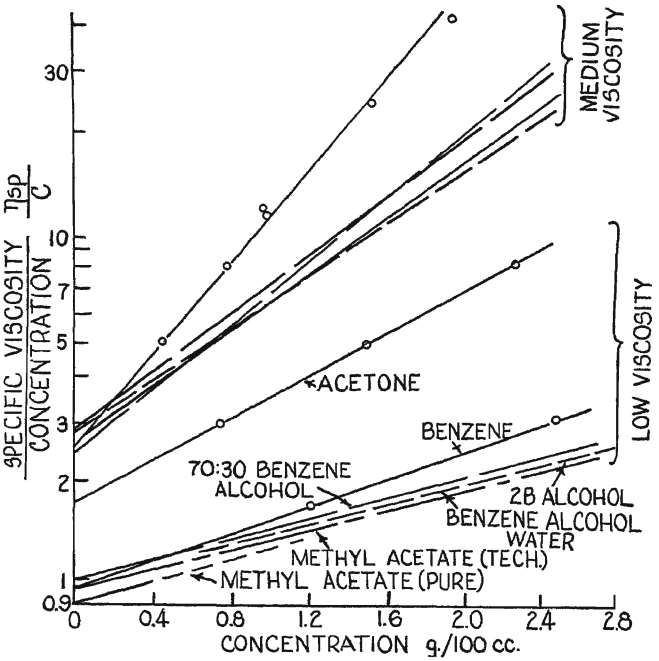

FIG. 7

Effect of Solvent on Slope and Intercept of Viscosity-Concentration Curves of Medium- and Low-Viscosity Ethylcellulose. (Ref. 14)

ethylcellulose, and benzene is a poor one. The particular sample of ethylcellulose which gave a horizontal curve in benzene was more insoluble than that represented in the viscosity curves in Fig. 7. In fact, it precipitated on dilution of a concentrated solution. The viscosity-concentration curve for this sample was very steep, but extrapolation showed that the relation between the intrinsic viscosities in benzene and methyl acetate was the same as in the case of the more soluble ethylcellulose. Thus, the slope of the reduced viscosity-concentration curve is a useful measure of the solvent power even in those cases in which the miscibility range is limited.

The variation of intrinsic viscosity with solvent power may also give information of interest in plasticizer-polymer systems. In Fig. 7, the curves for medium-viscosity ethylcellulose all intersect the vertical axis at nearly the same point, as do the curves for the low-viscosity polymer, with the exception of the one for the acetone solution. The conclusion is that the intrinsic viscosities of these systems do not vary much with solvent power. On the other hand, Table I shows that there is a regular decrease in the intrinsic viscosity of polyisobutylene as the solvent power decreases. This behavior has been

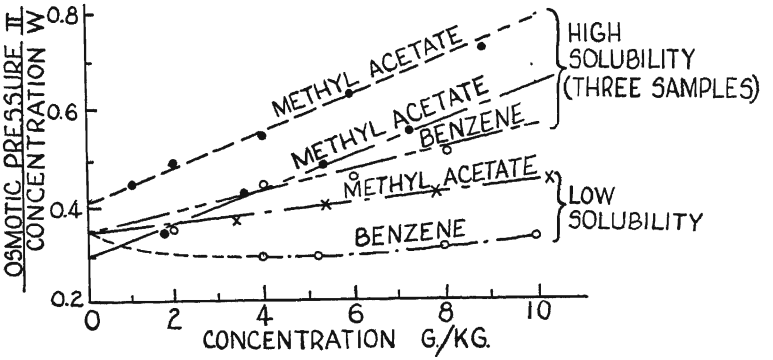

FIG. 8

Effect of Solvent on Slope of Ethylcellulose Osmotic Pressure-Concentration Curves. (Ref. 14)

ascribed to changes in the extent to which these very flexible molecules are coiled in the various solvents. Coiling to a compact shape is favored in poor solvents because forces between segments of polyisobutylene molecules do not have to compete with the strong polymer-solvent forces characteristic of good solvents. The intrinsic viscosity varies by a factor of 16 in contrast to that of ethylcellulose, which varies by a factor of 2. This indicates that cellulose derivatives do not change much in the extent to which they are coiled in solution when the solvent power of the solvent is changed.

Another reason for the fact that the absolute value of intrinsic viscosity is not a satisfactory measure of solvent power is that, if the law $[\eta] = KM^a$ is followed, $[\eta]$ will be proportionately higher with poor solvents as the molecular weight is lowered. This is seen to be the case with acetone in Figs. 6 and 7.

The influence of polymer-polymer association and similar deviations from non-ideal behavior upon the bulk properties of polymer-plasticizer systems becomes very much more marked as the concentration of polymer increases. While dilute solution measurements can give much information about these deviations, use of this information to predict concentrated solution properties is not yet feasible. Measurements covering the entire concentration and temperature ranges will be necessary to establish, for example,

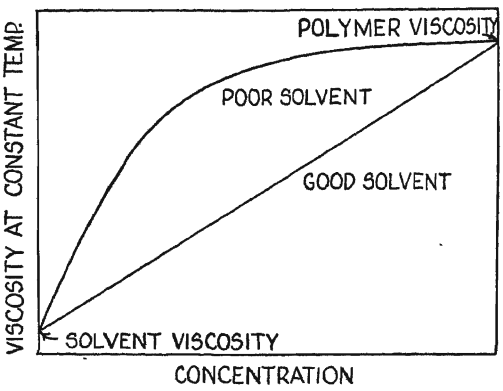

FIG. 9

Complete Viscosity-Concentration Curve for Polymer Solutions. (Ref. 14)

the effects of these variables upon viscosity. Some conclusions of value can be drawn from information now available, however. The viscosity of a system must vary continuously with concentration from that of the solvent to that of the pure polymer, and it is unlikely that the effects of complex formation will be pronounced enough to cause maxima or minima to occur in intermediate concentration regions (Fig. 9). Therefore, that system in which the initial portion of the viscosity-concentration curve is steepest (poor solvent) will have a curve with the lowest slope at high concentrations. In proof of this deduction, Fig. 10 shows sections of the viscosity-concentration curves for cellu-

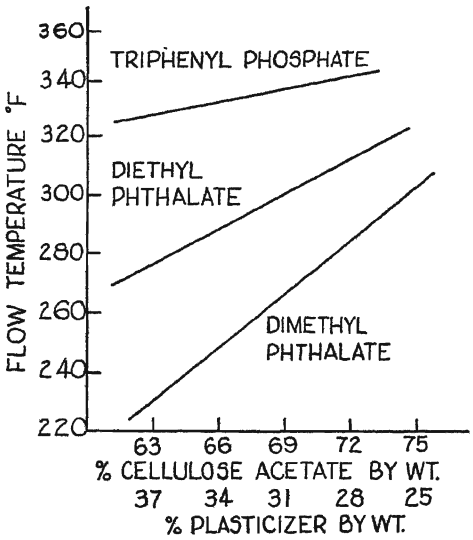

FIG. 10

Effect of Plasticizer on Cellulose Acetate Flow Temperature *vs.* Concentration Curves. (Ref. 14)

lose acetate-plasticizer formulations at normal plastic concentrations. (The assumption has been made that the logarithm of the flow temperature varies inversely with the viscosity. The flow temperature was measured according to ASTM D569–43.) It can be seen that the poorest solvent (triphenyl phosphate) has the flattest curve while the best solvent (dimethyl phthalate) has the steepest one.

Fig. 11, taken from the work of Frith (8) shows specific viscosity curves for cellulose acetate in 50% mixtures of acetone with three different plasticizers. It was reported that dimethyl phthalate and triacetin, which exhibit the high slopes, were both more compatible with cellulose acetate than diethyl phthalate which shows the low slope. Another very

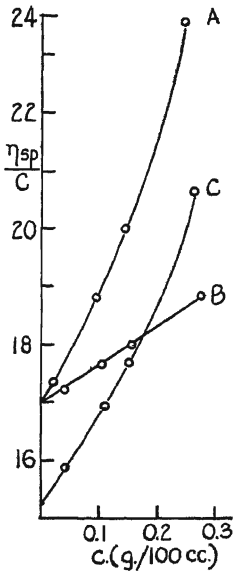

FIG. 11

Viscosities of Dilute Solutions of Cellulose Acetate in 50% Mixtures of Acetone and Plasticizer, 25°C. (Ref. 8).

A. Dimethyl phthalate; B. Diethyl phthalate; C. Triacetin.

interesting set of curves are shown in Fig. 12 corresponding to solutions of polyvinyl chloride in 50% mixtures of cyclohexanone with a series of alkyl phthalates. The intrinsic viscosities observed in all cases were within experimental error identical but the slopes varied over a wide range. Again, the highest slope was reported to correspond to the best solvent and *vice versa*. The structure of polyvinyl chloride would hardly allow us to attribute this behavior to stiffness of the chain but must have its origin in some other factor. (It is interesting to compare these results with the observations of Doty and others concerning the intrinsic viscosities of associated polyvinyl chloride solutions.) Frith also reported similar re-

sults in the case of polyvinyl acetate solutions in a number of mixed solvents.

To conclude this very incomplete survey of "anomalous" viscosity behavior, let us consider the results reported by Doty, Wagner, and Singer (4) on polyvinyl chloride. These authors studied the association of polyvinyl chloride in poor solvents. Their results can be summarized as follows:

In a poor solvent (*e.g.*, dioxane) polyvinyl chloride molecules associate to form clusters. These clusters are numerous enough and large enough to increase the weight average molecular weight by as much as eight-

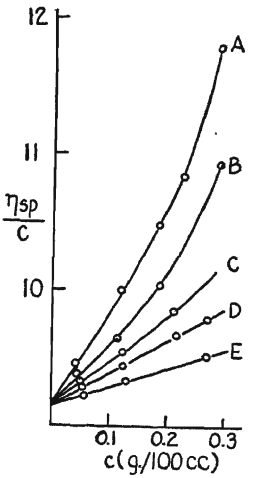

FIG. 12

Viscosities of Dilute Solutions of Polyvinyl Chloride in 50% Mixtures of Cyclohexanone and Alkyl Phthalates, 25°C. (Ref. 8).

A. Dibutyl phthalate; B. Dihexyl phthalate; C. Dioctyl phthalate; D. Diethyl phthalate; E. Dimethyl phthalate.

fold. This association was studied by means of osmotic pressure, light scattering, ultracentrifuge, and viscosity measurements. The interesting fact for our purposes is that this association has very *little* effect on the specific viscosity of the solution. The authors interpret this as meaning that the clusters are much more dense than the individual polymer molecules.

The view is taken that the fact that the specific viscosity is essentially unchanged when the amount of association is altered is coincidental and not particularly significant. The important feature is that observed viscosity is very considerably less than would have been predicted if the configuration of the molecules in the cluster was nearly identical with the configuration of the individual molecule except for the effect of molecular weight. For example, if the association were of the end to end type, then the viscosity

would surely have been decreased several-fold when the associated molecules were broken up. Here in the viscosity measurements there is evidence that the cluster must be of about the same size as the individual molecules for it is the largest average dimension more than any other factor which determines the specific viscosity. Consequently, it appears that the molecules are so highly coiled and packed in the cluster that the viscosity is greatly reduced and by coincidence is nearly equal to that of the unassociated molecules at the same weight concentration. . . . Investigation of the forces holding the molecules together in the cluster has not been carried out. However, . . . certain explanations of the phenomenon can be eliminated and a self-consistent description can be postulated.

It is possible to decide at once whether or not the association observed is the result of a dynamic equilibrium between individual molecules and clusters. In other words, is it possible to explain the observed behavior by assuming that there is a dynamic equilibrium between individual molecules and a cluster composed of a number of molecules? Such an explanation is fundamentally incompatible with two observations. First, it was noted both with osmotic pressure and turbidity that the equilibrium value of either of these quantities was obtained at once upon heating but, upon cooling, a very long time was required for the return of either of these properties to its equilibrium value at the lower temperature. This microscopic irreversibility cannot result from a dynamic equilibrium where individual molecules would be associating and clusters would be breaking up at a reasonably fast rate.

The second objection to the dynamic equilibrium hypothesis is found in the straight lines obtained in the osmotic pressure plots at any temperature measurement, for, if this association resulted from a dynamic equilibrium, the equilibrium constant, being defined in terms of the concentrations, would demand that the apparent molecular weight would vary enormously with the concentration. This would lead to strongly curved lines of π/c *vs.* c.

The alternative explanation requires that the equilibrium be of the static type and that the temperature dependence of the amount of association results from the presence of secondary bonds of many different strengths. In other words, if the points of binding in the cluster are of different strength then upon heating the dioxane solution to say 45°, about the weakest 15% of the secondary bonds would be broken and a certain number of individual molecules set feee. Upon heating to a higher temperature, the weakest fraction of the secondary bonds remaining would be broken and more individual molecules would result. When the solution is cooled the individual molecules would return to clusters only when the portions of the molecule in which the seocndary binding could arise diffuse together. Such a diffusion-controlled reaction would, of course, be very slow. The spectrum of secondary bond strengths required in this description may perhaps arise from a cooperative phenomenon in which regions of varying length of the polymer chains could fit together in such a sterically favorable pattern as to enhance greatly the dipole-dipole interaction or hydrogen bonding. The strength of such an attachment would depend upon the length of the chains participating at the region of binding. It thus appears that qualitatively the observations on polyvinyl chloride solutions can be explained if the association originates in secondary bonds in varying degrees of strength.

From the sedimentation diagrams it would appear that a significant critical number of molecules are necessary to form a cluster because there is always a large gap between the two peaks indicating the absence of clusters of intermediate size. There is some basis for further speculation, but in view of the complexity of the phenomenon it would scarcely serve a useful purpose.

In view of these observations it is clear that the specific viscosity of such a polymer solution (in which the intermolecular forces vary in

magnitude from point to point along the chain) is a very involved problem, and that extreme caution should be used in drawing conclusions as to the molecular mechanisms involved unless the phenomenon is studied with a number of distinct experimental techniques.

References

1. Alfrey, Bartovics, and Mark, *J. Am. Chem. Soc.* **64**, 1557 (1942).
2. Alfrey, Justice, and Nelson, *Trans. Faraday Soc.* (in press).
3. Dobry, *J. chim. phys.* **36**, 102 (1939).
4. Doty, Wagner, and Singer, *J. Polymer Science* (in press).
5. Evans and Young, *Ind. Eng. Chem.* **34**, 461 (1942).
6. Ewart, *Recent Adv. Colloid Sci.* **2**, 197 (1946).
7. Flory, *J. Chem. Physics* **10**, 51 (1941).
8. Frith, *Trans. Faraday Soc.* **41**, 90 (1945).
9. Frith, *Trans. Faraday Soc.* **41**, 17 (1945).
10. Gee, British Rubber Producers Research Association, Publ. No. **10**; *India Rubber J.* **108**, 349 (1935); *Trans. Faraday Soc.* **40**, 463 (1944); *ibid.* **40**, 480 (1944).
11. Huggins, M. L., in Cellulose and Cellulose Derivatives, E. Ott, Editor, pp. 893–909, especially pp. 902 *et seq.* Interscience Pub., Inc., N. Y., 1943.
12. Huggins, *J. Phys. Chem.* **46**, 151 (1942).
13. Janssen and Caldwell, *Polymer Bull.* **1**, 120 (1945).
14. Spurlin, Martin, and Tennent, *J. Polymer Science* **1**, 63 (1946).

RHEOLOGICAL PROPERTIES OF POLYMERS AND PLASTICS*

W. O. Baker

From the Bell Telephone Laboratories, New York, N. Y.
Received December 5, 1946

During the years of Professor E. C. Bingham's high activity, probably the most extensive rheological studies, in countless laboratories, were on high polymers. This does not mean that, for example, more measurements were not made on lubricating oils or low polymeric paints. Rather, it is significant that a particularly wide range of variables, such as shearing stress, rate of shear, temperature, and the time dependences of observations, was found to affect strikingly the flow of polymers. Often there was evidence of complex behavior. The apparently unique quality of long chain molecules allowing gross (several hundred *per cent*) strain of a sample by *high elasticity* rather than *fluidity* has principally contributed this intricacy to polymer rheology.

Therefore, it was natural that the phenomenology first drew attention. The early suggestion of Maxwell has been widely modified and applied to polymers. Here

$$\Im = \gamma G e^{-t/\tau}; \eta = G\tau,$$

where $\Im$ = shearing stress, γ = strain, G = modulus of rigidity, t = time, τ = relaxation time. A more general expression includes a (perhaps quite artificial) series of terms $\Sigma_i e^{-t/\tau_i}$ in which a distribution of relaxation times occurs. This general attack has at least aided statement of the problem of specifying the reaction of a chain polymer to external stress.

More recently, the detailed mechanism of polymer deformation has been probed. Stimulation has come especially from Eyring and coworkers. By happy coincidence, it has also lately become possible to prepare polymers of known structure and average molecular weight. Likewise, new techniques for studying very small displacements, such as the oscillations of a dipole in an alternating electric field, the vibrations of small domains in a compressional, ultrasonic field, and very recently, in a field of ultrasonic *shear* waves, have come in. From these techniques, knowledge of the viscous contributions from specific chemical groups, such as C-Cl in polyvinyl chloride or the ester linkage in polyesters, is

* Because the title assigned involved primarily a review discussion, the author did not feel that space in print taken by more than an abstract was justified.

gained. In complementary fashion, molecular weights tell how the macromolecule as a whole influences viscosity, through such relations as Flory's, wherein $\eta = N \exp (aZ_w^{\frac{1}{2}})$, where η = viscosity of polymer at given temperature, a and N are characteristic constants, and Z_w is the weight average chain length of given polymer. The viscosity of long chains in *dilute solution* is also being interpreted in terms of chain configuration.

Hence, it is encouraging, in thinking of Professor Bingham's many contributions to "anomalous" viscosity, that the rheology of high polymers, the special realm of anomalies, is gradually being tied to their *molecular* traits.

CONCENTRATED SOLUTION VISCOSITY OF POLYSTYRENE

R. S. Spencer and J. L. Williams

From The Dow Chemical Company, Midland, Michigan

Received Nov. 27, 1946

Introduction

Solutions of high polymers exhibit a wide range of properties. Quite dilute solutions are very similar in their behavior to simple liquids; very highly concentrated solutions differ only slightly from the pure polymer in their properties. As the polymer concentration is increased from the dilute region the viscosity increases and the solution becomes non-Newtonian in its flow behavior. At still higher concentrations the polymer chains become intertangled to form a more or less netlike structure throughout the solution, giving it some of the properties of the solid polymer. The solution exhibits rubberlike elasticity and elastic memory and is quite rigid under rapid periodic stresses.

If attention is confined to a single polymer-solvent system the major factors determining viscosity, other than concentration, are temperature and polymer molecular weight. The individual effects of these three variables have been discussed at considerable length, both experimentally and theoretically. The effect of temperature has been found to be similar for both concentrated and dilute solutions, the viscosity being exponentially dependent on the reciprocal of absolute temperature, with an activation energy of anywhere from a few kcal. to 20–30 kcal. In dilute solutions the dependence of viscosity on molecular weight is perhaps best expressed by the power law relationship between intrinsic viscosity and molecular weight due to Mark (1). Many formulae have been proposed for the influence of concentration upon dilute solution viscosity, recent surveys of the more important ones having been made by Huggins (2) and Pfeiffer and Osborn (3). For concentrated solutions, Flory has developed relationships showing how viscosity is dependent upon molecular weight (4) and concentration (5).

In this paper we are concerned only with concentrated solutions of polystyrene and the dependence of their viscosities upon the variables mentioned above. In addition to applying the relationships above mentioned we have also studied the concurrent effect of all three variables and set forth an empirical formula representing this behavior. Some space is also devoted to a consideration of the activation energy of viscous flow of pure polystyrene and a comparison of values reported in the

literature with those obtained by extrapolation from the concentrated solution region.

Concentration Dependence of Viscosity

Numerous equations have been proposed to represent the concentration dependence of viscosity, each having its own range of applicability. Most of these relationships are equivalent in the very dilute region, as has been shown by Huggins (6), differences appearing as the concentration is increased. That due to Martin (7) has found wide use as being the most generally applicable in both the dilute and more concentrated regions, good fits being obtained up to 5% polymer in many cases. The systems studied by Martin included polystyrene in various solvents, and

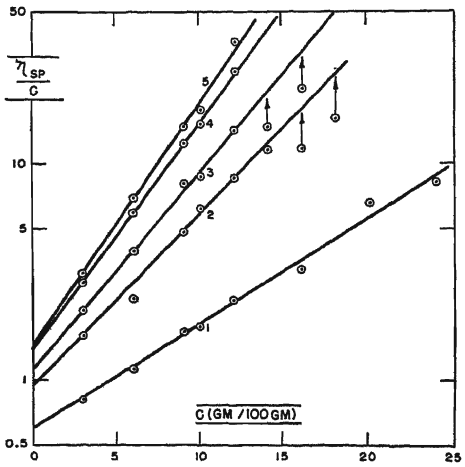

Fig. 1

Viscosities of Solutions of Polystyrene in Toluene at 25°C. (Martin's Equation)

it was thought to be of interest to extend his study to include higher concentrations and a range of molecular weights.

For this purpose a series of five commercial-type polystyrenes were chosen to give a representative range of molecular weights. Viscosities of solutions of varying concentration in toluene were determined at 25°C. with an Ostwald viscosimeter. The resulting data are plotted in Fig. 1 as the logarithm of the reduced viscosity against the concentration in g. of polymer/100 g. of solution. It is seen that a resonably good fit is obtained up to 12% polymer, and probably up to in the neighborhood of 20% polymer. Table I lists the intrinsic viscosities and k' values taken from the curves of Fig. 1, together with viscosities at 10% polymer for comparison. Good agreement was found between the k' values for the

TABLE I

Application of Martin's Equation to Polystyrene in Toluene

10% Viscosity *centipoises*	$[\eta]$	k'
15	0.585	0.190
35	0.935	0.1935
50	1.10	0.195
85	1.37	0.178
100	1.45	0.177

three lower molecular weight materials, with the two higher molecular weight materials giving a somewhat lower value. These may be compared with a value $k' = 0.235$ reported by Martin. Certain of the data of Bredee and de Booys (8) on the viscosities of benzene and tetralin solutions of polystyrene also fit Martin's equation up to 15% polymer.

Martin's equation, together with a suitable k' value, may be used to calculate intrinsic viscosities from 10% solution viscosities. The viscosity of a 10% solution of polystyrene in toluene at 25°C. is listed as part of the ASTM specifications for polystyrene molding compounds (D703–43T) and has been used in the industry as a rough measure of the polymer molecular weight. It would perhaps be preferable, however, to use the intrinsic viscosity as an index of molecular weight, as it varies more

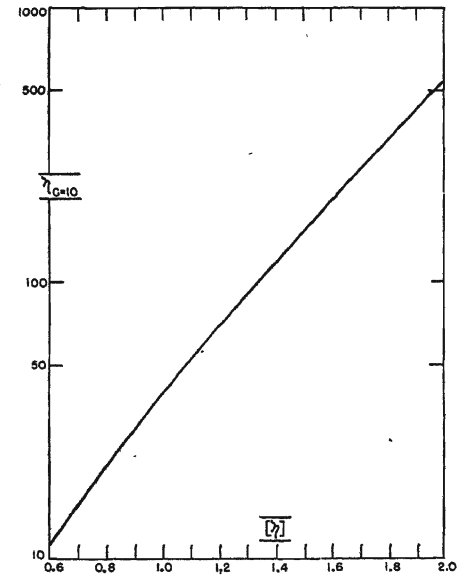

FIG. 2

Relationship Between 10% Viscosity and Intrinsic Viscosity of Polystyrene in Toluene at 25°C. (From Martin's Equation with $k' = 0.193$)

nearly linearly with molecular weight than does the 10% solution viscosity, which is more nearly exponential with molecular weight. At the same time, 10% solution viscosity is rather well established in practice and is a fairly convenient quantity to obtain. With these ideas in mind we have prepared Fig. 2, which shows the relationship between 10% solution viscosity and intrinsic viscosity, as calculated from Martin's equation with $k' = 0.193$.

At concentrations beyond the range of applicability of Martin's equation it is still possible to adequately represent the data. Flory (5)

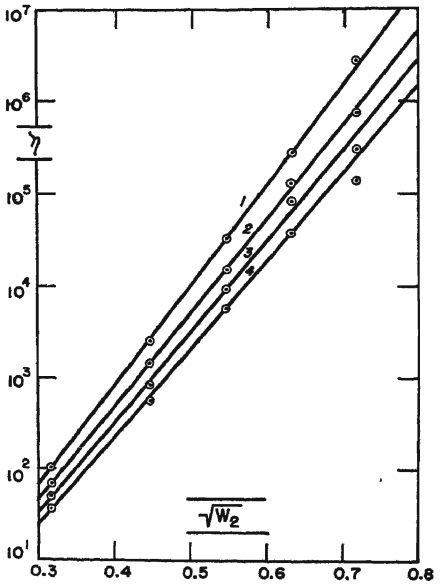

FIG. 3

Concentration Dependence of the Viscosity of Solutions of Polystyrene in Isopropyl Benzene. (Molecular Weight = 101,000) (1) 25°C.; (2) 50°C.; (3) 75°C.; (4) 100°C.

has shown that a polymer solution can be considered as a homogeneous polymer of lowered average molecular weight, and by applying his relationship for the influence of molecular weight on viscosity (4) arrived at the fact that the logarithm of the viscosity should be a linear function of the square-root of the weight fraction of polymer. In Fig. 3 the viscosities of solutions of polystyrene in isopropyl benzene at different temperatures are plotted against concentrations in this fashion, and it is seen that Flory's relationship gives a fairly good representation of the data.

Concurrent Effect of Concentration, Molecular Weight and Temperature

The individual effects on viscosity of concentration, molecular weight and temperature are well known. Many workers have observed that the viscosity of a molten polymer depends exponentially on the reciprocal of the absolute temperature, and Kauzmann and Eyring (9) have shown this to be the limiting case, for vanishing shearing force, of the more general theoretical expression. Flory found the viscosity to depend exponentially on the square-root of polymer molecular weight (4) and exponentially on the square-root of the weight fraction of polymer (5). All of these relationships have been confirmed experimentally by holding all conditions constant except the variable being considered. It remains to inquire into the dependence of viscosity upon these three parameters when all are varying simultaneously.

To this end three commercial polystyrenes of different molecular weights were selected, solutions of each in isopropyl benzene made up, of

TABLE II

Viscosities of Isopropyl Benzene Solutions of Polystyrene

W_2	25°C.	50°C.	75°C.	100°C.
	centipoises	*centipoises*	*centipoises*	*centipoises*
0.1	67.6	45.3	31.9	22.9
0.2	1,093.	547.8	415.5	299.4
0.3	15,300.	7,450.	4,370.	2,730.
0.4	156,100.	61,300.	29,500.	17,060.
0.5	1,293,000.	357,600.	142,900.	66,500.
		(M = 101,000)		
0.1	104.5	69.8	49.4	35.9
0.2	2,524.	1,447.	827.2	566.4
0.3	32,940.	16,170.	9,370.	5,830.
0.4	287,500.	134,700.	84,100.	38,200.
0.5	2,789,000.	755,700.	306,100.	151,300.
		(M = 113,500)		
0.1	167.0	108.7	73.2	52.3
0.2	4,138.	2,363.	1,503.	984.7
0.3	61,300.	31,660.	18,100.	11,220.
0.4	774,800.	300,500.	145,700.	79,800.
0.5	5,767,000.	1,569,000.	633,200.	313,500.
Isopropyl Benzene	0.747	0.554	0.434	0.351

concentration 10, 20, 30, 40 and 50% by weight of polymer, and viscosities determined at 25, 50, 75 and 100°C. with a falling-ball viscosimeter. These data are listed in Table II in the form of absolute viscosities in centipoises. The influence of the individual variables is indicated in Figs. 3, 4 and 5. In Fig. 3 the molecular weight is held constant and the effect of concentration shown at the four temperatures mentioned above. Fig. 4 presents the influence of temperature, molecular weight again being

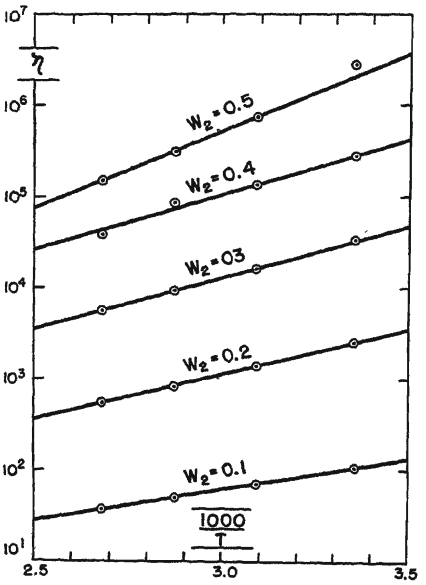

FIG. 4

Temperature Dependence of the Viscosity of Solutions of Polystyrene in Isopropyl Benzene. (Molecular Weight = 101,000.)

constant, at the five concentrations used. The temperature was held constant in Fig. 5 and the dependence of viscosity on molecular weight shown at the different concentrations. This was done for all of the data obtained and the numerical coefficients appropriate to each plot computed. The variation of these numerical coefficients with the other two variables was then studied, and the following relationship finally obtained as expressing the concurrent effect of concentration, molecular weight and temperature:

$$\eta = 3.63 \times 10^{-10} \exp. \left\{ .0572\sqrt{M} + \sqrt{W_2}\left(22.54 - .045\sqrt{M} + \frac{5000}{T} \right) \right\},$$

where η is viscosity in centipoises, M is the Staudinger molecular weight, W_2 is the weight fraction of polymer, and T is the absolute temperature.

It should be emphasized that this relationship is an approximate one giving only a fair representation of all the data obtained, since not all of the dependencies found could be expressed exactly by simple functions. However, it may be considered as at least a first approximation giving an indication of the general behavior of the system. It must also be remembered that this analysis was carried out only for the system isopropyl benzene-polystyrene and that other systems would certainly re-

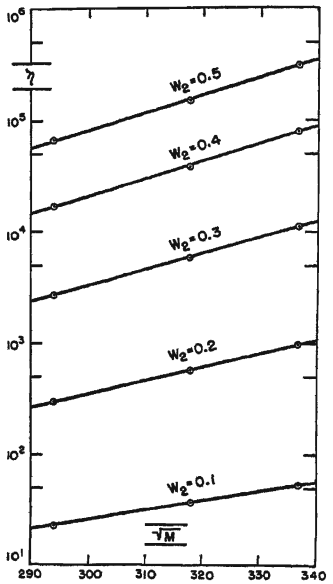

FIG. 5

Molecular Weight Dependence of the Viscosity of Solutions of Polystyrene in Isopropyl Benzene. (Temperature = 100°C.)

sult in different numerical coefficients and very possibly even in different types of relationship. As an indication of this, Fig. 6 shows what happens to the viscosity-concentration relationship as the solvent is changed gradually from isopropyl benzene to methyl ethyl ketone. The Flory equation is apparently still fairly well obeyed and these data merely illustrate the well known fact that the viscosity of a solution is quite dependent on the choice of solvent.

The equation given above brings out the fact that the effects of temperature and molecular weight upon viscosity are independent of each other but do depend upon the concentration, at least within the ranges of variables studied. This behavior seems quite reasonable when one considers that variations in both temperature and molecular weight do not change the system in any very fundamental way. The magnitude of the intermolecu-

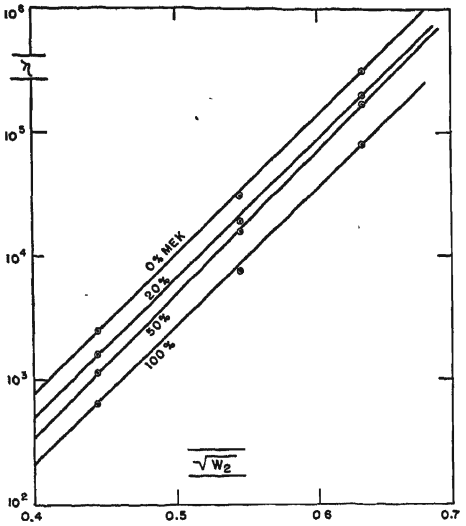

FIG. 6

Concentration Dependence of the Viscosity of Solutions of Polystyrene in Mixtures of Isopropyl Benzene and Methyl Ethyl Ketone at 25°C. (Viscosity in Centipoises. Molecular Weight = 101,000).

lar forces is altered but the system is still very nearly the same chemically. A change in concentration, on the other hand, is really a change to a different system, in spite of the success of the relationship derived by Flory (5) on the assumption that a change in concentration is equivalent to a change in average molecular weight.

The influence of concentration upon the temperature coefficient has been observed for properties of polymers other than viscosity. The data of Davies, Miller and Busse (10), discussed by Kauzmann (11), show that the activation energy of dielectric relaxation of polyvinyl chloride decreases as tricresyl phosphate is added, as shown in Table III. The

TABLE III

Activation Energy of Dielectric Relaxation of Polyvinyl Chloride Plus Tricresyl Phosphate (Davies, Miller and Busse)

W_2	E kcal.	$E/\sqrt{W_2}$ kcal.
1.0	116	116.0
0.9	88	92.7
0.8	74	82.8
0.7	66	78.9
0.6	57	72.3
0.5	59	82.3
0.4	49	77.5

data of Alexandrov and Lazurkin (12), discussed by Eley (13) and Simha (14), show a similar behavior of the activation energy of the elastic orientation of plasticized polymethyl methacrylate, as set forth in Table IV.

One further point of interest appears from the data of Tables III and IV. If the activation energies were to depend upon the concentration in the same manner as given by our relationship for isopropyl benzene-polystyrene, the quantity $E/\sqrt{W_2}$ should be a constant, and this is not the case. Instead $E/\sqrt{W_2}$ decreases with increasing solvent, becoming constant only after an appreciable amount of solvent or plasticizer is added. We should like to suggest that this region of decreasing $E/\sqrt{W_2}$ represents a region of incomplete solvation of the polymer and that the subsequent constancy of $E/\sqrt{W_2}$ is indicative of a mixture of more or less mobile solvent and solvated polymer. Thus the variation of activation

TABLE IV

Activation Energy of Elastic Orientation of Polymethyl Methacrylate Plus Plasticizer (Alexandrov and Lazurkin)

W_2	E *kcal.*	$E/\sqrt{W_2}$ *kcal.*
1.0	75	75
0.9	59	61.9
0.7	52	62.1

energy with concentration may serve to determine the point of complete solvation of the polymer and yield valuable information on the interaction between polymers and plasticizers. If this viewpoint were correct, one would not expect the Flory relationship between viscosity and polymer weight fraction to hold in the region of incomplete solvation, and this point is being investigated in more detail.

Activation Energy of Viscous Flow of Polystyrene

The temperature dependence of the viscosity of polystyrene is of considerable practical interest in connection with certain types of fabrication. The meager data available in the literature on this point are not in complete agreement and it therefore seemed pertinent to consider the possibility of extrapolating such data on concentrated solutions as appear in this paper to 100% polymer. Such extrapolated values may then be compared with those reported for pure polystyrene.

Ferry (15) has studied the viscosity of solutions of polystyrene in xylene over approximately the same range of concentration as was covered in this work. He found the typical variation of activation energy with concentration, as shown in Table V. Ferry observed that, except for the highest concentration, the activation energy was approximately linear

TABLE V

Activation Energy of Viscous Flow of Polystyrene in Xylene (Ferry)

W_2	E	$E/\sqrt{W_2}$	$(E-2.1)/W_2+2.1$
	kcal.	*kcal.*	*kcal.*
0.154	3.8	9.65	13.14
0.210	4.6	10.00	14.00
0.257	4.6	9.04	11.83
0.318	5.3	9.38	12.15
0.523	10.7	(14.8)	(18.53)
	Average	9.52	12.78

with weight fraction and obtained in this manner an extrapolated value of 12 kcal. This corresponds to the fourth column of Table V, resulting in an average value for the activation energy of 12.78 kcal., neglecting the highest concentration. In column three we have listed $E/\sqrt{W_2}$, as suggested by our work, which gives an average value of 9.52 kcal. At this point little can be said as to the relative merits of these two procedures.

Table VI presents our data on polystyrene-isopropyl benzene in the same manner, and Table VII lists some additional observations on the system polystyrene-ethylbenzene. It will be noted that xylene and isopropyl benzene result in activation energies in fair agreement, and that the values extrapolated from the ethylbenzene data are somewhat lower.

It has been generally supposed, on the basis of the few values reported in the literature, that the activation energy of viscous flow of polystyrene was considerably higher than the values found above. For example, Foote (16) states that a temperature variation of 1° at 150°C. produces a change in the apparent viscosity of polystyrene of about 50%, and calculates an activation energy of 40 kcal. from measurements of

TABLE VI

Activation Energy of Viscous Flow of Polystyrene in Isopropyl Benzene

W_2	E	$E/\sqrt{W_2}$	$(E-2.22)/W_2+2.22$
	kcal.	*kcal.*	*kcal.*
0.1	3.1	9.80	11.02
0.2	4.4	9.83	13.12
0.3	4.9	8.94	11.15
0.4	5.72	9.05	10.97
0.5	7.78	11.00	13.34
	Average	9.72	11.92

flow in capillary molds. However, as Foote himself points out, the highly elastic deformation present in his measurements was not corrected for, and this would result in a higher value of the activation energy. The observations of Wiley (17) permit the calculation of an activation energy of 31.6 kcal., which again is considerably higher than our values. In this case also, however, highly elastic deformation is a complicating factor that has not been corrected for, as was pointed out by Tuckett (18).

On the other side of the picture Spencer and Boyer (19) obtained an activation energy of 12 kcal. for the isothermal volume changes associated with the thermal expansion of polystyrene. This process is intimately connected with the viscous behavior of the polymer. The data of Nason

TABLE VII

Activation Energy of Viscous Flow of Polystyrene in Ethylbenzene

W_2	E	$E/\sqrt{W_2}$	$(E-2.1)/W_2+2.1$
	kcal.	*kcal.*	*kcal.*
0.1	2.78	8.80	8.90
0.2	3.24	7.25	7.80
0.3	4.42	8.07	9.83
0.4	5.17	8.18	9.77
	Average	8.08	9.08

(20) are exceedingly interesting in themselves, as showing very clearly the non-Newtonian behavior of polystyrene at high pressure gradients. These data were obtained in a special Bingham-type viscosimeter designed by Nason and are thus well adapted to the calculation of viscosity, if the non-Newtonian behavior is correctly taken into account. One way of doing this is to use the Eyring equation for viscosity (9), written in the form

$$\eta = \frac{\eta_0 kf}{\sinh (kf)},$$

where η_0 is the limiting viscosity at zero shear, f is the shear force per unit of area, and k is a lumped constant dependent upon the temperature but independent of shear force. Using this expression an equation analogous to Poiseuille's was derived and used to evaluate Nason's data. The values of η_0 and k obtained are listed in Table VIII and must be regarded as approximate only, as the flow rates used were estimated from Nason's published curves and not from original data. From the viscosities at zero shear an activation energy of 15.5 kcal. was computed.

Table IX summarizes these values of the activation energy of viscous flow of polystyrene. Pending further investigation, the most that can be said at present is that it has a value in the neighborhood of 12 kcal.

TABLE VIII

Viscous Flow of Polystyrene (Nason)

	175°C.	200°C.	225°C.
64,000 M.W.	$\eta_0 = 1.24 \times 10^5$ poises $k = 1.682 \times 10^{-6}$	3.54×10^4 2.206×10^{-6}	1.81×10^4 2.733×10^{-6}
103,000 M.W.	$\eta_0 =$ —— $k =$ ——	7.9×10^{-4} 1.671×10^{-6}	5.1×10^{-4} 2.167×10^{-6}

Activation Energy = 15.5 kcal.

TABLE IX

Activation Energy of Viscous Flow of Polystyrene

Reference	E
This Paper (Isopropyl Benzene)	9.72 (11.92)
This Paper (Ethylbenzene)	8.08 (9.08)
Ferry (14) (Xylene)	9.52 (12.78)
Spencer and Boyer (18) (Thermal Expansion)	12.0
Nason (19) (Melt Viscosity)	15.5
Wiley (16) (Melt Viscosity)	31.6
Foote (15) (Melt Viscosity)	40.0

Summary

Data have been presented on the viscosity, under various conditions, of solutions of polystyrene in the range from a few *per cent* to 50% by weight of polymer. It was shown that Martin's equation gives a good representation of the effect of concentration up to about 20% polymer, and that Flory's relationships for the individual effects of concentration and molecular weight hold over the entire range covered. A study of the concurrent effects of temperature, molecular weight and concentration on the viscosities of isopropyl benzene solutions of polystyrene showed that both the temperature coefficient and molecular weight coefficient depend on the concentration.

This influence of concentration on activation energy has been noted by other workers for the cases of rubberlike elasticity and dielectric relaxation. It was suggested that a study of activation energy versus concentration may be a method of investigating the interaction of polymers and solvents. Extrapolation to obtain the activation energy of viscous flow of pure polystyrene was discussed, and a comparison made between the values thus obtained and those reported in the literature. It was concluded that this quantity has a value in the neighborhood of 12 kcal.

References

1. Mark, H., Der feste Korper, 103. S. Hirzel, Leipzig, 1938.
2. Huggins, M. L., Cellulose and Its Derivatives, 950. Interscience, New York, 1943.
3. Pfeiffer, G. H., and Osborn, R. H., *ibid.*, p. 962.
4. Flory, P. J., *J. Am. Chem. Soc.* **62**, 1057 (1940).
5. Flory, P. J., *J. Phys. Chem.* **46**, 870 (1942).
6. Huggins, M. L., Cellulose and Its Derivatives, 951. Interscience, New York, 1943.
7. Martin, A. F., Am. Chem. Soc. Meeting, Memphis, April 20–24, (1942).

$$\frac{\eta_{sp}}{c} = [\eta] \exp \{k'[\eta]c\}.$$

8. Bredee, H. L., and de Booys, J., *Kolloid-Z.* **79**, 31 (1937).
9. Kauzmann, W., and Eyring, H., *J. Am. Chem. Soc.* **62**, 3113 (1940).
10. Davies, J. M., Miller, R. F., and Busse, W. F., *J. Am. Chem. Soc.* **63**, 361 (1941).
11. Kauzmann, W., *Rev. Modern Phys.* **14**, 12 (1942).
12. Alexandrov, A. P., and Lazurkin, Y. S., *Acta Physicochim. U. R. S. S.* **12**, 647 (1940).
13. Eley, D. D., *Trans. Faraday Soc.* **38**, 299 (1942).
14. Simha, R., *Ann. N. Y. Acad. Sci.* **44**, 297 (1943).
15. Ferry, J. D., *J. Am. Chem. Soc.* **64**, 1330 (1942).
16. Foote, N. M., *Ind. Eng. Chem.* **36**, 244 (1944).
17. Wiley, F. E., *Ind. Eng. Chem.* **33**, 1377 (1941).
18. Tuckett, R. F., *Trans. Faraday Soc.* **39**, 158 (1943).
19. Spencer, R. S., and Boyer, R. F., *J. Applied Phys.* **17**, 398 (1946).
20. Nason, H. K., *J. Applied Phys.* **16**, 338 (1945).

VISCOELASTIC PROPERTIES OF THERMOPLASTICS AT ELEVATED TEMPERATURES *

G. J. Dienes

From the Development Laboratory, Bakelite Corporation, Bound Brook, N. J.

Received Nov. 25, 1946

Abstract

A method of measurement and analysis, based on the parallel plate plastometer, has been developed for the determination of the viscoelastic properties of plastic materials at elevated temperatures. It is shown theoretically and verified experimentally that, for linear viscoelastic materials, measurements from constant load and constant plate separation experiments may be expressed, using the appropriate normalization factors, as deformation-time and stress-time curves respectively. The necessary criteria for interpreting such measurements in terms of a mechanical model are discussed. The method has been applied to vinyl chloride-acetate resin, polyethylene resin compounds, and a cellulose ester compound. The data show that these compounds are linear viscoelastic materials, that is, the deformation (or any of its components) is proportional to the applied stress at a fixed value of the time. Data are presented which show that at elevated temperatures the viscoelastic properties of these materials are representable by a simple mechanical model consisting of a pure elastic spring, a retarded Voigt element, and a pure viscous dashpot coupled in series. The elastic, delayed elastic, and viscous components of the deformation are, therefore, quantitatively separable and are completely characterized by four constants, two elastic moduli and two viscosity coefficients. High temperature stress-strain curves at various rates of loading, and recovery behavior after periods of continuous deformation, are predicted theoretically and verified experimentally. The variation of the viscoelastic constants with temperature and composition has been evaluated. The principal viscosity (viscosity of pure dashpot) is the only viscoelastic constant which obeys a linear $\log \eta_3$ *vs.* $1/T$ relation over wide ranges of temperature, thus permitting the calculation of activation energies for viscous flow. It is shown that the disappearance of elastic effects is associated with a sharp decrease of the retardation time (time constant of the delayed elastic deformation). A study of polyethylenes of various molecular weights shows that the effect of increasing molecular weight is to increase the resistance to both the elastic and the viscous types of deformation and to increase the temperature at which elastic effects become negligible. The principal viscosity varies with the molecular weight according to Flory's relation (linear $\log \eta_3$ *vs.* $M^{\frac{1}{2}}$). The variation of the other viscoelastic constants with the molecular weight is more complex.

Introduction

It is well known that the behavior of plastic materials under the action of stresses is very complex because elastic and viscous deformations take place simultaneously (7, 8, 4). A substance showing such behavior

* Presented at the Annual Meeting of the Society of Rheology, New York, N. Y., November, 1946.

may be referred to as a viscoelastic material. The complex, over all deformation is usually divided up into three main types as follows:

(1) Sudden elastic deformation. This deformation is reached almost immediately upon application of the load and is completely recoverable upon release of the load.

(2) Delayed elastic deformation. This type of deformation is developed in the material at a continuously decreasing rate. It may take from a few seconds to months or years to reach the complete delayed elastic deformation, depending on the temperature and the properties of the material. Most of this deformation is recoverable.

(3) Viscous deformation (or flow). This deformation is developed in a material at a rate proportional to the applied stress and will continue until the specimen is ruptured or the test conditions are altered. This type of deformation is irrecoverable.

A quantitative separation and description of the above deformation components are essential for an understanding of the mechanical and flow properties of plastic materials.

At low and moderate temperatures the delayed elastic type of deformation is the most important. This phenomenon is most conveniently studied *via* creep and stress relaxation curves. The phenomenon is very complex for most materials due to the fact that apparently many delayed elastic processes or mechanisms differing in response or relaxation time are superimposed on each other. A mathematical description, which would be useful in practice, has not been devised as yet for this type of deformation.

At high temperatures some plastic materials show almost pure viscous flow. The study of these is relatively simple, the only problem being the measurement of high viscosities. Such measurements are conveniently made in a parallel plate plastometer and have been described in a previous paper (3). Most plastic materials, however, show a mixture of viscous and "elastic" deformations even at high temperatures. Delayed elastic processes may become simple enough at high temperatures to be amenable to analysis, usually since many of the complicating processes, important at low temperatures, become negligible or disappear altogether. The subject of this report is the measurement and analysis of combined viscous and "elastic" deformations at elevated temperatures based on parallel plate plastometer methods.

Experimental Procedures

Several types of experiments can be performed with the parallel plate plastometer:

1. Constant Load Experiment. This type of experiment has been described in detail in a previous paper (3). Briefly, the desired test load is

applied to a right circular cylindrical specimen and the plate separation, h, is measured as a function of time. The load on the Bakelite plastometer may be varied from 0 to 60 kg. and the specimen volume may be varied from about 1 cc. to 2 cc. Loads and volumes must be adjusted to give plate separation readings between 0.010 and 0.100 inches; otherwise the data are not simply interpretable. The resulting test data are plotted in the form of a $1/h^4$ *vs.* time curve where h is expressed in centimeters and time in seconds. The resulting $1/h^4$ *vs.* time curves, which are essentially deformation-time curves obtained at constant load, are analyzed for the fundamental viscoelastic constants by the methods given in the section on theory.

2. Stress Relaxation Experiment. It is well known that for a viscoelastic material held under constant strain, the load or stress required to maintain this strain decreases with time. The parallel plate plastometer was not designed for a measurement of this kind but can be adapted for the purpose. In this test the sample is quickly deformed to the desired value of h and the load is manually adjusted to keep this value of h constant. Here again the value of h is to be between 0.010 and 0.100 inches. The resulting test data are plotted in the form of a load *vs.* time curve. The resulting load *vs.* time curves, which are essentially stress relaxation curves obtained at constant deformation, are analyzed for the fundamental viscoelastic constants by the methods given in the section on theory. The precision of this type of experiment is rather low due to lack of sensitivity of the load measurement. It is important, however, from the standpoint of interpretation of viscoelastic behavior to have stress relaxation data at elevated temperatures. The test described above served this purpose.

3. Load Deflection Experiments. Manual manipulation of the loading weights makes it possible to obtain a "load-deflection" curve at constant rate of loading with the parallel plate plastometer. The loading weight is pushed manually along the loading beam at a constant rate and the plate separation, h, is measured at convenient intervals. These experiments were found to be quite reproducible.

4. Recovery Experiments. In this test the sample is allowed to deform under a constant load. After the desired time of continuous deformation the load is reduced to a nominal value of 0.1 kg. and plate separation readings are taken at convenient time intervals. The 0.1 kg. load was found necessary to maintain contact between the upper plate and the sample. From these data the residual strain is expressed as a normalized $1/h^4$ *vs.* time curve in recovery. Such an experiment is not highly reproducible because:

(a) The zero reading of the dial gage, which measures h, depends on the load used and requires a correction. This amounts to about 0.001 in. at 10 kg. and 0.0025 in. at 50 kg. but is difficult to determine accurately.

(b) Any friction in the machine or any irregularity in the sample has a large effect on recovery since very small changes in h must be measured. Due to the difficulties above it is more reliable, in practice, to calculate the recovery properties from constant load experiments.

Theoretical Considerations

Plastic materials under stress exhibit a behavior which combines simultaneously the properties of an elastic solid and a viscous liquid, that is, the total deformation is a more or less complex superposition of elastic and viscous deformations. A quantitative separation of the various components of the deformation and a mathematical description of viscoelastic properties are of great importance in the study of the flow properties of plastic materials.

In a parallel plate plastometer the plate separation, h, is measured as a function of time at a given load and specimen volume. From such experimental data it is desired to obtain fundamental material constants which will describe the intrinsic properties of the material. It was shown in a previous paper (3) that, if the data obtained in a constant load experiment are plotted as a $1/h^4$ *vs.* time curve, then the straight line portion of this curve represents pure viscous flow. The early, non-linear portion of the curve was attributed to elastic and delayed elastic effects. The fact that a $1/h^4$ *vs.* time curve becomes linear and has the general shape of a typical deformation-time curve suggests, that, in fact, it may be a deformation-time curve. If such is the case it may be possible to determine the viscoelastic constants of a material at elevated temperatures by parallel plate plastometer data and to interpret such data in terms of mechanical models. Before such an interpretation can be made the behavior of a viscoelastic material in a parallel plate plastometer must be investigated and the necessary criteria for a mechanical model representation established. This can be done theoretically for linear, incompressible viscoelastic materials and all further discussion will be restricted to such substances.

1. Viscoelastic Behavior in the Parallel Plate Plastometer

Several methods have been employed to define the properties of viscoelastic materials. A critical summary of these methods has been given recently by Alfrey and Doty (2). For the purposes of this paper the "Operator equation" method has been adopted. The properties of a linear, incompressible, isotropic viscoelastic material are conveniently specified by a single differential equation (2).

$$\vec{P}s = 2\vec{Q}\epsilon, \tag{1}$$

where s = deviatoric stress tensor, ϵ = deviatoric strain tensor, and $\vec{P}$ and $\vec{Q}$ are the differential operators

$$\vec{P} = \frac{\partial^m}{\partial_t m} + p_{m-1}\frac{\partial^{m-1}}{\partial_t m - 1} + \cdots + p_0,$$

$$\vec{Q} = q_n\frac{\partial^n}{\partial_t n} + q_{n-1}\frac{\partial^{n-1}}{\partial_t n - 1} + \cdots + q_0.$$

Alfrey has shown that, for small strains, the laws of the Theory of Elasticity must be obeyed by such a material with respect to the spatial coordinates. For the purpose of this paper it is convenient to restate his results in terms of "normalization factors." In a constant stress experiment the strain, $\epsilon(t)$, is measured as a function of time. Since, in a linear viscoelastic material, the strain (and time derivatives of the strain) at any fixed value of the time is proportional to the stress, s, the deformation-time, or creep, function, $\psi(t)$, may be written

$$\psi(t) = \frac{2\epsilon(t)}{s}$$

$$= Ff(t), \tag{2}$$

where F = normalization factor which involves the geometry of a given specimen and instrument, *i.e.*, is a function of the spatial coordinates but not of the time; $f(t)$ = solution of the general stress-strain relation, Eq. (1), with respect to the time under conditions of constant stress. Similarly in a stress relaxation experiment, the relaxation function, $\phi(t)$, will be given by

$$\phi(t) = \frac{s(t)}{2\epsilon}$$

$$= F'g(t), \tag{3}$$

where F' is the appropriate normalization factor. Alfrey's result, in terms of normalization factors, is:

The normalization factor for any linear, incompressible viscoelastic material which obeys Eq. (1) is the same as for a Hookean elastic material [$\epsilon \neq f(t)$] under the same experimental conditions (provided the experimental conditions satisfy the boundary and initial conditions of the theory of elasticity).

These results can be carried over directly to experiments which satisfy the boundary and initial conditions of the Theory of Newtonian viscous flow. Since Alfrey's results are true for any $\vec{P}$ and $\vec{Q}$ they will certainly

hold for

$$\vec{P} = 1,$$
$$\vec{Q} = \eta \frac{\partial}{\partial t},$$

where η = coefficient of viscosity.

This, is, of course, the well known viscosity-elasticity analogy. Application of the reasoning outlined above to a viscosity type experiment gives the result:

A normalization factor determined for an incompressible Newtonian viscous material applies also to an incompressible linear viscoelastic material under the same experimental conditions (provided that the experimental conditions satisfy the boundary and initial conditions of the theory of Newtonian viscosity).

According to these theoretical considerations, therefore, the normalization factors for a parallel plate plastometer experiment, involving the applied load and the volume of the specimen, can be applied directly to viscoelastic materials provided the corresponding equations are known for Newtonian viscous fluid. In a previous paper (3) it was shown that the viscosity can be calculated from the linear portion of the $1/h^4$ *vs.* time curve using the equation

$$1/h^4 = \frac{8.21 \times 10^6 W}{V^2} \frac{1}{\eta} t + C, \tag{4}$$

where $1/h^4$ is expressed in cm.$^{-4}$; V = volume of sample, cm.^{3}; W = applied load, kg.; η = viscosity, poises; and C = constant of integration. The constant C is effectively zero due to the fact that before the load is applied $1/h^4$ is very small. The general theory leading to this equation and the general conditions of applicability were described in the previous paper.

The general operator equation, Eq. (1), as applied to a parallel plate plastometer experiment, becomes now

$$\frac{8.21 \times 10^6}{V^2} \vec{P} W = \vec{Q} 1/h^4, \tag{5}$$

or letting $y = 1/h^4$ for convenience

$$\frac{8.21 \times 10^6}{V^2} \vec{P} W = \vec{Q} y. \tag{6}$$

For $\vec{P} = 1$, $\vec{Q} = \eta \frac{\partial}{\partial t}$, Eq. (6), of course, reduces to Eq. (4). Thus, all components of the deformation will follow the same law with respect to load and volume as is followed by the viscous deformation. Any point

along a $1/h^4$ *vs.* time curve, therefore, will vary linearly with the load and inversely with the square of the volume. Such a normalization then transforms a $1/h^4$ *vs.* time curve, obtained at constant load, into a normalized deformation-time curve and permits the calculation of both elastic moduli and viscosity coefficients.

2. Mechanical Model Representation of Viscoelastic Behavior

Whenever possible it is very convenient to use mechanical models for representing viscoelastic behavior. A large amount of experimental information can be summarized by such a representation, and the behavior of the material under various conditions can be quickly predicted from the model.

Whenever an attempt is made to describe viscoelastic behavior in terms of a mechanical model certain restrictions are put on the general operator Eq. (1). Any mechanical model made up of Hookean elastic and Newtonian viscous elements is a special case of this equation. The great advantage of a mechanical model representation is that individual rheological constants may be identified with very definite physical processes, such as elastic deformation, viscous flow, relaxation time, *etc.* The constants of the general operator equation, on the other hand, are composite constants, and while they define completely the behavior of the material their physical interpretation is usually not simple.

It was shown above that the operator equation, Eq. (1), for a parallel plate plastometer experiment becomes Eq. (6). All further discussions will be concerned with special forms and solutions of Eq. (6) and their representation in terms of mechanical models and fundamental rheological constants. It is assumed in Eq. (6), of course, that the experimental conditions obey all the restrictions particular to a parallel plate plastometer experiment (3).

From parallel plate plastometer studies it was found that a relatively simple model accounts for the behavior observed experimentally. The model to be considered consists of two Hookean springs and two Newtonian dashpots. Two types of mechanical models can be constructed from these elements: (1) Voigt elements in series, (2) Maxwell elements in parallel. It was shown by Alfrey and Doty (2) that the two types of models are mathematically equivalent. The constants of one system are transformable into the constants of the other, numerically they are not equal. The Voigt type of model is more convenient to use in interpreting a constant stress experiment while the Maxwell type is more useful in stress relaxation studies. The characteristic constants for the elements of the Voigt specification, moduli for the springs and viscosity coefficients for the dashpots, are denoted by G_1, G_2, η_2, and η_3. Let the equivalent ele-

ments of the Maxwell specification characteristic constants be denoted by primed quantities G_1', G_2', η_1', and η_2'.

By superposition of strains (Voigt type) and superposition of stresses (Maxwell type) it is easily shown that these models obey, in a parallel plate plastometer test, the following differential equations:

Voigt specification:

$$\eta_2\eta_3\frac{d^2W}{dt^2} + (G_1\eta_3 + G_1\eta_2 + G_2\eta_3)\frac{dW}{dt} + G_1G_2W = \frac{V^2}{8.21 \times 10^6} G_1\eta_2\eta_3\frac{d^2y}{dt^2} + G_1G_2\eta_3\frac{dy}{dt}; \quad (7)$$

Maxwell specification:

$$\frac{1}{G_1'G_2'}\frac{d^2W}{dt^2} + \left(\frac{1}{G_1'\eta_2'} + \frac{1}{G_2'\eta_1'}\right)\frac{dW}{dt} + \frac{1}{\eta_1'\eta_2'}W = \frac{V^2}{8.21 \times 10^6}\left(\frac{1}{G_1'} + \frac{1}{G_2'}\right)\frac{d^2y}{dt^2} + \left(\frac{1}{\eta_1'} + \frac{1}{\eta_2'}\right)\frac{dy}{dt}, \quad (8)$$

where $y = 1/h^4$.

The mathematical descriptions given by Eqs. (7) and (8) are identical provided certain relations are obeyed by the constants of the Voigt and of the Maxwell type models. These relations are obtained by equating the coefficients of like terms (for example the coefficients of d^2y/dt^2). Some of these relations will be used in testing for the applicability of a model representation and are, therefore, set down here.

$$G_1 = G_1' + G_2', \quad (9)$$

$$\eta_3 = \eta_1' + \eta_2', \quad (10)$$

$$-\frac{1}{\tau_1'}, -\frac{1}{\tau_2'} = \frac{-\gamma \pm \sqrt{\gamma^2 - 4\beta}}{2}, \quad (11)$$

where

$$\gamma = \frac{G_1}{\eta_2} + \frac{G_1}{\eta_3} + \frac{G_2}{\eta_2}, \quad \text{and} \quad \beta = \frac{G_1G_2}{\eta_2\eta_3}.$$

The complete set of transformation equations are given by Alfrey and Doty (2); these become quite complicated even for such a simple model. The complexity of the transformation equations increases as the number of elements used in the model increases, and the numerical computation of the constants of one type model from those of the other becomes very difficult.

The general equations (7) and (8) can be solved for a variety of experimental conditions. For a determination of the rheological constants (G_1, η_1) it is simplest to use constant load and constant $1/h^4$ (*i.e.*, constant strain) experiments. Either Eq. (7) or (8) is easily solved for these condi-

tions. It is convenient and mathematically simpler, however, to use the Voigt specification, Eq. (7), for a constant load, and the Maxwell specification, Eq. (8), for a constant strain experiment.

Under a constant load (W = constant) the Voigt specification, Eq. (7), gives the solution

$$F1/h^4 = \frac{1}{G_1} + \frac{1}{\eta_3} t + \frac{1}{G_2} (1 - e^{-\frac{t}{\tau_2}}), \tag{12}$$

where

$$\tau_2 = \text{retardation time} = \frac{\eta_2}{G_2},$$

and F is the normalization factor given by

$$F = \frac{V^2 \times 10^{-6}}{8.21W} \tag{13}$$

with V expressed in cm.^{3}, h in cm., W in kg., and t in seconds. This will give G_1 and G_2 in dynes/cm.^{2}, η_3 and η_2 in poises, and τ_2 in seconds. Dimensional analysis will immediately show that F/h^4 has the dimensions of (stress)$^{-1}$ so that all the constants of the right hand side of Eq. (12) have the proper dimensions to be interpreted as moduli and viscosity coefficients. Equation (12), therefore, represents a normalized deformation-time curve. The use of the Maxwell specification, Eq. (8), will yield an equivalent expression with the constants expressed in terms of G_1', G_2', η_1', and η_2'.

For a constant plate separation (or stress relaxation) experiment ($1/h^4$ constant, units as above), the Maxwell specification, Eq. (8), gives the solution

$$F'W = G_1' e^{-\frac{t}{\tau_1'}} + G_2' e^{-\frac{t}{\tau_2'}}, \tag{14}$$

where

$$\tau_i' = \text{relaxation time} = \frac{\eta_i'}{G_i'},$$

and F' is the normalization factor given by

$$F' = \frac{8.21 \times 10^6}{V^2 1/h^4}. \tag{15}$$

Both types of equations, Eqs. (12) and (14), are easily fitted to experimental data and the constants determined by graphical methods, namely by the method of successive residues (5, 6). The applicability of Eq. (12) and (14) is thereby automatically tested.

It must be emphasized that numerically, as well as in their variation with, say temperature, the constants G_i, η_i of one specification are different from the corresponding constants G_i', η_i' of the other specification. One set of constants are calculable, however, from the other via a set of

transformation equations, three of which are given in Eqs. (9), (10), and (11).

It is evident from Eq. (6) that the operator specification is very general and is *a priori* not connected with any model. As a matter of fact, a model representation restricts the general operator equation. It is also evident that a constant load experiment studies one side of the general differential equation (6), while a constant strain experiment studies the other side. Thus, at least two types of experiments—constant load and stress relaxation—are necessary for the complete determination of a given differential equation. From Eqs. (12) and (14) it is seen that the assumption of a mechanical model representation predicts very specific results for both types of experiments. Unless the results of both experiments follow the predicted relations the model description cannot be justified. In addition, if the model representation is correct, the derived constants of one type of experiment must be calculable from the derived constants of the other type. This can be tested by using Eqs. (9), (10), and (11).

In summary then, the use of a mechanical model representation consisting of Hookean springs and Newtonian dashpots for describing viscoelastic behavior is justified only if

a. The correct normalization factor is predicted. This tests the "linearity" of the material (see Eqs. (6), (12), and (14));
b. the equations predicted for constant load and stress relaxation experiments are consistent;
c. the transformation equations from a Voigt type model and *vice versa* are obeyed by the viscoelastic constants.

Once a model is set up and its use justified it is possible, on the basis of Eqs. (7) and (8), to predict the behavior of the viscoelastic material under more complicated load or strain sequences (this can also be done, of course, on the basis of the operator equation without any model representation). Stress-strain curves at constant rate of loading and constant rate of straining are of particular interest. Experimentally it was possible to obtain constant rate of loading. The mathematics of this case is of interest and it was found convenient to use the Voigt specification for this purpose. Thus, Eq. (7) is to be solved subject to the condition

$$\frac{dW}{dt} = c = \text{constant}.$$

The solution of the differential equation is

$$\left(\frac{V^2}{8.21 \times 10^6}\right) y = \left(\frac{1}{G_1} + \frac{1}{G_2}\right) W + \frac{1}{2c\eta_2} W^2 + \frac{c\eta_2}{G_2^2} \left(e^{-\frac{G_2}{\eta_2}\frac{W}{c}} - 1\right), \quad (16)$$

where, as before, $y = 1/h^4$.

The resulting $W - y$ curve may be interpreted as a sort of normalized load-deflection curve (normalized with respect to sample size, V) and theory compared with experiment at various rates of loading. Thus, when a model representation is applicable, the "stress-strain" curve can be predicted theoretically at various rates of loading (and by a similar mathematical development at constant rates of straining) from constant load and stress relaxation experiments. This is a "stress-strain" curve in which all deviations from Hooke's law may be attributed directly to time effects. All the elements of the mechanical model are Hookean and Newtonian. It is the combination of these elements which leads to the "stress-strain" relation of Eq. (16).

The main assumption in the whole theory outlined above concerns the nature of the various components of the total deformation. Thus, it is desirable to investigate experimentally whether the elastic and delayed elastic deformations are actually recoverable, and the viscous deformation irrecoverable in character. For this purpose the equations for a recovery experiment have to be worked out. These are completely determined by the general Eqs. (7) and (8).

Let the sample be continuously deformed for a certain length of time and then let the load be removed at the end of this time interval. The response of the Voigt model, Fig. 2A, will be as follows:

(a) The sudden elastic deformation, represented by the spring of modulus G_1, will be recovered immediately upon release of the load and will not contribute, therefore, to the residual deformation.

(b) The delayed elastic element, represented by a spring (G_2) and dashpot (η_2) in parallel, will show a gradual recovery. The normalized residual deformation at any time, t', after load removal will be given by

$$(F1/h^4)_{\text{Res.}} = \frac{1}{G_2}\left(1 - e^{-\frac{t_1}{\tau_2}}\right)e^{-\frac{t'}{\tau_2}}, \tag{17}$$

where t_1 = length of time of load application, t' = time elapsed since load removal, *i.e.*, the recovery time,

$$F = \frac{V^2 \times 10^{-6}}{8.21W}.$$

This equation was obtained by solving the differential equation describing a Voigt element

$$\frac{8.21 \times 10^6}{V^2} W = G_2 y + \eta_2 \frac{dy}{dt}$$

under condition of zero load ($W = 0$) and the initial condition at t_1 (or $t' = 0$):

$$\frac{V^2 \times 10^{-6}}{8.21W} y = \frac{1}{G_2}\left(1 - e^{-\frac{t_1}{\tau_2}}\right).$$

The residual deformation due to this element decays exponentially to zero, the rate of decay depending on the duration of previous load application. Complete recovery of this element, in the same length of time as the duration of load application, will be obtained only if t_1 is very large compared to τ_2.

(c) The viscous deformation is irrecoverable and will contribute to the residual deformation an amount given by

$$(F1/h^4)_{\text{Res.}} = \frac{1}{\eta_3} t_1. \tag{18}$$

The total normalized residual deformation is the sum of these and is given by

$$(F1/h^4)_{\text{Res.}} = \frac{1}{G_2}(1 - e^{-\frac{t_1}{\tau_2}})e^{-\frac{t'}{\tau_2}} + \frac{1}{\eta_3} t_1. \tag{19}$$

The complete residual deformation-time curve can be calculated, therefore, from the known viscoelastic constants and the results compared with experiment.

Presentation and Interpretation of Results

It was shown in the theory that for linear viscoelastic materials a parallel plate plastometer experiment at constant load yields a deformation-time curve while a constant plate separation experiment gives a stress relaxation curve. The necessary criteria for interpreting such measurements in terms of a mechanical model representation are also given in the theory. Experimental evidence supporting the above interpretation is presented in this section, and the viscoelastic properties of some plastic materials, as determined by this technique, are also discussed. Thus, it becomes possible to study deformation-time and stress relaxation phenomena at elevated temperatures where the more usual type of experimental approaches, such as tension, flexure, compression, *etc.*, cannot be used.

1. Experimental Evidence for Model Representation

In the theory three major criteria of applicability were established for a simple mechanical representation of viscoelastic behavior. A mechanical representation is a convenient way of summarizing a large amount of experimental data. From the model one can tell at a glance how the material will behave under a variety of conditions. Experimental evidence will be presented to show that the materials treated in this report follow, in fact, the Voigt and Maxwell models.

The first step is to show that the correct normalization factor is predicted. Equations (13) and (15) of the theory give the theoretical normalization factors, F and F', for a constant load and a stress relaxation

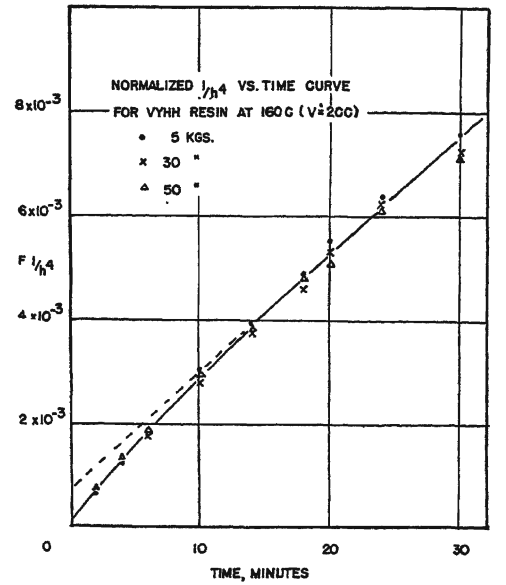

FIG. 1

Normalized $1/h^4$ *vs.* Time Curve for Vinyl Chloride-Acetate Resin VYHH at 160°C. Obtained at Various Loads

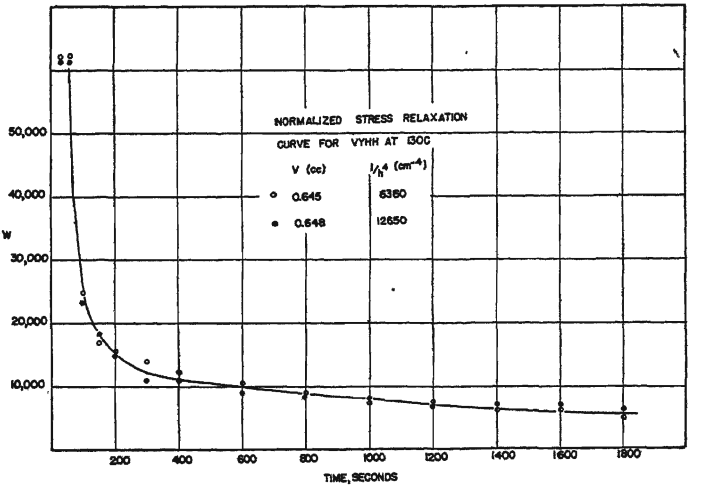

FIG. 2

Normalized Stress Relaxation Curve for Vinyl Chloride-Acetate Resin VYHH at 130°C. Obtained at Various Deformations

experiment respectively. If these are correct, then at any load and volume a single $F \times 1/h^4$ *vs.* time curve should describe the constant load data, and a single $F' \times W$ *vs.* time curve should fit the stress relaxation data. These predictions were experimentally verified as shown in Figs. 1–2. Typical $F \times 1/h^4$ *vs.* time curves were obtained at various loads and volumes for VYHH resin, polyethylene DE-3401, and a commercial cellulose ester. All of the data are evidently well represented by a single line. An $F' \times W$ curve is presented in Fig. 2 for VYHH resin at 130°C. showing that proper normalization is obtained also in stress relaxation. All of the data given in this paper were obtained from such

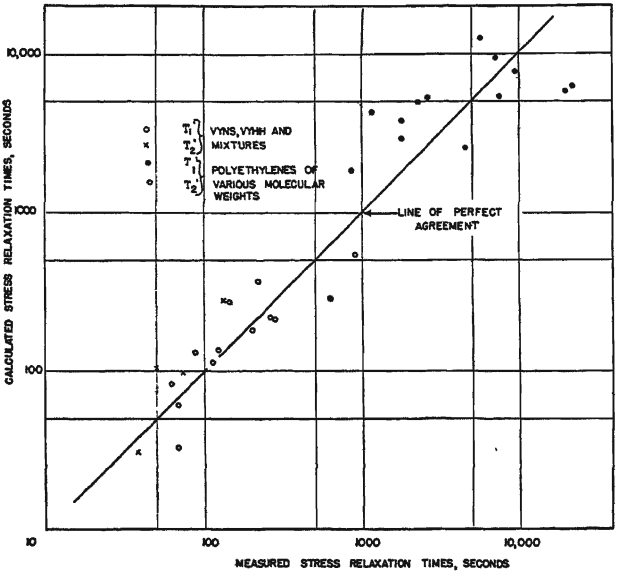

FIG. 3

Comparison of Calculated and Measured Stress Relaxation Times

average normalized curves, that is, the applicability of normalization was verified for all compounds at all temperatures.

The second criterion is the prediction of the correct equations for a $1/h^4$ *vs.* time curve (constant load equation) and a stress *vs.* time curve (stress relaxation equation). The appropriate equations for the Voigt and Maxwell models are given by Eqs. (12) and (14) of the theory. It was found that all the experimental data, without a single exception, could be fitted well by these relations, thus permitting a calculation of all the viscoelastic constants. It is realized that in fitting the experimental curves the constant term, $1/G_1$, of Eq. (12) may or may not be a true constant. The first reading is taken at 30 or 60 seconds and any delayed

elastic processes which are fully developed by this time will give rise to an apparently constant deformation and $1/G_1$, therefore, may be the sum of several very rapid delayed elastic deformations. The fact that a second exponential term for these materials did not show up at any of the temperatures investigated suggests, however, that $1/G_1$ is essentially a simple constant. As the temperature is lowered more exponential terms will, of course, appear since it is well known that at, say, room temperature a whole series of Voigt or Maxwell elements (or a continuous distribution of them) is necessary to describe the deformation-time and stress relaxation properties of many thermoplastic materials.

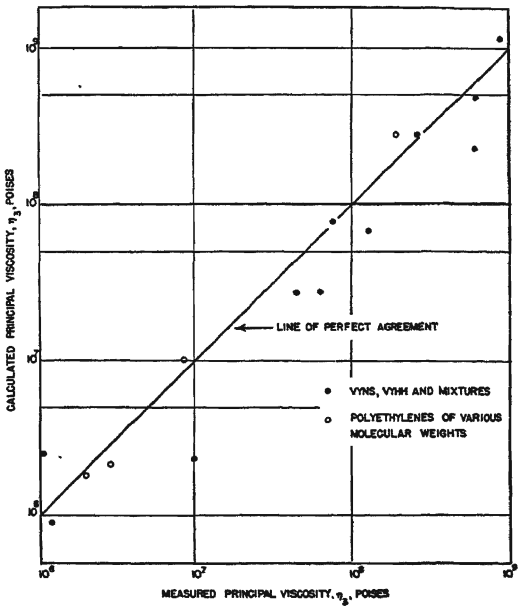

FIG. 4

Comparison of Calculated and Measured Principal Viscosities

A third criterion of the applicability of mechanical representation is the validity of the transformation equations for calculating the constants of the Voigt type of model representation from those of the Maxwell type. Three of the simplest transformation relations are given by Eqs. (9), (10), and (11). These equations permit the calculation of the Voigt elastic modulus G_1 from the Maxwell moduli G_1', G_2'; the principal Voigt viscosity from the Maxwell viscosities η_1', η_2'; and the Maxwell stress relaxation times τ_1', τ_2' from the constants of the Voigt model. Thus experimental and calculated constants can be compared when both constant load and stress relaxation data are available.

There are some experimental difficulties in measuring stress relaxation properties, due to the fact that the present plastometer was not designed for this purpose, as described earlier in this report. A sufficient number of stress relaxation experiments have been run, however, to provide a good test of the transformation equations.

Fig. 3 shows the correlation between calculated and measured stress relaxation times for VYNS, VYHH and mixture compounds, and several polyethylene resin compounds at various temperatures. It will be seen that the points lie quite evenly distributed about the line of perfect agreement so that no trend is shown in the deviations. The conclusion is that good order of magnitude agreement is obtained. It may be pointed

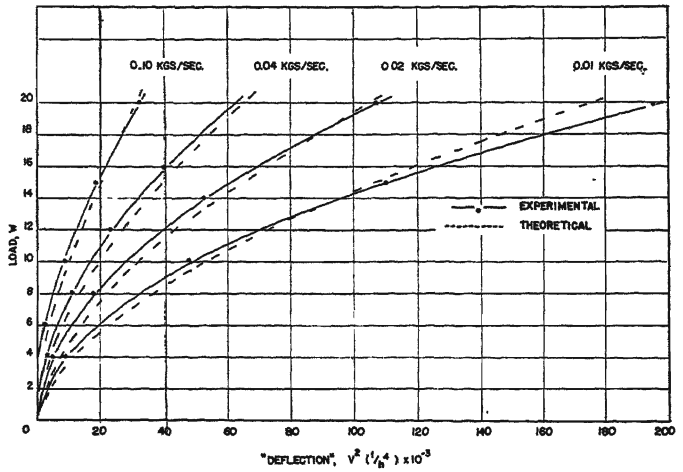

FIG. 5

Comparison of Experimental and Theoretical Load-Deflection Curves. Polyethylene, DE-3401 Nat., at 130°C

out that in these calculations a quadratic equation must be solved (see Eq. (11)) which is quite sensitive to any error in the Voigt viscoelastic constants G_i, η_i. In this case, therefore, discrepancies are to be attributed to experimental errors in G_i, η_i as well as lack of precision of stress relaxation experiments leading to errors in the measured G_i', η_i'.

A similar correlation is shown for the principal viscosity, η_3, in Fig. 4. Again good order of magnitude agreement is obtained for η_3. The calculated values are generally somewhat lower than predicted by the line of perfect agreement. This constant is calculated from stress relaxation experiments which are known to be far less precise than constant load experiments and probably account for most of the deviations.

The general conclusion is that a mechanical model representation, as

judged by the applicability of the transformation equations, is essentially justified.

In a few cases an additional test of the mechanical model is provided by "load-deflection" relations obtained at constant rate of loading. As shown in the theory, such a normalized load-deflection relation may be calculated from the known viscoelastic constants by the use of Eq. (16). A comparison of theoretical and experimental "load-deflection" curves is shown in Fig. 5 for polyethylene DE-3401 at four rates of loading (at 130°C.). The agreement is seen to be very good. In these "load-deflec-

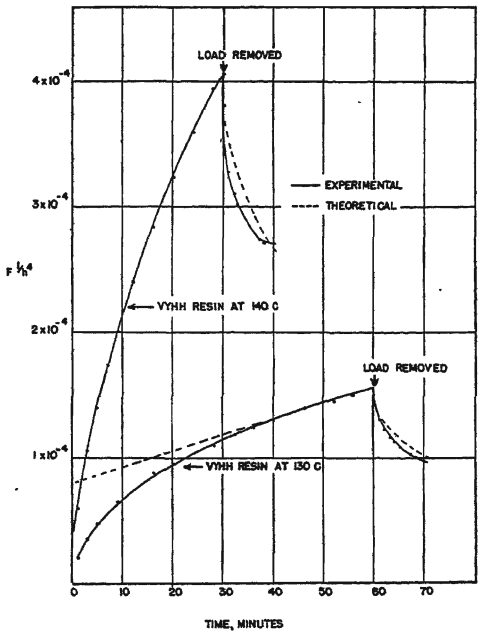

FIG. 6

Comparison of Theoretical and Experimental Recovery Curves for Vinyl Chloride-Acetate Resin VYHH at 130°C. and 140°C.

tion" curves all deviations from linearity are directly attributable to time effects since all the elements of the mechanical model are Hookean and Newtonian. It is the combination of these elements which leads to the "load-deflection" relations shown here.

Similar results were obtained for a 50:50 mixture of VYNS and VYHH at 160°C. at three rates of loading, although the agreement between theoretical and experimental curves is less satisfactory in this case. This may be explained by the fact that the viscosity of this compound is quite high (1.7×10^7 poises at 160°C.), and the values of h in the early

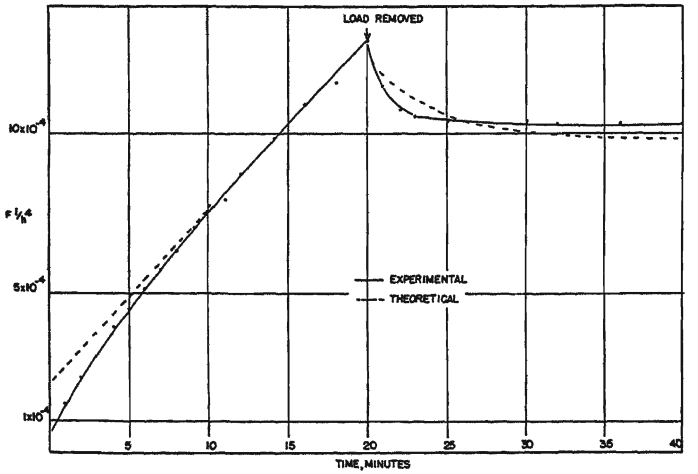

FIG. 7

Comparison of Theoretical and Experimental Recovery Curves for Polyethylene DE-3401 at 130°C.

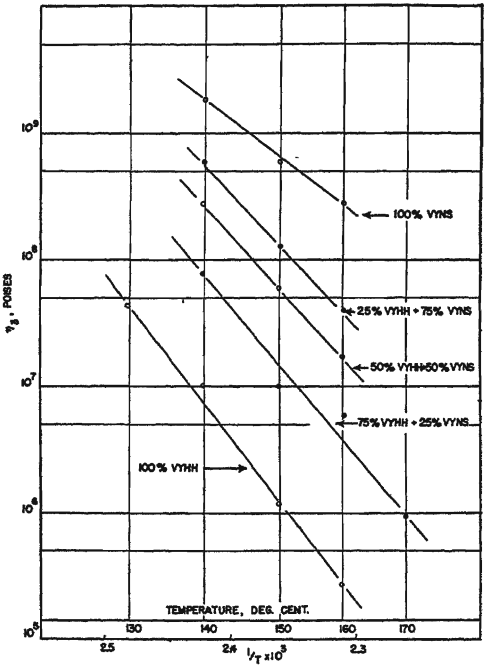

FIG. 8

Principal Viscosity-Temperature Characteristics for Vinyl Chloride-Acetate Resins VYHH, VYNS and Their Mixtures

portion of the stress-strain curve do not fall within the specified limits. If this is the case better agreement would be obtained at higher rates of loading, which was observed.

Recovery measurements are also in agreement with this picture and present, perhaps, the most direct proof of the validity of attributing the initial part of the $1/h^4$ *vs.* time curve to the presence of elastic and delayed elastic deformations. Precise experimental measurement of recovery by present experimental techniques is difficult due to the fact that very small

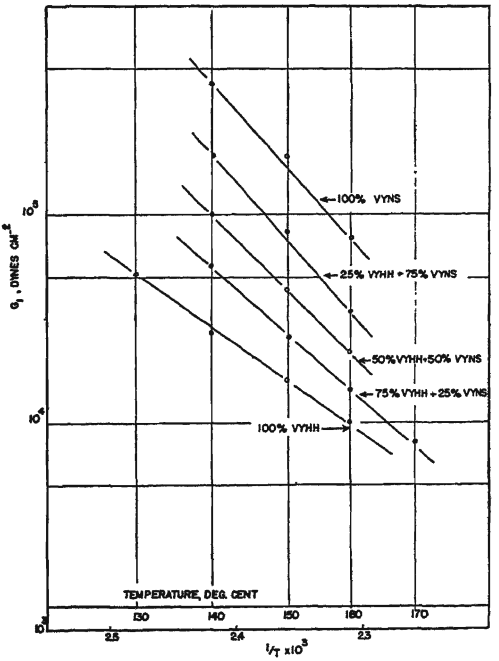

FIG. 9

Elastic Modulus, G_1, *vs.* $1/T$ Curves for Vinyl Chloride-Acetate Resins VYHH, VYNS and Their Mixtures

changes in h must be determined, and therefore only a few studies of this type have been made. It was shown in the theory that the residual strain *vs.* time curve after load removal can be calculated from the viscoelastic constants of the material. Thus, a comparison between experiment and theory can be made. Fig. 6 shows the results for vinyl chloride-acetate resin VYHH at 130°C. and at 140°C. in the form of normalized $1/h^4$ *vs.* time curves under load and in recovery. At 130°C. the load was removed at 60 minutes and the recovery measured for 10 minutes. The theoretical recovery curve was calculated from Eq. (19). In this case the

straight line portion of the $1/h^4$ *vs.* time curve has been reached and, therefore, the delayed elastic deformation was fully developed while under load. At 140°C. the load was released shortly before the straight line portion of the curve would have been reached, and therefore, in this case, the delayed elastic deformation was not fully developed. In both cases quite good agreement is shown with the theory. A similar curve is shown for polyethylene DE-3401 (M.W. = 20,000) at 130°C. in Fig. 7. It may be pointed out that the discrepancy between the experimental

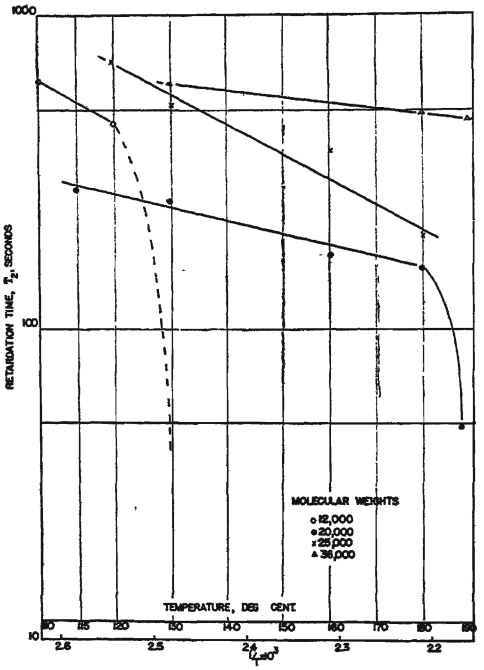

FIG. 10

Retardation Time-Temperature Characteristics for Polyethylenes of Various Molecular Weights

and theoretical recovery curves in all three cases corresponds to an error in h of less than 0.0005 in.

This agreement between theoretical and experimental recovery curves lends strong support to the general interpretation of superimposed elastic and viscous deformations and to the model representation employed for the materials treated in this paper.

2. Viscoelastic Behavior at Elevated Temperatures

a. Vinyl Chloride-Acetate Resin Compounds. The viscoelastic properties of vinyl chloride-acetate resins VYHH, VYNS and VYNS and VYHH-

VYNS resin mixture compounds were determined in the 130–170°C. temperature range. All samples were made from the same blend of resins VYNS and VYHH and had the composition, in *per cent* by weight:

Resin	97.5%
Stabilizer, lubricant, *etc.*	2.5%
	100.0%

with the resin composition varying from pure VYHH to pure VYNS.

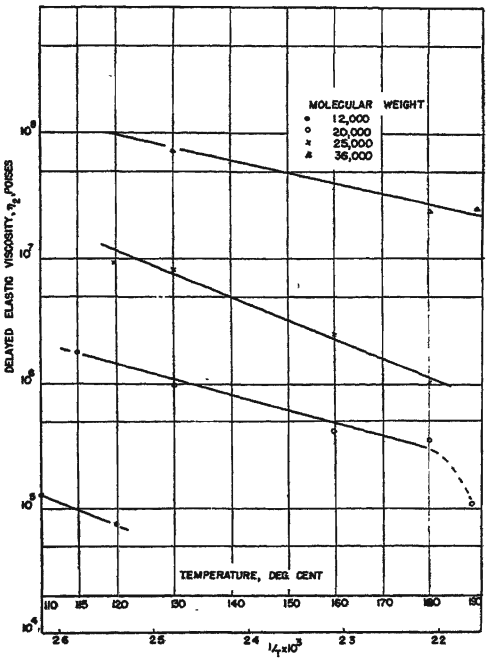

FIG. 11

Delayed Elastic Viscosity-Temperature Characteristics for Polyethylenes of Various Molecular Weights

The viscoelastic constants were determined from constant load experiments as well as from stress relaxation experiments. The correlation of the two sets of constants on the basis of the model representation was discussed in the previous section. Discussion here will be limited to the constants of the Voigt model as affected by temperature and composition. The detailed data are shown in Tables I and II.

The principal viscosity, η_3, varies with the temperature in the normal manner, that is, $\log \eta_3$ is linear in $1/T$, as shown in Fig. 8. Resins VYHH and VYNS are widely separated on the viscosity scale with the mixture

TABLE I

Viscoelastic Constants from Constant Load Experiments Vinyl Chloride-Acetate Resins VYHH-VYNS Series

Temp. °C.	η_1, Poises $\times 10^6$	η_2, Poises $\times 10^6$	G_1, Dynes $cm^{-2} \times 10^4$	G_2, Dynes $cm^{-2} \times 10^4$	τ_2, seconds
100% VYHH Resin					
130	44	11	5 3	1.8	595
140	10	3.4	2.8	0.48	709
150	1.1	1.2	1.7	0 42	291
160	0.28	0.49	1.0	0.13	394
75% VYHH+25% VYNS Resin					
140	75	9.2	5.6	1.7	549
150	9.9	2.1	2.6	0.26	806
160	5.7	0.66	1.4	0.11	621
170	0 95	0.16	0.80	0.03	637
50% VYHH+50% VYNS Resin					
140	270	63	9.3	9.5	658
150	63	8.3	4.6	1 4	610
160	17	1.1	2.2	0 20	543
25% VYHH+75% VYNS Resin					
140	600	96	20	14	694
150	120	24	8.3	3.9	613
160	40	3.3	3.5	0.50	658
100% VYNS Resin					
140	1800	310	43	37	820
150	600	63	20	8 6	735
160	290	22	7.7	3 2	690

compounds falling in between. The slopes of the lines, and therefore the activation energies for viscous flow, also vary in a regular manner, as shown below:

Per cent VYHH	*Per cent* VYNS	Activation energy for viscous flow, cal./mole
100	0	60,000
75	25	54,000
50	50	50,000
25	75	48,000
0	100	35,000

TABLE II

Viscoelastic Constants from Constant Plate Separation Experiments
Vinyl Chloride-Acetate Resin VYHH-VYNS Series

Temp. °C.	G_1', Dynes $cm^{-2} \times 10^4$	G_2', Dynes $cm^{-2} \times 10^4$	τ_1', Seconds	τ_2', Seconds
100% VYHH Resin				
130	1.4	3.2	1800	87
140	0.098	1.4	1700	62
150	0.064	0.52	870	68
75% VYHH+25% VYNS Resin				
140	0.38	1.7	19800	116
150	0.06	1.7	2030	68
50% VYHH+50% VYNS Resin				
140	1.6	2.9	18100	266
150	0.58	3.9	4350	84
25% VYHH+75% VYNS Resin				
140	5.1	15	9400	150
150	0.93	2.0	7500	202
100% VYNS Resin				
140	16	20	7000	221
150	3.7	4.3	5600	280

It was also found that the logarithm of viscosity is approximately linear with percent composition in the 0% to 75% VYHH content region; VYHH itself is less viscous than the extrapolation would predict. Since the viscosity-temperature curves are not parallel the relations will not apply at temperatures much outside the 140°C. to 160°C. range.

The other viscoelastic constants, that is, the moduli G_1 and G_2, the delayed elastic viscosity η_2, and the retardation time τ_2, exhibit a similar behavior. Over the temperature range available for plastometer studies they show a linear log—$1/T$ relation and an approximate logarithmic additivity with respect to concentration at these temperatures. As an illustration Fig. 9 is presented showing the elastic modulus G_1 as a function of the temperature and composition. It will be seen in connection with other compounds that this type of behavior is not generally true over wide ranges of temperatures.

The retardation time, τ_2, for these compounds varies very slowly with the temperature and the composition. In general, τ_2 decreases with increasing temperature and increasing VYHH content. This is the expected behavior, that is, the importance of elastic effects decreases as the temperature is raised or the content of the lower viscosity component is increased. The slow variation of τ_2 with temperature means that a considerably higher temperature would have to be reached before the elastic effects disappear. These compounds cannot be studied at higher temperatures due to thermal instability.

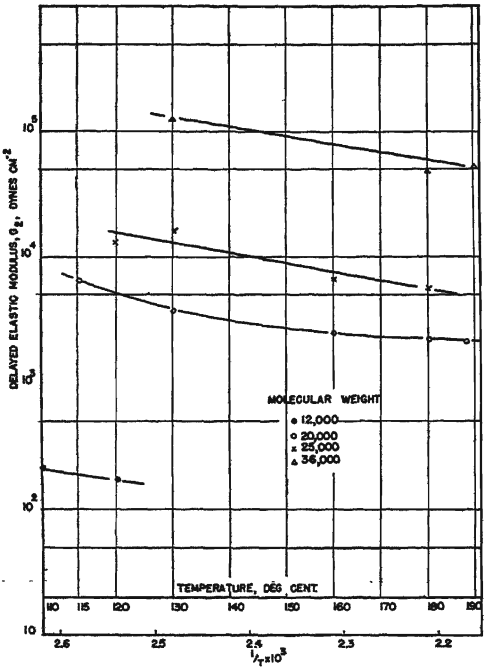

FIG. 12

Delayed Elastic Modulus-Temperature Characteristics for Polyethylenes of Various Molecular Weights

b. Polyethylene Resin Compounds. The viscosity characteristics of polyethylene resins of various molecular weights have been studied previously by parallel plate plastometer methods (3). It was shown that polyethylene resins and polyethylene resin-paraffin wax mixtures obey Flory's relation, that is, log (viscosity) varies linearly with the square root of the weight average molecular weight. Viscosity-temperature characteristics followed the straight line log $\eta_3 - 1/T$ relation with the slopes being essentially independent of the molecular weight. The visco-

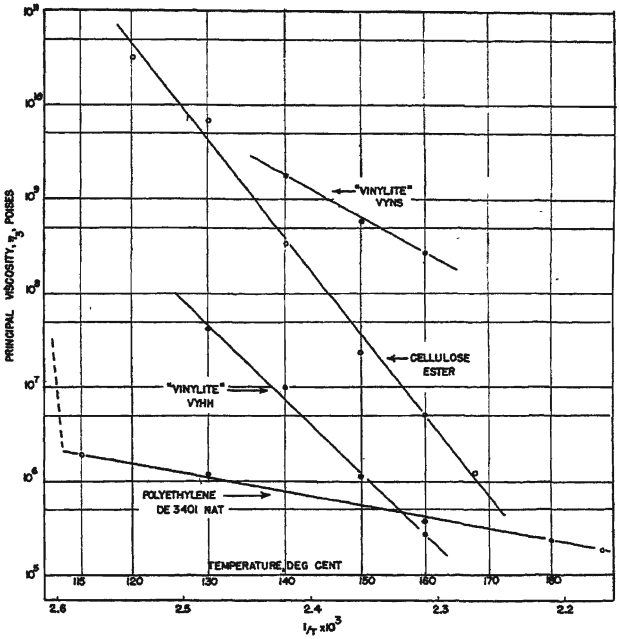

FIG. 13
Principal Viscosity-Temperature Characteristics for Several Plastic Materials

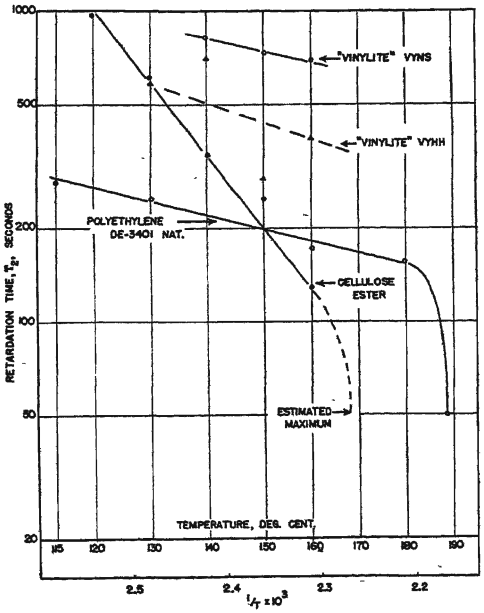

FIG. 14
Retardation Time-Temperature Characteristics for Several Plastic Materials

elastic properties of four polyethylene compounds, taken from the series investigated before (polyethylene resins stabilized with 0.2% Akroflex C), of widely different molecular weights have now been studied over a wide temperature range. All these compounds obeyed the normalization laws described earlier. Stress relaxation experiments showed that the model representation was applicable to these materials. The same or better agreement between measured and calculated constants was obtained as for the VYHH-VYNS series (Figs. 3–4). One of these materials, DE-3401 Natural (M.W. = 20,000), exhibited excellent agreement between cal-

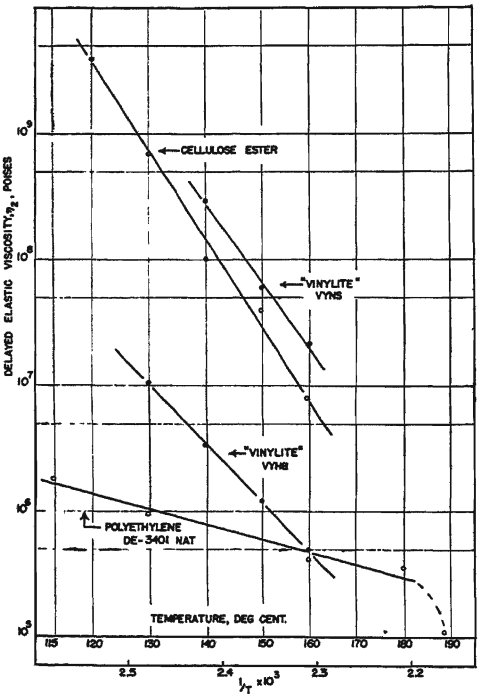

FIG. 15

Delayed Elastic Viscosity *vs.* $1/T$ Curves for Several Plastic Materials

culated and experimental load deflection curves as shown previously in Fig. 5. The detailed data are given in Tables III and IV.

The study of these materials throws more light on the behavior of delayed elastic effects, particularly in connection with the variation of the retardation time, τ_2, with temperature and molecular weight. Fig. 18 is a plot of log τ_2 *vs.* $1/T$ for the polyethylene compounds of four different molecular weights over a wide temperature range. The elastic effects disappear at 130°C. for the low molecular weight compound (12,000),

TABLE III

Viscoelastic Constants from Constant Load Experiments Polyethylene Resin Series

Temp. °C.	η_2, Poises $\times 10^6$	η_2, Poises $\times 10^6$	G_1, Dynes cm$^{-2} \times 10^4$	G_2, Dynes cm$^{-2} \times 10^4$	τ_2, seconds
		Wt. Av. Mol. Wt.: 12,000			
110	0.11	0.13	0.50	0.021	617
120	0.075	0.075	—	0.017	453
130	0.042	—	—	—	<50
160	0.012	—	—	—	—
		Wt Av. Mol. Wt.: 20,000			
115	2.0	1.8	2.2	0.67	281
130	1.3	0.97	2.5	0.38	259
160	0.38	0.43	2.0	0.25	172
180	0.24	0.36	1.8	0 23	159
188.5	0.19	0.11	1.5	0.22	49
		Wt. Av. Mol. Wt.: 25,000			
120	13	9.5	5.9	1.3	710
130	8.8	8.4	5.5	1.6	523
160	2.9	2.5	2 5	0.67	372
180	1 4	1.1	2.3	0.58	199
		Wt. Av. Mol. Wt.: 36,000			
130	190	76	33	13	610
180	59	24	12	4.9	490
190	40	25	7.3	5.3	472

TABLE IV

Viscoelastic Constants from Constant Plate Separation Experiments Polyethylene Resin Series

Wt. Av. Mol. Wt.	Temp. °C.	G_1', Dynes cm$^{-2} \times 10^4$	G_2', Dynes cm$^{-2} \times 10^4$	τ_1', Seconds	τ_2', Seconds
20,000	115	4.7	13	2600	137
25,000	130	0.14	4.1	1180	72
25,000	160	0.055	1.0	862	50
36,000	130	0.10	5.0	625	39

i.e., the $1/h^4$ *vs.* time curve at this temperature is straight from the start. Thus, all delayed elastic effects are "wiped out" within 1 minute (first h reading after load application). This means that τ_2 has to be less than 40–50 seconds, as otherwise the delayed elastic effects could be observed. A sharp drop occurs, therefore, in the log $\tau_2 - 1/T$ curve between 120°C. and 130°C. Similarly a sharp drop will be observed for the 20,000 molecular weight material (DE-3401 Natural) between 180°C. and 190°C. At 188.5°C. the elastic effects are still measurable with a 50 second value for τ_2. Thus, the effect of increasing molecular weight is to raise the tempera-

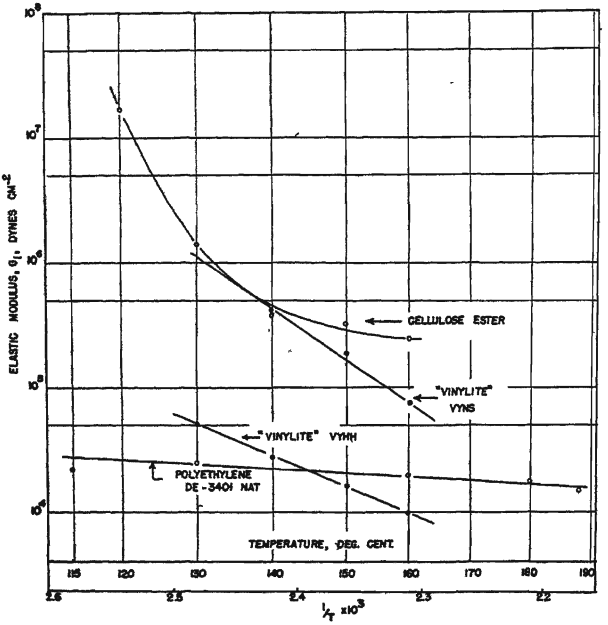

FIG. 16

Elastic Modulus, G_1, *vs.* $1/T$ Curves for Several Plastic Materials

ture at which delayed elastic effects become negligible. Up to this temperature, τ_2 shows an essentially linear log τ_2 *vs.* $1/T$ behavior. The higher molecular weight compounds fall in line with this interpretation as shown in Fig. 18. The log $\tau_2 - 1/T$ curves are not parallel, however, and a simple "retardation time-molecular weight" relation is not apparent.

A more regular behavior with changing molecular weight is observed for the delayed elastic viscosity (η_2) and modulus (G_2). The temperature characteristics for these constants are shown in Figs. 11 and 12. The modulus of the sudden elastic deformation, G_1, follows the same pattern. The values of the viscoelastic constants are increased by increasing the

molecular weight. The curves are not parallel and do not, in general, follow a linear log-$1/T$ relation over wide ranges of temperature. The η_2 and G_2 curves give somewhat of a clue concerning the mechanism by which elastic effects disappear. A rather sharp drop in η_2 is observed between 180°C. and 190°C. for the 20,000 M.W. compound which is associated with the corresponding change in τ_2. Since

$$\tau_2 = \eta_2/G_2$$

a sudden change in τ_2 means a sudden change in η_2 or G_2. Since G_2 changes very slowly in this range (Fig. 12) a decrease in η_2 is apparently primarily responsible for the disappearance of delayed elastic effects. Since the viscoelastic constants-temperature characteristics are usually not parallel, nor are they always straight lines (G_2 curve for 20,000 M.W. compound, for example), a simple interpretation of variation with molecular weight will only hold over limited ranges of temperature. It was found that G_2 at 120°C., and η_2 at 130°C. follow quite closely Flory's relation, *i.e.*, log G_1 (or η_2) linear in $1/T$. At other temperatures, deviation from this relation are observed. G_2 did not follow this relation at any temperature where experimental data were available.

As far as the empirical determination of weight average molecular weights is concerned, the only reliable method for these compounds is the measurement of the principal viscosity, η_3. This viscoelastic constant exhibits linear and essentially parallel log $\eta_3 - 1/T$ relations and obeys Flory's relation closely over a wide temperature range (3).

The effect of heterogeneity (distribution of molecular weights) on the viscoelastic constants was not investigated in this work. Some recent work by Zapp and Baldwin (9) on butyl polymers indicates that polymolecularity has a considerable effect on the elastic and delayed elastic components of the deformation.

c. Plasticized Cellulose Ester. The viscoelastic properties of a commercial cellulose ester were also determined (cellulose acetate butyrate (37% butyryl, 12% acetyl) plasticized with dibutyl sebacate). This work was done on molded pellet samples which were submitted by Committee D-20 of ASTM for round robin tests on flow temperature measurements. This material shows very interesting viscoelastic properties which are best considered in comparison with typical properties of vinyl chloride-acetate and polyethylene resin compounds.

The principal viscosity-temperature characteristics are shown in Fig. 13. Since all these materials show the proper normalization, average values only as obtained at various loads and volumes, are shown. Cellulose ester exhibits the usual linear log $\eta_3 - 1/T$ relation with a very high slope. A comparison of activation energies for viscous flow shows in a

very convenient manner the differences in temperature sensitivities:

Material	Activation energy for viscous flow, cal./mole
Cellulose ester	78,000
Vinyl chloride-acetate resin VYHH	60,000
Vinyl chloride-acetate resin VYNS	35,000
Polyethylene, DE-3401 Natural (M.W. 20,000)	11,000

The $1/h^4$ *vs.* time curves for cellulose ester are linear from the start above about 165°C. showing that delayed elastic effects become neg-

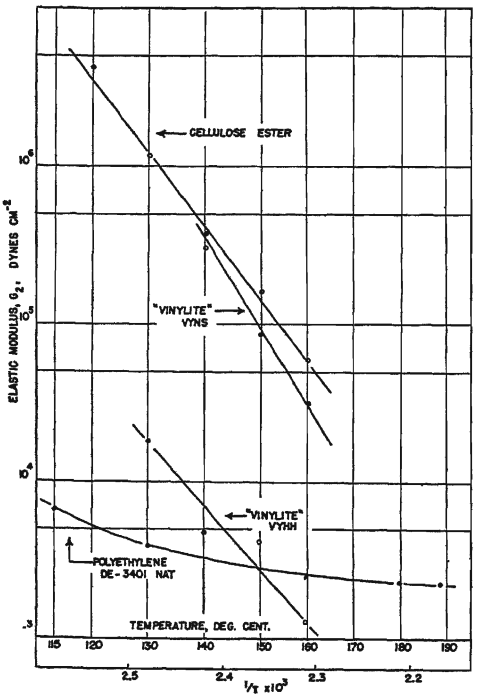

FIG. 17

Elastic Modulus, G_2, *vs.* $1/T$ Curves for Several Plastic Materials

ligible between 160°C. and 170°C. τ_2 at 170°C., therefore, must be less than 50 seconds. Below this temperature this material shows a linear log $\tau_2 - 1/T$ curve as shown in Fig. 14. The characteristics of the other curves have already been discussed.

The delayed elastic viscosity (η_2)-temperature relations are shown in Fig. 15. A typical viscosity behavior is shown for each compound. The sharp drop in the polyethylene curve between 180°C. and 190°C. was discussed earlier.

Figs. 16 and 17 illustrate the variation of the elastic moduli, G_1 and G_2, with temperature. The G_1 curve for cellulose ester and the G_2 curve for polyethylene are not straight while the others exhibit straight line behavior when plotted logarithmically *vs.* $1/T$ over the temperature range studied. It is possible that over a wider temperature range these constants would exhibit the well known typical inverted "S"-shaped stiffness-temperature curves.

Acknowledgments

The writer is indebted to Mr. F. D. Dexter for carrying out the high temperature stress-strain studies. Grateful acknowledgment is also made to R. F. Clash, Jr., and A. P. Wangsgard for many helpful discussions on various phases of this work.

Note: The necessity of correcting the sample volume in Eq. 4 to allow for thermal expansion is recognized.

References

1. Alfrey, T., *Quant. Appl. Math.* **2**, 113 (1944); **3**, 143 (1945).
2. Alfrey, T., and Doty, P., *J. Applied Phys.* **16**, 700 (1945).
3. Dienes, G. J., and Klemm, H. F., *J. Applied Phys.* **17**, 458 (1946).
4. Leaderman, H., Elastic and Creep Properties of Filamentary Materials and Other High Polymers. The Textile Foundation, 1943.
5. Lipka, J., Graphical and Mechanical Computation. J. Wiley and Sons, 1918.
6. Pendleton, W. W., *J. Applied Phys.* **14**, 170 (1943).
7. Reiner, M., Ten Lectures on Theoretical Rheology. Nordeman Publishing Co., 1943.
8. Tuckett, R. F., *Trans. Faraday Soc.* **39**, 158 (1943).
9. Zapp, F. L., and Baldwin, F. P., Am. Chem. Soc. Meeting, Atlantic City, April, 1946.

THE FUNDAMENTALS OF TACKINESS AND ADHESION

J. J. Bikerman

Present Address: Research and Development Division, Merck & Co., Inc., Rahway, New Jersey

Received Nov. 21, 1946

1. Introduction

Why does glue stick?

The reply to this query is given usually either in "chemical" and "molecular" terms, or in terms of mechanics and rheology. In the present paper an attempt is made to trace the relative importance of molecular and rheological effects at different stages of the adhesive action.

2. Application of Adhesives

Application of an adhesive to two solid surfaces transforms a system solid–surface layer–air–surface layer–solid into a system solid–surface layer–adhesive–surface layer–solid. Its primary function is displacement of air by the adhesive, but the adhesive can also mechanically displace or chemically alter one or both of the surface layers.

Displacement of air can be achieved always if one of the several known (more or less cumbersome) methods is resorted to, but usually capillary forces take care of this displacement without any deliberate assistance by the man in charge. Air is displaced by the adhesive because the latter wets the solids to be joined, *i.e.*, forms with them a contact angle of 0° or thereabout. The contact angle observed in a given system under given conditions often is determined by the previous history of the system and depends also on the roughness of the solid, but, nevertheless, it is above all a function of the chemical nature of the three phases in contact (*i.e.*, air, liquid adhesive, solids). Hence, the displacement of air is brought about primarily by molecular forces.

Chemical forces are responsible also for the interaction, if any, between the adhesive and the solids or their surface layers. A familiar example of such an interaction is met with in soldering various steels by means of tin solders: the interface between steel and solder contains crystals of $FeSn_2$ (1). According to Gurney (2) the adherence of rubber to brass is due to formation of copper sulfide crystals along the boundary of rubber (which contains sulfur) and brass (which contains copper).

3. The Tackiness

The term *tackiness* is used in different industries with slightly different meanings. Here the resistance is meant which must be overcome when separating two solids joined by an adhesive still in its liquid state.

For simplicity's sake we assume that the separation is achieved by a pull normal to the adhesive layer, see Fig. 1. In it, A and E are the solids jointed by the adhesive C, and B and D are the surface layers. When a pull (see the arrow) is applied to the system, equal tensions are produced at various cross-sections of the specimen, and the results of the experiment depend on the behavior of the various components of the system at the given stress.

When the adhesive is still liquid, the most probable result is "necking" and, finally, breaking of the adhesive film. For the initial stage,

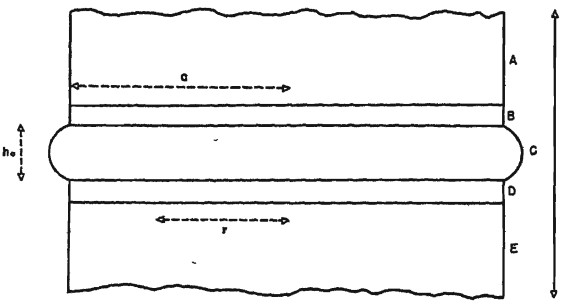

Fig. 1

Scheme of an Adhesive Joint.

A and E—solids. B and D—surface layers. C—the adhesive layer. The pulling force is applied in the direction of the arrow. h_0 is $\fallingdotseq$ the thickness of the adhesive layer, r is the variable distance of a point from the axis, and a is the radius of the specimen.

which is also the most important one of this process, J. Stefan (3), see also O. Reynolds (4) and H. Green (5), derived the following equation:

$$Ft = \frac{3\eta a^2}{4}\left(\frac{1}{h_1^2} - \frac{1}{h_2^2}\right). \tag{1}$$

F is the stress applied (*e.g.*, in g. cm.$^{-1}$ sec.$^{-2}$), t is the duration of its action (*e.g.*, in sec.), η is the viscosity of the liquid C (*e.g.*, in g. cm.$^{-1}$ sec.$^{-1}$), a is the radius of the specimen, h_1 the initial thickness of the adhesive layer, and h_2 that after the time interval t.

Since Stefan's paper is not easily accessible and Reynolds' mathematics too difficult, a proof of Eq. (1) is given here. It differs somewhat from those published previously.

When the distance h_0 between the plates A and E, see Fig. 1, is increased, the liquid flows from the bulges shown in the figure toward the

central part of the adhesive layer, and the stress F is that required to keep up the flow at the rate determined by the magnitudes h_1, h_2 and t.

Consider within the adhesive layer a cylinder, the axis of which coincides with that of the plates A and E and the radius of which is r. When h_0 increases by dh_0, the volume of this cylinder increases by $\pi r^2 dh_0$. Consequently, through the cylindrical surface of this part, the liquid volume $\pi r^2 dh_0$ must pass in dt sec., if the movement dh_0 is accomplished in time dt. The flow of liquid is nearly horizontal and centripetal. Obviously, some liquid rises when the upper plate is lifted but, as long as r is much greater than h_0, the vertical component of the flow may be neglected.

If the pressure within the liquid is P at the distance r from the axis and $P - dP$ at $r - dr$, then the centripetal movement is due to the pressure difference dP. The force on a ring confined between the vertical cylindrical surfaces r and $r - dr$ and the horizontal planes h and $h + dh$, is $2\pi r dh \cdot dP$. When the flow takes place without acceleration, this force must be equal and opposite to the viscous force acting on the same volume. The latter force is $\eta \frac{d^2u}{dh^2} \cdot 2\pi r dr \cdot dh$. Here u is the linear velocity of flow at the point (r, h). Equating the two forces yields relation (2):

$$\frac{d^2u}{dh^2} = -\frac{1}{\eta}\frac{dP}{dr}. \tag{2}$$

The right hand term of Eq. (2) is independent of h so that integration readily gives

$$u = -\frac{1}{2\eta}\frac{dP}{dr}h^2 + bh + c,$$

b and c being integration constants. Since du/dh must be equal to zero at $h = h_0/2$ from symmetry reasons, $b = \frac{h_0}{2\eta}\frac{dP}{dr}$. Since u is zero at $h = 0$ (no gliding along the wall), $c = 0$. Hence,

$$u = \frac{1}{2\eta}\frac{dP}{dr}h(h_0 - h). \tag{3}$$

The volume of liquid which traverses the cylindrical surface at r in dt sec. is

$$dt\int_0^{h_0} u \cdot 2\pi r \cdot dh = \frac{\pi r}{\eta}\frac{dP}{dr}dt\int_0^{h_0} h(h_0 - h)dh = \frac{\pi r}{\eta}\frac{dP}{dr}\frac{h_0^3}{6}dt. \tag{4}$$

It is equal to the volume increase per dt sec., *i.e.*, to $\pi r^2 dh_0$. Hence,

$$\frac{dh_0}{h_0^3} = \frac{1}{6\eta r}\frac{dP}{dr}dt. \tag{5}$$

Eq. (5) shows the relation existing between the rate of rise of the upper plate and the pressure gradient within the liquid. But Eq. (1) connects the rate of rise with the stress F. Consequently, the relation between P and F has to be found first.

The total force lifting the upper plate is $\pi a^2 F$ because πa^2 is the area of the plate. It is equal to P multiplied by the area on which P acts, *i.e.*,

$$\pi a^2 F = \int_a^0 P \cdot 2\pi r dr, \tag{6}$$

if the atmospheric pressure is set equal to zero.

As Eq. (5) shows, $\frac{1}{r}\frac{dP}{dr}$ is independent of r (because $\frac{1}{h_0^3}\frac{dh_0}{dt}$ is independent of r). Hence $P = kr^2 + m$, k and m being constants. Since $P = 0$ at $r = a$, $m = -ka^2$, *i.e.*, $P = -k(a^2 - r^2)$. Introducing this expression into (6) we obtain

$$\pi a^2 F = -2\pi \int_a^0 k(a^2 - r^2) r dr = \frac{\pi k a^4}{2}.$$

Hence, $k = 2F/a^2$, $P = 2F\left(\frac{r^2}{a^2} - 1\right)$, and $\frac{1}{r}\frac{dP}{dr} = \frac{4F}{a^2}$.

Equation (5) then gives

$$\frac{dh_0}{h_0^3} = \frac{2F}{3\eta a^2} dt$$

or, after integration,

$$\frac{1}{h_1^2} - \frac{1}{h_2^2} = \frac{4F}{3\eta a^2} t$$

which is identical with (1).

The tackiness equation (1) has several important implications.

(a) There is no definite force opposing the breaking of the joint. The resistance to separation depends on the rate of separation.

(b) The whole process of separation occurs within the liquid layer so that the forces between the adhesive and the solids A and E are not involved at all. The phenomenon is of purely rheological nature.

(c) The product Ft is greater the smaller the original clearance between the solids A and E, *i.e.*, the magnitude h_1. Presumably, in very many tests—as in the original experiments by Stefan—the product Ft is inversely proportional to the square of the thickness of the adhesive layer.

(d) The product Ft is proportional to the viscosity of the adhesive. This again shows the importance of displacing air from the surface of the solids to be joined. If there is a channel, open to air, between a solid and

the adhesive, air may move into it and equalize the pressure before the liquid is forced in. Since the viscosity of air is some 10,000 or 100,000 times smaller than that of usual adhesives in the moment of application, the rate of the infiltration of air is 10,000 to 100,000 times that of the adhesive, for equal dimensions of the channel.

The limits of the applicability of Stefan's equation are important. One of these limits is discussed in Section 4. Another is indicated by the assumption that the viscosity η is independent of the gradient of velocity. An analog of Eq. (1), valid for non-Newtonian liquids, has not been derived as yet. A third limitation is dealt with in the following paragraph.

The right-hand side of Eq. (1) is independent of time t. Hence, F is inversely proportional to t. When t is very small, *i.e.*, when the joint is broken with a jerk, F as given by Eq. (1) may become greater than the ultimate tensile strength of one of the solids jointed: in this case the rupture occurs within the solid, not within the adhesive. Instances of this behavior are very common when the solids have low strengths, *e.g.*, when paper or cardboard are used. Slow peeling movement may separate a freshly applied adhesive stamp from the envelope, but a rapid movement will tear either the stamp or the envelope. A numerical example will show the position of this limit. Let η be 10 g. cm.$^{-1}$ sec.$^{-1}$, h_1 10^{-3} cm., h_2 very large, and a^2 13.33 cm.^{2}; then Ft is 10^8 g. cm.$^{-1}$ sec.$^{-1}$. If t is 1 sec., F is 10^8 g. cm.$^{-1}$ sec.$^{-2}$, *i.e.*, within the region of the tensile strength of structural carbon or hard rubber. A further reduction of h_0 or t would readily shift F into the region of the strength of metals.

If surface layers on the solids were not eliminated, that is, if the solids were not "clean," the rupture may occur within one of these layers.

4. The Setting of Adhesives

The processes taking place in the layer of adhesive after its application can have any of several different mechanisms. Glue can be applied hot and "set" because of cooling. It can be applied dilute and "set" because of evaporation of the solvent or its diffusion into porous solids. Setting can be due to chemical reactions either between the components of the adhesive (as in plaster of Paris or some synthetic resin adhesives) or between the adhesive and an adjacent solid. Often two or more of the above mechanisms operate simultaneously

Whatever the mechanism, the setting of an adhesive results in an increase in its viscosity or, more generally, its resistance to deformation and rupture. When the viscosity becomes very high, even if it continues to be a true Newtonian viscosity, Stefan's equation (1) loses its validity.

For highly viscous substances Eq. (1) predicts values of F much in excess of the tensile strength of the best structural materials. Assuming

again h_2 to be very large, h_1 to be 10^{-3} cm. and $a^2 = 13.33$ cm.^{2}., but taking η equal to 10^5 g. cm.$^{-1}$ sec.$^{-1}$, we find $Ft = 10^{12}$ g. cm.$^{-1}$ sec.$^{-1}$. Some bitumens and slightly plasticized rosins, see, *e.g.*, (6), have Newtonian viscosities of the order of 10^5. Hence, a bitumen or rosin joint should be able to withstand a stress of 10^{12} g. cm.$^{-1}$ sec.$^{-2}$ for 1 sec. or a stress of 10^9 g. cm.$^{-1}$ sec.$^{-2}$ for 16 min. The ultimate tensile strength of copper is about 3×10^9, and of steel about 7×10^9 g. cm.$^{-1}$ sec. $^{-2}$. Common experience shows that bitumen, rosin and similar joints are not stronger than copper for 5 min. or stronger than steel for 2 min. They fail immediately at much smaller stresses.

Inspection of these joints after rupture shows that the mechanism of rupture was totally different from that postulated in Stefan's theory. There was no inward flow of the adhesive from the periphery of the joint; there was no visible flow at all; the adhesive did not move but a crack advanced along the whole layer.

Stefan's theory assumes the adhesive to be "liquid," but in these tests it behaves like a "solid." The difference revealed here between "liquid" and "solid" has no connection with any yield point. As mentioned above, the adhesive is a Newtonian liquid also after setting. When the stress applied is small, the adhesive flows according to the laws of hydrodynamics. The difference between "liquid" and "solid" in these tests is of another kind which, perhaps, has not received sufficient attention so far.

When stress is applied to a "liquid," the whole liquid sample becomes involved. The changes caused by the stress depend on the bulk properties of the liquid and also on the shape and dimensions of the sample. In Eq. (1) the relation between the effects of a stress and the dimensions of the sample is disclosed by the magnitude a^2 in the right-hand term. The stress F is force divided by area, but this division does not make F independent of a. The ultimate tensile strength of "solids," *i.e.*, breaking force divided by cross-section, is at a first approximation independent of the cross-section. It is determined above all by the properties of the weakest spot of the "solid." Rupture occurs when this weakest spot breaks down, although the bulk of the specimen is still undamaged and is capable of supporting much higher stresses. Foreign inclusions in a "solid" very often form its weakest spots and reduce its tensile strength. Foreign inclusions (air bubbles, dust particles, *etc.*) in a "liquid" usually increase its viscosity, if they alter it at all.

Perhaps the above difference between "liquids" and "solids" can be formulated as follows: resistance to separation of "liquids" is a bulk property, and resistance to separation of "solids" is a topical property. In this respect the latter is similar to many instances of corrosion resistance. Corrosion often starts at the boundary of the parent metal and

an inclusion and can be very extensive although the inclusion is quite small.

I made some experiments[1] to study the frontier between liquids and solids as just defined. The apparatus, which is called the penetroviscometer and which will be described in detail elsewhere, consists of a small vertical brass rod sinking in a vertical glass tube filled with an adhesive. The axis of the rod coincides with that of the tube. The theory of the instrument is similar to that of coaxial cylinder viscometers, see, *e.g.*, (7), except that the area of contact between the rod and the adhesive increases in time. From this point of view the instrument is similar to penetrometers. Hence its long and compound name.

When the brass rod slowly descends in plasticized rosin, the rate of its movement agrees quantitatively with the theory derived for Newtonian liquids. Plasticized rosin is a true liquid when tested by slow penetration.

To test the adhesiveness of rosin, the instrument was turned upside down. Now the system can be described as brass rod glued to coaxial glass tube with a rosin adhesive, and, when because of gravitation the rod gradually slid out of the tube, that was a slow rupture of an adhesive joint.

In theory, the movement of liquid in this second experiment is almost exactly the inverse of the movement taking place in penetration experiments, and the time required for, say, 1 cm. of the rod to emerge from the adhesive should be nearly equal to that required to increase the penetration by 1 cm. This consequence of the theory is confirmed by experiment for the very beginning of the sliding out. If the brass rod required t sec. to increase the immersion from x to $x + 0.05$ cm. and the instrument was reversed immediately afterwards, then again t sec. elapsed before the immersion decreased from $x + 0.05$ cm. to x cm. However, the two time intervals were not identical if, say, the movement from x to $x + 1$ cm. was compared with that from $x + 1$ cm. to x cm. The withdrawal always was more rapid than the penetration, just as the rupture of a rosin or bitumen joint takes place in a time shorter than t in Stefan's equation.

Just as a crack in a solid grows "autocatalytically" and finally causes rupture, a casual indentation of the lower glue surface shows an "autocatalytic" growth, and the brass rod falls out soon after the "crack" has reached its front and an air bubble has formed above the rod. Fig. 2 schematically shows four stages in the propagation of a "crack."

The mechanism of this effect seems clear. Since the vertical distance between the apex of the indentation and the front of the rod is smaller than that between the front of the rod and any other point of the air-

[1] In the Laboratories of The Printing and Allied Trades Research Association, London, England.

adhesive interface, the pressure gradient above the indentation has a maximum value. Therefore, the air rises here more rapidly than in other parts of the adhesive. The difference of the pressure gradients above the indentation and elsewhere increases when the depth of the indentation increases, *i.e.*, the growth is self-accelerating.

On the contrary, when the rod immerses deeper into the liquid (pene-

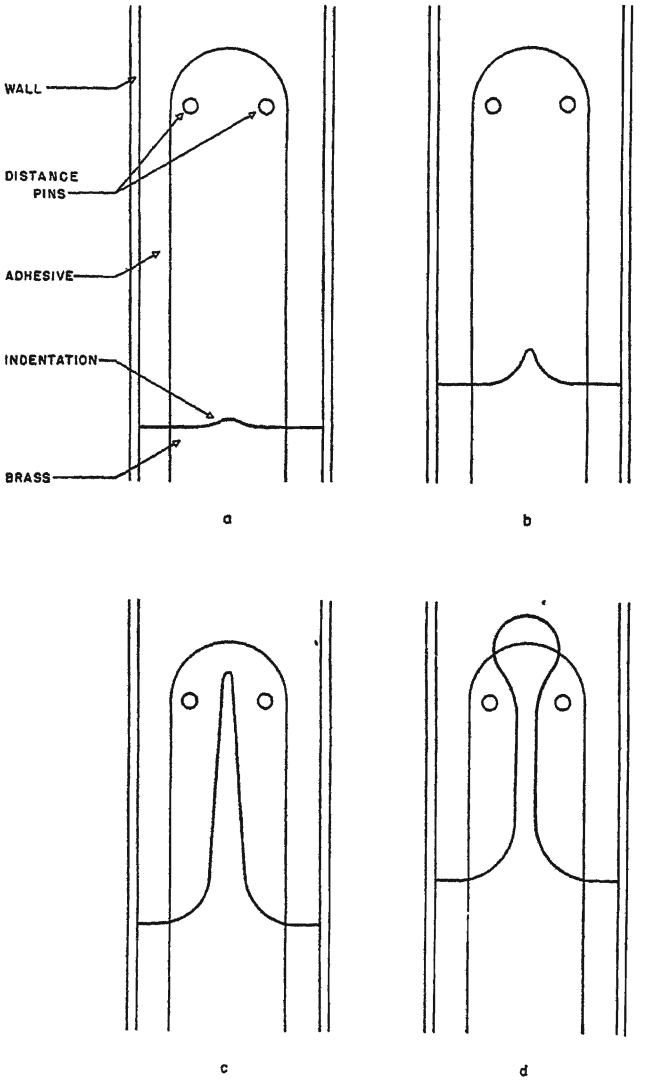

FIG. 2

Four Consecutive Stages in the Growth of an Indentation in the Adhesive Column.

tration experiment), the difference in pressure gradients along the air-adhesive interface helps to fill up the hollows and depress the hills. The geometry of the experiment makes the adhesive behave as a liquid in the penetration test and as a solid in the withdrawal test.

In addition to the geometry, the speed of the experiment determines whether the adhesive behaves as a "liquid" or a "solid." If the deformation caused by the external agent is so slow that the intrinsic forces can keep up the continuity of the specimen, the specimen is a "liquid"; otherwide, the deformation is topical and the specimen is a "solid." The intrinsic forces tending to preserve the continuity include above all gravitation (this force is proportional to the difference in the specific gravities of specimen and air) and surface tension. The movement caused by the intrinsic forces is the more likely to be as rapid as that caused by the external agent, the weaker this agent and the smaller the viscosity of the specimen. All the cumbersome reasoning of this paragraph is intended to give physical interpretation to the following 3 simple observations: (a) when a glass rod is withdrawn from water, no hole remains where it was, (b) when a glass rod is very slowly (say, within a month) withdrawn from an asphalt or plasticized rosin, there again is no hole, and (c) a more rapid (say, within an hour) withdrawal of the rod from asphalt or rosin leaves a hole behind. When gravitation, surface tension and other forces of preservation are assisted by hydrostatic pressure, solids lose some of their brittleness. P. W. Bridgman's paper (8) read at the present meeting contains examples of this effect.

5. The Final Strength of Adhesive Joints

The state of the adhesive in a joint rapidly changes after application because of cooling, evaporation of the solvent, chemical reactions, *etc.*; but after a while any further changes usually become so slow that it is possible to speak of the final state of the joint and its final strength.

When a joint is stressed to determine its final strength, the rupture occurs within the weakest link which can be in one of the solids, in one of the surface layers, or in the adhesive. An identical remark has been made in Section 3 in regard to tackiness.

When the rupture takes place within a solid—this happens as a rule with paper or cardboard—the properties of the adhesive and its adhesion to the solid are not involved. When a surface layer breaks, this generally indicates insufficient cleaning of the original solid. The strength of the adhesive is determined only when the break passes through the adhesive.

In this case it seems obvious that, in tensile tests, the final strength of a joint is the tensile strength of the solidified adhesive in it. Then two observations require interpretation. One is that the thinner the joint the

greater its strength. The other is that the joint strength often is greater than the tensile strength of solidified adhesive in bulk, see, *e.g.*, (9, 10, 11).

The increase in strength observed on diminishing the thickness of the adhesive layer was attributed (12) to attractive forces between the two solids A and E, see Fig. 1. If such forces exist, and if their intensity increases when the distance between the solids is reduced within the limits of, say, 0.1 cm. to 0.001 cm., then both above-mentioned observations would find their explanation. Then the joint strength would not be identical with the tensile strength of the solidified adhesive.

However, the inducement to postulate long-range molecular attractions vanishes as soon as it is realized that tensile strength depends on the length of the specimen (13). The tensile strength of textile threads (14, 15, 16), of glass fibers and yarns (17), *etc.*, is greater the shorter the specimen. Statistical analysis of the data shows that the effect is due entirely to the higher probability of a very weak spot in a longer specimen (14, 16, 17). The shortest specimens used in these experiments were of the order of 1 cm., but there is no reason to doubt the validity of the probability laws also for much shorter specimens, such as the films of solidified adhesive within joints. On this view thin joints are stronger than thick joints because the presence of a bad flow is more probable the bulkier the specimen; and the adhesive *in situ* is stronger than an independent specimen of the same adhesive because the independent specimens are much bulkier.

Apparently only one attempt to check this view was published (13). Paraffin wax joints of two thicknesses (roughly 0.005 and 0.05 cm.) were prepared between a steel rod and a brass plate. As usual, the thinner joints were stronger, and statistical analysis demonstrated that about $\frac{2}{3}$ of the difference between thick and thin joints was accounted for by the probability alone. The rest was attributed to the different conditions of setting in thick and thin joints. New experiments to test the theory would be highly welcome.

As far as the available evidence goes, the strength of adhesive joints is nothing but the strength of the solid adhesive in the joint. Since, according to the prevalent opinion, the strength of solids is determined by the flaws more than by molecular forces, the strength of joints, too, has a "mechanical," not a "molecular," nature.

Rupture within the adhesive layer is a very common phenomenon, but sometimes the break seems to occur at the boundary between the adhesive and one of the solids jointed. In this case, it might be inferred, the strength of the joint would be a direct measure of the molecular attraction between solid and adhesive. However, closer examination shows that "boundary breaks" occur practically only when a wrong adhesive was used, *e.g.*, a dextrin paste on ordinary (*i.e.*, greasy) metals.

In such instances failure can be due, among other causes, (a) to insufficient wetting; then the adhesive in many places is from the very beginning separated from the solid by air, and the rupture surface passes from one air inclusion to another; (b) to the presence of grease on the metal surface; then the grease (a surface layer) gives way; or (c) to changes which took place during the course of setting.

As to (c): If the contact between adhesive and solid was good in the beginning, it can deteriorate later on. Shrinkage processes associated with the drying of the adhesive, alterations of its dimensions caused by variable humidity and variable temperature, crystallization phenomena and so on, can create in the system stresses which may result in cracks within one of the solids, within the adhesive, or between the adhesive and one of the solids. The necessity of adjusting the thermal expansion coefficients of metal and glass when sealing metal wire into glass tubing was recognized long ago. This is a good indication of the perils attending upon the solidification of an adhesive. The unyielding metal does not follow the shrinkage and swelling of dextrin paste, and the link between the two is readily broken before any external force is applied.

That still leaves us with the problem of why a clean separation between adhesive and a solid (in the absence of surface layers) apparently never occurs. Does this mean that the forces between two dissimilar compounds are always greater than those between identical molecules?

The reply is *no*. To support this reply in the negative it seems profitable first to look into another problem. When a solid (say, a metal rod) is broken and the freshly exposed ends are brought in contact again, why does no healing occur? The molecular forces known to us are reversible. If a row of metal atoms is first removed from, and then again placed next to another similar row, the forces between the neighboring rows are exactly as great as before separation. It should be possible, then, to restore the original metal rod simply by fitting together the fracture faces.

The reason for the very different behavior observed is obvious. Immediately after separation the exposed surfaces adsorb air, moisture, *etc.* When the fragments are brought into "contact," only air touches air, or water touches water, *etc.*, and for a new separation only an air or water film needs to be broken.

This cause can sometimes be eliminated by persistent degassing of the rod before the rupture and by carrying out the rupture and contact in a high vacuum. Under these conditions some physicists succeeded in observing sticking between two pieces of metal (18). However, the force required to overcome this sticking was a small fraction of the breaking load of a similar unbroken metal. Here another cause operates. In all probability, the attraction between the fragments is small compared with that within a metal because the fragments touch each other only in relatively few

points. The rupture faces are rough, and it is impossible to fit every elevation on one face into the corresponding depression on the other. Probably, there is very often no "corresponding" depression at all, since rupture releases stresses within the solid and these stresses alter the profile of the surface.

The roughness of solid surfaces seems to supply the explanation also for the general absence of separation between adhesive and a solid. The boundary between adhesive and solid is a complicated surface, and its area is considerably greater than the cross section of the solid or the adhesive layer. Near the adhesive-solid boundary a butt joint is a multitude of scarved joints. The stress (force:area) is consequently smaller there than within the bulk phases. The truth of this explanation is evident when the solid is porous (*e.g.*, paper, fabrics), but the phenomena on non-porous surfaces probably differ only in the degree.

Presumably, the area effect is not the only one connected with roughness. It is improbable that the rupture follows any one predetermined surface, whether within a bulk phase or at their boundary, but a quantitative treatment of this probability has not been attempted yet.

6. Summary

The paper compares the importance of "molecular" forces with that of "rheological" forces on different stages of making and breaking adhesive joints.

Adhesives usually are applied in liquid form, and the perfection of the contact between the adhesive and the solids to be joined depends above all on the wetting power of the liquid toward the solids. This wetting power is primarily a "molecular" phenomenon.

The resistance which must be overcome to separate two solids jointed by a liquid adhesive is tackiness. Its mechanism is purely rheological, and tackiness is a function of viscosity. When in the course of its setting the viscosity of an adhesive becomes very high, the resistance to separation is still rheological, but is smaller than would be expected from the viscosity. Some new experiments concerning this intermediate region between tackiness and final strength are reported.

When the adhesive has set, the resistance to separation is determined by the final strength of the adhesive, which (for tensile tests) is identical with the tensile strength of the adhesive film of the given thickness; the final strength, too, is a rheological property. The experiments which are claimed to prove disagreement between final strength and tensile strength are given a different interpretation. The rupture occurs usually within the set adhesive, not between the adhesive and a solid, and consequently molecular forces are not involved in the determination of final strength, probably because of the universal roughness of solid surfaces.

References

1. Romig, O. E., *Metal Progress* **42**, 899 (1942).
2. Gurney, W. A., *Trans. Inst. Rubber Ind.* **20**, 205 (1945); *Chem. Abstracts* **39**, 5543 (1945).
3. Stefan, J., *Sitzber. Akad. Wiss. Wien, Math.-naturw. Kl., Abt. II* **69**, 713 (1874).
4. Reynolds, O., *Trans. Roy. Soc. (London)* **177**, 190 (1886).
5. Green, H., *Ind. Eng. Chem., Anal. Ed.* **13**, 632 (1941).
6. Traxler, R. N., Schweyer, H. E., and Moffatt, L. R., *Ind. Eng. Chem.* **29**, 489 (1937).
7. Lawaczeck, F., *Z. Ver. deut. Ing.* **63**, 677 (1919); Bridgman, P. W., *Proc. Am. Acad. Sci.* **61**, 57 (1926).
8. Bridgman, P. W., *J. Colloid Sci.* **2**, 7 (1947).
9. Crow, T. B., *J. Soc. Chem. Ind.* **43**, 65T, 69T (1924).
10. Konstantinova, V. P., *Acta Physicochim. U. R. S. S.* **1**, 286 (1934).
11. Van Roy, L., *Paper Ind. and Paper World* **25**, 1102 (1944).
12. McBain, J. W., and Lee, W. B., 3rd Report of the Adhesives Research Committee, Dept. Sci. & Ind. Res., London, 1932.
13. Bikerman, J. J., *J. Soc. Chem. Ind.* **60**, 23 (1941).
14. Peirce, F. T., *J. Textile Inst.* **17**, T355 (1926); **18**, T475 (1927).
15. Brown, K. C., Mann, J. C., and Peirce, F. T., *J. Textile Inst.* **21**, T186 (1930).
16. Bellinson, H. R., *Textile Research* **10**, 287 (1940).
17. Bikerman, J. J., unpublished.
18. Holm, R., and Kirschstein, B., *Wiss. Veröffent. Siemens-Werken* **15** I, 122 (1936); **18** II, 73 (1939).

THE BINGHAM VISCOMETER AND VISCOSITY STANDARDS [1]

James F. Swindells [2]

From the National Bureau of Standards, Heat and Power Division, Washington, D. C.

Received Nov. 25, 1946

Introduction

For a number of years the National Bureau of Standards has been concerned with precise viscosity measurements in connection with the issuance of Standard Viscosity Samples for use in the calibration of viscometers. The viscosities of these samples are determined by the variable-pressure method, employing the Bingham viscometer. The value of 0.01005 poise for the absolute viscosity of water at 20°C. is used as the primary standard, and the viscosity values of the Standard Samples are based upon this value for water.

A critical study of the various factors involved in viscosity measurements by this method has resulted in some departures from the usual techniques described in the literature. The method described is not intended for routine work but is adapted rather to conditions where speed or simplicity can be subordinated to accuracy.

Technique with the Viscometer

General

The general construction of the Bingham viscometer is illustrated in Fig. 1. A detailed description of its advantages and use is given by Bingham and others (1–6) and, primarily, only departures from the usual techniques with the instrument will be dealt with here.

With the usual procedure the mean rate of flow during a determination is measured by the time required for the left bulb, A (Fig. 1), to empty or fill depending upon the direction of flow in the viscometer. Measurements made in this manner involve drainage errors (7, 8) which are complicated to evaluate with sufficient accuracy. To avoid the necessity of such corrections, the flow is always made in the right-to-left direction and into a dry bulb. To accomplish this the sample is introduced from a pipette into the bulb B, sufficient liquid being added to fill the viscometer, at the temperature of test, between the marks d and g. Care is taken to avoid wetting the bulb above the line d. The liquid is

[1] Presented before the Society of Rheology, New York, Nov. 2, 1946.

[2] Associate Physicist, National Bureau of Standards.

drawn back and held below the line d until the temperature of test is reached. Pressure is then applied to the right limb and the time required for the meniscus to pass between the two fiducial marks c and d is observed. For each viscosity measurement the viscometer is cleaned and dried, and a fresh sample is introduced. By this procedure the volume of flow is kept constant regardless of the viscosity or rate of flow.

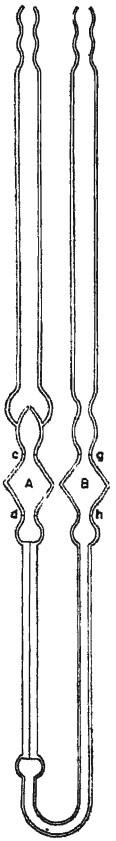

FIG. 1
The Bingham Viscometer

While the importance of accurate temperature and time measurement can hardly be emphasized too strongly, the precautions to be taken are well known and will not be repeated here.

Pressure is applied to the liquid in the viscometer by means of air supplied from a tank having a capacity (about 60,000 cm.^{3}) sufficiently large that the increase in volume in the pressure system during the flow of liquid from bulb B (about 4 cm.^{3}) causes no significant reduction in pressure. The tank is thermally lagged to prevent rapid changes in its temperature with fluctuations in the ambient temperature. This method of controlling the applied pressure has been found more satisfactory than the usual methods involving pressure regulators. Pressures are generally limited to a minimum of 200 mm. Hg to assure sufficiently accurate measurements by means of a mercury manometer and to eliminate the necessity of correcting for the varying head of liquid in the viscometer (3). Most of the measurements are made with pressures in the range 300 to 600 mm. Hg.

Calibration with Water

One of the important advantages of the Bingham viscometer is that its constants can be evaluated using a single calibrating liquid at a single temperature. It is general practice at the present time to assume the value of 0.01005 poise for the viscosity of water at 20°C. and to base subsequent viscometric measurements upon this value.

The usual form of the modified Poiseuille equation for the calculation of viscosity by the capillary method is

$$\eta = \frac{\pi r^4 P t}{8V(l+\lambda)} - \frac{m\rho V}{8\pi(l+\lambda)t}, \qquad (1)$$

where r = radius of capillary, P = mean effective pressure difference across the capillary, V = volume of flow, t = time for volume V to flow, l = length of capillary, λ = correction to length of capillary, m = coefficient of the second or "Kinetic Energy" term, and η and ρ are the viscosity and density of the liquid whose viscosity is to be determined. Since m and λ can be taken as constant for square-cut capillaries over a

considerable range of flows (9), certain of the quantities in Eq. (1) may be grouped to give two constants for the instrument. Eq. (1) then takes the form

$$\eta = CPt - C'\rho/t, \tag{2}$$

where

$$C = \frac{\pi r^4}{8V(l + \lambda)} \text{ and } C' = \frac{mV}{8\pi(l + \lambda)}.$$

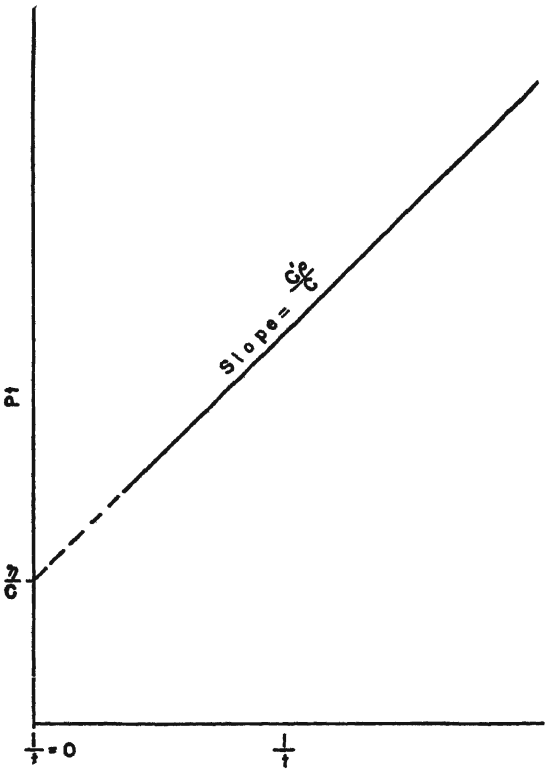

FIG. 2
Graphic Solution of Instrumental Constants

With water at 20°C. in the viscometer, times of flow are measured for various applied pressures. The product Pt is then plotted against $1/t$, and the two constants are evaluated from the resulting straight line as illustrated in Fig. 2. The solid line which represents the data points is extrapolated to the Pt axis, at which $1/t = 0$, as is shown by the broken line in the figure. The value of Pt at this intercept is then η/C and the slope of the line is $C'\rho/C$. Substituting the value of η, the instrumental constants C and C' are readily calculated. The value of C is independent

of temperature and the change of C' with temperature is usually not significant.

Calibration of the Viscometers with Larger Capillaries

In order to cover any considerable range of viscosity measurement, a series of viscometers having larger capillary diameters than are suitable for calibration with water must be employed. The dimensions of these viscometers are such that the second term in Eq. (2) can usually be neglected and only the constant C is evaluated. In the few cases where the value of this second term is not negligible an approximate value for C' is obtained from the dimensions of the instrument and taking $m = 1.12$. The viscosities of the oils used in calibrating these viscometers are based upon determinations made in the water-calibrated instrument.

Change of Viscosity with Pressure

When viscosities of petroleum oils are being determined in viscometers where an external pressure is applied, consideration must be given to the change of viscosity of the oils with pressure and values of viscosity reduced to some standard pressure such as atmospheric. To introduce this effect of pressure as a correction to the viscosity equation, use is made of a relation for the change of viscosity of petroleum oils with pressure developed by Cragoe (10). His investigation of the available data on the viscosity of oils at high pressures shows that such data are well represented in terms of the pressure coefficient β, defined by

$$\beta \equiv \frac{L_{p=l} - L_p}{L_p(p - l)} \text{ or } \frac{-\Delta L}{L\Delta p}, \tag{3}$$

where p is in atmospheres and L is defined by

$$\eta = Ae^{B/L}, \tag{4}$$

in which $A = 5 \times 10^{-4}$, $B = 1000 \ln 20 = 2995.74$, and η is in poises. Writing Eq. (4) as $\ln \eta = \ln A + \frac{B}{L}$ and differentiating gives

$$\frac{d\eta}{\eta} = -\frac{B}{L^2} dL \tag{5}$$

or using small finite changes and Eq. (3)

$$\frac{\Delta\eta}{\eta} = -\frac{B\Delta L}{L^2} = \frac{B\beta\Delta p}{L}. \tag{6}$$

From Eq. (4), $\frac{B}{L} = \ln 2000\,\eta$ which gives

$$\frac{\Delta\eta}{\eta\Delta p} = \beta \ln 2000\,\eta = F, \tag{7}$$

where F is a factor representing the fractional change in η for unit change in pressure. Thus the fractional correction to η depends upon η and also upon β, which is found to be approximately constant, independent of both pressure and temperature. With p expressed in atmospheres, β is found to vary from 2.7 to 3.9×10^{-4} for a wide variety of petroleum oils (kerosene to cylinder oil). As a rough approximation β is taken as 3×10^{-4} with some indication that this value is good to about 10% except for strongly naphthenic or asphaltic oils where it may be in error by as much as 30%. From Eq. (7), converting to common logarithms, with Δp in mm. of Hg and η in poises, $F = 3.00 \times 10^{-6} + 0.91 \times 10^{-6} \log \eta$. Since the effective pressure in the capillary is one-half the observed pressure with one arm open to the atmosphere, for the Bingham viscometer $F = 1.50 \times 10^{-6} + 0.455 \times 10^{-6} \log \eta$. Introducing this correction in Eq. (2), the viscosity at a pressure of one atmosphere is calculated by

$$\eta = CPt - \frac{C'\rho}{t} - FP\eta. \tag{8}$$

For convenience η is plotted against F on semi-logarithmic paper and, from the straight line which results, F is obtained for any desired value of η.

This correction is always small, 0.1% being about the maximum encountered, so that an uncertainty in β of even 30% would mean an uncertainty of only 0.03% in the viscosity.

Change of Viscosity with Dissolved Air

While the viscosity of water is not significantly affected by the solution of air under the conditions encountered here, consideration must be given to changes in the viscosity of oils from this cause. In practice it has been found that, unless relatively high pressures are applied to the more fluid oils, the rate of diffusion of air into the samples apparently will be so slow as to have no significant effect upon the viscosities.

Viscosity Standards

Assuming the value of 0.01005 poise for the absolute viscosity of water at 20°C. as a primary standard, it is often required to calibrate viscometers with capillaries of the larger sizes in terms of this standard without the necessity of first calibrating a smaller capillary with water. Where this is desirable the calibrations may be effected with certain other liquids of known viscosity.

The viscosity of solutions of sucrose in water are known with considerable accuracy in the temperature range 0 to 40°C., and these solutions may be used as calibrating fluids. Viscosity values for various concentrations of sucrose in water are given in the National Bureau of Stand-

ards Circular 440 (Polarimetry, Saccharimetry and the Sugars). The useful range covered is roughly 0.01 to 40 poises. However, in some cases the use of these solutions may not be entirely satisfactory due to the extreme precautions which must be taken in their preparation and in guarding against changes in concentration caused by evaporation during use.

It is considered more satisfactory, where possible, to employ one of the viscosity standards available either from the National Bureau of

TABLE I

Approximate Viscosities of Standard Viscosity Samples Available from the National Bureau of Standards

Oil	Absolute viscosity, poises		Kinematic viscosity, stokes	
	20°C.	100°C.	20°C.	100°C.
D	0 021	0.0064	0.026	—
H	.075	.014	.091	0 018
I	.12	.018	.15	.023
J	.21	.024	.25	.030
K	.41	.032	.48	.041
L	1.0	.048	1.2	.060
M	2.7	.096	3.1	.12
N	13.	.24	15.	.30
OB	350.	1.7	390.	2.1
P*	(490. at 30°C.)	5.0	(550. at 30°C.)	5.9

* Not supplied for use at temperatures lower than 30°C.

Standards or the American Petroleum Institute. These standards are reasonably stable hydrocarbon oils whose viscosities are known accurately based on the value of 0.01005 poise for the absolute viscosity of water at 20°C. Approximate viscosity values at 20 and 100°C. for the National Bureau of Standards oils are given in Table I. Values at intermediate temperatures are also available. Approximate viscosity values for the oils available from the American Petroleum Institute are given in Table

TABLE II

Approximate Viscosities of Oils Available from American Petroleum Institute Kinematic Viscosity in Centistokes

Oil	100°F.	122°F.	210°F.
Alpha	66	—	8
Beta	380	87	24
Gamma	3	—	—

II. Values for these oils are supplied only at the temperatures indicated in the Table.

The viscosity of water at several temperatures is commonly used for calibrating kinematic viscometers of the Ostwald type having small capillaries. Unfortunately the reliability of some of the data appearing in the literature on the viscosity of water at various temperatures is open to question. Probably the most accurate values available are defined by Cragoe's equation which is given by Coe and Godfrey (11). Viscosity values for water in the range 10–60°C., based upon this equation, are given in Table III.

TABLE III

Viscosity of Water at Various Temperatures

Temp., °C.	Viscosity		
	Relative[a] η/η_{20}	Absolute[b] centipoises	Kinematic[c] centistokes
10	1.3035	1.3100	1 3104
15	1.1358	1.1415	1.1425
20	1.0000	1.0050	1.0068
25	0.8885	0.8929	0.8956
30	0.7959	0.7999	0.8034
40	0.6518	0.6551	0.6602
50	0.5460	0.5487	0.5554
60	0.4659	0.4682	0.4762

[a] Values defined by

$$\log \frac{\eta}{\eta_{20}} = \frac{1.2348(20 - t) - 0.001467(t - 20)^2}{t + 96}.$$

[b] Computed from (*a*) with $\eta_{20} = 1.0050$ cp.

[c] Computed from (*b*) using densities from International Critical Tables in *g./ml.* and converting to g./cm.^{3}, using 1 ml. = 1.000027 cm.^{3}

Summary

The technique used with variable-pressure viscometers of the Bingham type for evaluating the viscosities of Standard Viscosity Samples at the National Bureau of Standards is described. Corrections for internal head, drainage and change of viscosity with pressure are accounted for or rendered negligible. A graphical solution of the equation for laminar flow in capillary tubes is employed to determine the instrument constants.

The value of 0.01005 poise for the absolute viscosity of water at 20°C. is used as a primary standard in the measurement of viscosity. Sucrose solutions, Standard Viscosity Samples from the National Bureau of Standards and the American Petroleum Institute, and water in the temperature range 10 to 60°C. are discussed as liquids for the calibration of viscometers.

References

1. Bingham, Fluidity and Plasticity. McGraw-Hill,
2. Bingham, Schlesinger, and Coleman, *J. Am. Chem. Soc.* **38**, 27 (1916).
3. Bingham and Jackson, *Natl. Bur. Standards, (U. S.) Bull.* **14**, 59; *Sci. Paper No.* **298** (1917).
4. Bingham and Thompson, *J. Rheology* **1**, 418 (1930).
5. Bingham and Geddes, *Physics* **4**, 203 (1933).
6. Spooner and Serex, *Physics* **6**, 162 (1935).
7. Bingham and Young, *Ind. Eng. Chem.* **14**, 1130 (1922).
8. Jones and Ferrell, *J. Chem. Soc.* **1939**, 325.
9. A discussion of these constants is given by Barr, A Monograph of Viscometry, Ch. II., Oxford Univ. Press.
10. Cragoe, *Proc. World Petroleum Congress, London*, **2**, 529 (1933).
11. Coe and Godfrey, *J. Applied Phys.* **15**, 625 (1944).

MECHANISM OF FRACTURE OF BRITTLE SOLIDS *

Nelson W. Taylor

Research Dept., Minnesota Mining and Mfg. Company, St. Paul, Minn.

Received Dec. 5, 1946

ABSTRACT

A theory is proposed which connects the stress, f, required to break a brittle material in simple tension, with its duration of application, t. The slow process preceding fracture is shown to be the orientation of the atomic network contained in an elementary prism of length $r = \lambda_0 E/f$, where E is Young's Modulus and λ_0 is the critical elongation required for fracture. The rate-controlling factor is the activation energy, $E\alpha/f$, for the orientation or rearrangement of the atomic network under the stress, f. Moisture in glass, and oxygen in metals, are important catalytic or fatigue-promoting factors because they reduce the unit activation energy, α. The theory leads to the equations

$$t = \frac{1}{k_0} e^{E\alpha/fkT}$$

and

$$\log t = -\log k_0 + \frac{1}{f}\left(\frac{E\alpha}{2.3kT}\right),$$

where t is the time for fracture (duration of the stress), k is the Boltzmann constant, T the absolute temperature, and α and k_0 are experimentally determined constants. The logarithmic expression has the same form as the Glathart-Preston (*J. Applied Phys.* 17, 189 (1946)) empirical relation $\log t = -a/m + 1/fm$, which, in the case of glass, appears to be valid over a time factor of 10^7.

The theory shows why a solid object does not have a single characteristic breaking strength, and how it adjusts its fracture mechanism to whatever stress is applied. Quantitative tests of the theory are made, using fracture data on various glasses and on one glass at various temperatures. Applicability of the theory to certain aspects of fatigue of metals under stress-corrosion conditions, as well as to failure by fracture of the more rigid organic plastics, is indicated.

(This abstract is a revision and correction of an earlier one which appeared in *Rheology Bulletin*, Nov. 1946.)

* Presented at the Annual Meeting, Society of Rheology, New York, November 2, 1946.

STATISTICAL ANALYSIS OF PLASTICITY MEASUREMENTS OF NATURAL AND SYNTHETIC RUBBER

M. C. Throdahl

From the Rubber Service Department, Monsanto Chem. Co., Nitro, W. Va.

Received Nov. 11, 1946; Revised Ms. received Jan. 6, 1947

Introduction

The reliability of plasticity data of rubber is affected by (a) variance in precision of measurement of the instrument used and (b) heterogeneity of the rubber. While the relative precision of the instrument and observer error must be considered, the problem is somewhat complicated by the fact that each sample is used only once. Thus a single measurement is made on "*n*" like things rather than "*n*" like measurements on a single thing. Methods commonly used are the Williams parallel plate (1), Dillon and Johnston extrusion (2) and Mooney shear (3).

Rather meager data have been published on plasticity measurements of large numbers of samples (200–300) of elastomers. Riebl (4) and Martin, Davey and Baker (5) have reported no dispersion values, only averages of D_{30} plasticity values of smoked sheet and crepe being shown using a parallel plate plastometer. Aside from Mooney plasticity values of GR-S on 45–50 samples given in recent papers by Heide (6) and Vila and Gross (7) no statistical data for GR-S plasticity are available in the literature.

It is the purpose of this paper to present a simple statistical analysis of the three types of plasticity measurements for GR-S and natural rubber (Hevea smoked sheets) based on 256 specimens.

Experimental

The three standard plastometers (1, 2, 3) were used under the conditions set forth in Table I. GR-S specimens were prepared from randomly selected 100 g. pieces cut from a single 75 lb. bale (U. S. Rubber Co., Institute, W. Va.). These were milled for eight minutes on a 6 × 12 in. mill at a 45°C. roll temperature using an 0.08 nip width. Each piece was sufficient for two extrusion specimens rolled into cylindrical form from very thinly sheeted stock. Specimens were cut to weigh 19 g. Owing to high shrinkage of GR-S, these were made up 15 minutes before preheating, wrapped in varnished cambric and held together tightly with rubber bands. Mooney slabs were prepared according to the method of

* Ed. Note: This paper was given before the Society of Rheology on Nov. 1, 1946.

Taylor (8) from GR-S milled in the previously described manner. Williams pellets were drilled from a 500 g. milled slab. Smoked sheet specimens were prepared from randomly selected 100 g. pieces cut from a 250 lb. bale. A total of 2,500 g. was masticated 5 minutes in a type OO Banbury mixer running 76 r.p.m. at a stock temperature of 80°C. This masticated batch was divided into 5 parts and further mixed 2 minutes on the mill. Sheeted stock was plied up evenly to a thickness necessary for each type of specimen. Extrusion and Williams specimens were bored from thick slabs using a cork borer fitted to a power drill. Mooney slabs were cut from stock sheeted off to the desired thickness. Preparation of specimens was as previously described.

TABLE I

Plastometers Used and Conditions of Test

Type	Conditions
Williams	5 Kg. load, 2 ml. specimen, 100°C. temperature, 6 minutes preheat.
Extrusion	*GR-S* (0.703 Kg./cm.^{2}) 10 lb./in.^{2} air pressure, six minutes preheat at 90°C. in air. Running temperature of 82°C., one minute preheat in plastometer. *Smoked Sheets (Hevea)* (0.843 Kg./cm.^{2}) 12 lb./in.^{2} air pressure, six minutes preheat at 82°C. Running temperature of 82°C., one minute preheat in plastometer.
Mooney	One minute preheat at 100°C.; reading taken after four minutes running, using large rotor.

Results and Discussion

All statistical quantities shown in Table II were calculated from equations commonly expressed in any standard reference on mathematical statistics. A value of $t_{0.01}$ of 2.597 derived from the Normal Law Integral was taken from a table (9) of values of t.

In parallel plate plasticity, the thickness of the specimen is read at different times, plasticity being denoted by K in the following equation:

$$K = Yx^n,$$

where Y is the specimen thickness, x is time in minutes and n is a constant. According to Williams (1) the data fit the theoretical curve fairly well at Y values taken at approximately three minutes. The curve is tangent to the x and y axes at infinity but, since the specimen originally has measurable thickness, the readings taken over the first very short interval will not fall along the curve. To test this, appropriate $Y_{0.5}$ and Y_3

readings were taken for each specimen along with the Y_5 values. Frequency distribution of the $Y_{0.5}$ values (not given here) showed that they had but slight tendency to group themselves about a central mean in a symmetrical manner which would allow use of Normal Error Law treatment. The Y_3 values were considerably more precise than the $Y_{0.5}$ but were not used—the Y_5 values being preferred.

The data obtained indicate that the Mooney plasticity data are the most precise with Williams plasticity reasonably close. The extrusion

TABLE II

Statistical Quantities for Two Sets of Plasticity Measurements on Different Lots of Hevea (Smoked Sheets) and GR-S

Set 1		Williams				Extrusion		Mooney	
Number of Specimens	Statistical Quantity	Hevea Y_5	Hevea Y_∞	GR-S Y_5	GR-S Y_∞	Hevea	GR-S	Hevea	GR-S
256	$\overline{X}$	272.6	385.5	343.5	464.3	48.5	18.6	79.5	48.7
	$^{\prime}0.01\ \sigma_{\overline{X}}$	4.6	4.1	3.5	8.3	2.7	0.7	0.3	0.3
	σ^2	806.0	642.0	468.0	2586.3	282.0	18.7	3.8	4.28
	σ	28.4	25.3	21.6	50.9	16.8	4.3	1.95	2.06
	$\sigma_{\overline{X}}$	1.78	1.58	1.35	3.18	1.05	0.27	0.12	0.13
	V	10.4	6.6	6.3	10.9	34.6	23.1	2.4	4.2
Set 2									
25	$\overline{X}$	467.2	795.0	396.0	949.0	73.0	26.2	96.3	68.9
	σ^2	300.9	3453.3	79.4	9415.0	79.9	12.3	0.8	0.6
	σ	17.3	58.8	8.9	97.0	8.9	3.5	0.9	0.8
	$\sigma_{\overline{X}}$	3.46	11.80	1.78	19.45	1.79	0.70	0.18	0.16
	V	3.7	7.4	2.3	10.3	12.2	13.3	0.9	1.1

data showed this type of measurement to have the greatest variability; precision was affected appreciably by the less effective temperature control.*

Surprisingly the coefficient of variability was less for GR-S than Hevea in the Williams and Extrusion plastometer measurements. The Mooney values, however, were more precise for Hevea than for GR-S.

Probably the most significant factor influencing results was the cleanliness of the rubber chambers of the extrusion and Mooney plastometers, and more especially with the latter. It was found, for example, that meticulous care was necessary in punching the proper sized hole in

* Special installation of Superior Electric Co. Powerstats for this instrument have held the temperature change over a range of about ± 4°C.

the Mooney specimen for the rotor, or else the rubber would work between the rotor shaft and its bearing, thus causing wild fluctuation of the dial gauge. This may have occurred occasionally during the running of the series; however, after 256 readings were taken the instrument was dismantled and inspected for collected rubber. None was found.

Addendum

Dr. M. Mooney (U. S. Rubber Company) has suggested to the author that, in addition to the precision measures employed in the paper, a rating of practical significance would be one based on the ". . . ability of the instrument to distinguish between two samples which are not very different." Thus, both methods of rating would give the same relative standing only if the same percentage difference existed between two different samples, by different methods.

To apply this suggestion a group of 25 samples were prepared from a different lot of Hevea and GR-S (the GR-S used was of an experimental type of known divergence from regular GR-S) in a similar manner and tested as before. The various statistical calculations are shown in set 2 of Table II.

Dr. Mooney used the term "coefficient of discrimination" as applied to a specific test for two specific samples and defined it as

$$D = \frac{\bar{X}_1 - \bar{X}_2}{\sigma},$$

where $\bar{X}_1$ = arithmetic mean for samples of set 1, $\bar{X}_2$ = arithmetic mean for samples of set 2, σ = standard deviation within samples which would be calculated from

$$\sigma = \sqrt{\frac{n_1\sigma_1^2 + n_2\sigma_2^2}{n_1 + n_2}},$$

where n_1 and n_2 are the numbers of measurements in the respective samples and σ_1^2 and σ_2^2 are the respective variances. To illustrate, typical values are tabulated from the calculations supplied by Dr. Mooney:

Discrimination between sets of samples	Williams				Extrusion		Mooney	
	Hevea		GR-S		Hevea	GR-S	Hevea	GR-S
	Y_5	Y_∞	Y_5	Y_∞				
D_{1-2}	7.1	13.7	2.5	8.6	1.5	1.8	8.9	10.2

These show the extrusion plastometer to have less discriminating ability than the others. However, as Dr. Mooney has pointed out, this is not as

low as the precision measures indicate. These results lead to a somewhat different conclusion than that reported by Dillon (10) who used the term "selectivity" (percentage difference between two observations on different mixtures divided by the average maximum percentage error) and found that the extrusion plastometer ranged from twice to twenty times that of the Williams plastometer when the two instruments correlated. When they failed to correlate, the relative sensitivity of the two instruments had no meaning.

References

1. Williams, I., *Ind. Eng. Chem.* **16**, 362 (1924).
2. Dillon, J. H., and Johnston, N., *Physics* **4**, 225 (1933); *Rubber Chem. Tech.* **7**, 248 (1934).
3. Mooney, M., *Ind. Eng. Chem., Anal. Ed.* **6**, 147 (1934).
4. Riebl, *Arch. Rubbercultuur* **14**, 223 (1930); in Davis and Blake, Rubber Chemistry and Technology, p. 53, Table 34. Reinhold, New York, 1937.
5. Martin, G., Davey, W. S., and Baker, H. C., Rubber Research Scheme (Ceylon), *Bull.* **52** Peradeniya (1932); Dayson and Porritt, Research Assoc. Brit. Rubber Mfrs., p. 48, Table 194. Croyden, England, 1935.
6. Heide, J. D., *Ind. Rubber World* **114**, 653 (1946).
7. Vila, G. R., and Gross, M. D., *Rubber Age* **57**, 551 (1945).
8. Taylor, R. H., Natl. Bur. Standards, (U.S.), Circ. **C-451**, Nov. 8 (1945).
9. Snedecor, G. W., Statistical Methods, p. 65, Table 3.8. Iowa State College Press, Ames, 1946.
10. Dillon, J. H., *Physics* **7**, 73 (1936); *Rubber Chem. Tech.* **9**, 496 (1936).

THE INITIATION AND PROPAGATION OF THE PLASTIC ZONE ALONG A TENSION SPECIMEN OF NYLON

Julius Miklowitz

From the Westinghouse Research Laboratories, East Pittsburgh, Penna.

Received November 29, 1946

ABSTRACT

A study of the mechanical factors influencing the initiation and propagation of the plastic zone in nylon is presented.* Nylon, a material exhibiting a well-defined yield point, is extremely valuable in studying localized yielding (the well-known property of mild steel), since, with its enormous strain values, the details of discontinuous flow are greatly magnified. Specifically, the effects of the speed of stretching and the rigidity of the testing machine on the initiation and propagation of the plastic zone and the accompanying phenomena were studied. Along with the studies concerning the influence of the speed and of the rigidity of the force measuring parts of the testing machine, an investigation of yielding along the test bar under one and two traveling plastic boundaries (advancing yield fronts) gave conclusive evidence of, and data on, the factors influencing the shape of the plastic boundary and the extent of the yield-point elongation.

I. INTRODUCTION

It is a well-established fact that mild steel when tested in tension exhibits a definite yield point. Frequently associated with this phenomenon is a drop of the load after the yield point has been reached, followed by a "yield-point elongation"[1] during which the material within the gage length of the specimen is yielding discontinuously under approximately a constant load. Several special investigations in the past have dealt with this phenomenon of mild steel both from a metallurgical and mechanical viewpoint. This paper presents the results of an investigation of the circumstances under which plastic discontinuities travel along a tension specimen under static loading, provided the material exhibits a sharply defined yield point.

W. H. Carothers and J. W. Hill (1), in their early work with superpolymers, stated that these artificial fibers exhibited the cold-drawing phenomenon, during which the fibers transformed from an unoriented

* This paper is based on an investigation done for the National Defense Research Committee (Division 2) of the Office of Scientific Research and Development, under O.S.R.D. Contract OEMsr-891 (O.S.R.D. Report No. 3864 (1944)). Acknowledgment is due Division 2 for permission to publish parts of the investigation.

[1] On the stress-strain diagram of mild steel, the yield-point elongation is that amount of strain between the yield point and the point at which uniform strain begins (increased resistance to stress).

molecular structure to an oriented[2] one. In these early experiments, a stress was gradually applied to the unoriented fiber and, instead of breaking apart, it separated into two sections joined by a thinner section having the oriented structure. As the pulling was continued the oriented section grew in length at the expense of the unoriented sections. A very noticeable feature of this experimentation was the sharpness of boundary between the unoriented sections and the oriented section. It was noted then that the shape of this boundary did not change, but that the boundary merely advanced through the unoriented sections changing them to oriented material of uniform cross section. During the process of orientation the stress gradually increased to a definite flow point, where considerable elongation occurred, followed by increased resistance to stress.

In 1938 at the Westinghouse Laboratories, J. Boyd and A. Nadai observed that filaments of unoriented nylon presented stress-strain characteristics in tension similar to those of mild steel. Their observations were similar to those of Carothers and Hill. Nylon shows an upper and lower yield-point at the formation of the yield constriction. A yield-point elongation is produced under a constant load as the boundaries of this constriction travel along the filament. Since the strain values during this orientation process are of the order of 100 times those of mild steel during its yielding process, Dr. Nadai suggested a study of these phenomena in nylon with a view toward obtaining useful information concerning the mechanical influences on discontinuous yielding in metals. Although the fundamental process causing the abrupt starting of yielding in the polycrystalline structure of a soft low carbon steel is different from the process of the orientation of the chain-like molecules in filaments or strips of unoriented nylon, the behavior of these two materials shows striking analogies in their stress-strain curves.

II. Material and Specimens

Two forms of nylon material were used, the first being rolled sheet of approximately 0.009 in. thickness, from which flat strip specimens were cut. The other supply was in the form of fiber, 0.0385 in. in diameter.

C. P. Kidder states that superpolymers under the group name of nylon have been known to stretch from 4 to 7 times their original length during the orientation process, the exact amount of stretching depending upon the composition of the particular fiber (2). Although it is well established that nylon properties, both physical and chemical, vary somewhat with the particular polyamide, these variations did not come

[2] In superpolymeric substances an unoriented molecular structure is one in which the long-chain molecules are in a state of random orientation. Upon drawing the originally unoriented fiber into its oriented structure, the long-chain molecules arrange themselves in a definite pattern parallel to the longitudinal axis of the specimen.

into account in this investigation since only two types of nylon were investigated, one independently of the other.

Both materials naturally had to be of unoriented long-chain molecular structure, as the investigation depended on the process of orienting these long-chain molecules.

On advice of the du Pont Company, the nylon was kept under a constant relative humidity of 65%, which is the best possible testing condition for the material. The temperature variable was dismissed since tests were performed under fairly uniform conditions at room temperature. A preliminary test proved that the volume of the nylon remains practically constant when strained permanently in tension. Ordinary strain calculations, based on the constancy of volume, were therefore considered accurate for this material.

Another preliminary test determined the modulus of elasticity of the unoriented fiber as 6.9×10^4 lb./in^2. This figure was obtained by directly loading a long piece of fiber, and measuring the extension per unit load by the use of a microscopic eyepiece. As a check on this modulus figure, the same method gave the modulus of the oriented fiber as 2.69×10^5 lb./in^2. This value lies between the 4.5×10^5 and 1.7×10^5 given[3] in the Handbook of Plastics (3).

Nylon is a material which, after being pulled into its oriented condition, experiences the phenomenon of recovery. The measure of recovery is the amount of contraction that a tensile specimen exhibits after it has been stretched permanently and unloaded. The recovery action could be neglected in this investigation, since tests indicated a recovery of only 2% over a period of 24 hours.

Fig. 1 shows the two types of flat strip specimens that were used. The specimen of Fig. 1a is slightly undercut at the center, while that of Fig. 1b is undercut at one head. The first was used to develop two yield fronts (plastic boundaries) at the undercut, which would advance toward the heads as the test proceeded. The other specimen would initially form two yield fronts also, but the advance of one of them would be prevented by the larger cross-sectional area of the head. Both types of flat strip specimens were carefully prepared, being cut by hand. Due to the variance of thickness of material and the difficulty of obtaining a uniform width by cutting, the cross-sectional areas along the tensile axis of the specimen varied as much as 5% in some cases. This, of course, presented difficulties in the control of yielding, as will be described later.

Although the fiber tests required no specimen cutting, difficulties arose in the means of gripping the round fiber. Fig. 2b is a sketch of the drum method that was used. Gripping the fiber in this way minimized the

[3] The 4.5×10^5 figure refers to a dry nylon fiber, while the 1.7×10^5 value is the modulus of a wet fiber.

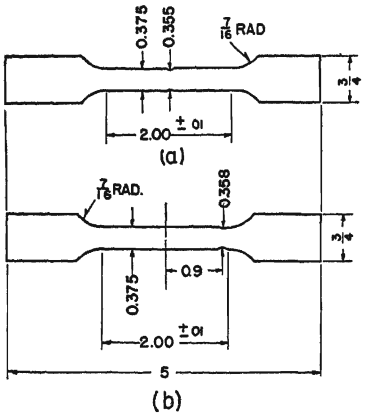

FIG. 1
Flat Strip Specimens Made from Thin Nylon Sheet. (Dimensions in Inches)

stress concentration at the contact point between the grip and specimen. This method was used only where interest centered about the initial portion of the stress-strain diagram. It was not suitable when testing proceeded into the region of uniform strain, because the material of the specimen on the drum would also strain; therefore the recorded elongation

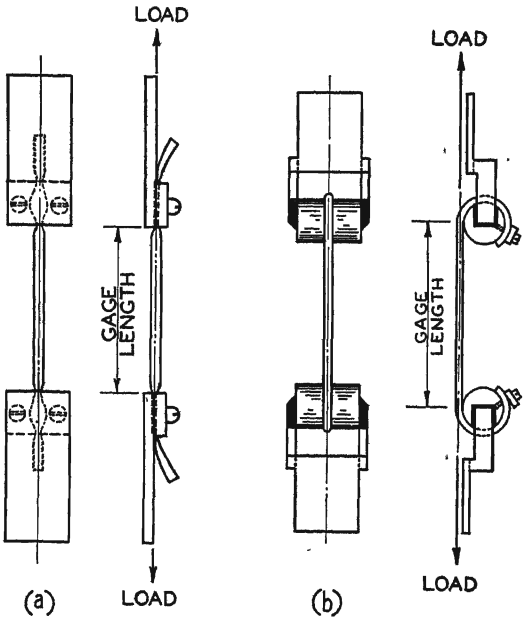

FIG. 2
Two Types of Grips for Nylon Fiber Tensile Specimens

would no longer be a measure of strain based on the original gage length. Fig. 2a shows the grips used when complete tensile tests were run. The fiber was initially strained laterally at the two gripping places before testing, and this high stress concentration at the grips initiated two yield fronts, which traveled toward the center of the specimen during the test.

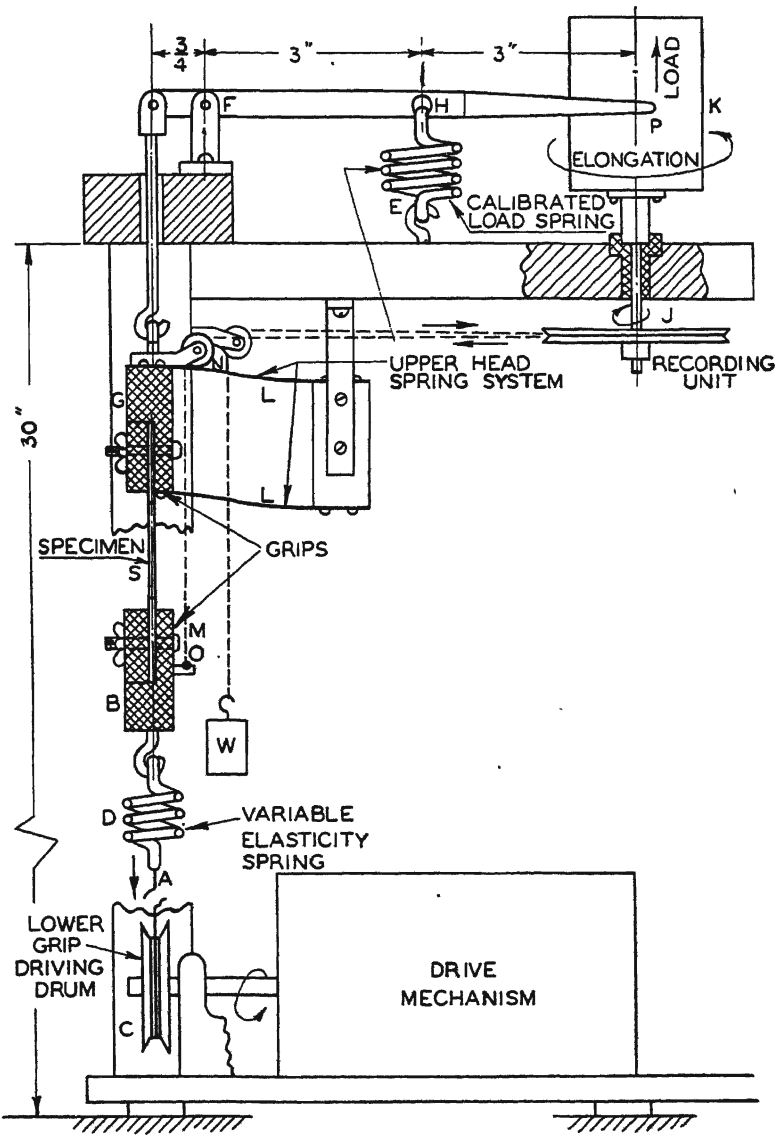

FIG. 3
Diagrammatic Scheme of Nylon High-Speed Tension Machine

FIG. 4
Nylon High-Speed Tensiòn Machine

The gage length was, as shown in the figure, the distance between grip faces.

III. The Nylon High-Speed Tension Machine

A variable-speed, tensile-testing machine, capable of pulling nylon specimens under comparatively high rates of strain and suitable for loads of the order of 10 lb. was designed. The scheme of this machine is shown diagramatically in Fig. 3.

A piece of piano wire A connected to the lower grip B at one end, and to the driving drum C at the other end, applies tension to the system.

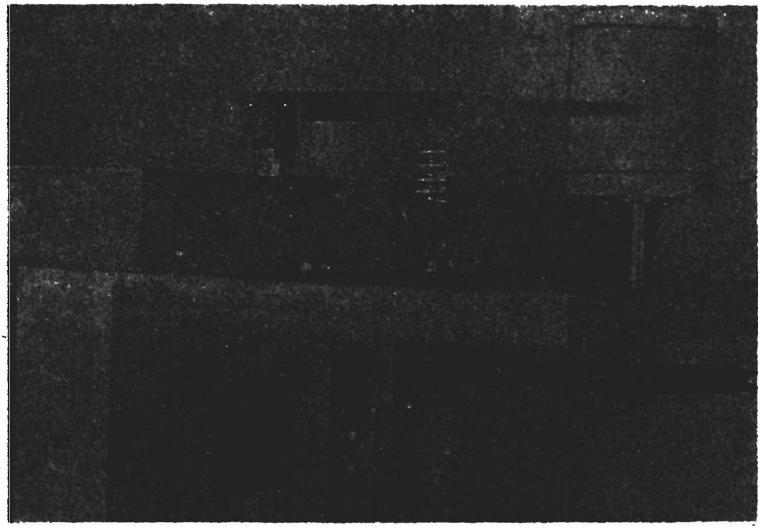

Fig. 5
Tension Machine Upper Head-Spring System and Recording Unit

To vary the rigidity of the testing machine, different springs D could be inserted below the lower grip. A calibrated load spring E balances the tension load and serves to measure this load in the recording system. A pivot F placed $\frac{3}{4}$ in. from the tension axis, and 3 in. from the axis of the load spring, makes the movement of the upper grip G only one-quarter that of the load spring hinge H and only one-eighth that of the indicator point P which is 6 in. from the pivot F. Four leaf springs L tie the upper grip G to the machine and serve as part of the upper head-spring system.

A large pulley J on the same shaft as the recording drum K is driven by the cord M. Cord M is fixed to the lower grip B at point O and passes over the pulley N which is connected to the upper grip G. From pulley N the cord passes around pulley J and is weighted on its other end. As the specimen S is stretched, the cord follows the elongation of the specimen,

rotating pulley J. Pointer P records this elongation on wax paper fitted to the drum K. The movement of pointer P revolving about pivot F and the simultaneous rotation of the drum due to elongation give a recorded load-elongation diagram. Due to the ratio of the diameter of pulley J to the diameter of drum K, the elongation is recorded in a 1 to 1.53 reduced value. The movement of pointer P depends upon the load on spring E which has been calibrated, so that for any point on the diagram, the corresponding load value may be read from a linear calibration curve.

Through suitable gear reducers and pulleys connected to the lower-grip driving drum C it is possible to vary the speeds of the lower grip B from 0.004 to 8.700 in./sec. At the higher speeds, controlled stopping of the lower grip is accomplished by dynamically braking the d.c. shunt motor, which is used as the basic drive of the testing machine. Fig. 4 is a picture of the machine and Fig. 5 a close-up of the upper head-spring system and recording unit.

IV. The Influence of Speed of Stretching on the Stress–Strain Characteristics of Nylon

The stress-strain characteristics of mild steel have been found to be influenced to a great extent by the speed of stretching. This effect in mild steel has been frequently investigated in the past. The reader is referred to papers concerned with the influence of speed of deformation (4).

As mentioned previously, it has been observed by the writer and others that a yield constriction forms on a nylon filament during the drop from upper to lower yield load, producing a stress concentration, and, under the constant lower yield load, the plastic boundaries (referred to as yield fronts in this paper) of this constriction travel along the filament yielding the material they traverse. When the yield fronts have traversed the whole gage length, the load begins to increase. This means that the yield-point elongation is produced during the travel of the fronts. Therefore, the advancing front produces the yield-point elongation of a section of material in the filament by passing over that section.[4] This is shown in Fig. 6. The material in a section such as "AA" is about to yield, and the material in a section such as "BB" has yielded. The material within the advancing front (between these two sections) undergoes its yield-point elongation as the front advances.

The plastic boundaries in nylon are sufficiently long to assume that a state of uniaxial tension exists in the boundary. Therefore the above conception of yield-point elongation can be used in the plot of the true

[4] This is not actually the full yield-point elongation. Neglected is the small amount of strain of the section due to the continuation of the load on this section as the front advances to yield other sections of material. This was verified by the tests dealing with progressive yielding.

stress-conventional strain diagram. The section "AA" has the stress $\sigma_0 = P/A_0$ (neglecting the elastic strain) on it, where σ_0 is the lower yield-load stress, A_0 the original area of the specimen, and P the lower yield load. Section "BB" has the stress $\sigma = P/A$ on it, where σ is the true stress. Therefore, $\sigma = \sigma_0(A_0/A)$, and, since the conventional strain at any particular section is given by $\epsilon = (A_0/A) - 1$, $\sigma = \sigma_0(1 + \epsilon)$. This relation, a straight line passing through the points ($\epsilon = -1$, $\sigma = 0$) and ($\epsilon = 0$, $\sigma = \sigma_0$), will define the yield-point elongation part of the true stress-conventional strain diagram. The automatic load-elongation records provided sufficient data to produce the curves shown in Fig. 7.

The four tests, F_1, F_2, F_3, and F_4, were run at the lower-head speeds of 8.700, 1.270, 0.030 and 0.004 in./sec., respectively. These tests were carried almost to fracture.

Two important conclusions were drawn from the tests, namely, that both the yield-point elongation and yield stresses (upper and lower)

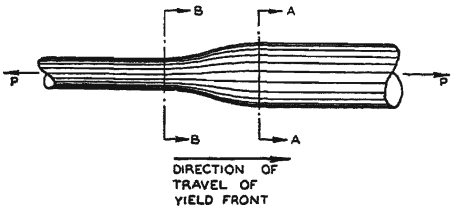

FIG. 6
An Advancing Yield Front in Nylon Fiber

increased with an increase in speed of stretching. The yield-point elongation increased from a conventional strain $\epsilon = 0.84$ to $\epsilon = 2.16$; 2.6 times. It is believed that the yield-point elongations of F_1 and F_2 have not fully developed. In test F_2 it was observed that the drop in load or stress in the vicinity of $\epsilon = 0.9$ occurred simultaneously with the formation of an additional neck or constriction. Since F_1 exhibits a similar drop in stress in the vicinity of $\epsilon = 1.0$, it is supposed that an additional neck formed there too. The formation of an additional neck causes twice as much material to strain, since 4 advancing fronts yield the specimen now instead of 2 fronts. With the additional material straining, the strain rate[5] decreases, assuming that the speed of the lower head remains constant. This drop in strain rate in tests F_1 and F_2 has caused the drop in load (Fig. 7) and has made the latter part of the yield-point elongations of these tests equivalent to the yield-point elongations of slower tests. It is therefore believed that the increase of 2.6 times should have been larger.

[5] Strain rate here refers to the mean strain rate of the material within the advancing front; it is directly dependent on the lower-head speed.

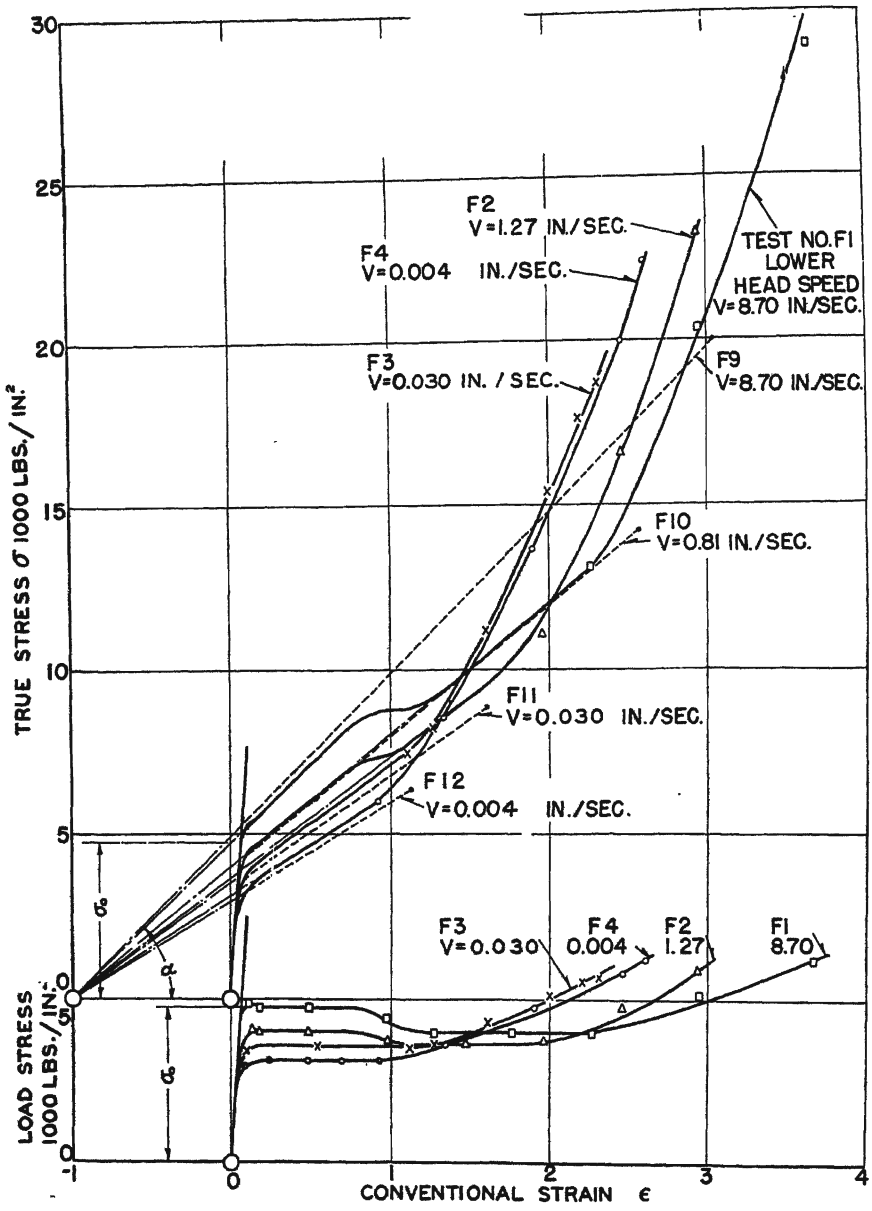

FIG. 7

Nylon True Stress—Conventional Strain and Corresponding Load Stress—Conventional Strain Curves at Different Speeds of Stretching

In another group of fiber tests (F_9, F_{10}, F_{11} and F_{12}) the yield-point elongation increased from $\epsilon = 1.04$ to $\epsilon = 2.96$; 2.8 times, the speed range being the same as before. Just the yield-point elongations are plotted in Fig. 7. They are the dashed lines with large black dots at their terminal points.

In their tests on mild steel, Winlock and Leiter (5) found that the yield-point elongation increased with the rate of deformation. A comparison of Fig. 7 of this report and Fig. 16 of the Winlock and Leiter paper (5) reveals that, although in the nylon tests the yield-point elongations were of a much greater magnitude than those in steel, the relative

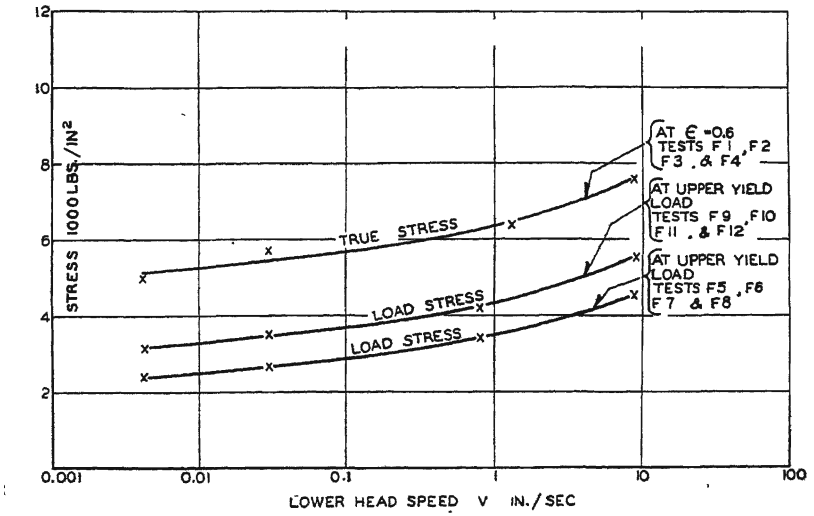

FIG. 8

Stress as a Function of Head Speed

increase of yield-point elongation over a 4-cycle speed range[6] was much greater for steel, the increase in one case being 10 times.

The true yield stresses for tests F_1, F_2, F_3 and F_4, increased from 3230 to 5360 lb./in.². over the 4-cycle speed range (see Fig. 7). This is an increase of 1.7 times. Since the true stress increases linearly with the conventional strain throughout the yield-point elongation, this increase holds for stresses at any value of strain within the yield-point elongation. The true stresses σ at a vertical section through the conventional-strain value $\epsilon = 0.6$ (Fig. 7) are plotted against the lower-head speed on semilog paper in Fig. 8.

The upper yield-load stresses of the tests F_9, F_{10}, F_{11} and F_{12} showed

[6] This range of speed was from 0.000076 to 0.168 in./sec. (lower-head speed).

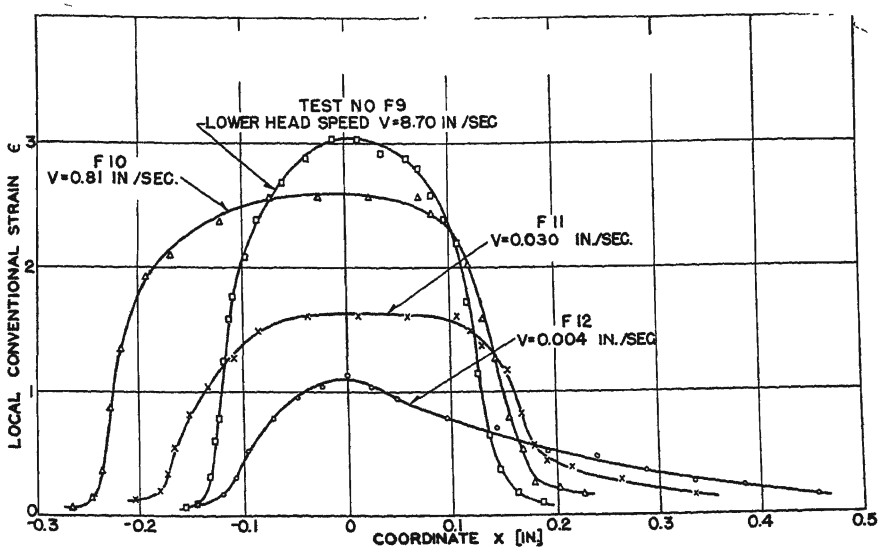

FIG. 9
Distribution of Conventional Strains in the Plastic Zone
of a Nylon Fiber Tensile Specimen

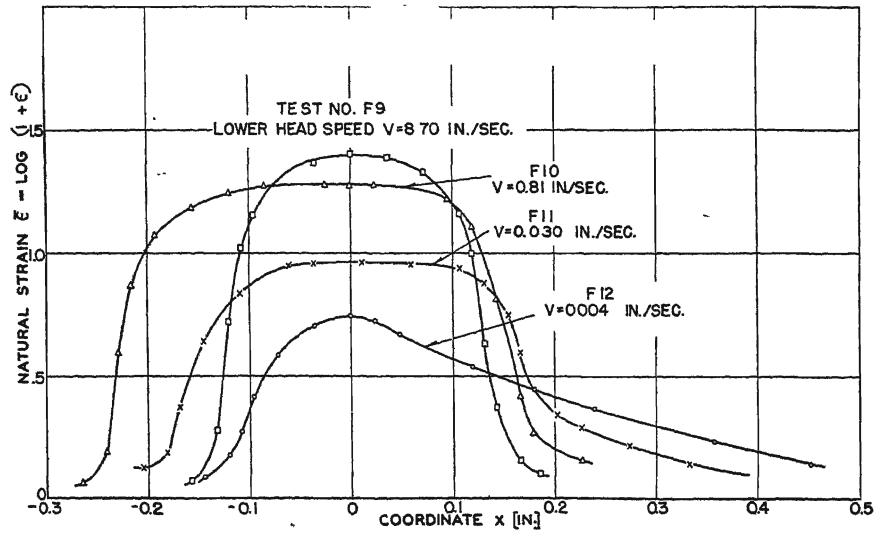

FIG. 10
Distribution of Natural Strains in the Plastic Zone
of a Nylon Fiber Tensile Specimen

an increase of 1.8 times; varying from 3100 to 5500 lb./in^2. over the stated speed range.

Several investigators have found a similar speed effect in mild steel,[7] but again, nylon shows this phenomenon in a much more pronounced form.

It is interesting to note that while for steel practically the same curve is obtained in the uniform strain region at all speeds of deformation, in nylon there is a shift of the uniform strain region to larger strain values with an increase in speed of deformation. Test F_3 is an exception to this statement but the yield-point elongation of test F_{11} (pulled at the same speed as F_3) seems to confirm the statement.

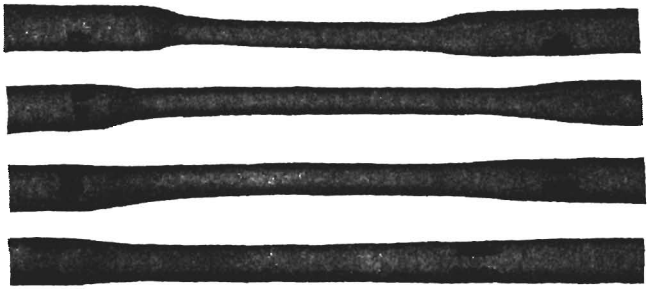

FIG. 11
Influence of Speed of Stretching on the Shape of the Yield Fronts of Nylon Fiber

For the sake of comparison with the true-stress curves of Fig. 7, the corresponding load-stress curves are plotted in the lower part of the figure.

The tests F_9, F_{10}, F_{11}, and F_{12} were used in a study of the strain distribution in the plastic zone. The specimens held by the drum grips (see Fig. 2b) were stretched just beyond the yield point and values of local conventional strain corresponding to the diameters within the plastic zone that had formed at the upper drum[8] were plotted as shown in Fig. 9. All the strain curves in Fig. 9 are aligned so that the maximum strain values lie on the same vertical line at $x = 0$[9]. Negative x-values represent positions along the restricted front of the zone. This front

[7] See Refs. 4 b, c, d, e and 5.

[8] Whenever the circular drum grips were used, a neck formed on the specimen at the point of contact of specimen and drum, due to a stress concentration at this point caused by the contact.

[9] The coordinate x is in terms of the Lagrangian system of coordinates, stating the value of the coordinate of a point of the fiber which in the original unstrained condition was identified by the coordinate x^*.

is called restricted since its movement along the specimen is prevented by the drum. Positive x-values represent positions along the advancing front of the zone. These curves show that, as the speed of deformation increases, (a) the length of the advancing front decreases, or, stated in other words, the maximum strain of a cross section of material due to the front passing over the section occurs more abruptly; and (b) this maximum strain in the cross section increases.

The natural strains for the plastic zones shown in Fig. 9 are plotted in Fig. 10 for comparison. The corresponding fibers are shown in Fig. 11. The sharpness of the fronts in the specimens subjected to the faster tests is very evident from the photographs shown.

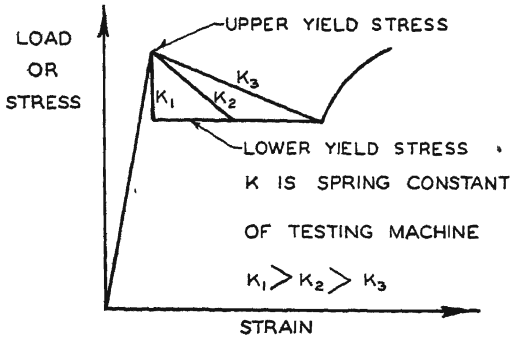

FIG. 12

Resulting Curves of Siebel and Schwaigerer Rigidity Tests

V. THE INFLUENCE OF THE RIGIDITY OF TESTING MACHINE ON THE DROP OF LOAD AND UPPER YIELD STRESS OF NYLON

The drop from the upper to lower yield load in mild steel depends on a number of circumstances (6).

In their tests with mild steel, Siebel and Schwaigerer (7) varied the rigidity of their tension-testing machine by inserting helical springs of different elasticities in series with the specimen. They found that the stiffer or more rigid the inserted spring (more rigid the machine), the steeper was the load drop from upper to lower yield load. This is shown in Fig. 12.

To investigate the rigidity influence in nylon, three tests with flat specimens (see Fig. 1a) were run, each with a different spring in series with the specimen. The spring constant K of the machine in each of the tests is given in Table I. These spring constants refer to a point on the piano wire just below the inserted spring (see Fig. 3) and are exclusive of the elasticity of the specimen. The three tests 1A, 1B and 1C were all pulled at a lower-head speed of 3.6 in./sec. The machine was stopped as

the recorded diagram showed a leveling off of load at the upper yield value. The load dropped immediately.

Fig. 13 shows the recorded load-elongation diagrams of the tests. A comparison of the 3 diagrams reveals that, as the spring constant of the machine increases, the load drop-off line becomes steeper, and this line appears linear. This checks the results found by Siebel and Schwaigerer.

TABLE I

Specimen	Spring Constant K (lb./in.)	Upper Yield Load Stress (lb./in^2.)
1A	115.6	4620
1B	61.8	4680
1C	24.2	4360

The value of the upper yield-load stress (see Fig. 12) for each of the tests is given in Table I.

The results of test 1B indicate that cutting the rigidity of the machine in half had no noticeable effect on the upper yield load stress, but in test

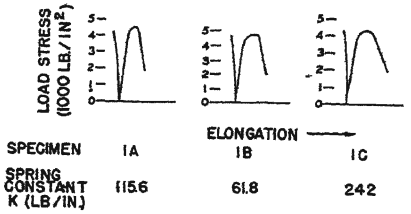

FIG. 13
Tensile Tests of Nylon Strip under Different Machine Rigidities

1C, where the rigidity of the machine was cut to one-fifth that of test 1A, a smaller value came about. Davis found that the yield stress of mild steel increased with the load rate.[10] Since in a less rigid machine the load rate is smaller, head speeds being equal, the results of tests 1A and 1C seem to check Davis' results and it may be concluded that nylon acts similarly to mild steel in this respect also. The specimens are shown in Fig. 14.

VI. Progressive Yielding by One Advancing Front

To study local conventional strains while stretching produced a yield-point elongation, a series of three tests were run using a specimen of the type shown in Fig. 1b. If inaccuracies are neglected, this gave a series where yielding was produced by one advancing front. The speed of stretching was made the same for each test—lower-head speed, 3.6 in./sec.

[10] See Ref. 4d.

Strain values in these tests were plotted under the Lagrangian system of coordinates, x^* being the coordinate of a point on the specimen in its original unstretched condition.

Fig. 15 shows the elongation to which each specimen was subjected before strain measurements were made. Each successive stage was a test in which the observed traveling front produced a greater elongation of

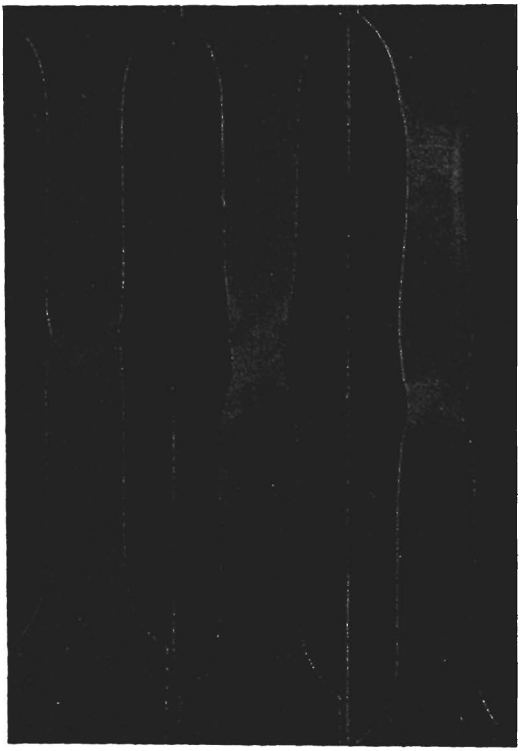

FIG. 14
Nylon Tensile Specimens Pulled under Different Machine Rigidities

specimen than the stage or test preceding it. The results of this series of tests are presented in Fig. 16 (Tests 2A, 2B and 2C). The curves labeled A_0 are curves of the original area of cross sections perpendicular to and along the tensile axis of the specimen. The curves labeled ϵ are the local conventional-strain curves corresponding to the A_0 curves. As shown by the small dip in the A_0-curves, the specimens were undercut at $x^* = 0.9$.

Actually, two yield fronts are produced at the initial necking down of this type of specimen, but one front is prevented from moving by the large cross-sectional area of the head adjacent to it. So finally only one front travels along the specimen in the negative x^*-direction.

Test 2A showed a maximum strain at $x^* = 0.9$ (the undercut section), and the strain had dropped to 0.14 at $x^* = 0.6$. The difference between these two values of x^* from maximum strain to minimum strain—0.3 in.—is the length of the yield front. The lower maximum at $x^* = -0.7$ where $\epsilon = 0.89$ was probably due to the low original area in that vicinity.

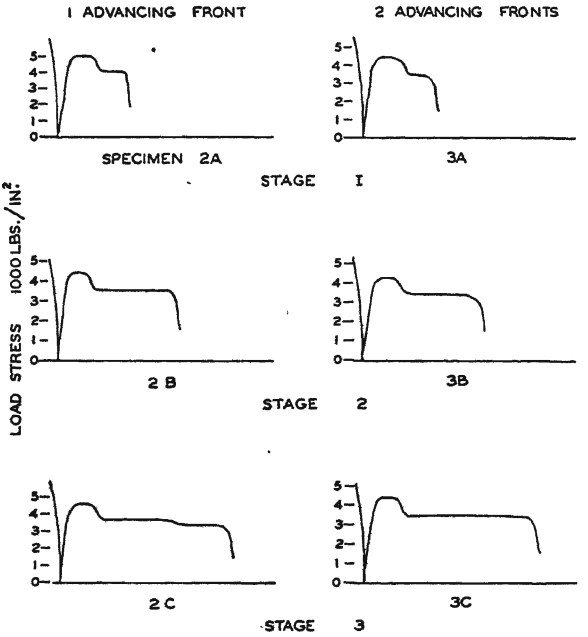

FIG. 15

Progressive Yielding in Nylon Strip Tensile Tests

Specimen 2B (Fig. 16) was stretched approximately twice as far as specimen 2A. A maximum strain of 3.90 was produced at $x^* = 1.0$. In this case the yield-front length is considerably greater than in test 2A. It lies between the strain value of 0.43 at $x^* = 0.1$ and the 3.35 strain value at $x^* = 0.7$, a length of 0.6 in. The results of this test give convincing evidence of the validity of a previous statement; namely, that a certain section of material does not undergo its complete yield-point elongation due to the passing of the yield front over it, but that the total yield-point elongation is composed of two parts, the strain that is produced by the yield front and the strain that is produced by the continuous

action of the load on the section while the front is advancing to yield other sections of the specimen. The front advance in test 2B was approximately 0.2 in. (based on the position of the front in test 2A).

Fig. 16 (Test 2C) shows a minimum in the original area in the vicinity of $x^* = -0.2$. Due to this minimum, a second necking started in this vicinity after the initial necking at the undercut section had occurred.

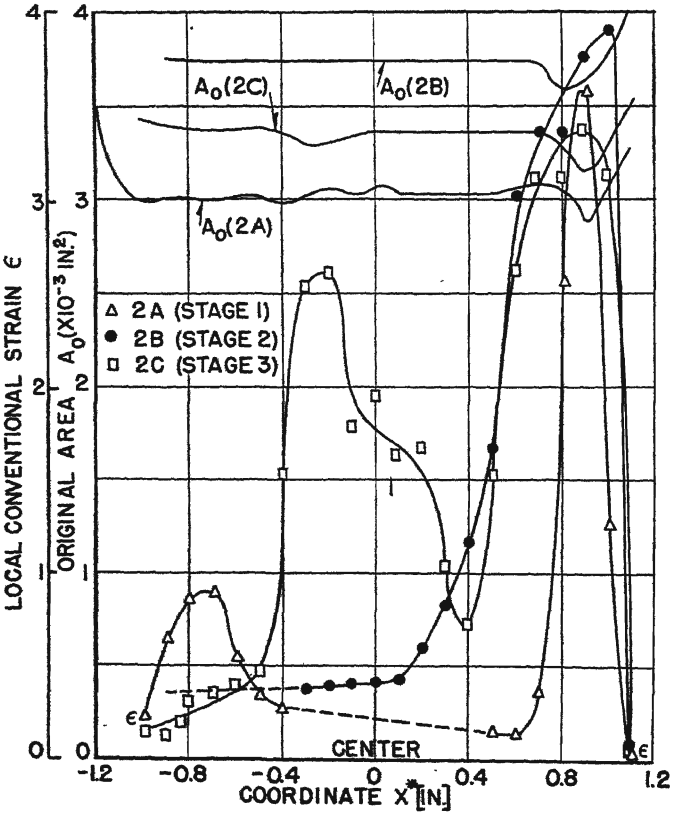

FIG. 16

Conventional Strain Distribution along the Axis of a Stretched Nylon Strip Tensile Specimen. (1 Advancing Front)

This second necking probably came simultaneously with the drop in load line as shown in the recorded diagram of Fig. 15. The formation of an additional neck caused a drop in strain rate and a corresponding load drop.[11] The maximum strain produced at the undercut section was 3.37. This value is well below the maximum strain of test 2B, which, according

[11] A similar phenomenon was observed in the tests on nylon fiber. (See explanation, Sec. IV, p. 201.)

to the theory of strain due to load continuation, should be higher than that of test 2B, since specimen 2C was under load for a longer time. But due to the drop in load produced by the formation of the additional neck, further straining of this maximum-strain section stopped. The shape of the advancing front of specimen 2C, which extended from $x^* = 0.8$ to

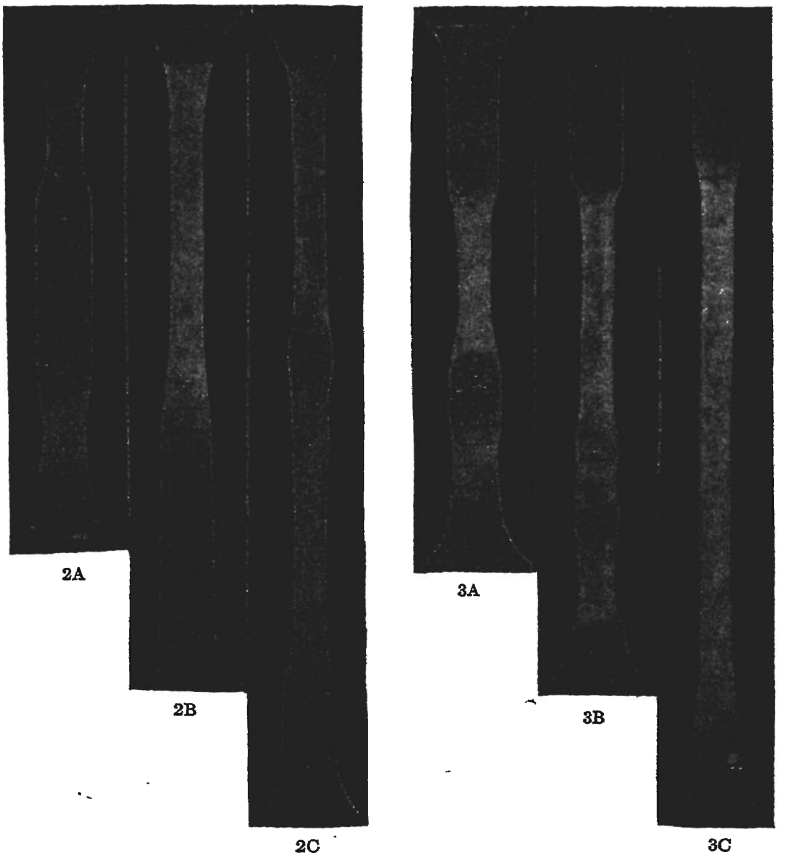

FIG. 17
Specimens Showing Progressive Yielding

$x^* = 0.4$, is very similar to the front of specimen 2B. The lower portion of the front has been cut off by the strain curve of the additional neck at $x^* = 0.4$.

The stretched specimens 2A, 2B, and 2C are shown in Fig. 17.

VII. Progressive Yielding by Two Advancing Fronts

As in the preceding group of tests, a study of local conventional strains, as stretching produced a yield-point elongation, was the object

of this last set of tests. The specimens used were of the type shown in Fig. 1a. With this type of specimen the initial neck formed at the central undercut section, and two advancing fronts proceeded to yield the specimen in both the negative and positive x^*-directions. The specimens were stretched at a lower-head speed of 3.6 in./sec. Fig. 15 shows the progressive stages of elongation (recorded diagrams). Fig. 18 presents the results of tests 3A, 3B, and 3C.

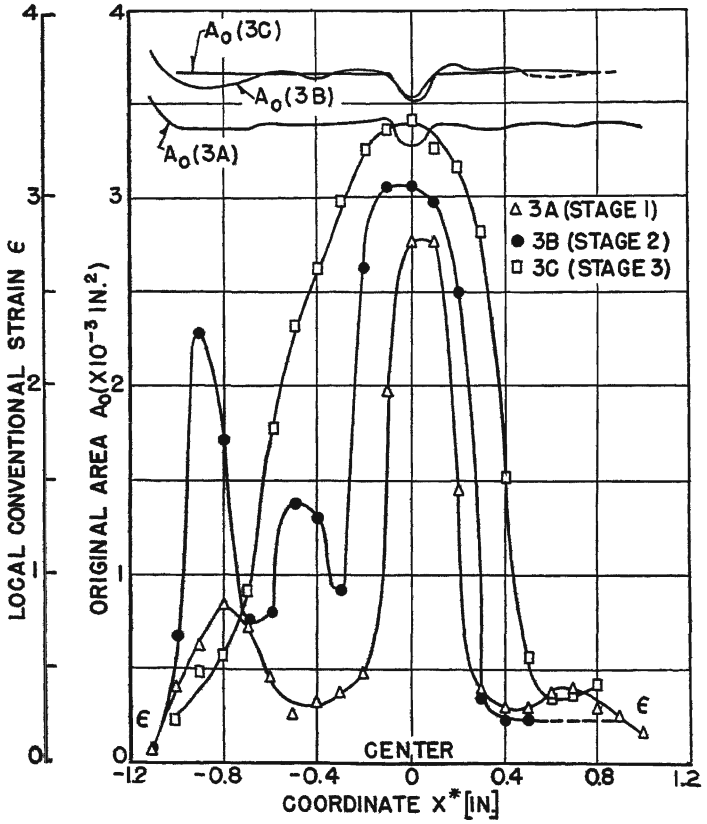

FIG. 18
Conventional Strain Distribution along the Axis of a Stretched Nylon Strip Tensile Specimen (2 Advancing Fronts)

As in test 2A, the stretching of specimen 3A was stopped as soon as its load-elongation diagram showed a leveling off of load at the lower yield value. The strain value at the undercut center section was 2.76 and dropped to 0.30 at $x^* = -0.4$, making the negative yield front 0.4 in. long. The positive front was also 0.4 in. long. The maximum strain of 2.76 is considerably lower than the 3.57 maximum of test 2A and the recorded

diagram (Fig. 15) of test 3A shows the lower yield load to be much less than that of test 2A. This again can be attributed to the speed effect in nylon, since two yield fronts instead of one reduced the mean strain rate[12] to one-half of its former value.

Specimen 3B shows three maximum strain values. These were produced by small local reductions in the original area. Two major necks formed, probably simultaneously, since no sudden drop in lower yield load was recorded. The recorded diagram does show a small gradual drop in lower yield load which was probably caused by the gradual formation of the third neck which did not fully develop. The stretched specimen is shown in Fig. 17. The main strain maximum of 3.05 (at $x^* = 0$) is lower than the 3.90 maximum of test 2B, which was expected, according to former reasoning. Again the load continuation on this main neck has produced a greater maximum strain than that of test 3A. The positive yield front of the main neck is 0.3 in. long. This front and that portion of the negative front that was not cut off by the rest of the strain curve, are very similar to the fronts of test 3A.

Specimen 3C has a maximum strain value of 3.40 at $x^* = 0$. The positive front has a length of 0.3 in. (from $x^* = 0.3$ to $x^* = 0.6$). This front is very similar to the positive fronts of specimens 3A and 3B. The maximum strain of 3.40 conforms to the presented theory, being greater than the maximum of test 3B. A comparison of the maximum strains of tests 3C and 2C show them nearly equal. This was to be expected since the maximum-strain section of specimen 2C was not subjected to load continuation strain, as stated before. The negative portion of the curve shows a rather peculiar shape, but close study of the curve and load-elongation diagram reveals the reasons for this shape. Approximately half way along the lower yield-load line (on the load-elongation diagram), a gradual dropping of load begins. This means that material, in addition to the initial neck, has evidently yielded a short time after the formation of the initial neck. This has caused irregularities in the shape of the progressive negative front. The stretched specimens are shown in Fig. 17.

From the foregoing analysis and theory, a conclusion may be drawn as to how an idealized set of progressive strain curves would look. Fig. 19 shows these shapes. In the time t the initiation of the plastic zone has come about. Its strain curve consists of a positive and negative front connected by a small portion of uniform strain (due to load continuation on the specimen) in the region of the maximum A. The line aa defines the mean of this uniform strain. In the time $2t$ the fronts remain practically of the same shape, but have moved out to new positions. Further uniform straining in the region of the maximum has increased the maximum to B, and raised the mean uniform-strain line aa, to a new position bb. Finally

[12] See Ref. 5.

at time $3t$ the fronts have advanced to the positions shown. The maximum is now at C, and the mean uniform-strain line is now cc. The fronts have remained practically of the same shape in every position. Below the strain-curves, one-half of the ideally stretched specimen corresponding to each curve is shown.

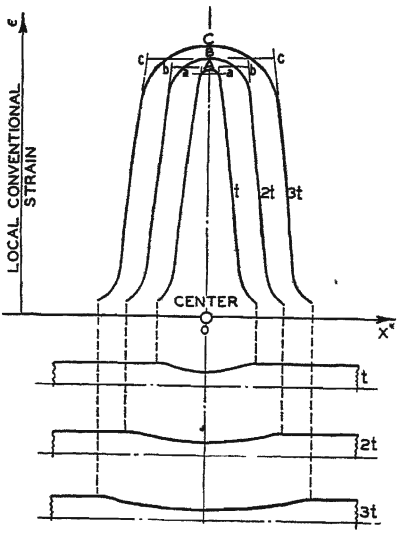

FIG. 19
Idealized Shapes of Advancing Strain Fronts Corresponding to Equal Time Intervals During Progressive Yielding

ACKNOWLEDGMENTS

The author's acknowledgments are due to Dr. A. Nadai of the Westinghouse Research Laboratories for guidance offered in this investigation, to Division 2 of the National Defense Research Committee, and to the E. I. duPont de Nemours Company (Nylon Division) for supplying the needed materials, and for advice concerning the same.

VIII. SUMMARY AND CONCLUSIONS

It was found that in nylon the yield-point elongation increased almost 3 times for a 10,000-fold increase of the speed of stretching. The true yield stresses and yield load stresses increased almost 2 times over the same range. It was observed that the first sharp drop of load, or any succeeding drop of load after the visible beginning of the yielding process, came simultaneously with the formation of a double yield front (a double yield front refers to the boundaries of the neck or constriction that form on a nylon fiber when the yield point has been reached). As the speed of deformation increases, the length of the advancing yield front decreases, or, stated in other words, the maximum strain of a cross-section of material due to the front passing over the section occurs more abruptly.

This maximum strain was found to increase with the speed of stretching.

The test results gave proof that, as the rigidity of the testing machine increases, the load drop becomes steeper from upper to lower yield point; this load-drop line appears linear. The upper yield-load stress was found to increase with an increase in machine rigidity.

The full yield-point elongation of nylon is composed of two parts, first, the strain in a section of material due to the plastic yield front passing over it, and second, the strain due to the continuous action of the load on this section as the plastic discontinuity advances to yield other sections of material; the longer the load is allowed to remain on the section the greater the strain of that section becomes. Yielding by two advancing fronts differs from the single-front yielding in that twice as much material is straining in the former type. This means that for the same relative head speed, the mean strain rate in the two-front yield is cut in half. This makes the maximum strain of a section of material due to the front passing over it less than it is in the single-front yield. The shape of the plastic yield front remains approximately the same throughout the yielding process provided the relative speed between the heads of the specimen remains the same.

References

1. Carothers, W. H., and Hill, J. W., *J. Am. Chem. Soc.* **54**, 1579 (1932).
2. Kidder, C. P., *Mech. Eng.* **63**, 287 (1941).
3. Simonds, H. R., and Ellis, C., Handbook of Plastics, p. 381. Van Nostrand, New York, 1943.
4. a. Korber, F., *Mitt. deut. Verbandes Materialprüfung* **8**, 91 (1926).
   b. MacGregor, C. W., *Trans. Am. Soc. Mech. Engrs.* **53**, APM-187 (1931).
   c. Elam, C. F., *Proc. Roy. Soc. (London)* **165**, 568 (1938).
   d. Davis, E. A., *Trans. Am. Soc. Mech. Engrs.* **60**, A-137 (1938).
   e. Nadai, A., and Manjoine, M. J., *Trans. Am. Soc. Mech. Engrs.* **63**, A-77 (1941).
5. Winlock, J., and Leiter, R. W. E., *Trans. Am. Soc. Metals* **25**, 163 (1937).
6. a. Nadai, A., Plasticity, pp. 85, 92–96. McGraw-Hill, New York, 1931.
   b. Winlock, J., and Leiter, R. W. E., *Trans. Am. Soc. Mech. Engrs.* **61**, 581 (1939). Also the two preceding References.
7. Siebel, E., Schwaigerer, S., Esser, H., *et al.*, *Arch. Eisenhüttenwesen* **11**, 630 (1937–38).

THE STRESS-STRAIN RELATIONSHIP OF NYLON UNDER BIAXIAL STRESS CONDITIONS

Julius Miklowitz

From the Westinghouse Research Laboratories, East Pittsburgh, Penna.

Received November 29, 1946

ABSTRACT

In a previous paper the writer describes and discusses the stress-strain characteristics of nylon, under an applied-uniaxial tensile stress (1). The present paper describes a method by which the stress-strain characteristics of nylon under equi-biaxial tensile stress were investigated. The results of the tests made are used for comparison with the applied single-stress condition, under which nylon showed a well-defined yield point and localized yielding.

I. INTRODUCTION

Nylon in its unoriented molecular structure is a material that exhibits a well-defined yield point when stressed in ordinary tension[1]. In a previous study by the writer the stress-strain characteristics of nylon under an applied-uniaxial tensile stress have been investigated (1). The enormous strain values in nylon (in some cases up to 400% or more at fracture) make it an extremely valuable material in studying localized yielding, a phenomenon which is so well known to be a property of mild steel. Nylon yields under the action of two or more plastic discontinuities (in the form of pronounced necks or constrictions on the fiber which travel the length of the specimen, producing a yield-point elongation[2] under a constant load. In the previous work (1) the initial plastic flow and the accompanying phenomena in nylon were compared with those in mild steel.

The present paper discusses the stress-strain characteristics of nylon under equi-biaxial tensile stress. It was believed that the comparison of the mode in which this material is suddenly reoriented under these

[1] In superpolymeric substances an unoriented molecular structure is one in which the long-chain molecules are in a state of random orientation. Upon drawing the originally unoriented fiber or strip into its oriented structure, the long-chain molecules arrange themselves in a definite pattern parallel to the longitudinal axis of the specimen. In the orientation process in the present case of the membrane subjected to biaxial stress, it is believed that the long-chain molecules arrange themselves in a pattern parallel to the plane tangent to the membrane.

[2] In materials that yield discontinuously the yield-point elongation denotes the amount of strain on the stress-strain diagram between the yield point and the point at which uniform strain begins.

conditions with that of the yield-point phenomenon under ordinary tension would be of considerable interest.

II. Material

The nylon membrane specimens were cut from a rolled sheet of approximately 0.009 in. thickness. This material naturally had to have the unoriented molecular structure. The nylon was kept under a constant relative humidity of 65%, which is its best testing condition. The temperature variable was not taken into account since all tests were made at a fairly uniform ambient temperature. A preliminary tensile test proved that the volume of the material remained practically constant when strained permanently. The following strain calculations were based on this fact. The recovery of 2% in 24 hours was small enough to neglect.

III. Method

Fig. 1 shows the device used to subject the thin nylon membrane to approximately equi-biaxial tensile stress. It consists of a base plate of steel upon which an unstretched nylon membrane was clamped. The base plate was undercut a small amount to allow for an initial volume of air between the membrane and plate. A bicycle tire pump served to inflate the region between membrane and plate, increasing the pressure and volume simultaneously.

The following nomenclature has been used to develop expressions for stress and strain:

Symbol	Meaning
ϵ_1, ϵ_2 and ϵ_3	Principal conventional strains
σ	Equi-biaxial true stress (lb./in.^{2})
σ_0	Equi-biaxial load stress (lb./in.^{2})
p	Internal pressure (lb./in.^{2})
h_0	Original thickness of membrane
h	Final thickness of membrane
s	Length of arc of deflected membrane along meridian plane
w	Deflection, measured at the vertex of the membrane
a	Radius of undeflected membrane
z, r	z is deflection of membrane over a chord of length $2r$ in meridian plane
ρ	Radius of curvature of the deflected membrane in meridian plane.
α	Central angle of arc s

In the initial small inflations it was assumed that the membrane took the shape of a segment of a sphere, and that a meridian section through

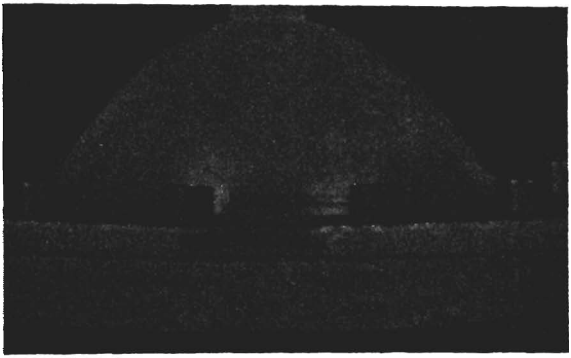

FIG. 1

Device for Subjecting Nylon Membrane to Equi-Biaxial Stress (Specimen M_2)

this segment looked like Fig. 2a. From the geometry of the deflected membrane

$$\epsilon_1 = \epsilon_2 = \frac{s}{a} - 1 \tag{1}$$

$$s = \rho\alpha \tag{2}$$

$$\tan \alpha = \frac{a}{\rho - w} \tag{3}$$

$$\rho^2 = (\rho - w)^2 + a^2 \tag{4}$$

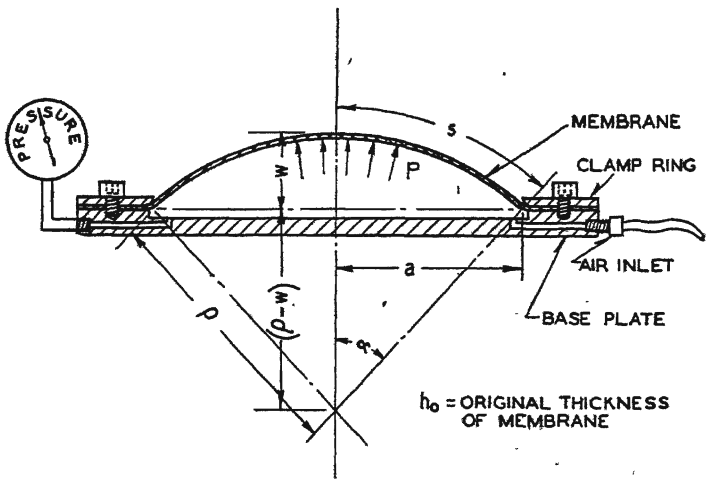

FIG. 2a

A Nylon Membrane Under Small Deflections

If we assume that angle α is sufficiently small for the approximation $\alpha = \tan \alpha$ to be used, from Eqs. (2), (3) and (4), Eq. (1) becomes

$$\epsilon_1 = \frac{2w^2}{a^2 - w^2} \tag{5}$$

From Eq. (4), and the relation $\sigma_0 = p\rho/2h_0$ for the stress in a thin spherical membrane, the equi-biaxial load stress σ_0 is given by

$$\sigma_0 = \frac{p(w^2 + a^2)}{4wh_0} \tag{6}$$

Eqs. (5) and (6) gave a means of obtaining ϵ_1 and σ_0 by simply measuring the deflection of the membrane at small pressures. The plot of equi-biaxial load stress-conventional strain, due to deflections given membrane

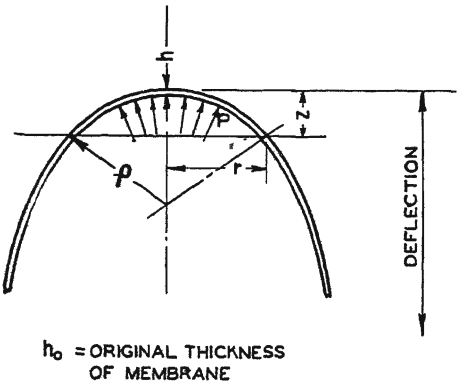

FIG. 2b
A Nylon Membrane Under Large Deflections

M_1, is shown in Fig. 3. The curve of a tension test of nylon fiber (test run at a machine head speed of 0.030 in./sec.) is shown in Fig. 3 also.

When the deflections are made large, the foregoing method of determining stress and strain does not remain valid since the surface of the membrane now becomes a more complicated surface of revolution. Fig. 2b is a sketch of the new conditions. Replacing the region near the vertex by the osculatory spherical membrane, in the plastic state the following relation holds:

$$(1 + \epsilon_1)(1 + \epsilon_2)(1 + \epsilon_3) = 1 \tag{7}$$

Since, near the vertex of the membrane under the equi-biaxial stress, $\epsilon_1 = \epsilon_2$, Eq. (7) may be written as

$$(1 + \epsilon_1)^2 = \frac{1}{1 + \epsilon_3} = \frac{1}{1 + \dfrac{h - h_0}{h_0}}$$

Finally,

$$\epsilon_1 = \sqrt{\frac{h_0}{h}} - 1 \tag{8}$$

From former reasoning (see Eqs. (4) and (6)), we may write the equi-biaxial true stress as

$$\sigma = \frac{p(z^2 + r^2)}{4zh} \tag{9}$$

By taking a photograph of the contour of the inflated membrane (the contour being the profile of the membrane in the meridian plane, see Figs. 1 and 4) simultaneously with a pressure reading, and then cutting the membrane and directly measuring h at the vertex point, it was possible, by Eqs. (8) and (9), to plot an equi-biaxial true stress-con-

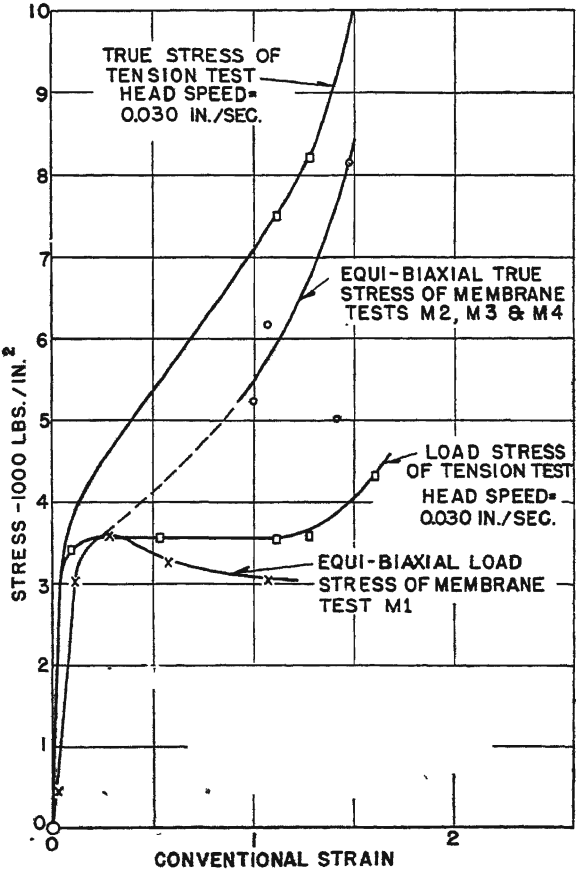

FIG. 3

A Comparison of the Equi-Biaxial Stress-Strain Relationship with That in the Ordinary Tensile Test of Nylon

ventional strain curve for a series of three tests—M_2, M_3 and M_4. Specimen M_2 is shown in Fig. 1, M_4 in Fig. 4. These tests are numbered in order of increasing applied deflections. Each test gave one point on the curve, which is shown in Fig. 3. The true stress curve of the fiber tension test is used for comparison.

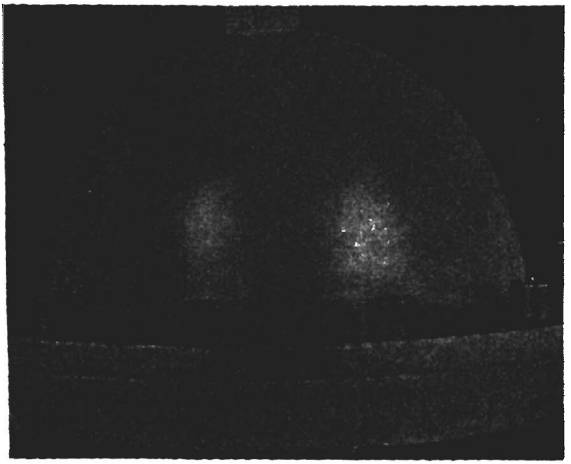

FIG. 4
Nylon Membrane Under Equi-Biaxial Stress (Specimen M_4)

ACKNOWLEDGMENTS

Acknowledgments of the author are due to Dr. A. Nadai of the Westinghouse Research Laboratories for guidance in this work, to Division 2 of the National Defense Research Committee for supporting and permitting publication of the work, and to the E. I. duPont de Nemours Company (Nylon Division) for supplying the material, and for advice concerning the same.

IV. RESULTS AND CONCLUSIONS

As shown in Fig. 3, membrane M_1 yielded under an equi-biaxial load stress of 3600 lb./in.^{2} at 0.3 strain. The stress gradually dropped to 3050 lb./in.^{2} at 1.08 strain. Comparing this test with that of the nylon fiber in tension, it may be said that both experience practically the same flow point. The essential difference is the drop in stress during the yield-point elongation of the membrane, whereas the fiber yields under a constant stress.

Comparing the true stress curves of ordinary tension and equi-biaxial tension, it may be seen that the former has points all of which are above those of the latter.

REFERENCES

1. MIKLOWITZ, J., *J. Colloid Sci.* 2, 193 (1947).

SOME RHEOLOGICAL MEASUREMENTS ON THE SURFACE OF SAPONIN IN WATER

John R. Van Wazer [1]

From the Department of Manufacturing Experiments, Eastman Kodak Company, Rochester, New York

Received December 5, 1946; Revised copy received January 10, 1947

Introduction

Although work has been reported on the mechanical properties of saponin surfaces, no study has been made in which the concepts and methods of modern rheology have been employed to full advantage. It is known that surfaces of saponin solutions are rigid and have a measurable shear modulus (9). The superficial viscosity of saponin has also been studied (11), and the surface concentration of saponin in water has been experimentally demonstrated (12) to be greater than the bulk concentration. The object of the work presented in this paper has been to measure as many mechanical properties of saponin surfaces as could be readily interpreted and to attempt to correlate these properties qualitatively.

In all the experiments reported here the solutions were prepared from one batch of commercially pure saponin powder which was carefully mixed before any samples were taken. Stock solutions of 0.1–0.5% were prepared and diluted to smaller concentrations when required. Since saponin is strongly adsorbed at interfaces, it is doubtful whether the concentrations around 0.001% are at all correct because, in the process of dilution and pouring from one container to another, saponin is probably lost by adsorption on the walls of the containers.

Surface Viscosity [2]

Apparatus and Procedure

A rotational viscosimeter was used to measure the surface viscosity. It appeared that by use of this method the viscosity of the body of the fluid could be subtracted from the viscous resistance of the fluid plus the surface, so as to obtain the flow characteristics of the surface alone.

[1] Present address: Research Laboratory, Rumford Chemical Works, Rumford, Rhode Island.

[2] The term "viscosity" is used here in the general sense of internal friction and does not mean the coefficient of viscosity. Thus a non-Newtonian fluid can be said to have viscosity although a physically real viscosity coefficient cannot be computed for it.

Several types of cylinder systems were used with an improved McMichael viscosimeter having variable speeds of rotation. In preliminary experiments a wire ring was attached to the torsion wire and allowed to just touch the surface of the fluid contained in an annular space. Later a hollow brass cylinder, open at the bottom, was dipped in the fluid contained between an inner and outer cylinder rotated together as is shown in Fig. 1. In this set-up the height of the liquid could be varied by means of a leveling bulb outside the cylinder, and measurements of the viscous torque could be made at different heights of the liquid ranging from 0 to 4 cms. submergence of the suspended cylinder. Some experiments were also performed with a set of concentric cylinders furnished with the McMichael instrumen.. The shape of the consistency curves

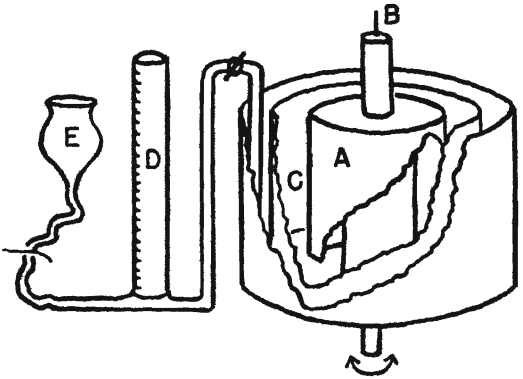

FIG. 1

Viscosimeter cups consisting of a hollow cylindrical shell, A, suspended from a torsion wire, B, and dipping into an annular volume of fluid, C.D is an arrangement for adjusting the height of the fluid by means of the leveling bulb E.

obtained with these various set-ups was the same, although the instrumental constants were different.

The data obtained with the two concentric cylinders were computed according to the usual relationship (1), and those obtained with the ring or cylinder dipping into an annular space were computed according to an equation which has been published recently (4). All the measurements reported were made after the solution had stood in the apparatus for several hours, as the rigid surfaces formed rather slowly.

Data and Results

When measurements of viscosity were made in a set of Ostwald capillary tube viscosimeters, it was found that the ratio of the viscosity coefficient of 0.1% saponin solution to the viscosity coefficient of pure

water at 25°C. was constant and equal to 1.03, although the tubes in the viscosimeter were of different sizes, giving a variation in shearing rate of *ca.* 8:1. In comparison with this, the consistency curve of saponin solutions obtained by rotational methods was similar to that characteristic of a plastic material as can be seen in Fig. 2A. The angle θ of Fig. 2A was practically the same for pure water as for saponin solutions, and when this angle was changed by varying the depth of submergence of the cylinders, it changed in the same way for pure water and the saponin solutions. This implies that the viscous resistance of the surface lamina is similar to solid friction or to that of an extremely thick gel (Fig. 2B)

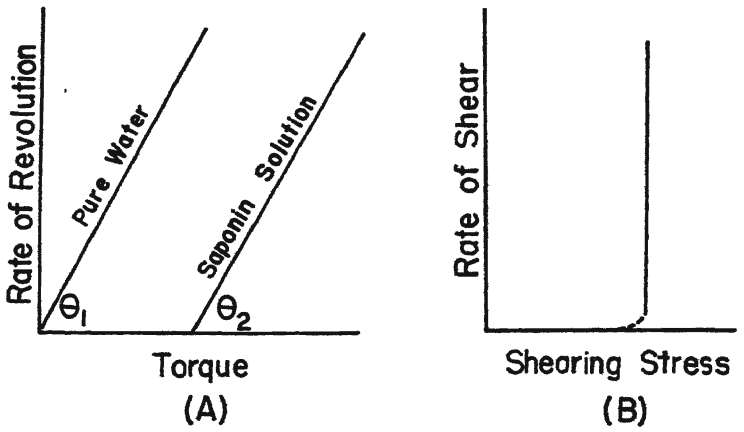

FIG. 2

(A) Consistency Curves for Saponin Solutions and Water
Angle θ_1 is very slightly greater than θ_2.

(B) Theoretical Consistency Curve for the Saponin Surface
Superposition of this curve on that for pure water results in the consistency curve of the solution.

since the shearing force is essentially independent of the rate of shear. After the rotation was stopped, the torque slowly diminished from a value near the extrapolated yield value to a much lower yield value. This final yield value remained constant for a period of over 24 hours. Within an experimental variation of *ca.* 10%, the yield values and consistency did not appear to change with concentration over the range of 0.005% to 0.5% saponin. However, the extrapolated yield value appeared to decrease by about 12% when the height of the liquid was raised from zero to 3 cm. submergence. When the saponin solutions were allowed to age for a week or so, the value of the yield point became much greater and was quite irreproducible. This is in accord with the findings of Wilson and Ries (11). When distilled water was allowed to stay in the apparatus

for about 24 hours, a slight yield point was found (3) due to insoluble and surface active material settling out of the air. Since no adequate method was devised for correcting the data on saponin solutions for the effect of traces of material settling from the air, results on aged solutions cannot be interpreted with respect to the adsorbed saponin. The values of the yield points as determined in the several experimental arrangements are given below. The consistency is not tabulated because it is only a few percent larger than the viscosity coefficient of pure water, and it was measured with greater accuracy in the capillary tube experiments.

TABLE I

Surface Yield Values of Saponin Solutions

Experimental set-up	Concentration (*Per cent* saponin)	Age of sample	Extrapolated yield value (*dynes/cm.*)	Final yield value (*dynes/cm.*)
Wire ring in annulus	0.1	fresh	.96	.35
	.2	2 weeks	1.64	.71
Cylinder in annulus (varying depths of submergence)	0.1	fresh	1.03	.34
	0.01	fresh	1.01	.34
	0.002	fresh	1.05	.34
Concentric cylinders	0.1	fresh	1.92	.30

Surface Shear Modulus by a Resonance Method (7)

Apparatus and Procedure

The important parts of the apparatus used in these experiments is shown in Fig. 3 and is quite similar to the arrangement used in the preliminary measurements of surface viscosity. The saponin solution was contained between two concentric cylinders which were rigidly coupled together and made to perform sine wave oscillations of small amplitude (*ca.* 10°) about their axis. A wire ring was allowed to touch the surface of the fluid so that it was concentric with the cylindrical walls of the container. This ring was rigidly attached to a small mirror and the whole ring system was suspended by a long, thin, silk fiber. The moment of inertia of the ring system could be measured by allowing it to oscillate from a wire of known rigidity. Photographic tracings of the motion of the wire ring as a function of time were made by reflecting a narrow, horizontal beam of light from the small mirror onto a camera consisting of a vertical slit behind which a strip of photographic paper was passed at constant speed. One of these traces is shown in Fig. 4, and it can be seen that at a certain frequency of oscillation the amplitude went through a maximum and resonance occurred.

Let us assume that the surface is a mathematical plane and express the data as a surface shear modulus. This surface shear modulus is numerically equal to the shear modulus which would be obtained by assuming that the thickness of the surface layer was equal to unity. Thus the true shear modulus can be obtained from the surface shear modulus by dividing by the thickness of the surface. It can be shown that the surface shear modulus, G_o, is given by the following relationship where I is the moment of inertia of the ring of radius r_2 suspended be-

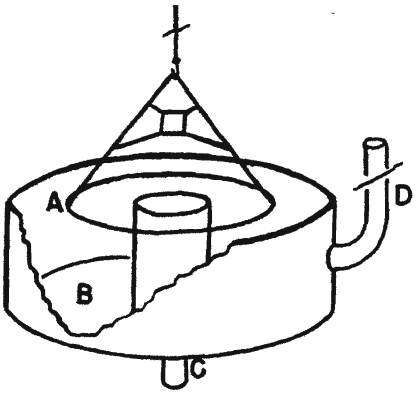

FIG. 3

Wire ring, A, suspended in an annular cup, B, which can be made to oscillate around a shaft, C. The surface can be renewed by flushing the solution through tube, D.

tween cylinders whose radii are r_1 and r_3 with $r_3 > r_2 > r_1$; f is the resonance frequency:

$$G_o = \pi f^2 I \frac{\left(\frac{1}{r_1^2} - \frac{1}{r_2^2}\right)\left(\frac{1}{r_2^2} - \frac{1}{r_3^2}\right)}{\left(\frac{1}{r_1^2} - \frac{1}{r_3^2}\right)}. \qquad (1)$$

The calculation of the shear modulus given above holds true only for an undamped or slightly damped system. When the damping is great, the shear modulus calculated by Eq. *1* is too small. However, if the magnification factor, which is the ratio of the amplitude at resonance frequency to the amplitude at zero frequency, is known and a model is assumed for the elastic system, the correct shear modulus (10) can be obtained from G_o. The simplest models consist of an elastic element with series damping, or an elastic element with parallel damping, in which the dampers are assumed to be filled with Newtonian liquids. The data in this work are reported as the uncorrected surface shear modulus and also as the moduli corrected for series and for parallel damping.

Data and Results

From traces similar to Fig. 4 the magnification factor and resonance frequency can be obtained. It will be noted that both the amplitude and frequency at resonance increase with the time elapsed since the surface

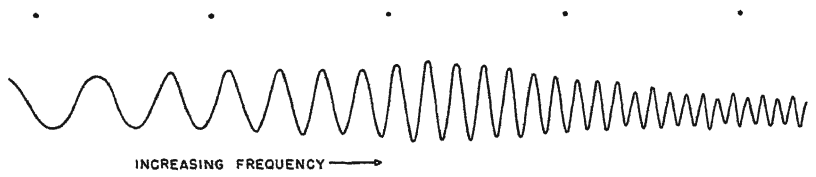

FIG. 4

Photographic Tracing of Amplitude of Oscillation Changing with Frequency
The dots above the tracing were made by a light flashing 1.46 times per sec.

was formed. The resonance frequency does not depend on the way the ring is placed in the surface although the damping does. This can be seen from the following table which gives data obtained on a 0.2% saponin solution, the surface of which had formed for about 5 minutes:

TABLE II

Variation of Resonance Data With Position of Ring

Position of ring	Magnification factor	Resonance frequency (*cycles/sec.*)	G_o (*dynes/cm.*)
Just touching surface, concentric	2.00	8.4	194
Lowered so that there is very little meniscus showing, concentric	1.85	8.3	188
Almost out of the surface, not concentric	2.00	8.3	188
Just below surface	1.00	None	—

The increase of resonance amplitude and frequency with the age of the surface is given below for several different bulk concentrations of saponin. The resonance frequency that is finally reached in the aging process is constant from 0.01% to 0.2% saponin concentration, and the final value of the magnification factor seems to increase slightly with concentration. However, this latter effect is questionable since the magnification factor varies with the placement of the ring.

If we take a magnification factor of 2.00 and an uncorrected surface shear modulus of 305 dynes/cm. as the values finally reached in the aging

TABLE III

Resonance Data

Bulk concentration (*Per cent* saponin)	Moment of inertia of ring (*g.-cm.²*)	Age	Magnification factor	Resonance frequency (*cycles/sec.*)	G_o (*dynes/cm.*)
0.0	1.00	—	—	none	—
0.005	1.00	2 min.	1.30	7.8	168
0.01	1.00	flowing[a]	1.05	*ca.* 5.0	70
		2 min.	1.28	5.3	80
		27 min.	1.48	7.4	150
		5 hr.	1.53	10.5	304
		7 hr. 10 min.	1.48	10.5	304
0.1	3.90	1 min.	1.83	4.93	225
		25 min.	2.05	4.36	178
		3 hr.	1.95	5.70	305
	1.00	flowing	1.05	5.5	85
		30 sec.	1.78	6.7	122
		90 sec.	1.83	6.3	106
		3 min.	1.67	6.8	127
		52 min.	1.97	8.5	198
		100 min.	1.90	9.2	233
		2 hr. 15 min.	1.83	8.4	194
		2 hr. 45 min.	2.05	10.3	293
		4 hr. 22 min.	1.75	11.9	387
		5 hr.	1.78	10.7	320
0.2	1.00	flowing	1.55	6.5	116
		1 min.	1.98	7.5	154
		30 min.	2.00	9.4	242
		3 hr.	2.00	9.8	262
		4 hr.	1.78	10.5	304
		15 hr.	1.95	10.5	304

[a] In the experiments marked "flowing" the surface was continually refreshed by allowing the solution to flow over the edge of the outer cylinder.

process, the final surface shear modulus corrected for parallel damping is 350 dynes/cm. and the final surface shear modulus corrected for series damping is 530 dynes/cm. Since the damping decreases as the ring is raised from the surface of the solution and since the internal damping in many gels with a consistency curve like that shown in Fig. 2B is very low, it is probable that the correct value of the surface shear modulus is about 310 dynes/cm. The increase in surface shear modulus with time after the surface was formed is probably due to an increase in the thickness of the elastic surface lamina. Using the value of 10–40 μ for the final

thickness of the surface lamina obtained by Wilson and Ries (11), the real shear modulus is found to be about 9×10^4 to 35×10^4 dynes/cm^2. This is in the order of magnitude of the elastic moduli of a medium stiff gel (2).

Experiments with the Langmuir Balance

Some experiments have been performed with a Cenco Hydrophil balance [3] which was modified so that the motion of the float along the fluid surface, as well as the force necessary to cause this motion, could be measured. This was effected by attaching a small mirror to the arm which held the float and reflecting a light beam from the mirror to amplify the motion of the float approximately 15 times. Although the interior of the trough and all the barriers were waxed, the contact angle between the saponin solutions and paraffin is such that a high meniscus cannot be formed, and thus great care must be taken in filling the trough. In order to record the variation of the force due to the torsion wire with time, a potentiometer (radio) was attached to the torsion head, and the amplifier and recording mechanism of a Brush Surface Analyser [4] was used. The width of the trace formed by the Brush recorder was proportional to the angle through which the torsion head on the Langmuir balance was turned. Before each experiment the surface was swept clean in the usual manner.

Surface Young's Modulus

To measure Young's modulus, the movable barriers were placed quite close to the float so that the distance from the float to the barriers was small with respect to the length of the float. Under these conditions the effect of the sides of the trough can be neglected and we can assume that the float is attached to the barrier on either side of it by an elastic membrane. Then, by simultaneously measuring the displacement of the float and the force necessary to cause this displacement, Young's modulus can be computed by the following formula:

$$E = \frac{f}{d\left(\frac{1}{l_1} - \frac{1}{l_2}\right)}, \qquad (2)$$

where E is the surface Young's Modulus, f is the applied normal force per unit length of float which causes a motion of the float $= d$, and l_1, l_2 are the distances from the float to the barrier on either side of it.

[3] Central Scientific Co., Chicago, Ill.

[4] Manufactured by the Brush Development Co., Cleveland, Ohio.

At large deflections, the force decays with time since there is some flow, as can be seen in Fig. 5. The true value of the elastic deflection was found by extrapolating these decay curves back, according to a logarithmic law, to the time at which the deflection was started. From traces such as Fig. 5, stress-strain curves were constructed, one of which is shown in Fig. 6. The surface Young's modulus computed from these curves is given in Table IV.

It can be seen that the surface Young's modulus increases with time for about 150 minutes after the surface was first allowed to form, and

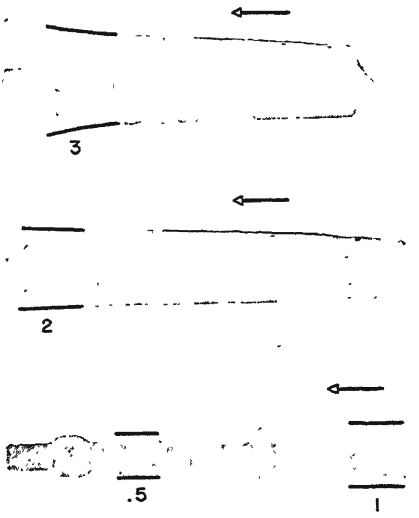

FIG. 5

Force-Time Curves from the Langmuir Surface Balance

The amplitude is proportional to the force and the charts moved at a constant rate in the direction of the arrow. The numbers on the graphs are the float deflections in 10^{-2} cm. corresponding to the charted force.

then becomes constant. This rate of increase of the modulus is poorly reproducible and can be fitted approximately to a first order rate equation. The increase of the surface Young's modulus with time is probably due to an increase in the thickness of the rigid surface layer and does not mean that the real Young's modulus increases with time. If we accept the value 10–40 μ for the final thickness of the surface layer, we see that the real Young's modulus of the surface must be 6×10^4 to 25×10^4 dynes/cm^2. At concentrations of 0.1–0.2% saponin the equilibrium surface Young's modulus is smaller than the equilibrium value of 240 dynes/cm. found at lower concentrations. This can be explained if we assume that the surface layer is more brittle at the higher concentrations and is folded

or broken during an experiment. Then a new surface with a very low surface-modulus would form at the points of rupture, thus causing the measured equilibrium surface modulus to be too small. This explanation is substantiated by the fact that when the calculated equilibrium modulus is low, there is very little change of the modulus with the age of the surface.

Also, the experiments performed on the 0.2% solution with $l_1 = l_2 = 8$ cm. gave a surface modulus which increased with time and approached the correct equilibrium value. In this case the length of the surface being

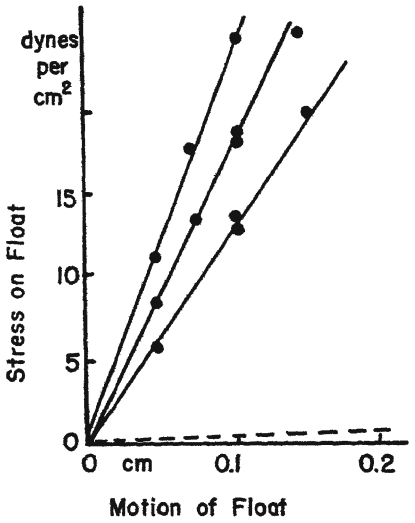

FIG. 6

Stress-Strain Diagrams for Saponin Surfaces

The dashed line at the bottom of the graph is the curve which is found for pure water and results from the fact that the center of gravity of the float system does not lie on the torsion wire. Corrections are made for this effect in the calculations.

stretched was great enough to withstand the motion of the float without rupturing. However, the effect of the edge causes the calculated value of the modulus to be high for large values of l.

Destroying the Surface

Some experiments were performed by moving one of the barriers toward or away from the float while the float was kept stationary and measuring the resultant force against the float. Thus when the barrier was moved away from the float, the float tended to be pulled along, and a certain force had to be applied to keep it stationary. When the barrier

TABLE IV

Surface Young's Modulus

(The trough is 14 cm. wide; and the float length is 12.2 cm.)

Concentration (*Per cent*)	l_1 (*cm.*)	l_2 (*cm.*)	Age of surface (*min.*)	Surface Young's modulus (*dynes/cm.*)
0.001	4	4	15	117
			65	220
			125	270
0.005	4	4	6	100
			76	180
			200	210
	2	4	420	230
	2	2	5	110
			100	170
			200	240
.01	4	4	5	110
			10	150
			90	190
			210	250
	3	3	420	220
	2	2	5	140
			98	190
			180	230
			210	240
			420	230
			1,200	240
			50,000	240
0.1	4	4	5	90
			28	110
			105	145
			150	160
	4	2	5	110
			78	110
			120	130
			150	110
	2	2	5	72
			58	77
			115	55
			175	63
0.2	8	8	3	110
			65	165
			115	230
	4	4	8	135
			56	145
			81	160
			120	160
	3	3	4	60
			30	115
			75	140
	2	2	4	85
			35	95
			140	110
			180	110

was moved toward the float, the surface was compressed and tended to move the float also. After the barrier had been moved from one position to another, the force on the barrier decayed according to a logarithmic law. This rate of decay is presumably a measure of the rate at which equilibrium is obtained between the body of the solution and the surface, since in all these experiments the surface area was increased or decreased by a factor of from 2 to 10. As might be imagined, these measurements were poorly reproducible, but they do show that the surface film is formed within a few minutes. When lycopodium powder was sprinkled on the surface and then the barrier was moved away from the float, an indication of the way in which the rigid surface ruptures under a tangential stress could be obtained. As the barrier was moved, rupture would occur at different spots on the surface so that, after the surface had been expanded several-fold, it was covered with a coarse web of powder filaments separated by clear spaces. After rupture would occur at a point, a round space, free of lycopodium, immediately formed due to the elastic forces. When the surface was compressed, the lycopodium powder appeared to show that the surface layer folded, buckled, and then slid over itself.

Discussion

From its mechanical properties, it is quite apparent that the surface of a solution of saponin is covered by an adsorbed layer of saponin molecules which are so close to each other that there is a great deal of interaction between them. Studies, *e.g.* (5), on gelatin and other gel-forming materials indicate that a gel of the type found at a saponin surface is a three-dimensionally bonded network of large molecules. Such a network, once it is formed, is a relatively unalterable entity, as is illustrated by the fact that the rate of formation of a gel from a gel-forming material and excess solvent is usually much faster than the subsequent dissolution of the gel itself in the remaining solvent. Since saponin surfaces exhibit a yield value which persists for several days, there cannot be a dynamic equilibrium between the body of the solution and the surface layer. However, when the surface layer is ruptured or swept away, a new, rigid surface is formed within a few minutes. This surface continues to strengthen for several hours.

It is noteworthy that the values of the rheological properties reported in this study were found to be independent of the bulk concentration of saponin, even though this concentration was varied by several powers of ten. This behavior is in accord with the idea that the rigid surface layer and the bulk of the solution are not in equilibrium.

Thus, we must conclude that the mechanism of formation of these

rigid surfaces is somewhat as follows: The saponin molecules in the body of a solution with a freshly cleaned surface diffuse to the surface region because of the difference in chemical potential. When enough molecules are present at the surface, a three-dimensional network is formed. This network, which is most irregular at first, slowly re-forms into a stronger, more regular arrangement. During this process, however, the molecules making up the gel network are not in equilibrium with the body of the solution, although it may be supposed that the molecules in the solution can interchange rather quickly with those at the lower boundary of the gel. It would thus appear that the mechanically rigid surface layer does not correspond with the usual types of sorption (6), obeying the Gibbs equation. In fact, it might best be considered as a separate phase. A study of these types of surface-bulk interactions using isotope tracer techniques would be advisable to substantiate the above hypotheses.

In the preceding experiments the value of the shear modulus was found to be slightly larger than that of Young's modulus. Since this result is not in accord with elastic theory (8)—which indicates that Young's modulus for a material of this type should be approximately three times as great as the shear modulus—the data are either unreliable or incomparable. Probably the discrepancy is due to the latter reason. The shear modulus resulted from a dynamic measurement, whereas Young's modulus was measured statically. It is well known (2) that static and dynamic measurements do not give the same values for a modulus of elasticity because of the possible existence of several bands of relaxation times for the material being studied, and the fact that static measurements are isothermal and the dynamic ones are essentially adiabatic.

Acknowledgment

I would like to thank Dr. E. K. Carver of the Department of Manufacturing Experiments at Eastman Kodak Company for the many informative discussions that we had on the subject of this paper. I also wish to thank Mr. Herbert Goldberg of the Kodak Research Laboratories for his helpful suggestions about measuring surface shear modulus.

Summary

By the use of new experimental techniques, values have been found for the shear modulus, Young's modulus, and the yield point of the adsorbed layer of solute on dilute aqueous solutions of saponin. These values are consistent with the concept that the surface consists of a stiff gel 10–40 μ thick.

The viscosity studies were made in a rotational viscosimeter devised so that the flow properties of the surface alone could be obtained by extrapolation. The shear modulus was measured in an instrument for investigating resonance frequencies in shear at the surface. Also, a Lang-

muir surface balance was so arranged that the force corresponding to a given motion of the float could be recorded as a function of time. This latter instrument was used to measure Young's modulus of the surface and to study the bulk-surface interaction of the solution.

References

1. Barr, Monograph of Viscometry, p. 222. London, 1931.
2. Ferry, *Ann. N. Y. Acad. Sci.* **44**, 313 (1943).
3. Gurney, *Phys. Rev.* **26**, 121 (1908).
4. Mooney, *J. Colloid Sci.* **1**, 195 (1946).
5. Poole, *Trans. Faraday Soc.* **21**, 114 (1925).
6. Ramsden, *Trans. Faraday Soc.* **22**, 484 (1926).
7. Sandvick and Goldberg, Unpublished results.
8. Scott Blair, Survey of General and Applied Rheology, p. 19. New York, 1944.
9. Shorter, *Phil. Mag.* **17**, 560 (1909).
10. Van Wazer and Goldberg, *J. App. Phys.* **18** (1947), in press.
11. Wilson and Ries, *Colloid Symposium Monograph*, **1**, 145 (1923).
12. Zadwidski, *Z. phys. Chem.* **42**, 613 (1903).

THE SUBMICROSCOPIC STRUCTURE OF PLANT CELL WALLS

Otto Treitel

From the Botanical Laboratory, University of Pennsylvania, Philadelphia, Pa.

Received Nov. 21, 1946

Introduction

In a recent paper (9) a theory was presented concerning submicroscopic structure in the cell walls of higher plants. The theory was supported by elasticity experiments on cylindrical plant tissues. According to this theory, the greater the ratio between the moduli of elasticity the greater is the ratio between crystalline and amorphous cellulose, the greater the percentage of cellulose, and the greater the orientation of the cellulose molecules. To support this theory on the submicroscopic structure of cell walls, a new experiment was performed.*

It is of importance to know that the cell walls of certain plants contain a great amount of amorphous cellulose, whereas the cell walls of other plants contain a great amount of crystalline cellulose. As plant tissues differ, it is necessary to refer to specific material. Here reference is made only to the average secondary cell wall, and only to the cylindrical plant tissues which were investigated (9).

The case of much amorphous cellulose is to be expected for petioles of *Nymphaea* because the ratio of the moduli of elasticity is small. In this case the ratio is 3 (9). The chain molecules deviate greatly from the direction of the axis of the tissue.

The case of much crystalline cellulose, is to be expected for woody branches of *Salix babylonica* because the ratio of the moduli of elasticity is great. In this case this ratio is 33 (9). Here most of the chain molecules of cellulose are about parallel to the axis of the tissue. It is probable that the ratios of the moduli of elasticity already reported (9) will have to be slightly changed if the real modulus of elasticity in transverse direction is to be used.

In 1925 L. Hock (7) proposed a theory of the Gough-Joule effect in raw rubber. He stated:

(a) Stretched rubber has a fibrous structure because the rubber molecules are in parallel direction.

(b) In greatly stretched rubber heat is produced, and forces of cohesion, van der Waal's forces, are acting.

* I wish to thank the Samuel Fels Fund for the grant which has made these investigations possible. I wish also to express my appreciation to Dr. William Seifriz for the use of laboratory facilities.

(c) The forces of cohesion are weak at high temperature because of the thermal motion of the rubber molecules. At low temperature the forces of cohesion are in equilibrium with the elastic forces in rubber.

The importance of Hock's work lies in the fact that he tried by experiment to prove the fibrous structure of stretched rubber which is expected from his theory of the Gough-Joule effect.

Method and Results

In the experiment of Hock (7) a stretched rubber strip was first fixed in a freezing mixture and then firmly frozen in liquid air. Thus frozen, the rubber strip may be split into fibers by striking with a hammer. These fibers, which were separated from each other by striking, represent parallel bundles oriented in the direction of stretching. It is to be assumed that each bundle is composed of long chain molecules. The possibility of such chain molecules was proved by H. Staudinger on the basis of chemi-

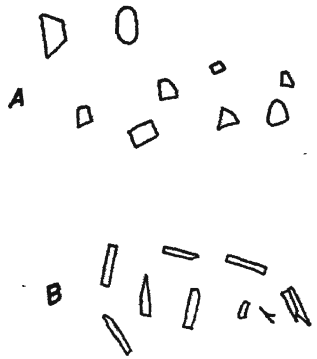

Fig. 1

Particles of Plant Tissue Frozen with Liquid Air

A. Petioles of *Nymphaea gladstonia* (slightly magnified); B. branches of *Salix babylonica.*

cal experiments. The foregoing facts prove that stretched rubber can have micelles. If, now, undeformed rubber is frozen in liquid air and struck by a hammer, it breaks into irregular pieces similar to glass, and this proves that undeformed rubber is amorphous with a network structure (7).

Hock's method of freezing with liquid air was used in the investigation on the submicroscopic structure of cell walls here reported. The tissues studied were petioles of *Nymphaea gladstonia* and branches of *Salix babylonica.*

First, a piece of the cylindrical petiole of *Nymphaea gladstonia* was treated with liquid air. By striking the firmly frozen petiole with a hammer, irregularly shaped particles were produced (Fig. 1A). A section

of a woody branch of *Salix babylonica* was likewise treated with liquid air. By striking the firmly frozen branch with a hammer, linear particles were formed. These particles were roughly parallel to the axis of the branch (Fig. 1B).

Discussion

The question of interpretation of the last two experiments now arises. According to Berkley (1) it has been repeatedly demonstrated by the use of X-ray technique that the dimensions of the unit cell of the cellulose crystal of a cotton fiber do not change with changes in moisture content. It is not likely, therefore, that the dimensions of cellulose crystals will change under the same conditions. But Berkley believes that, although the submicroscopic cellulose crystals of cell walls cannot be altered by humidity, the amorphous cellulose may be so changed.

According to Treitel (9) none of the submicroscopic structure of cell walls of plant tissues generally is changed because of the influence of humidity.

On freezing in liquid air the solid material of plant tissues becomes rigid because the liquid parts of the tissue freeze. This is proved by a simple experiment. Dry cotton-wool treated with liquid air does not become rigid because in this case no water freezes.

On freezing plant tissues in liquid air the contents of the cells and the water in the crevices between parts of the submicroscopic structure of the walls will freeze but the solid structural material of the cell walls does not change.

So we may assume that the particles of frozen plant tissue produced by striking with a hammer give a rough picture of the submicroscopic structure of the secondary cell wall, at least in all cases where the cell wall contains much cellulose.

In the case of the frozen petiole of *Nymphaea gladstonia* irregularly shaped particles are observed after crushing.

Interpreted in the light of Hock's experiment with undeformed rubber, the submicroscopic structure of the secondary cell wall consists mainly of amorphous cellulose. In this case the submicroscopic structure is chiefly a network of cellulose molecules. This is in accordance with the fact that the ratio of the moduli of elasticity is 3 for petioles of *Nymphaea* (9).

In the case of the frozen branch of *Salix babylonica*, linear particles are observed. Again, interpreted in the light of the experiment with stretched rubber, the submicroscopic structure of the average secondary cell wall consists mainly of micelles of cellulose. The micelles are almost parallel to the axis of the branch. This is in accordance with the fact that the ratio of the moduli of elasticity is 33 for woody branches of *Salix babylonica* (9).

An experiment on the elastic stretching of wet petioles of *Nymphaea* showed that the particles obtained by using liquid air were a little more elongated in the case of stretched material than in the case of undeformed material. This result was to be expected because of the small strain, 0.02, at the elastic limit of wet petioles of *Nymphaea* (9).

If petioles of *Nymphaea* are stretched, the same result is to be expected as when undeformed rubber is stretched because of the similar structure of undeformed rubber and undeformed secondary cell walls of petioles of *Nymphaea*. Therefore, influence of water in vessels, or turgor, probably does not play a very great part in the stretching of petioles of *Nymphaea*. Most of the stretching will take place because of the elasticity of the cell wall. According to Freundlich and Hauser (4) droplets of liquid in raw rubber play a great part in the Gough-Joule effect in rubber. But according to L. Hock (7) the real explanation of the Gough-Joule effect is only possible by considering solid rubber. The Gough-Joule effect is to be observed for petioles of *Nymphaea* according to measurements not yet published. Hence there is another reason for believing that humidity or turgor probably play a small role in the elasticity of petioles of *Nymphaea*.

A measurement similar to the measurement of the influence of humidity on Young's modulus of branches of *Salix babylonica* (9) was carried out for petioles of *Nymphaea gladstonia*.

According to Treitel (9) for woody branches of *Salix babylonica* it was found that

$$E_1 = 1.2 \times E.$$

Young's modulus E refers to the wet branch, Young's modulus E_1 refers to the dry branch. Hence humidity does not play a great part in stretching of branches of *Salix babylonica*.

The petiole of *Nymphaea gladstonia* investigated had a weight of 9.100 g. at the beginning of the experiment. After 4 hours the weight was 6.040 g. This means that 3.060 g. of water evaporated from the petiole during 4 hours. The limp petiole now began to change its cylindrical shape by shrinking. Probably there was no more turgor in the cells and no more water in the vessels of the limp petiole. By using the equation:

$$EI = k(F/d) \quad (9)$$

it was found that, for a small tension,

$$E_1 = 2.2 \times E$$

where E refers to the wet petiole and E_1 to the limp petiole. During the experimental 4 hour period the evaporation of water produced a change of humidity in the petiole, and therefore the diameter of the petiole

became smaller. F/d was changed because of change of humidity and change of diameter. The change of diameter had the consequence that the moment of inertia, I, for solid plant material was also changed. The result $E_1 = 2.2 \times E$ is obtained by change of humidity and by change of the shape of the petiole. Because of the small value $E \sim 5 \times 10^8$ dynes/cm.^{2} for wet petioles of *Nymphaea* (9), E_1 also remains small. Thus, influence of humidity does not greatly change the order of size of Young's modulus of petioles of *Nymphaea*. Young's modulus for the "dry" petiole is $\sim 10 \times 10^8$ dynes/cm^2. In this case of the "dry" petiole the stretching is only effected by the elasticity of the cell walls.

In the computation it is assumed that turgor acts like the water in the vessels, because all water has gravity. It might be assumed that turgor as pressure plays no part in elastic stretching.

In the case of cylindrical tissues of *Salix babylonica* and *Nymphaea*, decrease in the amount of water increases the value of Young's modulus (9). The same rule also holds for plant fibers (9), and, according to Valkó (11, p. 119), for animal fibers such as wool.

In any case the ratio of moduli of elasticity is about the same for wet or dry cylindrical plant tissues.

According to Treitel (9) this ratio between Young's modulus and the transverse modulus of elasticity for rubber-like elastic dry cylindrical plant tissues is less than 10. The ratio is greater than 10 for metal-like elastic dry cylindrical plant tissues. This definition for rubber-like elastic and for metal-like elastic cylindrical plant tissues is better than the definition which uses curves (9).

The "dry" petioles of *Nymphaea* contain much water in the cell walls. Therefore, the cell walls probably contain a great deal of amorphous cellulose. The dry branches of *Salix* contain practically no water in the cell walls. Therefore, these cell walls probably contain much crystalline cellulose. Hence the results obtained for submicroscopic structure are well supported.

The conclusions here reached on chiefly amorphous cellulose in "dry" petioles of *Nymphaea* and on highly crystalline cellulose in dry branches of *Salix* are probable because of experimental work on cotton fibers by Berkley and Kerr (2).

According to these authors X-ray patterns of undried cotton fibers show little or no evidence of crystalline cellulose. Undried cotton fibers contain chiefly amorphous cellulose, and dried cotton fibers mostly contain crystalline cellulose. Amorphous cellulose in undried cotton fibers is formed by water molecules which separate cellulose chains. When cotton fibers are dried, the water molecules between the cellulose chains disappear, and the cellulose chains become closely parallel, with formation of cellulose crystals in dry cotton fibers.

"Dry" petioles of *Nymphaea* correspond to undried cotton fibers, dry branches of *Salix* correspond to dry cotton fibers. On the basis of these experiments the results mentioned above were obtained.

In the case of undried cotton fibers the water is between the chains of amorphous cellulose, but in the case of "dry" petioles of *Nymphaea* the amorphous cellulose is hydrated (see later). In hydrated cellulose the OH groups are surrounded by water molecules.

The correctness of the theory of submicroscopic structure for cell walls of higher plants depends greatly on a knowledge of the occurrence of amorphous and crystalline cellulose in cell walls.

There have been several theories on cellulose structure proposed.

(a) In 1864 Nägeli concluded, on the basis of the physical properties of cellulose, that the crystals or micelles were of submicroscopic dimensions, and that the water which penetrated between them caused swelling.

(b) In 1937 Mark, investigating regenerated cellulose, suggested that a given cellulose molecule may extend through a large number of crystals with the intermittent segments existing in the amorphous state.

(c) According to Frey-Wyssling (1936) the micellar cellulose rods of Mark are fused together in a colloidal particle of crystalline structure.

(d) In 1942 Berkley (1) investigated shrinkage and swelling of cotton fibers and concluded that the cellulose crystals in the cell wall have a molecular length of 15,000 Å. These crystals are surrounded by an amorphous matrix which, in the case of the secondary wall of the cotton fiber, at least, appears to be cellulose itself, from which Berkley deduced that amorphous cellulose may occur in plant cell walls. Bailey (9), on the contrary, is quite skeptical regarding the whole matter of the occurrence of amorphous cellulose in cell walls.

The cellulose pictures of Mark and Frey-Wyssling are in best agreement with the measurements made by the author of this paper. In addition, the picture for amorphous cellulose of Berkley and Kerr (2) was used.

The submicroscopic structure of average secondary cell walls of cylindrical plant tissues of higher plants may be represented by the schematic drawings in Fig. 2. These drawings give only a schematic picture of what is possible on the basis of experimental facts. Fig. 2 represents the general submicroscopic structure; micellar and amorphous cellulose alternate. In the second row of Fig. 2A amorphous cellulose is below the micellar cellulose of the first row, and the micellar cellulose of the second row is below the amorphous cellulose of the first row. The third row of Fig. 2A is like the first row, and so on. Thus, all cross sections of the average secondary cell wall are very much alike. Seifriz has a similar picture for the distribution of micelles (8, p. 5, Fig. 4), but he does not use an intermediate substance, which in the case of cellulose might be amorphous

cellulose. Fig. 2B represents the first row of the submicroscopic structure in the average secondary cell wall of a petiole of *Nymphaea*. This figure shows that, on the basis of the experiments, the submicroscopic structure in this case consists chiefly of amorphous cellulose. Amorphous cellulose of *Nymphaea* petioles probably contains more water in the case of Young's modulus equaling 5×10^8 dynes/cm.^{2} (fresh, wet tissue) than when

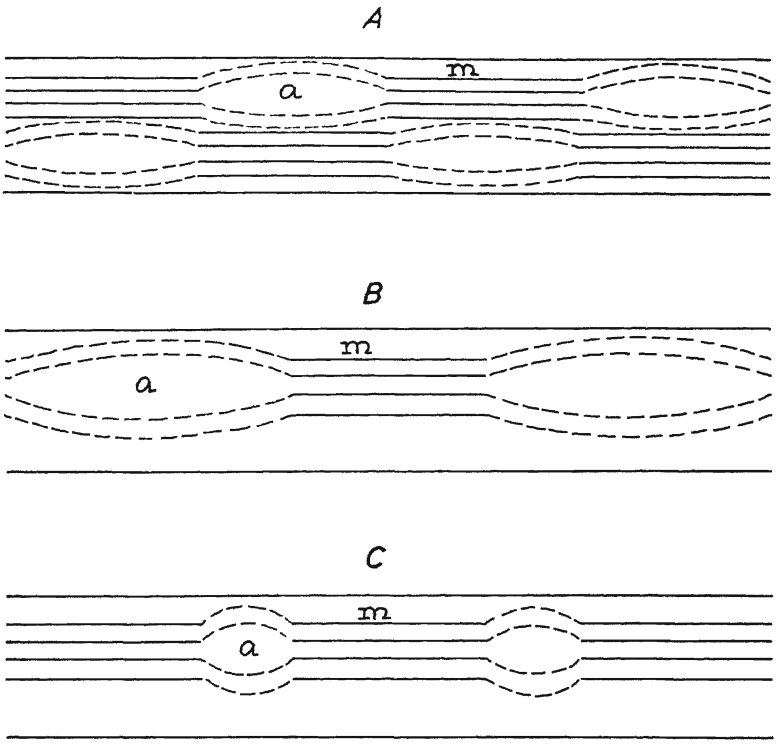

FIG. 2

Schematic Drawings of the Submicroscopic Structure of the Average Secondary Cell Wall of Cylindrical Plant Tissue

A. General scheme; B. petioles of *Nymphaea;* C. branches of *Salix babylonica.* a = amorphous cellulose; m = micellar cellulose.

Young's modulus equals 10×10^8 dynes/cm.^{2} ("dry" tissue). In both cases the stretching may be due to the elasticity in the cell wall. It is to be expected that hydrated cellulose produces rubber-like elasticity, since, according to Guth (5), flexible chain molecules exhibit such elasticity. Generally, cellulose molecules are long but not flexible. At room temperature the ring structure of the glucoside residues of cellulose does not produce enough internal mobility for rubber-like elasticity. At higher

temperature, however, or in a swollen state, cellulose may exhibit some rubber-like elasticity. This remark supports Treitel's observations of rubber-like elastic tissues in higher plants (9). All these plant tissues observed grow in wet locations and contain water to a great extent. Hence, rubber-like elasticity of plant tissues may be at least partly exhibited by hydrated cellulose in the cell walls.

According to Hermans (6) greatly swollen fibers of cellulose exhibit large extensibility like rubber. These cellulose fibers contain only a small amount of micelles as in the case of rubber. Flexible protein fibers and hydrated cellulose fibers have rubber-like elasticity. The extensibility of cellulose fibers in relation to their degree of hydration (their swollen condition) acts similarly to the extensibility of rubber in relation to temperature. The extension of cellulose is less reversible than the extension of rubber. This can be explained because the forces of cohesion between carbohydrate chains of cellulose are much greater than the forces of cohesion between the hydrocarbon chains of rubber. Stretched rubber may be fixed too by cooling the rubber.

Therefore, swollen cellulose fibers may have the same properties as high polymer fibers which are rubber-like. On the contrary, dry cellulose fibers of ramie and cotton are metal-like (9).

Fig. 2C represents the first row of the submicroscopic structure in the average secondary cell wall of a woody branch of *Salix babylonica*. This figure shows that the submicroscopic structure in this case consists mainly of micellar cellulose. The second row in both Figs. 2B and 2C would be similar to the first row.

Fig. 2 does not take into account the percentage of cellulose and the exact orientation of cellulose molecules in the cell wall.

According to Treitel (10), Young's modulus of cylindrical plant tissues which he has investigated increases with specific gravity. This specific gravity is mainly determined by cellulose because, in many cases, the greater portion of the weight in higher plants is made up of cellulose. Therefore, the percentage of cellulose in average secondary cell walls of cylindrical plant tissues will probably increase with the ratio of the moduli of elasticity (Young's modulus divided by the transverse modulus) (9).

Summary

(1) L. Hock investigated the Gough-Joule effect for rubber. In proving the effect, rubber was stretched. In this stretched rubber, parallel fibers were formed. These fibers were made visible by pouring liquid air over the stretched rubber and striking this rubber with a hammer. By treating undeformed rubber in a similar way, L. Hock found that this rubber was amorphous.

(2) The liquid air method used by L. Hock for rubber, was applied

to the petioles of *Nymphaea* and woody branches of *Salix babylonica*. In the case of *Nymphaea*, the petiole on being struck with a hammer breaks up into irregularly formed particles. Therefore, the submicroscopic structure of the average secondary cell wall of petioles of *Nymphaea* consists mainly of amorphous cellulose. In the case of *Salix bablyonica*, on striking with a hammer, linear particles which lie nearly parallel to the axis of the branch were observed. Therefore, the submicroscopic structure in the average secondary cell walls of woody branches of *Salix babylonica* consists mainly of micellar cellulose.

(3) Certain cylindrical tissues of higher plants are more or less isotropic. These tissues are rubber-like in their elasticity and contain large amounts of amorphous cellulose in the average secondary cell walls. Other cylindrical plant tissues are anisotropic. These tissues are metal-like in their elasticity and contain a great deal of crystalline cellulose in the average secondary cell walls.

These conclusions were reached mainly from two experimental facts. The first was the ratio of the moduli of elasticity, the second, the observation based on freezing the material with liquid air. In addition, the conclusions were supported by the occurrence of different cellulose in dried and undried cotton fibers.

(4) Schematic drawings were made of the submicroscopic structure of the average secondary cell wall of the petioles of *Nymphaea gladstonia* and the woody branches of *Salix babylonica*.

(5) Rubber-like elasticity of plant tissues is at least partly exhibited by hydrated cellulose in the cell walls.

(6) Swollen cellulose fibers may have the same properties as high polymer fibers which are rubber-like. Dry cellulose fibers of ramie and cotton are metal-like. Hence, it is to be understood that not only cellulose fibers, but also cylindrical tissues of higher plants, are either rubber-like elastic or metal-like elastic.

(7) From specific gravity measurements, it is found that the percentage of cellulose in average secondary cell walls of cylindrical plant tissues increases with the ratio of the moduli of elasticity.

(8) From the ratio of the moduli of elasticity (9), the liquid air experiment, and measurements of specific gravity (10), it is found that the submicroscopic structure in all secondary cell walls of higher plants is determinable by the percentage of cellulose and the ratio of amorphous and crystalline cellulose. The primary cell wall is highly plastic and contains a molecular network of cellulose (9).

References

1. Berkley, E. E., *Am. J. Bot.* **29**, 416 (1942).
2. Berkley, E. E., and Kerr, T., *Ind. Eng. Chem.* **38**, 304 (1946).
3. Flory, P. J., *Chem. Rev.* **35**, 51 (1944).

4. FREUNDLICH, H., AND HAUSER, E. A., *Kolloid Z.* **36**, 33 (1925).
5. GUTH, E., *Am. Assoc. Adv. Sci. Pub.* **21**, 103.
6. HERMANS, P. H., *Naturwissenschaften* **28**, 223 (1940).
7. HOCK, L., *Elektrochem. Z.* **31**, 404 (1925).
8. SEIFRIZ, W., A Symposium on the Structure of Protoplasm. The Iowa State College Press, Ames, Iowa, 1942.
9. TREITEL, O., *J. Colloid Sci.* **1**, 327 (1946).
10. TREITEL, O., *Trans. Kansas Acad. Sci.* **48**, 186 (1945).
11. VALKÓ, E., Colloidchemische Grundlagen der Textilveredlung. Julius Springer, Berlin, 1937.

LIBERATION OF H^+, AL^{+++} AND FE^{+++} IONS FROM HYDROGEN CLAYS BY NEUTRAL SALTS *

J. N. Mukherjee, B. Chatterjee [1]† and B. M. Banerjee [1]

From the Physical Chemistry and Colloid Research Laboratories, University of Calcutta, India

Received July 11, 1946

Acidity is developed in the interaction between a hydrogen clay and neutral salts and the clear salt extracts usually contain Al^{+++} ions and, in a secondary measure, Fe^{+++} ions. The mechanism of this reaction has been the subject of much discussion. Daikuhara (1), Kappen (2), and Paver and Marshall (3) hold that Al^{+++} and Fe^{+++} ions are directly exchanged for the cations of an added salt and the subsequent hydrolysis of the aluminum and iron salts gives rise to the observed acidity of the supernatant liquid. On the other hand, Page (4), Magistad (5), Kelley and Brown (6), Wilson (7) and Mattson (8) are of the opinion that the chief replacement is one of H^+ ions associated with the colloidal particles. According to them, a hydrogen clay or an acid soil reacts with neutral salts to give rise to free acid which then dissolves aluminum and iron oxides present in the soil or clay. Differences of opinion also exist regarding the total amount of Al^{+++} and Fe^{+++} which can be displaced on the addition of neutral salts to hydrogen clays. Thus, while Paver and Marshall (3) observed that there is a limit to the amount of Al^{+++} and Fe^{+++} ions which can be displaced from a hydrogen clay by leaching with neutral salts, Mattson (8) found that Al^{+++} and Fe^{+++} ions are liberated as often as the clay is rendered unsaturated by leaching with dilute hydrochloric acid and then treated with neutral salts.

Several publications (9–12) from this laboratory have dealt with the liberation of Al^{+++} and Fe^{+++} ions from hydrogen clays isolated from typical Indian soils by neutral salts. At a given equilibrium pH the amount of Al brought into solution by HCl has been found to constitute a small fraction of that liberated by $BaCl_2$ (10, 12). At a constant pH and concentration of barium the same amount of Al is liberated both when the pH of the hydrogen clay decreases as a result of the addition of the salt as when the pH is kept constant by the use of a suitable buffer along with

* The work has been carried out under the scheme of "Research into the Properties of Colloid Soil Constituents" financed by the Imperial Council of Agricultural Research, India.

† Assistant Soil Chemist under the scheme.

[1] Experimental work done by these co-authors.

the salt or by the addition of the requisite amount of a base. The amount of Al liberated at a constant pH increases with the concentration of the added salt and the relation between the two is given by a curve which closely resembles an adsorption isotherm. *All these facts might indicate that Al^{+++} ions are directly exchanged for the cations of an added salt* and is not brought into solution by a secondary dissolution process. An exchange of H^+ ions along with Al^{+++} ions for the added cations has also been observed (9, 11). At very low concentrations of salts, especially with NaCl, very little Al^{+++} ions are present in the neutral salt extract and the neutralizable acidity of the latter is mainly due to displaced H^+ ions. With an increase in the concentration of the added salt, the amount of displaced H^+ ions (*i.e.*, the excess of the amount of neutralizable acidity of the salt extract over that of Al^{+++} ions present in it) progressively decreases in the case of hydrogen clays having a low base exchange capacity (*b.e.c.*), but its amount gradually increases when hydrogen clays having a comparatively high *b.e.c.* are considered. Using *very low concentrations, e.g.*, 0.001 *N*, of salt it has been observed (13) that the ratio of displaced H^+ to Al^{+++} ions has a value much greater than 1.0 with hydrogen clays having montmorillonite as their dominant clay mineral, while those having kaolinite as their major clay mineral show values less than 1.0 for this ratio. A relation has been found (14) between the amount of exchangeable Al^{+++} ions, *i.e.*, which can be displaced by neutral salts, and the *b.e.c.* of hydrogen clays prepared from subfractions isolated from the same entire clay fraction of soils. The amount of exchangeable Al^{+++} ion, as also the *b.e.c.*, increases with decreasing particle size. Any deviation from this regular variation of one is also reflected in similar deviation of the other.

The present paper deals with the question as to whether there is a limit to the amount of Al^{+++} and Fe^{+++} ions present on the surface of hydrogen clays, that is, whether the liberation of these ions by the action of neutral salt on a hydrogen clay can be repeated indefinitely. Estimations have been made of the amounts of H^+, Al^{+++} and Fe^{+++} ions displaced from 2 hydrogen clays on repeated leaching with $BaCl_2$ until these substances could not be detected in the salt extract. The Ba-clay thus obtained has been unsaturated into H-clays by leaching with 0.02 *N* HCl followed by washing with distilled water, and again treated with $BaCl_2$ as described above. This sequence of unsaturation and leaching with $BaCl_2$ has been repeated 7 times with one hydrogen clay and 5 times with the other. Their base exchange capacities have also been determined both before and after the series of leachings and unsaturations. The hydrogen clays Satara-F and Jorhat-F used in the present work have been prepared respectively from a black cotton soil from Satara, Bombay, and and acid soil from Jorhat Farm, Assam. X-ray analyses of Satara-F and

Jorhat-F revealed that the dominant clay mineral present in the former is montmorillonite while the latter contains kaolinite as its major mineral (15).

Details of the experimental technique and of the various methods used for the estimation of (*1*) neutralizable acidity of the salt extract; (*2*) amounts of Al^{+++} and Fe^{+++} ions present in the leachates; and (*3*) the base exchange capacity of the hydrogen clays will be published in a later paper. Brief outlines of these methods are, however, given below:

(*1*) Aluminum was precipitated by adding a solution of 8-hydroxyquinoline (16) weakly acidified with acetic acid. The precipitate was washed free from excess hydroxyquinoline with hot water. A sufficient quantity of 2 *N* hydrochloric acid and a little ethyl alcohol were added to dissolve the precipitate. Excess of a standard solution of potassium bromide-bromate mixture was added and then back titrated with standare thiosulphate solution. The amount of Al was calculated from the amount of *N*/10 bromate-bromide mixture used up according to the equation:

$$1 \text{ cc. } N/10 \ (KBrO_3 + KBr) \equiv 0.2248 \text{ mg. of Al.}$$

(*2*) Iron was estimated by matching the intensity of the red color produced on the addition of a few cc. of a solution of ammonium thiocyanate and a few drops of nitric acid to a given volume of the salt extract against that of the color produced in the same volume of a standard iron solution containing the same amounts of nitric acid and ammonium thiocyanate.

(*3*) The neutralizable acidity of the neutral salt extract, as also the base-exchange capacity, of the hydrogen clays were determined by potentiometric titration against standard solutions of bases.

Results and Discussion

(*a*) *The Total Amount of Acid Displaced from Hydrogen Clays on Repeated Leaching with Salt Solutions*

Hydrogen clays Satara-F (3.23 g.) and Jorhat-F (2.84 g.) were repeatedly leached with 100 cc. portions of *N* $BaCl_2$ solution until the leachate gave practically no acidity when titrated with $Ba(OH)_2$. The Ba-clay was unsaturated, again repeatedly leached with *N* $BaCl_2$ solution and the acidity of the clear salt extract was estimated in each leachate (see p. 250). The results are shown in Tables I and II and calculated for 100 g. oven dried material.

It will be seen that the neutralizable acidity of the leachate decreases with the progress of leaching to a negligible value and that its amount is reduced markedly in the very first unsaturation. With successive unsatu-

TABLE I

Hydrogen Clay—Satara-F, Acidity in the Leachates

Serial No. of treatment	*Me.*/100 g. hydrogen clay								Total acid displaced, *me.*/100 g.
	1st	2nd	3rd	4th	5th	6th	7th	8th	
1	2	3	4	5	6	7	8	9	
Original hydrogen clay	54.5	8.0	0.5	0.4	nil	—	—	—	63.4
1st unsaturation	43.2	4.3	1.8	0.8	0.2	nil	—	—	50.3
2nd unsaturation	39.5	5.8	2.2	1.4	1.0	nil	—	—	49.9
3rd unsaturation	41.5	5.9	2.9	1.7	0.7	nil	—	—	52.7
4th unsaturation	34.7	5.5	3.2	2.2	1.2	nil	—	—	46.8
5th unsaturation	34.8	6.1	3.6	1.6	0.9	nil	—	—	47.0
6th unsaturation	32.2	6.2	1.9	1.5	1.1	0.9	nil	—	43.8
7th unsaturation	26.2	6.3	2.4	1.5	1.3	0.7	0.7	nil	39.1

TABLE II

Hydrogen Clay—Jorhat-F

Serial No. of treatment	Acidity of the clear leachates *Me.*/100 g. colloid						Total acid displaced, *me.*/100 g.
	1st	2nd	3rd	4th	5th	6th	
Oirginal hydrogen clay	20.2	1.6	0.9	0.6	nil	—	23.3
1st unsaturation	13.6	2.8	1.4	1.0	0.2	nil	19.0
2nd unsaturation	13.9	2.8	1.6	0.9	nil	—	19.2
3rd unsaturation	12.6	3.7	1.3	1.1	nil	—	18.7
4th unsaturation	12.1	2.1	1.3	0.8	0.3	nil	16.6
5th unsaturation	12.1	2.5	0.8	0.7	nil	—	16.1

rations it decreases regularly in the case of Satara-F but with Jorhat-F it decreases tending to a constant value. An exception is observed in the third unsaturation of Satara-F in that the total acidity of the leachates is greater than that estimated in the preceding one.

(*b*) *The Total Amount of Al^{+++} and Fe^{+++} Ions Displaced from Hydrogen Clays on Repeated Leaching with Solutions of Neutral Salts*

Tables III and IV give the results of the estimation of the amount of Al^{+++} and Fe^{+++} ions displaced from hydrogen clays Satara-F and Jorhat-F after each successive leaching with $N/BaCl_2$ until no Al^{+++} and Fe^{+++} ions could be detected in the leachate and also after repeated unsaturations each time followed by leaching with $N/BaCl_2$ as in the previous case.

The amount of displaced Al^{+++} and Fe^{+++} ions decreases with the progress of leaching to an almost negligible value indicating that there is a limit to the amount of Al^{+++} and Fe^{+++} ions which can be displaced by repeated leaching of a hydrogen clay with a neutral solution of $BaCl_2$. The amount of Al^{+++} and Fe^{+++} ions thus obtained, however, does not correspond with the total amount of exchangeable Al^{+++} and Fe^{+++} ions present. As often as the clay is unsaturated and then treated with $BaCl_2$, Al^{+++} and Fe^{+++} ions are liberated (*cf.* Mattson (8)). However, the total amount of Al^{+++} plus Fe^{+++} displaced by leaching with the salt decreases markedly when the Ba-clay is unsaturated (1st unsaturation) by treating with dilute acid.

Exchange of Al^{+++} Ions. Satara-F shows a gradual decrease in the total amount of displaced Al^{+++} ions up to the fourth unsaturation

TABLE III

Hydrogen Clay Satara-F

Data are expressed in *me.*/100 g. hydrogen clay

Serial No. of treatment	Displaced Al in leachates					Displaced Fe in leachates	
	1st	2nd	3rd	4th	Total	1st	2nd
Original hydrogen clay	37.8	6.0	0.4	0.2	44.4	0.5	nil
1st unsaturation	20.8	0.7	nil	—	21.5	1.3	nil
2nd unsaturation	14.7	0.6	nil	—	15.3	1.7	nil
3rd unsaturation	15.7	0.6	[illegible]	—	16.3	2.9	nil
4th unsaturation	8.2	0.5	[illegible]	—	8.7	3.1	nil
5th unsaturation	8.6	1.0	[illegible]	—	9.6	2.9	nil
6th unsaturation	9.9	0.5	nil	—	10.4	1.4	nil
7th unsaturation	11.2	0.7	nil	—	11.9	0.7	nil

TABLE IV

Hydrogen Clay Jorhat-F

Data are expressed in *me.*/100 g. hydrogen clay

Serial No. of treatment	Displaced Al in leachates					Displaced Fe in leachates	
	1st	2nd	3rd	4th	Total	1st	2nd
Original hydrogen clay	12.1	0.4	nil	—	12.5	0.4	nil
1st unsaturation	6.3	0.4	nil	—	6.7	0.4	nil
2nd unsaturation	6.3	0.4	nil	—	6.7	0.3	nil
3rd unsaturation	4.7	0.7	0.4	nil	5.8	0.3	nil
4th unsaturation	4.9	0.2	nil	—	5.1	0.3	nil
5th unsaturation	4.6	0.5	nil	—	5.1	0.3	nil

TABLE V

Hydrogen Clay Satara-F

Serial No. of treatment	*Me.*/100 g. of hydrogen clay			$H^+/Al^{+++}+Fe^{+++}$
	Total amount of acid displaced	Total amount of $Al^{+++}+Fe^{+++}$ displaced	Total amount of H^+ displaced	
Original hydrogen clay	63.4	44.9	18.5	0.4
1st unsaturation	50.3	22.8	27.5	1.2
2nd unsaturation	49.9	17.0	32.9	1.9
3rd unsaturation	52.7	19.2	33.5	1.8
4th unsaturation	46.8	11.8	35.0	3.0
5th unsaturation	47.0	12.5	34.5	2.8
6th unsaturation	43.8	11.8	32.0	2.7
7th unsaturation	39.1	12.6	26.5	2.0

TABLE VI

Hydrogen Clay Jorhat-F

Data are expressed in *me.*/100 g.

Serial No. of treatment	Total amount of acid displaced	Total amount of $Al^{+++}+Fe^{+++}$ displaced	Total amount of H^+ displaced	$H^+/Al^{+++}+Fe^{+++}$
Original hydrogen clay	23.3	12.9	10.4	0.8
1st unsaturation	19.0	7.1	11.9	1.6
2nd unsaturation	19.2	7.0	12.2	1.7
3rd unsaturation	18.	6.1	12.6	2.0
4th unsaturation	16.	5.4	11.2	2.1
5th unsaturation	16.1	5.4	10.7	2.0

followed by an increase which has been found to continue till the seventh unsaturation. The amount of total displaced Al^{+++} ions obtained at the third unsaturation is, however, slightly greater than that displaced in the second stage. The displaced acid also shows a similar increase at the third unsaturation (see p. 251). Jorhat-F, on the other hand, shows a decrease in the total amount of displaced Al^{+++} ions up to the fourth unsaturation but the same quantity has been obtained in the fifth as in the fourth.

Exchange of Fe^{+++} Ions. Fe^{+++} ions displaced from the original hydrogen clay by $BaCl_2$ is very small. Similar observation has been made by Turner (17); mere traces (never exceeding 0.2 *me.*/100 g. of soil) of Fe^{+++} were found to be displaced by leaching a number of soils with solutions of *N*/NaCl. With Satara-F the amount of displaced Fe^{+++} ions increases with successive unsaturations up to the fourth one for which the amount of displaced Al^{+++} ions is minimum. Displaced Fe^{+++} ions then begin to

decrease. The amount of Fe^{+++} ions liberated from Jorhat-F by $N/BaCl_2$ remains practically constant throughout, the variation being from 0.4 *me.* to 0.3 *me.*/100 g.

It is rather interesting to note that the sum of the displaced Al^{+++} and Fe^{+++} ions decreases with progressive unsaturations tending to a constant value with both hydrogen clays (Tables V and VI).

The displacement of Al^{+++} ions by $BaCl_2$ from the hydrogen clay Latekujan-F prepared from an acid soil from Assam (India) has been studied previously by Mukherjee, Chatterjee and Goswami (18). Late-

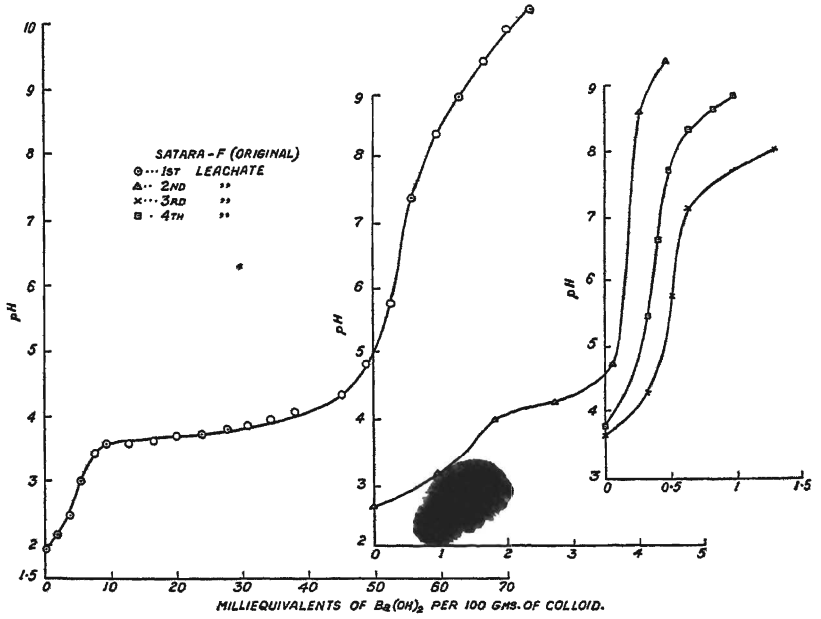

FIG. 1

Titration Curves of Leachates of Hydrogen Clay from Satara-F Soil

kujan-F and Jorhat-F show a similar behavior in this regard. It is also significant that kaolinite is the dominant clay mineral present in both of them. On the other hand, montmorillonite constitutes the major clay mineral in Satara-F. It appears, therefore, that the difference in the behavior of the 2 hydrogen clays Satara-F and Jorhat-F may be ascribed to the difference in the nature of the clay minerals present in them.

An inspection of the data presented in Tables III and IV will show that the third leachate practically contains no Al^{+++} and Fe^{+++} ions except in the case of the original Satara-F and the third unsaturation with Jorhat-F. H^+ ions, however, continue to be displaced even after the third leaching (see Tables I and II). The titration curves (see Fig. 1) of

the third and consecutive leachates also show this in that they resemble that of a dilute solution of hydrochloric acid. The flat portion of the titration curves with bases representing the zone of precipitation of

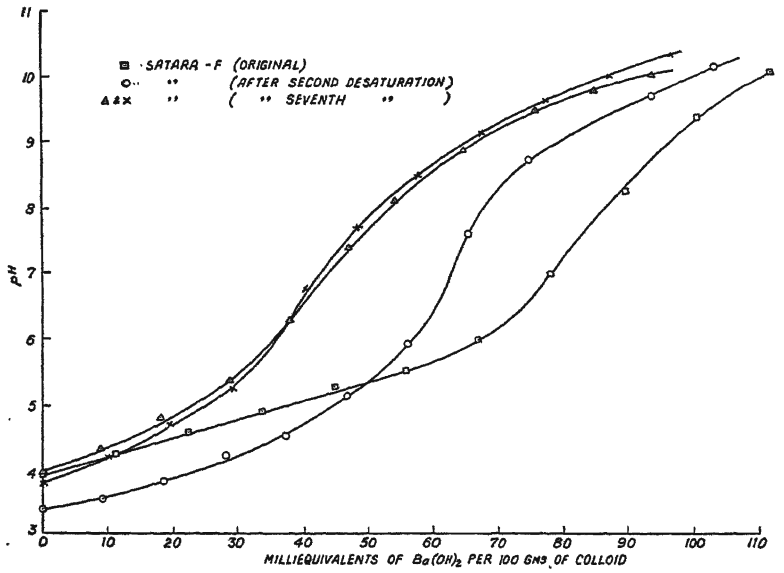

FIG. 2

Titration Curves of Hydrogen Clay from Satara Soil Before and After Desaturation

$Al(OH)_3$ and $Fe(OH)_3$ as obtai[redacted] the first and second leachates is also absent in the titration curves of the third and following leachates.

The Variation in the Ratio of Displaced H^+ Ions to Al^{+++} plus Fe^{+++} on Successive Unsaturations

It will be seen (Tables V and VI) that the total amount of neutralizable acid displaced from the hydrogen clays is greater than the sum of the amounts of Al^{+++} and Fe^{+++} ions liberated in the same treatment. *Obviously H^+ ions, in addition to Al^{+++} and Fe^{+++} ions, are exchanged for the added Ba^{++} ions.* The relation between the amounts of H^+ ions and Al^{+++} plus Fe^{+++} ions displaced on the addition of $BaCl_2$ to the hydrogen clays is shown in Tables V and VI. The excess of the total amount of neutralizable acidity of the leachates in any treatment over that of Al^{+++} plus Fe^{+++} ions has been taken to be the amount of displaced H^+ ions.

The amount of displaced H^+ ions at first increases with successive unsaturations, up to the third (Jorhat-F) or fourth (Satara-F) where it has a maximum value and then decreases. The increase as well as the

final decrease are more marked in the case of Satara-F, *viz.*, 89.1% and 23.3%, respectively, compared to the corresponding values of 20.2% and 14.4% observed with Jorhat-F. With Satara-F the ratio of displaced H^+ ions to Al^{+++} plus Fe^{+++} ions at first increases with successive unsaturations, attains a maximum in the fourth unsaturation and then decreases, while in the case of Jorhat-F this ratio increases with progressive unsaturations tending to a constant value.

The Effect of Successive Treatment with Neutral Salts and Unsaturations on the Base Exchange Capacity of Hydrogen Clays

The base exchange capacity (*b.e.c.*) of the 2 hydrogen clays have been calculated from the inflection points in the titration curves with $Ba(OH)_2$ (Fig. 2 *) before and after several unsaturations with a view to having fuller information on the stability of the absorption complex under repeated treatments with salt and acid respectively. The results obtained have been shown in Table VII.

TABLE VII

Figures in Brackets give pH at Inflection
Data are expressed in *me.*/100 g. of hydrogen clay

Hydrogen clay	Base exchange capacity at		Reduction in *b.e.c.*
	1st inflection	2nd inflection	
Satara-F (Original)	80.5 (7.25)	—	—
Satara-F (after two unsaturations)	62.0 (6.70)	—	23%
Satara-F (after seven unsaturations)	42.0 (6.8)	—	48%
Jorhat-F (Original)	20.5 (6.15)	32.5 (7.7)	—
Jorhat-F (after five unsaturations)	18.5 (6.3)	32.0 (8.45)	10%; 1.5%

It will be seen that whereas the *b.e.c.* of Satara-F diminishes very rapidly on repeated leaching with salt and unsaturations, that of Jorhat-F calculated at the first inflection point shows a much smaller decrease, but the *b.e.c.* at the second inflection † point remains practically unaffected even after 5 unsaturations. The results obtained with Jorhat-F again agree with those observed with hydrogen clay Latekujan-F (18). The *b.e.c.* of Latekujan-F was found to be equal to 31.0 *me.* while that of this hydrogen clay after 8 unsaturations was found to be equal to 31.6 *me.*/100 g.

* The titration curves of Satara-F only are shown in Fig. 2.

† Kaolinitic clays like Jorhat-F have been found to have a dibasic acid character while H-clays like Satara-F having montmorillonite as their dominant mineral constituent usually behave as a monobasic acid (19, 20).

The results presented in this paper appear to indicate that montmorillonitic and kaolinitic clays behave differently judged from the effect of treatment with neutral salts and unsaturations on the displacement of Al^{+++} and Fe^{+++} ions. In the light of these observations work on similar lines with pure specimens of clay minerals, *e.g.*, montmorillonite, kaolinite and pyrophyllite has already been undertaken. The results of these investigations will shortly be communicated for publication.

References

1. Daikuhara, G., *Bull. Imp. Central Agr. Exp. Sta. Japan* **2**, 18 (1914).
2. Kappen, H., *Landw. Vers.-Sta.* **88**, 96 (1916); see also Kappen, H., Die Bodenaziditat (1929).
3. Paver, H., and Marshall, C. E., *J. Soc. Chem. Ind.* **53**, 750 (1934).
4. Page, H. J., *Trans. Second Comm. Intern. Soc. Soil Sci.*, Gröningen, 232 (1926).
5. Magistad, O. C., *Soil Sci.* **20**, 181 (1925).
6. Kelley, W. P., and Brown, S. M., *Ibid.* **21**, 289 (1926).
7. Wilson, B. D., *Ibid.* **21**, 411 (1929).
8. Mattson, S., *Ibid.* **25**, 345 (1928).
9. Chatterjee, B., *Bull. Indian Soc. Soil Sci.* No. 4, 148 (1942).
10. Mukherjee, J. N., and Chatterjee, B., *Indian J. Agr. Sci.* **12**, 105 (1942).
11. Chatterjee, B., and Paul M., *Ibid.* **12**, 113 (1942).
12. Mukherjee, J. N., and Chatterjee, B., *Nature* **155**, 268 (1945).
13. Chatterjee, B., and Das, M., Unpublished work.
14. Chatterjee, B., and Majumdar, S., Unpublished Work.
15. Bagchi, S. N., Unpublished work.
16. Berg, R. *Z. anal. Chem.* **71**, 369 (1927).
17. Turner, P. E., *Soil Sci.* **32**, 447 (1931).
18. Mukherjee, J. N., Chatterjee, B., and Goswami, P. C., *J. Indian Chem. Soc.* **19**, 405 (1942).
19. Mukherjee, J. N., Mitra, P. R., and Mitra, D. K., *J. Phys. Chem.***47**,543(1943).
20. Mitra, R. P., Bagchi, S. N., and Ray, S. P., *Ibid.* **47**, 549 (1943).

KINETICS OF THE FORMATION OF MONODISPERSED SULFUR SOLS FROM THIOSULFATE AND ACID

Victor K. LaMer and Allen S. Kenyon

From the Department of Chemistry, Columbia University, New York

Received January 24, 1946

INTRODUCTION

Recent studies from this laboratory (1, 2) on the production of monodispersed sulfur sols prepared by the action of very dilute solutions of strong acids and sodium thiosulfate have made it possible to study the formation of these sols by optical methods. Although the action of acid upon sodium thiosulfate has been used extensively as a method of preparation of sulfur sols (3, 4, 5) previous preparations remained polydispersed even after extensive fractionation by peptization and reprecipitation. LaMer and Barnes (1) found that when very dilute thiosulfate and acid (approximately 0.001 *M*) are mixed, the resultant solution remains transparent for a varying period after mixing, depending upon the initial concentration. After this induction period, discrete particles suddenly form as indicated by the appearance of the Tyndall beam.

Foss (6) has concluded recently that the mechanism of the acid decomposition of thiosulfate takes place as follows:

$$HS_2O_3^- \rightleftarrows HSO_3^- + S.$$

Jahlezynsky and Rytel (7) studied the decomposition of considerably more concentrated solutions, namely 0.025 *N* thiosulfate in the presence of 0.125, 0.25 and 1.25 *N* HCl. They followed the increase in turbidity with a Koenig-Marten spectrophotometer. The induction period for the appearance of the Tyndall beam was of the order of 30 seconds. The formation of sulfur was attributed to the reaction written as

$$S_2O_3^{=} + H^+ \rightleftarrows HSO_3^- + S.$$

Their results, however, are complicated by the rapid coagulation of the concentrated sol at these higher concentrations. When coagulation was inhibited by the addition of 1.5% solution of gum arabic, the rate of decomposition of thiosulfate was first order in respect to the disappearance of thiosulfate, until the presence of increasing numbers of sulfur nuclei produces an additional autocatalytic reaction.

Experimental

One cc. of 1.0 *M* $Na_2S_2O_3$ was diluted with distilled water to 998 cc., to which was added 1 cc. of 1.5 *M* H_2SO_4 by a hypodermic syringe. All solutions were brought to constant temperature (25°C.) in a thermostat before mixing. Zero time was taken when the syringe had delivered the acid. An aliquot portion was then transferred to the quartz cells (10 cm. long) of a Beckman quartz spectrophotometer, model DU. The I_0 reading was adjusted by using .0010 *M* thiosulfate.

The molecular absorption of sulfur was determined by measuring the transmission of sulfur dissolved in various organic solvents at various concentrations. The sulfur was purified by the method of Bacon and Fanelli (8). One cm. quartz absorption cells were used for these measurements.

Discussion

In order to interpret the data at different wave lengths, we measured the transmittance of the various possible species that may be present in

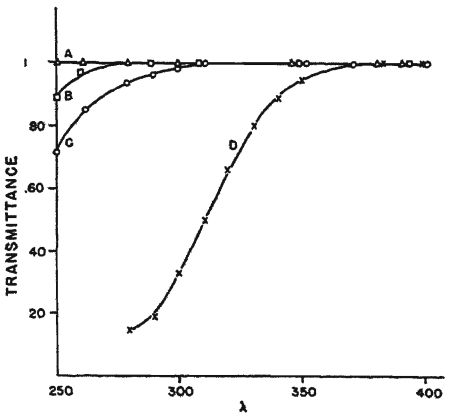

Fig. 1

Transmittance of the Various Compounds Involved as a Function of λ

△—△—△ = $NaHSO_3$ ○—○—○ = $Na_2S_4O_6$

□—□—□ = $Na_2S_2O_3$ ×—×—× = Sulfur

the solution. The transmittance data for 0.0015 *M* $NaHSO_3$, $Na_2S_2O_3$, $Na_2S_4O_6$, in water and .001 *M* sulfur in organic solvents (an average curve for the solvents CCl_4, $CHCl_3$, CH_3COCH_3, and CS_2) are given in Fig. 1 for the 1 cm. cell.

It will be observed that the various ions do not absorb for wave lengths above $\lambda = 300$ mμ (in air), whereas sulfur absorbs appreciably below $\lambda = 390$ mμ.

Transmission measurements made at $\lambda = 300$ mμ should therefore measure only the appearance of sulfur, whereas at $\lambda = 450$ and 600 mμ the decrease in transmittance is due only to the scattering produced by the sulfur droplets and not to molecular absorption by sulfur. By working above $\lambda = 300$ mμ all complications due to ions are eliminated.

In Fig. 2 the transmittance decreases to a value of 0.988 in about 35

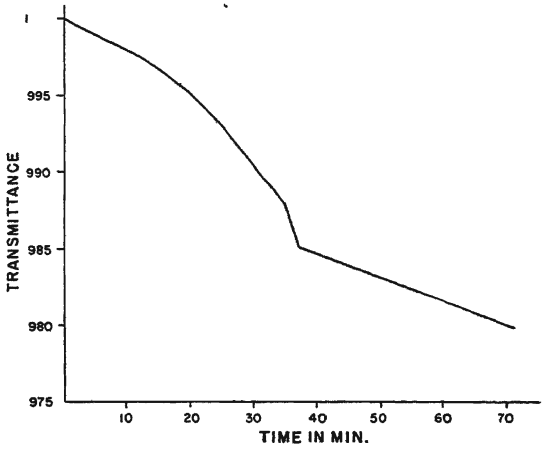

FIG. 2

Transmittance of the Acid-Thiosulfate Reaction as a Function of Time
1 cm. absorption cell
$\lambda = 300$ mμ

minutes after mixing of thiosulfate and acid. At 35 minutes the transmittance drops sharply from 0.988 to 0.985 in approximately two minutes, after which the transmittance decreases nearly linearly with time at a slower rate, reaching a value of 0.975 in 90 minutes.

This observation was repeated 4 times. The break in transmittance could be reproduced to $\pm$ one minute. This break in the curve coincided with the appearance of a faint blue Tyndall beam when observed vertically through a polaroid H filter No. 330, and hence arises from the appearance of discrete scattering particles.

These experiments were repeated using the 10 cm. quartz cells with the same type results, except that the curves were more accurately determined. Table I shows the measured values of the transmittance at $\lambda = 300$ mμ as a function of time for the reaction of 0.0010 *M* $Na_2S_2O_3$ and 0.003 *M* HCl for 10 cm. cells. When the data are plotted in terms of

TABLE I

0.0015 M $Na_2S_2O_3$; 0.003 M HCl

Time after mixing	I_0/I	Log I_0/I	Conc. of sulfur $\times 10^6$
min.			*g.-at./l.*
4½	.990	.0044	0.69
6	.988	.0052	0.82
8	.984	.0070	1.10
10	.982	.0079	1.24
13	.979	.0092	1.45
16	.975	.0110	1.73
18	.968	.0141	2.22
20	.967	.0146	2.30
22	.961	.0173	2.73
24	.954	.0205	3.23
26	.950	.0223	3.51
28	.943	.0255	4.02
30	.938	.0278	4.38
32	.930	.0315	4.96
34	.922	.0353	5.57
36	.907	.0424	
38	.892	.0496	
40	.885	.0531	
42	.880	.0555	
44	.877	.0570	
46	.871	.0600	
50	.863	.0640	
55	.854	.0685	
60	.848	.0716	
65	.838	.0768	
70	.829	.0814	

the optical density, log I_0/I, the break does not appear to be as sharp.

Fig. 3 shows the plot of log I_0/I against time for $\lambda = 300$, 435 and 560 mμ for 0.0015 *M* thiosulfate and 0.003 *M* HCl, and for $\lambda = 300$ and 450 mμ for 0.0010 *M* thiosulfate and 0.0015 *M* H_2SO_4. A discontinuity occurs at 70 minutes for 0.001 *M* thiosulfate and 0.0015 *M* H_2SO_4 and at 35 minutes for 0.0015 *M* thiosulfate and 0.003 *M* HCl for each wave length, indicating the rapid formation and growth of sulfur particles.

In order to use Beer's Law to determine the sulfur concentration during the homogeneous part of this reaction, it is necessary to know the molecular absorption coefficient for sulfur as a function of wave length. Wigand (9) measured the absorption of saturated solutions of sulfur in several organic solvents at wave lengths from 430 to 380 mμ. He observed shifts in the transmittance curves due to solvent effects. His measurements, however, were not applicable in the present investigation because of the disturbing effects that enter at these high concentrations.

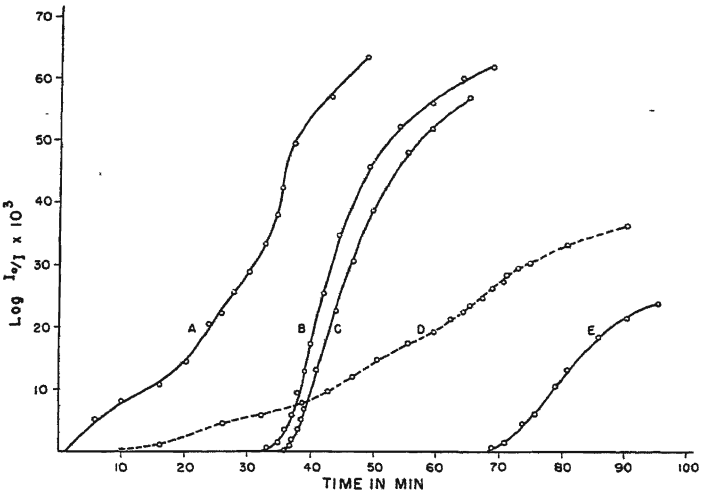

FIG. 3

Optical Density of Reaction Mixture as a Function of Time, Concentration and Wave Length

	λ	
A	300	.0015 *M* Thio
B	435	.003 *M* HCl
C	560	
D	300	.0010 *M* Thio
E	450	.0015 *M* H_2SO_4

The molecular absorption coefficient of sulfur was accordingly determined by measuring the transmittance of pure sulfur dissolved in

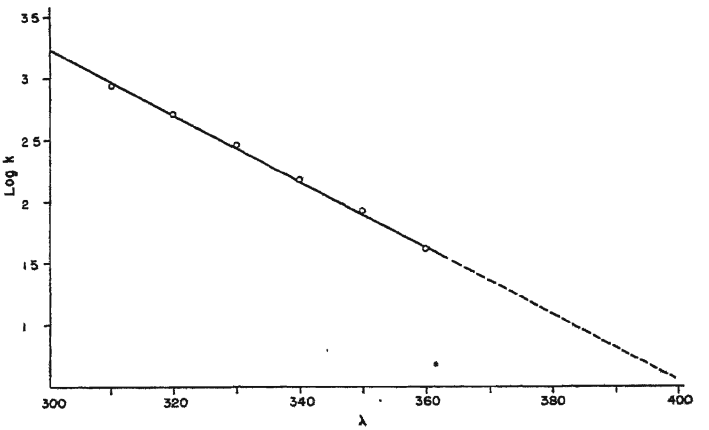

FIG. 4

Molecular Absorption Coefficient of Sulfur

carbon tetrachloride, chloroform, acetone and carbon bisulfide at concentrations of 0.001 M, 0.002 M and 0.003 M in each solvent. The absorption measurements were extended to as short a wave length as the organic solvent would permit. The values of log I_0/I for each wave length were plotted against the concentration. Beer's Law holds accurately for sulfur for the wave lengths investigated; namely, 370 mμ to 300 mμ.

The logarithms of the absorption coefficient as plotted against wave length are shown in Fig. 4. The points on this curve were obtained from

TABLE II

Molecular Absorption Coefficient, k, for Sulfur Dissolved in Organic Solvents as Function of Wave Length

mμ	Solvent			Average
	CCl_4	$CHCl_3$	CH_3COCH_3	
360	23.4	51.2 58.2	36.6 46.1	43.0
350	59.6	97.6 127.0	66.5 87.3	87.4
340	113.8	175.0 207.4	126.5 155.1	155.8
330	224	304.2 355.0		294.3
320	411.5	528 580		507
310	680	844 995		850
300	1105	1289 1413		1268

the average value of the absorption coefficient for all of the solvents given in Table II. It is seen that the logarithm of the molecular absorption coefficient varies linearly with wave length and extrapolates to a zero value at approximately $\lambda = 400$ mμ. Since it is impossible to dissolve sufficient sulfur in water to determine the value of k for that solvent, we are assuming that the value for water can be estimated with sufficient accuracy from the averaged values for the available solvents.

The concentration of the sulfur in g.-atoms/l. in the homogeneous part of the reaction has been calculated from the absorption coefficient

at $\lambda = 300$ mμ which has a value of 1460 cm.^{2}/g.-atom. The concentration of sulfur is tabulated in the last column of Table I and plotted as a function of time in Fig. 5. At the time of the appearance of the Tyndall beam, the concentration is approximately 5.5×10^{-6} g.-atoms of sulfur/l. of solvent. This is the concentration of sulfur at the highest point of supersaturation.

Although the initial concentration changes the time of appearance of the Tyndall beam, the concentration of sulfur as indicated by the value

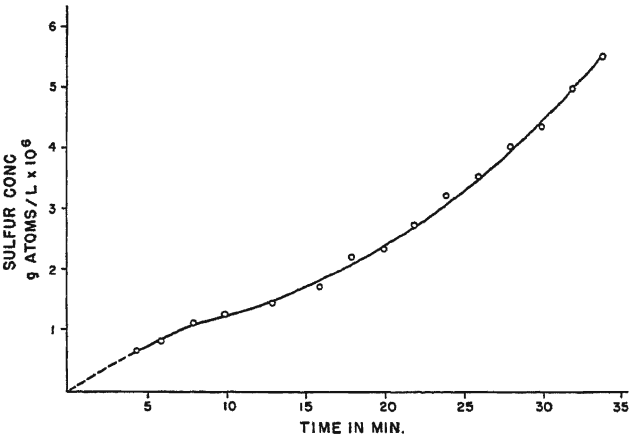

FIG. 5

Concentration of Sulfur Produced by the Reaction as a Function of Time

of log I_0/I at which the curve exhibits a discontinuity appear to be remarkably constant. The dependence upon concentration of time of appearance and of sulfur concentration at the break is being investigated more intensively by Miss Zaiser of this laboratory.

SUMMARY

1. The optical absorption of 0.0015 *M* $NaHSO_3$, $Na_2S_2O_3$, and $Na_2S_4O_6$, in aqueous solution and of sulfur (0.001–0.003 *M*) in $CHCl_3$, CCl_4, CH_3COCH_3 and CS_2 have been measured with the Beckman quartz spectrophotometer, model DU, over the range $\lambda = 390$ to 270 mμ. The ions do not absorb above $\lambda = 300$ and sulfur does not absorb above 390 mμ. Hence the absorption at $\lambda = 300$ can be used to determine sulfur in the presence of these ions.

2. The transmittance of mixtures of dilute thiosulfate and acid has been studied as a function of the time elapsing after mixing at wave lengths of 300, 435 and 560 mμ.

3. The solutions remain crystal clear in the visible (λ = 435 and 560 mμ) for a period of time which depends upon the initial concentrations of acid and of thiosulfate. During this period, however, the transmittance at λ = 300 shows conclusively that sulfur is being continuously formed during the homogeneous period of this reaction. Coincident with the visual appearance of a Tyndall beam, the optical density curves (log I_0/I) at all wave lengths exhibit a discontinuity, which is interpreted as corresponding to the formation of discrete sulfur particles from the supersaturated homogeneous solution of sulfur in water.

4. Although the time of appearance of the Tyndall beam depends upon the initial concentrations of thiosulfate and acid, the optical density at that time remains constant, indicating that the transition from true solution to colloidal dispersion of sulfur occurs at a fixed value of supersaturation of sulfur in water, which corresponds approximately to 5×10^{-6} g.-atoms of sulfur/l. of water.

5. Insofar as this method of preparing monodisperse colloids has been investigated, the results are in harmony with von Weimarn's conclusions on "corresponding crystallization conditions." We intend shortly to discuss the results in terms of the more elaborate theory of Becker and Doering (*Ann. Physik* **24**, 719 (1935)).

References

1. LaMer and Barnes, *J. Colloid Sci.* **1**, 71; 79 (1946).
2. Johnson and LaMer, *J. Am. Chem. Soc.* In press.
3. Freundlich, Kapillarchemie, English Ed., p. 615. Dutton, 1922.
4. Thomas, Colloid Chemistry, p. 117. McGraw-Hill, 1934.
5. Oden, *Kolloid-Z.* **8**, 186 (1911).
6. Foss, *Saertryki av Tidsskrift for Kjini, Bergoesem oy Mettalurgi* **1**, 3 (1946).
7. Jablezynski and Rytel, *Bull. soc. chim.* [4] **39**, 409 (1926).
8. Bacon and Fanelli, *Ind. Eng. Chem.* **34**, 1043 (1942).
9. Wigand, *Z. physik. Chem.* **77**, 423 (1911).

GELS AND JELLIES OF ALUMINUM DILAURATE IN CYCLOHEXANE AND BENZENE EXAMINED BY X-RAY DIFFRACTION *

Sullivan S. Marsden, Jr., Karol J. Mysels † and Gerould H. Smith ‡

From the Department of Chemistry, Stanford University, Palo Alto, Calif.
Received July 30, 1946; Revised manuscript received January 27, 1947

Introduction

Aluminum dilaurate in cyclohexane may form transparent coherent jellies, or opalescent lumpy gels of swollen soap. The differentiation of these two forms and their reversible transformation upon heating and cooling has already been described (1), based mainly on visual observations and X-ray diffraction of dry soap obtained from gels and jellies.

Considerable uncertainty was attached, however, to the interpretation of these latter results because of the possibility of deep changes occurring during the freezing and evaporation of solvent. To obtain reliable information on the nature of the systems, the gels and jellies themselves had to be examined. This presented considerable difficulty because of the weakness of the diffraction pattern and the need for excluding atmospheric moisture.

The method evolved allows examination of relatively concentrated systems and provides further justification for the distinction drawn between gels and jellies. The gel contains crystallites of original soap which are not observed in the jelly, where a new micellar structure appears.

Apparatus and Materials

The source of X-rays was a 1944 model General Electric XRD-1 unit operating at a potential of about 40 kv. and tube current 20 ma., with a Cu target and Be window tube. Powder (Debye-Scherrer) photographs were obtained in a flat cassette film holder at a sample to film distance of 50 mm. Six hour exposures were necessary.

The aluminum dilaurate, $AlOH \cdot L_2$, was prepared by a method previously described

* Study conducted under contract OEMsr-1057 between Stanford University and the Office of Emergency Management, recommended by Division 11.3 of the National Defense Research Council, and supervised by Professor J. W. McBain.

† Present address: Department of Chemistry, New York University, University Heights, New York 53.

‡ Present address: Union Oil Company of California, Oleum, Calif.

(2). The cyclohexane was Eastman Kodak Company's best, dried over Drierite (anhydrous calcium sulfate); the benzene was of C.P. quality, and also dried over Drierite.

Systems of soap and hydrocarbons were prepared in evacuated, thin-walled soft glass capillaries by a method already described (3). The capillary when heated above the boiling point of the solvent was enclosed in a wider, strong tube containing some solvent, to avoid bursting.

Results

Aluminum Dilaurate-Cyclohexane. A number of diffraction patterns have been made of 30% aluminum dilaurate in cyclohexane. Several diffraction patterns were then obtained from a single system after various

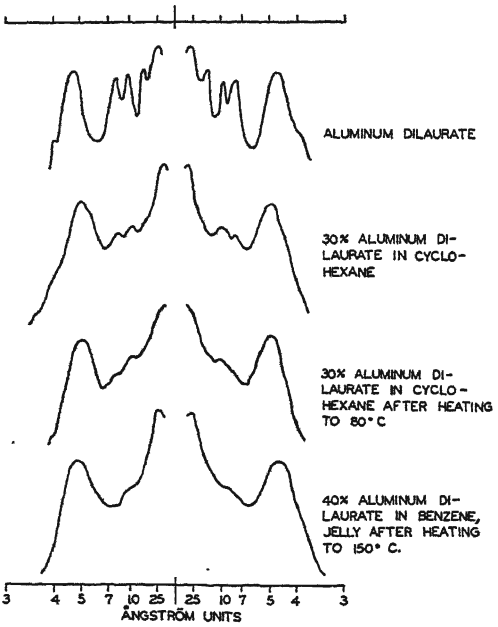

Fig. 1

Microphotometer Tracings of X-ray Diffraction Patterns

Distance—sample to plate—5 cm.; magnification—2 ×; photographed at room temperature.

thermal treatments and some of their microphotometer tracings are shown in Fig. 1. Curve 1 of Fig. 1 from pure solid aluminum dilaurate shows essentially a broad, short spacing diffraction at about 4.5–4.6 Å., a long spacing at 28–30 Å., and several higher orders of the long spacing in the intermediate region. An inhomogeneous gel, obtained at room temperature by mixing as well as possible aluminum dilaurate with

cyclohexane, consisted of opaque particles in a translucent to transparent medium. Its diffraction showed that the pattern of the soap had not been measurably altered when it formed a gel in cyclohexane at room temperature (Fig. 1, curves 1 and 2). The only apparent differences were a weakening and greater diffuseness due, partly at least, to scattering of X-radiation by the cyclohexane.

After heating the capillary and contents to 38°C., the whole of the excess solvent was taken up or thickened, and a stiff, opalescent system resulted. Diffraction by this system immediately after it had cooled to room temperature showed that the Bragg spacings, d/n, and the sharpness of the lines were the same as before heating (not given in Fig. 1).

The same system was then heated to 80°C.; after cooling to room temperature, it consisted of a stiff, birefringent material showing no apparent opalescence. An X-ray diffraction pattern made just after this latter treatment (Fig. 1, curve 3) was not as well defined as before but still showed the same Bragg spacings. The various orders of the long spacing were relatively less distinct than those of the short or side spacings. These lines are clearly visible to the naked eye and readily measured although blurred in the microphotometer tracing.

After standing at room temperature for 18 days the material in the capillary remained birefringent but had become visibly opalescent, indicating a reorganization of the gel. An X-ray photograph (not given in Fig. 1) showed that the spacings were the same as before, but the sharpness of the lines had increased, as compared with those in the previous photograph, and was practically the same as in the original system before heating.

Reheating to 80°C. reproduced the same changes as described above. The capillary system was then heated to 150°C. After cooling to room temperature, a diffraction pattern was again obtained. The lines of this pattern were still spaced as in the original system (or the dry soap) but the sharpness and density were considerably reduced.

Aluminum Dilaurate-Benzene. A system of 40% aluminum dilaurate in benzene was prepared in the thin capillary and then heated to 150°C. After cooling to room temperature, its diffraction pattern was obtained and is included in Fig. 1 (curve 4). The pattern consisted of two very diffuse halos, in approximately the positions of the most prominent side spacings of crystalline aluminum dilaurate, together with a more intense and less diffuse halo corresponding to a Bragg spacing of 25 Å. (The long spacings of aluminum dilaurate are 28–30 Å for the various types of crystal (4).) There were also no indications of the presence of the various higher order spacings of aluminum dilaurate in this photograph as there has been in those of the system of aluminum dilaurate and cyclohexane.

Discussion

The series of observations on the aluminum dilaurate-cyclohexane system indicated that *gel* formation does not affect the structure of the bulk of the soap crystallites and must, therefore, be either a surface phenomenon, or a partial disintegration accompanied by the disappearance of the most amorphous crystallites, or an arrangement of the gross particles with respect to each other, leaving the fine structure of the particles, as revealed by X-rays, still unchanged. The method of heating the systems with subsequent cooling before photographing probably resulted in reorganization of the soap into a gel, if it actually became a jelly during the heating. Observations of systems in larger tubes containing not more than 10% of aluminum dilaurate in cyclohexane have shown that such systems can, on cooling, revert to the gel from a clear system (1). Examples of this phenomenon have been observed even though the final heating exceeded the gel-jelly transition temperature by 50–60°C. The diffraction patterns of the system after it had been allowed to stand for 18 days showed that the reversion to an opalescent, birefringent material was actually a recrystallization of the aluminum dilaurate.

Systems of benzene and aluminum dilaurate containing about 5% of soap have been reported as stable jellies at about 25°C. (1). Therefore, the system prepared in benzene should have a markedly lesser tendency to revert from a jelly to a gel upon cooling from 150°C. to room temperature. Considering this, together with the differences in the patterns of the soap-cyclohexane and soap-benzene systems, the change to jelly from gel probably results in the complete disappearance of the original crystallites of soap. The new long spacing must arise from colloidal micelles of oriented soap molecules present in the jelly. These would be expected to be analogous to the well known lamellar X-ray micelles of aqueous soap solutions.

Summary

Aluminum dilaurate, $AlOH \cdot L_2$, swells to a gel in cyclohexane without greatly disturbing the crystalline diffraction pattern of the soap. After heating and cooling the system, the lines of the pattern for the gel are less distinct but the spacings are the same as before.

However, a jelly formed by heating a system of 40% aluminum dilaurate in benzene to 150°C. gives a pattern at room temperature that indicates the disappearance of the original crystallites of soap and the probable formation of micelles of oriented soap layers.

References

1. McBain, J. W., Mysels, K. J., and Smith, G. H., *Trans. Faraday Soc.* In press.
2. Smith, G. H., Pomeroy, H. H., McGee, C. G., and Mysels, K. J., *J. Am. Chem. Soc.* (communicated).
3. Marsden, S. S., Jr., *Rev. Sci. Instruments* **16**, 192 (1945).
4. Marsden, S. S., Jr., Mysels, K. J., Smith, G. H., and Ross, S., *J. Am. Chem. Soc.* (communicated).

THE DEPOSITION OF CHARGED PARTICLES IN TUBES, WITH REFERENCE TO THE RETENTION OF THERAPEUTIC AEROSOLS IN THE HUMAN LUNG

Irwin B. Wilson

From the Department of Chemistry, Columbia University, New York 27, New York
Final revision received January 29, 1947

Introduction

As a result of mutual electrical repulsion an aerosol, all of whose particles carry electrical charges of the same sign, expands. If such an aerosol is confined in a vessel, the flight of particles outward from the center of the cloud will bring them in contact with the walls of the container. The deposition resulting from this contact is calculated for cylindrical tubes and for aerosols of uniform charge and particle size.

Calculation

It is assumed that no particles are reflected from the wall and that the charge distribution may be considered as continuous and initially uniform. It is further assumed that the wall material is sufficiently conducting that a deposited particle will not form a center of repulsion for other particles.

The depositions calculated are those due to electrical repulsion alone. The electric field intensity inside a charged infinitely long cylinder at a distance r from the center, when the charge distribution is characterized by radial symmetry, is $E = \frac{2Q}{Dr}$, where D is the dielectric constant of the medium and Q is the charge per unit length of cylinder lying *interior* to the distance r.

Let

R = radius of cylinder
a = radius of particle
r_o = initial position of droplet
N_o = initial number of particles per unit volume
N = number of particles per unit volume
q = electrical charge per particle
η = viscosity of dispersing medium
ρ = fraction of aerosol deposited
r = variable of distance from center of cylinder
v = velocity
t = time.

1. Deposition under Conditions of no Disturbance. The Aerosol is Stationary in the Container

At time $=0$ the number of particles per unit length inside a cylindrical shell of radius r_o is $\pi r_o^2 N_o$, and the charge per unit length interior to r_o is $Q = \pi r_o^2 N_o q$.

Now at some later time all particles at r_o will have moved outward to some distance $r (r > r_o)$ but the charge interior to this new distance will be the same as that which had been interior to the distance r_o.

Therefore, the field intensity at the time t and position r is $E = \frac{2\pi r_o^2 N_o q}{rD}$, and the force F experienced by a particle at distance r is $F = \frac{2\pi r_o^2 N_o q^2}{rD}$. The resulting velocity, by Stokes' Law, will be

$$v = \frac{F}{6\pi\eta a} = \tfrac{1}{3}\frac{r_o^2 N_o q^2}{\eta a D r} = \alpha \frac{r_o^2}{r} \text{ where } \alpha = \frac{N_o q^2}{3\eta a D}.$$

Now

$$dr = vdt = \alpha \frac{r_o^2}{r} dt.$$

$$\int_{r_o}^{R} r dr = \int_{o}^{t} \alpha r_o^2 dt,$$

$$\tfrac{1}{2}(R^2 - r_o^2) = \alpha r_o^2 t,$$

$$r_o^2(1 + 2\alpha t) = R^2.$$

The amount deposited in time t is that confined between r_o and R and the fraction deposited is $P = \frac{R^2 - r_o^2}{R^2} = \frac{2\alpha t}{1 + 2\alpha t}$ which is independent of R.

The above formula is expected to hold for streamline flow since in such flow there is no radial motion and no stirring of the aerosol.

2. Deposition under Conditions of Continuous Perfect Stirring

Under conditions of perfect stirring the number of particles per unit volume will be the same for all radial positions in the tube and will have the initial value N_o but will decrease as particles are deposited.

The change in the number of particles per unit volume in time interval dt is dN and the change in the number of particles per *unit length* of cylinder is given by $\pi R^2 dN$ and also equals $-2\pi RNdr$ where dr is the distance traversed radially by the expanding cloud in the time dt at $r = R$.

$$\pi R^2 dN = -2\pi RNdr.$$

Now

$$Q = \pi R^2 Nq \text{ (interior to } R \text{ since } r = R)$$

and

$$E = \frac{2\pi R^2 Nq}{RD},$$

$$F = \frac{2\pi R^2 Nq^2}{RD},$$

$$v = \frac{F}{6\pi\eta a} = \frac{R^2 Nq^2}{3\eta aDR} = \alpha \frac{N}{N_o} R.$$

Therefore

$$dr = vdt = \alpha \frac{N}{N_o} Rdt.$$

So

$$\pi R^2 dN = -2\pi\alpha \frac{N^2}{N_o} R^2 dt,$$

$$\int_{N_o}^{N} \frac{dN}{N^2} = -\int_{o}^{t} \frac{2\alpha}{N_o} dt,$$

$$\frac{1}{N} - \frac{1}{N_o} = 2\alpha/N_o t,$$

$$N = N_o/1 + 2\alpha t$$

and

$$P = 1 - \frac{N}{N_o} = \frac{2\alpha t}{1 + 2\alpha t}$$

which is identical with the fractional deposition for the static case.

The above equation is expected to hold for turbulent flow in a cylindrical tube. In turbulent flow there is a continuous radial mixing of fluid so that conditions approach that of perfect stirring.

Application to the Retention of Aerosols in the Human Lung

It is believed that best results in the therapeutic use of aerosols will be obtained if deposition can be caused to occur in the finer passageways of the lung. The problem is essentially to pass the aerosol through wide tubes in which relatively little deposition is desired and then through smaller tubes in which we desire large deposition.

Since we have shown deposition to be independent of the diameter of the passageway, we can hope to obtain greater deposition in the finer tubes only if the aerosol spends more time there. This is the case for the human lung.

The lung may be divided into three regions. The first consisting of the relatively large air conduits; trachea, primary bronchi, and first order bronchi. The second region is made up of the second order bronchi, third

order bronchi, and terminal bronchi and the third group of the respiratory bronchi, alveolar ducts, alveolar sacs, and alveoli.

The terminal bronchi are not included in the third group on the basis of difference of wall structure and presumable absorption capabilities rather than on the basis of size.

Since deposition is the same under conditions of non-stirred and stirred flow, we are relieved of the problem of deciding which flow condition prevails.

In applying the electrical deposition formula to the lung, we must consider that not all of the inspired aerosol reaches each group and that a fraction of the aerosol particles have been removed by the preceeding group. The deposition equations are:

$$P_1 = 2\alpha t_1/1 + 2\alpha t_1,$$

$$P_2 = \frac{v_2}{v_o}\left(\frac{2\alpha(t_1 + t_2)}{1 + 2\alpha(t_1 + t_2)} - \frac{2\alpha t_1}{1 + 2\alpha t_1}\right),$$

$$P_3 = \frac{v_3}{v_o}\left(\frac{2\alpha(t_1 + t_2 + t_3)}{1 + 2\alpha(t_1 + t_2 + t_3)} - \frac{2\alpha(t_1 + t_2)}{1 + 2\alpha(t_1 + t_2)}\right),$$

where v_1 is the air volume reaching each group and v_o is the volume of inspired air, t_1 is the transit time for each group, and P_1 is the fraction of the aerosol *entering the trachea* which is deposited in each group. V_o is generally given as 550 cc. at room temperature and wet. The volumes of regions 1 and 2 are 26 and 56 cc., respectively, from data given by Findeisen (1). A respiration rate of 18 cycles per minute corresponds to 3.3 seconds per cycle and, assuming equal times for inspiration and expiration, an air intake rate of (550/3.3/2) 330 cc./sec. Thus $t_1 = \frac{26}{330}$ $= .08$ sec., $t_2 = \frac{56}{330} = .17$ sec., and $t_3 = 1.6$ sec., including exhalation.

Maximum deposition should be obtained in group 3 under conditions such that $\frac{\partial P_3}{\partial \alpha_5} = D$; $\alpha = \frac{1}{2\sqrt{(t_2 + t_1)(t_3 + t_2 + t_1)}} = .74$. The deposition in groups 2 and 3 is a maximum when $\frac{\partial(P_3 + P_2)}{\partial \alpha} = o$; $\alpha = 1.3$ (neglecting the slight difference between v_2 and v_3).

Expected depositions for various values of α are tabulated below. A small addition deposition (.01) is obtained in groups 1 and 2 on exhalation. Group 3 values include exhalation. Deposition in group 1 is expected mostly in the trachea and in group 2 largely in the respiratory bronchioles. Additional deposition is expected in group 3, due to mixing of inspired air with the large reservoir of air in region 3.

The predicted depositions are moderately promising. Although re-

tention occurring predominantely in group 3 cannot be achieved, it may be that the more even depositions will produce therapeutic results. Greater deposition in group 3 could be obtained by holding one's breath for a few seconds.

Therapeutic aerosols generally have a concentration of about 0.03 g./l., and the gaseous medium is usually oxygen or air. A particle size of 0.5 μ in radius and a particle density of unity will require a charge of 55 electronic units to yield an α of 1.3. With a particle radius of 0.3 μ, 20 electronic units of charge are required. Charges of this order may be obtained with a brush discharge.

TABLE I

The Calculated Effect of Electric Charge upon Fraction Deposited in Respiratory Regions 1, 2, and 3

α	Fraction deposited in respiratory regions 1, 2, and 3			
	1	2	3	Total
0.00	0.00	0.00	0.00	0.00
0.35	0.05	0.10	0.35	0.50
0.75	0.11	0.16	0.39	0.66
1.00	0.14	0.18	0.39	0.71
1.30	0.17	0.21	0.38	0.76
2.00	0.24	0.25	0.32	0.82
3.00	0.32	0.27	0.27	0.86

Findeisen has shown that with uncharged aerosols of sufficiently large particle size (3 μ diameter), impingement and sedimentation are the important mechanisms of deposition, and that by control of particle size a wide range of deposition distributions can be predicted. There is considerable uncertainty about the geometry of the lung and it may be that these predictions will not be realized. Nevertheless, they hold out promise of success. If charged aerosols must be used, it will be because impingement causes too much deposition in the larger vessels. Therefore, with charged aerosols, particles as small as are practical should be used.

Acknowledgments

The author wishes to express his appreciation to Prof. V. K. LaMer, under whose guidance this research was carried out, and to the American Medical Association for a grant for studies on the physics and chemistry of aerosols.

Summary

1. The deposition of charged aerosol particles upon the walls of a cylindrical conducting container as a result of electrical repulsion alone has been calculated for two cases:

(a) A non-stirred condition of the aerosol; streamline flow.

(b) A continually stirred condition of the aerosol: turbulent flow.

The results for both cases are the same.

2. The deposition equation has been considered in connection with the problem of the retention of aerosol particles in the human lung.

Reference

1. Findeisen, W., *Pflug. Arch. ges. Physiol.* **236**, 367 (1933).

ELECTRON DIFFRACTION STUDY OF OLEOPHOBIC FILMS ON COPPER, IRON AND ALUMINUM*

L. O. Brockway

University of Michigan, Ann Arbor

and

J. Karle

U. S. Naval Research Laboratory, Washington, D. C.

Received February 3, 1947

Introduction

The discovery and subsequent study by Zisman *et al.* (1) of oleophobic films adsorbed from solutions indicated that a variety of long hydrocarbon chains having polar end groups can be adsorbed from solutions in hydrocarbon solvents to give oriented films which are not wet by the solution. These films were readily made on a variety of solids. The films on platinum were demonstrated by Brockway and Livingston (2) to consist of layers of molecules oriented with their long axes approximately normal to the surface (usually less than 25° from the normal) by using the electron diffraction technique.

The extension of diffraction studies of films to those on metals which are more reactive than platinum introduced several new factors. In the preparation of the surfaces the highly corrosive cleaning agents suitable for platinum could not be used, but new cleaning methods had to be developed. The surfaces after preparation were not the pure metal but a coating produced by the action of the cleaning agent or an oxide due to reaction with the atmosphere. The present study is concerned with three problems: (a) the preparation of smooth surfaces on copper, iron and aluminum and an electron diffraction examination of the surfaces for impurities, (b) the formation of films of stearic acid and *n*-octadecylamine on these surfaces and a diffraction examination of their structures, and (c) the comparison of these films with similar films on platinum. Previous electron diffraction examinations made on organic films on solids have not used adsorption from solution in the preparation of the films.

* The investigation reported here was part of a study of films on metals carried out at the University of Michigan for the Naval Research Laboratory under Contracts N173s-9051 and N173s-10452.

Murison (3) studied films prepared by melting or spreading organic compounds on the surface and wiping off the excess. Germer and Storks (4) prepared uni- and multimolecular films of barium stearate and stearic acid by the Langmuir-Blodgett technique. Neither of these methods makes use of the property which is of special interest in the present investigation, *i.e.*, the formation of oleophobic films from solutions of the film-forming material. The technique of dipping the metal into the solution, as was used in the work on platinum (1), had to be modified here as described below.

The Preparation of Smooth Metal Surfaces

The advantage of using smooth, flat metal surfaces in adsorbed film experiments is readily appreciated on consideration of the problem of determining the orientation of the hydrocarbon molecules composing such a film. Electron diffraction photographs provide data on the orientation of the molecules relative to a set of axes fixed in the specimen. With a flat surface the orientation between the surface and the molecule at the point of attachment is immediately deduced. It is apparent, however, that on a wavy or slightly rough surface it would not be possible to distinguish in an electron diffraction study between those variations in orientation which are characteristic of the attachment of the molecules and those variations due to non-uniformity of the surface. In fact, on a sufficiently rough surface an adsorbed film cannot maintain a regular orientation even over a small area because of the interference from abrupt changes in surface contour.

Another advantage of flatness is that it facilitates the determination of the chemical composition of the metal surface. From a surface uniformly covered by a thin layer of oxide, the electron diffraction pattern obtained will be characteristic of the oxide. If the surface is uniformly coated but rough, however, the pattern obtained may be characteristic of the metal as well as the oxide and under some circumstances the oxide pattern may be almost entirely obscured. This is due to the fact that a considerable portion of the electron scattering arises from transmission through the oxide-coated metal peaks which occur on a rough surface.

Metallographic polishing techniques were employed for the purpose of obtaining flat surfaces. The physical appearance of these surfaces was observed in a metallographic microscope and their chemical composition determined from electron diffraction reflection photographs. The identification of the diffraction patterns was accomplished by comparison with patterns obtained from known reference materials and with X-ray data published by the American Society for Testing Materials.

Procedure

The metals studied in the polishing experiments were copper, iron and aluminum. The copper and aluminum were at least 99.90% pure. The iron was cold rolled steel—SAE 1020 (99.0% iron). Metal samples about a centimeter square were polished on a metallographic wheel with selvyt cloths and shamva, levigated alumina or rouge. The same metal samples were used throughout the experiments.

Three different procedures were followed subsequent to the treatment with polishing agents. The metal samples were (a) rinsed with distilled water and dried in a stream of air, (b) rinsed with distilled water, wiped on a damp, grease-free paper towel, rinsed again with distilled water and dried in a stream of air, or (c) rinsed in distilled water, finished on a clean, damp selvyt polishing cloth running at about 200 r.p.m. for about 10 seconds and dried in a stream of air.

The samples examined by the electron diffraction technique were photographed within 15 minutes of their preparation with electrons accelerated by about 30 kilovolts.

Results

The study of the various polishing techniques has shown that the polishing agents adhere strongly to the metal surfaces and that vigorous action is required to remove the last traces. If a metal sample is only rinsed with distilled water following the polishing treatment, adhering particles of the polish are often seen with the naked eye and invariably under the microscope. This is true for the three metals studied, copper, iron and aluminum, and the three polishing agents, shamva, alumina and rouge. A gentle wipe with a damp paper towel removes most of the adhering polish but here and there small isolated clumps could be located under the microscope. The ten second finish on a clean selvyt cloth was sufficient to remove all visible traces of the polishing materials. These observations were substantiated by the electron diffraction studies of the surfaces as can be seen from the results included in Table I. The patterns obtained after a 10 second treatment on the auxiliary cloth showed the absence of polishing material. In the case of iron and copper, only a few vague indications of a crystalline pattern appear. After a somewhat longer treatment on the auxiliary cloth, 1–2 minutes, good crystalline patterns appear which are due to characteristic oxides of copper and iron. Since the vague arcs in the diffraction patterns appearing after the shorter standard treatment on copper and iron correspond to the darkest lines in the patterns after the longer treatment, it was concluded that the chemical nature of the surface after the standard treatment corresponds to that after the longer treatment and could thus be determined. For the

short or long treatment on aluminum only an amorphous pattern is obtained. It is known that the natural oxide on aluminum which forms in air at room temperature is amorphous. The ability of the surfaces to form oleophobic films is independent of whether a short or long treatment time is used on the auxiliary cloth.

Typical diffraction results from the shamva polishing technique on copper and also some comparison data are shown in Fig. 1 as examples of

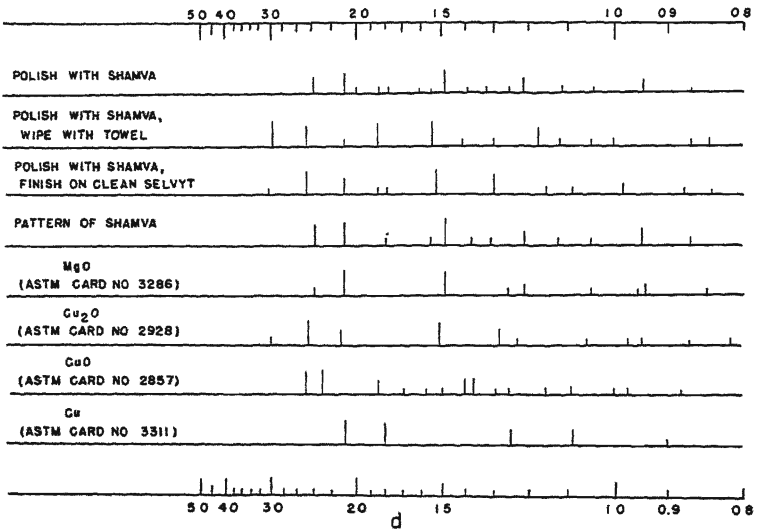

FIG. 1
Diffraction Patterns from Copper Surfaces Polished with Shamva and Patterns from Standard Comparison Materials

the information from which the results of Table I were compiled. The first pattern corresponds mainly to that of shamva, the polishing agent. The second and third patterns correspond mainly to a mixture of cuprous and cupric oxides. In no case was a pure metal surface obtained.

THE FORMATION OF OLEOPHOBIC FILMS

For the investigation of oleophobic film formation, metal surfaces were used which were prepared as described in the previous section. These surfaces were treated with solutions of stearic acid and *n*-octadecylamine in cetane forming adsorbed films which consisted of the polar additive. The orientation of the hydrocarbon chains in these adsorbed films is of considerable interest because of its relation to the physical properties of the films and to the nature of the binding to solid surfaces. Electron diffraction studies are able to give the orientation and packing of the mole-

TABLE I

The Nature of the Electron Diffraction Patterns from the Polished Metal Surfaces

Polishing technique	Copper	Iron	Aluminum
Shamva I	shamva	shamva	shamva
Shamva II	CuO and Cu_2O or shamva	iron oxide or shamva	shamva
Shamva III	CuO and Cu_2O*	γ-FeOOH*	amorphous, no pattern
Rouge I	rouge	rouge	rouge
Rouge II	rouge	rouge	rouge
Rouge III	CuO and Cu_2O*	γ-FeOOH*	amorphous, no pattern
Alumina I	alumina	alumina	alumina
Alumina II	CuO and Cu_2O or alumina	iron oxide or alumina	alumina
Alumina III	CuO and Cu_2O*	γ-FeOOH*	amorphous, no pattern

I Metallographic polishing followed by distilled water rinse.
II Metallographic polishing followed by wipe with towel and distilled water rinse.
III Metallographic polishing followed by further treatment for about ten seconds on clean polishing wheel and distilled water rinse.
* See text.

cules in adsorbed films. The theory of electron scattering from hydrocarbon films and its application to the determination of their structure has already been worked out (3, 4, 5).

Procedure

Solutions were prepared of *n*-octadecylamine in cetane, 0.05%, 0.01% and 0.001% by weight and of stearic acid in cetane, 0.1%, 0.05%, 0.01% and 0.001% by weight. A drop of the 0.001% solution contains about enough polar molecules to cover the surface of the metal samples. The octadecylamine used was obtained from Armour and Company and further purified by recrystallizing the hydrochloride 4 times from ether. The amine was then obtained from its hydrochloride. The stearic acid used was obtained from the Eastman Kodak Company and the cetane was obtained from the du Pont Company. The stearic acid was not further purified but the cetane was recrystallized several times and percolated through alumina and silica to remove polar impurities. However, it contained a mixture of hydrocarbons with a range of chain lengths, m.p. 17.7–17.8°C. The solutions were stored in pyrex glass-stoppered bottles

which had been cleaned in a chromic-sulfuric acid bath, rinsed several times with hot distilled water and dried in a drying oven.

A drop of solution sufficient to cover the surface was placed on the specimens of copper, iron and aluminum by the following technique. A platinum scoop made of thin sheet was flamed, allowed to cool 15 seconds and then dipped into the desired solution. The drop picked up was then transferred to the metal surface. After an oleophobic film formed, the drop would draw away from the surface and occasionally roll off the edge to a considerable extent. With the more dilute solutions, the tendency to draw away from the surface was much less than that for concentrated solutions and would often need to be encouraged by tilting the metal sample. Any remaining liquid could readily be removed by touching the edge of a grease free paper towel to the edge of the drop. The technique of placing a drop of solution on the metals rather than dipping them into the liquid was chosen because of the danger of contaminating the solution with foreign material from the unpolished metal surfaces. No attempt was made to control the temperature of the experiments. It varied from 20–23°C.

Some additional experiments were performed on thin rolled platinum, thin platinum soldered to a piece of steel so that it could be metallographically polished, and on metal surfaces abraded with 4/0 emery paper. The possibility of forming oleophobic films from molten stearic acid was investigated and also some films were made with cerotic acid to study orientation effects with longer chains.

Results

The only polishing technique which gave good uniform results in oleophobic film formation was polishing technique (c) which involved a final treatment with a clean auxiliary polishing cloth. Copper and iron formed oleophobic films with all concentrations of the amine and acid solutions except 0.001%. This result holds for each of the polishing agents, rouge, alumina and shamva. After a shamva polish using technique (c), aluminum forms films with all the solutions except the 0.001%. No oleophobic films could be formed after using alumina or rouge on the aluminum, owing, presumably, to a roughening of the surface. If the polished metal was rinsed with distilled water or wiped with a paper towel after polishing, oleophobic films were not readily made and showed a lack of uniformity. The drop of solution would draw up slowly from the surface and leave it wet in spots. The polished metal surfaces used in film-forming experiments were wet by both water and cetane. The adsorbed films which were oleophobic to their parent solutions were also oleophobic to pure cetane and were not wet by water.

It is interesting to note that a drop of pure cetane or of a very dilute solution of a polar additive, *e.g.*, 0.001%, can seriously interfere with the formation of an oleophobic film on a metal surface. If, after the drop is added, the excess liquid is drained from the surface and then a drop of concentrated solution which ordinarily gives a film in less than 20 seconds is added, it may taken an hour before an oleophobic film is formed. Apparently considerable time is required for the polar molecules to replace the cetane.

The time required to form oleophobic films on the copper, iron and aluminum is shortest for the more concentrated solutions. No great difference in speed was noted between the amine and acid. With the 0.1% and 0.05% solutions, the drop drew up on the metal surfaces within 30

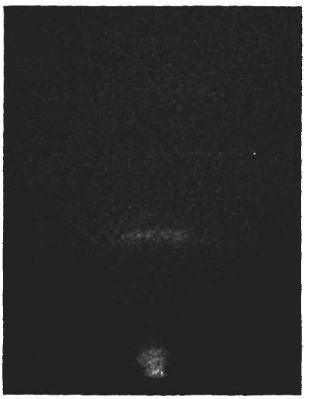

FIG. 2
Film from 0.01% Stearic Acid in Cetane on Metallographically Polished Iron

seconds at about 20°C., whereas it took the 0.01% solutions from 2 to 10 minutes to do the same. The 0.001% solutions showed no tendency to form films after 24 hours in contact with a metal surface. There is a higher concentration limit in these experiments than in those of Bigelow, Pickett and Zisman (1) since the drop technique rather than the dipping technique was used here and the total available polar material is therefore less.

Whenever oleophobic films were formed from *n*-octadecylamine and stearic acid, the electron diffraction photographs showed layer lines nearly parallel to the shadow line. The odd orders showed intensity minima at their centers and the even orders showed maxima at their centers. No spots of high intensity appear on the layer lines (Fig. 2). From measuring the spacing between the layer lines it was found that the tilt of the axes of the molecules varies between 0° and 10° from a normal to the surface of attachment. The distribution of intensity within the orders of reflection

shows that the molecules are oriented randomly about the surface normal and that they have a sufficiently random distribution on the surface so that there is no detectable intermolecular interference effect. Their distribution about their molecular axes cannot be discerned.

To investigate the effect of considerable roughness on oleophobic film formation, iron, copper and aluminum surfaces were abraded with 4/0 emery paper and attempts were made to form films. It was found that oleophobic films could be formed with 0.05% *n*-octadecylamine and stearic acid solutions within a half hour to an hour at about 20°C. only on copper and iron. Electron diffraction photographs give the surprising result that the molecules have a tilt which varies between 0° and 10° from a normal to the surface.

FIG. 3

Film from 0.05% Cerotic Acid in Cetane on Metallographically Polished Platinum

The possibility of forming oleophobic films on copper, iron and aluminum from molten stearic acid was investigated. The metals were polished with shamva and finished on an auxiliary cloth (technique (c)). If these metals are placed into molten stearic acid at 75°C. a film is formed which is oleophobic to the molten acid and the metal may be removed dry. The film is also not wet by cetane or water. Electron diffraction photographs indicate that the molecules are tilted no more than 10° from a vertical position.

In previous experiments on thin platinum having a bright and apparently smooth surface produced by rolling, oleophobic films were formed by dipping the metal into the desired solution. This technique was suitable since the platinum could be readily cleaned in a chromic-sulfuric acid bath and subsequently rinsed and flamed. A comparison of the dipping technique with the drop technique used on copper, iron and

aluminum was considered desirable. In addition, an investigation was made to determine the role played by the previous preparation of the platinum surface by comparing some results on thin flamed platinum with those on metallographically polished platinum. With both the drop and dipping techniques on thin flamed platinum an oleophobic film is formed with 0.05% *n*-octadecylamine in cetane or 0.1% stearic acid in cetane in a few seconds. The electron diffraction results show that the axes of the molecules vary from 0° to 30° from a normal to the surface as a whole. However, the drop technique on metallographically polished platinum gave films in a few seconds in which the axes of the molecules were oriented within 10° of the surface normal. This is similar to the results on metallographically polished copper, iron and aluminum. It was

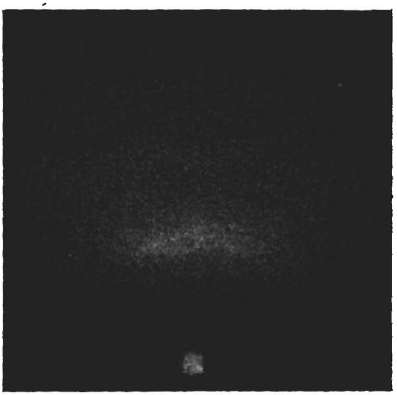

FIG. 4
Film from 0.05% Cerotic Acid in Cetane on Thin Rolled Platinum

also found that 0.05% cerotic acid solution in cetane produces an oleophobic film on metallographically polished platinum in which the molecular axes are parallel within a degree or two to the surface normal whereas on thin rolled platinum it forms a film in which the molecular axes vary from 0° to 30° from the surface normal (5b) (Figs. 3 and 4). A practically vertical orientation was also found for the molecules in a film of cerotic acid on metallographically polished iron.

DISCUSSION AND CONCLUSIONS

An important surface feature for facilitating the formation of oleophobic films is smoothness. The role played by smoothness can be understood from a consideration of the structure of oleophobic films. In the experiments performed on copper, iron and aluminum and metallographically polished platinum the molecules in the films formed from *n*-

octadecylamine and also stearic acid showed an average tilt of 5° from the surface normal. The electron diffraction results comparing the structure of films on thin rolled platinum to that on metallographically polished platinum indicate that the larger deviations from a vertical position on thin platinum is not due to an inherent structural characteristic of the film but is rather a measure of the submicroscopic unevenness of the platinum surface. If film formation is carried on for several hours on the thin platinum, a film is formed whose molecules are parallel to the normal to the surface as a whole (2). In addition it should be noted that it is not impossible to obtain oleophobic films on roughened surfaces as was shown with surfaces abraded with 4/0 emery paper. However, the time of formation is about 0.5 hour for a 0.1% solution of stearic acid in cetane instead of a few seconds and the molecules in the resulting film show a variation in orientation no greater than 10° from the normal to the surface as a whole. It is quite apparent from the experiments on the thin platinum and the abraded surfaces that the final equilibrium orientations of the molecules in an oleophobic film are not completely governed by the underlying surface contour. The significance of an orientation normal to the surface as a whole is that the molecules of such a film are perpendicular to the film-oil interface. Since this structural requirement is readily satisfied on a smooth surface, the importance of smoothness is now clear. It may be noted that, from observations on oleophobic behavior, Bigelow, Pickett and Zisman (1) suggested that such films consist of fairly closely packed molecules standing normal to the surface.

It has been found, in agreement with previous results, that with smoother surfaces, lower temperatures and more concentrated solutions the rate of oleophobic film formation is increased. A precise study of rate was not made, however, as some of the variables upon which the rate depends were not carefully controlled. The rate is not critically dependent upon the chemical nature of the solid surfaces investigated nor the nature of the end group on the polar molecules considered. The smooth surfaces of copper, iron and aluminum consisted of oxides of the metals, but neither the rate of film formation nor the structure of the film on these surfaces differs appreciably from the films on really smooth platinum. The similarity of the results from copper, iron, aluminum and platinum surfaces indicates a lack of any specific chemical effect in the adsorption.

Before a complete understanding of oleophobic behavior may be obtained several additional questions concerning the structural features of the adsorbed films need to be answered. These concern whether the film is a uniform monolayer free from solvent molecules and, if so, whether all its constituent molecules occur with their polar groups oriented toward the surface of the solid. The hydrocarbon end of the polar molecule may have a considerable attraction for the surface, as is indicated by the

poisoning effect of cetane and dilute solutions made with cetane mentioned above. So far it has not been possible to decide in general upon the number of layers, the position of the polar groups, nor the amount of solvent in oleophobic films. An experiment performed with a solution of *n*-octadecylamine in dicyclohexyl has indicated that oleophobic films formed from this solution consist of mono-layers (1).

Acknowledgments

This investigation has benefited largely from frequent conferences with Dr. W. A. Zisman whose continued interest has been most stimulating. Mr. W. C. Bigelow purified the cetane and *n*-octadecylamine used in these experiments. The interest and support provided by the Naval Research Laboratory in the study of films on surfaces is gratefully acknowledged.

References

1. Bigelow, W. C., Pickett, D. L., and Zisman, W. A., *J. Colloid Sci.* 1, 513 (1946); Part II, to be published.
2. Brockway, L. O., and Livingston, R. L., to be published.
3. Murison, C. A., *Phil. Mag.* 17, 201 (1934).
4. Germer, L. H., and Storks, K. H., *J. Chem. Phys.* 6, 280 (1938).
5. (a) Karle, J., *J. Chem. Phys.* 14, 297 (1946). (b) Karle, J., and Brockway, L. O., to be published.

NOTE ON A NEW MODE OF SOL-GEL TRANSFORMATION

Tominosuke Katsurai and Mitsuoki Nakahira

From the Institute of Physical and Chemical Research, Hongo-ku, Tokyo, Japan

Received October 10, 1946

In this article we should like to mention the reversible sol-gel transformation of silica sol which reminds us of thixotropy but is not quite similar to it. Some time ago we found that a silica sol became a gel when heated in an autoclave and that the resulting gel became a sol on shaking. This transformation, shown by

$$\text{sol} \underset{\text{shaking}}{\overset{\text{autoclaving}}{\rightleftharpoons}} \text{gel}, \qquad (1)$$

is reversible and can be repeated. The details of the experiment are as follows:

The sol is prepared by dialyzing a dilute solution of Na_2SiO_3 against dilute HCl. The commercial water glass (the Konishi product) is diluted 10 times with water, placed in a bladder, and dialyzed against 0.12 *N* HCl. The HCl is renewed from time to time. After 2 days the content of the bladder appears as an opalescent sol. The sol is not homogeneous and contains floating particles. The sol is transferred from the bladder to a stoppered bottle. The bottle is shaken for a couple of hours and allowed to stand overnight. The content of the bottle separates into two layers, *viz.*, an upper layer of opalescent sol and a lower layer of precipitate. By decanting the upper layer, a stable sol is obtained which gives no precipitate even after a week. The sol is acid to litmus and shows no cataphoresis. By determining the SiO_2 content of the sol we find that 0.0175 g. SiO_2/cc. = 0.29 mol SiO_2. This value corresponds to the composition $SiO_2 \cdot 190\ H_2O$, assuming that the sol consists only of SiO_2 (sp. gr. 2.66) and H_2O.[1] When the sol is diluted with an equal volume of water and mixed, a stable sol is also obtained. This sol was used in the experiment.

The sol undergoes no change on boiling at atmospheric pressure, but a distinct transformation into gel takes place when it is subjected to autoclaving.[2] The sol is kept in a test tube of fused quartz and heated to 200°C. in an autoclave. By this procedure the sol sets to a gel which does not flow even on inverting the test tube. If we stopper the test tube and

[1] *Cf.* Katsurai, T., and Kita, T., *Kolloid-Z.* **95**, 42 (1941).

[2] For the technique of autoclaving, *cf.* Katsurai, T., *Sci. Papers. Inst. Phys. Chem. Research (Tokyo)* **35**, 191 (1939).

shake, the gel becomes a sol which flows as easily as the original one. This behavior is similar to thixotropy. This second sol does not become a gel simply on standing. To transform this sol to a gel we must repeat the autoclaving. The transformation as is shown in the scheme (1) can be repeated.

To decide whether the change is a colloidal property only of silica sol or one of the general properties of colloids, as thixotropy, further study is required.

LIGHT SCATTERING FROM POLYMERIZING AND COAGULATING SYSTEMS *

Gerald Oster

From the Department of Animal and Plant Pathology, Rockefeller Institute for Medical Research, Princeton, N. J.

Received Feb. 7, 1947

Introduction

Recent experiments have shown that the size and shape of high polymeric molecules, colloidal particles, and viruses can be conveniently determined by measuring the light scattered by solutions of these substances. The purpose of this paper is to extend the usefulness of the light scattering method to the study of some kinetic processes frequently encountered in high polymer and colloid chemistry.

According to a theory of Lord Rayleigh (1), the intensity of light scattered by a system of N (per unit volume) independent, transparent, spherical particles of volume V with radii small compared to the wavelength of light is given by the expression

$$\alpha = ANV^2. \tag{1}$$

If the intensity of light scattered is expressed in terms of the coefficient of attenuation, α (also called the "turbidity"), then

$$A = \frac{24\pi^3}{\lambda^4} n_o^4 \left(\frac{m^2 - 1}{m^2 + 2}\right)^2, \tag{1'}$$

where λ is the wave length in air of incident light, m the ratio of the indices of refraction of the solute and solvent, and n_o the index of refraction of the solvent. For metallic particles in suspension the index of refraction of the solute is complex.

The intensity of light scattered from a polydispersed system is the sum of the contributions from each of the components of the mixture and is given by

$$\alpha = A\Sigma_j N_j V_j^2, \tag{2}$$

where N_j is the number of particles per unit volume of the jth kind each having a volume V_j. From equations 1 and 2 it follows that, although the number of particles decreases with time for a polymerizing or coagulating process, the intensity of light scattered by such a system will increase

* Paper presented before the Chemistry Section of the American Association for the Advancement of Science, 113th meeting, Cambridge, Mass., Dec. 27, 1946.

with time because the volume, which is also increasing with time, appears as the second power. In this paper the light scattering as a function of time will be determined for various kinetic processes from an evaluation of the sum in equation 2.

Equations 1 and 2 hold for spherically shaped particles. For deviations from sphericity the light scattered is reduced by a factor which is, at most, equal to 3 (2). However, since the intensity of light scattered by the systems to be considered here may change by as much as a thousand times, this factor is not important in these cases. In addition, equations 1 and 2 should not be expected to hold for solutions deviating from thermodynamic ideality. The correct expression for real solutions has been obtained by Einstein (3). However, this present discussion will be confined to ideal solutions. It has been found (4) that solutions of viruses exhibiting easily measurable turbidities are ideal, so that colloidal systems are probably ideal. However, the formulae derived here must be used with caution when applied to solutions of high polymeric molecules where large deviations from ideality have been observed (5).

The discussion below is confined to particles whose size is small compared to the wavelength of incident light. For particles whose size is comparable to the length of light, more light is scattered in the forward direction than in the backward direction with an overall reduction in the intensity of scattered light (6). The light scattered from a polydispersed system of large particles is difficult to evaluate.

Light Scattered by Polymerizing Systems

Condensation Polymerization

Linear condensation polymerization may be regarded as the combination of any size polymer with any other size polymer. In such a combination the loss in weight due to the elimination of, for example, water is negligible compared with the molecular weight of the polymer. By an argument based on the equal reactivity of all functional groups during linear condensation polymerization, Flory (7) has shown from probability considerations that the number of j-mers at any time is given by

$$N_j = N_o(1 - p)^2 p^{j-1}, \tag{3}$$

where N_o is the initial concentration of monomers and p is the extent of the reaction, *i.e.*, the fraction of all functional groups which have reacted after a given time.

Since the volume of the j-mer is j times the volume of the monomer, equation 2 becomes

$$\alpha = AV_o^2 \Sigma_j j^2 N_j, \tag{4}$$

where V_o is the volume of the monomer and N_j is given by equation 3.

By successive differentiation of the sum of p^j it can be shown that

$$\Sigma_j j^2 p^j = \frac{p(1+p)}{(1-p)^3}$$

and substituting in equation 4, we obtain for the light scattering for a linear polymerization process

$$\alpha = AN_oV_o^2 \frac{1+p}{1-p}. \tag{5}$$

Since linear condensation polymerization is a second order reaction, it is easy to show that the extent of reaction is $p = \frac{\frac{1}{2}kt}{1+\frac{1}{2}kt}$, where k is the reaction rate content. Substituting this value of p in equation 5, we obtain

$$\alpha(t) = AN_oV_o^2(1+kt), \tag{6}$$

i.e., the intensity of light scattered is proportional to the time with a slope determined by the rate of the elementary step reaction. Thus, from a knowledge of the refractive indices of the solute and solvent, of the concentration of the monomeric units, and of the light scattering as a function of time, the rate constant for the polymerization process taking place in dilute solution may be calculated.

The above discussion can be generalized for condensation polymerization of molecules with functionality greater than 2, such as encountered in gel formation, by the use of the more general distributions derived by Flory (8) and by Stockmayer (9).

Depolymerization

The distribution given by equation 3 also holds for depolymerization of linear polymers, but the extent of the reaction is given by $p = e^{-kt}$ (10). By inserting this value of p in equation 5 we obtain

$$\alpha(t) = AN_oV_o^2 \coth(kt/2), \tag{7}$$

i.e., the intensity of light scattered is decreasing approximately exponentially with time.

For systems in which the initial chain lengths cannot be considered infinitely long compared with the degradation products, the distribution function given by equation 3 is not exact (11) and for such cases the above discussion must be modified.

Addition Polymerization

Addition polymerization consists of the building up of high polymeric molecules on active nuclei or centers. According to Dostal and Mark (12) and to Flory (13) the size distribution for monomer addition is given by

the Poisson distribution

$$N_j = N_o e^{-kt} \frac{(kt)^{j-1}}{(j-1)!}, \tag{8}$$

where N_j is the number of species with $j - 1$ monomers and N_o is the number of active nuclei. The rate constant, k, is independent of time when the concentration of the monomers is sufficiently large.

The active nuclei are approximately of the same size as the monomeric units, and the problem consists of an evaluation of the sum given by equation 4 where the distribution is given by equation 8. If, in the sum, only those terms involving j are retained, the problem reduces to a mathematical one of evaluating the sum

$$\Sigma_j j^2 \frac{x^{j-1}}{(j-1)!}.$$

By a rearrangement of subscripts in the sum for the exponential this can be shown to be equal to $e^x(1 + 3x + x^2)$. The light scattering as a function of time becomes for this process

$$\alpha(t) = AN_o V_o^2[1 + 3kt + (kt)^2], \tag{9}$$

i.e., the intensity of light scattered is quadratic in time with a curvature determined by the rate constant.

Since the dependence of light scattering with time is different for condensation and for addition polymerization, the light scattering method should provide a convenient means for distinguishing between these two processes for a given system and should also enable a determination to be made of the rate constant for the elementary step process.

In practice, the formation of active nuclei for addition polymerization may be comparatively slow, so that inception of polymerization and the accompanying increase in light scattering may take place after a lag period.

Light Scattered by Coagulation Systems

Coagulating or polymerizing processes may be regarded as polymerization processes. Thus, droplet formation may be regarded as addition polymerization, *i.e.*, a building up of large particles about active nuclei. Rapid coagulation of colloids is essentially a linear condensation polymerization since any aggregate of "monomeric" colloidal units may combine with any other aggregate. According to Smoluchowski (14) coagulation proceeds in this manner with a rate constant determined by the rate at which the particles diffuse into the sphere of influence of each other and then stick (or have a constant probability of sticking). An analysis shows that the theory of Smoluchowski is identical with that used to describe condensation polymerization with the rate constant

given by $k = 8\pi D_o R_o N_o$, where D_o, R_o and N_o are the diffusion constant, radius of sphere of influence (approximately the diameter of the particle), and the number concentration of the original colloidal units. The expression for the rate constant must be multiplied by a factor less than unity if the particles do not stick on each collision. The rate constant is that for the steady state solution of the diffusion equation and is theoretically correct for time intervals greater than about 10^{-4} second and, therefore, is appropriate for the time of observations considered in coagulation.

Substitution of the diffusion rate constant in the expression for the light scattering for linear condensation polymerization, equation 6, gives

$$\alpha(t) = AV_o^2 N_o(1 + 8\pi D_o R_o N_o t), \tag{10}$$

i.e., the light scattered is linear in time and proportional to the square of the number concentration of the original colloidal particles. Since the diffusion constant for a sphere is inversely proportional to its diameter ($D_o \simeq \frac{KT}{3\pi\eta R_o}$, K is Boltzmann's constant, T the absolute temperature, and η the viscosity of the medium) and for a given weight of material the volume of the particles are inversely proportional to their number, the size of the original colloidal particles can be eliminated from equation 10 and the slope is given by

$$\frac{d\alpha}{dt} = \frac{8}{3}\frac{KT}{\eta d^2} Ac^2, \tag{11}$$

where d is the density of the particles and c is the weight concentration. It follows, therefore, that all rapidly coagulating systems should exhibit the same slope when the weight concentration, density, and refractive index of the colloid are taken into account.

Three rather diverse processes, the salting out of tomato bushy stunt virus with high concentrations of ammonium sulfate, the precipitation of ovalbumin with its antiserum, and the formation of sulfur sols by the acidification of sodium thiosulfate solution, were all found to show, after a lag period, light scattering linear in time and proportional to the square of the weight concentration in agreement with equation 10. The case of the antibody-antigen reaction will be considered in detail elsewhere.

Various volumes of a 1 N sodium thiosulfate solution were added to an equal volume of 1 N sulfuric acid solution in nearly 100 cc. of water. The total volume was quickly brought to 100 cc. with water while the mixture was shaken and the light scattering measured at intervals of one half minute. The light scattering was determined by measuring the optical density (the attenuation coefficient, α, is 2.303 times the optical density and the decrease in transmission is due only to the light scattered by the sulfur since sulfur is colorless at the wave length used) of the solu-

tion in a Klett-Summerson colorimeter using a filter transmitting almost monochromatic light of a wave length of 440 mμ. The results are given in Fig. 1 where the numbers on the curves express the volume in cc. of 1 *N* sulfuric acid and sodium thiosulfate solutions in 100 cc. of the mixture. After a lag period which decreases with increasing concentration of the

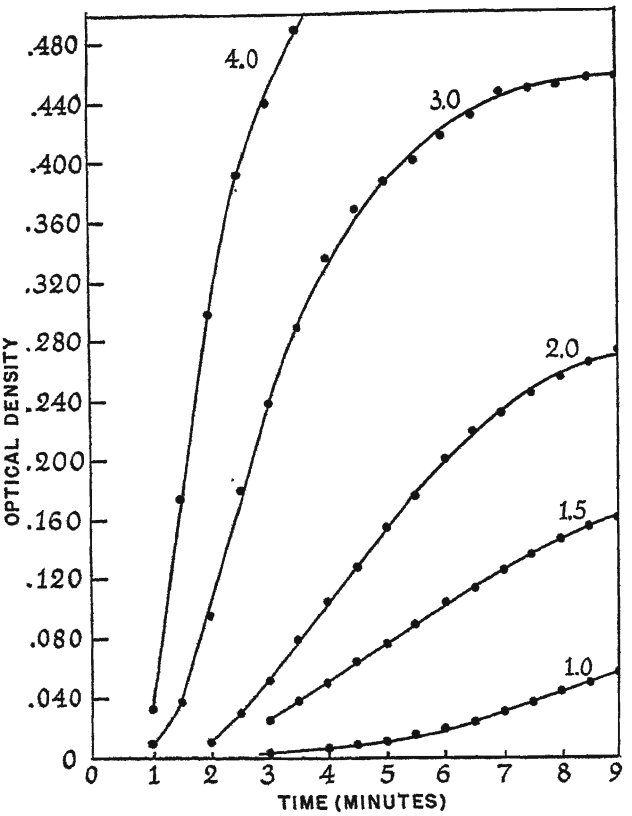

FIG. 1

Light Scattering ($\lambda = 440$ mμ) as a Function of Time for an Acidified Solution of Sodium Thiosulfate

Numbers on the curves indicate the equal volumes (in cc.) of 1.0 *N* sodium thiosulfate and 1.0 *N* sulphuric acid in 100 cc. of the aqueous mixture.

constituents, the light scattering is linear in time and the slopes are proportional to the square of the concentrations in agreement with equation 10. For longer periods of time the slope decreases because the particles become comparable with the wave length of light and the scattering is less than that given by equations 1 and 2 (6). During the times given by the straight line dependence, the solutions show, on examination with

white light, typical Tyndall appearance, namely, the scattered light at 90° is blue and polarized, and become whitish at later times which correspond to regions with lesser slopes in Fig. 1.

The slopes of the straight line portions of the curves in Fig. 1 are considerably less than those calculated from equation 11, assuming that the amount of sulfur precipitated is given by the reaction

$$Na_2S_2O_3 + H_2SO_4 = S + SO_2 + Na_2SO_4 + H_2O.$$

The sulfur precipitation reaction is probably more complicated than

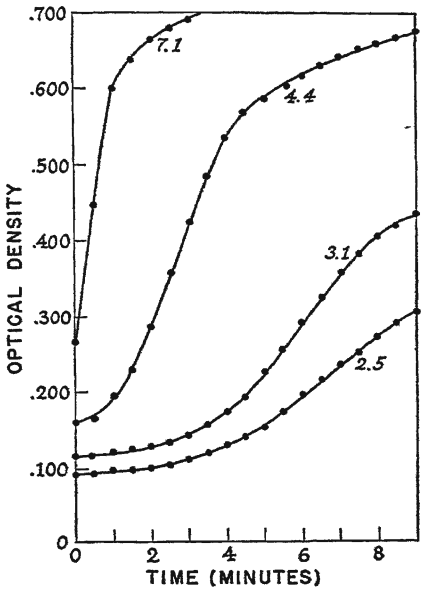

FIG. 2

Light Scattering (λ = 440 mμ) as a Function of Time for Bushy Stunt Virus Salted out of Aqueous Solution with Ammonium Sulfate

Numbers on the curves indicate the concentrations, in mg./cc., of the virus solutions.

this; the type of reaction produced depends on the initial concentration of the reactants (15). The amount of precipitable sulfur produced is very small. In fact, LaMer and his co-workers have shown (16) that the lag period in Fig. 1 is due to the time necessary for the production of a sufficient amount of sulfur to produce a supersaturated solution, which is of the order of 5×10^{-6} M/l.

Whatever the details of the chemistry of the sulfur reaction may be, it seems clear that after the initial lag period the sol formation with the high concentrations of the reagents used (nearly ten times that used by LaMer and Barnes (17) in their production of monodispersed sulfur sols)

follows the kinetics according to Smoluchowski since the light scattering is of the form expressed in equations 10 and 11.

Tomato bushy stunt virus purified by differential ultracentrifugation as described by Stanley (18) was salted out from aqueous solution by the addition of a concentrated solution of ammonium sulfate. The results are given in Fig. 2 where 0.6 cc. of saturated ammonium sulfate was added to 4.0 cc. of the virus solutions of concentrations, in mg. virus/cc., indicated on the curves. Initially the solutions were quickly shaken and the light scattering determined as described above. The virus particles have a molecular weight of about 9,000,000 and therefore scatter a considerable amount of light even in dilute solution (4); thus the curves in Fig. 2 do not commence at the origin. After the initial lag period the light scattered is linear in time and proportional to the weight concentration in agreement with equations 10 and 11.

For coprecipitating systems (the colloidal analog of copolymerization) the light scattered would not be expected to be the sum of that for the individual systems since the concentration appears as the square in equation 10.

The treatment given here for a coagulating system can be further generalized by the use of the results of theoretical studies by Müller (19) on the kinetics of coagulation of initially polydispersed colloids.

Summary

The intensity of light scattered as a function of time from a system undergoing polymerization is calculated by combining Rayleigh's theory with the size distribution functions for various polymerization processes. For linear condensation polymerization the light scattering increases linearly in time with a slope proportional to the rate constant of the elementary step reaction. For monomer addition polymerization the light scattering is quadratic in time with a curvature determined by the rate constant. Light scattered from depolymerizing linear molecules decreases with time and is proportional to the hyperbolic cotangent of the time.

Rapid coagulation of colloids, which may be regarded as a linear condensation polymerization with a rate constant determined by diffusion process, shows by calculation light scattering linearly increasing in time with a slope proportional to the square of the concentration of the colloidal substance. All rapidly coagulating systems should show the same behavior when the weight concentration, refractive index, and density of the colloid is taken into account.

When acid and sodium thiosulfate are mixed, colloidal sulfur is produced after a short induction period of from 1–3 minutes. In the first few minutes following the production of sulfur particles, they are small

enough to show Rayleigh scattering. For this period of time, the intensity of scattered light depends on time and initial concentration in agreement with the theory developed in this paper. Solutions of purified tomato bushy stunt virus exhibit a similar dependence of light scattering on time and concentration when salted out with ammonium sulfate.

References

1. Lord Rayleigh, *Phil. Mag.* **47**, 375 (1899).
2. Gans, R., Handbuch der Experimentalphysik, vol. **XIX**, Leipzig (1928); Cabannes, J., La diffusion moleculaire de la lumière, Paris (1929).
3. Einstein, A., *Ann. Physik.* **33**, 1275 (1910); Raman, C. V., and Ramanathan, R., *Phil. Mag.* **45**, 213 (1923); Debye, P., *J. Applied Phys.* **15**, 338 (1944).
4. Oster, G., *Science* **103**, 306 (1946).
5. Doty, P., Zimm, B., and Mark, H., *J. Phys. Chem.* **13**, 159 (1945).
6. Mie, G., *Ann. Phys.* **25**, 377 (1908); Debye, P., *Ann. Phys.* **30**, 57 (1909); Lord Rayleigh, *Proc. Roy. Soc. (London)* **90A**, 219 (1914); Debye, P., lecture given at the Polytechnic Institute of Brooklyn, Nov. 25, 1944, *J. Chem. Phys.* (in press) (see Zimm, B. H., Stein, R. S., and Doty, P., *Polymer Bull.* **1**, 90 (1945)).
7. Flory, P. J., *J. Am. Chem. Soc.* **58**, 1877 (1936). See also Mark, H., and Raff, R., High Polymeric Reactions, New York, 1941.
8. Flory, P. J., *J. Am. Chem. Soc.* **62**, 3038 (1941); *Chem. Rev.* **39**, 137 (1946).
9. Stockmayer, W. H., *J. Chem. Phys.* **11**, 45 (1943).
10. Kuhn, W., *Ber.* **63**, 1503 (1930).
11. Montroll, E., and Simha, R., *J. Chem. Phys.* **8**, 721 (1940).
12. Dostal, H., and Mark, H., *Trans. Faraday Soc.* **32**, 54 (1936).
13. Flory, P. J., *J. Am. Chem. Soc.* **62**, 1561 (1940).
14. Smoluckowski, M., *Z. physik. Chem.* **92**, 129 (1917). See also Thygesen, J. E., *Kgl. Danske Videnskab. Selbskab, Math.-fys. Medd.* **17**, (2) (1939), and Debye, P., *Trans. Electrochem. Soc.* **82**, 265 (1942*z*.
15. See, for example, Bassett, H., and Durrant, R. G., *J. Chem. Soc.* **1931**, 2929.
16. La Mer, V. K. (Personal communication).
17. La Mer, V. K., and Barnes, M. D., *J. Colloid Sci.* **1**, 71 (1946).
18. Stanley, W. M., *J. Biol. Chem.* **135**, 437 (1940).
19. Müller, H., *Kolloidchem. Beihefte* **26**, 257 (1928).

EFFECT OF TEMPERATURE ON MICELLE FORMATION AS DETERMINED BY REFRACTION

It has been reported that the critical concentration for the formation of micelles (*cmc*) increases with increasing temperature as determined by conductivity (1) and decreases with increasing temperature as determined by density (2) and by the use of changes occurring in the spectra of various dyes (3). In addition, it has also been stated that the *cmc* is temperature-independent (4). However a recalculation of the data of Bury and Parry and those of Ekwall indicates that the *cmc* increases slightly with temperature. In addition, the variation in *cmc* with temperature as determined by corresponding changes in dye spectra has been shown to be a property of this particular method and to involve a change in the aggregation of the dye rather than in the formation of micelles (3).

The use of refraction (5), in which the *cmc* is determined by the intersection of two straight lines, does not involve the application of an external field of force, an electric field in the case of conductivity, or of a solubilized or oriented dye as in the spectral method. In the application of the change in the refractive indices of soaps and detergents at the *cmc*, no external forces are applied or impurities added unless one considers as impurities those soap molecules or ions which are added to bring the total concentration of like ions to the *cmc*. However, this latter effect occurs in all methods under discussion. Because of the apparent lack of direct influence of this method on the *cmc*, it was believed that the application of refraction to *cmc* determinations as a function of temperature would yield additional evidence as to the temperature effect.

For these measurements, use was made of a Haber-Löewe type of interferometer with a cell having a layer thickness of 160.290 mm. To prevent evaporation at elevated temperatures and, thus, changes in concentration, the cell was sealed with a special glass plate containing a ground glass stopper through which the cell was filled. Details of this cell will be presented later but it should be mentioned that a cell of this type was found suitable to measure refractive indices of volatile liquids. The sodium alkyl sulfonates were kindly supplied by Professor H. V. Tartar and were the same materials used by him for conductimetric measurements (1). The potassium laurate and potassium myristate were prepared by multiple fractionation of the methyl esters of the two acids followed by saponification and repeated recrystallizations. They are

identical with the soaps which have been used for similar measurements of *cmc* in this laboratory.

The values of *cmc* at various temperatures of sodium decyl sulfonate, sodium dodecyl sulfonate, potassium laurate, and potassium myristate are given in Table I. For comparison, data obtained from conductivity measurements (1) for the alkyl sulfonates and from the dye-spectral method (3) for the laurate and the myristate are included. It should be noted that even at the lowest temperature the *cmc* values determined by the dye-spectral method are lower than those obtained from other

TABLE I

Critical Micelle Concentrations as Determined by Various Methods at Different Temperatures

Refraction		Conductivity		Temp. (°C.)	Refraction	Dye Spectra
Temp. (°C.)	*CMC* (*M*/l)	Temp. (°C.)	*CMC* (*M*/l)		*CMC* (*M*/l)	*CMC* (*M*/l)
	Sodium decyl sulfonate				*Potassium Laurate*	
25	.041	40	.040	25	.0255	.0215–.0235
35	.042	60	.043	35	.0270	.0205–.0220
45	.045	80	.058	45	.0305	.0200–.0215
55	.049			55	.0350	.0200–.0215
65	.055			65	.0420	
	Sodium dodecyl sulfonate				*Potassium Myristate*	
35	.010	40	.011	25	.0066	.0060–.0067
45	.011	60	.012	35	.0070	.0054–.0060
55	.012	80	.014	45	.0074	.0053–.0057
65	.014			55	.0079	.0053–.0057
				65	.0086	

measurements. This is due probably to the fact that the use of a dye involves a degree of solubilization which, similar to the effects of added hydrocarbons, will decrease the *cmc* (6), or else the dye acts like a salt causing a similar decrease (1).

The data in Table I indicate without a doubt that the *cmc* increases with increasing temperature as measured by refraction and is symbatic with the changes observed by measurement of conductivity and antisymbatic with the measurements made with the dye-spectral method. These data seem to agree with our conception that most aggregations are temperature-dependent and that they will have less tendency to aggregate at elevated temperatures due to increased thermal agitation of the coalescing units.

References

1. Wright, K. A., Abbott, A. D., Sivertz, V., and Tartar, H. V., *J. Am. Chem. Soc.* **61**, 549 (1939); Ralston, A. W., and Hoerr, C. W., *J. Am. Chem. Soc.* **64**, 772 (1942).
2. Bury, C. R., and Parry, G. A., *J. Chem. Soc.* **1935**, 626.
3. Klevens, H. B., *J. Phys. Chem.* (1947) (In print).
4. Ekwall, P., *Z. physik Chem.* **161A**, 195 (1932); *Kolloid-Z.* **101**, 135 (1942).
5. Hess, K., Philippoff, W., and Kiessig, H., *Kolloid-Z.* **88**, 40 (1939); and Klevens, H. B., *J. Chem. Phys.* **14**, 567 (1946).
6. Lingafelter, E. C., Wheeler, O. L., and Tartar, H. V., *J. Am. Chem. Soc.* **68**, 1490 (1946); and Klevens, H. B., unpublished data.

University of Chicago,
Chicago, Illinois.
January 6, 1947

H. B. Klevens
Present address:
Chemical and Physical Research Laboratories,
Firestone Tire and Rubber Co.,
Akron, Ohio.

VISCOSITIES OF SOLUTIONS OF CELLULOSE ACETATE IN SOLVENT-PRECIPITANT MIXTURES

Sir:

We wish to report briefly the results of experiments performed in this laboratory in collaboration with M. H. Forsyth and G. A. Hanks. Viscosities of dilute solutions of cellulose acetate fractions in acetone-methanol mixtures were each measured at 10°C., 25°C., and 35°C. The fractions were prepared and kindly furnished to us by A. M. Sookne and M. Harris of Milton Harris Associates. The osmotic molecular weights measured by these authors were 110,000, 53,000, and 24,000, and the acetyl contents were approximately 38.6%.[1] Solvent composition was varied from pure acetone to 60 vol.-% methanol. This latter composition is very close to the precipitation point.

The changes in intrinsic viscosities with changes in solvent composition are less pronounced than those shown by some vinyl-type polymers. For solvents containing up to 50% methanol the intrinsic viscosities are nearly constant; further increase in the methanol content leads to a sharp decrease in intrinsic viscosity. The relative change is largest for the lowest molecular weight fraction at a given temperature, and for a given molecular weight is less pronounced at the highest temperature. Nevertheless, from the available data no significant trend in the value of the exponent "a" of the modified Staudinger equation can be demonstrated. A similar sharp change in intrinsic viscosity with solvent composition has been reported by Staudinger and Sorkin[2] for the system cellulose nitrate-acetone-water.

The limiting slopes of the plots of η_{sp}/c *vs.* c increase continually with increasing methanol content of the solvent mixture for the lowest fraction; in the higher ones the increase is pronounced only beyond a methanol content of 50%. These results are in qualitative agreement with the findings of Spurlin, Martin, and Tennent,[3] who found that the slopes associated with ethyl cellulose in poor solvents are greater than the slopes associated with good solvents.

The temperature coefficients of intrinsic viscosity for the temperature interval 25–35°C. are all negative in the range of solvent compositions studied. However, as the methanol content of the solvent mixtures is

[1] Sookne, A. M., and Harris, M., *Ind. Eng. Chem.* **37**, 475 (1945).

[2] Staudinger, H., and Sorkin, M., *Ber.* **70**, 1993 (1937).

[3] Spurlin, H. M., Martin, A. F., and Tennent, H. G., *J. Polymer Sci.* **1**, 63 (1946).

increased, the temperature coefficients become less negative. The absolute magnitudes of the coefficients increase with increasing molecular weight.

It should be of interest to compare the behavior described above with that exhibited by fully esterified samples under analogous conditions.

S. G. Weissberg
Robert Simha

National Bureau of Standards,
Washington, D. C.
November 29, 1946

HEAT OF WETTING OF CHARCOAL AND ITS RETENTIVITY FOR ETHYL CHLORIDE

Saul Hormats, B. M. Zeffert, and F. E. Dolian*

Contribution of the Chemical Corps Technical Command, Edgewood Arsenal, Md.

Received February 6, 1947

Introduction

The heat evolved on the immersion of a unit quantity of an adsorbent in an excess of a liquid is known as the heat of wetting, or more precisely as the integral heat of wetting, of the adsorbent. The measurement of the total heat evolvable is a lengthy procedure which requires specialized technique and equipment. However, with well activated adsorbents, a large and fairly constant fraction of the heat is liberated immediately following immersion and can generally be measured with satisfactory reproducibility using simple procedures and apparatus. The simplicity with which reproducible heat of wetting tests can be conducted has attracted a number of investigations of the possibility of using such tests as a measure of the quality of an adsorbent.

The heat evolved on immersing activated charcoal in organic liquids has been found to be dependent upon the type of charcoal (1) and approximately independent, over a wide range, of the liquid used for immersion (2). By comparing the heats of wetting in several series of samples with various adsorptive characteristics, correlations have been shown between the adsorptive capacity and retentivity of charcoal for benzene and chloropicrin vapors (3, 4, 5) and the adsorption from solution of crystal violet, brucine, and iodine (6), among others. Empirical equations have been developed which permit calculating the sorptive capacity and retentivity of activated coconut charcoal from its heat of wetting in *m*-xylene (7). The relationship found between the heat of wetting of charcoal by benzene and the retentivity of charcoal for benzene and chloropicrin vapors has led to the inclusion of a heat of wetting requirement in some specifications for activated charcoal for military respirators, the assumption being that those charcoals having a heat of wetting above an experimentally determined value would have a good retentivity for those toxic gases and vapors which are removed from an air stream by physical adsorption.

Most of the work reported on retentivity has been concerned with the vapors of chloropicrin, carbon tetrachloride, or benzene, all of which are

* Formerly Major, Chemical Corps, present address, Commercial Solvents Corp., Terre Haute, Indiana.

medium boiling liquids in the range 75–115°C. Little has been reported on lower boiling liquids in this respect. Since extension of the heat of wetting test to cover the adsorption of lower-boiling materials would be of value, it appeared desirable to determine the relative retentivities for low boiling liquids of a variety of activated charcoals, and to compare these retentivities with the heats of wetting of the charcoals to determine whether a relationship between retentivity and heat of wetting existed with compounds of this class. Ethyl chloride (b.p. 12.2°C.) was chosen as a representative low boiling liquid for this work. The charcoals selected were commercially produced gas-adsorbents, and were chosen to cover as wide a range of activated materials and processes as are available commercially for producing respirator charcoals.

Experimental Method

A. Materials

1. *Activated Charcoals.* The charcoals used were 12–16 U. S. Standard mesh samples of the materials shown in Table I.

TABLE I

Types and Characteristics of Charcoals Used

Charcoal	Source	Process of activation	Apparent density	Heat of wetting in benzene (5,7)
			g./cc.	*cal./cc.*
A	Bituminous Coal	Steam	0.532	8.6
B	Pine	$ZnCl_2$	0.314	7.7
C	Mixed Nut Shell	Steam+CO_2	0.464	8.1
D	Walnut Shell	Steam+CO_2	0.512	7.9
E	Douglas Fir	Steam	0.458	8.0

2. *Ethyl Chloride.* Eastman's ethyl chloride (Catalog No. 1075), b.p. 12.5–13°C., was used in this work.

B. Procedure

Ground glass-stoppered U-tubes of approximately 1.8 cm. diameter and 75 ml. capacity were used as the charcoal containers. The empty tubes were weighed, then filled with 32 ml. of charcoal which had been dried 3 hours at 150°C. The tubes were then placed in a water bath regulated at 30°C. ± 0.1°C., and air, dried with H_2SO_4, $CaCl_2$, and $CaSO_4$ successively, was passed through until two successive weighings of the stoppered tube varied by less than would correspond to 0.01 mg./l. of air. The airflow used was the same as later used in the desorption of ethyl chloride from the charcoal.

After being brought to constant weight, the charcoal was saturated with ethyl chloride at room temperature (*ca.* 25°C.). Liquid ethyl chloride was introduced into a 250 ml. Erlenmeyer flask fitted with a stopper connected to one arm of the charcoal-filled U-tube. Saturation was considered to have been approached closely enough when the charcoal returned to room temperature with ethyl chloride vapor continuously passing through.

Desorption was effected by passing measured volumes of dry air at measured rates of flow through the saturated charcoal in the water bath at 30°C. in the same direction as was used for absorption of the ethyl chloride. Weighings were made at intervals until the amount of ethyl chloride being desorbed became less than 0.01 mg./l. of influent air. Volume of sample-airflow ratios used cover about the same range as is normally encountered with respirators.

Results

The data obtained are plotted on graphs indicating the relative retentivity of the charcoals over a range of concentrations of ethyl chloride being desorbed. Semi-logarithmic paper is used in order to extend the range of the plot.

Data obtained on desorptions run at an influent air flow rate of 2.70 l./min. are given in Fig. 1; this figure includes data on all the charcoals

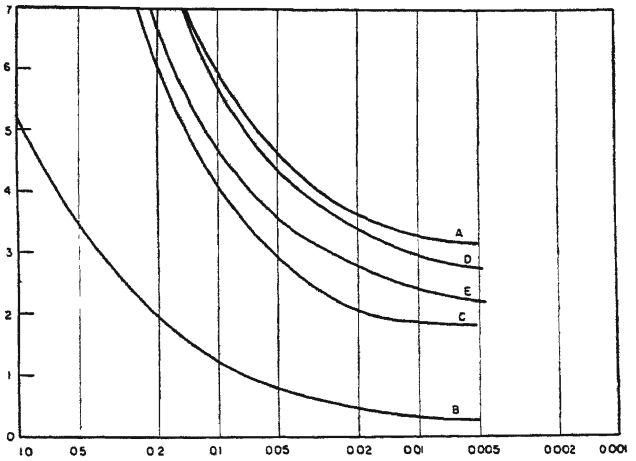

Fig. 1.

Retentivity of Ethyl Chloride by Activated Charcoals at 30°C. and Airflow Rate of 2.70 l./min.

Letters refer to the charcoals described in this paper.

Ethyl Chloride on Charcoal, mg./ml. of Charcoal

Concentration of Ethyl Chloride in Air, mg./l.

used in the work. The effect of air flow rate on retentivity is shown in Fig. 2 for charcoals B and C at influent air flow rates of 1.35 and 2.70 l./min. The reproducibility of determinations is indicated in Fig. 2 by two separate runs with charcoal B at the same air flow rate. Two runs with charcoal A at the same flow rate, one on a small (13.9 ml.) sample

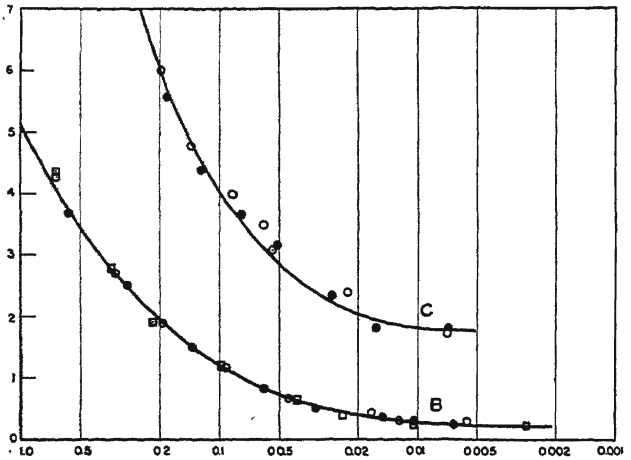

FIG. 2.

Effect of Air-Flow Rate on Retentivity of Ethyl Chloride at 30°C.; ⊙, 1.35 l./ min. ●, 2.70 l./min.; ⊡, duplicate run with charcoal B at 1.35 l./min.

Ethyl Chloride on Charcoal, mg./ml. of Charcoal

Concentration of Ethyl Chloride, in Air, mg./l.

in a straight tube, 1.95 cm. diameter, and one on a large (32.4 ml.) sample in a U-tube, are shown in Fig. 3.

DISCUSSION

Retentivity of an adsorbent has been variously defined as: the amount of sorbate retained at 100°C. and 2 mm. Hg pressure (8); as the value obtained by plotting rate of desorption at 2 mm. Hg. pressure and 100°C. (9) or 20°C. (7) and extrapolating the linear portion of the curve to the zero-time axis; and as the amount of sorbate retained by a 10 cm. layer of adsorbent contained in a tube 1.4 cm. in diameter after saturation at 25°C. followed by desorption by passing air at the rate of 1000 cm./min. through the sample for 2 hours at 25°C. (5). These definitions are arbitrary, and others could be proposed on the basis of intended use of the characteristic, or reproducibility or ease of measurement. For adsorbents intended for use in respirators, retentivity may be defined as the weight of adsorbed gas or vapor in equilibrium with a concentration of gas or

vapor in air just below that of physiological significance. Properly, retentivity as thus defined should be obtained from adsorption isotherms in air, but, as has been shown (10), these can be closely approximated by measuring the rate of evolution or the desorbing concentration of an adsorbed vapor in a current of air, as was done in this work.

As the data, particularly of Fig. 1, show, there is an appreciable difference among commercial gas-adsorbent charcoals in the amount of ethyl chloride retained at low desorbing concentrations. The zinc chloride-activated sample B is poorer in this respect than any of the other charcoals studied. This difference would be important in selecting adsorbents

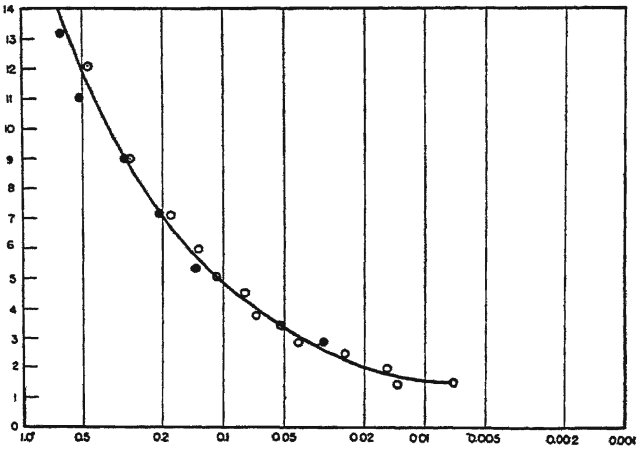

FIG. 3.

Effect of Size and Shape of Container on Retentivity; ⊙, 32 ml. of charcoal A in U-tube; ●, 14 ml. of charcoal A in straight tube; conditions were 30°C. and air-flow of 1.35 l./min.

Ethyl Chloride on Charcoal, mg./ml. of Charcoal

Concentration of Ethyl Chloride in Air, mg./l.

for use in military respirators. Toxic gases are of value in warfare only if of physiological significance at concentrations of the order of the desorbing concentrations considered in this work. If it is assumed that a toxic gas exists which is effective at a concentration of 0.01 mg./l., with a boiling point similar to ethyl chloride, and which is not destroyed by charcoal either catalytically or otherwise, then a canister filled with charcoal B would permit the passage of effective concentrations when it has taken up only 10–20% as much of this hypothetical toxic agent as the other charcoals examined. From Figs. 2 and 3, the relative merits of the charcoals would not be changed by variations in flow rate or in size and shape of the respirator canister.

Significance of Heat of Wetting and Retentivity

No relationship is indicated between heats of wetting and the relative retentivities for ethyl chloride with the charcoals examined in this work. On immersing a unit quantity of an adsorbent in a liquid the total heat liberated (2)

$$U_i = \int_o^{x_b} U_x dx = q_{im} - q_L, \tag{1}$$

where x_b is the weight of adsorbate per unit adsorbent at saturation pressure, U_x is the differential heat of wetting, q_{im} is the integral heat of adsorption, and q_L the heat of evaporation of the adsorbate. The integral heat of adsorption, q_{im}, includes (11) that due to the addition of the first portions of adsorbate to the most active parts of the surface, in which the differential heat of adsorption is generally high, plus that due to adsorption on the more uniform part of the surface, E_1, to the building up of monolayers, in the filling of capillaries, and in the immersion of the saturated granules.

Ethyl chloride gives a Langmuir unimolecular adsorption-type isotherm on charcoal (12). The total surface areas of well activated gas-adsorbent carbons range from 500–700 m.^{2}/cc. Assuming a close-packed, liquid monolayer, the surface coverable by ethyl chloride is of the order of 500 m.^{2}/g. Obviously, the 0.3–3 mg./cc. retentivities for ethyl chloride of concern in this work relate to but a small fraction of the total surface of the charcoal and a small fraction of the total heat evolved. Although the differential heats of adsorption on this most active part of the surface may be relatively high, any reasonable variations in activity and in heat effects within this region with different charcoals could not be expected to influence noticeably the heats of wetting of the charcoals. An indication of the relative smallness of the heat concerned with adsorption in this region may be obtained by applying the empirical equation of Lamb and Coolidge (13),

$$q = ma^n, \tag{2}$$

where m and n are constants, and q is the heat evolved on the adsorption of a cc. of sorbate/g. Assuming the same constants as found by Lamb and Coolidge, the equation

$$q = 0.7385a^{0.915}$$

yields 0.002 cal. for the adsorption of 3 mg. ethyl chloride/cc. of charcoal, as compared with heats of wetting obtained of 7.7–8.6 cal./cc.

Those correlations which have been reported between heats of wetting and gas-adsorptive properties of charcoal are concerned, as was stated earlier, for the most part with the vapors of comparatively high-boiling liquids. The adsorptions correlated are of the order of 100–200 mg./cc.

charcoal. It might be presumed that variations in heat effects in this region are of sufficient magnitude to be indicated by differences in the heat liberated. However, if the Lamb and Coolidge Eq. (2) is even approximately applicable, any reasonably expected variations in heat effects would still be too low to change appreciably the heat of wetting. From Eq. (1), heat of wetting is a measure of the saturation capacity of an adsorbent, that is, of its porosity. For a series of activated charcoals in which the pores are similar geometrically, variations in porosity or total pore volume within the series would be accompanied by directly corresponding variations in total pore surface. A 100–200 mg. adsorption, if assumed unimolecular, would correspond to an active surface one-fifth or more of the total surface, which may explain the correlations which have been reported. Closest correlation should be obtained with adsorptive characteristics which utilize a large fraction of the total surface or porosity of the charcoal, and with charcoals made from the same carbonaceous material activated in the one way, *e.g.*, the coconut shell charcoals of reference (7), since then the pores would be expected to be of the same shape and to vary uniformly over a wide range of activation.

Summary

a. For adsorbents for use in respirators, retentivity may be defined as the weight of adsorbed gas or vapor per unit volume of adsorbent in equilibrium in air with a concentration of the gas or vapor just below that of physiological significance. There is a considerable variation in the retentivity, thus defined, for substances of the type of ethyl chloride among gas-adsorbent activated charcoals of different manufacture.

b. Within the limits studied, changes in the flow rate of desorbing air, or changes in the volume of charcoal and the shape and dimensions of the bed, do not affect the relationship between the amounts of ethyl chloride retained and desorbed.

c. No correlation is indicated between the heats of wetting of various activated charcoals in benzene and the retentivities of the charcoals for ethyl chloride. This is attributed to the smallness of the heat effects and small proportions of adsorbent surface concerned with retentivities in this case as compared with the total quantities of heat evolved on the immersion of the adsorbent in a liquid.

References

1 Razouk, I., *J. Phys. Chem.* **45**, 179 (1941).
2. Brunauer, S., The Adsorption of Gases and Vapors (1943), pp. 238–239.
3. Burstin, H., and Winkler, J., *Brennstoff-Chem.* **10**, 121 (1929); *Chem. Abstracts* **23**, 3613[8] (1929).
4. Bell, S. H., and Phillip, J. C., *J. Chem. Soc.* **1934**, 1164.

5. MACY, R., *J. Phys. Chem.* **35**, 1399 (1931).
6. BERL, E., AND WACHENDORF, E., *Kolloid-Z., Zsigmondy Festschr.* **36**, 36 (1925); *Chem. Abstracts* **19**, 2766 (1925).
7. STONE, H. W., AND CLINTON, R. O., *Ind. Eng. Chem., Anal. Ed.* **14**, 131 (1942).
8. RAY, A. B., *Chem. & Met. Eng.* **28**, 981 (1923).
9. CHANEY, N. K., RAY, A. B., AND ST. JOHN, A., *Ind. Eng. Chem.* **15**, 1245 (1923).
10. ALLMAND, A. J., AND MANNING, J. E., *J. Soc. Chem. Ind.* **47**, 369 (1928).
11. BRUNAUER, *ibid.*, p. 252.
12. GOLDMANN, F., AND POLANYI, M., *Z. physik Chem.* **132**, 321 (1928).
13. LAMB, A. B., AND COOLIDGE, A. S., *J. Am. Chem. Soc.* **42**, 1146 (1920).

ELECTROPHORESIS IN AN ULTRACENTRIFUGAL FIELD

E. Reed Lang,* Quentin Van Winkle, and Wesley G. France

From the Department of Chemistry, The Ohio State University, Columbus

Received April 5, 1947

Introduction

The ultracentrifuge has been used with noteworthy success in the study of many colloid systems and high molecular weight compounds. Most of this work has, however, been devoted to proteins or related substances and only a small amount to inorganic colloid systems. It was, therefore, thought desirable to resume the centrifugal and ultracentrifugal studies on various inorganic colloid systems, begun a number of years ago in this laboratory by France (1), Morgan (2) and Marshall (3). Also, in view of the importance of the electrical properties of these systems in determining their stability, a study of such properties together with the determination of sedimentation constants should prove valuable in characterizing inorganic colloid systems. Accordingly, an attempt has been made in this investigation to develop a simple method for the simultaneous determination of sedimentation constants and electrophoretic mobilities in the ultracentrifuge. This can be accomplished by applying a potential to two electrodes placed in the cell of the ultracentrifuge rotor and adjusting the polarity so that the electrophoretic force acts in opposition to the centrifugal force. The magnitude of the electrical force is governed by the potential applied to the electrodes and the charge on the colloid particle. The centrifugal force is a function of the mass of the particle, the rotational velocity, and the distance from the center of rotation. A knowledge of the magnitude of the two forces, (*a*) the centrifugal force tending to produce sedimentation and (*b*) opposing electrical force tending to prevent sedimentation, offers a new approach for the simultaneous determination of mobility and sedimentation constant. Previously, McBain and Williams (4) balanced an electrical force against the gravitational force acting on microscopic air bubbles in an aqueous medium as a means of determining the number of electrical charges on the air bubbles.

Theory

When a colloidal particle is suspended in a viscous medium and placed in a high centrifugal field, the particle will attain a definite settling ve-

* Present address Rohm and Haas, Bristol, Pennsylvania.

locity which is a function of the centrifugal force, the viscosity of the medium, and the dimensions of the particle (5).

$$v_{\text{sed.}} = s\omega^2 x \tag{1}$$

and

$$v_{\text{sed.}} = \frac{m(1 - V\rho)\omega^2 x}{f} \tag{2}$$

where

s = sed. velocity in unit field (sed. constant),
ω = angular velocity (radians/sec.),
m = mass of a single particle,
f = frictional coefficient per particle,
V = partial specific volume of the particle,
ρ = density of the medium,
x = distance in cm. from center of rotation.

When the particle is acted upon by an electrical field, the velocity which it attains is dependent on its electrical mobility, μ, and the field strength (X).

$$v_{\text{elect.}} = \mu(X). \tag{3}$$

The combination of a centrifugal field opposed by an electrical field will result in a sedimentation velocity which is given by the equation:

$$v_{\text{obs.}} = v_{\text{sed.}} - v_{\text{elect.}} \tag{4}$$

$$v_{\text{obs.}} = s\omega^2 x - \mu(X). \tag{4a}$$

For a constant ω and for very small changes in the distance of the particle from the center of rotation, the term $s\omega^2 x$ in Eq. (4a) is essentially a constant. Therefore, a plot of $v_{\text{obs.}}$ *vs.* field strength (X) should yield a straight line whose slope is equal to $-\mu$, Fig. 1. The intercept of this line at zero field strength is equal to $s\omega^2 x$.

Therefore, measurement of settling velocity at various values of field strength provides a means of determining sedimentation constant and mobility in a single run in an electrophoretic ultracentrifuge.

In an actual run in the ultracentrifuge, the distance x from the particle to the center of rotation is continually changing, and a simple plot of $v_{\text{obs.}}$ *vs.* (X) will not give a true straight line. Therefore, a method of plotting the data must be used which will correct for the variation in x.

The simplest procedure for correcting the data for variations in x is to plot a preliminary curve of $v_{\text{obs.}}$ *vs.* (X), draw the best straight line through the points and observe the velocity intercept V_0 at (X) = 0.

It will be assumed that

$$V_0 = s\omega^2 x_{\text{ref.}} \tag{4b}$$

where $x_{ref.}$ is the average distance of the particle from the center of rotation during the period of observation.

At any given field strength, $v_{obs.}$ is related to field strength by the following equation:

$$v_{obs.} = s\omega^2 x_{obs.} - \mu(X). \tag{4a}$$

It is our purpose to plot a corrected velocity of settling *vs.* field strength, where the corrected velocity is a velocity of settling in a centrifugal field of $\omega^2 x_{ref.}$ and an electric field (X). The equation is:

$$v_{corr.} = s\omega^2 x_{ref.} - \mu(X). \tag{4c}$$

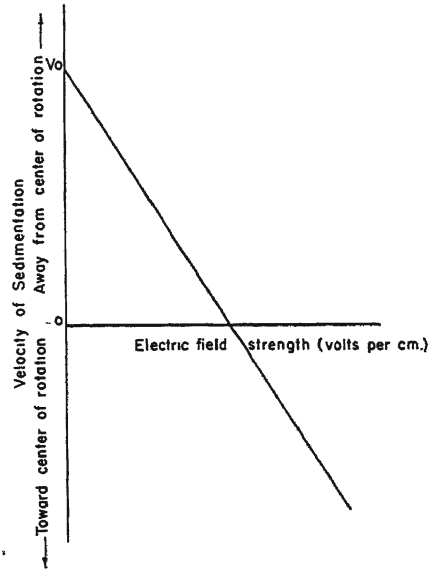

FIG. 1
Velocity of Sedimentation

Equations (4a), (4b) and (4c) can be combined to give:

$$v_{corr.} = v_{obs.} - \left(\frac{x_{obs.} - x_{ref.}}{x_{ref.}}\right) V_0. \tag{5}$$

This equation is then used to obtain values of $v_{corr.}$ from data on $v_{obs.}$, $x_{obs.}$ and a calculated $x_{ref.}$.

On inspection of Eq. (5), it can be seen that the graphical method of obtaining an approximate value for V_0 is sufficiently accurate, because V_0 occurs only in the correction term, which, in itself, is quite small.

A plot of $v_{corr.}$ *vs.* field strength then gives a straight line whose slope equals $(-\mu)$ and whose intercept at $(X) = 0$ is equal to $(s\omega^2 x_{ref.})$. In

this manner, the graphical method outlined above provides a means of determining sedimentation constant and mobility simultaneously.

Description of Apparatus

The Ultracentrifuge. To study sedimentation in an electrical field, it was necessary to design an ultracentrifuge in which two electrodes could be placed in the rotor cell and a suitable type of electrical contact main-

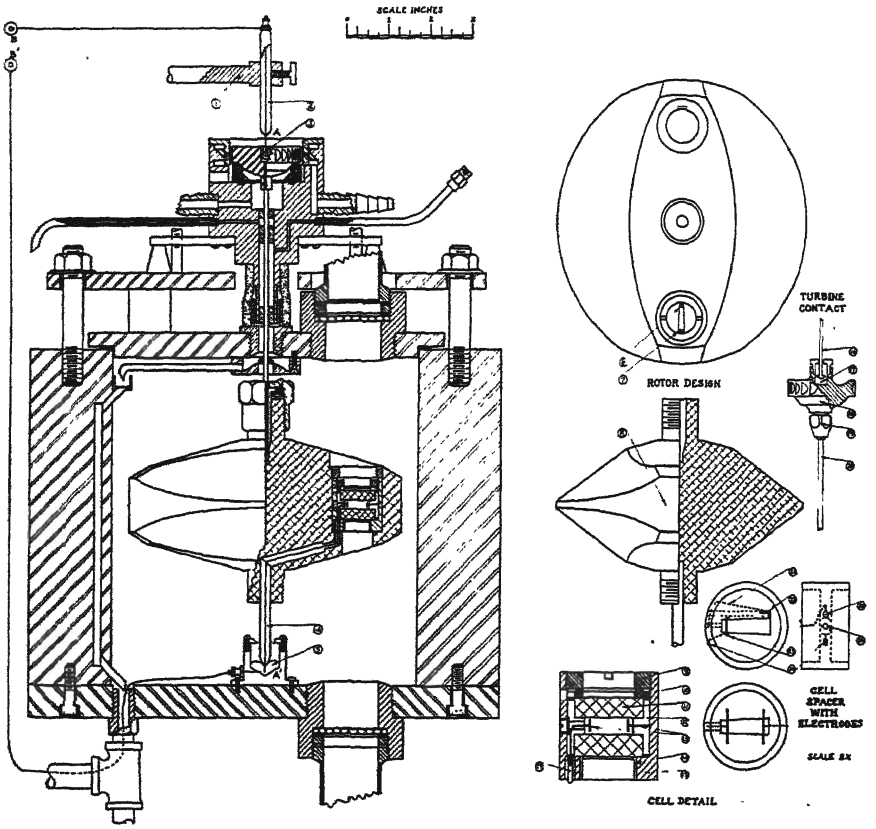

Fig. 2
Air-Driven Ultracentrifuge

tained while the machine is turning many thousands of r.p.m. A modified Beams type machine with a special rotor and turbine has proved to be very satisfactory. A detailed drawing of the apparatus is shown in Fig. 2. Electrical contacts are made at the center of rotation through mercury at points 3 and 5. This forms an almost frictionless, yet very efficient, type of rotating contact. Details of two different types of cells are also

shown in Fig. 2. The following description is for the one used in this investigation.

The cell consists of a sectorial slot cut into a Lucite spacer 0.350 cm. thick. The slot subtends a circular arc of approx. 3.5°. Smooth platinum electrodes are sealed into the spacer at points 22 and 23 and make direct contact with the solution contained in the spacer slot, or centrifuge cell. One of the electrodes, 23, is grounded to the rotor and an external connection to the rotor is made through a mercury pool in the center of the turbine, 3, and the flexible steel shaft which is connected to the turbine and the rotor. The other electrode, 22, is placed in a channel drilled alongside the sector opening in the spacer and is well insulated from the rotor. This channel is connected to the main cell sector by a small opening just opposite the electrode. This makes essentially a U-tube out of the cell spacer, one arm of which is the sectorial opening in which the boundary is followed. A platinum wire, 21, runs through the spacer and makes contact between the electrode in this chamber and the insulated wire which runs through the rotor and out the stem to the lower mercury contact, 5. It is thus possible to vary the potential on the electrodes and maintain electrical contact even though the rotor is turning at a very high velocity producing fields as high as 200,000 *g*.

To prevent the mercury from being thrown out of the recess in the turbine, 18, a special type of cup, 17, was machined. Centrifugal force causes the mercury to line the sides of this receptacle when it is revolving at high speeds and electrical contact is established through a small disc attached to a wire, 16, which cuts into the mercury as it rotates with the turbine. The pool of mercury in the lower contact reservoir remains stationary while the wire and iron tip on the stem rotate in it.

The process of sedimentation and electrophoresis was followed and recorded photographically through an optical system designed in this laboratory and described elsewhere by Lang and France (6). A six-inch aluminized telescope mirror is used in place of the customary long focal length lens and the image of the cell is brought to focus on 35 mm. film in the camera after being enlarged with a Leitz *f*. 3.5 Elmar lens. A special automatic camera mounted on a Leica copying attachment is used to record the sedimentation process. The shutter is controlled by a magnetic timing device and the film is wound automatically after each exposure.

The ultracentrifuge was operated at a reduced pressure (10^{-2} mm. Hg) and the temperature rise was less than 0.5°C./hour. Two high capacity 6 volt Willard storage batteries wired in series were used as the source of electrical energy. The voltage was varied by means of a volt-box and the potential applied to the electrodes was measured by means of a type K potentiometer with a sensitive galvanometer.

Hydrous Ferric Oxide Sols. The hydrous ferric oxide sols used in this investigation were prepared by Graham's method. In preparing Sol No. 1, about 100 g. of $Fe(OH)_3$ was precipitated from a $FeCl_3$ solution with an excess of NH_4OH. This precipitate was repeatedly washed with boiling water until free from electrolyte. It was peptized with the least possible amount of $FeCl_3$ solution and diluted to one liter. This sol was then hot dialyzed for a week after which traces of chloride ion could no longer be detected by sensitive tests. When freshly prepared the sol was very concentrated, analyzing 48 g. of Fe_2O_3/l. During the three years this sol had aged, some of the heavier material settled to the bottom of the container. For this investigation only 150 ml. of the uppermost clear fraction was removed and diluted to make a sol containing 14.2 g. of Fe_2O_3/l.

Sol No. 2 was prepared by the same procedure as was used for Sol No. 1, and the dialysis, which was carried out at room temperature, was not allowed to proceed to the minimum obtainable specific conductivity. Some of the properties of the two sols are listed in Table I.

TABLE I

Properties of Sols No. 1 and No. 2

	Conc. Fe g./l.	pH	Specific conductivity	g. at. Cl/1000 g. H_2O
Sol No. 1	9.9	4.8	5.6×10^{-5}	
Sol No. 2	2.1	5.5	5.0×10^{-5}	0.0025

Manipulation. The sol. was placed in the rotor cell containing the two electrodes across which a potential could be applied. After thermal equilibrium had been established, the centrifuge was started and the sol. subjected to a constant centrifugal force of about 25,000 times the force of gravity.

At this force the colloid micelle was thrown out of suspension with a certain sedimentation velocity. The rate of sedimentation was followed by the photographic means described under the section on apparatus. About 8 pictures at 158 second intervals were made initially in each series, before a potential was applied, in order to obtain data for the determination of the sedimentation constant. After this normal sedimentation period of about 20 minutes a potential of 1.5 volts was applied to the electrodes in such a way that the electrical force acted in opposition to the centrifugal force. Since the colloidal hydrous ferric oxide used in this investigation had particles which were positive they migrated toward the negative electrode and, therefore, by making the electrode nearest to the center of rotation negative the electrical force acted in opposition to the centrifugal force. After three pictures of the sedimenting boundary

were taken at this field strength, the potential difference was increased by a small amount and three more pictures taken. This process was repeated until a potential was attained under which the electrical force equalled the centrifugal force and the boundary became stationary. At this equilibrium, a further increase in potential caused the boundary to move back against the centrifugal force, clearly showing that the electrical force was of a greater magnitude than the sedimenting force. The boundary was then brought back by a sufficient increase in potential to its original position at the start of the sedimentation and the entire process repeated again. The number of times which the process could be repeated was limited by the coagulation which occurred during the application of the electrical field. After coagulation had proceeded beyond a certain

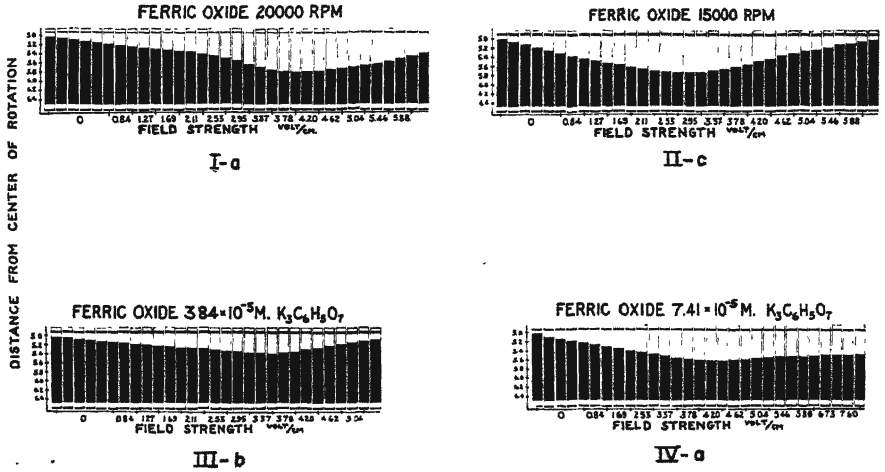

FIG. 3
Sedimentation in an Electric Field

point, application of fields as high as 10 volts/cm. was not effective in bringing the boundary back to its original position.

The runs have been numbered I-a, I-b, II-a, II-b, II-c, *etc.* The Roman numeral indicates the number of the run and the letters a, b, c, *etc.*, apply respectively to the 1st, 2nd, 3rd, *etc.*, times which the boundary is brought back to its original position by application of an electric field. Actual enlargements of the negatives taken of the cell during several runs are shown in Fig. 3. The first few pictures in each series (I-a, I-b, *etc.*) were taken without an opposing electrical field in order to determine the effect of the previously applied electrical field on the sedimentation constant. It is evident from these pictures that the sedimentation velocity increases after a prolonged passage of current through the cell.

Runs III and IV show the results obtained when a small amount of citrate ion is added to the ferric oxide sol. A decrease in mobility is observed. Further consideration of these runs will be made in the discussion of the results.

For runs I to IV inclusive, the electric field strength applied to the colloidal system during ultracentrifugation was determined by measuring the total applied e.m.f. with a potentiometer and dividing this measured e.m.f. by the distance between the smooth platinum electrodes (distance = 1.5 cm.). It is recognized that overvoltage effects introduce error in the value of the field strength which is obtained by this procedure. For runs V-a, b, c, and d both the current through the cell and the applied e.m.f. were measured. The values of field strength used in plotting the curves in Fig. 8 were obtained by using the following relationship:

$$X = \frac{I}{qK_{sp.}} = \text{volts/cm.} \tag{6}$$

where

I = current passing through the cell (amps.),
q = cross-sectional area of the cell (q varies with distance from center of rotation for a sectorial cell),
$K_{sp.}$ = specific conductivity of the colloidal system.

The measured currents passing through the centrifuge cell were of the order of 5×10^{-6} amps.

Results

The results of five runs are shown graphically in Figs. 4, 5, 6, 7 and 8. The curves were obtained by plotting observed velocities of sedimentation *vs.* applied field strength and correcting the straight line portion of the curves for the variation in centrifugal force ($\omega^2 x$) with the distance x of the boundary from the center of rotation, by means of Eq. (5).

The curves all have the same general shape, graphically illustrated in Fig. 9.

In the absence of complicating effects, the normal course of the curves should be along the straight line a-e (in Fig. 9). However, it is postulated that coagulation of the colloidal particles results in a shift of the line a-e to some new position such as f-g. As coagulation proceeds further the straight line is finally shifted to the position b-c, where apparently coagulation ceases. It is assumed that no coagulation occurs along the line b-c because the chance of obtaining a straight line relationship between velocity of sedimentation and electric field strength should be very small during the time in which coagulation is occurring. It should also be pointed out that, for runs 1, 2, 3, and 4, part of the shift of the line a-e to the

position b-c is the result of polarization effects at the platinum electrodes and the method used in evaluating the field strengths.

The slope of the straight line portion (b-c) of the curve in Fig. 9 is equal to the mobility of the partially coagulated and momentarily stable sol. Also, the sedimentation constant of this sol can be obtained by extrapolating the line b-c back to zero field strength and obtaining the velocity of settling in the absence of the electric field as an intercept on the ordinate axes. Since the straight line portion of the curve has always been observed to cross the x-axis (velocity of settling equal to zero), the

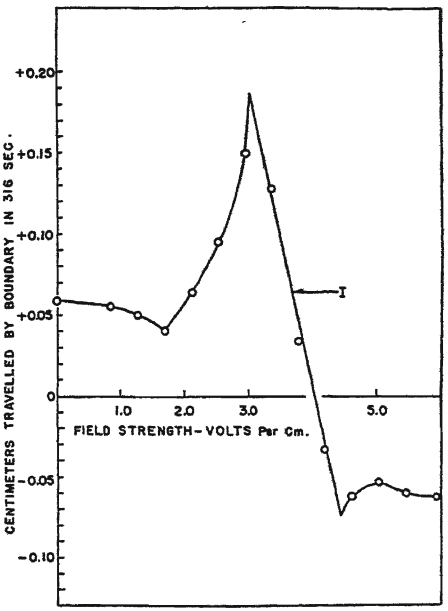

FIG. 4

Variation of Sedimentation Velocity with Electrical Field Strength for Hydrous Ferric Oxide Sol No. 1. R.P.M. = 20,000

value of the sedimentation constant at the point where electrical and centrifugal forces acting on the colloidal particles are in exact balance is designated as S_{balance}.

The deviation from the straight line of the portion of the curve c-d (Fig. 9) is again the result of coagulation of the colloidal particles.

Since coagulation effects were observed to occur, four quantities were measured or calculated from a single run: (1) sedimentation constant before application of the electric field (S_{initial}); (2) sedimentation constant at the balance point (S_{balance}); (3) mobility at the balance point; (4) sedimentation constant after the electric field has been removed (S_{final}).

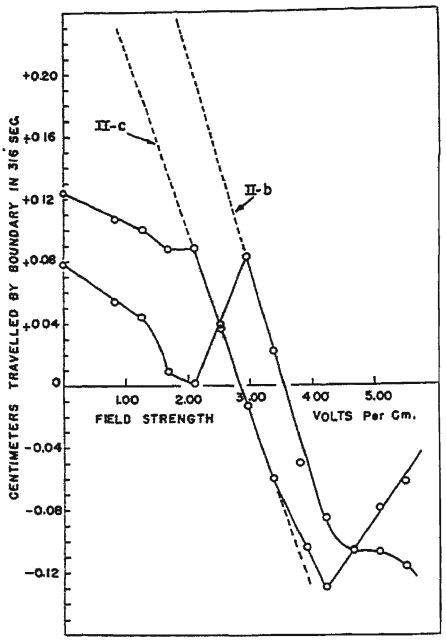

FIG. 5

Variation of Sedimentation Velocity with Electrical Field Strength for Hydrous Ferric Oxide Sol No. 1. R.P.M. = 15,000

TABLE II

Mobilities and Sedimentation Constants of Hydrous Ferric Oxide Sols from Ultracentrifugal Measurements

Run	Sol	Temp. °C.	R.P.M.	Molarity K-citrate $\times 10^5$	Mobility cm.^{2} sec.$^{-1}$ volt^{-1} $\times 10^4$		Sedimentation constant $\times 10^{13}$ T = 20°C.		
					obs'd	T = 20°C	$S_{init.}$	S_{final}	$S_{bal.}$
I-a	1	26.0	20,000	zero	5.8	5.0	71	454	794
II-a					—	—	52	167	—
II-b	1	27.5	15,000	zero	4.5	3.8	167	266	1000
II-c					3.8	3.2	266	368	644
III-a	1	27.0	15,000	3.84	3.3	2.8	97	332	720
III-b					2.4	2.1	332	411	417
IV-a	1	25.0	15,000	7.41	2.8	2.5	192	613	779
V-a					3.1	2.8	113	162	333
V-b	2	24.8	14,000	zero	3.4	3.0	162	158	225
V-c					3.4	3.0	158	212	223
V-d					3.4	3.0	212	231	220

These quantities have been calculated for the five runs represented in Figs. 4, 5, 6, 7, 8, and the results are listed in Table II. Table II also contains the above data corrected to the viscosity of water at 20°C. The sedimentation constants S_{initial} and S_{final} were calculated by the method described by Pedersen (7).

Mobilities. A review of the results tabulated above shows that the mobilities obtained are in the same range of values as those reported for hydrous ferric oxide sols by other investigators, Table III.

The mobilities measured in the ultracentrifuge and recorded in Table II are not mobilities of the original unaltered sol, however, since partial coagulation of the sol occurs before a stable particle size is attained. Also, these mobilities are somewhat compromised by (a) formation of products of electrode reactions in the colloidal system and (*b*) the change in conductivity which occurs at the boundary between the sedimenting colloidal system and the clear supernatant solution. The latter effect arises from the fact that the conductivity of the colloidal material amounts to about 20% of the total conductivity of the solution for Sol 1 and about 6% for Sol 2. Sedimentation of the colloidal material results in the formation of a clear supernatant which has a lower conductivity than the solu-

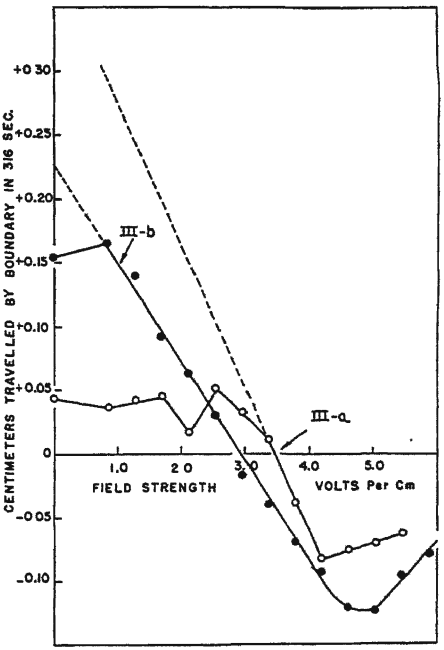

FIG. 6

Variation of Sedimentation Velocity with Electrical Field Strength for Hydrous Ferric Oxide Sol No. 1. Molarity Potassium Citrate = 3.84×10^{-5}. R.P.M. = 15,000

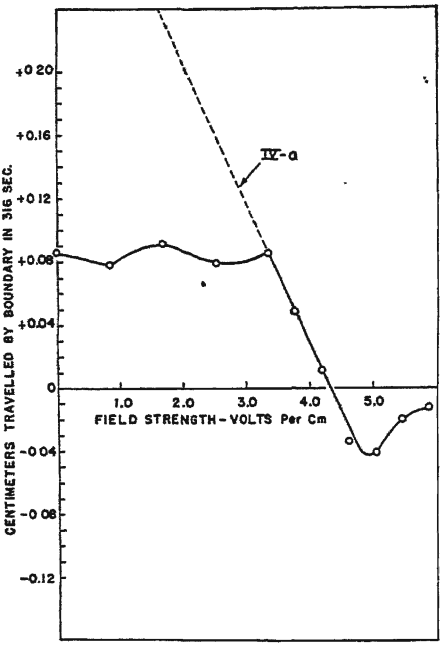

FIG. 7

Variation of Sedimentation Velocity with Electrical Field Strength for Hydrous Ferric Oxide Sol No. 1. Molarity Potassium Citrate = 7.41×10^{-5}. R.P.M. = 15,000

tion below it which contains the colloidal material. When current is passed through such a system, a greater field strength is developed in the clear supernatant than in the colloidal solution below it, as can be seen

TABLE III

Mobilities of Hydrous Ferric Oxide Sols

Mobility cm.^{2} sec.$^{-1}$ volt^{-1} $\times 10^4$	pH	Conc. of Fe g./l.	Reference
2.5–5.0	4.8	9.9	Table II, Runs, 1, 2, 3, and 4.
3.0	5.5	2.1	Table II, Run 5.
5.2	3.2		Sen-Gupta and Sinha, *J. Indian Chem. Soc.* 18, 489 (1941).
3.1		1.3	Whitney and Blake, *J. Am. Chem. Soc.* 26, 1339 (1904).
3.7	5.8	0.006	Hazel and Ayers, *J. Phys. Chem.* 35, 2930 (1931).
6.0	4.5	3.3	Mukherjee, *J. Phys. Chem.* 36, 595 (1932).
4.5	4.2	17.4	McBain and Thomas, *J. Phys. Chem.* 40, 997 (1936).

by application of Eq. (6). Therefore, a colloidal ion moving into the clear supernatant layer is speeded up and its concentration near the boundary is reduced. The observed mobility is then higher than the true mobility for this case. As shown by Henry and Brittain (8), the rate of migration of the boundary is equal to the true mobility of the colloidal particles when the colloidal solution contains sufficient dissolved electrolytes to render negligible the contribution of micelle ions to the total conductivity of the solution.

Sen-Gupta and Sinha (9) observed that by using ultra-filtrate as a leading electrolyte for a hydrous ferric oxide sol (determination of mobilities by the moving boundary method) in which the micelle ions (including gegen-ions) contributed at least 38% of the conductivity of the colloidal solution, the observed mobility was 25% higher than the true mobility of the sol. Thus the conductivity error involved in the mobility determinations on Sols 1 and 2 could be small.

Comparison of S_{initial}, S_{final} *and* S_{balance}. Comparison of the initial sedimentation constants (S_{initial}), sedimentation constants at the balance point (S_{balance}), and sedimentation constants after the electric field is removed (S_{final}) for runs I to IV inclusive, shows that while the electric

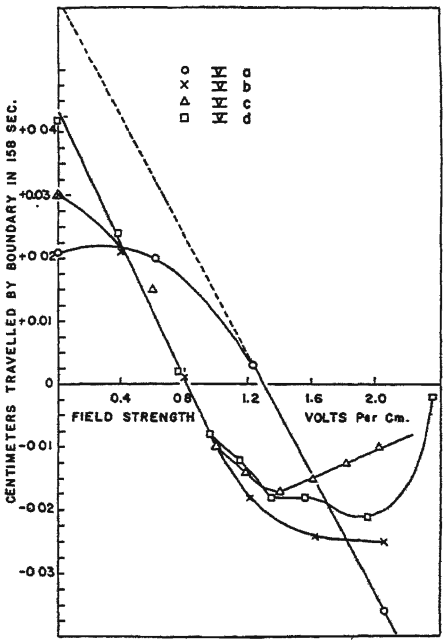

FIG. 8

Variation of Sedimentation Velocity with Electrical Field Strength for Hydrous Ferric Oxide Sol No. 2. R. P. M. = 14,000

field is applied to the sol its sedimentation constant is considerably larger than either before or after the electric field has been applied. This seems to indicate that a coagulation occurs during the application of the electric field, which is partially reversed by a decoagulation after the electric field is removed. However, it is possible that the apparently large values of S_{balance} are the result of polarization at the platinum electrodes and/or the result of any phenomenon which introduces a high resistance into the centrifuge cell circuit. Such a high resistance would cause the

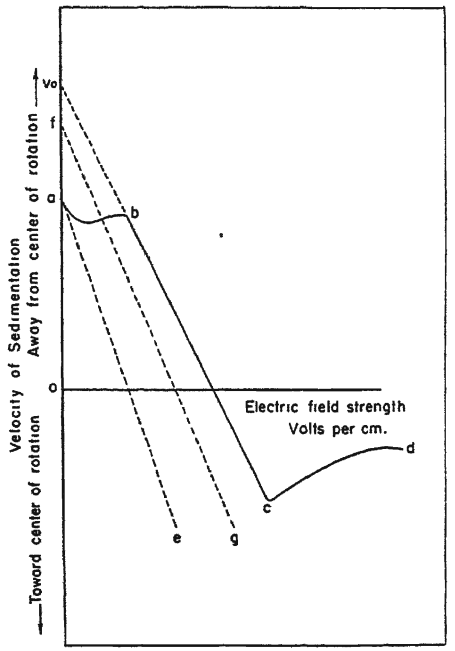

FIG. 9
Variation of Sedimentation Velocity with Electrical Field Strength for Hydrous Ferric Oxide Sols

effective field strength in the centrifuge cell to be much lower than the value obtained by dividing the applied e.m.f. by the distance between the electrodes.

For Runs V-a, b, c, and d, where field strength was calculated from the current passing through the cell, the values of S_{balance} are more nearly equivalent to the values obtained for S_{final}. The applied e.m.f.'s were also measured for Runs V-a, b, c, and d, and the curves of applied e.m.f. *vs.* current were coincident straight lines which extrapolated to 1.7 volts for zero current flow. This indicates that significant changes in the specific

conductivity of the colloidal solution in the centrifuge cell did not occur, nor could there have been any appreciable change in the overvoltage characteristics of the platinum electrodes during the application of the electric field.

Effect of Potassium Citrate. Referring to Table II, it can be seen that potassium citrate decreases the mobility of hydrous ferric oxide sol. at the balance point and increases the initial sedimentation constant. The increase in the initial sedimentation constant is the result of two effects: (1) coagulation of the sol due to the influence of the citrate ions, and (2) repression of the "primary charge effect" due to the addition of electrolyte, as discussed by Pedersen (10). In the following section it will be shown that repression of the primary charge effect can account for only a minor fraction of the total increases observed.

Primary Charge Effect. The primary charge effect which reduces the sedimentation rate of colloidal ions is of considerable importance when sedimentation velocities of highly dialyzed sols are being measured. Pedersen (10) has derived an equation which relates the observed sedimentation constant to the true sedimentation constant for colloidal systems in which primary charge effects are involved:

$$S_{\text{obs.}} = S_{\text{true}} \left(1 - \frac{QC_k\mu_k}{K_{\text{sp.}}} \cdot F \right), \tag{7}$$

where

Q = net units of charge on the colloidal particle,
C_k = number of colloidal particles/ml. $\div$ 6.0×10^{23},
μ_k = mobility of the colloidal particle (cm.^{2} $\times$ sec.$^{-1}$ $\times$ volts^{-1}),
F = Faraday's constant (coulombs),
$K_{\text{sp.}}$ = specific conductivity of the colloidal solution.

In the case of Sols 1 and 2, it is possible to calculate in an approximate manner the ratios between $S_{\text{obs.}}$ and S_{true} with the aid of a few assumptions. The simplest procedure is to assume that the sol particles are spheres. According to Abramson, Moyer and Gorin (11) for spheres in solutions of low ionic strength:

$$Q = 6\pi\eta r\mu_k \tag{8}$$

where

η = viscosity of the medium (poises),
r = radius of the particles (cm.),
μ_k = mobility of the particles $\left(\text{cm.}^2 \times \text{sec.}^{-1} \times \text{volts}^{-1} \dfrac{300}{4.77 \times 10^{-10}} \right)$,
ρ_p = density of the particles = 5.0 g./ml.,
ρ_m = density of the medium (H_2O).

Also—

$$r = \sqrt{\frac{9\eta s}{2(\rho_p - \rho_m)}}.$$

A value for the number of colloidal particles/ml. can be calculated from the density of the colloidal particle, its radius, the concentration of iron expressed as g./ml., and an assumed constitutional formula for the colloidal micelle. Then, using Eqs. (7) and (8), the *per cent* deviation of $S_{obs.}$ from S_{true} is obtained. For Sol 1, the *per cent* deviation was 2–6% for $S_{balance}$ and approximately 20% for $S_{initial}$ in the two Runs I-a and II-a. Carrying the calculations further, it is estimated that addition of potassium citrate in the amounts used in Runs III-a and IV-a increases the initial sedimentation constant from 5 to 10% through the reduction of the primary charge effect which results when the specific conductivity of the solution is increased, whereas the experimentally observed increases amounted to 50% for Run III-a and 300% for Run IV-a.

Acknowledgments

Grateful acknowledgment is made to the National Research Council for its generous Grant-in-Aid, which made possible the development and construction of the ultracentrifuge used in this investigation. Thanks are also due to Technical Assistants John F. Betz and Percy Gordon Laverack for service rendered in the construction of this equipment.

Summary

1. An air-driven electrophoretic ultracentrifuge designed for the investigation of the electrophoresis of colloidal systems in an ultracentrifugal field has been described.

2. A graphical method for simultaneously determining the mobilities and sedimentation constants of colloidal particles from electrophoretic ultracentrifugal data has been developed.

3. The electrophoretic mobilities of hydrous ferric oxide sols have been determined by the use of the electrophoretic ultracentrifuge.

4. The particle size or sedimentation constant of hydrous ferric oxide sols increases with continuous exposure to the combined effect of an electrical and ultracentrifugal field.

5. Low concentrations of potassium citrate lower the mobility of hydrous ferric oxide sols and increase their particle size and sedimentation constant.

References

1. France, W. G., Division of Physical and Inorganic Chemistry, Milwaukee Meeting, Am. Chem. Soc., 1923.
2. Morgan, S. J., Dissertation, The Ohio State University, 1928.
3. Marshall, M. L., Dissertation, The Ohio State University, 1937.

4. McBain, J. W., and Williams, R. C., *Colloid Symposium Annual* **7**, 105 (1930).
5. Svedberg, T., and Pedersen, K. O., The Ultracentrifuge, p. 5. Oxford Univ. Press, 1940.
6. Lang, E. R., and France, W. G., *Rev. Sci. Instruments* **12**, 32–4 (1941).
7. Svedberg and Pedersen, *l. c.*, p. 17.
8. Henry, D. C., and Brittain, J., *Trans. Faraday Soc.* **29**, 798 (1933).
9. Sen-Gupta, N. C., and Sinha, P. R., *J. Indian Chem. Soc.* **18**, 489 (1941).
10. Svedberg and Pedersen, *l. c.*, pp. 24–25.
11. Abramson, H. A., Moyer, L. S., and Gorin, M. H., Electrophoresis of Proteins, p. 121. Reinhold Publishing Corp., New York, 1942.

THE STRUCTURE AND PROPERTIES OF COLLOIDAL SULFUR[1]

Wolfgang Pauli

From the Chemical Institute, University of Zurich, Switzerland
(Translated by Ralph E. Oesper, University of Cincinnati)
Received September 25, 1946

This discussion of the relationship between the structure and the properties of colloidal sulfur may appear to be concerned with a very restricted section of colloid chemistry, but it reflects so clearly the type of problem that confronts the modern colloid chemist, and the methods by which he attacks his task, that the discussion actually possesses considerable general interest.

I

The history of sulfur sols extends back to the beginning of colloid chemistry as a special field of study. Wackenroder (2) in 1846 described the production of a milky dispersion of sulfur by passing sulfur dioxide and hydrogen sulfide into water. In 1850 Selmi (3) noted that this "pseudo-solution" of sulfur exhibits peculiar properties, an observation that antedates by eleven years Graham's division of materials into two worlds of matter, colloid and crystalloid, which are distinguished on the basis of their membrane-permeability and rates of diffusion. In 1908 Raffo (4) reported a second procedure for preparing S sols, namely, by the action of thiosulfate and sulfuric acid. The unstable thiosulfuric acid decomposes, forming colloidal sulfur along with polythionic acids.

The reactions which occur when hydrogen sulfide and sulfur dioxide interact in aqueous solution were not cleared up until many years after Wackenroder and Selmi had published their observations. The elucidation of this reaction was due to Foerster and his collaborators (5) and to Stamm and his associates (6). The decomposition reactions of the liberated thiosulfuric acid were studied by Foerster, especially. The Wackenroder reaction proceeds through thiosulfurous acid as an intermediate stage, with production of polythionic acids and thiosulfuric acid along with the Selmi S sol.

After preliminary work of Riesenfeld and Gruenthal (7), according to Foerster (8), the following reactions take place when thiosulfuric acid

[1] This paper originated in a lecture delivered on May 15, 1944, before the Chemical Society of Zurich. Details of the experiments can be found in ref. (1).

breaks down to give the Raffo S sol. These equations give a picture of the interplay that leads to the formation of polythionic acids and to the regeneration of thiosulfuric acid from these products.

$$
\begin{aligned}
S_2O_3^{=} + H^+ &\rightarrow HSO_3^{=} + S \\
5S_2O_3^{=} + 6H^+ &\rightarrow 2S_5O_6^{=} + 3H_2O \\
S_5O_6^{=} + HSO_3^{-} &\rightarrow S_4O_6^{=} + S_2O_5^{=} + H^+ \\
S_4O_6^{=} + HSO_3^{-} &\rightarrow S_3O_6^{=} + S_2O_3^{=} + H^+ \\
S_3O_6^{=} + H_2O &\rightarrow SO_4^{=} + S_2O_3^{=} + 2H^+
\end{aligned}
$$

The Raffo and the Selmi sols make up the group of hydrophilic sulfur sols. They display their hydrophilic nature in the following characteristics: 1. relatively low electrolyte sensitivity toward coagulation by alkali salts and acids; 2. reversible coagulation by neutral salts; 3. slight sensitivity toward electrodialysis (even at 25–30 V/cm.). Sven Oden (8) noted that Raffo S sols display a characteristic which is reminiscent of a property of water-soluble proteins, namely, their fractional precipitation by salts is dependent on particle size.

The general theory that the charge on colloidal particles is due to ionogenic complexes (10) was advanced in 1920. This was applied in 1922 by Freundlich and Scholz (11) in a study of the structure of the Raffo S sol. Two important statements evolved from this work: 1. The sulfur of the sol is present as the carbon disulfide-insoluble modification $S\mu$; 2. The charge-conferring group of the sol is pentathionic acid, $H_2S_5O_6$. The proof that this complex is responsible for the charge is based on the finding that treatment of the coagulum with hot ammonia water furnished considerable thiosulfate that can be titrated with iodine, whereas only slight reduction of iodine to iodide was detectable in the sol before this treatment.

Freundlich's postulate that pentathionic acid is the charge-conferring component in these sulfur sols was accepted by all the subsequent workers insofar as this function was ascribed to a polythionic acid. Bassett and Durrant (12) suspected that hexathionic rather than pentathionic acid was involved. Verstraete (13) found tetrathionic and pentathionic acid in the ultrafiltrate. He also determined, as K_2SO_4, the contra-ions K^+ in the separated coagulum produced by the addition of KNO_3, or the contra-ions H^+ from the titration differences in the negatively charged sol and the ultrafiltrate. The difference of the contra-ions was assumed to be associated with the sol particles and at the same time, accepting Freundlich's postulate, the contra-ions determined in this way were assigned to the corresponding quantity of polythionic acid bound in the sol.

In the following discussion of the constitution of the S sol and its relations to the properties and peculiarities of this colloid, it will be found useful to assume in advance a viewpoint that has developed from the

writer's investigations and then to test it with respect to the individual findings. As a preface, it will be well to call attention to certain difficulties or contradictions which have not yet been adequately accounted for by the previous assumptions. 1. Freundlich's proof that pentathionic acid is the charging complex takes cognizance of only one possibility with respect to the action of hot ammonia on the sol, namely, that the $H_2S_5O_6$ is thus converted into thiosulfuric acid which can be determined by means of standard iodine solution. It turns out that this is not the only conceivable possibility. 2. According to Freundlich, the hydrophilic character of the S sol is to be ascribed to the charging pentathionic acid. However, determinations (12, 13, 14) of the ratio of acid to sulfur gave values of 1–2:100, which is inadequate. The writer has found values within these same limits for the corresponding ratio of the ionogenic charging complex in the majority of highly purified hydrophobic sols (noble metals, sulfides, metal oxides). 3. All the procedures employed to determine the contra-ions, and from whose results the concentration of the charging polythionic acid was deduced, reveal only the contra-ions that are accessible to the particular reaction employed, *e.g.*, H^+ titration. Occluded portions, or those that are incorporated in the particles, are not reached in these procedures unless the sol particles are broken down beforehand. 4. Bassett and Durrant (15) found that in S sols, the decomposition of the polythionate by means of sodium hydroxide is apparently 24 times as fast as that of pure tetra- or pentathionate. They tried to account for this great divergence by assuming that the sulfur acted as catalyst, an hypothesis that has no factual basis.

The writer's own experience with a series of highly purified sols showed that certain acids, which normally are unstable, become stable when they are bound to colloids, and may form stable charging complexes. Examples are $H(AuCl_2)$, $H(AgCl_2)$, H_3AsS_3, H_3SbS_3. Consequently, there is considerable likelihood that the process of forming the S sols proceeds, in a certain sense, in two stages: 1. decomposition of thiosulfuric acid to produce sulfur; 2. binding of thiosulfuric acid to sulfur, with mutual stabilization. The bound portion of the thiosulfuric acid would thus be shielded from the decomposition, whereas the polythionic acids, formed as by-products, would be contained in the intermicellar fluid, where they would be free and molecularly dispersed.

II

Raffo S sols, prepared by a thoroughly tested, reliable procedure, were subjected to electrodialysis and electrodecantation. The electrode potential was gradually raised to 220 volts over a period of several days, with no visible damage to the sol. In fact, the most highly purified sols were the best with respect to color and transparency. Although the relative con-

ductivities of the segregated sol and the upper layer could be raised to above 99%, a portion of the molecularly dispersed acid, which decreased only gradually [2], remained in the sol. The S sol, after purification by this method, contained only H^+ as contra-ions and hence was strictly negative. Conductometric titrations, further developed for this purpose, were used to study the variation of the counter-ions and the prolonged reactions of various reagents. This proved to be an excellent method of analyzing S sols. This methodology was first used in the study of colloids in 1924 (16). It was subsequently developed into a satisfactory procedure for the investigation of counter-ion substitution in metal oxide sols (17), and provided a sufficiently accurate micro method (18) for analyzing purified sols of noble metals (19) and sulfides (20).

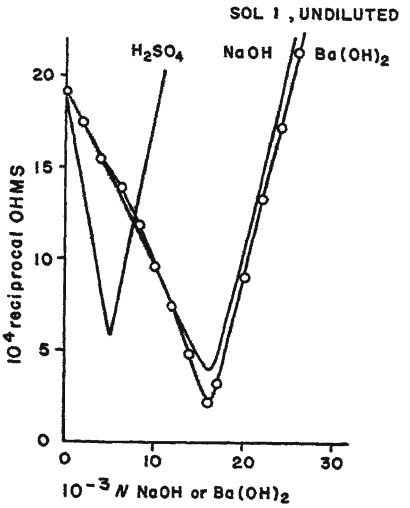

FIG. 1

Conductometric Titrations of Sol 1 and H_2SO_4

Several essential features will be apparent, when the conductometric titration curves of the S sol shown in Fig. 1 are compared even cursorily with the results usually obtained with negative sols. The curves show a minimum; the ascending and descending branches have no abrupt deflections, such as would indicate rather strongly divergent dissociation stages of polybasic charging acids, such as are found in sols of As_2S_3, Sb_2S_3, or Pt. Some additional points should be noted: 1. The titrated H^+ is proportional to the dilution. Only when the dilution is 100–150 times

[2] The possible prevention of this disturbing condition by improvement of electrodecantation is discussed on page 347.

the original volume of the sol does the hydrolysis of the latter become evident in the region of almost complete neutralization as a spreading and flattening of the curve, which can still be corrected graphically. (Titration curves for diluted sols are not shown here.) 2. A comparison with a solution of sulfuric acid that has the same conductance is instructive (see Fig. 1). At this dilution, the conductivity coefficient can be taken as $f_\lambda \sim 1$, and the titrated H^+ agrees closely with that calculated from L (the specific conductance). In contrast, the titrated H^+ in the comparable S sol is about three times as great as that computed from L, corresponding to $f_\lambda \sim 0.3$. This may mean two things: for a weak acid it may be essentially a degree of dissociation; for a strong acid it may be a true conductivity coefficient, expressing a considerable interionic action with appreciable Debye retarding forces. 3. The decision was reached here by comparing the acid and the salt with respect to their conductivities or the corresponding f_λ values. The figures derived for $f_{\lambda\,\text{acid}}$ and $f_{\lambda\,\text{salt}}$ showed a scattering of only a few *per cent* in both directions. Consequently, f_λ of the acid appears as a true deviation coefficient and its low value, despite the high dilution ($N \approx 10^{-4}$–10^{-3}) is the expression of a high charge density and field strength of the colloid ion. Accordingly, the charging complex of the S sol is a strong acid and occupies the particle surface in considerable density. 4. The titrations of the negative S sol with NaOH and $Ba(OH)_2$ agree with respect to the form of the curve and the minimum point (except for a stronger inactivation of the barium ions). Consequently, there are no additional groups present that react with barium hydroxide, or that build themselves up into complex acids, as is markedly the case in sulfide or platinum sols. This is also in line with the finding that treatment of these latter sols with salts of barium or lanthanum, for instance, causes the liberation of considerably greater quantities of H^+ than were originally determined in the sol with sodium hydroxide. In contrast, the S sol gives exactly the same amount of titratable H^+ after the addition of these salts as it did before. The expulsion of the H^+ from the field of the colloid ion is reflected in a sharp rise in the conductivity. The end of this process is indicated by a deflection in the L curve. Fig. 2 shows, on the one hand, the concordant behavior of barium, copper, and lanthanum with respect to the expulsion of H^+; [3] in contrast, the addition of silver nitrate presents an entirely different picture, since several times the original H^+ content is now shown to be present by increases in both L and titratable H^+. For instance, one hour after silver nitrate was added to the most highly purified sols, the titrated H^+ had risen to 4–6 times the original value (from 12.4×10^{-4} N to 75×10^{-4} N) (*cf.* Fig. 3). Longer action of $AgNO_3$ on the S sol results in progressive destruction of the sol, with

[3] The differences in the forms of the curves after reaching the minimum are connected with the formation of insoluble hydroxides in the excess alkali.

milky turbidity, brown coloring, and finally blackening. A similar behavior with respect to the liberation of acid and the destruction of the sol is shown by mercurous nitrate.

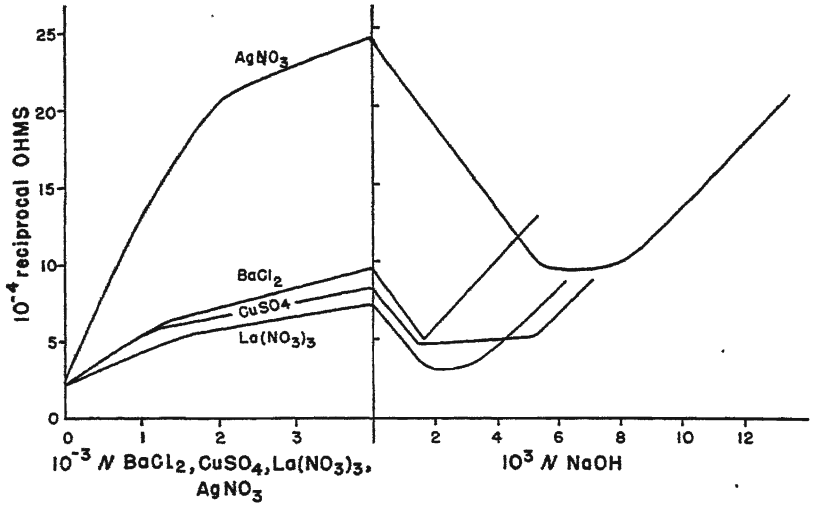

FIG. 2

Liberation of H^+ by Heavy Metal Salts

The relation between the consumption of silver and the formation of acid proved to be important to an understanding of the structure of the sol. For this purpose a combination of conductometric titrations was employed. Known quantities of silver nitrate were first added continuously until the rapid rise in conductance had ceased. The excess silver nitrate was back-titrated with KCl., and the difference between the total silver nitrate and the back-titration gave the silver consumption of the sol. The liberated H^+ was then determined with NaOH. The whole procedure, which is illustrated in Fig. 3, might be termed a "conductometric chain titration." In these solutions the liberated strong acids are

TABLE I

Sol	1	1 (10× dil.)	2	2 (10× dil.)	2A	3	3A*
Sulfur g./l.	19.0	1.9	8.3	0.83	2.0	3.25	0.39
$L\times10^4$	17.5	1.83	10.3	1.2	2.97	2.66	1.56
$C_H\times10^4$ (titrated)	160	16	76	7.6	14.8	12.4	4.6
f_λ	0.27	0.29	0.34	0.39	0.51	0.54	0.85

* Sol 3A was quite insufficiently purified by electrodecantation. It contained 0.39 g. S/l., and served only for purposes of comparison.

molecularly dispersed; the dilutions are so great that it may be assumed that $f_\lambda \sim 1$. A study of Table II shows that the H^+ values derived from the conductivities agree very satisfactorily with the values of H^+ actually determined by titration. Some data regarding the original sols used are given in Table I.

TABLE II[1]

Sol	Consumption of N $AgNO_3$	Excess of N $AgNO_3$	L'_{calc} [3] for excess $AgNO_3$	L_{obs} at maximum	ΔL $L-L'$	N H^+ calc.[4] from ΔL	N H^+ titr.
1[2]	23	17	2.0	23.9	21.9	55	55
2[2]	12	18	0.9	11.9	11.0	28	28
2A	31	19	2.3	27.2	25.0	63	64
3	35	15	1.8	29.8	28.0	70	75

[1] All values are to be multiplied by $10.^{-4}$

[2] Diluted 10 times.

[3] for $u + v = 120$.

[4] For $u + v = 400$.

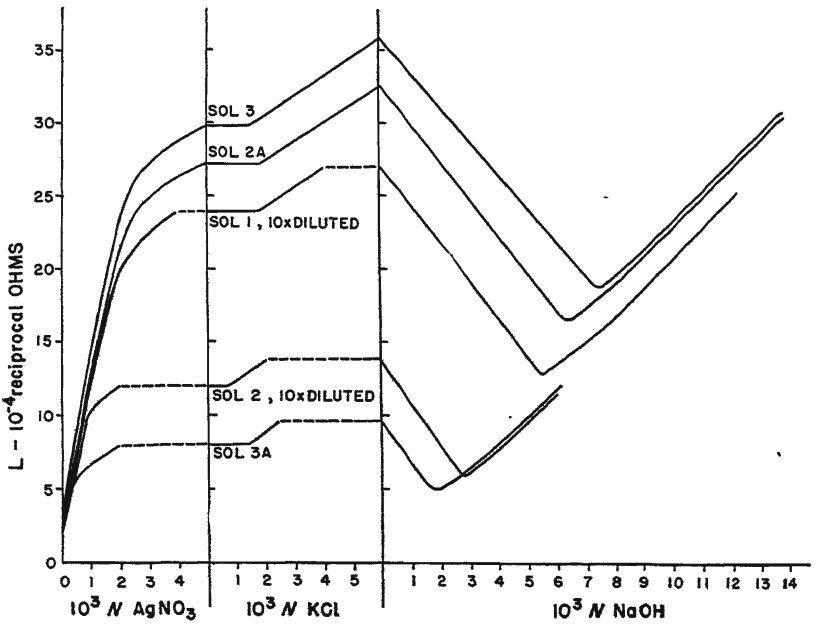

FIG. 3

Conductometric Chain Titrations

The following equations show that in the case of $H_2S_2O_3$ the relation of silver consumed to liberated H^+ is 1 Ag:2 H^+, whereas for $H_2S_XO_6$ [4] the

[4] H_2SxO_6 is a general formula for polythionic acids, in which X equals or is greater than 3.

relation is 1 Ag:3 H^+. When the titration is made immediately after adding the silver salt, it may be safely assumed that no attack on the sulfur by the silver occurs within this short period. In fact, tests showed that this assumption is justified (*vide infra*). The following relationships hold under these conditions.

$$H_2S_2O_3 + 2AgNO_3 + H_2O \rightarrow Ag_2S + 2HNO_3 + H_2SO_4 \quad (1)$$

$$H_2S_xO_6 + 2AgNO_3 + 2H_2O \rightarrow Ag_2S + 2HNO_3 + 2H_2SO_4 + S_{x-3} \quad (2)$$

Translated into equivalents, these become the general relations:

a $H_2S_2O_3$ consume a $AgNO_3$ and yield $2a$ H^+

b $H_2S_XO_6$ consume b $AgNO_3$ and yield $3b$ H^+

In mixtures a $H_2S_2O_3 + b$ $H_2S_xO_6$ consume $(a + b)$ $AgNO_3$ and yield $(2a + 3b)$ H^+.

The composition of a mixture consisting of a $H_2S_2O_3$ and b $H_2S_XO_6$ can be calculated from the silver consumed and the H^+ liberated. If N $Ag^+ = a + b$ and N $H^+ = 2a + 3b$, then $b = N$ $H^+ - 2N$ Ag^+ and $a = 3N$ $Ag^+ - N$ H^+. Table III gives the relation, determined in this fashion,

TABLE III

Sol (S g./l.)		
1 (1.9)	$a + b = 23$ N Ag^+ $2a + 3b = 55$ N H^+ $b = 9$ $a = 14$	14 N $H_2S_2O_3$ 9 N $H_2S_XO_6$
2 (0.83)	$a + b = 12$ N Ag^+ $2a + 3b = 28$ N H^+ $b = 4$ $a = 8$	8 N $H_2S_2O_3$ 4 N $H_2S_XO_6$
2A (2.0)	$a + b = 31$ N Ag^+ $2a + 3b = 64$ N H^+ $b = 2$ $a = 29$	29 N $H_2S_2O_3$ 2 N $H_2S_XO_6$
3 (3.2)	$a + b = 35$ N Ag^+ $2a + 3b = 75$ N H^+ $b = 5$ $a = 30$	30 N $H_2S_2O_3$ 5 N $H_2S_XO_6$
3A (0.39)	$a + b = 6$ N Ag^+ $2a + 3b = 17$ N H^+ $b = 5$ $a = 1$	1 N $H_2S_2O_3$ 5 N $H_2S_XO_6$

of thiosulfuric acid to polythionic acid in the sols, and in sol 3A, which had been but slightly purified. All values are to be multiplied by 10^{-4}.

The connection between the purification of the sols by electrodecantation and the ratio of thiosulfuric acid to polythionic acid in the sol is clearly shown in Table III. The lowest content of polythionic acid was found in sols 2A and 3, which had been the most thoroughly purified. In fact, the relation of Ag^+ consumed to H^+ formed averaged 1:2.2 for all the sols, which corresponds to a considerable preponderance of thiosul-

furic acid. The relations are reversed in the dilute, only slightly purified sol 3A. These findings harmonize best with the postulate that a free molecularly dispersed polythionic acid is a component of the intermicellar fluid, which is removed by electrical purification, whereas the thiosulfuric acid bound on the particles of the sol remains unaffected.

An independent proof of the existence of these relationships was secured by *freezing out the sol.* This coagulation of highly purified sols, which consist of practically nothing but colloid ion and counter-ion, involves an "auto-electrolyte coagulation" as a consequence of the extensive concentration of the sol and the overlapping of the fields of the counter-ions [5]. Table IV presents the data for L, the H^+ titrated in the original sol and in

TABLE IV*

	L	H^+ titr.	N Ag^+ consumed	N acid after silver	N $H_2S_2O_3$	N $H_2S_xO_6$		N $H_2S_xO_6$
Sol 2A (2 g. S/l.)	7.35	15.6	31.0	64.0	29.0	2.0	Sol 1 10× dil. 1.9 g. S/l.	8.0
Liquidus after freezing	5.5	10.8	6.0	22.0	—	6.0	*Liquidus*	9.0
Sol 3 (3.2 g. S/l.)	6.3	13.2	35.0	75.0	30.0	5.0	Sol 2 10× dil.	4.0
Liquidus	3.7	7.2	7.0	21.5	—	7.0	0.83 g. S/l *Liquidus*	4.0

* All values are to be multiplied by 10^{-4}.

the *liquidus* obtained by freezing, and also the silver consumed and the liberated H^+ in this liquid. These figures show that the addition of potassium salt to the sol causes the displacement of some H^+ from the sphere of the colloid ions, and this is reflected in a slight rise in the L of the sol. On freezing, most of the acid goes along with the sol particles into the coagulum; hence L and the titrated H^+ fall off sharply. In the *liquidus* the ratio of the silver consumed to the H^+ liberated is 1:3. This shows that this liquid contains only polythionic acids. The quantity of these acids agrees satisfactorily with the amounts originally found in the sol (Table III). The slight incidental admixture of nitric acid due to the addition of potassium nitrate, is easily measured by a separate determination. The acid removed from the solution along with sol particles when the sol is frozen out is thiosulfuric acid.

[5] Because of the slight sensitivity of the S sol towards H^+ ions, a small quantity of a salt had to be added to bring about complete, irreversible coagulation on freezing (0.002 N KNO_3 was sufficient).

III

A study of the course of the reaction of the S sol with silver nitrate over a period of time proved interesting. Prolonged action resulted in direct attack on the sulfur. In this event, the following reactions occur:

$$H_2S_2O_3 + 2AgNO_3 + H_2O \rightarrow Ag_2S + 2HNO_2 + H_2SO_4 \quad (1)$$

$$H_2S_XO_6 + 2AgNO_3 + 2H_2O \rightarrow Ag_2S + 2HNO_2 + 2H_2SO_4 + S_{X-3} \quad (2)$$

$$S + 2AgNO_3 + H_2O \rightarrow Ag_2S + 2HNO_3 + 0 \quad (3)$$

In terms of equivalents:

a $H_2S_2O_3$ consume a $AgNO_3$ and produce a H_2SO_4 and a HNO_3
b $H_2S_XO_6$ consume b $AgNO_3$ and produce $2b$ H_2SO_4 and b HNO_3
c S consume c $AgNO_3$ and produce c HNO_3

$a + b + c = N$ Ag^+ consumption $\qquad 2a + 3b + c = N$ H^+ production

Difference (N H^+ production $-$ N Ag^+ consumption) $= N$ H_2SO_4
$= 2b + a$

$c/2$ = atomic (pure) S portion

The results of the conductometric chain titration can be used for a calculation in the sense of these equations, if the following assumptions are accepted: 1. because of their reactions with silver nitrate the reaction between thiosulfuirc acid and polythionic acids does not occur, and hence there is no subsequent formation of the latter; 2. there is no attack on the sulfur during the brief period required to make the titration; 3. the anion bound to the sol particles is that of the thiosulfuric acid.

Experiments on the time course of the silver consumption and H^+ liberation in the case of sol 3 showed that the sol reaction with the silver salt is still going on after 1,500 hours. Figs. 4 and 5 present the calculated quantity, as *per* the foregoing equations, of thiosulfuric acid with progressive silver reaction, and also the increase with time of the attacked sulfur.

All the findings that have been cited in the foregoing are in harmony with the assumptions that underlay the preceding calculation. According to these postulates, the quantity of sulfuric acid produced by the prolonged action of silver should be $2a + b$. Consequently, a further check on the validity of these assumptions was obtained by actually determining the sulfuric acid formed. Table V contains the results for sols 1, 2, 2A, and 3, after an average exposure of 1390 hours to the action of silver nitrate. The agreement between the calculated and found values is excellent.

IV

The S sol was found to *consume iodine progressively* as the period of reaction was lengthened. After several hours a turbidity appeared, and

TABLE V

Sol	g. $BaSO_4$ found in 10 cc.	g. H_2SO_4 found in 10 cc.	g. H_2SO_4 calc. in 10 cc.
1 (10× dil.)	0.0090	0.0038	0.0037
2 (10× dil.)	0.0040	0.0017	0.0016
2A	0.0108	0.0045	0.0046
3	0.0112	0.0047	0.0046

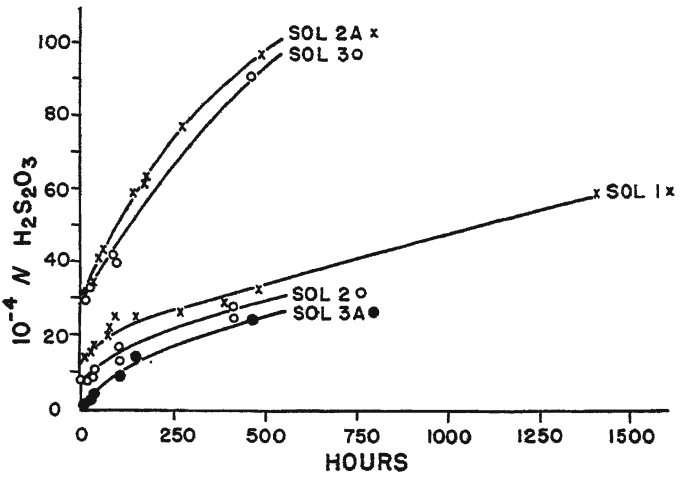

FIG. 4

Increase in Calculated $H_2S_2O_3$ with Time

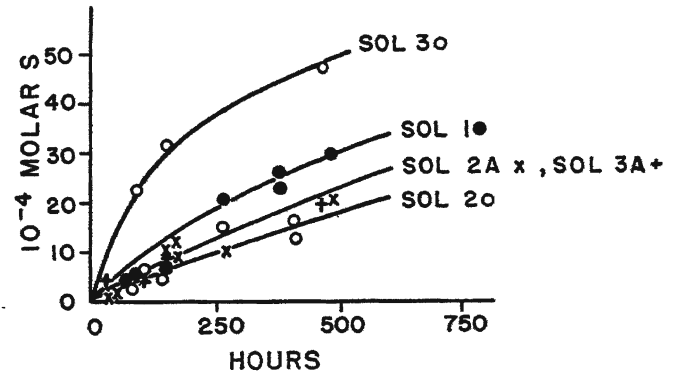

FIG. 5

Time Course of $AgNO_3$ Attack on Sulfur

eventually the sol settled out. This observation proved to be quite useful in the elucidation of the structure of the sol because it provided a direct method for determining the thiosulfuric acid in the sol without previous addition of alkali. The time course of the reactions was followed by titrimetrically measuring the iodine consumption and the liberation of H^+. The results are shown in Fig. 6, and it can be seen that the reaction is practically over after 250 hours.

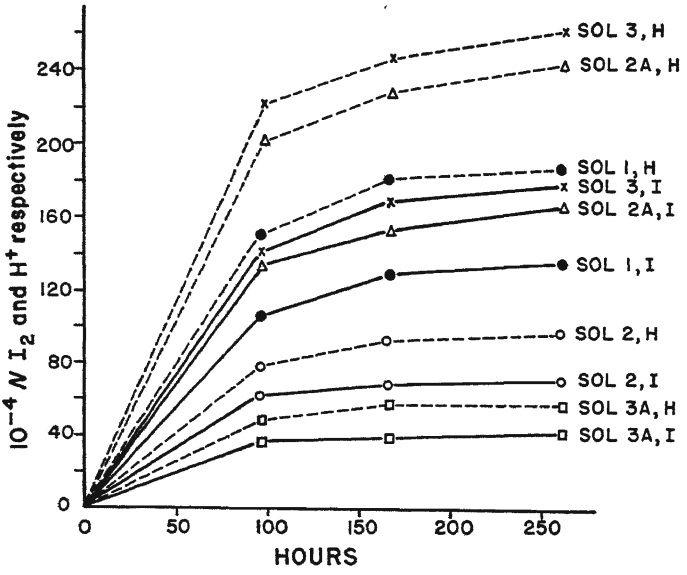

FIG. 6

Iodine Consumption and H^+ Liberation

For all the acids that may be involved here, the ratio of I consumed to H^+ liberated is 1I:2H^+. This relation conforms to the equations:

$$2H_2S_2O_3 + I_2 \rightarrow H_2S_4O_6 + 2HI$$
$$H_2SO_3 + I_2 + H_2O \rightarrow H_2SO_4 + 2HI$$

Actually, the iodine consumed was found to be more than the amount corresponding to half the acid equivalents formed. The only explanation of this excess consumption (about 25%) is the assumption that iodine combines with sulfur. This supposition is supported by other findings.

Warren and Burwell (21) found by X-ray studies that rhombic sulfur consists of 8-membered rings, whereas according to Meyer (22) plastic sulfur is made up of zig-zag chains. The latter are produced by rupture of the rings and recombination of the fragments into long chains, which are responsible for the high viscosity of the melt. Rotinjanz (23) found that

small amounts of iodine bring about a tremendous lowering of this viscosity. For example, as little as 0.02% iodine is enough to decrease it 90%. Meyer assumes that this effect is due to a breaking of the chains into small segments whose ends are occupied by iodine, Be that as it may, this would still give 40,000 S to 1 I_2 in his case. In our experiments, calculation shows that only very short sulfur chains are concerned, under any circumstances, in the addition of iodine. If, at the end of the reaction, the excess iodine, as calculated from the liberated H^+, is assigned to the elementary S, which equals the total sulfur minus that contained in the acids, the ratio of I:S turns out to be 1:8 for sols 2 and 2A, and 1:16 for sol 3. This result is quite remarkable in view of the possible connection between elemental 8-membered chains and 8-membered rings of the sulfur.

Particular interest attaches to the completeness of the prolonged action of iodine on the components of the sol. In contrast to the action of silver, which is complicated by the formation of interfering silver sulfide coatings, the iodine reaction leads to final limiting values for the reactive thiosulfuric acid in the sol. This culminates in an average ratio of 1 *M* $H_2S_2O_3$:4.2 S in the four purified sols. This relation corresponds to an extraordinarily abundant penetration of the sol particles by ionogenic complexes, whose total weight nearly equals that of the sulfur.

Foerster and Vogel (24) succeeded in preparing pure $H_2(S_2O_3 \cdot SO_2)$. The presence of this coordination addition compound is revealed in weakly acidified solutions of thiosulfuric acid by a yellow coloration. It may possibly be present as an impurity in the sulfur sols and be partly responsible for their yellow color. The results of long-continued *action of alkalies* on the S sol likewise agree admirably with those of the previous studies in which thiosulfuric acid was found to be the ionogenic component of the sol particles. Here again, useful information is gained by measuring the iodine consumption, the consumption of silver, and the corresponding production of acid. In these studies it is necessary to differentiate between the *pure neutralization* effect, and the action of the *excess alkali.*

The following relationships hold with respect to the neutralization:

$$2H_2S_2O_3 + 4NaOH \rightarrow 2Na_2S_2O_3 + 4H_2O$$
$$2Na_2S_2O_3 + I_2 \rightarrow Na_2S_4O_6 + 2NaI$$
$$Na_2S_2O_3 + 2AgNO_3 + H_2O \rightarrow Ag_2S + Na_2SO_4 + 2HNO_3$$

Accordingly, on neutralization: 1. half as many equivalents of iodine as of sodium hydroxide are consumed; 2. the number of equivalents of silver consumed and of acid produced are equal. The results obtained with sols 1 and 2, after dilution 1:10, are given in Table VI.

Distinct evidence of the effect of excess alkali appears when the excess amounts to about two-thirds of the amount necessary for neutralization.

Under these conditions the reaction

$$Na_2S_2O_3 + 2NaOH \rightarrow Na_2S + Na_2SO_4 + H_2O$$

occurs, and is revealed by the evolution of hydrogen sulfide when the liquid is acidified. On the addition of silver nitrate, the sulfide portion does not react to form acid, but produces $NaNO_3$ instead. Consequently, the acid liberated by the silver is not equivalent to the silver consumption, but is less by an amount corresponding to the sulfide. Excess alkali invaribly produced this result.

TABLE VI*

Sol	NaOH addition 100				
	Time of action	N OH^- consumed	Iodine consumed	N Ag^+ consumed	N Acid after Ag^+
	hr.				
1	19	64	31	68	67
2	20	32	15.2	40	42
	Without addition of alkali				
1	22		24	32	66
2	19		12	17	33

* All values are to be multiplied by 10^{-4}.

V

All of the findings obtained by these quite varied and independent methods indicate definitely that thiosulfuric acid is the ionogenic component of these S sols. The polythionic acid is a free, molecularly dispersed constituent of the intermicellar fluid and can be removed by electrodecantation, or as *liquidus* on freezing, or (according to Verstraete) as ultrafiltrate. If this viewpoint is accepted, all the former difficulties and contradictions disappear.

The tremendous difference in the speed of reaction of polythionate and S sol on treatment with alkali (Bassett and Durrant) finds a natural explanation in the fact that two entirely different processes occur. Only the thiosulfate which is already present in the sol is accessible for reaction, and not that which is formed later. The *ad hoc* hypothesis of a sulfur catalysis is entirely unnecessary.

The molar ratio 1 S_2O_3:approx. 4 S explains directly the hydrophilic properties of these S sols, and also gives an insight into their topographical structure. In most hydrophobic sols (noble metals, As_2S_3, metal oxides, *etc.*) the ratio of the charging complex to the neutral portion is 1:50 to 1:100. In such systems, there is a large particle nucleus with isolated or

film-like coherent ionogenic surface groups. In the S sols, the particle surface is not large enough to house the ionogenic component; most of the latter resides within the particle. Accordingly, the whole particle consists of a mosaic-like structure composed of the sol components. At the same time, the colloid ion has a high field strength, which manifests itself in small deviation coefficients even at high dilutions. Prolonged exposure to a silver salt, iodine, or alkali breaks down the sol and the interior of the particles becomes accessible to reaction. Accordingly, it becomes clear why the quantity of thiosulfate which is titratable with iodine is increased by treating the sol with hot ammonia water. However, this observation (Freundlich) is no proof that the thiosulfuric acid is formed from pentathionic acid.

In 1909 Svedberg (25) described a peculiarity of Raffo sols which has, as yet, no analog among inorganic colloids. The sols were precipitated by means of sodium salts. The resulting precipitates were then in an unusual temperature equilibrium with the supernatant sols. For instance, the sulfur content of the sol (in 0.2 *N* NaCl) rose from 0.16% to 29.4% over a temperature range 0.8°–25°C.; or (in 0.2 *N* Na_2SO_4) from 0.21% to 18.9% when the temperature was raised from 10.2° to 23.9°C. This behavior is also readily explained by the new concept of the composition of the S sols. In short, the sol behaves as though it were a complex salt with a high positive temperature coefficient of solubility.

The present findings give an interesting insight into the question as to the origin of the carbon disulfide-insoluble colloidal sulfur. Because of this insolubility, Freundlich regarded it as belonging to the $S\mu$ type. According to Warren (*loc. cit.*) the formation of $S\mu$ at 160°C. is due to the breaking down of the 8-membered rings of crystalline sulfur into zig-zag chains. This would be a thermomechanical effect. Since there is 1 mol of acid to about 4 mols of sulfur in the sol, about 8 atoms of sulfur would be the share of two molecules of thiosulfuric acid, which suggests the possibility that the ring closure is prevented by steric hindrance. In any event, the present sols probably contain short sulfur chains in distinction to the thread-like form described by Meyer. Furthermore, the ratio of 1 I:8 or 16 S atoms, which is finally attained in the prolonged action of iodine on the sol would be no accident; it is what might be expected from short molecular chains of S_8.

For the present, all our reported observations can be taken merely as valuable suggestions or starting points for future studies. Supplementary investigations on a highly purified sulfur sol doubtless will shed interesting light on the subject. New possibilities and ways of attack will be provided by 1. improvement of electrodecantation through the use of positive anodic membranes (or membranes which can be made positive by H^+); 2. an extension of the investigation to Selmi sols; 3. an analysis

of the strong oxidizing action of light on S sols, which would be analagous to the photochemical sensitivity of other sulfide sols, which have been more closely studied by the writer and his associates.

By virtue of its many physicochemical peculiarities, which correspond in every respect to its constitutive properties, the sulfur sol appears now to provide convincing testimony in favor of regarding colloids and their reactions from a strictly electrochemical-constitutive point of view. The laying of the firm foundations of this concept was made possible only through the valuable aid through the years of a series of competent collaborators.

References

1. Pauli, W., Russer, E., and Balog, P., *Helv. Chim. Acta* **27**, 585 (1944).
2. Wackenroder, H. W., *Arch. Pharm.* **48**, 40 (1846); *Ann. chim. pharm.* **60**, 189 (1846).
3. Sobrero, A., and Selmi, F., *Ann. chim. phys.* [3] **28**, 210 (1850).
4. Raffo, M., *Kolloid-Z.* **2**, 358 (1908).
5. Foerster, F., and Vogel, R., *Z. anorg. allgem. Chem.* **155**, 161 (1926); Foerster, F., *Ber.* **57**, 258 (1924).
6. Stamm, H. and, Wintzer, M., *Ber.* **71**, 2212 (1938); Stamm, H., and Goehring, M. *Z. anorg. allgem. Chem.* **242**, 413 (1939); **247**, 277 (1941).
7. Riesenfeld, E. H., and Gruenthal, E., *Medd. K. Vetenskapsakad. Nobelinst.* **6**, No. 9, 1; *Chem. Ztg.* **1924II**, 288.
8. Foerster, F., *Z. anorg. allgem. Chem.* **177**, 66 (1929).
9. Oden, S., Der kolloide Schwefel, *Nova Acta Upsala* (IV) **3**, No. 4 (1913).
10. Pauli, W., *Trans. Faraday Soc.* **16**, 14 (1920); *Kolloid-Z.* **28**, 49 (1921).
11. Freundlich, H., and Scholz, P., *Kolloidchem. Beihefte* **16**, 234 (1922).
12. Bassett, H., and Durrant, R. G., *J. Chem. Soc.* **134**, 2919 (1931).
13. Verstraete, E. O., *Kolloid-Z.* **102**, 251 (1943); **103**, 25 (1943).
14. Freundlich, H., and Scholz, P., *loc. cit.*
15. Bassett, H., and Durrant, R. G., *loc. cit.*
16. Pauli, W., and Semler, A., *Kolloid-Z.* **34**, 146 (1924).
17. Pauli, W., and Valko, E., *Z. physik. Chem.* **121**, 161 (1926); Pauli, W., and Schmidt, E., *ibid.* **129**, 199 (1927); Pauli, W., and Peters, A., *ibid.* **135**, 1 (1928).
18. Pauli, W., and Schild, T., *Kolloid-Z.* **72**, 165 (1935).
19. Pauli, W., and Baczewski, A., *Monatsh.* **69**, 204 (1936).
20. Pauli, W., and Laub, A., *Kolloid-Z.* **78**, 295 (1937); **80**, 175 (1937).
21. Warren, B. E., and Burwell, J. D., *J. Chem. Phys.* **3**, 6 (1935).
22. Meyer, K. H., and Go, Y., *Helv. Chim. Acta* **17**, 1081 (1934); Meyer, K. H., in Meyer, K. H., and Mark, H., Hochpolymere Chemie, 2nd ed. **2**, 59 (1944).
23. Rotinjanz, L., *Z. physik. Chem.* **62**, 609 (1908).
24. Foerster, F., and Vogel, R., *Z. anorg. allgem. Chem.* **155**, 161 (1926); Foerster, F., *Ber.* **57**, 258 (1924).
25. Svedberg, T., *Kolloid-Z.* **4**, 49 (1909).

MONODISPERSED SULFUR SOLS.[1] IV. COMPARISON OF THE PARTICLE RADIUS DETERMINED BY TRANSMITTANCE AND BY THE ANGULAR POSITIONS OF HIGHER ORDER TYNDALL SPECTRA FROM THE MIE THEORY

Marion D. Barnes, A. S. Kenyon, E. M. Zaiser, and V. K. LaMer

From the Department of Chemistry, Columbia University, New York

Received February 10, 1947

Introduction

In Ref. II of this series it was shown that both the particle number and the particle radius of monodispersed sulfur sols could be determined by comparing the experimental curve for the transmittance of the sol as a function of the wave length of the scattered light with a theoretical curve based upon the scattering area coefficient K_s computed from the Mie Theory (for the definition of K_s see the Note under Ref. II in this issue).

In the third paper of the series, the particle radius was determined by measuring the angular position of the "red orders" of the higher order Tyndall spectra which these monodispersed sols exhibit. The radii so determined were checked in part by theoretical calculations of the order position based upon the Mie theory and by direct measurement of the rate of sedimentation in those ranges of particle size in which sedimentation proceeds.

The transmittance measurements in Ref. II were made with a Coleman spectrophotometer and consequently were restricted to the visible spectrum. Meanwhile, a Beckman quartz spectrophotometer became available. This superior instrument permits extension of the transmittance measurements into the ultraviolet. Accordingly, it becomes possible to

[1] To facilitate references to the literature, the papers of this series on monodispersed sulfur sols will be designated as follows:

I. Preparation—LaMer and Barnes—*J. Coll. Sci.* **1**, 71 (1946).
II. Transmittance in visible—Barnes and LaMer—*J. Coll. Sci.* **1**, 79 (1946). See also Note on symbols and definitions involved in light scattering equations—*J. Coll. Sci.* **2**, 361 (1947).
III. Higher order Tyndall spectra in visible—Johnson and LaMer—*J. Am. Chem. Soc.* **69**, 1184 (1947), also **67**, 2055 (1945).
IV. Transmittance in visible and ultraviolet—present paper by Barnes, Kenyon, Zaiser, and LaMer.
V. Kinetics of formation—LaMer and Kenyon—*J. Coll. Sci.* **2**, 257 (1947).
VI. Higher order Tyndall spectra in ultraviolet and effect of consumptive absorption —Kenyon and LaMer (forthcoming).

check the Mie theory more adequately and to investigate more carefully whether or not the curious "wiggles" near the first maximum in the computed K_s curve (see Fig. 1, Ref. II) really exist. Furthermore, in the previous work, the concentrations of reactants used in II were not exactly the same as in III, and it was accordingly desirable to repeat the measurements using both methods simultaneously upon aliquots of the same sol.

Experimental

Monodispersed sulfur sols were prepared according to the method of LaMer and Barnes (I) by mixing 9 cc. of 1.0 *M* $Na_2S_2O_3$ with 9982 cc. of distilled water, and adding to this 9 cc. of 1.5 *M* H_2SO_4, which brought the final concentration to 0.0010 *M* $Na_2S_2O_3$ and 0.0015 *M* H_2SO_4. Although all experiments on the formation of these sols have not shown thus far any perceptible dependence upon the presence of foreign nuclei, nevertheless, a large volume of a given sol was prepared at one time to insure the presence of the same number of nuclei in all aliquots. At these concentrations colloidal sulfur appears approximately 60 minutes after mixing. At various intervals from 2 to 14 hours after mixing, the growth of particles in aliquot portions was stopped and the sol stabilized by partial removal (60–70%) of the thiosulfate with iodine. Stoichiometric removal of the thiosulfate causes a reversal of the reaction with consequent instability and solution of the sulfur particles during their measurement.

Transmittance measurements were made with a Beckman quartz spectrophotometer, Model DU, over a range of wave lengths λ(air) = 285 to 1000 mμ with λ'(water) = 215 to 750 mμ with an accuracy of $\pm$ 0.1%. To cover this range with a minimum of experimental error it was necessary to use two different pairs of absorption cells, namely, quartz cells of 10 $\pm$ .001 cm. length were used from λ = 285 to 320 mμ and 19.86 $\pm$ .01 cm. pyrex cells from λ = 320 to 1000 mμ. The cell housing assembly on the spectrophotometer was modified so that it would accommodate interchangeably either pair of absorption cells. All transmittance measurements were corrected for the difference in the lengths of the tubes and other apparatus variables. In some of the initial experiments (not reported here) the Beckman spectrophotometer was used for ultraviolet wave lengths only, the visible region being studied with the Coleman apparatus described previously (II). When the transmittance curves obtained with the two instruments were superimposed the overlapping portions did not coincide exactly. We believe this discrepancy results largely from the distribution of intensity in the different sources of the light employed in each instrument. The Coleman double grating spectrophotometer, which was used as a monochromator, has a fixed slit width of 7.5 mμ, while the Beckman permitted the use of slits as narrow as 1 mμ. The availability of the Beckman instrument increased not only the rapidity and accuracy

of the measurements, but also the resolution of fine structure in the curves. The reference solvent for the transmittance measurements was 0.0010 M $Na_2S_2O_3$ to which was added the same amount of iodine used to stop the growth of the sol.

The angles of the red orders of the Tyndall spectra were measured by the method of Johnson and LaMer (III) on an aliquot of the sol used for the transmittance measurements. The intensity of the vertical component of the scattered light J_2 was measured at 5° intervals from 25° to 170° using Wratten filters, numbers *29* and *58*, having transmittance maxima at $\lambda_{red} = 676$ mμ and $\lambda_{green} = 560$ mμ, respectively.

Results

In their report on angular scattering as a method for the determination of the size of monodispersed sulfur particles, Johnson and LaMer state that a relative index of refraction $m = 1.44$ gave better agreement between the Mie theory and experiment than for $m = 1.55$. No tabulated values for dependence of intensity upon angle are available for refractive indices intermediate between these values. The theoretical computations available at present for angular dependence do not go beyond $\alpha = 2\pi r/\lambda' = 6$ so that an independent method, applying the rate of sedimentation based upon Stokes' law, was used to check the experimental values corresponding to $\alpha > 6$. The angular positions of the orders for radii beyond the theoretical values were thus calibrated by the rate of sedimentation. Our experience confirms Johnson and LaMer's conclusion that the determination of the angles of maximum red scattering is an accurate method for the determination of particle size to within $\pm$ 0.005 μ for the range checked, namely $r = 0.2$ to 0.5 μ.

The ratio of the intensities $J_{\lambda 676}/J_{\lambda 560}$ passed by these filters was calculated for all measured angles and plotted in Figs. 1 and 2. The radius in microns was read directly from the theoretical plot of order angle *vs.* radius (see Fig. 4 of Johnson and LaMer (III).

In Fig. 3, $\log(I_0/I)$ is plotted against λ' (wave length in medium), using a plotting increment to separate the curves. These curves were obtained from transmittance data on aliquot samples from a typical run. It is clear that, as the monodispersed particles steadily grow in size, the characteristic points of the transmittance curve are shifted toward longer wave lengths. The principal minimum in transmittance for sols with radii less than 0.3 μ would occur in the ultraviolet ($\lambda < 400$) where molecular absorption by the sulfur becomes appreciable. The influence of molecular absorption upon scattering intensity and transmittance is under investigation and will be reported in Ref. VI.

The presence of a fine structure in the transmittance curves reported by Barnes and LaMer has also been confirmed. The theoretical computa-

tions do not show as much fine structure as the experimental curves, probably because the former are not sufficiently detailed. The detailed structure in the experimental curves is to be interpreted as an extension rather than a contradiction of existing theory. It is also possible that the sulfur droplets are not strictly isotropic.

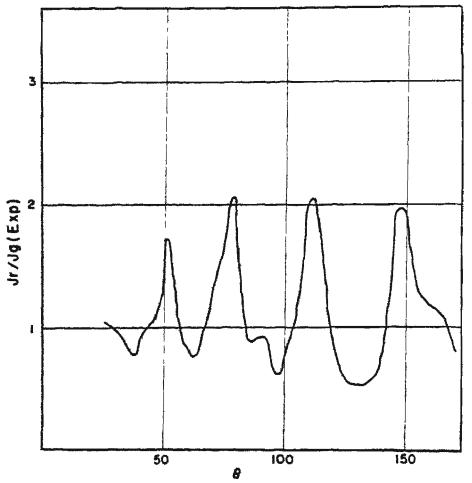

FIG. 1
Angular Scattering 4 orders $r = .35\mu$

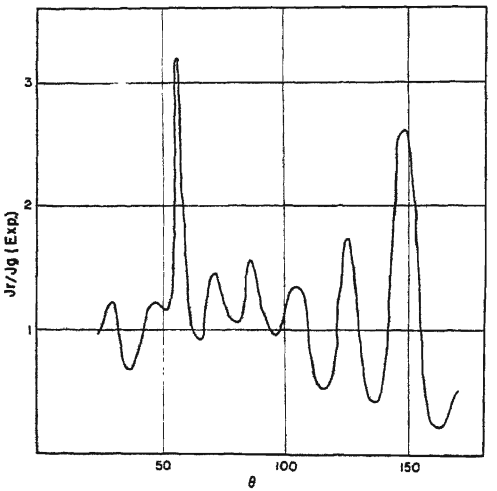

FIG. 2
Angular Scattering 7 orders $r = .45\mu$

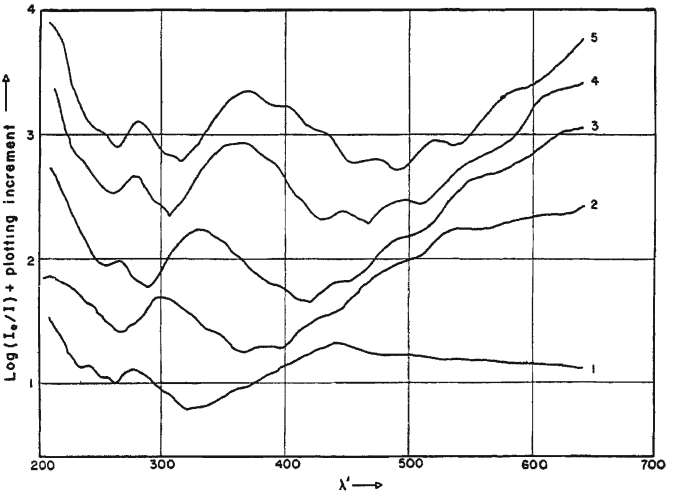

FIG. 3

Optical Density of Monodispersed Sulfur Sols as a Function of Wave Length

Sol. No.	*P. I.*
1	0
2	.02
3	.05
4	.10
5	.14

TABLE I

Determination of α_{minimum}

Sol. No.	Time after mixing in minutes	Angular positions of orders $\theta_1, \theta_2, \theta_3$, *etc.*	Radius (μ) from angular scattering	$\lambda'_{\text{minimum}}$ from transmittance	α_{min}	$10^6 n/cc.$
1	208	45, 82, 120, 151	.352	.321	6.90	1.2
2	328	37, 57, 76, 106, 132, 160	.413	.365		
3	510	36, 50, 70, 92, 115, 140, 165	.448	.418	6.75	1.0
4	722	30, 47, 56, 72, 87, 103, 126, 147	.492	.467	6.65	0.9
5	840	28, 43, 55, 77, 96, 110, 131, 150	.514	.489	6.65	0.8
6	208	47, 76, 110, 152	.345	.311	6.95	
7	849	32, 46, 60, 78, 100, 119, 146	.485	.473	6.48	
8	180	51, 81, 110, 146	.323	.307	6.65	
9	180	51, 78, 112, 147	.323	.310	6.55	

It is evident from the definition of α that the Mie theory for scattering by spherical transparent isotropic particles predicts that the principal minimum in the $\log(I_0/I)$ *vs.* λ' curve will always correspond to the same α value for a given system, that is, the $\lambda'_{\text{minimum}}$ is linearly proportional to the chosen radius, if the dependence of K_s upon λ has been correctly computed.

In Table I the radius determined from the angular scattering data and the corresponding α value computed from the wave length yielding a minimum in the transmittance data, are tabulated for 9 monodispersed sols. The values prove to be constant, with an average $\alpha = 6.8$. This constancy of the α value is a proof that angular scattering (based on the Mie theory and confirmed by sedimentation) and the characteristics of transmittance (based on theory alone) furnish equally reliable methods for the determination of particle radius.

Table II gives the scattering coefficient $K(m, \alpha)$ as a function of α for $m = 1.50$ as computed by Dr. Arnold Lowan (1) and his staff and verified

TABLE II

Scattering Coefficient $K_s(m, \alpha)$ as a Function of α for $m = 1.50$

α	Lowan	Langmuir
0.5	0.01456	
0.6	0.03018	
1.0	0.2150	0.2163
1.2	0.3949	
1.5	0.7528	0.7527
1.8	1.348	
2.0	1.798	1.7984
2.4	2.338	
2.5	2.539	2.540
3.0	3.418	3.4181
3.2	3.531	3.535
3.4	3.878	3.873
3.6	4.184	4.181
3.8	4.126	4.127
4.0	4.052	4.052
4.5	4.202	4.2025
4.8	3.819	
5.0	3.927	3.933
6.0	2.903	2.903
7.0	1.848	
7.2	1.771	
8.0	1.777	1.7781
8.4	2.012	
9.0	2.238	
9.6	2.798	
10.0	2.882	2.829
10.8	2.981	
12.0	2.476	

in part by Dr. Irving Langmuir (2). The calculated values are plotted as circles in Fig. 4. To compare the experimental curves with the theoretical, it was necessary to reduce the transmittance curves to functions of the scattering coefficient K_s and α. The particle radii were then recalculated, using the average α_{minimum} and the $\lambda'_{\text{minimum}}$ values. With the aid of these radii, values were computed for the abscissa values corresponding to every measured point on the $\log(I_0/I)$ *vs.* λ' curves.

Since $\log(I_0/I) = K_s(\pi r^2 nl/2.3)$, division by r^2 yields a quantity, proportional to the number of particles, which depends only upon the scattering coefficient K_s, for a given length l provided n remained constant during growth in the different sols. A plot of $\log[\log(I_0/I)/r^2]$ against $\log\alpha$

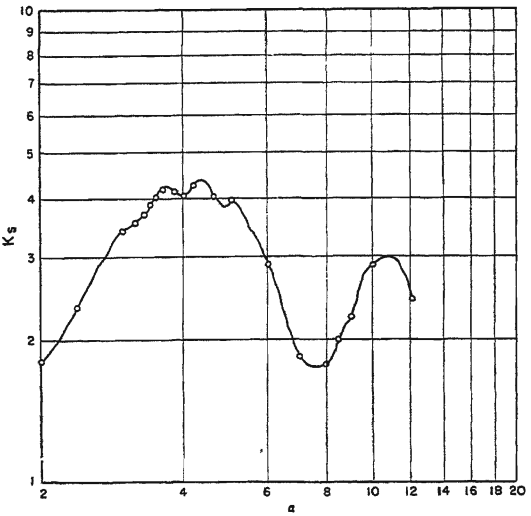

FIG. 4

Theoretical Scattering Coefficient as a Function of α. $m = 1.50$

should accordingly be of the same form as a plot of the theoretical $\log K_s$ against $\log\alpha$. When the experimental curves were superimposed upon the theoretical plot, it was found that they were indeed almost identical in shape (see Fig. 5), except that they were displaced in the direction of the ordinate by amounts equal to $\log(\pi nl/2.3)$. This displacement is attributable to small decreases in the particle number n, arising possibly from coagulation as the sol grew.

It is noteworthy that the characteristics of both curves are nearly identical for α values up to 6. For $\alpha > 6$ there is a lack of agreement. The experimental points are as accurately determined for α values larger than 6 as for smaller ones. The deviation of the experimental curve is not due to molecular absorption, since the transmittance measurements on which

it is based were made only at wave lengths where no absorption occurs. It is proposed, therefore, to extend the theoretical curve beyond $\alpha = 6$ by using experimental rather than computed points. It is believed that a curve so obtained provides a more reliable basis for the calculation of

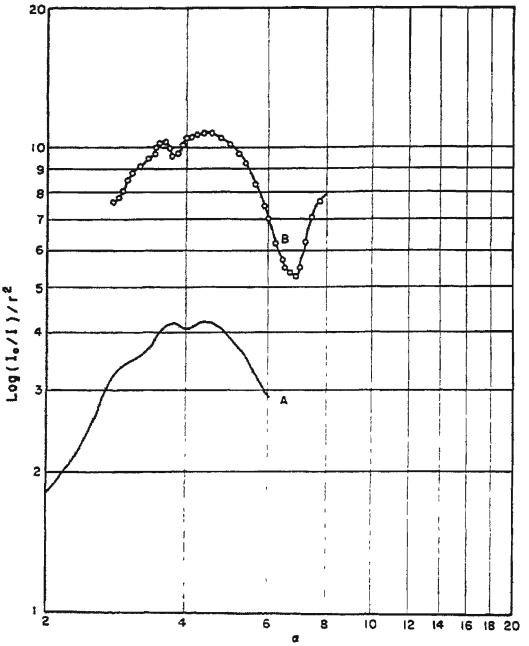

FIG. 5

Scattering Coefficients as a Function of α
Curve A = Theoretical; Curve B = Experimental

particle radius in the particular systems under study. Fig. 6 shows the result of extending the theoretical curve with experimental points.

The deviation of the experimental from the theoretical curve for $\log K_s$ *vs.* $\log\alpha$ above $\alpha = 6$ could occur because the index of refraction $m = 1.50$ does not fit this system exactly. It may well be that the sensitivity of the scattering coefficient to different indices becomes appreciable only at large α values. The refractive index of molten sulfur has been reported as 1.927 at a wave length of 568 mμ (3). This corresponds to a relative index of 1.44. The n_D^{20} for sulfur in an Oden sulfur sol has been reported to be from 1.951 to 2.157 (4), corresponding to $m = 1.47$ to 1.52. A reinvestigation of the dispersion of refractive index is under investigation and will be reported in Reference VI.

Using the curve in Fig. 6 as the "theoretical" curve for $m = 1.5$, the particle numbers were determined on aliquot portions of a single growing

sol over a period of several hours. The last column in Table I shows the number of particles/cc. for 5 samples. The small decrease in number with time cannot be entirely attributed to settling. Other causes will be investigated.

In the previous papers (I, II, III), angular scattering and transmittance measurements were made on sulfur sols of different initial concentrations of reactants, and no exact comparisons could be made between the results. This explains why the difference between the experimental and theoretical $\log K_s$ *vs.* $\log\alpha$ curves above $\alpha = 6$ went unnoticed. Some results of the use of the experimentally adjusted "theoretical" curve (Fig. 6) are shown in Table III. These measurements were made on 10

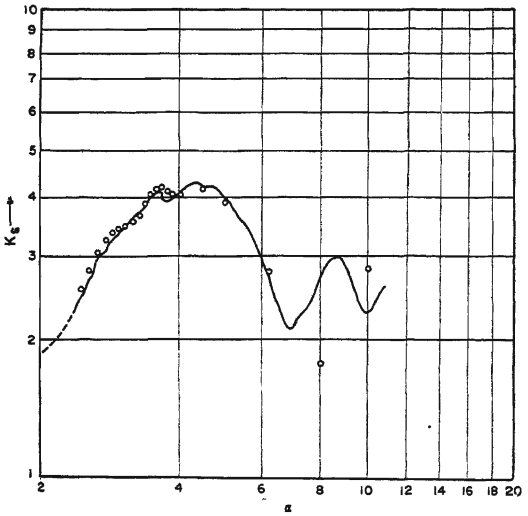

FIG. 6

Scattering Coefficient as a Function of α
Experimental reduced to theoretical by eliminating parameters r and n
o = Theoretical; — = Experimental

separate sols on different days. The excellent agreement of the radii calculated from transmittance and angular scattering data is an indication that the α_{minimum} value that was experimentally determined is accurate for this system.

LIMITS OF ERRORS

In r from angular scattering:

The error arises not in the measurements of angles, which are accurate to $\pm$ 1°, but in the interpretation of the theoretical order position *vs.* radius curves. This error is not more than $\pm$ 0.005 μ in r, but the method

TABLE III

Comparison of Radius in Microns (μ) Determined from Angular Scattering and Transmission Data

Sol. No.	Time after mixing in minutes	Angular positions of orders	Angular scattering	$\lambda'_{min.}$	Transmittance
10	208	50, 81, 105, 141	.31	.298	.33
14		47, 70, 110, 146	.33	.306	.33
19		50, 77, 110, 146	.33	.313	.34
11	322	51, 71, 119, 149, 176	.33	.337	.35
15		43, 73, 97, 121, 155	.38	.358	.39
12	502	41, 56, 81, 100, 130, 159	.39	.359	.39
16		36, 55, 80, 105, 131, 161	.43	.374	.41
13	622	39, 55, 71, 106, 125, 159, 172	.41	.380	.41
17	788	31, 46, 64, 91, 113, 141, 167	.47	.428	.46
18	904	31, 47, 62, 81, 96, 120, 145, 168	.49	.450	.49

requires monodispersed sols, whereas an average radius can be more readily calculated for a polydispersed sol using transmittance.

In r for transmittance:

The transmittance can be measured to 0.1%, and the wavelength to $\pm$ 3 mμ which corresponds to an error of $\pm$ 1% in r. Since the calculation of r is based on an average value of α_{minimum} which contains all the errors of angular scattering, the error in r from transmittance is about $\pm$ 0.01 μ.

In n from transmittance:

The 0.1% error in transmittance measurements is negligible compared to an error of uncertain size which arises because the K_s at the minimum in the "theoretical" curve (Fig. 6) is not accurately located. Certainly the order of magnitude ($n = 10^6$/cc.) is correct, and reliable relative values of n, n_0 can be obtained. Even granting the error that may be present, this method allows a better estimate of relative particle number than any other known method. The establishment of the α_{minimum} enables transmittance measurements to be made very quickly since it is only necessary to measure a few points on either side of the minimum. The angular scattering method is somewhat tedious. Transmittance measurements can be completed in approximately one-third the time required by angular scattering.

Conclusions

1. The transmittance of monodisperse sulfur sols has been investigated with a Beckman quartz spectrophotometer over the range of wavelength

λ = 285–1000 for particle radii of the range 0.3–0.5 μ. The position of the minimum in the curve for the scattering coefficient K_s as a function of the particle radius has been located experimentally for these monodispersed sulfur sols. This permits more reliable calculations of particle number and radius from transmittance data than previously.

2. The Mie theory for the dependence of K_s on $\alpha = 2\pi r/\lambda'$ has been verified experimentally in a region where very few theoretical calculations of K_s are available, that is, for $\alpha \leq 6$.

3. Close agreement ($\pm$ 0.01 μ) is obtained when the radii calculated from angular scattering data are compared with those from transmittance data when the experimentally determined K_s *vs.* α curve for this system (Fig. 6) is used.

4. The presence of a fine structure in the transmittance curves of monodispersed sulfur sols over and above that predicted by the presently available computations based on the Mie theory and noted previously by Barnes and LaMer has been confirmed.

References

1. Lowan, Arnold, Div. 10 O. S. R. D. Report 1857 by LaMer and Sinclair.
2. Langmuir, Irving, private communication.
3. Mellor, J. W., A Comprehensive Treatise on Inorganic and Theoretical Chemistry, Vol. X, 70. Longmans, Green & Co., London (1930).
4. Lifschitz, V., and Brandt, Jens, *Kolloid-Z.* **22**, 133 (1918).

A NOTE ON THE SYMBOLS AND DEFINITIONS INVOLVED IN LIGHT SCATTERING EQUATIONS

Victor K. LaMer, and Marion D. Barnes

From the Department of Chemistry, Columbia University, New York

Received April 11, 1946

Symbols and units used in the description of the intensity of light scattered by systems of small particles which scatter or scatter and absorb light are varied and confusing (1, 2, 3, 4). This difficulty in notation could be eliminated by the consistent use of a standard set of symbols and a clear definition of the coefficients used. It is the purpose of this note to recommend a convenient set of symbols and to bring one of our previous publications (5) into harmony with this proposed usage.

Mie (6) derived the following expression for the total scattered light for a beam of unit incident intensity striking a small particle.

$$S = \frac{\lambda'^2}{2\pi} \sum_{n=1}^{\infty} \frac{|A_n|^2 + |P_n|^2}{2n+1}, \tag{1}$$

where S is a function of m' (relative refractive index), and $\alpha = \frac{2\pi r}{\lambda'}$. S has the units of area and represents the watts scattered/watt/cm.^{2} of incident radiation. λ' = wave length of light in the medium in which the particle is suspended, r = radius of particle and A_n and P_n are complex functions of α and m'. If the particles absorb as well as scatter, the functions A_n, P_n involve the complex index of refraction of the particle, *i.e.*, $m'(1 - ik)$, where k is the absorption index, and Eq. 1 again gives the total scattering. The total scattering plus absorption is given by:

$$S = \frac{\lambda^2}{2\pi} Im\Big[\sum_{n=1}^{\infty} (-1)^n (A_n - P_n)\Big]. \tag{2}$$

For a clear, unambiguous description of scattering, we recommend the use of the definition of the scattering coefficient proposed by LaMer and Sinclair (4), with a modification as to name in order to avoid confusion with the usual definition of the scattering and absorption coefficients. The total scattering coefficient (5) is the energy scattered/second/unit cross sectional area of the particle for unit intensity of illumination. In terms of S, the total scattering coefficient is $\frac{S}{\pi r^2}$.

To describe the total scattering of a single transparent particle we propose the symbol K_s, called the scattering area coefficient, which is a

dimensionless number. For particles which absorb as well as scatter we propose the symbol K_e, called the extinction area coefficient, which is likewise dimensionless and describes the total dissipation of incident illumination (*i.e.*, scattering and absorption). It is assumed in the above definition that the radius of the particles is not exceptionally large compared to the wave length of light employed.

These coefficients are related to the incident and transmitted light intensities as follows:

$$\text{For transparent particles: } \log(I_o/I) = K_s\pi r^2 nl$$
$$\text{For colored particles: } \log(I_o/I) = K_e\pi r^2 nl$$

in both of which n = number of particles/cc., l = length of solution traversed in centimeters, and I_o/I is the ratio of incident to transmitted light.

The scattering coefficients of Stratton, Mie, and others may be expressed in terms of the coefficients proposed above. The scattering coefficient employed by Stratton (7) is defined as $K = \frac{S}{2\pi r^2}$ and applied to particles whose radius is not exceptionally large compared to the wave length of light employed. Under these conditions Stratton's K is equal to $K_s/2$.

The scattering coefficient of Mie may be expressed in terms of S as K (or K') $= S/V$, where V is the volume of the particle. Therefore, in Eq. 2, page 80, of Ref. 5, K is equal to $\frac{3}{4}\frac{K_e}{r}$, and, in Eq. 3, K' is equal to $\frac{3}{4}\frac{K_s}{r}$ (r being expressed in millimeters). K' becomes F_1 in Eq. 4, which is the Rayleigh equation divided by V.

In the article previously published in this Journal (8) we have referred to the equations of Mie, Stratton, and others. In view of the fact that no consistent set of symbols and units was available, we employed the same notation used in the original articles. It is now possible to bring our previous publication into harmony with the notation being proposed.

In the curve in Fig. 1, based upon Lowan's scattering functions, K corresponds to K_s. Values of K from this curve were used in the calculation of n (number of particles/cc.) on the assumption that the scattering coefficient calculated by Lowan was that defined by Stratton. However, since Lowan actually calculated values of K_s (9), the equation on page 89 should read $\log(I_o/I) = \frac{K_s\pi r^2 nl}{2.3}$ and a recalculation of values employing this equation shows that the n values (Tables II, column 3) should be: $n \times 10^{-6} = 1.6, 1.7, 1.6, 1.0$. Other values in the table are unchanged.

The authors wish to thank Dr. David Sinclair for his assistance.

The following corrections to Ref. 5 should be entered:

p. 80 (line 19) Read κ = absorption index.
(9 lines from bottom) K = extinction coefficient/unit volume of particle.
K' = scattering coefficient/unit volume of particle.
p. 81 (top) m_0 = real refractive index of medium.
p. 81 (Eq. 4) See above. This is the Rayleigh equation divided by V.
p. 81 (5 lines from bottom) $K = K_s/2$.
p. 82 (Fig. 1) ordinate is K_s and abscissa $\alpha = 2\pi r/\lambda$.
p. 89 Replace $2K$ by K_s in first equation and in logarithmic equation replace K by K_s and delete factor of two in last term. Also conventional *scattering* coefficient for *extinction*.

References

1. Mie, Gustav, *Ann. Physik* [4] **25**, 377 (1908).
2. Gribnau, Franciscus, *Kolloid-Z.* **77**, 289 (1936); **82**, 15 (1938).
3. Stratton, J. H., and Houghton, H. G., *Phys. Rev.* **38**, 159 (1931).
4. LaMer and Sinclair, O.S.R.D. Report 1857 (Sept. 29, 1943), Verification of the Mie Theory. References to O.S.R.D. reports dealing with the ambiguity of a factor of 2 in the definition of K. A fuller account is being presented by D. Sinclair to the *J. Optical Soc. Am.*
5. Barnes, M. D., and LaMer, V. K., *J. Colloid Sci.* 1, 79 (1946).
6. Mie, G. (Ref. 1, p. 436).
7. Ref. 3, p. 162, eq. 4.
8. Ref. 5, p. 80–81.
9. Lowan, A., unpublished communication.

Since this was written, H. C. Van de Hulsts' Dissertation, Utrecht (1946) has come to our attention. This author gives a table of equivalent symbols of the various authors. He also discusses the factor 2 in the definition of K, which was encountered in experimental work in 1941 and which David Sinclair and L. Brillouin have since clarified theoretically. Van de Hulsts' explanation appears to be identical in principle with Sinclair's treatment.

LATEX PARTICLE SIZES AS DETERMINED BY SOAP TITRATION AND LIGHT SCATTERING

H. B. Klevens*

Department of Chemistry, University of Chicago, Chicago, Illinois

Received Nov. 4, 1946

A discussion by Hartley (1), and a more recent one by Sheppard and Geddes (2), have shown that the change in spectra of various dyes could be used to follow changes in aggregation in detergent solutions. This has led to a series of researches involving the determination of the critical micelle concentration (cmc) of some fatty acid soaps (3), of the effects of salts on the cmc (4), of the change in cmc of soap mixtures (5), of the effect of temperature (6) and oils on the cmc, and of the cmc of some very pure sulfates and sulfonates (7), the latter to check this method against other more involved techniques. Further, it has recently been shown that this method can be applied to protein and to protein-detergent complexes.

For anionic soaps and anionic soap mixtures, cationic dyes such as pinacyanol chloride, Victoria Blue B, anisoline, and others have been shown to be suitable as indicator dyes (1, 4); cationic soaps require the use of anionic type dyes such as acidified indophenol (8), benzopurpurine 4B, Sky Blue FF, and various others as described by Baxendale and Lewin, and Neale (9).

The various dyes mentioned above were all water soluble but not soluble to any extent in various hydrocarbons such as benzene, styrene, and isoprene. Thus, one could follow various changes in soap concentration in the presence of these and other monomers. Various methods have been used to measure the amount of soap adsorbed from solution by both liquids and solids, for example by emulsion droplets, carbon blacks, high polymeric particles, *etc.* These include viscosity, surface tension, conductivity, density, and refractometry. These methods are usually time-consuming and it was found possible to apply the relatively simple dye method to surface area determinations. To determine the cmc by surface tension, by conductivity, or by viscosity measurements, it is necessary to obtain 2–3 points on either side of the cmc. In the case of the dye method, only one titration is necessary to find the cmc, although, in the determinations reported here, checks were run on all points.

* Present address: Chemical and Physical Research Laboratories, The Firestone Tire and Rubber Company, Akron 17, Ohio.

As has been previously mentioned (7), changes in both color and in fluorescence occur during micelle formation. In systems containing only soap and water, actual observation of color changes in the dyes during micelle formation could be made with an accuracy of 2–3% as determined by titration. However, in those which contain colored or turbid material in addition, as in the present experiments, it was found simpler to measure the end point by noting changes in fluorescence of the dye. It had been reported that fluorescence increased markedly at and above the cmc, due probably to preferential absorption and orientation of the dye on the soap micelle.

The dye method involved essentially the titration of a particular system containing an excess amount of soap with a solution of the appropriate type of dye until a color change occurred or until there was a corresponding change in fluorescence. These changes are indicative of a change of micellar to non-micellar soap at the cmc. It was necessary in all cases to use a cationic type of dye for anionic soap systems and an anionic type for the cationic soaps, for, as explained previously (8), a difference in charge on dye and soap was necessary. In certain cases illustrated, it was found advantageous to titrate the system under investigation, not with a dye solution, but with a soap solution containing the dye. When possible, as in the case of the various polymer particles studied, it was found interesting to titrate in both directions to check the two methods. As will be shown later, this is quite possible in certain systems, such as high polymer latices, but not possible in emulsion systems of certain types.

To check the soap dye titration method for the determination of surface areas and, from these, particle sizes and numbers of various latices, use was made of the spectrophotometric-interferometric procedure (10) for particles with diameters less than 800A (about 0.1–0.2 the wavelength of the incident light) in which the Rayleigh λ^{-4} law is valid, and of "Tyndall spectra"[a] to determine the diameters between 800–3000A (11). To

[a] "Tyndall spectra," defined as the variation of light scattering with the wavelength, λ, have been applied here for the determination of size of spherical dielectric particles. This term has been so defined and used previously (12) in attempts to determine size and shape of various colloid systems by optical means. In agreement with the conventional meaning of spectra, as applied to ultraviolet or infrared spectra, the term denotes scattering or absorption as a function of wavelength. The term, Tyndall effect or Tyndall phenomenon (13), usually means scattering of light of one wavelength similar to the way in which Raman effect is used. Raman spectrum is often used interchangeably with Raman effect and this has also occurred in the use of Tyndall spectrum in place of Tyndall effect. Thus LaMer and Barnes have shown the presence of various orders of scattered light which they designate as Tyndall spectrum (14). As long as these terms are defined, no confusion should arise. In one case, Tyndall spectrum denotes the color and intensity changes which occur when a parallel beam of plane polarized white light is scattered by a particle (14); in the other, it denotes the changes in intensity of scattered light when the wavelength of the initial monochromatic light is varied (12).

make use of available apparatus, transmission instead of scattering measurements were made. These are directly related, for the difference between the intensities of the incident and the transmitted light is the total scattered light.

The Tyndall spectra of these samples were measured with two instruments, the visual Pulfrich spectrophotometer and the Beckman photoelectric spectrophotometer, and involved the determination of $-n$, *i.e.*,

$$(\log K_1 - \log K_2)/(\log \lambda_1 - \log \lambda_2)$$

where K is the absorption coefficient at wavelength λ. The K values are not true "consumptive" absorptions but are "conservative" absorptions and therefore are equivalent to measurements of the total Tyndall effect. The $n(\lambda)$ relationships are of two types: n_{tc}, which are true consumptive absorptions and may vary between 0 and $\pm\infty$, and n_{ac}, which are apparent conservative absorptions and vary between 0 and 4.0, except where particles are much larger than the wavelength of the incident light. The solid angle in the Pulfrich spectrophotometer was defined as $\leqslant 4°$ depending on the slit width used. In the Beckman instrument, this angle was somewhat larger due to the construction of this spectrophotometer and the non-accessibility of its optical system. In the determination of large particle sizes, the Pulfrich photometer was used exclusively because of the relatively slight forward scattering as a result of its narrow solid angle.

The refractive index increments of the copolymers were determined by use of the mixture rule reported recently (15) and were found to be 1.21–1.23 for the latices measured. Calibration curves for systems of these increments had been determined previously by combined ultramicroscopic and light scattering measurements (11), and thus the particle diameters could be determined simply by measurements of the Tyndall spectra and of $-n$, the slope of the log K *vs.* log λ plot. It will be shown that there is about the same degree of agreement in the determinations of these larger particle sizes as was observed in those in which the λ^{-4} law is valid.

Synthetic latices were prepared at 50°C. using 2.5% potassium myristate as the emulsifier. To 180 parts by weight of soap solution, were added 100 parts of a 75–25 mixture of isoprene and styrene and a small amount of a mercaptan and a persulfate. Yields were determined gravimetrically. Preparations of samples for spectrophotometric-interferometric measurements were identical with those described by Heller and Klevens (10). Portions of the same latices were used for both the optical and the soap adsorption measurements. Since any area determination, as in the titration method, would require that the entire available area be covered by soap molecules regardless of the composition of the surface, it was necessary to remove any residual oil by centrifuging before meas-

urements were made. The presence of any monomer in the form of emulsion droplets would produce erroneous results since the area of these droplets could not be distinguished from those of the copolymer. In order to obtain concordant results by the two methods under comparison, it was also found necessary to strip off the residual monomers held by the polymer-monomer particle after centrifuging.

In Table I, the data of particle diameters as a function of yield for a series of styrene-isoprene copolymers are presented. The initial reaction mixture contained 2.5% (9.4 × 10^{-2} M) potassium myristate. The values

TABLE I

Diameter of Styrene-Isoprene Particles as a Function of Yield
(2.5% KC_{14}; C_i = 9.4 × 10^{-2}; centrifuged, stripped)

Per cent yield	$\frac{C_i}{m}\times10^4$	$C_a\times10^2$	$\frac{C_a}{m}\times10^4$	D(Å) (str.)
84.8	2.94	8.95	2.80	650
75.0	3.20	9.80	3.33	570
62.0	3.67	10.10	3.95	490
55.5	3.98	9.73	4.12	460
52.5	4.16	9.35	4.13	450
40.3	5.13	7.49	4.09	405
27.7	7.05	4.42	3.31	360
22.4	8.49	2.73	2.47	340
17.6	10.56	1.32	1.49	310
14.5	12.60	.172	.232	290
12.2	14.80	(.63)	—	270
8.5	20.83	(2.68)	—	250
5.3	32.86	(4.20)	—	205
3.0	57.30	(5.63)	—	160
0	—	(9.40)	—	—

of particle diameters in this table are for the centrifuged stripped samples. The terms C_i and C_a are the concentrations in moles/l. of initial and added potassium myristate and m is the g. polymer/l. To yields of between 12.2% and 14.5%, it was found that there was an excess of soap present and the values in brackets are those in which back titration with dye solution was found necessary to reach an end point. At higher yields, as mentioned previously, it was possible to determine the available surface area by titration with soap solution directly, or by back titration with a dye solution after an excess amount of soap solution had been added to the latices.

It was of interest to observe the loss of micellar soap with yield in the emulsion polymerization system. Fig. 1 shows this effect indicating that, at a yield of between 13–14%, all the micellar soap has disappeared, presumably forming a monolayer on the surface of the polymer particles.

This yield agrees fairly well with the surface tension-determined values of about 12–15%, reported by Adinoff and Harkins (16) at which micellar soap disappears. A correction term involving either the cmc of potassium myristate as measured in the absence of oils (the dot-dash curve in Fig. 1) (3), or the cmc as determined in the presence of excess hydrocarbon (the dotted curve in Fig. 1) (6), had to be applied to obtain the actual amount of residual soap. The corrections used were those obtained in the latter case. These corrections involve the amount of soap which might be termed

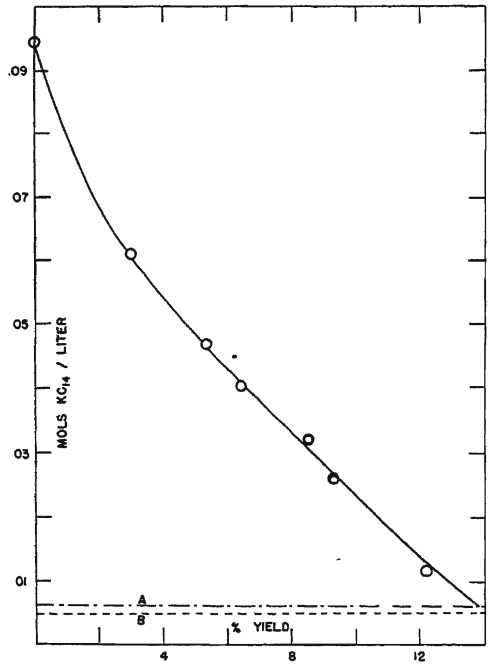

FIG. 1

Disappearance of micellar soap during polymerization (50°C., 2.5% KC_{14}). (A) CMC in absence of added hydrocarbon. (B) CMC in presence of added hydrocarbon.

free, *i.e.*, not adsorbed soap. The assumption is made that micelle formation begins only after the surface of the polymer particles has become completely saturated.

In Table II, data are presented showing the particle diameters of copolymers of various yields as determined by the spectrophotometric-interferometric method and by the soap titration-dye method. The values as determined by the former method in the cases of the stripped and unstripped samples agree well with those determined by the latter method on the stripped samples.

TABLE II

Particle Sizes of Styrene-Isoprene Copolymers as Determined by Soap Titration-Dye and by Spectrophotometric-Interferometric Methods
(2.5%, KC_{14}; centrifuged)

Soap Titration-Dye[a]				Spectro-Inter.	
Per cent yield	$D(A)$unstr.	$D(A)$str.	$\frac{D(A)\text{unstr.}}{D(A)\text{str.}}$	$D(A)$unstr.	$D(A)$str.
84.8	655	650	1.0	670	665
75.0	565	570	1.0	590	585
62.0	560	490	1.1	505	510
55.5	545	460	1.2	475	475
52.5	550	450	1.2	470	465
40.3	540	405	1.3	425	430
27.7	525	360	1.5	390	395
22.4	555	340	1.6	375	370
17.6	615	310	1.9	350	335
14.5	705	290	2.4	345	330
12.2	775	270	2.9	330	325
8.5	885	250	3.5	310	300
5.3	875	205	4.3	280	260
3.0	840	160	5.2	240	225

[a] Values checked by surface tension measurements.

The agreement in particle size in the stripped and unstripped samples has been reported previously (10) for numerous other latex systems and a more detailed explanation will be presented later by these authors. It is sufficient for the present case to note that, in the use of this optical method, the latices are often diluted to 1:10,000 at which concentration the excess monomer probably diffuses, to a great extent, into the water layer in which it is below its solubility limit. The much larger sizes determined by soap titration in the case of the unstripped latices are shown by noting the decrease in the ratio of the particle sizes of the unstripped to the stripped samples with increase in yield. Above 55% yield, the diameters determined by the two methods seem to be independent of stripping.

It would be of interest to try to use these data to determine the monomer-polymer ratio as a function of yield, for this ratio would give us additional evidence as to reaction rates, mechanism, and loci of reaction in copolymerization. However, no such attempt can be made with the values here, for the addition of micellar soap in the titration technique involves not only theoretical close packing of the soap molecules on the surface of the polymer particle, but possibly an indeterminate amount of solubilization of the monomer present. Further, it is probable that this titration technique does not involve equilibrium distribution of the hydro-

carbons, for it has been shown (17) that solubilization by soap solutions is a very slow process.

Fig. 2 shows a comparison of the stripped samples as determined by the two methods. The two curves are fairly symbat over the entire range, the largest divergence being at lower yields. The fact that the diameters determined by the spectrophotometric-interferometric method are larger than those determined by the titration technique can be explained by noting that the two methods determine different particle diameters. The

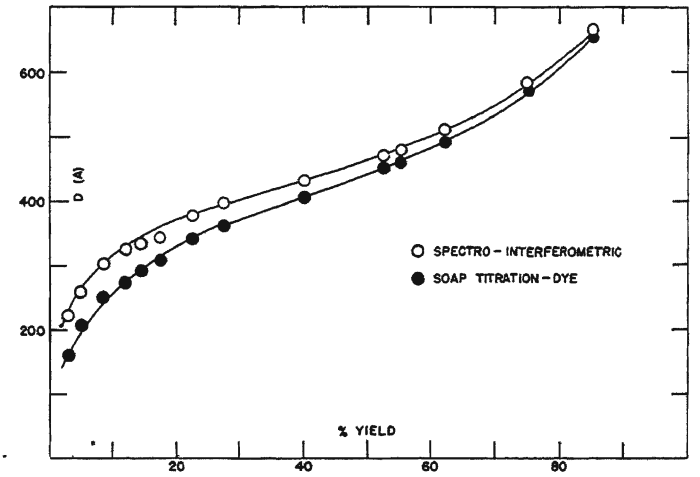

FIG. 2

Particle sizes of styrene-isoprene copolymers as determined by spectrointerferometric and soap titration-dye methods (50°C., 2.5% KC_{14}).

first method involves a weight-average determination which can be expressed by

$$D_w = \frac{\Sigma nd^4}{\Sigma nd^3}$$

and the second is a surface-volume or area average particle in which

$$D_a = \frac{\Sigma nd^3}{\Sigma nd^2}$$

(n = number of particles of diameter d). D_w is based on the total surface area of a unit weight of particles and D_a on the density and the specific surface (area/unit volume). In any determination of surface area or particle diameter, D_w is always larger than D_a and both are larger than the modal or mean diameter. However, this is not sufficient to explain the increase in divergency of the two sets of values at lower yields.

Electron micrographs of various high yield latices, obtained through the courtesy of the Research Laboratories of the U. S. Rubber Co., showed half-width of size distribution of about 100–150A. This type of distribution could not explain the variations of about 50% observed for the low yield latices as seen in Table II. An explanation of the divergency at low yields may be that these latices are more heterodisperse initially and that, as particles increase in size, their rate of growth decreases. If it would be possible to accept the idea that a portion of the polymer-monomer particles coalesce on impact, the apparent increase in homodispersity at higher yields could be due to the much larger Brownian movement of the smaller particles. It has been shown that at higher yields a certain amount of coalescence occurs in latices (10) and it is possible that this is happening during the entire course of the polymerization.

The data for the large particle size latices which do not obey the λ^{-4} law, and consequently were determined by the use of Tyndall spectra as well as by soap titration, are given in Table III. These latices were

TABLE III

Comparison of Particle Size of Various Latices as Determined by Tyndall Spectra and Soap Titration

(Styrene-isoprene copolymer; 0.05% KC_{14} + 1% KCl; samples centrifuged and stripped)

Yield Per cent	Diameter (A) Tyndall spectra	Soap titration
1.0	950	990
4.5	1400	1360
7.0	1450	1600
15.5	2050	1990
35.0	2550	2470
70.0	2900	2860

prepared using the standard formula given above except that 0.05% potassium myristate plus 1% potassium chloride were used in place of the 2.5% potassium myristate. In the preparation of these latices, it was necessary to allow the polymerization to proceed for as many as 3–15 days for the higher yields. As has been shown previously (10), larger particle size latices may be obtained by decreasing the soap concentration. The number of polymer particles produced were also shown to increase linearly with increasing soap concentration. Since these two sets of data are measures of different averages, the agreement noted in Table III is good for a heterodisperse system. The ultramicroscopic determinations from which the calibration curves for the measure of the slope, $-n$, are obtained, are essentially number averages, for they are counts of particles

in unit volumes. It is thus probable that these determinations were made on copolymers having narrow distribution of particle sizes.

The agreement that is observed in the determination of particle diameters by optical and by adsorption measurements indicates that these two methods may be used to supplement each other. It is unfortunate that these two sets of values lie on the high side of any distribution curve for it would be very useful if one could measure diameters which fall on the low side and thus obtain some indication as to particle size distribution.

The value, $28A^2$, that is used as the cross-sectional area of a potassium myristate molecule was that obtained from Dr. R. W. Mattoon from his extensive X-ray measurements on soap solutions (18). Since various other soaps and detergents are used in the preparations of synthetic latices as well as in other emulsifications, it seemed necessary to endeavor to obtain cross-sectional areas of other soaps. A carbon black whose surface area had been determined by N_2 adsorption was used in these studies. Dispersions of carbon black-soap solutions were shaken in a rotary shaker for 24–48 hours, centrifuged at about 20,000 *g* and the residual liquor was titrated with dye solutions. The areas determined for the various soaps were found to be considerably larger than those measured by other means. In the discussion of this problem with Dr. E. Schmidt, it was mentioned that in all probability incomplete dispersion of the carbon blacks was the contributing factor for the differences in soap areas. At present, work is in progress on this problem using a ball mill technique, a spark coil and ultrasonics to prepare more uniformly dispersed systems. It is possible that with the removal of some experimental difficulties, this simple method will find much use in the textile, emulsion, polymer, and other related fields.

Summary

Particle sizes of synthetic latices as determined by soap adsorption using various dyes as indicators of surface saturation agree with those determined optically. For diameters to 800A, values were determined by the spectrophotometric-interferometric method; for those between 800–3000A, a "Tyndall spectra" method was used. To obtain concordant results, it was found necessary to attempt removal by steam stripping and application of vacuum, of residual free monomer present either as emulsion droplets or in the polymer-monomer particle. It is proposed that, at all times during polymerization, a certain amount of coalescing of particles is taking place. Carbon black areas and, from these, the areas of other soaps could not be determined by the present technique due to difficulties involved in dispersing the blacks.

REFERENCES

1. HARTLEY, G. S., Aqueous Solutions of Paraffin-Chain Salts. Hermann et Cie, Paris. 1936.
2. SHEPPARD, S. E., AND GEDDES, A. L., *J. Chem. Phys.* **13**, 63 (1945).
3. CORRIN, M. L., KLEVENS, H. B., AND HARKINS, W. D., *J. Chem. Phys.* **14**, 216, 480 (1946).
4. CORRIN, M. L., AND HARKINS, W. D., *J. Am. Chem. Soc.* 69, 683 (1947).
5. KLEVENS, H. B., *J. Chem. Phys.* **14**, 742 (1946).
6. KLEVENS, H. B., *J. Phys. Colloid Chem.* **51**, (1947). (In press.)
7. KLEVENS, H. B., presented before the Division of Colloid Chemistry at the 110th meeting of the Am. Chem. Soc., Chicago, Illinois, September 9–13, 1946.
8. KLEVENS, H. B., *J. Am. Chem. Soc.* **69**, (1947). (In press.)
9. BAXENDALE, D. H., AND LEWIN, S., *Trans. Faraday Soc.* **42**, 126 (1946); AND NEALE, S. M., *J. Colloid Sci.* **1**, 371 (1946).
10. HELLER, W., AND KLEVENS, H. B., presented before the Symposium on High Polymers at the 110th meeting of the Am. Chem. Soc., Chicago, Illinois, September 9–13, 1946.
11. HELLER, W., KLEVENS, H. B., AND OPPENHEIMER, H., *J. Chem. Phys.* **14**, 566 (1946).
12. HELLER, W., AND VASSY, E., *Phys. Rev.* **63**, 65 (1943); *J. Chem. Phys.* **14**, 565 (1946); HELLER, W., Am. Chem. Soc. meeting, New York, N. Y., Sept. 11–15 (1944); HELLER, W., AND KLEVENS, H. B., *Phys. Rev.* **67**, 61 (1945); also Ref. 11 above.
13. FREUNDLICH, H., Colloid and Capillary Chemistry, 2nd Ed., p. 382. Methuen and Co., London.
14. LAMER, V. K., AND BARNES, M. D., *J. Colloid Sci.* **1**, 71, 79 (1946).
15. HELLER, W., *Phys. Rev.* **68**, 5 (1945).
16. HARKINS, W. D., *J. Chem. Phys.* **13**, 381 (1945).
17. HELLER, W., AND KLEVENS, H. B., *J. Chem. Phys.* **14**, 567 (1946).
18. HARKINS, W. D., MATTOON, R. W., AND CORRIN, M., *J. Am. Chem. Soc.* **68**, 220 (1946).

ERRATUM

On page 31, under Conclusions and Summary, in the article on "The Role of Psychophysics in Rheology" by G. W. Scott Blair, *J. Colloid Sci.* 2 (1947), the second sentence should read: For simple elastic bodies, the force may be determined by a dynamic method involving measurements of an acceleration, *e.g.*, an Atwood machine.

STUDY OF ALUMINUM SOAP-HYDROCARBON SYSTEMS: "CALOTROPY" AND TRUE STABILITY OF THE JELLY PHASE [1]

Karol J. Mysels [2]

From the Department of Chemistry, Stanford University, California

Received March 4, 1947

Introduction

All colloidal systems were at one time considered inherently unstable. This generalization had to be abandoned because some systems have been shown to be truly stable. It is now recognized that solutions of stable colloids, such as soap solutions, form true phases in the sense of Gibbs.

Jellies, the clear, elastic homogeneous colloidal systems which have high viscosities and may be even rigid, are sometimes unstable, being syneretic, or liquefying spontaneously to a thin sol, or precipitating out to form an inhomogeneous gel. The term *gel* is used in this laboratory to connote a two-phase system in which there is X-ray or other evidence of the presence of the crystalline solid, more or less disintegrated and enmeshing the second phase, that may be solvent, sol or jelly.

McBain and Laing investigated in 1920 (1) a stable jelly in the system sodium oleate-water but the temperature range of its stability was very narrow, only about 2°C. In the present paper a system is reported in which the jelly phase is stable over a wide range of temperature. McBain and Laing showed that a jelly may pass into a sol without change in refractive index, osmotic pressure, particle size, light scattering (opalescence), conductivity, E.M.F., or any property other than mechanical, such as viscosity and elasticity. This demonstrated, using aqueous sodium soaps as an example, that the properties of the jelly could be due only to loose contacts forming a framework consisting of the same colloidal particles that exist in the sols. Similarly, in the present paper, a smooth continuous transition from stable jelly to stable sol and *vice versa* has been observed viscometrically in an anhydrous aluminum soap dispersion upon changes of temperature.

[1] Study conducted under contract OEMsr-1057 between Stanford University and the Office of Emergency Management, recommended by Division 11.3 of the National Defense Research Council, and supervised by Professor J. W. McBain.

[2] Present address: University of Southern California, Los Angeles 7, Cal.

It is well known that the viscosity of jellies and many sols differs from that of true solutions and pure unassociated liquids. At a given temperature and pressure it depends markedly on the history of the sample, showing that the time necessary to form the structure is large compared with the duration of experiments. The most common type of such hysteresis is *thixotropy*, the reduction of viscosity by prior flowing, especially by rapid flowing, where the structure is broken down mechanically during the flow and then is gradually restored during rest.

Perhaps less generally known, though frequently occurring, is another type of hysteresis which may well be called "*calotropy*," the temporary reduction of viscosity by prior heating. Here the structure is loosened during the heating and then gradually restored at a lower temperature.

In both these hysteretic phenomena the structure of the jelly is restored *spontaneously* at constant temperature and pressure, in a quiet solution, after it has been disrupted and a flowing sol has formed. Thus the jelly is stable under these conditions with respect to the sol. The spontaneous formation of a jelly upon cooling of a sol proves, of course, the same point. Frequently, however, such a jelly is itself unstable with respect to a gel or a two phase gel-sol system, the form that is stable at lower temperatures. If, however, a jelly forms spontaneously, not only from the sol but also from the gel or gel-sol system, then its strict thermodynamic stability is demonstrated. The white opaque gels of aluminum dilaurate with cyclohexane set to a clear jelly on heating to between 45° and 50°C., the process taking time at 45°C. (3), and its sols form the jelly on cooling below 100°C., the latter is therefore stable at intermediate temperatures.[3]

Viscometric study of dispersions of aluminum dilaurate in cyclohexane provides clear illustrations in non-aqueous systems of the smooth transition from sol to jelly, of calotropy and of thixotropy, and of a thermodynamically stable jelly.

Experimental

The System Aluminum Dilaurate-Cyclohexane

To measure the viscosity of a system whose composition remained invariable over long times and wide ranges of temperature, a sealed tube containing it was inverted and the time of rise of a vapor bubble between two fixed points was observed. A forced draft air oven served as thermostat; its temperature remained constant to ±1°C.

[3] McBain and McClatchie (*J. Phys. Chem.* **36**, 2571, 1932) concluded that the jelly of sodium stearate in benzene above 105°C. is "the most stable state." G. S. Hattiangdi (*J. Sci. Ind. Research (India)* **4**, 491 (1946) likewise found that, with sodium oleate and sodium stearate in xylene, jelly is the most stable state between 80 and 90°C.

Formation of Sol. An approximate overall picture of the variation of viscosity of the jellies and sols of aluminum dilaurate in cyclohexane with temperature and concentration is given in Fig. 1. The lines drawn are smoothed estimates from many observations. For example, for 1% aluminum dilaurate-cyclohexane at 5°C., 29 readings were made of the time taken for movement through 4 cm., the maximum being 4.02, the minimum 3.87, the average 3.93 seconds for the 4 cm.

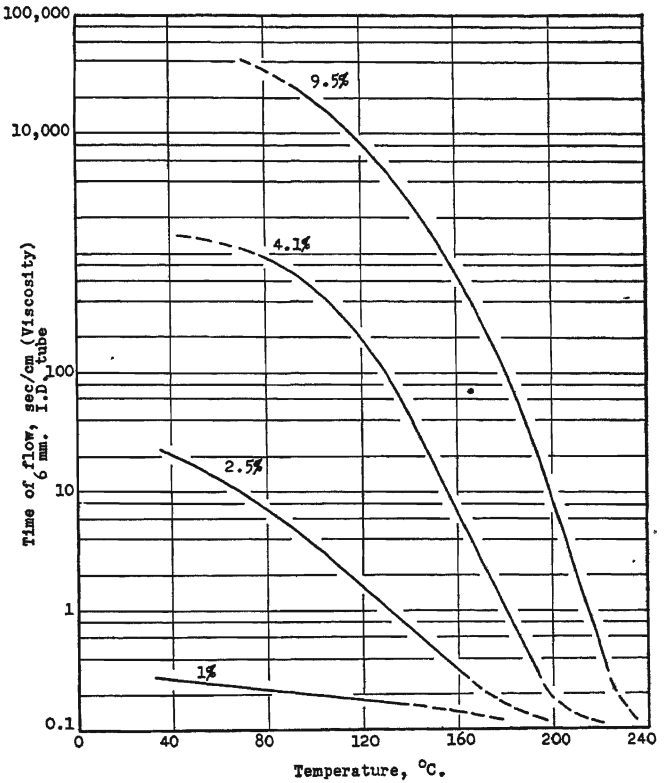

FIG. 1. Variation of viscosity of $Al(OH)L_2$-cyclohexane system with temperature.

All systems at sufficiently high temperatures are typical sols; and their viscosity is little more than that of the pure solvent. The temperature at which the viscosity approaches that of the pure solvent bears no relation to the melting point (4) of the pure soap. Dilute jellies become thin liquids far below that melting point while a 9.5% system is appreciably thickened even 10°C. above it. Fig. 2 shows the behavior of a 4.1% and a 9.5% system in the neighborhood of 196°C., the melting point of the soap. In the 9.5% system, particularly, the viscosity is much higher than

that of the pure solvent, and decreases uniformly about three-fold per 10°C. rise in temperature. There is, therefore, no scaffolding or felt of ordinary soap crystals disappearing as the soap melts, as was suggested by Höppler (2).

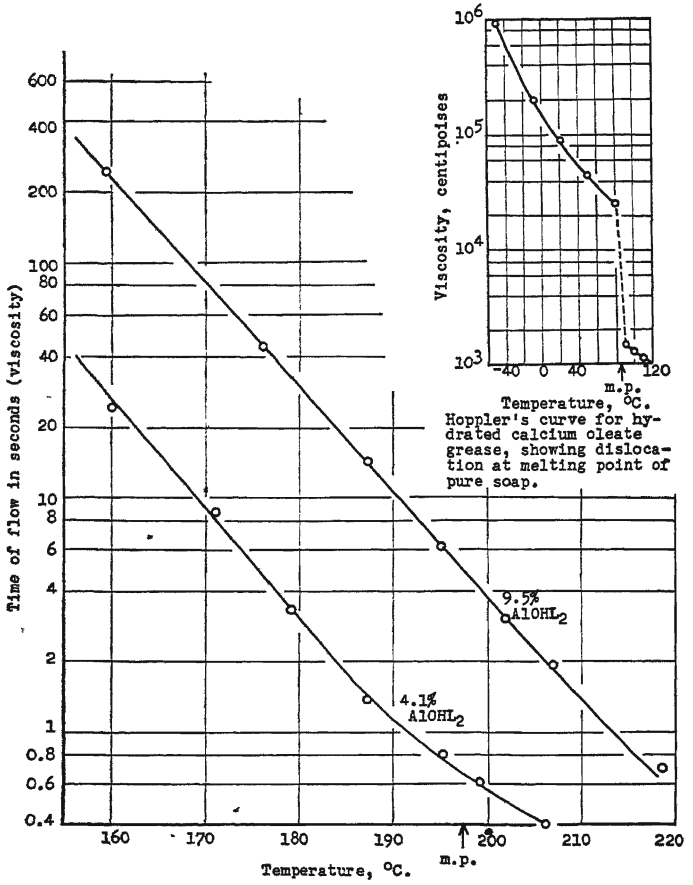

FIG. 2. Viscosity of $Al(OH)L_2$-cyclohexane systems as a function of temperature, showing no discontinuity at the melting point of the soap.

This agrees well with the view that soap molecules associate to colloidal particles which then stick together in loose aggregates, enmeshing and immobilizing large tracts of solvent, but also shows that the colloidal particles are *not* original soap but something that results from the interaction of solvent and soap (5).

Quite different behavior occurs for the system hydrated *calcium* oleate-hydrocarbon which might have been considered *a priori* closely related to the present one. Höppler found that in his system there was a

sudden discontinuity in the viscosity temperature curve, the viscosity changing suddenly by a factor of 15 at the melting point of the soap. This supported Höppler's view that the soap retained most of its original properties. This system is a *gel*, not a jelly. Below the melting point of the soap it is a dispersion of fine fibrillar crystallites of the soap itself, which, by interweaving, enmeshes the liquid and causes high viscosity with but small dependence on temperature. Above the melting point a dispersion of liquid droplets is present, showing little or no thickening. The sharply different behavior of the jelly of aluminum soap requires a correspondingly different explanation.

Calotropy. Both thixotropy and calotropy were apparent, but intermixed, in preliminary experiments. To separate them as far as possible the time of flow of a sealed system was measured once only at 82°C. after the structure had been substantially completely destroyed by heating to 200°C., and then rebuilt by slow cooling to 82° C., with residence at this temperature for various lengths of time. Slow cooling was necessary to avoid bubble formation in the jelly. It was realized with sufficient reproducibility by setting the thermostat for 82°C. (after it had been above 200°C. for at least 10 minutes) and allowing it to cool spontaneously, which took approximately one hour. After a given time at 82°C., the time of flow was determined once and the tube heated to 200°C. before the next measurement.

The results are shown by open circles in Fig. 3. The time of flow increases slowly but very markedly at 82°C., a five-fold increase being

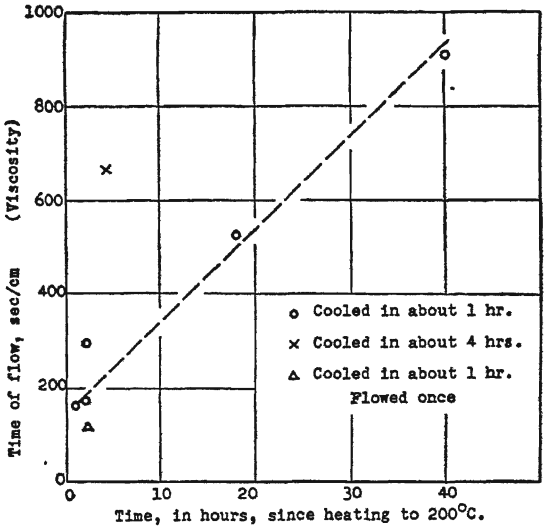

FIG. 3. Viscosity of 4.1% $Al(OH)L_3$-cyclohexane at 82°C. after previous heating to 200°C. as affected by cooling rate, time at 82°C., and thixotropy.

observed in 40 hours. If the cooling from 200° to 82°C. was slowed and extended over 4 hours, the time of flow became immediately more than 3 times that obtained with one hour cooling, as shown by the × of Fig. 3.

The results of Fig. 3 clearly suggest that the structure of the jelly is built up to an increasing *extent* as the temperature is lowered, but that the *rate* of building up is more rapid at higher temperatures. This was shown more strikingly when the tube was heated above 200°C. and then quenched by dropping it into cold water. Of course, obvious inhomogeneity was then produced but by the next day this 4.1% system became homogeneous; it was a *slightly* viscous liquid having a flow time of only about 10 sec./cm. It was kept at room temperature and its viscosity observed occasionally over nearly 40 days.

The viscosity increased slowly at first, then more and more rapidly at an almost exponential rate, but after some 20 days the rate was again reduced. On a linear graph this would give an S-shaped curve. On a semilogarithmic scale a rather regular pattern is obtained as shown in Fig. 4, suggesting that the structure being built up is proportional, not to the viscosity, but to its logarithm. The smooth line drawn is calculated on the hypothesis of a first order process and a final value of 1000 sec./cm.

When the time of flow became large, thixotropic effects again became disturbing and the points in the upper part of the curve were quite uncertain. The dotted line in Fig. 4 shows the recovery after repeated rapid flowing of the jelly in a centrifuge. The time of flow dropped appreciably below the smooth line and did not recover in a day. The recovery time from the thixotropic disturbance was much faster than from the calotropic effect, suggesting that the two may affect different elements of the structure.

Another striking manifestation of calotropy was an *increase* of viscosity as the temperature was raised. Thus, in one case the flow time of a jelly increased from 153 to 430 seconds after its temperature was raised from 82 to 101°C., showing that structure was being built up despite the warming up.

Stability of the Jelly Phase. The above experiments show the spontaneous formation of the structure characterizing the jelly, both upon cooling and isothermally, at temperatures of 80–150°C., and concentrations of 2–10% aluminum dilaurate in cyclohexane.

It has been shown previously (3) that, under some conditions of concentration, the stablest, most crystalline (4) form of aluminum dilaurate spontaneously formed a jelly in cyclohexane below 50°C. Thus there is a substantial range of temperatures and concentrations where this jelly forms spontaneously from both the gel and the sol. This demonstrates conclusively the true thermodynamic stability of a jelly, repeatedly asserted many years ago by McBain (6).

Outside of these ranges of concentration and temperature, the jelly may exist as an unstable or metastable phase such as has been frequently reported for other systems, or may not form readily. Thus, supercooled stiff jellies at room temperature were observed in the above systems for several months without any appearance of the gel and, on the other hand, no jellies were observed in the systems more dilute than 1%, the gel passing directly into a thin sol, and *vice versa.*

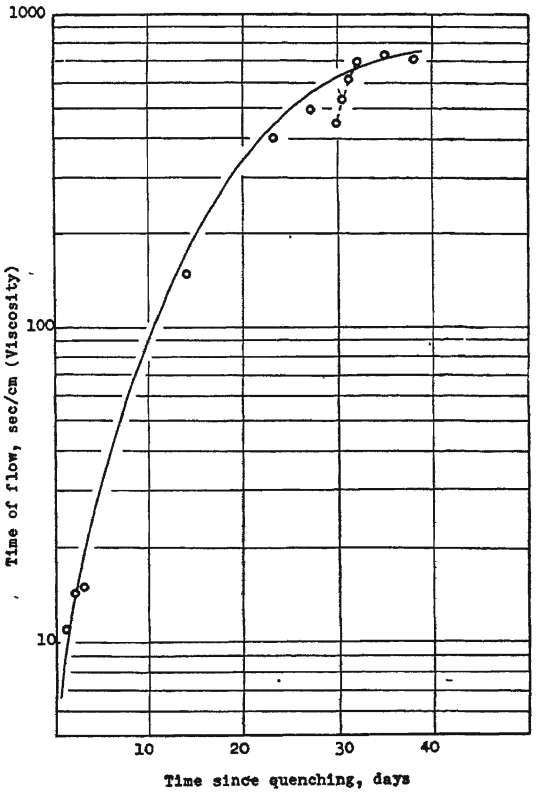

FIG. 4. The slow recovery of a quenched 4.1% sol of aluminum dilaurate in cyclohexane. (Quenched from 200°C. to room temperature.)

SUMMARY

1. Viscometric measurements showing the gradual transition from jelly to sol without phase change in aluminum dilaurate-cyclohexane systems are reported.

2. Observations of "calotropic" recovery, the slow increase of viscosity after cooling from a higher temperature, are reported for these

systems under conditions in which the *jelly*, a single phase, is stable with respect to *gel*, a two-phase system involving crystalline solid.

3. The existence of a large region in which a jelly phase is thermodynamically stable is thus demonstrated.

References

1. Laing, M. E., and McBain, J. W., *Trans. Chem. Soc.* (*London*) **117**, 1507 (1920); *Nature* **125**, 125 (1930).
2. Höppler, *Fette u. Seifen* **49**, 700 (1942).
3. McBain, J. W., Mysels, K. J., and Smith, G. H., *Trans. Faraday Soc.* **43**, (1947).
4. Mysels, K. J., and McBain, J. W., (communicated).
5. Marsden, S. S., Mysels, K. J., and Smith, G. H., *J. Colloid Sci.* **2**, 265 (1947).
6. McBain, J. W., 4th Colloid Symposium Monograph, Cambridge, 1926, p. 1; *Kolloid-Z.* **40**, 1 (1926).

THE SORPTION OF ORGANIC VAPORS BY MONOLAYERS OF SOAP*

R. B. Dean and James W. McBain**

Stanford University, California

Received June 30, 1947

Introduction

Monolayers of insoluble soaps on water can be considered as a limiting case of the sorption of soaps at the air-water interface. The question now arises as to whether such a layer can itself sorb additional material of a hydrocarbon nature. Schulman and co-workers (5) and Harkins (3) have investigated the sorption of substances in solution onto monolayers. In some cases they found evidence that both substances existed together in the monolayer, while other more surface-active substances displaced the first monolayer. Washburn and Keim (6) observed the displacement of monolayers by surface-active volatile liquids if the monolayer was at a pressure less than the spreading pressure of such liquid. They proposed to measure spreading pressure by this method since their values agreed satisfactorily with the values for spreading pressure obtained by Harkins (2).

In some preliminary experiments, which we are not at present able to continue, we found that organic vapors would cause an increase in the area of sodium stearate monolayers, which were held at constant surface pressure. Vapors of liquids which have a spreading pressure greater than the surface pressure on the monolayer would be expected to displace the monolayer and increase the total film area if the vapor were sufficiently close to saturation. We found, however, that the vapors of some substances with lower spreading pressures would also penetrate and expand the film. This indicates that the vapor is sorbed by, and forms a mixed monolayer with, the sodium stearate. Washburn and Keim (6) found no evidence for this behavior in their studies, although they admit the possibility of adsorption.

A few vapors failed to expand a film which was held at a lower pressure than the spreading pressure of the substance. This probably indicates that the vapor was not saturated. If this method were to be adapted

* The work reported in this paper was done in connection with the Government Research Program on synthetic rubber under contract with the Office of Rubber Reserve, Reconstruction Finance Corporation.

** Present address: University of Oregon, Eugene, Oregon.

to quantitative measurements it would, of course, be necessary to work at a constant pressure of the vapor.

Experimental

Sodium stearate monolayers were prepared by spreading a dilute solution of stearic acid (Eastman Kodak Company) in benzene on cleaned surfaces of 0.002 *M* aqueous sodium phosphates. The surface, of initial area 300 cm.^{2}, was held at constant pressure by a vaselined thread "piston" separating it from either tricresyl phosphate (9.5 dynes/cm.) or triolein (20 dynes/cm.). The technique is essentially that developed by Blodgett (1, 4) for the preparation of multimolecular films. The liquid whose vapor was to be examined was placed on a piece of absorbent paper about 6 cm. square, held immediately over the end of the trough furthest from the piston thread and about 0.5 cm. above the surface.

Many vapors were sorbed by the film and caused an expansion of from 2 to 20 cm.^{2} as estimated from the movement of the piston. Other

TABLE I

Sorption of Vapors on Monolayers of Sodium Stearate

(Room temperature, 22°C.)

Vapor	Spreading pressure (2)	Trisodium phos.		Disodium phos.	
		9.5 dyn.	20 dyn.	9.5 dyn.	20 dyn.
Isopropyl alcohol	49	+	0	−	−
Diethyl ether	45	+	+	+	+
sec-Amyl alcohol	(44)	+	−	+	0
Amyl acetate	(30)	+	−	+	+
Ethyl acetate	(>20)	+	+	+	+
Diisobutyl mercaptan	(>10)	+	0	+	+
Butadiene gas (unsat.)	(10)	0	−	−	−
Benzene	8.9	+	0	0	0
Xylene (mixed)	6.6	+*	−	−	−
Cyclohexane	(<10)	+	−	−	−
Isoheptane	(<5)	+*	−	0	−
Petroleum ether (b.p. 60–70)	(4)	+*	0	0	−
n-Hexane	3.4	+*	−	−	−
Carbon tetrachloride	−1.0	0	−	0	−
Carbon disulfide	−6.9	0	−	0	−
Dioxane	?	0	−	0	−

+, increase of area of at least 2 cm.^{2}

0, no detectable increase in area <0.2 cm.^{2}

−, no data

( ), estimated by analogy with other compounds

* appear anomalous

vapors produced no perceptible change in the film. The expansion when produced was always completely reversible following removal of the source of the vapors. The results are summarized in Table I together with the values for the spreading pressure. For substances not listed by Harkins (2) we have estimated values which are given in parenthesis.

The results indicate that many vapors can enter and expand monolayers of sodium stearate on trisodium phosphate. Acid soap films on disodium phosphate are more resistant to penetration. At lower film pressures more substances would probably be taken up by the film because increasing the film pressure from 9.5 to 20 dynes always decreased the extent of vapor sorption and in some cases completely prevented any sorption.

Summary

A new method for studying molecular interactions at surfaces is to expose an insoluble monolayer on water to the vapor of a volatile liquid. Some vapors produce no change in area. Others increase the area of the monolayer, those with high spreading pressure being usually most effective, some even doing so under a higher pressure than their own spreading pressure.

References

1. Blodgett, K., *J. Am. Chem. Soc.* **57**, 1007 (1935).
2. Harkins, W. D., *Colloid Symposium Monographs*, **VI**, 26 (1926). Chemical Catalog Co., New York.
3. Harkins, W. D., Colloid Chemistry, J. Alexander, Ed., V, 12 (1944). Chemical Catalog Co., New York.
4. Langmuir, I., and Schaefer, *Chem. Revs.* **24**, 181 (1939).
5. Schulman, J. H., and Hughes, A. H., *Biochem. J.* **29**, 1243 (1935).
6. Washburn, E. R., and Keim, C. P., *J. Am. Chem. Soc.* **62**, 1747 (1940).

DIFFUSION WITH DISCONTINUOUS BOUNDARY (1)

J. J. Hermans *

N. V. Onderzoekingsinstituut Research, Arnhem, Holland

Received Jan. 22, 1947

Introduction

In recent work on the penetration of various substances into gels, we have encountered a phenomenon of penetration with a sharp boundary line. For example, if sulphide ions diffuse into a gel containing ions of a heavy metal, the boundary line separating the metal sulphide from the rest of the gel remains perfectly sharp during the entire diffusion process. A similar sharp boundary line is observed when copper ions diffuse into a cellulose xanthate gel.

Both theory and experiment show that this phenomenon is quite general in all cases in which the diffusing particles react with the medium to form a precipitate and are thus withdrawn from the diffusion process (see below). Earlier experiments on the penetration of water into dry cellulose (2), and more recent observations on the diffusion of various solvents into high polymers (3), have shown the very general character and the practical significance of the phenomenon. We do not claim that the occurrence of a sharp boundary line in a diffusion process necessarily indicates a reaction between the diffusing substance and the medium. As pointed out by several authors (2, 3, 4), a very high concentration gradient will always result if the diffusion coefficient increases rapidly with the concentration of the diffusing substance. Nevertheless, it is noteworthy, that some solvents are known to give stoichiometric compounds with the polymer into which they diffuse (5), and, in these cases at least, the anchoring of the solvent molecules by the polymer may play some part in the phenomenon.

1. Theory

a. The Medium Does Not Take Part in the Diffusion Process

Let us first consider the diffusion of particles into a medium which can bind a certain amount of the diffusing substance but does not itself take part in the diffusion process. We may say that the medium contains a number of "holes" in which the diffusing molecules can be caught. Once a molecule is caught in a hole, it has lost its diffusibility. We assume diffusion in one dimension, the x-coordinate. Let b be the total number of holes in unit volume.

* Present address: Lab. Inorg. Phys. Chem., University of Groningen, Holland.

Suppose, now, that in a certain unit of volume at time t there are c freely diffusing molecules, *i.e.*, molecules which have not yet been caught in a hole. Let m holes in this volume be empty. Then, obviously, c will change with time for two reasons. To begin with, c changes as a result of ordinary diffusion:

$$\left(\frac{\partial c}{\partial t}\right)_1 = D\frac{\partial^2 c}{\partial x^2},$$

D being the diffusion coefficient. In addition, a certain number of the freely diffusing molecules in this volume are caught in a hole. For this process some such law as proportionality with c and with m may be expected to hold good:

$$\left(\frac{\partial c}{\partial t}\right)_2 = -Kcm,$$

K being a constant. In which case we get

$$\frac{\partial c}{\partial t} = D\frac{\partial^2 c}{\partial x^2} - Kcm; \quad \frac{\partial m}{\partial t} = -Kcm. \tag{1}$$

It can be shown on the basis of these equations, that the concentration c of freely diffusing particles shows a steep gradient, which is steeper the larger the value of K. Unfortunately, however, since both c and m are dependent on x and t, the system (1) is not linear. For this reason we introduce the following simplification.

In those cases in which a very sharp boundary is observed, we may take it that K is very large and, therefore, m is practically zero in all points which have been reached by the diffusing molecules. We assume, therefore, that at any point x, either all holes are filled, or none. Freely diffusing molecules exist only in those volume elements in which all holes are filled. The boundary line indicates the abrupt change from "all holes filled" to "all holes empty." Fig. 1 gives a diagrammatic representation of the situation. In this figure it is assumed that at the boundary $x = 0$ a constant concentration a of the diffusing substance is maintained.

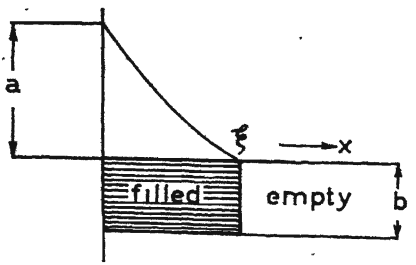

FIG. 1. Diffusion of particles which are trapped in non-diffusible holes

From this boundary onwards the concentration c drops gradually to become zero in a point ξ. The slope of the c-x-curve at this point is determined by the condition

$$-D\left(\frac{\partial c}{\partial x}\right)_{\xi} = b\frac{d\xi}{dt}. \tag{2}$$

In fact, the left hand side of this equation gives the number of particles diffusing through ξ in unit time, and the right hand side determines the amount needed to fill the holes in the region covered. This boundary condition can be transformed to

$$D\left(\frac{\partial c}{\partial x}\right)_{\xi}^{2} = b\left(\frac{\partial c}{\partial t}\right)_{\xi} \tag{3}$$

because

$$\left(\frac{\partial c}{\partial x}\right)_{\xi} d\xi + \left(\frac{\partial c}{\partial t}\right)_{\xi} dt = 0. \tag{4}$$

Consequently, the problem to be solved is a simple diffusion:

$$\frac{\partial c}{\partial t} = D\frac{\partial^2 c}{\partial x^2} \quad (x < \xi) \tag{5}$$

with the boundary conditions

$$c(\xi,t) = 0 \text{ and } D\left(\frac{\partial c}{\partial x}\right)_{\xi}^{2} = b\left(\frac{\partial c}{\partial t}\right)_{\xi}. \tag{6}$$

The further boundary conditions to be met are determined by the conditions of the experiment. We have not investigated the requirements these conditions must fulfil to make a solution of the problem possible. It is easy to show, however, that a very simple solution exists under the following circumstances. Let us assume, as in Fig. 1, that the concentration a is maintained at the boundary $x = 0$, and that contact between the two media at the left and at the right of the origin is established at time $t = 0$. Hence

$$c(0,t) = a;\ c(x,0) = 0 \text{ for } x > 0. \tag{7}$$

The solution runs

$$c = a - AG(x/2\sqrt{Dt}) \text{ for } x \leqslant \xi;\ c = 0 \text{ for } x \geqslant \xi \tag{8}$$

where we abbreviate

$$G(y) = \frac{2}{\sqrt{\pi}}\int_0^y ds e^{-s^2}. \tag{9}$$

The constant A is determined by the condition $c(\xi) = 0$, which gives

$$AG(\xi/2\sqrt{Dt}) = a. \tag{10}$$

This is possible only if $\xi/\sqrt{t}$ is constant. The second boundary condition

at $x = \xi$ must, therefore, also reduce to a condition of this form. In fact, we find

$$\frac{2}{\sqrt{\pi}} A e^{-\xi^2/4Dt} = b \frac{\xi}{\sqrt{Dt}}. \tag{11}$$

For convenience let us introduce the quantity

$$z = \frac{\xi}{2\sqrt{Dt}}. \tag{12}$$

Eliminating A from (10) and (11), we may then write

$$ze^{z^2}G(z) = \frac{1}{\sqrt{\pi}} \frac{a}{b}. \tag{13}$$

This means: the boundary line moves into the gel according to the simple relation $\xi/\sqrt{t}$ = constant. The value of this constant is determined by the solution of Eq. (13). The relation between z^2 and the ratio a/b is represented in Fig. 2. It is clear from this figure that, with increasing

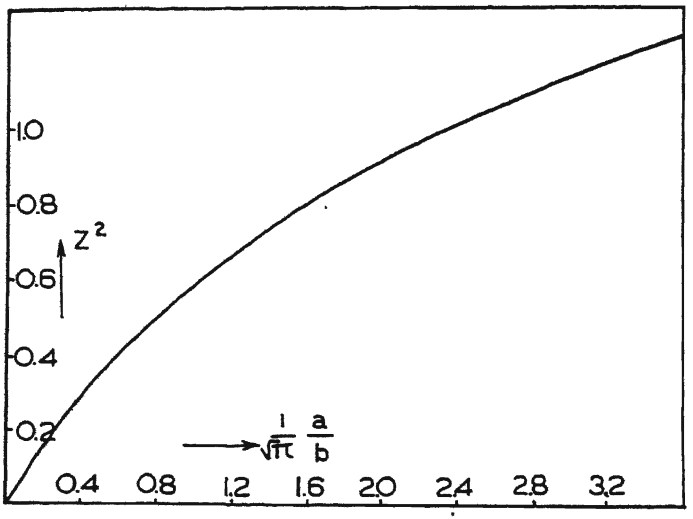

FIG. 2. Relation between z^2 and a/b according to Eq. (13).

ratio a/b, the value of z, and hence the velocity of penetration, increases less and less rapidly, without, however, asymptotically reaching a finite value.

A similar simple solution is possible if the boundary conditions (7) are replaced by the following:

$$c(x,0) = a \text{ for } x < 0 \text{ and } 0 \text{ for } x > 0. \tag{14}$$

This means that at zero time the two media are brought together, the concentration being a at the left and 0 at the right of the origin. At time $t = 0$ a diffusion in *both* media sets in, the diffusion coefficient having the same value throughout the system from $x = -\infty$ to $x = \xi$. However, we shall not elaborate this case, since all experiments carried out conformed to the boundary conditions (7).

Finally, it is to be noted, that D is the diffusion coefficient at the left of the boundary line, that is, in a medium in which all the "holes" are filled.

b. The "Holes" Themselves are Mobile

If, say, $S^{=}$ ions penetrate into a gel containing Pb^{++} ions, PbS precipitates. If the lead ions are mobile, they will take part in the diffusion process. Here, again, the conditions for a sharp boundary are fulfilled. The concentration v of the lead ions, however, in contrast to that of the "holes" in the former case, will now decrease with decreasing x and reach the value zero at $x = \xi$ (see Fig. 3, drawn curve).

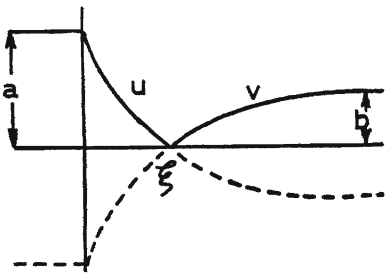

FIG. 3. Diffusion of particles which are caught by mobile holes.

This problem can be solved in much the same way as that discussed previously. However, we found later that Adair (6) had already derived the solution of the problem in a somewhat intuitive manner. We shall, therefore, simply quote Adair's formula, indicating the argument, and discussing in more detail one particular point which has given rise to confusion. The problem to be solved is the following:

$$0 < x < \xi: \frac{\partial u}{\partial t} = D_1 \frac{\partial^2 u}{\partial x^2}; \quad u(0,t) = a; \quad u(x,0) = 0; \quad u(\xi,t) = 0; \quad v = 0.$$

$$x > \xi: \frac{\partial v}{\partial t} = D_2 \frac{\partial^2 v}{\partial x^2}; \quad v(\infty,t) = b; \quad v(x,0) = b; \quad v(\xi,t) = 0; \quad u = 0.$$

Further, at the boundary $x = \xi$:

$$-D_1 \frac{\partial u}{\partial x} = D_2 \frac{\partial v}{\partial x} \tag{15}$$

Adair shows that a solution exists in which both u and v have the simple form: $A + BG(x/2\sqrt{Dt})$. The boundary conditions give rise to equations from which the constants A, B and the ratio $\xi/\sqrt{t}$ can be solved. The condition $\xi/\sqrt{t} = \text{const.}$ is a

necessary condition for the solution to be self-consistent. The final equation for ξ runs:

$$\frac{a\sqrt{D_1}\, e^{-\xi^2/4D_1t}}{G(\xi/2\sqrt{D_1t})} = \frac{b\sqrt{D_2}\, e^{-\xi^2/4D_2t}}{1 - G(\xi/2\sqrt{D_2t})}. \tag{16}$$

This equation reduces to the condition (13) if the diffusion coefficient of the holes approaches zero, as of course it should. A very simple relation is obtained if $D_1 = D_2$, in which case Eq. (16) reduces to

$$G(z) = \frac{a}{a+b}, \tag{17}$$

z being the quantity defined by Eq. (12). Since $G(z)$ is the well-known error-integral, the relation between z and $a/(a+b)$ can be read from the usual tables or graphs. In this specially simple case the solution can be interpreted as follows. The penetrating particles diffuse as if their initial concentration in the gel were $-b$, and the holes diffuse as if their concentration were maintained at the level $-a$ at $x = 0$. This is symbolized in Fig. 3 by the dotted curve. A similar, but unsymmetrical, interpretation can be given if D_1 differs from D_2.

Further, there is no difficulty in finding an equally simple solution if, instead of a constant concentration at $x = 0$, we have a boundary condition of the type given by Eq. (14), *i.e.*, diffusion in the region $x < 0$ with uniform initial concentration in this region.

Duclaux (7) objects to condition (15), because this condition means that the amount of $S^=$ ions crossing the boundary towards the right is exactly the same as the amount of Pb^{++} ions crossing it towards the left, and there would seem to be no reason for a displacement of the boundary itself. This, however, is not true. If, to simplify the discussion, we take $D_1 = D_2$, we have equal slopes at the boundary line. The displacement of this boundary must not be attributed to a difference in slope; it is due to a difference between $\partial^2u/\partial x^2$ and $\partial^2v/\partial x^2$ at $x = \xi$. The situation is completely analogous to that in ordinary diffusion, where the change in concentration $\partial c/\partial t$ is not determined by the value of $\partial c/\partial x$ but by $\partial^2c/\partial x^2$. We may best explain the phenomenon if we imagine successive steps: Since $\partial^2u/\partial x^2 > \partial^2v/\partial x^2$, the slope of the u-curve somewhat to the left of ξ is a little greater than that of the v-curve at the right. Consequently, the number of $S^=$ ions transported toward the right in unit time across a section somewhat to the left of ξ is slightly larger than the number of Pb^{++} ions transported toward the left across a section somewhat to the right of ξ. If the boundary is kept at a fixed position, the slope $\partial u/\partial x$ at the left of ξ will, therefore, become a little higher than $\partial v/\partial x$ at the right. The next step will be a displacement of the boundary to readjust these slopes.

The validity of Eq. (15) is particularly obvious if we consider the case where $S^=$ ions diffuse in the whole region left of ξ (*i.e.*, from $-\infty$ to ξ). Since the numbers of $S^=$ ions and of Pb^{++} ions disappearing as a result of precipitation are the same, and the total number of both $S^=$ ions and

Pb^{++} ions is, of course, constant, we must have

$$\int_{-\infty}^{\xi} dx \frac{\partial u}{\partial t} = \int_{\xi}^{\infty} dx \frac{\partial v}{\partial t},$$

which leads at once to Eq. (15).

c. Diffusion into Cylindrical Filaments

So far we have considered linear diffusion into an infinite medium. In media of finite dimensions the solution of diffusion problems is much less simple and it is doubtful whether a simple solution of the problem hitherto considered can be given. In particular, for diffusion into a cylindrical gel the solutions of type (8) must be replaced by a series involving Bessel functions. In that case the simple relation $\xi/\sqrt{t}$ = constant will no longer hold true.

In one particular case, however, we may immediately write a solution of the cylindrical problem. For, if $D_1 = D_2$, we may make use of the symmetry principle indicated in Fig. 3. The diffusion of the penetrating particles for $x < \xi$ is that which would prevail if the initial concentration in the cylinder were $-b$, and is determined by (8)

$$u = a - A \frac{2}{R} \sum_{n=1}^{\infty} \frac{1}{\alpha_n} \frac{J_0(\alpha_n r)}{J_1(\alpha_n R)} e^{-D\alpha_n^2 t}, \tag{18}$$

$$A = a + b.$$

Here R is the radius of the cylinder, J_0 and J_1 are Bessel functions of zero and first order respectively; the quantities $\alpha_n R$ are the roots of the equation $J_0 = 0$. The concentration v of the holes for $x > \xi$ is given by $v = -u$. This solution is clearly in conformity with all the requirements of the problem.

Many years ago Bungenberg de Jong (9) carried out an experimental study on the phenomenon discussed here. He found, among others, that $\xi/\sqrt{t}$ in linear diffusion is constant. He observed further that the penetration into cylindrical media took place according to a curve such as that represented in Fig. 4, and recognized that this curve may be ap-

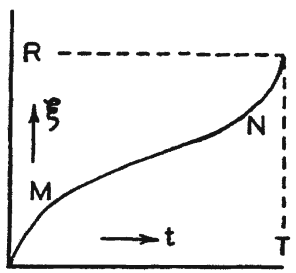

FIG. 4. Penetration of boundary line into cylindrical media.

proximated by a superposition of two parabolas as follows:

$$\xi = k[\sqrt{t} + \sqrt{T} - \sqrt{T - t}] \qquad (19)$$

where k and T are constants, T being the time needed to reach the center. The symmetry of this curve requires that the time needed for the boundary line to travel half the distance R to the center is exactly one-half of the total time T needed to reach the center:

$$\tfrac{1}{2}R = k\sqrt{T} \text{ and } R = 2k\sqrt{T}. \qquad (20)$$

The parameter T used by us to check the equation, was always twice the time needed to reach $\xi = R/2$. Our experiments have shown that Eq. (19) represents the process quite satisfactorily in its intermediate phases. Deviations occur in the initial phase (below point M) and in the final phase (beyond N). Equation (19) must, therefore, be considered as an empirical approximation to a part of the process, and we have no reason to believe that the value of k derived from the first of Eq. (20) is the same as that which would have been found in a linear diffusion. In fact, a few experiments in which both linear and cylindrical diffusion could be examined (see experimental part) revealed that k in the cylindrical process was about 40% lower than the value of $\xi/\sqrt{t}$ in the linear process. For practical reasons the experiments could not be continued, and no systematic investigation on the relation between k and $\xi/\sqrt{t}$ could be carried out. We hope to return to this point in later work. For the time being we shall make use of the velocity constant k defined by (20), taking into account that the $\xi/\sqrt{t}$ value in a linear experiment might be larger by a factor 1,4, or perhaps even more. If the diffusion coefficient is to be derived from the experimental k value, we shall have to compare k with the value of z derived from Eqs. (13), or (16), or (17). In other words, we shall obtain $\sqrt{D}$, and an error of 40% in $\xi/\sqrt{t}$ will then give rise to an error of 100% in D. For this reason the values of D derived from cylindrical diffusion have as yet only relative value.

2. Experiments

a. General remarks

The theory should be applicable to any diffusion process in which the diffusing particles are withdrawn as a result of reaction with the medium into which they diffuse. It is not essential that this medium be a gel. However, in all cases in which a precipitate is formed, we need the gel frame as a support for this precipitate. Otherwise, the boundary line would be seriously disturbed by the sedimentation of the precipitate.

The occurrence of a precipitate is not a necessary condition. It is sufficient if the diffusing particles are consumed by the medium or by other diffusing particles. No precipitate is formed, for example, if thio-

sulphate diffuses into a gel containing iodine. All $S_2O_3^=$ ions, however, which are converted into $S_4O_6^=$ ions no longer contribute to the diffusion of $S_2O_3^=$ ions, and the effect is, therefore, the same as if the $S_2O_3^=$ ions had disappeared into holes. It is obvious, however, that great precautions against convection currents must be taken to maintain the sharp boundary line if the process were to take place in a liquid, the more so because the chemical reaction which takes place at the boundary will usually be accompanied by production of heat. This applies in particular to the reaction between H^+ and OH^- ions. Attempts to obtain a sharp boundary line in the diffusion of an acid into an alkaline gel, or conversely of a base into an acid gel, were only successful when the boundary line traveled very rapidly. Whether this is due to disturbing effects or to complications arising from the interaction of H^+ ions with the gel frame, or to still other factors, could not be further examined. All the experiments described were of a preliminary character and no great accuracy was aimed at. Plans for more accurate work had to be abandoned for technical reasons.

b. Linear Diffusion

Capillaries of 1–2 cm. length and 0.8–1.6 mm. inner diameter were filled with a hot solution of gelatin (10%), containing iodine and some starch. The starch was added to make sure that the iodine molecules acted as non-diffusible holes. A large excess of neutral salt was added to the mixture to suppress diffusion potentials. After cooling, the gel-filled capillary was cut out of the mass and introduced into a small vessel containing a solution of thiosulphate in the same amount of additional neutral salt as that in the gel. The penetration of the boundary line was followed under the microscope. It was found that the speed of this penetration was independent of the inner diameter of the capillary. A plot of ξ versus $\sqrt{t}$ proved to be perfectly linear. The slope of this line was compared with the value of z derived from Eq. (13). This leads immediately to the diffusion coefficient D of the thiosulphate in the gel (compare Table I).

TABLE I

Diffusion of Thiosulphate of Concentration a *into a Gel of Iodine Content* b = *0.040 M/l.*

a ($M/l.$)	0.14	0.090	0.045	0.023
z (Eq. (13))	0.95	0.83	0.64	0.49
$10^3 \times \xi/\sqrt{t}$ obs. (cm./sec.$^{\frac{1}{2}}$)	2.4	2.35	1.65	1.35
$10^6 D$ (cm.^{2}/sec.)	1.6	2.0	1.7	1.9

This diffusion coefficient was also determined directly. To that end the hot gelatin solution was poured into a tube which ended in a thin glass filter. After solidification the gel formed a layer 9 mm. thick, of which 1 mm. consisted of the gel-filled glass filter. In this way we obtained a 9 mm. layer of gel at the end of the tube. This tube was then immersed in the solution of the neutral salt and filled to the same level with 0.5 *M* thiosulphate in the same salt solution. The difference in level between inner and outer solution may have been about 1 mm. It was shown experimentally, however, that the effect of this difference on the experimental results was negligible. The inner solution was stirred by means of a slow current of small nitrogen bubbles, the outer solution by

means of a motordriven small glass paddle. After 3–7 hours the total amount of thiosulphate in the outer solution was determined by titration. It proved to be proportional to the time of the experiment within reasonable limits, provided this time was long compared with the time needed for establishment of stationary diffusion (3–4 hours always sufficed). The diffusion coefficient determined in this way was $(2.2 \pm 0.3) \times 10^{-6}$ cm.²/sec. In view of the fact that no correction was made for the volume occupied by the glass filter, the agreement between this value and that of Table I must be considered as satisfactory.

A further example is given by the diffusion of Na_2S into agar gel containing lead acetate. Here again we added an excess of neutral salt ($NaNO_3$, 10%). The results are given in Table II. In view of the SO_3H groups in the agar, it was first expected that the

TABLE II

Diffusion of Na_2S of Concentration a *into a Gel of Lead Acetate Content* b = *0.05 M/l.*

a ($M/l.$)	0.25	0.125	0.062	0.030
z (Eq. (13))	1.04	0.86	0.665	0.50
z (Eq. (17))	0.97	0.74	0.54	0.345
$10^3\ \xi/\sqrt{t}$ (observed)	4.7	3.7	2.45	1.38
$10^6\ D$ (Eq. (13))	5.1	4.6	3.4	1.8
$10^6\ D$ (Eq. (17))	5.8	6.2	5.2	4.0

Pb^{++} ions would be fixed in the gel and that Eq. (13) would be applicable. However, it was observed that the boundary lines at the two ends of the capillary, although very sharp for the first 2 hours, gradually deteriorated as the lines approached each other. The PbS precipitate in the middle part of the tube was distinctly less dense, and finally a zone remained in which no precipitate occurred at all. This proves that the lead ions took part in the diffusion process and gradually disappeared from the middle part of the capillary. This is confirmed by Table II. Application of Eq. (13), which assumes non-diffusible Pb^{++} ions, leads to a diffusion coefficient of the $S^{=}$ ions which decreases systematically with the concentration, whereas Eq. (17) gives almost constant D values. It may be remembered that Eq. (17) assumes equal diffusion coefficients for $S^{=}$ and Pb^{++}, and it is obvious that a perfect agreement would easily be obtained by adjusting the two coefficients D_1 and D_2. In fact, it can even be shown that there are several different sets of D_1–D_2 values which fit in with the data of Table II within experimental error. A choice from these different sets would be possible only if the experiments were more accurate.

c. *Cylindrical Diffusion*

The diffusion of $Na_2S_2O_3$ into gelatin gels with iodine was also studied in cylindrical filaments. The gel was simply pushed out of the capillary and the filament obtained was then immersed in the diffusing substance. The value of k, introduced in the theoretical section on cylindrical diffusion, was determined by plotting the depth to which the discoloring effect of thiosulphate had penetrated against the time elapsed since immersion. The time needed to reach a depth $R/2$ is $T/2$ and thus determines the parameter T. The value of k is nothing but $R/2\sqrt{T}$. As mentioned already in the theoretical part, it was found in these experiments that k was some 40% lower than the $\xi/\sqrt{t}$ value in linear diffusion.

We were interested in this cylindrical diffusion because of a series of experiments with model filaments of cellulose xanthate. If these filaments are introduced into a solu-

tion containing copper ions, a dark-brown precipitate is formed. Analysis shows that 1 Cu atom is bound by 2 CS_2 groups. Here again the penetration of the copper ions is marked by a sharp boundary line, and as the CS_2 groups in the cellulose xanthate are fixed to the gel frame, we should apply Eq. (13).

The diffusion took place in the presence of excess neutral salt. The concentration of the CS_2 groups in the gel was determined by direct analysis; b is half as large, because 2 CS_2 groups are needed to bind 1 Cu. The results are shown in Tables III and IV. To

TABLE III

Diffusion of Cu^{++} Ions of Concentration a *into Cellulose Xanthate of CS_2 Content · 0.126 M/l.* (b = *0.063*) *in the Presence of $(NH_4)_2SO_4$, 1 M/l.*

a ($M/l.$)	0.40	0.20	0.133	0.10	0.050	0.025	0.018
z (Eq. (13))	1.12	0.93	0.81	0.74	0.56	0.42	0.35
10^3 k exp. (cm./sec.$^{\frac{1}{2}}$)	1.65	1.35	1.08	0.98	0.72	0.53	0.47
10^6 D (cm.^{2}/sec.)	0.54	0.53	0.44	0.45	0.41	0.41	0.43

TABLE IV

Diffusion of Cu^{++} Ions of Concentration a = *0.2 M/l. into Cellulose Xanthates of Various CS_2 Contents in the Presence of Na_2SO_4, 1 M/l.*

b ($M/l.$)	0.165	0.135	0.125	0.095	0.095	0.065
z (Eq. (13))	0.66	0.71	0.74	0.81	0.81	0.92
10^3 k exp. (cm./sec.$^{\frac{1}{2}}$)	0.83	0.86	0.90	1.05	1.09	1.19
10^6 D (cm.^{2}/sec.)	0.40	0.37	0.38	0.41	0.44	0.42

calculate the diffusion coefficient D, we identified k with $\xi/\sqrt{t}$. The D values found prove to be constant within a large range of concentrations. We know from the theoretical part that the actual D value will be about twice as large. However, even if this is accounted for, the D values found are remarkably low.

For this reason we have also carried out a direct determination of D. A test tube was covered evenly with a thin layer of viscose and then dipped into 1 M ammonium sulphate. After solidification to a gel and washing with ammonium sulphate, the skins were stripped off and hung from a glass tube by means of a small rubber ring. The sacks thus formed had a thickness of about 0.2 mm. This thickness was determined after the experiment by cutting off the sack, converting the cellulose xanthate into cellulose, washing out the copper by means of dilute HNO_3, drying the gel and weighing. This dry weight determined the volume of the original gel, because its degree of swelling was known. From the dimensions of the sack it was thus possible to calculate not only its surface but also its thickness.

The experiment consisted in first dipping the cellulose xanthate sack into a copper solution for about 0.5 hour. The brown precipitate is formed in the entire gel, which is then rinsed with ammonium sulphate solution on the outside, filled with a solution of copper in ammonium sulphate solution and immersed in ammonium sulphate free from copper. Both outer and inner solutions are stirred. After about 30 minutes, the amount of copper in the outer solution is determined colorimetrically, using the blue color in excess ammonia. The concentration of copper in the sack was corrected for loss of copper by diffusion. The diffusion coefficient found in this manner was $(1.6 \pm 0.3) \times 10^{-6}$ cm.^{2}/sec. Even if we allow for a factor 2 in the D values of Table III, these values

are still off by a factor 2. It is possible that this discrepancy is due to a still larger difference between the cylindrical k value and the linear $\xi/\sqrt{t}$ value than that assumed. This problem must be reexamined in later work.

Summary

If the molecules of a diffusing substance react with the medium into which they diffuse in such a manner that they no longer take part in the diffusion process, a sharp boundary results which is displaced at a rate determined by the conditions of the experiment.

The theory of this phenomenon is discussed and the results compared with a few preliminary experiments.

References

1. Communication No. 34 from the Laboratory for Cellulose Research, AKU and Affiliated Companies, Utrecht, Netherlands.
2. Hermans, P. H., Contribution to the Physics of Cellulose Fibres, p. 23. Elsevier, Amsterdam, 1946; Hermans, P. H., and Vermaas, D., *J. Polymer. Sci.* **1**, 149 (1946).
3. Hartley, G. S., *Trans. Faraday Soc.* September meeting, 1946, to appear shortly. Robinson, C., *Trans. Faraday Soc.*
4. King, G., *Trans. Faraday Soc.* **41**, 479 (1945).
5. Calvet, E., *Compt. rend.* **212**, 542 (1941); **214**, 716, 767 (1942). Schulz, G. V., *Z. physik. Chem.* **180A**, 1 (1937); **52B**, 253 (1942). Hermans, P. H., and Weidinger, A., *J. Colloid Sci.* **1**, 185 (1946); Champetier, G:, *J. chim. phys.* to appear shortly.
6. Adair, G. S., *Biochem. J.* **14**, 762 (1920); **15**, 620 (1921).
7. Duclaux, J., Diffusion dans les gels et les solides, II, p. 13. Hermann, Paris, 1936.
8. Barrer, R. M., Diffusion in and through Solids, p. 32. Cambridge Univ. Press, 1941.
9. Bungenberg de Jong, H. G., unpublished research in 1926.

Note added in proof: Mr. Levison (Arnhem) kindly drew the author's attention to the fact that a diffusion problem similar to that considered in the present article was treated by A. V. Hill, *Proc. Roy. Soc. London* **B104**, 41 (1929).

DIFFERENCES BETWEEN SILICA AND SILICA-ALUMINA GELS I. FACTORS AFFECTING THE POROUS STRUCTURE OF THESE GELS

C. J. Plank and L. C. Drake

From Socony-Vacuum Laboratories (A Division of Socony-Vacuum Oil Company, Inc.), Research and Development Department, Paulsboro, N. J.

Received August 9, 1946; Revised July 9, 1947

Introduction

While an enormous amount of work has been done on the study of silica gels, it is very hard to find, outside the patent literature, any appreciable consideration of the properties of silica-alumina gels. In view of the known differences in the catalytic properties of these two types of gel—particularly in regard to catalytic cracking—it seems highly desirable to find the fundamental chemical and physical differences between them. The work here reported represents the start of such a study.

The preparation of a true gel of silica-alumina for catalytic purposes involves the following steps: (1) Preparation of a clear hydrosol by addition of a water glass solution to an acid solution. (2) Gelation of the sol. (3) Regulation of the final density of the gel by allowing the hydrogel to age. (4) Removal of the sodium ions by base exchange with cations such as NH_4^+ or AlO^+. (5) Washing the hydrogel free of excess anions, and (6) drying the gel. For comparative purposes, exactly the same processing steps were followed in preparing the silica gels, also. The present investigation represents an attempt to study the effects of variations in the first four steps. It is, of course, impossible to vary steps (1) and (2) independently, but otherwise the study involves changing a single variable at a time.

Certain very significant distinctions between silica and silica-alumina gels have been discovered by measurement of the particle densities and surface areas of the dried gel samples.

Experimental

The surface areas were determined by gravimetric measurement of the nitrogen adsorption isotherm using the McBain-Bakr quartz-spring balance method (1). The surface areas were then calculated by the B.E.T. method (2) from the adsorption isotherm. This method has been used in

our laboratories to determine surface areas of a great number of samples of highly porous materials. In this work it was found that the reproducibility of the results was about $\pm 2\%$.

The particle density (McBain's apparent density) (3) is defined as the density determined by mercury displacement. The apparatus used was suited to samples of about 5 g. The method consisted simply of a measurement of the weight of the sample followed by a determination of the volume of mercury displaced by the sample. The apparatus involved essentially a sample bulb connected by a spherical ground glass joint to one arm of a U-tube mercury reservoir. The other arm of the reservoir was graduated in 0.1 ml. divisions. The remaining parts of the apparatus provided for evacuation of the sample bulb. Thus the method of measurement was simply to evacuate the bulb, fill the bulb with mercury and record the volume of mercury in the graduated arm. The mercury was then forced out of the sample bulb into the reservoir, the weighed sample inserted and the process repeated. The volume displaced by the gel was then the difference between the two volume readings. Calibration of the apparatus with samples of known density showed its accuracy to be within $\pm 1\%$.

Due to very considerable difficulties which would have been encountered in trying to perform the complete gel processing under isothermal conditions, another method was employed to eliminate the effect of the temperature variable. This was to prepare simultaneously all gel samples made for investigating the effect of a given variable. Thus, all members of any given series were processed under identical temperature conditions.

The stock solutions used in making up the gels were a water-glass solution containing 0.210 g. SiO_2/cc. and a 3.75 N HCl solution. The water-glass solution was made by diluting the concentrated "N" brand sodium silicate sold by the Philadelphia Quartz Company. In preparing the gels for this study both of these solutions were further diluted to give the desired solids content. In specifying the solids content the term *pc* is used. This is an arbitrary unit of concentration used industrially by some catalyst manufacturers and means "product concentration." That is, *pc* is defined as the total weight of desired oxides $\times$ 100 divided by the total volume of the sol.

The general procedure used in making and processing the gels may be described as follows. The necessary amount of water was added to the desired quantities of the two stock solutions. The water-glass solution was then added to the acid solution with vigorous mechanical agitation. In making the silica-alumina gels the aluminum salt was dissolved in the acid solution prior to the mixing. The sols were perfectly clear and transparent and, in general, set to transparent hydrogels within a few minutes.

Usually in less than an hour the hydrogels were firm enough to be cut into cubes about $\frac{3}{4}$ in. on a side. They were then allowed to age for the desired length of time. Following this the cubes were transferred to Büchner funnels, stoppered at the bottom, and covered with the appropriate base exchange medium. Base exchange is essential, especially in the case of the silica-alumina gels, if the sodium content is to be reduced to trace amounts.

In this process the gel was covered with its own volume of base exchange solution. At the end of two hours the solution was drained off and the procedure was repeated twice. Then the fourth portion of exchange solution was allowed to sit in contact with the gel overnight (16 hours). The gel was then washed free of the excess anions introduced by the exchange medium. To standardize the washing process, exactly 25 washes were used. Each wash represented a volume of distilled water equal to the volume of the gel. This washing was more than sufficient to remove all undesired anions, a fact which was checked for each gel by testing the wash water in each of the last 8 washes. Finally, the washed gel was dried at 240°F. ± 10°F. for 16 hours. For the members of a given series the variation in drying temperatures was less than this indicated variation, for all of any one series were dried in one single drawer of the drying oven at the same time.

Following this procedure, and changing only one variable at a time, 6 different series of silica gels were prepared, as were an equal number of silica-alumina gel groups. The silica-alumina gels were all made to contain 93% SiO_2 and 7% Al_2O_3 on a dry basis.

The Effect of pH

Five 50-g. batches of silica gel were made at $pc = 4.0$. The quantity of acid was varied to give gels at pH = 5.5, 6.5, 7.5, 8.5, and 9.5 ± 0.1, respectively. After finding by trial experiments the exact quantities of acid to be added to give the desired pH, the solutions for all the gels were prepared and the sols then made almost simultaneously. In all cases the pH of the sols and gels was determined with the glass electrode. The gels were then allowed to age for 24 hours before being base-exchanged with 1% NH_4Cl.

In an identical manner an equivalent group of silica-alumina gels was prepared. The properties of the dried gels resulting from these two series are shown in Table I and Fig. 1.

The Effect of pc

Seven one-liter batches of silica gel were prepared at pH = 7.0 ± 0.1 varying the water content to give gels at $pc = 1.5, 2.0, 3.0, 4.0, 5.0, 7.0,$

TABLE I

The Effect of pH of Formation on the Porous Structure of SiO_2 and $SiO_2 - Al_2O_3$ Gels

A. Silica Gel: $- pc = 4.0$. Base-exchanged with 1% NH_4Cl after 24 hrs.

pH	Particle density	Surface area	Particle diameter	Pore diameter
	g./cc.	*m.²/g.*	*A.U.*	*A.U.*
5.5	0.95	625	44	56
6.5	0.84	526	52	84
7.5	0.83	516	53	87
8.6	0.86	529	52	82
9.5	0.86	526	52	82

B. Silica-Alumina Gel: $- pc = 4.0$. Base-exchanged with 1% NH_4Cl after 24 hrs.

pH	Particle density	Surface area	Particle diameter	Pore diameter
5.6	1.60	372	74	27
6.5	1.54	434	63	26
7.5	1.39	552	50	28
8.5	1.28	596	46	32
9.5	1.21	596	46	37

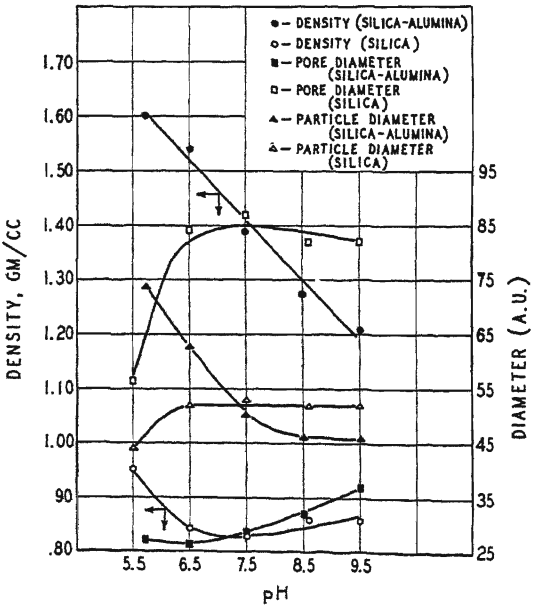

FIG. 1. Effect of pH on gel structure.

TABLE II

The Effect of pc on the Porous Structure of Silica and Silica-Alumina Gels

A. Silica Gel — pH = 7.0 ± 0.1. Base-exchanged with 1% NH_4Cl after 48 hrs.

pc	Particle density	Surface area	Particle diam. (Av.)	Pore diam. (Av.)
	g./cc.	$m.^2/g.$	*A.U.*	*A.U.*
1.5	0.90	633	43	63
2.0	0.87	587	46	70
3.0	0.90	568	48	69
4.0	0.89	544	50	73
5.0	0.82	464	59	99
7.0	0.81	439	62	106
10.0	0.69	362	75	164

B. Silica-Alumina Gel — pH = 7.0 ± 0.1. Base-exchanged with 1% NH_4Cl after 48 hrs.

pc	Particle density	Surface area	Particle diam. (Av.)	Pore diam. (Av.)
1.5	1.45	488	56	28
2.0	1.41	526	52	28
3.0	1.39	540	51	29
4.0	1.38	551	50	29
5.0	1.31	569	48	32
6.0	1.25	586	47	35

and 10.0, respectively. Due to the very wide variation in the gel times at the different *pc* values a rather long aging time had to be allowed. The longest gel time, occurring at $pc = 1.5$, was 16–20 hours to give a firm gel which could be cut into cubes. Therefore, all the gels of this group were allowed to age 48 hours from the time of mixing the sol before being base-exchanged. Thus, the assumption has tacitly been made here that the process of setting to a gel and the subsequent syneresis process are completely continuous in nature. Actually, this is hardly an assumption in view of the fact that no sudden change in the properties of hydrogels occurs at the time of setting to a firm gel. To a limited extent this has been proved for silica gel by Hurd, Frederick and Haynes (4) and by Prasad, Mehta and Desai (5) and for a wide variety of other hydrous oxide gels by Prakash (6).

Again an equivalent set of silica-alumina gels was prepared in an identical manner except that in this case no gel could be made above $pc = 6.0$. This was due to the fact that above this *pc* the gel time was too short to permit complete mixing of the acid and water glass solutions. Therefore, the silica-alumina series included gels made at $pc = 1.5$, 2.0, 3.0, 4.0, 5.0, and 6.0, respectively. The properties of the dried gels obtained from these two series are shown in Table I and Fig. 2.

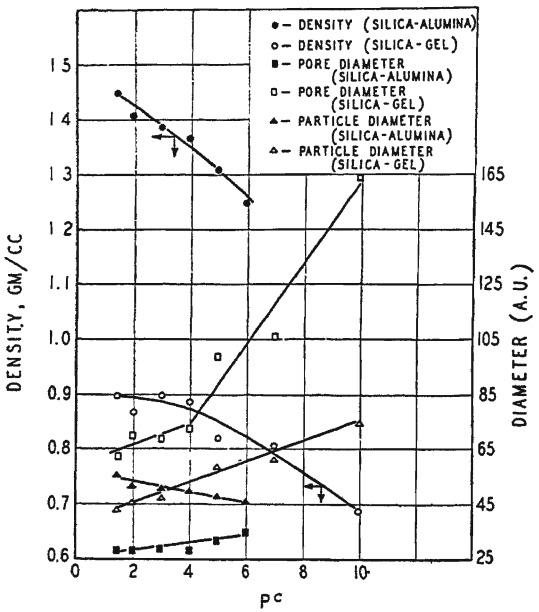

FIG. 2. Effect of *pc* on gel structure

The Effect of Aging Time and Base Exchange Medium

A single 150 g. batch of silica gel was prepared at pH = 7.0 and *pc* = 5.0. This was divided into 3 equal portions—one was base-exchanged immediately, the second after 24 hours and the third after 168 hours. Each of these portions was further divided into 4 equal batches, each of which was treated with a different base exchange medium. These base exchange solutions were (1) H_2O—as a blank, (2) 1% NH_4Cl, (3) 1% HCl and (4) 1% $Al_2(SO_4)_3$. Thus there were obtained 3 different series of gels showing the effects of different base exchange media at a constant aging time. Or looking at the group another way, there were 4 series of gels showing the effect of aging time with a given base exchange medium.

Exactly equivalent sets of silica-alumina gels were made from a single 150 g. batch of gel made at pH = 7.0 and *pc* = 5.0. The properties of the dried silica gels are shown in Table III (and Figs. 3, 4 and 5) and those of the dried silica-alumina gels in Table IV (and Figs. 3, 4 and 6).

After the effects of the base exchange media, 1% NH_4Cl, 1% $Al_2(SO_4)_3$, and 1% HCl, had been ascertained, it was decided that the relative effects of acidic and basic exchange media should be determined. For this purpose a single 100 g. batch of silica gel was prepared at pH = 7.0 and *pc* = 5.0. This gel was allowed to age 24 hours and was then divided into 4 portions which were base-exchanged with 1% HAc, 1% NH_4Cl, 1%

$(NH_4)_2CO_3$, and NH_3 at pH = 11, respectively. Again a comparable series of silica-alumina gels was made. The properties of the resultant gels are shown in Table V.

TABLE III

The Effect of Syneresis and Processing Variables on the Porous Structure of SiO_2 Gel

Syneresis time	Physical properties	Base exchange medium			
		H_2O	NH_4Cl	HCl	$Al_2(SO_4)_3$
hrs.		pH = 6–6.5	pH = 5.3	pH = 0.6	pH = 3.2
0	Particle Density (g./cc.)	0.88	0.88	1.23	1.14
	Surface Area ($m.^2/g.$)	400	478	694	755
	Av. Particle Diameter (A.U.)	68	59	39	36
	Av. Pore Diameter (A.U.)	102	86	32	33
24	Particle Density	0.86	0.86	0.97	0.81
	Surface Area	434	520	704	746
	Av. Particle Diameter	63	52	39	37
	Av. Pore Diameter	96	82	50	63
168	Particle Density	0.84	0.84	0.75	0.68
	Surface Area	444	509	524	566
	Av. Particle Diameter	62	53	52	48
	Av. Pore Diameter	94	82	100	108

TABLE IV

The Effect of Syneresis and Processing Variables on the Porous Structure of Silica-Alumina Gel

Syneresis time	Physical properties	Base exchange medium			
		H_2O	NH_4Cl	HCl	$Al_2(SO_4)_3$
hrs.					
0	Particle Density (g./cc.)	1.36	1.29	1.39	1.56
	Surface Area ($m.^2/g.$)	551	591	560	384
	Av. Particle Diameter (A.U.)	50	46	49	72
	Av. Pore Diameter (A.U.)	30	33	28	32
24	Particle Density	1.33	1.26	1.25	1.38
	Surface Area	546	614	695	514
	Av. Particle Diameter	50	44	40	54
	Av. Pore Diameter	32	34	30	32
168	Particle Density	1.22	1.13	1.13	1.20
	Surface Area	615	641	751	579
	Av. Particle Diameter	44	42	36	48
	Av. Pore Diameter	34	40	34	28

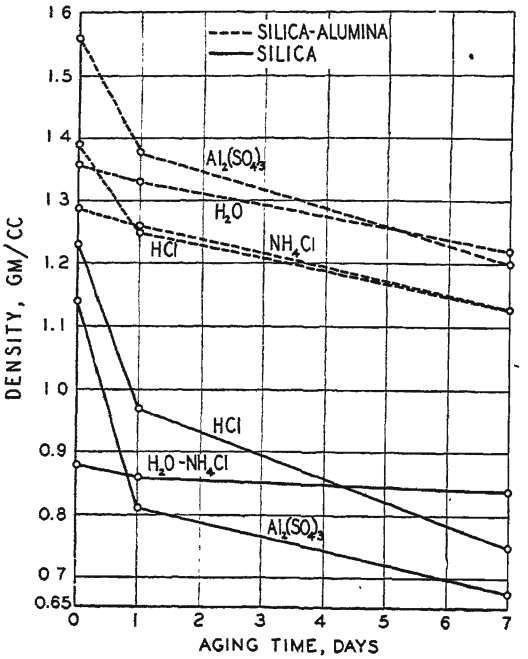

FIG. 3. Effect of base exchange and syneresis on density.

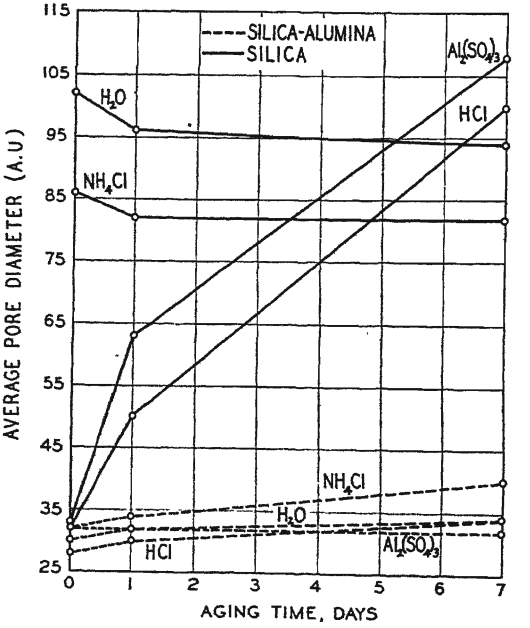

FIG. 4. Effect of syneresis and base exchange on pore diameter.

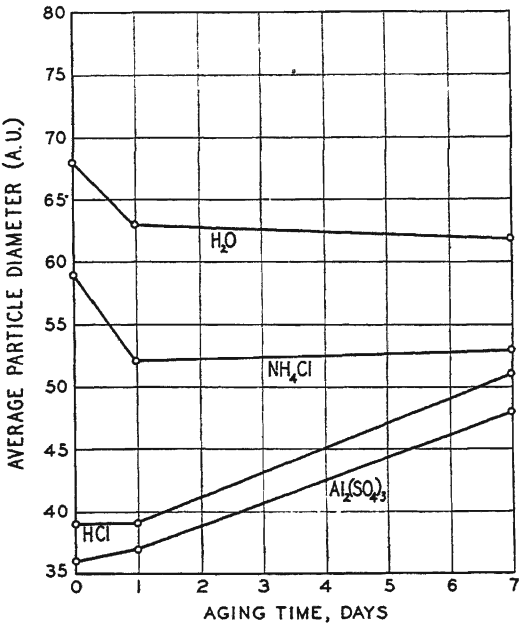

FIG. 5. Effect of syneresis and base exchange on particle diameter of silica gel.

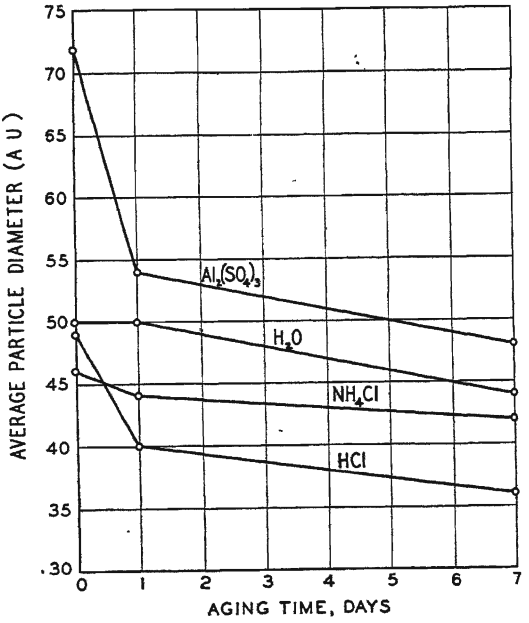

FIG. 6. Effect of syneresis and base exchange on particle diameter of silica-alumina gel.

TABLE V

Comparison of the Effects of Acidic and Basic Exchange Media on the Porous Structure of Silica and Silica-Alumina Gels

A. Silica Gel — pc = 4.0. Base-exchanged after 24 hrs.

Base exchange medium	pH	Particle density	Surface area	Particle diameter	Pore diameter
		g./cc.	*m.²/g.*	*A.U.*	*A.U.*
1% HAc	2.7	0.87	656	42	64
1% NH_4Cl	5.3	0.76	413	66	126
1% $(NH_4)_2CO_3$	8.7	0.77	404	68	125
1% NH_4OH	11.0	0.79	354	77	138

B. Silica-Alumina Gel — pc = 4.0. Base-exchanged after 24 hrs.

Base exchange medium	pH	Particle density	Surface area	Particle diameter	Pore diameter
1% HAc	2.7	1.42	478	56	31
1% NH_4Cl	5.3	1.32	540	51	33
1% $(NH_4)_2CO_3$	8.7	1.12	593	46	44
NH_4OH	11.0	0.97	535	51	64

Discussion of Results

The type of calculations made from these data is based on the concept of these gels as being composed of discrete particles of hydrous oxides. Obviously, to account for the mechanical strength of the dry gels the particles must be firmly interconnected. From the surface area measurements, and from the fact that the —OH content of such gels is probably less than 1% (7), it is clear that the bridges contribute a minor portion of the total surface area.

In the hydrogel stage the micelles are bonded together into chains, probably through hydrogen bonding. That such discrete particles make up the hydrogels seems conclusively proved by the drying characteristics of these gels. The regular shrinkage which accompanies syneresis and drying of the gels is certainly most easily explained as a loss of water between short chains of the hydrous oxide to form the micelles. Finally, at the latter stages of drying, actual cross-linking between the micelles occurs. For these gels the assumption that the micelles approximate a spherical shape seems justified by the equivalence of all four directions in the silica tetrahedra. There seems to be no reason for expecting polymerization in preferred directions to give chains or plates.

Although the assumption of a spherical shape of the micelles was used as a basis for calculating the average particle diameters the values obtained for these diameters are not at all arbitrary. A few simple calcula-

tions demonstrate the fact that exactly the same numerical results are obtained in each of the following cases:

(1) If the particles are spherical with diameter = d, Volume = $\pi d^3/6$ and Area = πd^2, then $d = 6\ (V/A)$.
(2) If the particles are cubes with length of side = d, Volume = d^3, Area = $6d^2$, then $d = 6\ (V/A)$.
(3) If the particles are cylinders with height = diameter = d, Volume = $\pi d^3/4$ and Area = $3\pi d^2/2$, then $d = 6\ (V/A)$.

Thus it is evident that so long as the micelles approximate any of these simple geometrical shapes, the values reported in the accompanying tables as average particle diameters are actually significant figures. They should give close approximations to the true average dimensions of the particles. These values are calculated from the surface area (A) and the reciprocal of the real density of the gel. For these calculations the real densities have been assumed to be constant—2.18 g./cc. for the silica-alumina gels and 2.20 g./cc. for the silica gels. This assumption is based on a large number of previous determinations of the real densities of comparable gels. From these measurements it can safely be stated that the assumed real densities are within 2% of the values which would have been determined by actual experiment. The method which has been used to determine the real density of such gels is a pycnometric measurement of the volume of water displaced by a known weight of the gel. The water penetrates all but the very tiniest of pores and thus the volume of water displaced by the gel represents very nearly the true volume of the gel. To obtain reasonable accuracy by this method a larger quantity of gel should be used than was available in the case of most of the samples prepared during this study.

The average pore diameters were calculated in a strictly comparable manner. Here, however, in the formula

$$d = 6(V/A)$$

the volume specified is the pore volume, which is numerically equal to the (particle density)$^{-1}$ − (real density)$^{-1}$.

The data in Tables I–V show some very striking differences between the two types of gel, with regard to the effects on the gel structure of preparational and processing variables. Since the second paper of this series attempts to present a unified explanation of these phenomena, it will suffice here merely to delineate the actual results.

The Effect of pH

Silica-alumina gels appear much more susceptible to property changes as a result of variations in the hydrosol pH than do silica gels. In fact,

in the pH range 6.5–9.5 the silica gel properties are constant within experimental error. However, between pH 6.5 and 5.5 a sudden change takes place in the silica gel resulting in greatly increased density and greatly decreased particle size. This effect of pH on particle size has been observed previously (8). In the case of the silica-alumina gel, however, throughout the pH range studied (5.5–9.5) a rise in the pH of the sol causes a regular decrease in density and a corresponding decrease in the particle size. Thus, at lower pH values both gels are increased in density but the average particle size is decreased for silica gel and increased for silica-alumina gel.

The Effect of pc

An increase in the solids content of the hydrosol has a marked effect on the properties of both types of gel. Again, however, the effects differ for the two gel types. In both cases the density decreases as the *pc* increases. However, the accompanying particle size change is toward an increase for silica gel and toward a decrease for silica-alumina gel. That is to say, as the *pc* of a silica hydrosol increases, the surface area decreases markedly, while for a silica-alumina gel the surface area increases substantially with increased *pc*.

The Effect of the Base Exchange Medium

To a great extent it was found that the effect of the base exchange medium depended on the pH of the medium. Thus, those solutions giving low pH resulted in higher densities and smaller particle sizes for silica gel, while the higher pH media reversed this effect. On the other hand, with silica-alumina gels those media giving low pH resulted in higher densities and larger particles. This is true, surprisingly, even in the case of HCl which dissolves practically all of the Al_2O_3. To this extent there is complete parallelism with the changes produced by variations in the pH of formation. There are, however, minor specific effects attributable to the media in themselves and not merely to the pH.

The results shown in Tables III and IV cannot be compared directly with those given in Table V, for the former were obtained from experiments performed several months prior to those reported in Table V. Thus, the room temperature conditions may have been decidedly different. In both cases, however, one of the base exchange solutions used was 1% NH_4Cl. Therefore, this solution can be used as a standard against which to compare the other media. Such a comparison shows that, although the acetic acid and $Al_2(SO_4)_3$ solutions are in the same pH range, they produced somewhat different results on silica gel. For example, $Al_2(SO_4)_3$ exchange gives a gel with lower density than one exchanged

with NH_4Cl (0.81/0.86). However, acetic acid exchange gives a denser gel than one exchanged with NH_4Cl (0.87/0.76). In this particular result, the HAc appears to resemble HCl as a base exchange medium more than it does $Al_2(SO_4)_3$.

In general, it is apparent that during base exchange silica gel is relatively insensitive to pH changes at pH above 5. However, silica-alumina gel appears quite sensitive to pH as high as 11. But somewhere in the pH range 8.5–11 there is a reversal in the general tendency of the particle size to decrease with increasing pH.

The Effect of Aging

From Tables III and IV it is clearly shown that the primary effect of prolonged aging is to moderate any change which might be produced by subsequent base exchange. This is true for both types of gel. There are cases, of course, where the aging effect may be overcome. If the exchange medium is sufficiently acid to dissolve the alumina from silica-alumina gels, as in the case of 1% HCl, the resultant gel has a high surface area even when exchanged after prolonged syneresis. The density, however, is not correspondingly high, showing that increased syneresis overcomes the tendency of low pH exchange to give high density.

Thus, when acidic base exchange media are used, the effect of increased aging prior to the exchange is to decrease the surface area and decrease the density for silica gels, but to increase the surface area and decrease the density in the case of silica-alumina gels.

Acknowledgment

The authors wish to express their appreciation for the assistance of J. L. Hammond, R. W. Sauer and M. Kaigh in performance of the experimental work. The encouragement and advice of R. C. Hansford in connection with this program of research is gratefully acknowledged.

Summary

By measurement of the particle densities and surface areas of a number of series of silica and silica-alumina gels the effects of several processing variables on their porous structure have been determined. From these data the average particle sizes and pore sizes of the dried gels were calculated. The calculations are based on an assumption that the ultimate particles making up the gels are essentially spherical in shape. The following preparational variables were studied: (a) the pH of the hydrosol, (b) the solids content of the hydrosol, (c) the length of the aging time prior to base exchange, and (d) the nature of the base exchange solution.

It was found that these factors had markedly different effects on the two types of gel. The following general conclusions were drawn: (1) Low

pH favors higher density and higher surface area for silica gel. This is true both in regard to the pH of formation of the hydrosol and with respect to the pH of the base exchange medium. (2) In the case of silica-alumina gel, lower pH favors higher density and lower surface area. (3) Increased solids content of the hydrosol gave decreased density with both types of gel. However, at the same time the surface area decreased for silica gel, but increased for silica-alumina gel. (4) The effect of increased aging time was to moderate any change which could be produced by subsequent base exchange treatment.

References

1. McBain, J. W., and Bakr, A. M., *J. Am. Chem. Soc.* **48**, 693 (1926).
2. Brunauer, S., Emmett, P. H., and Teller, E., *ibid.* **60**, 309 (1938).
3. McBain, J. W., The Sorption of Gases by Solids, p. 79. London, 1932.
4. Hurd, C. B., Frederick, K. J., and Haynes, C. R., *J. Phys. Chem.* **42**, 85 (1938).
5. Prasad, M., Mehta, S. M., and Desai, J. B., *ibid.* **36**, 1324 (1932).
6. Prakash, S., *ibid.* **36**, 2483 (1932).
7. Tamele, M. W., Paper presented at A.A.A.S. Conference on Catalysis, Gibson Island, 1945.
8. Prasad, M., Mehta, S. M., and Desai, J. B., *loc. cit.*

DIFFERENCES BETWEEN SILICA AND SILICA-ALUMINA GELS II. A PROPOSED MECHANISM FOR THE GELATION AND SYNERESIS OF THESE GELS

C. J. Plank

From Socony-Vacuum Laboratories (A Division of Socony-Vacuum Oil Co., Inc.), Research and Development Department, Paulsboro, N. J.

Received August 9, 1946; revised July 9, 1947

At the very outset of this discussion it must be admitted that no rigorous proof of the proposed mechanism of the gelation and syneresis reactions is possible at the present time. Considerably more detailed and exhaustive study needs to be given to the problem to prove or disprove the hypotheses essential to the theory presented. However, it seems to the author that before any worker in the field of siliceous gels can hope to correlate the multitudinous facts from the literature, he must have at least a tentative theoretical framework on which to build. It is with the purpose of establishing such a tentative framework and of stimulating more detailed work to confirm or negate the hypotheses accepted by the author, that this paper was prepared.

One of the fundamental properties of these gels is the sensitivity of the gel time to the pH of the hydrosol. Fig. 1 shows this relationship for sols prepared at $pc = 4.0$ and at 17.5°C. ± 0.2°C. In this experiment the acid and water glass solutions were cooled to temperatures sufficiently low that the heat of reaction raised the temperature of the sol to 17.5°C. In the lower pH range this meant cooling to about 15.5°C. However, as the pH increased, the temperature differential decreased. A stop-clock was started the instant mixing of the two solutions was begun, and it was stopped at the moment a tip stick (a 6 mm. glass rod 30 mm. long) was held upright by the gel. This is, of course, an arbitrary definition of the time of gelation, but it is completely satisfactory for comparative purposes. This is essentially the "tilted stick" method described by Hurd and Letteron (1).

In view of the extremely rapid gelation of these hydrosols under certain conditions and of the great sensitivity of the gelation time to small pH changes, it seems highly probable that the reaction is ionic in nature. The belief expressed by many authors (2,3) that the initial reaction is the formation of monosilic acid and that this is followed by condensation—splitting out water between molecules—is not sufficient to explain the above-mentioned properties. Equation A gives an example

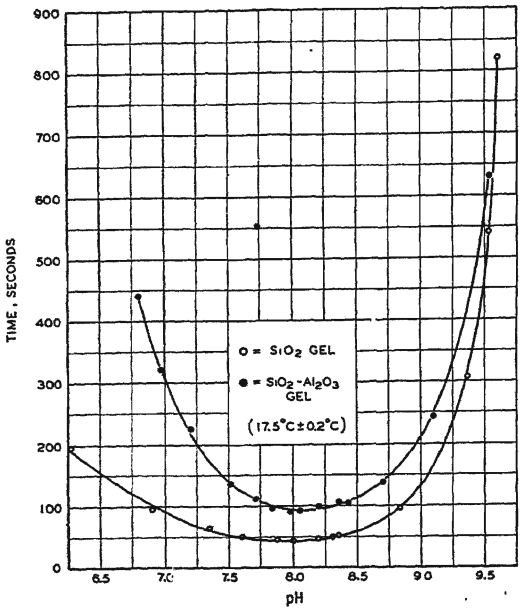

FIG. 1. The effect of pH on gel time.

of the type of reaction which we assume takes place in the formation of the micelles.

$$\text{—Si—O}^- + \overset{+}{\text{H}}_2\text{O—Si—} \xrightarrow{a} \text{—Si—O—H} < \begin{matrix}\text{H}\\ \text{—O—Si—}\end{matrix} \xrightarrow{b} \quad \text{(A)}$$

$$\text{—Si—O—Si—} + \text{H}_2\text{O}$$

Step *b* is probably the slow step in the reaction and is substantially irreversible. As shown in Fig. 1, the minimum gelation time occurs at about pH = 8. This is in agreement with the findings of Hurd, Raymond and Miller (4). Therefore, it is quite logical to expect the existence of both of these ions on mixing a water glass solution with an acid solution. In addition to the actual polymerization reaction (A) gelation involves, of course, linking of the micelles into chains. This linking undoubtedly occurs through hydrogen bonds between H_2O and —Si—OH groups of different micelles.

Thus, in the case of silica gel the initial reaction is the formation of micelles consisting of short silica chains linked together into a 3-dimensional network. Each chain is probably connected to others at only a few points. The slow reaction of syneresis—the setting and shrinking

process—involves essentially continued condensation between micelles and cross-linking (by condensation) between chains within the individual micelles, until finally the structure of a single micelle resembles the Zachariesen structure of glass (5).

From this picture it is evident that anything which can affect either the stability of the hydrogen bonds joining the micelles together or the rate of cross-linking will affect the density and surface area of the resulting gel after drying. Thus, any factor which causes disruption of the hydrogen bonds between micelles produces shorter chains of micelles which can rearrange to form a more closely packed system, and, in so doing, cause a higher density of the final dry gel. On the other hand, any factor which prevents cross-linking within the individual micelles gives greater surface area. That is to say, whenever complete cross-linking has occurred around any given Si atom, a certain amount of surface has been lost.

The results of two simple experiments are shown in Figs. 2 and 3, which illustrate some of the changes which take place in the hydrogels

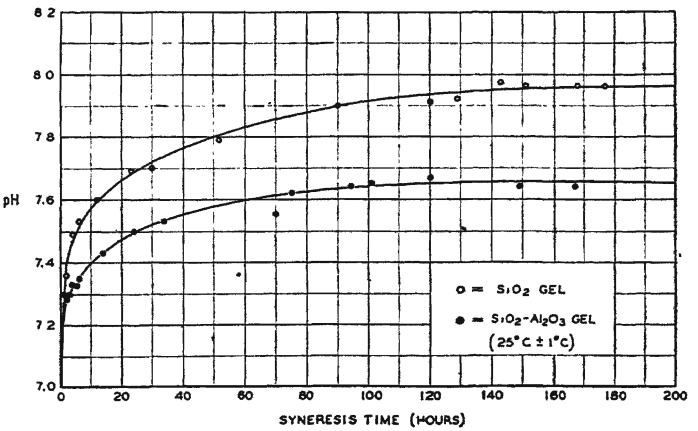

FIG. 2. The change of pH with syneresis.

of both silica and silica-alumina during syneresis. While such data have been given before for silica gel, the differences exhibited by silica-alumina gels have not been previously demonstrated. Fig. 2 shows that the pH of silica gel rises very rapidly to an equilibrium value considerably greater than that exhibited at the moment of forming the sol. As shown by Hurd and others (6,7) no break in the curve occurs at the moment of gelation. In the case of silica-alumina gels the pH rise is somewhat less. These experiments were carried out in a thermostatically controlled room which was held at 25°C. ± 1°C. Carefully calibrated electrodes (glass *vs.* calomel) were used, and the gels were kept in stoppered 3-neck flasks to prevent exposure to any atmospheric gases which might affect the pH.

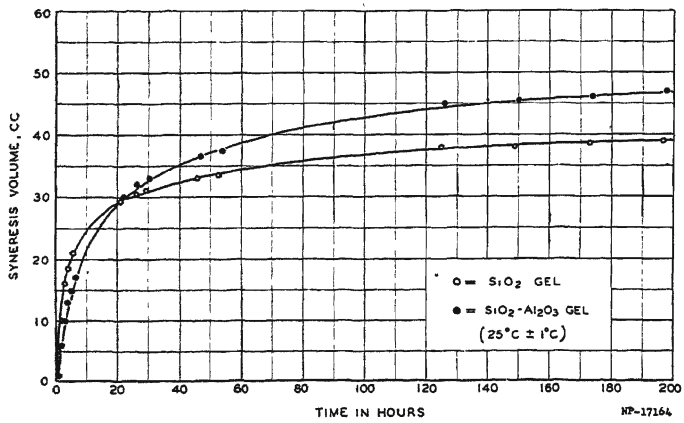

FIG. 3. Rate of syneresis.

Fig. 3 shows the rate of shrinkage of both types of hydrogels at 25°C. ± 1°C. in a closed system so that a condition of 100% relative humidity prevailed. Here it is seen that the initial rate of syneresis of the silica gel is considerably greater than that of the silica-alumina gel. However, this rate declines more rapidly for the silica gel, so that the actual shrinkage soon becomes equal for both types of gel, and finally the equilibrium shrinkage is greater for silica-alumina gel.

The actual experiment was performed as follows. Identical volumes (250 ml.) of 100% silica gel and a 93% silica-7% alumina gel were prepared in a waxed cylindrical mold. Both were made at $pc = 5.00$. The term pc is defined as the total weight of oxides (SiO_2 and/or Al_2O_3) $\times$ 100 divided by the volume of the sol. Using the same mold for both gels gave exactly the same external surface to both gels. After 20 minutes the gels were firm enough to be removed intact from the mold. Each gel was then suspended in a cheesecloth sling inside a waxed funnel which was connected to a graduated cylinder. The top from which the sling was suspended was waxed and sealed to the funnel. The funnel in turn was sealed to the graduate. Thus the whole set-up was air-tight. The process then consisted simply of reading the volume of liquid squeezed out by the syneresis process and correlating this with the time of syneresis. The whole experiment was carried out in a room thermostated to 25°C. ± 1°C.

Since the polymerization reaction itself involves no gain or loss of hydrogen ions the change of pH must be attributed to hydrolysis reactions of the type of equation (B).

$$\text{—Si—O}^- + \text{H}_2\text{O} \longrightarrow \text{—Si—OH} + \text{OH}^- \qquad \text{(B)}$$

The shrinkage of the gels can only be attributed to closer orientation of the micelles and cross-linking through the splitting out of H_2O.

The results of the experiments described in the first paper of this series (8) give a considerable insight into these processes and will form the basis for most of the present discussion. Table I shows data from the

TABLE I

The Effect of Syneresis and Processing Variables on the Porous Structure of SiO_2 Gel

Syneresis time	Physical properties	Base exchange medium			
		H_2O	NH_4Cl	HCl	$Al_2(SO_4)_3$
hrs.		pH = 6–6.5	pH = 5.3	pH = 0.6	pH = 3.2
0	Particle Density (g./cc.)	0.88	0.88	1.23	1.14
	Surface Area ($m.^2/g.$)	400	478	694	755
	Av. Particle Diameter (A.U.)	68	59	39	36
	Av. Pore Diameter (A.U.)	102	86	32	33
24	Particle Density	0.86	0.86	0.97	0.81
	Surface Area	434	520	704	746
	Av. Particle Diameter	63	52	39	37
	Av. Pore Diameter	96	82	50	63
168	Particle Density	0.84	0.84	0.75	0.68
	Surface Area	444	509	524	566
	Av. Particle Diameter	62	53	52	48
	Av. Pore Diameter	94	82	100	108

previous paper relevant to silica gel. From these data it is evident that if syneresis is allowed to proceed as long as a week before any further processing is done, variations in the processing have only minor effects on the final dry gel. The slightly lower density resulting from exchange with HCl or $Al_2(SO_4)_3$ can probably be attributed to the greater ionic volume of these hydrated cations (9); for in all cases the micelles will possess an adsorbed layer of ions. On the other hand, immediate base exchange prior to any appreciable syneresis produces very pronounced effects on the final silica gel. HCl or $Al_2(SO_4)_3$ exchange, for example, results in a great increase in the density and surface area of the dry gel. The surface area effect undoubtedly means that cross-linking within micelles is very greatly slowed down—probably due to adsorption of hydrogen or aluminyl ions on the —OH groups. The great increase in density indicates very definitely that the hydrogen bonds between micelles are loosened by the addition of these ions according to a reaction such as (C)

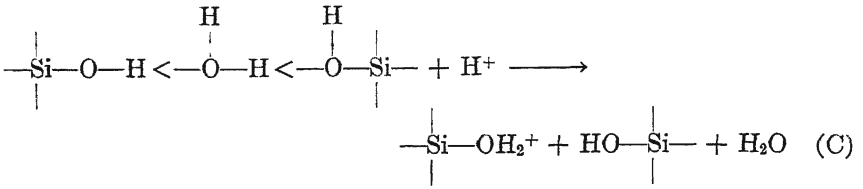

so that shorter micellar chains are formed, permitting a more closely packed arrangement of the chains.

The effect of varying the base exchange medium after 24 hours syneresis leads to two very important conclusions. With HCl and $Al_2(SO_4)_3$ exchange the density has dropped so far below the value for immediate exchange that one can only conclude that the intermicellar bonds (hydrogen bonding through water molecules) have been largely converted to more intimate bonds directly between $\begin{matrix}|\\-Si-\\|\end{matrix}$OH groups. Thus, the rate of condensation between micelles is evidently greatly retarded by an excess of H^+ ions. This is confirmed by the fact that the rate of syneresis of gels formed at pH = 8.5 is much faster than for gels formed at pH = 7.0. In contrast to this rapid condensation between micelles, the very slight change in surface area indicates very clearly that the cross-linking process (within the individual micelles) is very slow and that very little intramicellar condensation has occurred within 24 hours.

Thus, the picture which has been developed for the gelation and syneresis of silica gels is somewhat as follows. The micelles are formed according to an ionic reaction of the type of equation (A), and the bonds connecting the short chains within the micelle are hydrogen bonds of the type (D).

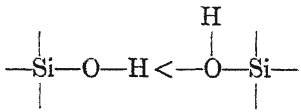

(D)

These bonds we have termed the intramicellar bonds. On the other hand, the micelles are joined into chains at the time of gelation by hydrogen bonding through water molecules giving a structure of the type (E).

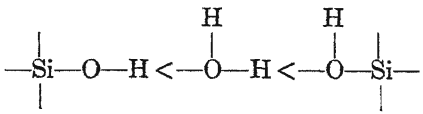

(E)

These we have termed the intermicellar bonds.

The most rapid reaction occurring during syneresis is the splitting

out of water from the intermicellar bonds, thus converting them to bonds of the intramicellar type. The rate of condensation is evidently decreased substantially in the case of both types of bonds by the presence of excess hydrogen ions. This means that the presence of acid promotes the peptization of intramicellar bonds giving a smaller average particle size. At the same time smaller micellar chains are produced (by peptizing the intermicellar bonds) which permits closer orientation of these chains to produce a much denser gel.

The density of the final gel is evidently determined by the average length of the chains connecting the micelles. Thus, once syneresis has proceeded far enough that a substantial proportion of the intermicellar bonds have been converted to bonds of type (D) a low density gel necessarily results. For then, even if a large number of small chains were produced by hydrogen bond rupture, the major gel structure would be unaffected. Ultimately these chains would condense at a few points thus creating a large number of small particles. Such a decrease in the average particle size would result in increased surface area. The total volume occupied by a given weight of gel, however, would be essentially unaffected by peptization at this stage of the aging process. Furthermore, once syneresis has proceeded practically to completion of reaction (A), step *b*, the introduction of acidic media, would have almost no effect at all.

The effects of increasing the silica concentration in the sol (*pc*) shown in the previous paper are (1) to decrease the density and (2) to decrease the surface area. Both of these effects are very readily explained in accordance with the foregoing discussion. With increasing silicate concentration one would certainly expect a greater amount of cross-linking. This factor would result in both lower density and lower surface area.

Silica-Alumina Gels

In the case of silica-alumina sols the gelation reaction itself follows a mechanism analogous to that involved in the formation of silica gels. The most important reaction is probably one of type (F).

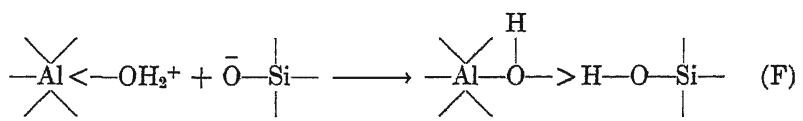

(F)

The experimental results on silica-alumina gels show that the presence of even the minor amount of alumina which these gels contain (atomic ratio Si/Al = 11.3) has a marked effect on the properties of the hydrogel. As a result, the porous properties of the dried products differ greatly. It is well known, of course, that the base exchange properties of the silica-

alumina gels are strikingly different from those of silica gel. Excellent synthetic zeolites, for example, may be prepared by forming silica-alumina gels above a pH of 8.5. Heretofore, it has generally been assumed that the explanation for this high base exchange capacity is the same as for natural zeolites. That is, it has been accepted that the Al atoms replace Si atoms in some of the tetrahedra, thus imparting a negative charge to the gel lattice and necessitating the presence of positive ions in the interstices for neutrality. The experimental results lead to the conclusion that this concept is probably not true.

The normal coordination number of the aluminum ion in acid solution is 6 (10). Since the aluminum ion is introduced into the gels from such a solution, it seems highly likely that the Al atoms should remain in this coordination state after gel formation. The percentage of base-exchangeable sodium contained in such an artificial zeolite (containing about 7% Al_2O_3) is about 4%. This requires an average charge of very nearly minus one (− 1) on each Al-containing group. Clearly, if the Al ions are then 6-coordinated, they must be terminal ions, *i.e.*, coordinated with —OH and OH_2 groups. Tetrahedral coordination for the aluminum atoms is not at all essential for producing zeolitic (*i.e.*, base exchange) properties. If four or more of the coordination positions be occupied by negative groups such as —OH or —O—Si(|)—, the group will possess an excess negative (−) charge. Thus, interstitial cations will be required for neutrality. Such an argument will, incidentally, explain how silica-zirconia gels possessing zeolitic activity can be produced. For it is obvious that replacement of Si in the tetrahedra (even if possible) by Zr would not result in a charged network. Examples of silica-zirconia gels possessing zeolitic capacity have been prepared in our laboratories.

This explanation is, further, consistent with the fact that silica gel, which possesses no catalytic cracking activity, may be converted to a very good catalyst by impregnating the gel with $Al(NO_3)_3$ and muffling the product. Obviously, in this material the Al atoms must be terminal atoms.

Referring again to Fig. 2, one can now explain the smaller rise in pH during syneresis of the silica-alumina gel as compared to that for silica gel. In both cases the rise is undoubtedly due to a reaction of the type (B). However, with the silica-alumina gels another reaction (G), proceeds simultaneously, using up part of the hydroxyl ions produced by reaction (B).

$$\text{—Al(—)—}OH_2 + OH^- \longrightarrow \text{—Al(—)—}OH^- + OH_2 \qquad \text{(G)}$$

One would be tempted to argue that this reaction should tend to increase the zeolitic capacity of the gel. However, if one calculates the actual extent of this hydrolysis from the pH rise, it is seen that it is much too small to be detected analytically.

Table II shows data, again from the first paper of this series (8), relevant to silica-alumina gels. The interpretation of these data in com-

TABLE II

The Effect of Syneresis and Processing Variables on the Porous Structure of Silica-Alumina Gel

Syneresis time	Physical properties	Base exchange medium			
		H_2O	NH_4Cl	HCl	$Al_2(SO_4)_3$
hrs.					
0	Particle Density (g./cc.)	1.36	1.29	1.39	1.56
	Surface Area (m^2./g.)	551	591	560	384
	Av. Particle Diameter (A.U.)	50	46	49	72
	Av. Pore Diameter (A.U.)	30	33	28	32
24	Particle Density	1.33	1.26	1.25	1.38
	Surface Area	546	614	695	514
	Av. Particle Diameter	50	44	40	54
	Av. Pore Diameter	32	34	30	32
168	Particle Density	1.22	1.13	1.13	1.20
	Surface Area	615	641	751	579
	Av. Particle Diameter	44	42	36	48
	Av. Pore Diameter	34	40	34	28

NA

parison with those of Table I for silica gel provides a definite picture of the differences between these two types of hydrogel. Due to the ionic nature of the micelles (SiO_2—Al_2O_3), it would be expected that the distance between micelles (pore diameter) would be essentially independent of the particle size. That is, the repulsion between the two Al-containing groups will depend only on the charge density on the groups and not on the size of the micelles. It is shown in Table II that such constancy of pore radius does hold for the silica-alumina gel.

The second very marked distinction between the effects of syneresis on the two types of gels is the fact that with silica-alumina gel the surface area increases steadily with increasing syneresis time. This shows a continued decrease in particle size, or, to put it another way, a decrease in cross-linkage, with increasing syneresis time. To explain this phenomenon it is necessary only to assume that the most important reaction involved in the syneresis of silica-alumina gels is a peptization reaction of the type of equation (H).

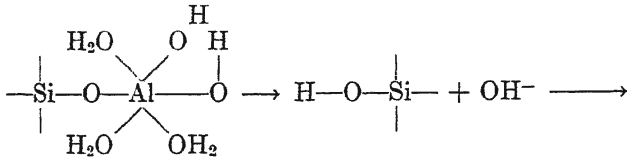

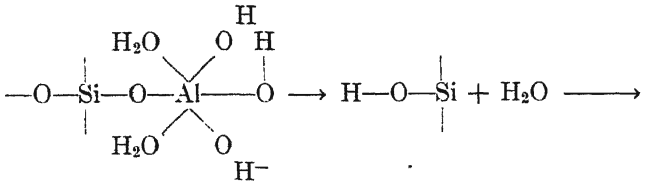

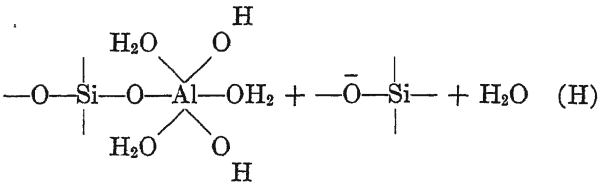

This reaction would tend to reduce the pH in the same manner as reaction (G). Such a reaction would result in shorter chains and decreased cross-linking (*i.e.*, decreased particle size). On the other hand, acidic media would reverse reaction (H) and actually promote condensation between the silica and alumina groups, according to a reaction of the type (I).

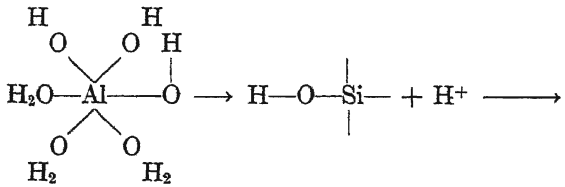

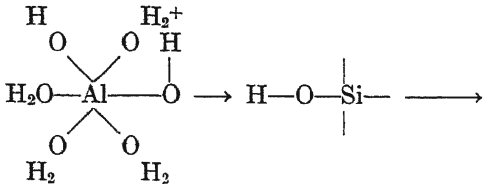

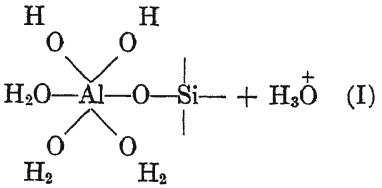

As a result of reaction (H) it is apparent that the alumina groups would be terminal groups. That is, the aluminum atoms would be connected to one or more $\leftarrow OH_2$ groups. To understand what is meant by this statement, it is probably simplest to contrast the proposed structure with that of pyrophyllite or montmorillonite. Fig. 4 shows the structure assigned by Pauling (11) to pyrophyllite. Here the gibbsite layer of alumina is condensed with two silicate layers. The alumina groups are definitely not what we are calling terminal groups, for condensation about the alumina is complete. On the contrary, in the case of the amorphous silica-alumina gels under discussion the evidence points toward a silicate

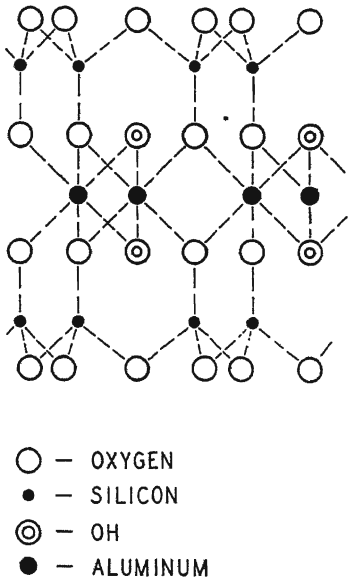

FIG. 4. Pyrophyllite and montmorillonite (ideal case).

structure condensed at random points with alumina groups. It is postulated that rather than entering the silicate structure in tetragonal coordination (and thus becoming part of a continuing lattice), the aluminum atom retains its octahedral coordination. Then, whether part of the coordination poisitions are filled by H_2O initially or only after the peptization reaction (H), the alumina necessarily becomes a terminating group in the lattice structure.

By occupying such a position the alumina groups should be much more readily subject to peptization or solution by acids than the gibbsite alumina in montmorillonite. The method of converting Bentonite clays to cracking catalysts, for example, involves dissolving the un-

desirable materials in acids (*e.g.*, 10% H_2SO_4). The remaining material contains generally around 20% Al_2O_3 by analysis, which shows the relative insolubility of this type of alumina.

On the other hand, the following experiment proved the fact that the alumina in amorphous silica-alumina gels is very soluble. Samples of a single batch of silica-alumina gel (90% SiO_2—10% Al_2O_3) were leached with HCl of varying strengths at three stages of the processing—(a) hydrogel stage after base exchanging with $Al_2(SO_4)_3$, (b) oven-dry stage—350°F., and (c)muffled stage—1275°F. In performing the leaching, a considerable excess of the acid solution was kept in contact with the gel at 16.0°C. ± 0.2°C. Small samples of the liquid were drawn off at certain intervals of time and analyzed colorimetrically for alumina. The results are shown in Table III. On washing samples A, B, C, and E

TABLE III

The Effect of HCl on Silica-Alumina Gel of Varying H_2O Content

	Hydrogel			Oven dried (350°F.)		Muffled (1275°F.)
	A	B	C	D	E	F
Normality HCl	0.101	0.338	0.522	1.008	.338	1.008
Time	Al_2O_3 extracted, %					
min.						
0	0	0	0	0	0	0
15	24.7	42.1	44.3	36.8	16.6	0.5
30	43.3	51.1	56.1	45.0	30.0	1.9
45	50.7	55.8	60.2	62.4	47.3	2.6
60	58.0	59.8	73.5	65.1	53.2	3.3
90	—	—	—	—	—	4.7
100	—	67.2	—	—	—	—
120	67.5	78.3	81.2	78.3	94.9	5.1
130	—	—	—	—	—	—
180	88.2	94.9	95.7	—	—	7.2
240	95.5	95.0	95.3	93.2	94.6	7.0
300	—	—	—	—	—	7.9
360	—	—	—		—	8.0
420	—	—	—		—	8.1
1440	—	—	—		93.1	
1500	95.3	94.9	95.6		—	

free of chloride and analyzing for residual Al_2O_3, it was found that less than 0.5% Al_2O_3 remained in the gel. After washing, sample E was dried and muffled and the particle density and surface area were determined.

These figures are compared with those for the corresponding unleached sample as shown in Table IV.

TABLE IV

The Effect of HCl-Leaching SiO_2-Al_2O_3 Gel

	Al_2O_3, %	Particle density	Surface area
Unleached Gel	10	1.02	560
Leached Gel*	<0.5	0.98	558

* Sample E from Table III.

From the speed with which dilute HCl removed the alumina even from the oven-dried gel and from the very slight effect which this leaching produced on the density and surface area, it seems certain that the aluminum atoms were indeed terminal. It has already been noted (Table I, col. 3) that HCl treatment of a silica gel after prolonged syneresis does not peptize the gel to any appreciable extent. Therefore, if the aluminum atoms had been completely condensed inside the lattice, they could not have been hydrolyzed with anywhere near the speed which was shown in this experiment. This principle is further supported by the very slight leaching of sample F (Table III) which had been muffled at 1275°F. prior to the acid treatment. In this case the aluminum atoms had evidently been converted into interior atoms by the splitting out of water between neighboring micelles, at the high temperature involved.

One consequence of equation (H) which may be subject to experimental confirmation by the electron microscope is the fact that the micelles of silica-alumina gels must decrease in size as syneresis proceeds. This is indicated by the results shown in Fig. 6 of the previous paper (8) —the effect of $Al_2(SO_4)_3$ or HCl exchange on the particle size of silica-alumina gels. If exchanged immediately after gelation, the average particle diameter is much greater than if the gel is aged for 24 hours. Further aging produces a much slower rate of change.

As already noted, the decrease in particle size according to equation (H) is accompanied by a pH decrease. This accounts, in part, for the smaller rise in pH during syneresis of the silica-alumina gel compared to that for silica gel. Since the major portion of the particle size change occurs during the first 24 hours aging, a large part of the pH differential should arise during that period. This effect is definitely shown in Fig. 2.

It will be noted that, although the density of the silica-alumina gel decreases with syneresis as does that of silica gel, the explanation is not the same. In the case of the silica gel the density depends on the rate of conversion of the hydrogen bonds between micelles to intramicellar bonds. However, in the silica-alumina gel the bonds between micelles are ionic

in nature. Therefore, as previously stated, the distance between the micelles is fairly constant. Thus, the density depends on the particle size. The smaller the particles, the less the density. It follows, then, that since increased syneresis results in increased hydrolysis and smaller particles, it must also result in lower density. This, of course, is in agreement with the facts.

The mechanism proposed for the syneresis of silica-alumina gels stresses the fact that the properties of the alumina groups overshadow those of the silica groups. First of all, due to coordination of at least 4 negative groups around each aluminum atom the micelles are negatively charged and an ionic structure is formed. Consequently, the properties of the resulting gels are determined very largely by the size of the micelles. This, in turn, is controlled primarily by the extent to which reaction (H) takes place. As the equation indicates, the rate of this reaction is greater the higher the pH.

In such a system of negatively charged micelles, rupture of even a relatively large number of hydrogen bonds between silica groups would have a very minor effect. Peptization would produce short silica chains which would ultimately recondense with other charged micelles, thus giving no overall change in the average particle size.

Summary

An ionic mechanism for the gelation of silica and silica-alumina gels is proposed as explanation of the very rapid gelation occurring within a certain pH range. The intermicellar bonds are hydrogen bonds and the condensation reaction is believed to be a slow reaction. This reaction is the essential feature of the syneresis, or aging, process in silica gel. Interruption of this process by introduction of an acidic medium causes rupture of the hydrogen bonds which, in turn, results in smaller particles, higher density and higher surface area.

In the case of silica-alumina gel the properties of the alumina overshadow those of the silica groups. Thus, the most important reaction occurring during syneresis is the rupture of the hydrogen bonds joining alumina groups to silica groups. This reaction, furthermore, is accelerated by hydroxyl ions. As a result, increased syneresis time and/or exchange with slightly basic media give smaller particles and, therefore, greater surface area. Acidic exchange media promote the condensation reaction, thus giving increased particle size.

In the case of silica-alumina gels decreased density invariably accompanies increased surface area (*i.e.*, decreased particle size). This is contrary to the effect found in silica gels. The explanation lies in the fact that the silica-alumina micelles are charged particles.

An important consequence of the proposed theory is that the alumina particles must be "terminal" groups. Thus the base exchange properties of such gels do not arise by substitution of Al for Si in tetrahedral groups.

REFERENCES

1. HURD, C. B., AND LETTERON, H. A., *J. Phys. Chem.* **36**, 604 (1932).
2. MYLIUS, F., AND GROSCHUFF, E., *Ber.* **39**, 116 (1906).
3. HURD, C. B., *Chem. Revs.* **22**, 403 (1938).
4. HURD, C. B., RAYMOND, C. L., AND MILLER, P. S., *J. Phys. Chem.* **38**, 663 (1934).
5. ZACHARIASEN, W. H., *J. Am. Chem. Soc.* **54**, 3841 (1932).
6. HURD, C. B., FREDERICK, K. J., AND HAYNES, C. R., *J. Phys. Chem.* **42**, 85 (1938).
7. HURD, C. B., AND MAROTTA, A. J., *J. Am. Chem. Soc.* **62**, 2767 (1940).
8. PLANK, C. J., AND DRAKE, L. C., *J. Colloid Sci.* 399 (1947).
9. JENNY, H., *J. Phys. Chem.* **36**, 2217 (1932).
10. WHITEHEAD, T. H., *Chem. Revs.* **21**, 113 (1937).
11. PAULING, L., *Proc. Natl. Acad. Sci. U. S.* **16**, 123 (1930).

PROPERTIES OF SAPONINS. SURFACE ACTIVITY AND DEGREE OF DISPERSION

R. Ruyssen and R. Loos

From the Laboratory of Physical Biochemistry, University of Ghent, Belgium

Received March 28, 1947

Introduction

The study of the properties of saponins was undertaken to obtain accurate information concerning their surface activity and the structure of their solutions. It was found that much of the available information in the literature was of limited significance, as it had been obtained with materials of ill-defined purity and origin, or with inadequate methods.

Definition of Saponins

The name saponin is given to substances whose properties have a certain analogy with those of soaps. A substance is termed a saponin, when it is a glucoside possessing to a greater or less degree the property of lowering the surface tension of water and producing a permanent foam by shaking. The detergent properties are associated with a strong hemolytic action (dilution of complete hemolysis ranging from a few thousand to several million cells).

The glucoside constitution is demonstrated by energetic hydrolysis with strong acids, which leaves a mixture of different glucides and an aglucon, called the sapogenin. Extensive studies on different sapogenins have been conducted by Ruzicka, Giacomello, Haworth, Kon (1) and others. They have proved that most saponins belong to two main groups:

(1) The steroid saponins, the genins of which are steroid compounds, *i.e.*, cyclopentanoperhydrophenanthrene derivatives. To this group belong digitonin (genin shown in Fig. 1), gitonin, sarsaponin.

(2) The triterpene saponins, the genins of which are pentacyclic triterpenes of the so-called β-amyrin group, which carry a carboxyl group. Representatives of this group are sapoalbin or *gypsophila* saponin (gypsogenin is shown in Fig. 2), α-hederin, *quillaia* saponin, glycyrrhizin.

The saponins of both groups have distinctly different behaviors. The steroid saponins are typically better crystallized, less soluble, and possess a higher genin content (44% for digitonin against 24% for sapoalbin). Their surface activity is influenced to a much lesser extent by the hydrogen ion activity. Senegin also belongs to the acid and more

soluble saponins, but the chemical constitution of the genin is not completely settled as yet. According to Jacobs and Isler (3) it is supposed to be a triterpene compound carrying two carboxyl groups. We could not

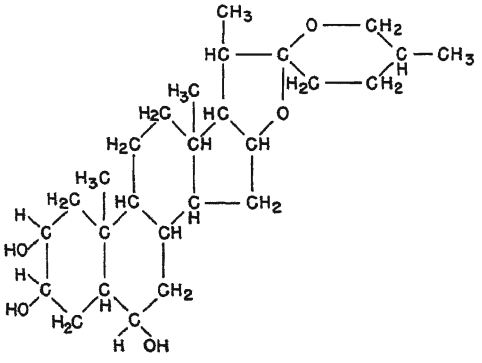

FIG. 1. The probable structure of digitogenin (2).

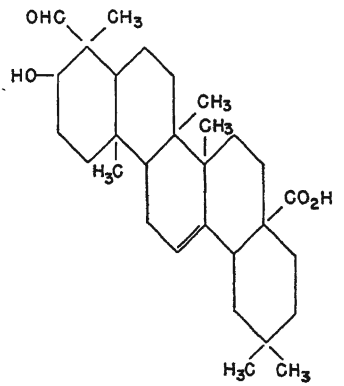

FIG. 2. Gypsogenin.

confirm this latter point, as our results tend to demonstrate that seneginic acid is monovalent. This contradiction may be due to a difference in the method of extraction.

EXPERIMENTAL

Preparation of the Saponins

A. Sapoalbin (*Gypsophila* saponin) was prepared from *Saponinum purum album* Merck. This product, commercially graded as pure, was stated by the manufacturer to have been extracted from the roots of *Gypsophila* species, mostly *Gypsophila struthium* L.

The concentrated dark brown solution was carefully neutralized with sodium hydroxide, the sodium sapoalbinate being easily reprecipitated from this solution with alcohol. The salt was dried *in vacuo*, dissolved in an equal weight of water and electrodialyzed for at least 24 hours. Nearly one-fourth of the substance was removed by diffusion through the dialyzing membrane. The solution thus obtained was acid (pH about 2) and the sapoalbinic acid was again precipitated with pure alcohol and ether. The saponin was further dried *in vacuo* at 30–40°C.

B. Senegin was prepared from the roots of *Polygala senega* L. by extraction with warm alcohol. When the solution was cooled to room temperature, a precipitate formed (this product was soluble in water but not in cold ethanol); from the remaining clear solution the senegin was precipitated by adding successively acetone and ether (not the reverse). The precipitate was collected by centrifugation and washed several times

with ether. The ether was evaporated *in vacuo* at low temperature. The product was dissolved in water (concentration 10%) and electrodialyzed for at least 24 hours until no more colored compounds passed through the membrane. The senegin was precipitated from the solution by adding an appropriate quantity of acetone followed by ether. The correct proportion of the organic liquids to be used was determined by a preliminary test on a small portion of the solution. The precipitate obtained was thoroughly washed with ether and dried *in vacuo* at low temperature.

Extraction of the roots was also tried with cold methanol; the product obtained and purified in the above described manner proved to be the same seneginic acid.

C. Digitonin was obtained from *Digitoninum* cryst. Merck by repeated precipitation with ether and recrystallization from hot water-alcohol mixture.

D. Blighiin or Blighia Saponin is an almost unknown saponin, which has been isolated for the first time in our laboratory (4). The saponin is extracted from the fruit shells of the congolese plant *Blighia Laurentii* (De Wildeman) with hot alcohol; after cooling, the saponin was repeatedly precipitated with acetone and ether. The precipitate was dried, dissolved in water and electrodialyzed; the blighiinic acid was precipitated with alcohol and ether and the purified product was dried *in vacuo* at 30–40°C.

This saponin is characterized by its high surface activity and hemolytic power. When hydrolyzed a crystallizable sapogenin was produced.

The Electrochemical Equivalent of the Saponins

As the exact chemical formula of the saponins is unknown, it is not possible to calculate their molecular weight beforehand. However, for some of our investigations it was sufficient to know their electrochemical equivalent.

The acid saponins are weak acids and, therefore, the determination of the equivalent by titration with alkali could not always be of the highest accuracy. We used both indicators and electrometric titration (glass electrode). The indicator method is subject to some difficulties, as the color change may be influenced by the presence of the saponin itself, as is the case for phenol red; phenolphthalein proved well adapted for our purpose.

For the equivalents, the following figures were found: sapoalbin, 1640; senegin, 1270; blighiin, 1510. If these three saponins are monobasic acids, the molecular weights should be equal to these values. That this really seems to be the case will be proved by measurement of their freezing point depressions. The weights of the saponin particles obtained by these measurements agree fairly well with the values obtained by electrometric titration.

The Surface Activity of Saponins

Method of Measurement. We are dealing with substances of relatively high molecular weight (1000–2000). Such large molecules will but slowly diffuse to the surface of the solution and the final value of the surface tension will only be reached after a certain lapse of time.

The choice of the method of measurement must take this low diffusion velocity into account. Dynamic methods were excluded. On the other hand, there are objections to some static methods such as the drop-weight and detachment methods.

In the drop-weight, or stalagmometric method, the liquid surface increases during the drop formation and the adsorption equilibrium is far from being realized at the moment the drop is detached. The same objection may be made against the maximum gas-bubble pressure method.

In the detachment method a circular disc, or better a thin ring, is pulled from the surface. Here one may wait until the surface equilibrium is established, but during the measurement this equilibrium is destroyed by the upward motion of the disc, or torus, causing an enlargement of the surface and a subsequent decrease in the surface adsorption. Wrong values for the surface tension are obtained unless the measurement is carried out very slowly, but even then that portion of the surface enclosed by the ring may have a different surface tension than the rest of the surface, as is stated by Harkins and Anderson (5).

The capillary rise method proved unsuitable in the case of saponin solutions. Usually, high results were obtained when measuring with receding angle; values obtained with advancing angle more nearly approached the correct ones.

From our standpoint there is but little objection against those methods in which the surface tension is computed from the shape of a sessile drop or of a gas-bubble in the liquid. The variations of the surface tension may be instantaneously observed. The difficulties of these methods reside in the rather elaborate measurements and calculations, the rather poor accuracy, and the difficulty of making a large number of successive measurements.

The most satisfactory method for measuring surface tension or interfacial tension was to determine directly the pull exerted by the liquid on an immersed vertical slide. A similar method, based on the principle of Wilhelmy, was used by Harkins and Anderson (5) and others.

The surface tension σ is computed from the formula:

$$F = 2(b + d)\ \sigma \cdot \cos\theta - bdhpg, \qquad (1)$$

F being the total force (in dynes) exerted on the slide (minus the weight of the slide and the hook), b and d the width and thickness of the slide, h the

depth of immersion, θ the contact angle, ρ the density of the liquid and g the acceleration due to gravity.

To avoid measurement of the depth h, one of us (6) has modified the method in the following way: The very thin slide (Fig. 3), suspended by a platinum wire EF and a glass rod FG, is suspended at one of the arms of a balance (a chainomatic, torsion or spring balance may be used). The vessel containing the liquid is raised until the liquid surface comes exactly into contact with the base of the slide and the latter is held in this position by properly equilibrating the balance. As now $h = 0$, the surface tension is calculated from:

$$F = 2(b + d)\ \sigma \cdot \cos\theta, \tag{2}$$

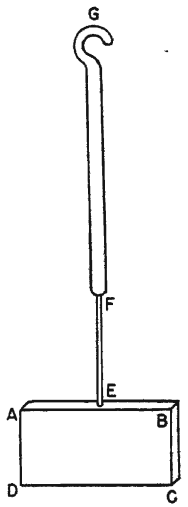

FIG. 3. System for the measurement of surface and interfacial tension in cases in which the meniscus is concave on the upper side. (Thickness of slide is exaggerated.)

while F is equal to the total charge on the balance minus the weight of the slide and its support. In the case of perfect wetting ($\theta = 0$), and formula (1) reduces to:

$$F = 2(b + d)\ \sigma. \tag{3}$$

One of us (7) has investigated the precautions which must be taken when the method is applied in this form, and the systematic errors which may be encountered. It was proved theoretically that the exactness of the formula is not affected by the fact that the line of contact between the liquid and the plate is not a horizontal curve (on the broad flat portions of the slide the liquid rises much higher than at the edges).

The exact knowledge of the angle θ is a fundamental condition for the application of the method, the most accurate results being obtained when it is zero.

The erect plane of the slide must be perfectly vertical and its base perfectly horizontal. The errors caused by a deviation from the ideal position depend upon the thickness of the slide. Therefore, the latter should be as thin as possible. With a slide 0.01 cm. thick a deviation of 2° from the vertical causes errors in σ or the order of 0.02–0.05 dyne/cm.

The construction of the slide and its support must be symmetrical, otherwise it would deviate from the vertical position when brought in contact with the liquid.

For correct measurements, the edges of the slide must be situated beyond a certain minimum distance from the walls of the vessel. Therefore, in the case of a slide 2 cm. broad the diameter of the vessel should be at least 5 cm. and the contact of the slide with the liquid surface must take place in the central (almost flat) part of the meniscus.

The vertical dimension of the slide should be larger than the constant $a = \sqrt{\frac{2\sigma}{g\rho}}$ (for water $a = 0.383$ cm).

The depth h in formula (1) is taken from the main level, which is situated at a certain distance below the liquid surface. In a wide vessel the main level coincides within a few hundredths of a millimeter with the lowest portion of the meniscus. When the slide is brought into contact with the liquid surface, the main level is lowered, and at first sight one would think the computation of the necessary correction is rather complicated. However, this computation is made very easily in the following manner. In a vessel of radius r the volume of liquid lifted above the main level is $2\pi r\sigma/\rho g$ (the contact angle being supposed equal to zero). After the slide has been brought in contact, the volume of liquid lifted above the new main level is: $[2\pi r\sigma + 2(b + d)\sigma]/\rho g$. As the total volume of liquid present remains constant, this means that the main level is lowered by the quantity:

$$l = \frac{2(b + d)\sigma}{\pi r^2 \rho g}. \qquad (4)$$

In our method, where the slide is brought exactly into contact with the surface its lower edge is at a height l above the main level and instead of formula (2) we must use formula (1), where h is now equal to minus l. Formula (1) becomes:

$$F = 2(b + d)\sigma + \frac{2(b + d)\sigma \cdot bd}{\pi r^2}. \qquad (5)$$

If we put

$$\sigma' = \frac{F}{2(b + d)}$$

formula (5) gives:

$$\sigma = \sigma' \frac{\pi r^2}{\pi r^2 + bd}. \tag{6}$$

To illustrate the importance of the correction, we write (7) in the approximate form:

$$\sigma = \sigma' \left(1 - \frac{bd}{\pi r^2} \right) \tag{7}$$

from which it appears that for $r = 2.5$ cm., $b = 0.01$ cm., $d = 2$ cm. and $\sigma = 72$ dyne/cm., the correction amounts to:

$$\frac{bd}{\pi r^2} \sigma' = 0.07 \text{ dyne/cm.}$$

For benzene it would be 0.03 dyne/cm. For a slide 1 mm. thick these corrections are 10 times larger. For thick slides it would be necessary to apply a correction for the fact that when the slide is not in contact with the liquid surface the main level does not coincide exactly with the lower part of the meniscus. However, for slides 0.01 cm. thick and a vessel of 5 cm. diameter this correction is insignificant, *viz.*, of the order of 0.01 dyne/cm.

The considerations above exemplify the advantage of using thin slides; not only do the possible errors become much smaller, but the sensitivity of the method is also increased, as the hydrostatic forces considerably diminish the deviations of the balance.

The same method of measurement may be used for the determination of the interfacial tension of two liquids (8). Here one must distinguish between the case where the interface is concave on the upper side and the case where it is concave on the lower side. The construction of the slide and its support must be adapted to each case.

If the interface is concave when viewed from above, we use the same construction as described above (Fig. 3). The system is suspended on the balance and the vessel containing the two liquids is raised until the interface comes exactly into contact with the base CD of the slide (at this moment the slide must be completely submerged by the upper liquid). The total force F measured, subtraction of the weight of the slide being made, is equal to

$$F = 2(b + d)\gamma \cdot \cos\theta - S + \Sigma,$$

b and d being the horizontal dimensions of the slide, γ the interfacial tension, S the buoyancy exerted on the slide, Σ the pull caused by the surface tension of the upper liquid working on the wire EF.

The terms $-S$ and Σ may be calculated. They may also be measured directly by weighing the slide completely immersed in the upper liquid,

but not in contact with the interface. To the value of $\Sigma - S$ thus determined a small correction $-\pi r^2 e\rho_1 g$ must be added for the slight increase e of the depth of immersion of the suspension wire (radius r) when the slide is in contact with the interface (ρ_1 is the density of the upper liquid). For thin wires a rather rough approximation of e is sufficient.

In the case of an interface, which is concave on the lower side, we use a thin parallelopiped slide ABCD, the base of which is attached to a frame of thin platinum wire KLMN (Fig. 4) The plane ABCD is perpendicular to the plane KLMN. The slide is completely immersed in the lower liquid and, by lowering the vessel, the upper side AB is brought exactly into contact with the interface. As the present work only deals

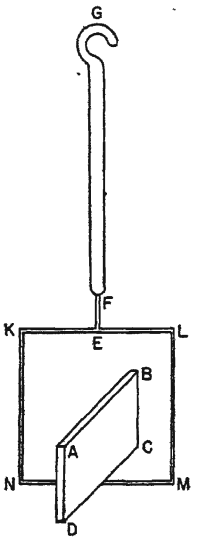

FIG. 4. System for the measurement of surface and interfacial tension in cases in which the meniscus is concave on the lower side. (Thickness of slide is exaggerated.)

with cases in which the interface is concave on the upper side (saponin solutions against benzene) we refer to the original work (8) for a more extensive description of the second case

The sources of error in using the described method for measuring nterfacial tension are almost the same as when measuring surface tension (see above).

Accurate results are only obtained when the contact angle is zero. Therefore, if water is one of the components of the binary system, the slide must be completely covered with a water film. In the system water/benzene, this is easily controlled by observing the total reflection of light at the interface: the surface of the slide appears very brilliant when the

water film is present. The formation of a stable water film is only possible when the second liquid is saturated with water, a state which is reached after a certain lapse of time (about 30 minutes).

The diameter of the vessel containing the two liquids must have a minimum value d_m, depending on the quantity $a' = \sqrt{\frac{2\gamma}{g|\rho_1 - \rho_2|}}$ (where $|\rho_1 - \rho_2|$ means the absolute value of the difference of the densities of the two liquids). When a' is not larger than the value of a of water (0.383 cm.) a vessel with a diameter of 5 cm. is sufficient (see above), but for larger values of a' larger vessels are needed. For the system water/benzene ($a' = 0.74$) the diameter must be at least 6 cm. The minimum height allowed (vertical dimension) h_m of the slide is equal to a'. For large values of a' (*e.g.*, caused by small values of $|\rho_1 - \rho_2|$) both d_m and h_m are large and the method becomes unsuitable in practice.

By reason of the lowering of the main level when the plate is put into contact with the interface, a correction must be applied, which can be calculated from formula (7).

In our measurements special care was taken in cleaning the platinum and the glass vessels. The slides were thoroughly washed with a hot solution of potassium dichromate and sulfuric acid and rinsed with hot doubly distilled water. The vessels were cleaned systematically with the concentrated chromic-sulfuric acid mixture and finally steamed.

The series of saponin solutions were made by dilution from a concentrated solution. After being poured into the various vessels for measurement, the solutions remained at rest (30 cc. of benzene was poured on each solution for measurement of interfacial tension). The vessels were placed in the correct position in the thermostat under the balance and all mechanical disturbances were carefully avoided.

Results

I. Surface Tension of Saponin Solutions

The surface tension of saponin solutions is subject to change with time. In the case of senegin, these variations come to an end about 2 hours after the solution is set aside to rest. In the case of digitonin and sapoalbin the surface tension diminishes during the first 5 hours and then rises to a constant value. Fig. 5 gives an example of changes observed with sapoalbin ($\Delta\sigma$ is the surface tension lowering).

Because of these variations, senegin solutions were measured after at least 2 hours, digitonin and sapoalbin after at least 10 hours rest.

Fig. 6 gives the surface tension-concentration curves of the four saponins studied dissolved in doubly distilled water (pH of the solutions about 5.5), the concentrations being given on a logarithmic scale. Senegin has the highest surface activity, sapoalbin the lowest.

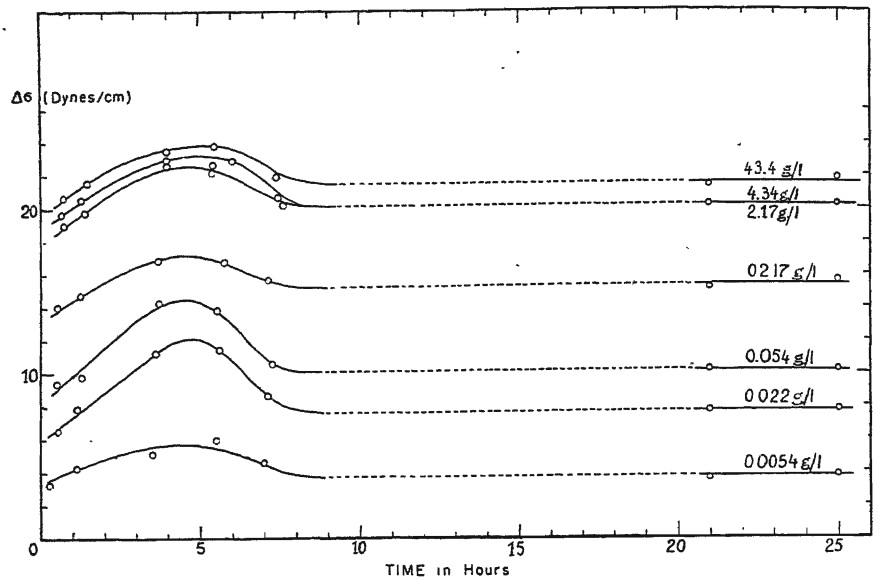

FIG. 5. Change with time of the surface tension of sapoalbin solutions (25°C.).

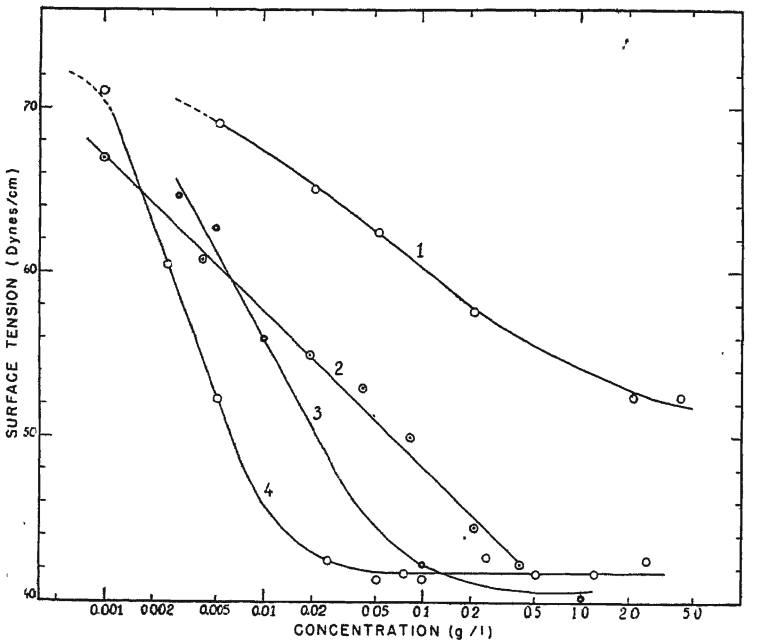

FIG. 6. Surface tension of saponin solutions in doubly distilled water (25°C.).

1. Sapoalbin.
2. Digitonin.
3. Blighiin.
4. Senegin.

Whereas the surface tension of digitonin solutions is practically independent of hydrogen ion concentration, the surface tensions of senegin, sapoalbin and blighiin solutions are strongly influenced by

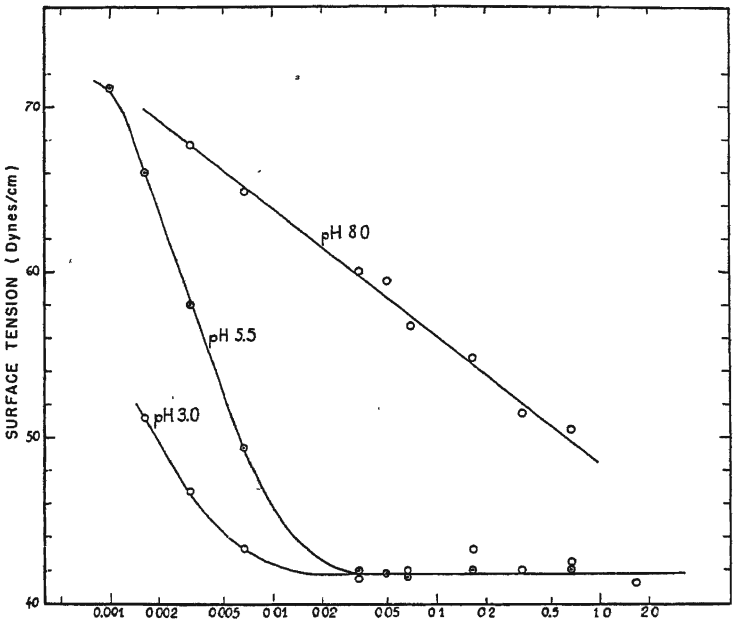

FIG. 7. Surface tension of senegin solutions (25°C.).

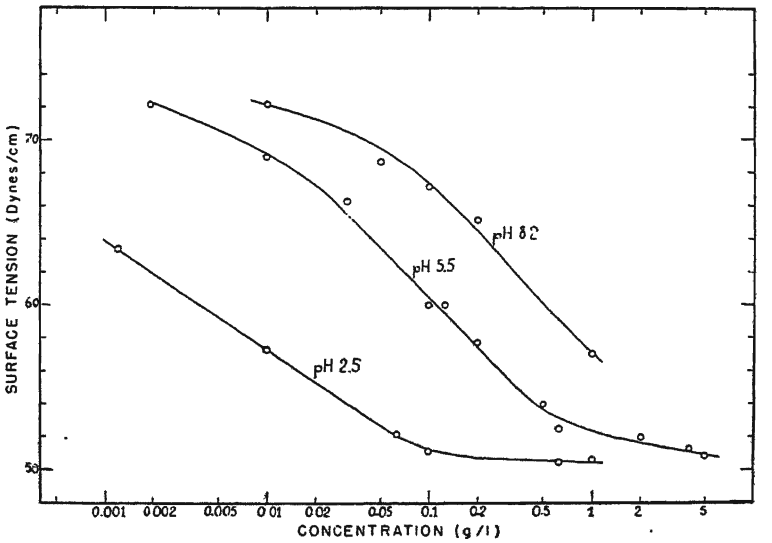

FIG. 8. Surface tension of sapoalbin solutions (20°C.).

changes in pH. Figs. 7, 8 and 9 give the surface tension of senegin, sapoalbin and blighiin for 3 values of the pH (logarithmic concentration scale), the acid and alkaline solutions being obtained by diluting with appropriate quantities of HCl or NaOH solution.

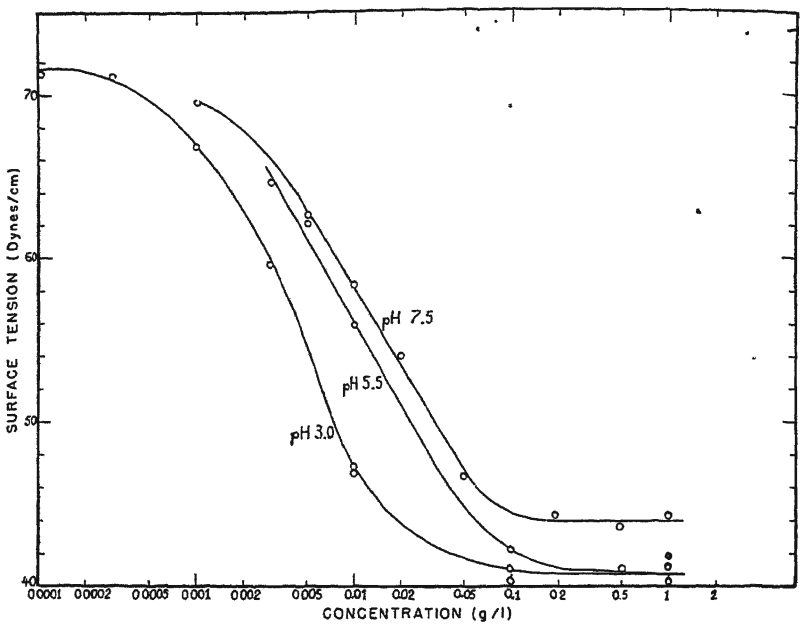

FIG. 9. Surface tension of blighiin solutions (25°C.).

The 3 acid saponins show the same general behavior, *viz.*, the raising of surface tension with higher pH, caused without doubt by the stronger electrolytic dissociation of the saponin salts. However, there are typical differences. The surface tension of senegin solutions increases greatly in passing from pH 5.5 to pH 8, and, at the same time, there is a marked diminution in the slope of the curve. For sapoalbin the increase is most pronounced in passing from pH 3 to pH 5.5, and for blighiin the 3 curves lie rather close to one another.

As one must avoid as much as possible the use of electrolytes (see below), it was impossible to make use of buffer solutions to obtain a given pH. On the other hand, for all points of a given concentration curve the pH must be the same, otherwise it has a limited significance. In each case experimentation was needed to find the correct quantity of HCl and NaOH to be added. Of course, the pH of the alkaline solutions could change during the time preceding the measurement, so that the final value of the pH had to be taken into account.

To avoid this uncertainty the surface tension of sapoalbin solutions of 3 fixed concentrations, but with different pH values, was measured (Fig. 10, curves 1, 2, 3). For each solution the pH was determined immediately after measurement of the surface tension, by means of the quinhydrone-calomel or antimony electrodes (of course the solutions were of no further use after this). The curves show the steep increase in the region pH 3–6 or 7; beyond pH 7 there is only a very slow decrease. We may say that for sapoalbin the entire change of surface tension occurs for pH values below 7.

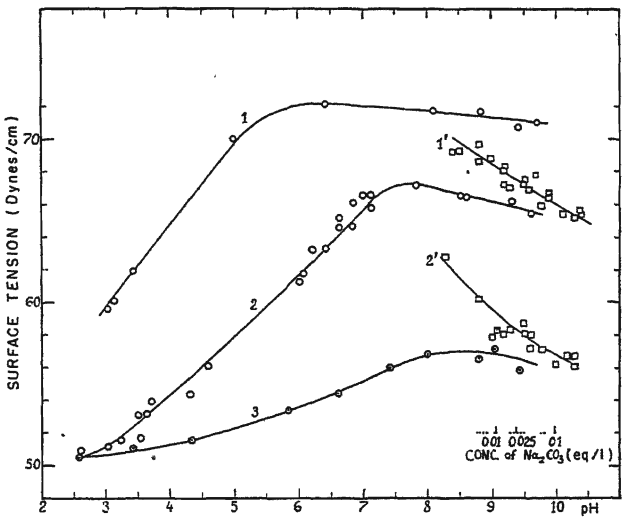

FIG. 10. Influence of hydrogen ion concentration and of electrolyte (Na_2CO_3) on the surface tension of sapoalbin solutions (20°C.).

1. c = 0.01 g./l.; 2. c = 0.1 g./l.;
3. c = 1 g./l.
1'. c = 0.01 g./l. (Na_2CO_3 added);
2'. c = 0.1 g./l. (*id.*)

In the above described measurements, one important factor was not taken into account, *viz.*, the influence of the atmospheric carbonic acid. The influence of pure CO_2 may be considerable on solutions which are not acid, as is shown by the following qualitative experiment: a senegin solution with a surface tension of, *e.g.*, 60 dyne/cm., was kept and measured in a special vessel in an atmosphere of purified nitrogen. The nitrogen was then replaced by carbon dioxide and in a very short time the surface tension was lowered to 48 dyne/cm. The carbon dioxide was then replaced by nitrogen again and the surface tension slowly rose to the original value. (It is our purpose to study this effect more closely.)

The presence of electrolytes has a marked influence on the surface tension of saponin solutions. In preparing the alkaline solutions with sodium carbonate instead of sodium hydroxide, larger quantities of the former than of the latter are needed in order to obtain a given pH. In Fig. 10 (curves 1′ and 2′) are shown the results when the pH series are prepared with Na_2CO_3 (the small auxiliary scale shows approximately the quantities used). There is a strong decrease of surface tension when Na_2CO_3 is used instead of NaOH. The same effect is observed with sodium chloride. When to a series of sapoalbin solutions (of 0.1 g./l.) Na_2CO_3 and NaCl are added in different ratios, but in such a manner that the total concentration of sodium is 0.2 g.-eq./l., the surface tension is nearly constant, *viz.*, 55.5 dyne/cm. These experiments clearly show that in alkaline sapoalbin solutions the surface tension is influenced more by electrolytes than by a change in pH.

Therefore, the use of electrolytes must be limited to the necessary amount. In some investigations, *e.g.*, when studying the surface active properties with respect to hemolysis, the electrolyte concentration has to be adapted to the demands of the problem (*e.g.*, isotonic solution).

II. Interfacial Tension of Saponin Solutions against Benzene.

The interfacial tensions were measured by the method described above. The results for the different saponins are shown in Fig. 11 (sapo-

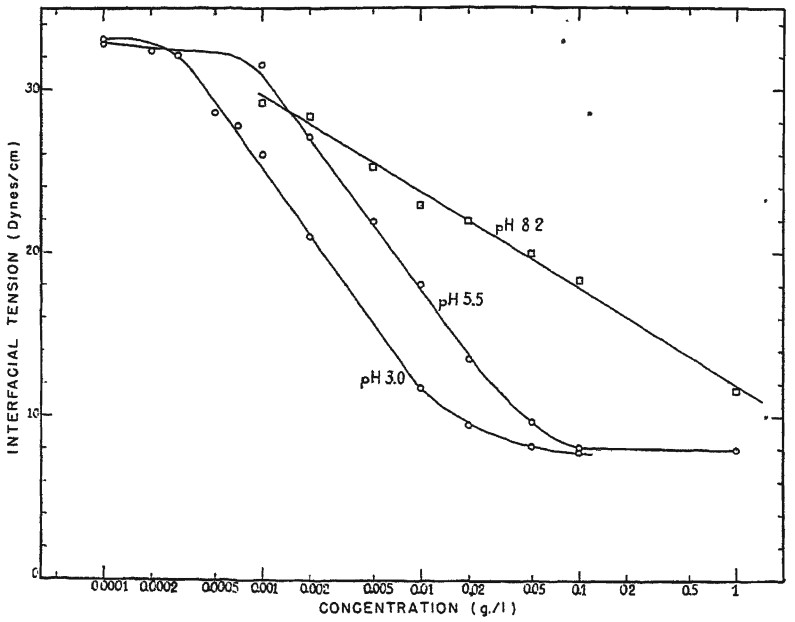

FIG. 11. Interfacial tension of sapoalbin solutions and benzene (20°C.).

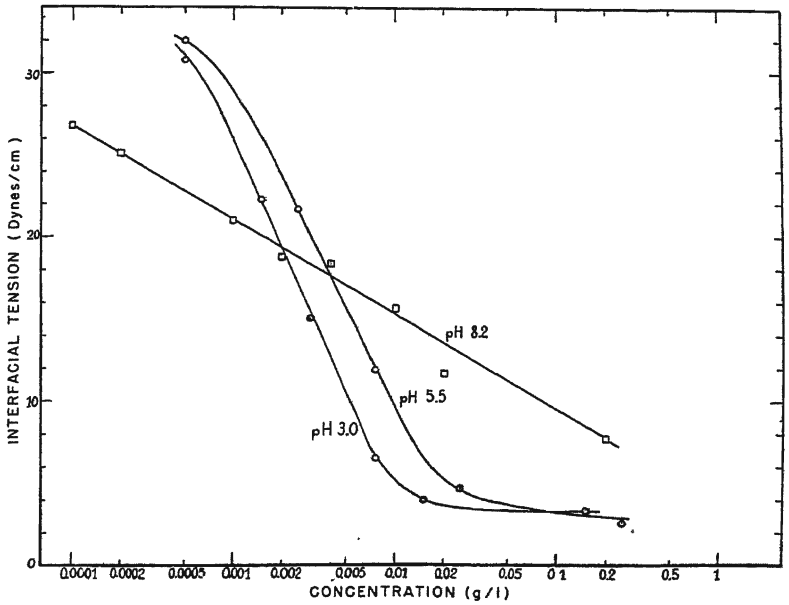

FIG. 12. Interfacial tension of senegin solutions and benzene (20°C.).

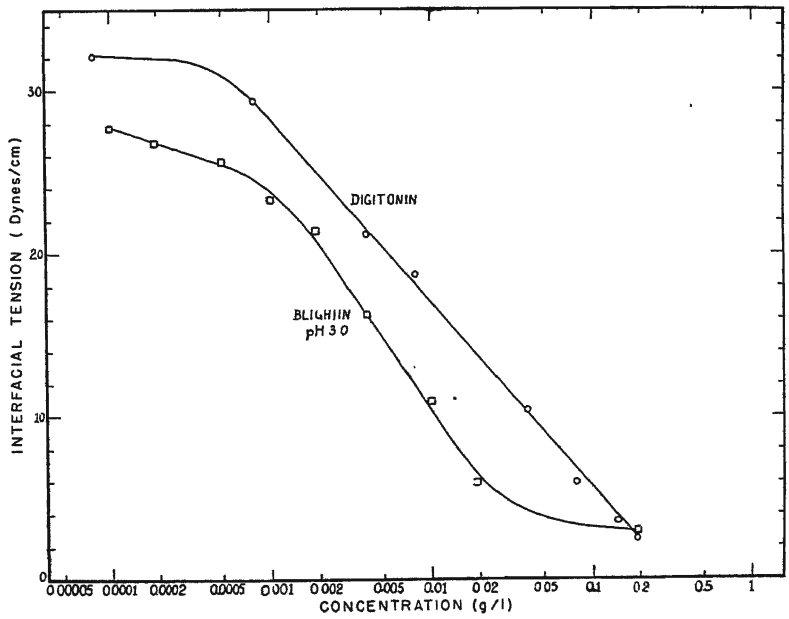

FIG. 13. Interfacial tension of digitonin and blighiin solutions to benzene (20°C.).

albin at pH 3.0, 5.5, and 8.2), Fig. 12 (senegin at pH 3.0, 5.5, and 8.2) and Fig. 13 (blighiin and digitonin at pH 3.0); the temperature was 20°C. (concentration scales are logarithmic).

The general shape of the curves is the same as for the surface tension curves. This becomes still more obvious in Fig. 14, where for each saponin the interfacial tension lowering and the surface tension lowering are included in the same diagram. For senegin at pH 5.5 both curves coincide almost entirely, as is also the case for blighiin at pH 3.0. This may be regarded as more than a mere chance and we may conclude that both

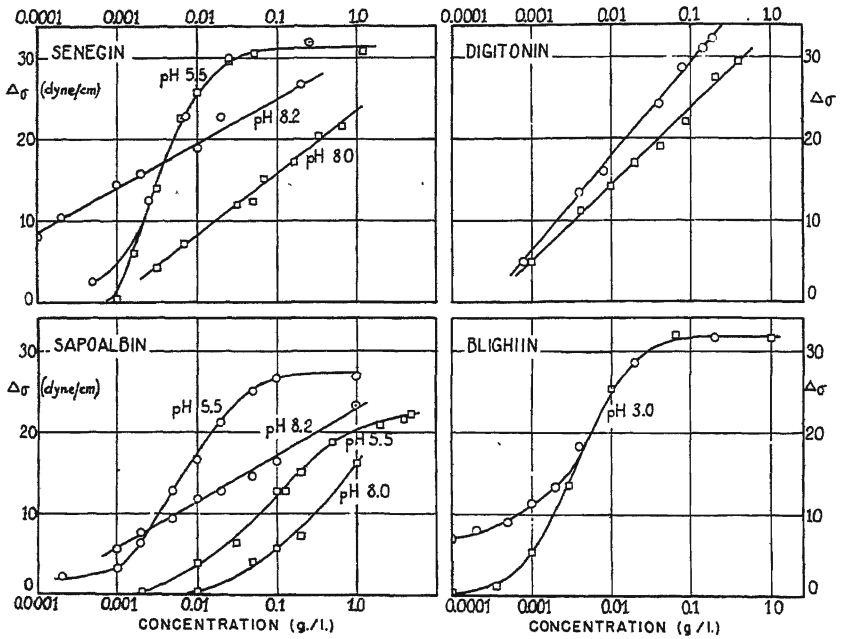

FIG. 14. Comparison of surface-tension lowering (squares) with interfacial tension lowering (circles).

saponins at the given pH show the same tensio-activity at the water surface as at the water-benzene interface (for blighiin there is a deviation at low concentrations, which might be due to minute quantities of some impurity). There is a certain difference between the two curves of digitonin. For sapoalbin at pH 5.5 and 8 and for senegin at pH 8.2, there is a very large difference, showing that, in these cases, the organic liquid has a strong influence on the adsorption of the saponin: the interfacial tension lowerings are of the same order as the surface tension lowerings obtained with 10–100 times higher concentrations.

Determination of Molecular Area by Spreading and by Application of Gibbs' Equation

Molecular area can be determined if it is possible to spread the substance as a monomolecular film. In the case of saponins the procedure is rather difficult because of their solubility. However, on 0.001 *N* HCl, films of senegin, and also of sapoalbin, could be obtained, which were sufficiently stable to allow measurements of their area.

With a volumetric pipette (after Harkins) the saponin solution in water was brought on the surface of the HCl solution in the trough. While compressing, the surface pressure was measured by the vertical plate method described above.

By extrapolation to pressure zero the area, *S*, occupied by 1 mg. of substance, was found, and by taking into account the equivalents of 1270 (senegin) and 1640 (sapoalbin), considered as true molecular weights, the molecular area *A* and molecular diameter *D* were determined. The thickness *E* of the film was calculated on the assumption of the density of the material in the film being the same as that of the dry substance, *viz.*, 1.47 for sapoalbin and 1.4 for senegin: (See Table I.)

TABLE I

Substance	S	A	D	E
	m.²/mg.	*A²*	*A*	*A*
Sapoalbin	0.569	154	12.3	12.0
Senegin	0.622	130	11.4	11.4

From these measurements the saponin molecules appear to be isodimensional particles.

It is of great interest to compare the results derived from spreading measurements with those obtained from the application of Gibbs' adsorption equation.

The general form of Gibbs' equations (*cf.* ref. 9) for a system of n components, with chemical potentials μ_i and surface excesses Γ_i, is

$$d\sigma = -\sum_{i=1}^{n} \Gamma_i d\mu_i, \tag{8}$$

where σ is the surface tension. If the mathematical surface is chosen so that the surface excess of the solvent vanishes, *i.e.*, $\Gamma_1 = 0$, (8) becomes:

$$d\sigma = -\sum_{i=2}^{n} \Gamma_i^{(1)} d\mu_i, \tag{9}$$

the indices (1) referring to the adopted position of the mathematical surface.

For a system of two components, solvent and solute, (9) reduces to:

$$d\sigma = - \Gamma_2^{(1)} d\mu_2 \tag{10}$$

and in dilute solutions, we obtain the approximate form of Gibbs' relation:

$$\Gamma_2^{(1)} = - \frac{1}{RT} \frac{d\sigma}{d\log_e c}, \tag{11}$$

where $\Gamma_2^{(1)}$ is expressed in mole/cm.^{2}, c in arbitrary units. The case of a system with three components (*e.g.*, saponin solution in contact with benzene) is more complicated by the presence of the term $\Gamma_3^{(1)} d\mu_3$. As this term may be small, either by $\Gamma_3^{(1)}$ or $d\mu_3$, or both, being small, equation (11) in this case may also be regarded as a first approximation.

In Table II are given the surface excesses Γ (in moles per sq. cm.) calculated from the maximum slope of the surface tension and interfacial tension curves. The molecular areas A are based on the assumption that the surface excess is equal to the real amount of substance per unit area; this is permissible when the solutions are very dilute.

TABLE II

Substance	Interface water/air			Interface water/benzene		
	pH	Γ Mol./cm.^{2}	A A^2	pH	Γ Mol./cm.^{2}	A A^2
Sapoalbin	5.5	1.20×10^{-10}	137	5.5	2.60×10^{-10}	63.5
Sapoalbin	8.2	1.20×10^{-10}	136	8.2	1.10×10^{-10}	150
Senegin	5.5	3.25×10^{-10}	37.0	5.5	3.25×10^{-10}	37.0
Senegin	8.0	1.38×10^{-10}	120	8.2	1.02×10^{-10}	162
Digitonin	—	1.56×10^{-10}	106	—	2.01×10^{-10}	82.4

These results show a few good agreements, but, on the other hand, there are also large differences. For sapoalbin the three values 137, 136 and 150 A^2 are nearly in agreement with the spreading value 154 A^2; but the value of 63.5 A^2 at the interface water-benzene at pH 5.5 is quite divergent.

Also for senegin there is some agreement between the two values at pH 8.0, *viz.*, 120 and 162, and the spreading value 130 A^2 (at pH 3), but at pH 5.5 the two values of 37 A^2 are too low.

Another difficulty is the diminution of the slope of the curves in Figs. 8, 9, and 10 with higher, although still small, concentrations. This would mean that the adsorption becomes smaller and is finally annihilated.

The non-applicability of Gibbs' approximate equation (11) for dilute solutions may be caused by the fact that the system may not be considered as a two-component system. Of course, in the system saponin solution-benzene, there are at least 3 components, and we have considered

equation (11) only as a first approximation. But even a saponin solution might by itself contain more than two components, either by electrolytic dissociation, or micelle formation, or due to the presence of an impurity.

Electrolytic dissociation plays an important part, and, if the undissociated molecules are more strongly adsorbed than the ions, its effect will be to give somewhat steeper curves, and thus absorption values which are too high. However, this effect does not explain the very steep curves for senegin in acid medium.

Micelle formation might explain the flat horizontal portion of the curves, but in the case of saponins no evidence of micelle formation was found by other methods (see below), even in much higher concentrations than those in which the surface tension remains constant.

The presence of an impurity would give rise to complicated effects analogous to those of detergents (9), and might possibly cause the observed behavior of the senegin solutions. As long as the saponins are not prepared as absolutely pure chemical individuals, this explanation remains plausible.

We must admit that Gibbs' law, although applicable in certain cases to saponins (*e.g.*, alkaline solutions), is, in its simple form (Eq. 11), not generally applicable to this kind of solution.

* * *

To determine whether the saponins show a micellar aggregation in water, as do the soaps, synthetic detergents and tensio-active biocolloids, we have measured their electrolytic conductivity and freezing point depression.

Electrolytic Conductivity of Saponin Solutions

Method of Measurement and Apparatus. The conductivity was determined by the Kohlrausch method. The alternating current, with a frequency of 1000 cycles/sec., was produced by a pentode oscillator; the potential difference in the bridge was amplified by a pentode amplifier, connected with the head phone. The absence of leakage currents (*e.g.*, through capacitive grounding) was verified by comparison with standard resistances. A variable condenser compensated the capacity of the conductivity cell. Two cells of the Washburn type were used. One cell had large electrodes 2 cm. in diameter and 0.1 cm. apart, and a cell constant of 0.0195. The second cell was cylindrical, 1.4 cm. in diameter, and had electrodes of the same diameter at a distance of 2.8 cm. Its cell constant was 1.788. In the regions where comparison was possible, both cells gave the same results.

Because of the pentode amplifier, great sensitivity was obtained. The

detectable differences were: under 100 ohms: 0.2%; from 100 to 1000 ohms: 0.1–0.05%; above 1000 ohms: down to 0.01%.

The measurements were made in a thermostat regulated at 25.00 ± 0.01°C.

The conductivity of the water was between 0.8 and 1.3 × 10^{-6} $ohm^{-1} \cdot cm^{-1}$, and was always taken into consideration for correction of the results.

In Fig. 15 are given the equivalent conductivities Λ of sapoalbinic and seneginic acids and of their salts as functions of $\sqrt{c}$ (the concentration c is expressed in eq./l., Λ in $ohm^{-1} \cdot cm.^{-1}/eq./cm.^3$).

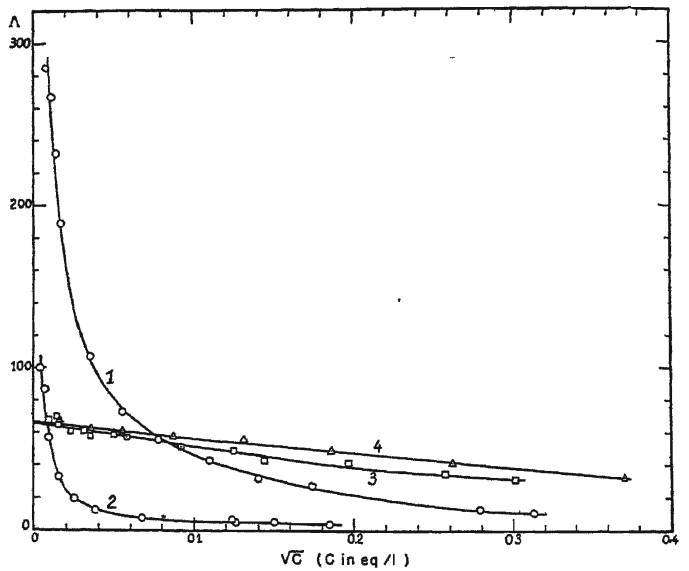

FIG. 15. Equivalent conductivity of sapoalbinic and seneginic acids and their sodium salts (25°C.).

1. Sapoalbinic acid;
2. Seneginic acid;
3. Sodium sapoalbinate;
4. Sodium seneginate.

In the case of the saponin salts, the extrapolation of the straight part of the curves gives for the equivalent conductivities at infinite dilution:

Sodium sapoalbinate, 66; Sodium seneginate, 67.

By substracting from these numbers the mobility of the sodium ion at 25°C., *i.e.*, $u = 51$, the mobilities of the saponin ions are obtained:

Sapoalbin ion, $u = 15$; Senegin ion, $u = 16$.

On the other hand, as the radii of the saponin particles are known from the spreading measurements, the mobilities of the saponin ions can be calculated from Stokes' law. We find:

Sapoalbin ion, (r = 6.0 A): u = 14.0;
Senegin ion, (r = 5.7 A): u = 15.0.

These theoretical values agree well with the experimental values.

The curves for sapoalbinic and seneginic acids are those of weak acids. Extrapolation to infinite dilution is not feasible. However, the limit, conductivity at infinite dilution, Λ_0, is obtained by adding the saponin ion mobilities to the mobility of the hydrogen ion at 25°C., *viz.*, 351. Λ_0 thus determined is 365 for sapoalbin and 366 for senegin. The dissociation constant is then calculated as $K = \frac{\Lambda^2 c}{(\Lambda_0 - \Lambda)\Lambda_0}$, where c is expressed in eq./l. The average dissociation constants are: 1.6×10^{-4} for sapoalbin and 2×10^{-6} for senegin, both being weak acids, although sapoalbinic acid is stronger than acetic acid.

On the whole the saponin and senegin acids and their sodium salts behave as electrolytes dispersed molecularly, and not as colloidal electrolytes. There is no indication of a steep decrease, nor of a minimum in the conductivity curves, as is found for soaps and synthetic detergents.

The Freezing-Point Depression of Saponin Solutions

The freezing-point depression was determined by Beckmann's method. Because of the high molecular weight, the precision was rather poor, even with concentrated solutions.

In the case of the sodium salts, extrapolation at infinite dilution and assuming complete electrolytic dissociation gave the following molecular weights: 1200 for senegin and 1600 for sapoalbin, in rather close agreement with the equivalent weights. For the acids the figures were somewhat higher, *viz.*, 1250 for senegin and 2000 for sapoalbin; the high result for sapoalbin may be caused by the difficulty of the extrapolation.

In Fig. 16 are given the values of the Bjerrum osmotic coefficient g, defined as:

$$g = \frac{i}{2} = 1 - j = \frac{\theta}{2 \times 1.859 \times m},$$

where i is van't Hoff's function, j is Randall's function, θ is the freezing-point lowering and m the molar concentration. The abscissas are $\sqrt{c}$, c being the molar concentration; the broken lines are the theoretical Onsager curve for strong electrolytes and the curve for a micellar detergent (dodecylsulfonic acid) (10).

The two curves for saponins show a deviation from the Onsager curve which is much smaller than is the case for soaps and synthetic detergents. This makes it probable that even in concentrated solutions the saponins are dispersed as single molecules and ions.

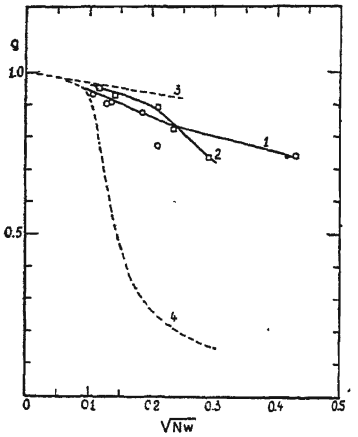

FIG. 16. Osmotic coefficients of 1. sodium sapoalbinate and 2. sodium seneginate, compared with dodecylsulfonic acid (curve 4) and with theoretical Onsager values (curve 3).

Furthermore, the fact that the electrochemical equivalents are in good agreement with the cryoscopic values makes it very probable that the sapoalbin and senegin acids are univalent.

The Viscosity of Saponin Solutions

The viscosity of the saponin solutions has also been studied for the purpose of obtaining some information about the shape and behavior of the dissolved particles (11). Some results can be summarized as follows.

The intrinsic viscosity $[\eta] = \left(\frac{d\eta_r}{dc}\right)_{c\to 0}$ for both sodium sapoalbinate and sodium seneginate is 0.036. This value is not much larger than the theoretical Einstein value 0.025, and small in comparison with the value for hydrophilic colloids (gelatin, 0.40; gum arabic, 0.24).

The viscosity of sapoalbin solutions is lowered in acid medium, that of senegin is raised in acid medium.

The viscosity of both sapoalbin and senegin solutions decreases with increasing pressure, an effect which can be explained by deformation of the saponin molecules in the glucidic part.

The results of the viscosity determinations seem compatible with a dispersion of the saponins as single molecules and ions.

Conclusion and Summary

The saponins in water solution are adsorbed similarly at the water-air and at the water-benzene boundary. The surface and interfacial tension lowering by the acid saponins is strongly influenced by the hydrogen ion concentration, the tension values being much lower in acid than in alkaline medium. We find it reasonable to ascribe this effect to a decrease in electrolytic dissociation.

In the case of sapoalbin the influence of electrolytes was studied; sodium salts considerably lowered the surface tension (in alkaline medium).

The molecular area obtained from the spreading measurements was compared with that derived from Gibbs' adsorption equation. Some data were in good agreement but, on the other hand, very large discrepancies were found, showing that, in this case, Gibbs' equation is not applicable in its simple form (probably because the system may not be considered as a two-component system).

From our measurements we were able to conclude that the saponins studied appear as large molecules, 10–12 A in diameter and with molecular weights ranging up to 1640. When dissolved in water, they are dispersed into single molecules and ions, and even in concentrated solutions there is probably no association into neutral or ionic micelles.

References

1. See *e.g.:* Ruzicka, L., and Giacomello, G., *Helv. Chim. Acta* **19**, 1136 (1936). Ruzicka, L., and Giacomello, G., *Helv. Chim. Acta* **20**, 299 (1937). Ruzicka, L., and Schellenberg, H., *Helv. Chim. Acta* **20**, 1553 (1937). Ruzicka, L., and Marxer, A., *Helv. Chim. Acta* **22**, 195 (1939). Bilham, P., and Kon, G. A. R., *J. Chem. Soc.* **1941**, 552. Elliott, D. F., Kon, G. A. R., and Soper, H. R., *J. Chem. Soc.* **1940**, 612. Haworth, R. D., *Ann. Repts. Progress Chem.* **34**, 327 (1937). Spring, F. S., *Ann. Repts. Progress Chem.* **37**, 332 (1940). Spring, F. S., *Ann. Repts. Progress Chem.* **38**, 187 (1941).
2. Gilman, H., Organic Chemistry, 2nd ed., pp. 1463, 1467. Wiley & Sons, New York, 1943.
3. Jacobs, W. A., and Isler, O., *J. Biol. Chem.* **119**, 155 (1937).
4. Braeckman, P., *J. pharm. Belg.* No. 14–15, 273 (1946).
5. Harkins, W. D., and Anderson, T. F., *J. Am. Chem. Soc.* **59**, 2189 (1937).
6. Ruyssen, R., *Mededeel. Koninkl. Vlaam. Acad. Wetenschap. Belg.* **4**, No. 1 (1942).
7. Loos, R., *Mededeel. Koninkl. Vlaam. Acad. Wetenschap. Belg.* **7**, No. 1 (1945).
8. Ruyssen, R., and Loos, R., *Mededeel. Koninkl. Vlaam. Acad. Wetenschap. Belg.* **7**, No. 2 (1945).
9. Adam, N. K., The Physics and Chemistry of Surfaces. Humphrey Milford, London, 1941.
10. McBain, E. L., Dye, W. B., and Johnston, S. A., *J. Am. Chem. Soc.* **61**, 3210 (1939).
11. Ruyssen, R. Loos, R., and Croes, R., *Mededeel. Koninkl. Vlaam. Acad. Wetenschap. Belg.* IX, No. 1 (1947).

THE THERMOELASTIC BEHAVIOR OF CYLINDRICAL PLANT TISSUES

Otto Treitel *

From the Botanical Laboratory, University of Pennsylvania, Philadelphia, Pa.
Received July 11, 1947

Introduction

The cylindrical tissues of higher plants are either rubber-like or metal-like in their elastic qualities (10). To understand the elasticity of plant tissues, a knowledge of the elasticity of rubber is necessary; in this, the S-shaped stress-strain curve and the following three thermoelastic phenomena (2, p. 306) are fundamental:

(1) Rubber exhibits a rise in temperature on rapid stretching.

(2) If stretched by a constant load (isotonically) rubber contracts visibly when heated.

(3) The stress in a rubber cylinder kept at constant extension (isometric stretch) increases with rising temperature.

Precise work on thermoelasticity reveals certain limits of the validity of these 3 thermoelastic effects for rubber.

Some of the best work on thermoelastic properties has been done by physiologists on muscle and allied material. It is notable also that the most delicate and accurate apparatus for measuring stress-strain relationships and small amounts of heat was developed, not by physicists, but by physiologists.

The second thermoelastic effect for rubber mentioned above is the Gough-Joule effect. The question arises whether or not there is a Gough-Joule effect for plant tissues.

The discovery of William Thomson (Lord Kelvin) that a rubber strip becomes heated when quickly elongated, marks the beginning of a series of fruitful investigations of the unusual thermal and elastic behavior of rubber. In contrast, a metal rod becomes cooler when greatly expanded (4). By applying thermodynamics Thomson concluded that a stretched rubber strip must be shortened if it is heated. This consequence was affirmed by an experiment of Joule in 1857, though he was preceded as

* I wish to thank the Samuel Fels Fund for the grant which has made it possible for me to carry out these investigations. I wish also to express my appreciation to Dr. William Seifriz, Professor of Botany at the University of Pennsylvania, for the use of laboratory facilities.

early as 1805 by Gough (6, p. 415). The phenomenon is therefore known as the Gough-Joule effect.

To obtain the Gough-Joule effect for vulcanized rubber, and the corresponding normal thermoelastic effect for metals, the following two experiments were performed.

(1) A rubber hose 10 inches in length was fixed in a vertical position. The hose was stretched under a load of 4200 g. After stretching, the length of the hose was $18\frac{1}{2}$ inches. By applying hot air along the hose, with a bunsen burner, the hose shortened one-half inch (Gough-Joule effect).

The explanation of the Gough-Joule effect, according to L. Hock (5), is as follows: when, in its original length (Fig. 1a), the hose is in an un-

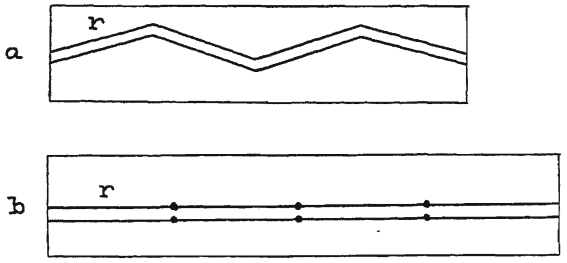

FIG. 1. Stretching and heating of a rubber hose. (a) Rubber hose in original condition and at the end after heating; (b) rubber hose stretched. r = rubber molecule.

stretched condition, the rubber molecules are folded. When the hose is stretched (Fig. 1b), the molecules are parallel to the axis, kept there by forces of cohesion. On heating the hose, the forces due to the thermal motion of the rubber molecules become stronger than the forces of cohesion. The hose, therefore, tends to return to its original condition with rubber molecules folded (Fig. 1a).

(2) When a vertically held spiral of iron is stretched under a load of 500 g. and is heated, lengthening of the spiral occurs: this is the normal thermoelastic effect.

The explanation of the normal thermoelastic effect is as follows: in Fig. 2a the iron spiral is in a stretched condition. The molecules of iron in Fig. 2 are represented by dots. After heating, the space occupied by the iron molecules is greater, because thermal motion has increased. The stretched spiral, therefore, elongates (Fig. 2b). Debye (8, p. 245) found a somewhat more exact explanation of the behavior of atoms at low and at high temperatures when an iron rod is heated. According to Debye, if A_1 and B_1, Fig. 2c, are the positions of two atoms at low temperature along the axis of the rod, A_2 and B_2 are the new positions after heating. A_2 has moved a short distance along the axis whereas B_2 has moved a

greater distance from its original position B_1. Thus, the lengthening of the iron rod on heating is explained. Similarly, if the stretched iron rod is cooled, it becomes shorter.

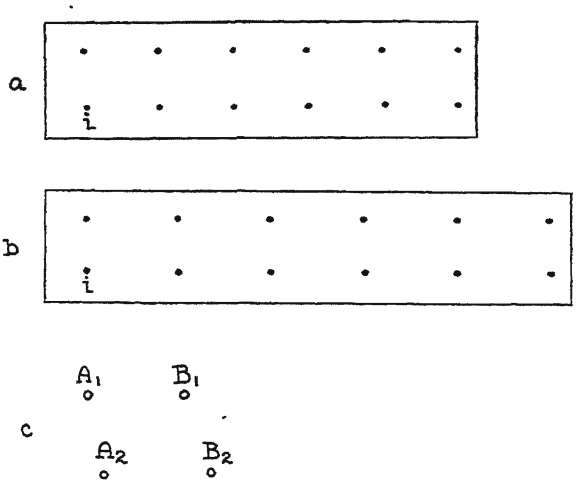

FIG. 2. Stretching and heating of an iron spiral. (a) Iron spiral stretched; (b) iron spiral after stretching and heating; (c) change of position of atoms at different temperatures according to Debye. i = iron molecule.

The derivation of the Gough-Joule effect, based on theoretical considerations, is as follows. The stress-strain relation for a rubber rod is, according to Wall (13),

$$\text{stress } f = \frac{NkT}{l_0}\left(\lambda - \frac{1}{\lambda^2}\right),$$

where N and k are constants, l_0 the original length, T the absolute temperature, and $\lambda = 1 +$ strain ϵ (see also 12). For small extensions the equation becomes:

$$\text{stress } f = \frac{NkT}{l_0}\left(1 + \epsilon - \frac{1}{(1+\epsilon)^2}\right)$$

$$= \frac{NkT}{l_0}(1 + \epsilon - 1 + 2\epsilon),$$

$$f = \frac{3NkT}{l_0} \cdot \epsilon = cT\epsilon,$$

where

$$\frac{3Nk}{l_0} = c.$$

According to Guth (2, p. 295), as the rubber rod is under strain ϵ and stress f, the isotonic stretch in the Gough-Joule effect is characterized by the thermal expansion coefficient:

$$\alpha = \frac{1}{\epsilon}\left(\frac{\partial \epsilon}{\partial T}\right)_f.$$

By using the equation of f for small extensions, it is found that

$$\alpha = -\frac{1}{T}.$$

The last equation explains why a rubber rod, stretched isotonically, contracts when heated (Gough-Joule effect).

According to L. Hock (4) the temperature of raw rubber must be below 18°C. for observing the Gough-Joule effect. The Gough-Joule effect in vulcanized rubber is to be observed near room temperature. Thus, the experiment performed with the rubber hose near room temperature showed the validity of the Gough-Joule effect.

Very accurate experiments on the thermoelastic behavior of rubber were made by Guth and Dart (1). The first law of thermoelasticity in rubber is thus accurately proved.

According to Guth (3) rubber-like elasticity occurs to a lesser or greater extent in most materials consisting of flexible long chain molecules. Therefore, proteins and cellulose esters are rubber-like materials. The same is true for cellulose molecules swollen with water. According to Treitel (10) there are cylindrical tissues of higher plants which have S-shaped stress-strain curves. Therefore, the cell walls of these tissues have rubber-like elasticity. Because cellulose forms a large percentage of the cell walls of higher plants, rubber-like elasticity must be a property of cellulose in certain plant tissues.* As cellulose centains many OH groups, a great amount of the cellulose in the walls of rubber-like elastic plant tissues may be hydrated (12). However, the rubber-like elasticity of cellulose is probably only partly due to hydration because, under this condition, only molecular water changes the elasticity.

According to Mark (9, p. 1019, Fig. 68) the stress-strain curve of a viscose rayon fiber may be S-shaped. This means that such a fiber is

* There is a linear relationship between spec. grav. and Young's modulus of woods. It must be assumed that cellulose is responsible for elasticity of woods. A similar linear relationship between spec. grav. and Young's modulus is valid for the cylindrical tissues of higher plants investigated in this article. Therefore, cellulose is again responsible for elasticity of cell walls. If all cell wall substances were responsible for elasticity, some other curve and not a straight line would give the relationship between spec. grav. and Young's modulus.

rubber-like in its elasticity. Besides, there is the fact that rayon contains hydrated cellulose (9). This is further support for the hypothesis that hydrated cellulose in the cell walls of plant tissues is the cause of their rubber-like elasticity.

Method and Results

Certain cylindrical plant tissues may show the Gough-Joule effect and other tissues may not.

Because rubber has an S-shaped stress-strain curve and three thermoelastic effects, it is to be expected that all plant tissues which have S-shaped stress-strain curves also show the Gough-Joule effect. Petioles of *Nymphaea gladstonia* have a parabola-like stress-strain curve which is a special case of the S-shaped curve. S-shaped stress-strain curves are also found for rhizomes of *Equisetum fluviatile* and for stems and rhizomes of *Brasenia schreberi*. The validity of the Gough-Joule effect remains to be proved in these three cases. As it is assumed that the submicroscopic structure of secondary cell walls in rubber-like plant tissues is similar to the structure of vulcanized rubber (11), it is to be expected that the Gough-Joule effect will hold for such plant tissues at room temperature.

The device used in the following experiments is the same as that used since 1942 (10). For heating the plant tissues, the material was covered with gauze and hot water poured over it.

1. Petioles of Nymphaea gladstonia

Five experiments showed that the Gough-Joule effect is valid for petioles of *Nymphaea gladstonia*. The results of one of these experiments is as follows: At a room temperature of 22°C., and under a load of 1200 g., a petiole of 15.50 cm. length elongates elastically 0.34 cm. At high temperature (hot water of 60°C.) and under a load of 1200 g., this petiole of 15.50 cm. length elongates 0.20 cm. The same petiole on cooling down to a room temperature of 22°C. elongates 0.34 cm. under a load of 1200 g. Hence, the Gough-Joule effect is valid for petioles of *Nymphaea gladstonia*. The full elongation at 22°C. is reached in 0.5 min., whereas at high temperature the elongation after 0.5 min. is only 0.20 cm. This is further evidence that the Gough-Joule effect is valid for petioles of *Nymphaea gladstonia*.

2. Rhizomes of Equisetum fluviatile

The Gough-Joule effect is valid for rhizomes of *Equisetum fluviatile* according to experiments carried out in 1943 (10).

3. Rhizomes of Brasenia schreberi

Again, several experiments similar to those for petioles of *Nymphaea* showed the validity of the Gough-Joule effect for rhizomes of *Brasenia schreberi*.

If plant tissues have metal-like elasticity a normal thermoelastic effect is to be expected. In such cases the stress-strain curves will be straight lines with a tail.

4. Roots of Rhus glabra

The average of four experiments showed the thermoelastic behavior of roots of *Rhus glabra*. The result was as follows:

First experiment: At a room temperature of 26°C., and under a load of 3000 g., a root 14.34 cm. long elongated elastically 0.28 cm. At a high temperature of 60°C., and under a load of 3000 g., the root (14.34 cm. length) elongated 0.40 cm. Validity of the Gough-Joule effect would demand a smaller elongation than 0.28 cm. Hence, the effect is not valid. The elastic behavior of the heated root is the same as that of the extended iron spiral. The first root shows a normal thermoelastic effect.

Second experiment: At a room temperature of 30°C., and under a load of 3000 g., a root 13.10 cm. long elongated elastically 0.32 cm. At 60°C. temperature, and under a load of 3000 g., the root (13.10 cm. length) elongated the same amount, *i.e.*, 0.32 cm. Hence the heated root shows neither anomalous nor normal thermoelastic behavior.

Third experiment: The result was the same as in the second experiment.

Fourth experiment: The result was validity of the Gough-Joule effect.

The average of these 4 experiments is that the roots show neither a normal nor an anomalous thermoelastic behavior. This is reasonable because the stress-strain curves of the roots look either S-shaped or straight with a tail (10). Roots of *Rhus glabra* thus have elastic properties on the boundary of rubber-like and metal-like elasticity.

5. Branches of Salix babylonica

Several experiments were conducted which showed that the Gough-Joule effect is not valid for branches of *Salix babylonica*. The results of one of these experiments were as follows: At room temperature of 30°C. and under a load of 4000 g., a branch 14.72 cm. long elongates elastically 0.18 cm. At 60°C., and under a load of 4000 g., the branch (14.72 cm. length) elongates 0.26 cm. Hence, the Gough-Joule effect is not valid for branches of *Salix babylonica*. These branches have normal thermoelastic behavior. Full elongation occurs in one-half minute. Two minutes after elongation at 60°C., the branch had, on cooling to room temperature,

returned to the original length when under a load of 4000 g. Therefore, on cooling, the stretched branch shortens. It is thus definite that branches of *Salix babylonica* show normal thermoelastic behavior.

Discussion

According to L. Hock (5) an explanation of the Gough-Joule effect is possible only when considered in relation to solid rubber. Therefore, it is to be expected that the thermoelastic behavior of cylindrical plant tissue is a property of the cell walls and not of the material within the cells.

According to Treitel (12) the submicroscopic structure of average secondary cell walls in cylindrical plant tissues consists of alternate layers of amorphous and micellar cellulose, which is in keeping with the modern view that natural cellulose consists of submicroscopic crystalline regions alternating with non-crystalline ones. Rubber-like elastic plant tissues have more amorphous cellulose*; metal-like elastic plant tissues have more micellar cellulose. The structure is further clarified by the thermoelastic behavior of plant tissues.

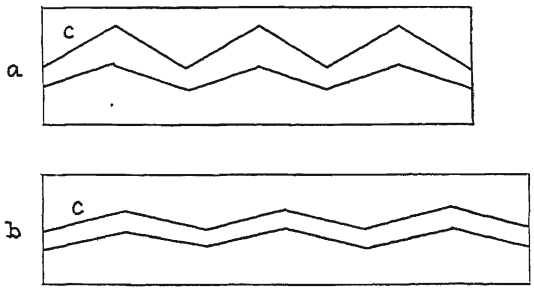

Fig. 3. The average secondary cell wall of rubber-like elastic cylindrical plant tissues. (a) Cellulose molecules in the undeformed cell wall and at the end after heating; (b) cellulose molecules in the cell wall after stretching of the tissue. c = cellulose molecule.

The anomalous thermoelastic behavior of rubber-like elastic tissues suggests that the tension in stretched rubber-like plant tissue is associated with a change of entropy in the material when it is deformed rather than with a change in internal energy. In the undeformed average secondary cell wall, the cellulose molecules are folded to a great extent (Fig. 3a). This is to be assumed because most of the cellulose molecules deviate greatly from the direction of the axis of the plant tissue (11). After stretching, the forces of cohesion keep the molecules parallel in a slightly folded condition

* It may be that not only amorphous cellulose but also non-cellulosic materials of the cell wall, most of which are amorphous, account for rubberlike elasticity. The influence of such small amounts of non-cellulosic material probably is not great and may be neglected.

(Fig. 3b). On heating the tissue there is contraction and the cellulose molecules in the wall are greatly folded as in Fig. 3a. This is the case if the thermoelastic behavior of the tissue is anomalous. The forces of thermal motion are stronger than the forces of cohesion, and the forces act in opposite directions. Hence, after heating, the molecules are greatly folded.

Metal-like elastic cylindrical plant tissues have normal thermoelastic behavior. Their normal thermoelastic behavior suggests that the tension in stretched tissue is mainly associated with a change in internal energy of the material when it is deformed. The cellulose molecules are slightly folded in the undeformed average secondary cell wall of the tissues

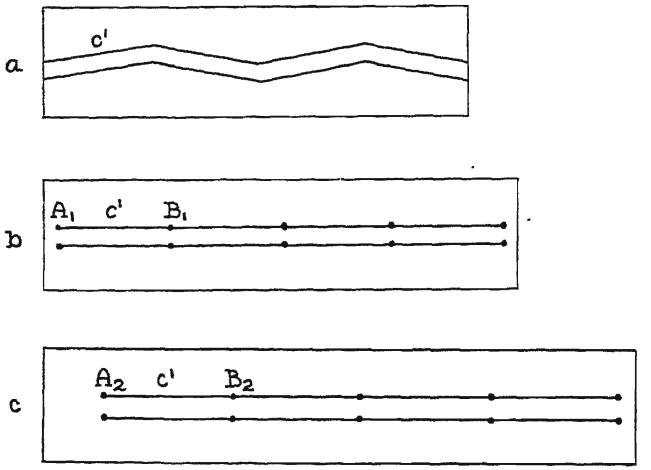

FIG. 4. The average secondary cell wall of metal-like elastic cylindrical plant tissues. (a) Cellulose molecules in the undeformed cell wall; (b) cellulose molecules in the cell wall after stretching of the tissue; (c) cellulose molecules in the cell wall after stretching and heating of the tissue. c' = cellulose molecule.

(Fig. 4a). This is to be assumed because most of the cellulose molecules deviate but little from the direction of the axis of the plant tissue (11). After the tissue is stretched, the forces of cohesion again keep the cellulose molecules in nearly parallel straight lines (Fig. 4b). On heating there is more elongation (Fig. 4c). In the case of metal-like plant tissues the forces of cohesion and of thermal motion act in the same direction. Debye (9, p. 245) assumed that A_1 and B_1 (Fig. 4b) are the ends of the cellulose molecule at low temperature, and A_2 and B_2 the ends of the same molecule at high temperature (Fig. 4c). Hence, after heating, the tissue is more elongated than after the first stretching.

The position assumed by the cellulose molecules in the undeformed cell wall suggests an explanation for the thermoelastic behavior of cylindrical plant tissue in the direction of length. The thermoelastic behavior of the tissues thus gives information about the submicroscopic structure of the cell wall. The same result is found for the orientation of cellulose molecules in average secondary cell walls by using the thermoelastic behavior as by using the ratio of the moduli of elasticity of the tissues (11). This result is as follows:

The average deviation of cellulose molecules in the average secondary cell wall from the direction of the axis of the cylindrical tissue is large in the case of rubber-like elastic tissues and small in the case of metal-like elastic tissues.

The thermoelastic behavior of cellulose ester films may now be considered. According to Guth (3) the thermoelastic behavior of cellulose nitrate and cellulose acetate films may be normal or anomalous. These films show a cooling effect at smaller extensions (normal behavior) and a heating effect at larger extensions (anomalous behavior) beyond the yield point.

It is of interest to compare the thermoelastic behavior of muscles with that of rubber and cellulose. Muscles may be investigated in the relaxed and in the activated state. According to Guth (3), muscles in the relaxed state resemble rubber. The stress-strain curves of the two are similar and the stretching forces have the same order of magnitude. Furthermore, both substances exhibit the same anomalous thermoelastic behavior. At small extensions, muscle absorbs heat. As we increase the extension we pass through an inversion point above which the muscle generates heat. This behavior is exactly like that of rubber. The inversion point for vulcanized rubber of constant extension is at $-50°C.$ (7). In the range between $-50°C.$ and $70°C.$ the tension in vulcanized rubber increases with temperature. At temperatures lower than $-50°C.$, vulcanized rubber becomes hard. Then the relation between tension and temperature is the same as for common solids.

In muscle there is a second inversion point, which is not the case for vulcanized rubber. At higher extension beyond this second inversion point the muscle again absorbs heat.

The molecular structure of rubber and relaxed muscles is the same in principle. Muscle consists of myosin, which is probably made up of long flexible polypeptide chains. We conclude this from its thermoelastic behavior which is similar to that of rubber.

The contraction of activated muscle is a phenomenon not present in rubber. Lengthening of the activated muscle is accompanied by heat absorption, contrary to the behavior of relaxed muscle and rubber. This

fact makes it plausible that activation transforms muscle into a substance with normal thermoelastic behavior.

It is interesting that both muscle and cellulose show both normal and anomalous thermoelastic behavior. The similarity of muscle and cellulose with respect to elasticity is to be expected because of the elastic relation which must exist between protoplasm and cell wall.

Summary

(1) The cell walls of rubber-like elastic plant tissues exhibit anomalous thermoelastic behavior (validity of the Gough-Joule effect). These cell walls contain hydrated cellulose. The cell walls of metal-like elastic plant tissues exhibit normal thermoelastic behavior. These cell walls contain cellulose which is not hydrated.

(2) The thermoelastic behavior of cylindrical plant tissues gives information about the submicroscopic structure in the average secondary cell wall. The average deviation of cellulose molecules in this wall from the direction of the axis of the cylindrical tissue is large in the case of rubber-like elastic cylindrical plant tissues, and small in the case of metal-like elastic cylindrical plant tissues.

(3) Relaxed muscles and hydrated cellulose exhibit anomalous thermoelastic behavior. Activated muscles and cellulose exhibit normal thermoelastic behavior.

References

1. Dart, S. L., and Guth, E., *J. Chem. Phys.* **13**, 28–36 (1945).
2. Guth, E., in J. Alexander's Colloid Chemistry, Theoretical and Applied, Vol. V. Reinhold Pub. Corp., New York, 1944.
3. Guth, E., The Problem of the Elasticity of Rubber and of Rubber-like Materials, *Am. Assoc. Adv. Sci., Pub. No.* **21**, 103–127.
4. Hock, L., *Kolloid-Z.* **35**, 40–47 (1924).
5. Hock, L., *Z. Elektrochem.* **31**, 404–409 (1925).
6. Memmler, K., The Science of Rubber. Reinhold Pub. Corp., New York, 1934.
7. Meyer, K. H., and Ferri, C., *Helv. Chim. Acta* **18**, 570–589 (1935).
8. Müller-Pouillet, Lehrbuch der Physik, III. Band, 2. Hälfte. Verlag Friedrich Vieweg und Sohn, Braunschweig, 1925.
9. Ott, E., Cellulose and Cellulose Derivatives. Interscience Publishers, New York, 1943.
10. Treitel, O., *Trans. Kansas Acad. Sci.* **47**, 219–239 (1944).
11. Treitel, O., *J. Colloid Sci.* **1**, 327–370 (1946).
12. Treitel, O., *J. Colloid Sci.* **2**, 237–246 (1947).
13. Wall, F. T., *J. Chem. Phys.* **11**, 527–530 (1943).

HIGHER ORDER TYNDALL SPECTRA WITH MIXTURES OF ANTIGEN AND ANTISERUM[1]

(A Note to the Editors of the *Journal of Colloid Science*)

Sirs:

At a seminar conducted in these Laboratories on May 5, 1947, Professor Victor K. La Mer of Columbia University described some interesting results which he and his collaborators have obtained in their study of the light scattering properties of monodispersed colloidal sulfur. The results of this study are summarized briefly in the following quotation from a recent article[2]:

"Monodispersed sols of small particle size exhibit the optical properties predicted by the Rayleigh equation, but in the case of sols of larger particles we have observed the higher order effects that can be predicted from the general electromagnetic theory of light scattering. These higher order effects are characterized by the dispersion of the scattered light resulting in bands (or spectra) of different colors whose intensity, polarization and angular distribution depend upon the particle size."

The following day, in the continuation of experiments along another line, I had occasion to examine by indirect illumination a number of slightly turbid supernatants which had been obtained in serological precipitation experiments involving the type-specific pneumococcal polysaccharide antigen SI and the corresponding horse antiserum.[3] To my intense surprise and delight, I noted that the scattered light, instead of being white, was dispersed into several confluent bands of different pastel colors; examination with approximately parallel white light quickly revealed the presence of two to three spectral orders.

The supernatants which showed these higher order Tyndall spectra were obtained in the following way. Mixtures consisting of 1 ml. 8% horse antiserum (antiserum diluted 12.5-fold with 1% NaCl in water) and 2 ml. 0.004% SI in 1% NaCl were prepared at 0°, 21°, and 37°C.; this proportion of the two reagents corresponded to a position near equiv-

[1] The investigation was supported by a grant from the U. S. Public Health Service to the California Institute of Technology.

[2] La Mer, V. K., and Barnes, M. D., *J. Colloid Sci.* 1, 71 (1946). See also Johnson, I., and La Mer, V. K., *J. Am. Chem. Soc.* (In press); La Mer, V. K., and Kenyon, A. S., *J. Colloid Sci.* 2, 257 (1947).

[3] This antiserum, which was kindly provided by the Lederle Laboratories, Pearl River, N. Y., was obtained from a horse which had been injected simultaneously with pneumococci of Types I and II and contained appreciable quantities of both anti-SI and anti-SII antibodies. The presence of the latter is not considered important in the present framework.

alence. The mutual precipitation reaction between SI and antibody protein of the serum was allowed to proceed for 3 hours at the temperature of mixing. At the end of this period, during which considerable precipitate[4] had formed and settled to the bottom, the mixtures were centrifuged for 15 minutes at 2,800 r.p.m. in a Clay-Adams angle-head centrifuge, and the supernatants were carefully obtained by decantation and stored in the refrigerator. At this time the supernatants were relatively clear. During the following days the supernatants were removed several times from the refrigerator and allowed to warm to room temperature so that various tests could be carried out, in accordance with the protocol of the experiment which was under way. Several days after their preparation it was noticed that some of the supernatants had developed an unwanted turbidity; and, indeed, it was to determine which of the mixtures required centrifuging that, on the tenth day following their preparation, the mixtures were held up to the light and the observation reported above was made. One has the feeling that the investigator was blind before Professor La Mer spoke.

Approximately 20 mixtures of the sort described above showed higher order scattering spectra. Uniformly, these mixtures were characterized by a noticeable turbidity, resulting from the presence of particles which failed to settle appreciably during a three-day period of observation. There were no large differences among these mixtures, either in the number of orders displayed or in the intensity of the bands. On the other hand, all of the control mixtures, consisting of serum solutions devoid of antigen and antigen solutions devoid of serum, remained relatively clear during the experimental period and failed to exhibit the spectral scattering.

We may, therefore, tentatively attribute the higher order scattering spectra to the presence of a relatively monodisperse immunochemical precipitate, produced by the continued slow reaction of small quantities of antigen and antibody, and perhaps of small antigen-antibody complexes, which remained in the supernatant when the initial precipitate was removed. We may explain the pastel quality of the spectral colors in terms either of the imperfect monodispersity of a single component or of a more complicated polydispersity, involving, for example, two relatively monodisperse components, or one relatively monodisperse component and one polydisperse component, the particle sizes of the two components falling into a bimodal distribution.[5]

[4] The amount of the washed precipitate, expressed in terms of its nitrogen content, was 57.6 γ at 0°, 49.5 γ at 21°, and 44.8 γ at 37°. Since the contribution of SI, which has a nitrogen content of approximately 5%, to the nitrogen of the precipitate cannot exceed 4 γ, these values correspond approximately to the precipitated antibody nitrogen.

[5] These notions are not completely the writer's own, but represent his assessment of the views expressed by interested associates.

Accepting this interpretation of the observed phenomenon, we may inquire briefly into its significance for our understanding of the process of serological precipitation. Recently, it was suggested[6] that this process may be effectively described in terms of the formation and consequent aggregation of microscopic particles of specific precipitate, called seromicrons. When homologous antigen and antibody are mixed in the usual concentrations, there follows a succession of events which are visible to the naked eye with the aid of indirect white illumination. In the initial period of the reaction a blue scattering appears and increases in intensity. Gradually the blue scattering is superseded by a white scattering which may be taken as a mark of the polydispersity of the developing precipitate.[2] Presently discrete particles may be discerned; by aggregating with one another these increase in size until they are large enough to settle to the bottom. Viewed under darkfield, these particles are seen to be aggregates of the microscopic particles referred to above. It is not possible at the moment to say how uniformly the process of seromicron formation proceeds under these conditions of rapid precipitation. We see, however, that when the precipitation is allowed to proceed slowly there may result particles sufficiently uniform to allow the observation which is the subject of this note. The customary determination of the amount of the formed precipitate reveals little of the morphology of its formation. The techniques for the study of this long-neglected aspect of serological precipitation are available, and it may be hoped that their application will soon provide interesting, and perhaps useful, information.

FRANK LANNI

National Institute of Health Research Fellow,
Gates and Crellin Laboratories of Chemistry,
California Institute of Technology,
Pasadena, Calif.
May 9, 1947

[6] Lanni, F., *J. Expil. Med.* **84**, 167 (1946).

BEHAVIOR OF SOME ALKALI SOAP SYSTEMS IN ORGANIC SOLVENTS

Mata Prasad, G. S. Hattiangdi * and B. K. Wagle

From the Chemical Laboratories, Royal Institute of Science, Bombay, India

Received April 15, 1946; revised Mss. received September 5, 1947

Introduction

There has been little systematic work on the behavior of alkali soaps toward organic solvents. Pioneer work on the subject was done by Fischer (3), who showed that typical lyophilic colloidal solutions of soaps are obtained in absolute alcohol, benzene, toluene, chloroform, carbon tetrachloride and ether. He also showed that the amounts of different alcohols taken up by a soap to form non-syneretic gels vary within wide limits. Fischer, McLaughlin and Hooker (4) prepared a large number of alkali soaps of the higher fatty acids and investigated systematically the behavior of several soap-water and soap-alcohol systems before, during, and after the process of gel-formation, with special reference to the physical condition of the soap mixtures. Miss Laing and McBain (6) report that the solutions of alkali soaps in anhydrous alcohol are true molecular solutions at the boiling point; on cooling, the soaps crystallize out in the form of flakes, and jellies are formed only if sufficient water is present.

von Weimarn (14) found that the gels of sodium oleate and sodium stearate in benzene, toluene, xylene, cumene and cymene appear to be isotropic when viewed through crossed nicols. McBain and Harris (10) noticed a similar behavior with the transparent jelly of sodium stearate in benzene which was formed when the soap-solvent system was heated in a closed tube to 105–110°C. They also observed that (1) below 105°C. the crystallization of the soap sets in, accompanied by the separation of the liquid, and (2) with a rise in temperature, the jelly is reformed, and appears to be most stable above 105°C. A similar behavior was noticed by von Weimarn in the case of soap gels in the several solvents mentioned earlier. McBain and McClatchie (10) have investigated the behavior of about 20 soaps toward xylene, and also of the palmitates of sodium, silver and aluminum toward 30 different organic solvents. The sodium soaps, although soluble in polar solvents, were found to dissolve and form jellies in non-polar solvents as well.

* Present address: Department of Chemistry, University of Southern California, Los Angeles 7, Calif.

Da Fano (1) was the first to observe that several sodium and potassium soaps dissolve in dense oils and other complex substances at a high temperature, and that soft jellies are obtained on cooling the resulting solutions. The firmness of the jellies increased with increasing temperature but depended mainly on the products used and the amount of the soap dissolved. Da Fano (2) has also prepared jellies of sodium and potassium palmitates, stearates, oleates, ricinoleates and linoleates in mineral oils, paraffin oil, vaseline, petroleum, resin oil, olive oil, tetrahydronaphthalene, decahydronaphthalene, pentachloroethane and hexachloroethane. He adds that the soaps of ricinoleic acid give gels in coal tar, but jellies are not obtained with resin soaps in dense mineral oils and in some vegetable oils.

Lawrence (7) has investigated the behavior of the stearates and oleates of several metals towards Nujol. He finds that the dry soaps pass, on heating, through a plastic or soft crystalline form between the solid crystalline and isotropic liquid states, and that the temperature range of the stable gels corresponds to this plastic range. Below the lower temperature limit and at concentrations above 0.5%, pseudo-gels are formed containing an opaque paste of micro crystals. In more dilute solutions, sedimentation of the crystalline soap takes place. Lawrence (8) has also prepared gels of sodium stearate in a number of organic solvents such as ethyl, propyl, butyl, amyl, octyl, cetyl and benzyl alcohols, phenol, *p*-cresol, glycol, glycerine and decalin, and finds that gelation is inhibited in methyl alcohol, naphthalene, α-bromonaphthalene, diphenyl, diphenylmethane and dibenzyl, from which the soap crystallizes out like an ordinary substance.

Leggett, Vold and McBain (9) have measured the solubility of sodium palmitate in 17 different organic solvents, including 4 alcohols and 3 hydrocarbons, over the whole range of composition from room temperature to 300°C., observing the phases formed and obtaining partial phase diagrams. They have correlated the results to the internal pressure and polarity of the solvents as well as to the size and shape of the solvent molecules and to the space relations of their polar groups.

Recently, Prasad, Hattiangdi *et al.* (11) have prepared gels of several alkali soaps in pinene, and have investigated several of their properties before, during, and after the process of gel-formation. They find that the soaps, which are insoluble in pinene at room temperature, swell on keeping for some time in contact with it; the swelling increases on increasing the temperature, and the soaps dissolve suddenly near the boiling point of pinene to give clear, mobile solutions. On cooling these solutions, clear transparent elastic gels are obtained, some of which exhibit the phenomenon of syneresis to a marked extent, whereas others develop opacity on standing. The effects of the addition of small amounts of different sub-

stances on the syneretic phenomenon exhibited by some of these gels have been investigated by Hattiangdi (5) and Prasad, Hattiangdi and Adarkar (12) who find that the stability of gel systems can be controlled by suitable added substances.

The review of literature given above shows that, although the data on the subject is not scanty, it cannot be correlated easily since the different investigations have not been carried out under identical experimental conditions. Further, the observed behavior of soaps toward organic solvents has not been explained adequately. An attempt in this direction has therefore been made in the present investigation which concerns a study of the behavior of sodium oleate, sodium stearate and sodium palmitate toward 40 different organic solvents. The data have been utilized to obtain an insight into the conditions necessary for the formation of soap gels under identical experimental conditions.

Materials Used

Sodium oleate, sodium stearate and sodium palmitate used were pure products of the British Drug House. The pinene used was a product of Eastman Kodak & Co., and the Nujol of Stanco, Inc. The other solvents employed were pure products of either E. Merck, Scherring-Kahlbaum, Reidel-Haen, or the British Drug House. All the soaps and solvents, except Nujol, were used after their purity was confirmed by means of standard methods.

Experimental Technique

A known amount of a dry soap was weighed out in a clean dry test tube, and 10 cc. of a solvent were added to it. The tube was corked well and the system was stirred thoroughly for some time. The soap-solvent system was then heated gradually to a temperature near the boiling point of the solvent when the soap dissolved completely to give a clear mobile solution. It was found in some cases, however, that even prolonged heating did not bring about the dissolution of the soap. The system was stirred constantly during the heating process. Air-bubbles present were removed carefully, and the solution was observed while it underwent cooling in an air thermostat at 30°C.

It was observed that, on cooling, the soap-solvent system ultimately existed in, or passed through, one or more of the following states: (1) homogeneous solution, (2) crystalline state, (3) pseudo-gel, and (4) true gel. A highly solvated mass, which appears like a true gel but possesses none of its characteristic properties, has been considered as a pseudo-gel. These systems are extremely weak and consist of a large number of microcrystallites which enmesh the dispersion medium at random.

The observations regarding the behavior of the 3 soaps toward the 40 different organic solvents are summarized in Tables I–VII.

TABLE I

Behavior of Soaps toward Hydrocarbons

Solvent	Sodium oleate	Sodium stearate	Sodium palmitate
ALIPHATIC			
Nujol	Insol. in cold; swells on warming and goes into a clear mobile solution at a high temperature; forms firm, transparent gels on cooling; syneresis very slight; no opacity developed on standing.	Behavior similar to that of oleate; gel is firmer and less syneretic than that with oleate; develops slight opacity on standing.	Insol. in cold; fairly sol. in hot; sets to firm, transparent gel; no opacity developed on standing; syneresis less than with stearate.
AROMATIC			
Benzene	Insol. in cold and hot; swells in contact with benzene; crystallizes on cooling; no gel obtained.	Same as oleate.	Same as oleate.
Toluene	Insol. in cold and sp. sol. in hot; swells with increasing temp.; forms opaque gel which synerizes markedly.	Insol. in cold and hot; swells considerably; no gel formed.	Same as stearate.
Xylene	Insol. in cold; sol. in hot; swells with increasing temp.; transparent gel obtained; marked syneresis.	Insol. in cold and hot; forms a transparent gel; syneresis less than oleate gel.	Insol. in cold; sp. sol. in hot; transparent gel; slight syneresis.
Mesitylene	Insol. in cold; sol. in hot; transparent gel; marked syneresis.	Same as oleate; gel is less syneretic.	Insol. in cold; sp. sol. in hot; transparent gel; little syneresis.
Cumene	Same as above.	Same as above.	Same as above.
Cymene	Same as above.	Same as above.	Same as above.
Pinene	Insol. in cold; sol. in hot; swells with increasing temp.; solution sets to a clear firm gel on cooling; marked syneresis.	Insol. in cold; sol. in hot; transparent gel; more rigid and less syneretic than oleate gel.	Insol. in cold; sp. sol. in hot; swells on increasing temp.; clear gel; firm and nonsyneretic.

DISCUSSION OF RESULTS

It will be seen from Tables I–VII that all three soaps are practically insoluble in all the solvents at low temperatures, and swell, and later dissolve, on gradual heating. Regarding the formation of gels on cooling the hot solutions of the soaps in the several organic solvents, it will be noticed that (a) for the same group of compounds, gelation is favored usually in aromatic rather than in aliphatic compounds; (b) among the 7 major groups of solvents, gelation is favored only in hydrocarbons, halogenated hydrocarbons, hydroxy compounds and ethers; and (c) in a homologous series of compounds, gelation is facilitated in the higher homologues, that is, the amount of gel-like material obtained increases roughly with the boiling point of the solvent used.

Further, the differences in the behavior of the soap gels in organic solvents of a different chemical character are quite marked in some cases.

For example,

(1) The soap gels in aliphatic hydroxy compounds are comparatively quick setting, soft, synerize profusely, and are usually translucent or opaque, whereas the corresponding gels in the aromatic hydroxy compounds are slow setting, rigid, non-syneretic, and are always transparent;

(2) Sodium oleate does not usually give rise to gels in aromatic hydroxy compounds, nor sodium palmitate in aliphatic hydroxy compounds.

Leggett, Vold and McBain (9), who have determined the solubility of sodium palmitate in numerous organic solvents, find that the solubility of the soap depends upon (1) the nature, number and space relationships of the polar groups of the solvent molecules, (2) the size and shape of the solvent molecules, and (3) the polarity of the solvent as measured by the

TABLE II

Behavior of Soaps toward Hydroxy Compounds

Solvent	Sodium oleate	Sodium stearate	Sodium palmitate
ALIPHATIC			
Methyl alcohol	Insol. in cold; sol. in hot; crystallizes on cooling; no gel.	Same as oleate.	Same as oleate.
Ethyl alcohol	Same as above.	Same as oleate.	Same as oleate.
n-Propyl alcohol	Same as above.	Same as oleate.	Same as oleate.
Isopropyl alcohol	Insol. in cold; sol. in hot; white opaque gel; slight syneresis.	Same as oleate; syneresis is less.	Insol. in cold and hot; no gel formed.
n-Butyl alcohol	Same as above.	Same as above.	Same as above.
Isobutyl alcohol	Same as above.	Same as above.	Same as above.
n-Amyl alcohol	Same as above.	Same as above.	Insol. in cold and hot; heterogeneous suspension; sets to opaque pseudo-gel on cooling.
Ethylene glycol	Insol. in cold; sol. in hot; crystallizes on cooling; no gel formed.	Insol. in cold; sol. in hot; white opaque gel; non-syneretic.	Same as oleate, but less soluble.
Glycerol	Insol. in cold; sol. in hot; neither crystallization nor gelation occurs.	Insol. in cold; sol. in hot; transparent, non-syneretic gel obtained.	Same as stearate.
AROMATIC			
o-Cresol	Insol. in cold; sol. in hot; crystallizes on cooling; no gel formed.	Same as oleate regarding solubility; but firm transparent gel formed on cooling and standing; non-syneretic and does not develop opacity on keeping.	Same as oleate.
m-Cresol	Same as above.	Same as above.	Same as stearate.
Phenol	Same as above.	Same as above.	Same as stearate, but less soluble.
Benzyl alcohol	Insol. in cold; sp. sol. in hot; swells; crystallizes on cooling; no gel.	Insol. in cold; sol. in hot; clear transparent non-syneretic gel formed on cooling; develops slight opacity on long standing.	Same as oleate.

TABLE III

Behavior of Soaps toward Halogenated Hydrocarbons

Solvent	Sodium oleate	Sodium stearate	Sodium palmitate
ALIPHATIC			
Chloroform	Insol. in cold and hot; swelling negligible; crystallizes on cooling; no gel.	Same as oleate.	Same as oleate.
Carbon tetrachloride	Same as above.	Same as oleate.	Same as oleate.
AROMATIC			
Benzal chloride	Insol. in cold and hot; swelling negligible; crystallizes on cooling; no gel formed.	Same as oleate.	Same as oleate.
Chlorobenzene	Insol. in cold; sol. in hot; gel formed on cooling; profuse syneresis; gel stable only at high temps.	Insol. in cold and hot; crystallizes on cooling; no gel formed.	Insol. in cold; sp. sol. in hot; loose pseudo-gel formed.
Bromobenzene	Same as above.	Insol. in cold; sol. in hot; loose gel.	Same as above, but firm true gel is obtained.
p-Chlorotoluene	Insol. in cold; sol. in hot; slightly syneretic gel obtained.	Insol. in cold; sol. in hot; gel obtained; syneresis less than with oleate.	Same as oleate and stearate; syneresis markedly less.

TABLE IV

Behavior of Soaps toward Ethers

Solvent	Sodium oleate	Sodium stearate	Sodium palmitate
ALIPHATIC			
Ethyl ether	Insol. in cold and hot; crystallizes and does not gelate.	Same as oleate.	Same as oleate.
AROMATIC			
Anisole	Insol. in cold; sol. in hot; gel formed; slight syneresis.	Same as above.	Same as stearate.
Phenetole	Insol. in cold; sol. in hot; transparent gel obtained.	Same as oleate; solubility is less.	Insol. in cold; sp. sol. in hot; does not gelate.

TABLE V

Behavior of Soaps toward Esters

Solvent	Sodium oleate	Sodium stearate	Sodium palmitate
ALIPHATIC			
Ethyl acetate	Insol. in cold and hot; swelling very slight; crystallizes and does not gelate.	Same as oleate.	Same as oleate.
Butyl acetate	Same as above.	Same as oleate.	Same as oleate.
AROMATIC			
Phenyl acetate	Same as above.	Same as oleate.	Same as oleate.

quotient of the dipole moment and the molecular volume. Since the solubility of the disperse phase in the dispersion medium is a factor which contributes largely toward gel-formation, it was considered that there might exist a relationship between the gel-forming capacity of a soap-solvent system and either the polarity or the dielectric constant of the

TABLE VI

Behavior of Soaps toward Aldehydes and Ketones

Solvent	Sodium oleate	Sodium stearate	Sodium stearate
Butyraldehyde	Sol. in cold and hot; yields white solution; neither crystallization nor gelation takes place.	Same as oleate.	Insol. in cold; sp. sol. in hot; no gel formed.
Benzaldehyde	Insol. in cold and hot; no gel formed.	Same as oleate.	Same as oleate.
Acetone	Insol. in cold; sol. in hot; crystallizes on cooling; no gel formed.	Same as oleate.	Same as oleate.
Methylethylketone	Same as above.	Same as oleate.	Same as oleate.

TABLE VII

Behavior of Soaps toward Nitro, Amino and Other Compounds

Solvent	Sodium oleate	Sodium stearate	Sodium palmitate
Nitrobenzene	Insol. in cold and hot; crystallizes on cooling; no gel formed.	Same as oleate.	Same as oleate.
Aniline	Same as above; swelling is slightly more.	Same as oleate.	Same as oleate.
Carbon disulphide	Insol. in cold and hot; crystallizes on cooling; no tendency to form a gel.	Same as oleate.	Same as oleate.

solvent molecules. It was found, however, that the amount of the gel-like material obtained, which increases roughly with the boiling point of the solvent, does not increase with either ϵ or μ/v, but that it increases roughly with an increase in the molar polarization, $\left(\frac{\epsilon - 1}{\epsilon + 2}\right)v$, of the solvents belonging to a homologous series. However, when solvents of the same value of molar polarization but of a different chemical character were considered, it was found that gelation takes place invariably in only one of them and not in the other, suggesting that there are other factors beside molar polarization which contribute toward the process of gel-formation. A quantitative investigation in this direction is under way.

It was observed during experimentation that, as the concentration of the soap is increased gradually, the soap-solvent system exists, on cooling, in different states. Consequently, the critical concentrations at which the systems pass from one state to another were determined carefully and the temperatures at which these states occur were also noted. Typical results obtained with soap-pinene systems are presented in Table VIII, and a summary of the results with 16 different organic solvents is given in Table IX. The terms C, PG and G in Table IX represent crystalline flaky or amorphous soap, pseudo-gels and true gels, respectively, and the temperatures (°C.) at which these forms are discernible are given in parentheses.

TABLE VIII

Effect of Concentration on the Behavior of Soap-Pinene Systems

Soap content (mg./10 cc. of pinene)	Temperature (°C.) at which		
	Crystallization starts	Pseudo-gels are obtained	True Gels are obtained
	Sodium Oleate		
5	110	—	—
10	110	—	—
20	110.5	?	—
25	110.5	80	—
30	110	80	—
35	108.5	80	—
36	110	80	—
37	110	80	—
38	109	80	—
39	109.5	80	—
40	—	—	40
50	—	—	43
60	—	—	45
80	—	—	50
100	—	—	56
	Sodium Stearate		
5	111.5	—	—
10	112	—	—
15	112	—	—
20	111	—	—
30	112.5	—	—
40	111.5	69	—
50	112	70	—
51	—	—	49
52	—	—	50
55	—	—	50
60	—	—	51
80	—	—	60
100	—	—	69
	Sodium Palmitate		
20			about 35
30			?
40			50
50			51
60			53
80			61
100			65

TABLE IX

Effect of Concentration on the Behavior of Soap-Solvent Systems

Solvent	Concentration of soap (mg./10 cc. of solvent)								
	Sodium oleate			Sodium stearate			Sodium palmitate		
	C	PG	G	C	PG	G	C	PG	G
Nujol	0–4	5–14 (*70*)	15–100 (>*93*)	0–15 (*185*)	20–30 (*105*)	30–100 (>*105*)	0–19	20–23 (*118.5*)	25–100 (>*67*)
Toluene		0–49	50–400 (>*42*)						
Xylene	0–20 (*94*)	30–39 (*30*)	40–100 (>*65*)	0–20 (*105*)	20–25 (*30*)	26–100 (>*29*)		0–34	35–100 (>*30*)
Pinene	0–19 (*110*)	20–39 (*80*)	40–100 (>*40*)	0–30 (*112*)	40–50 (*70*)	51–100 (>*49*)			20–100 (>*35*)
Isopropyl alcohol	0–60	65–75	80–100 (>*30*)	0–45	45–47	47–100 (>*32*)			
Isobutyl alcohol	0–100 (*35*)	105–165 (*36.5*)	170–250 (>*37*)	0–50 (*30*)	50–80 (*38*)	95–125 (>*30*)			
n-Butyl alcohol			150–300 (>*30*)	0–60 (*30*)	60–65 (*30*)	65–100 (>*30*)			
Ethylene glycol						300–375 (>*30*)			
Glycerol				0–40 (*40*)	40–45 (*30*)	50–100 (>*30*)	0–60 (*41*)	60–64	64–100 (>*30*)
Phenol					250–255 (*30*)	255–300 (>*30*)			
o-Cresol					150–170 (*30*)	175–200 (>*30*)	0–265	280–295 (*30*)	300–350 (>*30*)
m-Cresol						310–400 (>*30*)			
Benzyl alcohol				0–30 (*30*)	31–34 (*30*)	35–100 (>*30*)			
Bromobenzene	0–80 (*89*)	85–105 (*87*)	110–120 (>*90*)					40–70 (*85*)	75–100 (>*80*)
Chlorobenzene		60–95 (*67*)	100–200 (>*65*)						
Anisole		90–100 (*82.5*)	105–150 (>*67*)						

It will be seen from Table VIII that, within certain limits of concentrations, sodium oleate and sodium stearate crystallize out of the solutions in pinene on cooling. The mean temperatures at which sodium oleate and sodium stearate crystallize out are 110°C. and 112°C., respectively. Sodium palmitate is sparingly soluble in pinene and does not dissolve completely even at the boiling point of the solvent. It remains in the system in a finely dispersed and highly solvated state, and, on cooling, the soap sediments, not in the form of crystalline flaky or amorphous material, but as highly solvated aggregates. The temperatures of sedimentation were not noted as they would not have the usual significance. At soap contents above 20 mg./10 cc. of pinene, true gels of sodium palmitate are formed, but below this concentration lumps of solvated soap are obtained which do not show any tendency to form even a pseudo-gel.

Prasad, Hattiangdi and Vishvanath (13) conclude from their investigations on the viscosity of solutions of sodium oleate and sodium stearate in pinene that the values recorded above 110°C. are those for

true molecular solutions or for sols with little or no aggregation, whereas below this temperature, small rigid particles are formed which remain suspended in the system and vitiate the results. It is interesting to note that this temperature is almost identical with the temperature determined in the present investigation by direct visual measurements, indicating that the rigid particles, as reported by Prasad *et al.* to vitiate viscosity values, are in fact solvated micro-crystallites of the soap.

It will be seen from Tables VIII and IX that the changes of state from crystallization to pseudo-gelation and from pseudo-gelation to gelation are brought about by extremely small changes in the concentration of the soap, of the order of 1 mg. or less. This shows that the transition from the state of crystallization to that of the weak precarious pseudo-gels and subsequently to the typical stable gels is effected by very gentle gradations in the soap content of the system.

Summary

1. The behavior of sodium oleate, sodium stearate and sodium palmitate toward 40 different organic solvents has been examined. It is found that the soaps do not dissolve in most of the solvents at room temperature, but swell on heating and give clear mobile solutions near the boiling point of the solvent. On cooling these solutions, any one of the following phenomena takes place, depending upon the nature of the soap-solvent system: (1) the soap remains in solution, (2) the soap crystallizes out, (3) a pseudo-gel is formed, or (4) a true gel is obtained.

2. It is observed, in general, that the amount of the gel-like material obtained, that is, the gelating capacity of the soap-solvent system, increases roughly with the boiling point of the solvent.

3. The behavior of the soap-solvent systems giving rise to true gels has been examined with special reference to the degree of supersaturation. It is observed that, if the soap content is low, crystallization occurs when the hot soap-solvent system is cooled. With an increase in the concentration of the soap, a pseudo-gel is obtained at first, and a true gel is formed only when an optimum concentration of the soap is reached. Further, the transition from the crystalline state to the weak precarious pseudo-gels, and subsequently to the typical stable gels, is effected by very gentle gradations in the concentrations of the soap in the system.

4. The temperatures of crystallization and of the formation of pseudo-gels and true gels have been measured in the case of the three soaps in 16 different solvents. The zones of concentrations in which the soap exists in the three different states have also been determined.

References

1. Da Fano, E., *Giorn. chim. ind. applicata* **11**, 199 (1929).
2. Da Fano, E., *Ind. olii minerali e grassi* **9**, 105 (1929).
3. Fischer, M. H., *Science* **49**, 615 (1919).
4. Fischer, M. H., McLaughlin G. D., and Hooker, M. O., *Kolloidchem. Beihefte* **15**, 102 (1922).
5. Hattiangdi, G. S., *J. Sci. Ind. Research (India)* **4**, 489 (1946).
6. Laing, M. E., and McBain, J. W., *Kolloid-Z.* **35**, 19 (1924).
7. Lawrence, A. S. C., *Trans. Faraday Soc.* **34**, 660 (1938).
8. Lawrence, A. S. C., *ibid.* **35**, 702 (1939).
9. Leggett, C. W., Jr., Vold, R. D. and McBain, J. W., *J. Phys. Chem.* **44**, 1058 (1940); **46**, 429 (1942).
10. McBain, J. W., and McClatchie, W. L., *ibid.* **36**, 2567 (1932).
11. Prasad, M., Hattiangdi, G. S., *et al.*, *Proc. Indian Acad. Sci.* **21**, 1, 56, 105 (1945).
12. Prasad, M., Hattiangdi, G. S., and Adarkar, S. P., *ibid.* **22**, 320 (1945).
13. Prasad, M., Hattiangdi, G. S., and Vishvanath, C. V., *ibid.* **21**, 90 (1945).
14. Von Weimarn, P. P., Die Allgemeinheit des Kolloidzustandes, Bd. 1, Aufl. 2 (1925), pp. 352–363; *J. Russ. Phys. Chem. Soc.* **46**, 610, 624 (1914); **47**, 2163 (1915); **48**, 532 (1916).

VOLUMETRIC ANALYSIS OF COLLOIDAL ELECTROLYTES BY TURBIDITY TITRATION [1]

Joseph M. Lambert

From General Aniline & Film Corp., Central Research Laboratory, Easton, Penna.

Received June 26, 1947; Revised copy Sept. 4, 1947

Introduction

Interest in a method for the determination of colloidal electrolytes in dilute solutions is shown by several recent publications. The chemical determination of small amounts of soaps or fatty acids following conventional lines is described by Hoffpauir and Kettering (4). In an earlier article on the tensimetric analysis of surface-active electrolytes, Preston (9) described a method which depends upon the titration of an anionic material with a cationic material (or *vice versa*), determining the end-point by the change in surface tension. The organic sulfonate content of synthetic detergents can be determined, according to Marron and Schifferli (7), by a direct volumetric determination utilizing the chemical reaction of *p*-toluidine hydrochloride with organic sulfonates. Recently DuBois (2) gave a critical review of the various methods used specifically for the quantitative determination of cationic surface-active agents. One of the recommended test procedures developed by Hartley and Runnicles (3) is based on the titration of the cationic material with certain anionic agents in the presence of alkaline bromphenol blue as indicator.

None of the methods reviewed in the foregoing seemed to furnish a rapid and convenient procedure for determining small amounts of *different types* of surface-active agents. The turbidity titration method described here was worked out using equipment which is usually available in a chemical laboratory. The procedure consists of titrating an anionic agent with a cationic agent (or *vice versa*) under such conditions that a colloidal precipitate is produced near the equivalence-point and solubilized or coagulated by a small excess of reagent. The end-point of the titration is indicated by the maximum turbidity of the solution, which is easily detected with a conventional colorimeter.

A complication occurred with some surface active agents which gave a precipitate which was too permanent for solubilization by an excess of

[1] Presented Before the Division of Colloid Chemistry at the 111th Meeting of the American Chemical Society, Atlantic City, N. J.

the particular reagent used. However, sharp endpoints could be obtained with the synthetic agents by the addition of a non-ionic surface-active agent, and with soap by the addition of NH_4OH to the unknown solution. Using this modification, the turbidity titration method was universally applicable to a large variety of different colloidal electrolytes. Although the test measures the total amount of ionic surface-active materials in solution and is not specific, it was found to be useful. The method is simple, rapid, and sufficiently accurate to solve a number of problems which require the quantitative determination of one given detergent or wetting agent in dilute solution.

Description of Apparatus

A schematic view of the equipment is shown in Fig. 1. Almost any conventional type colorimeter is suitable, if it permits access to the absorption cell so that a buret and a stirrer can be mounted as indicated.

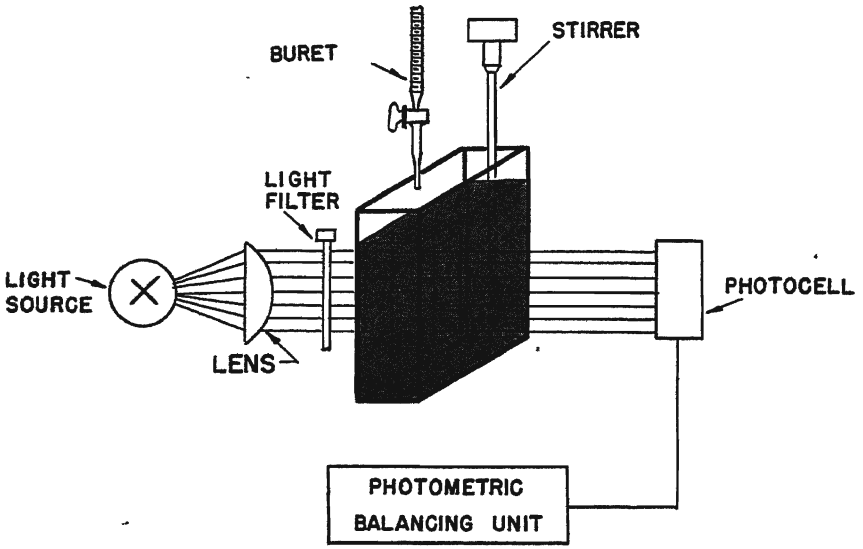

Fig. 1. Schematic view of equipment for turbidity titration.

The burettes used had a capacity of 10 ml. and were graduated in 0.05 ml. intervals. For routine determinations a Machlett automatic buret No. A8-525 proved very satisfactory. Stirring was accomplished by a glass rod which was placed in a part of the solution cell unexposed to the light beam of the photometer. For convenience the stirrer was operated by a foot switch.

Method of Turbidity Measurements

The arrangement shown makes it possible to stir the solution after each addition of reagent and to follow the subsequent changes in turbidity by measuring the amount of light transmitted by the solution. This method of turbidity measurement differs from the common nephelometric technique which is based on the measurement of the scattered light.

The following relations for the light transmitted by turbid solutions, containing colloidal particles much smaller than the wave length of light, show that a wide turbidity range can be covered by simply changing the filter in the colorimeter. Some typical solutions obtained by interrupting the turbidity titration near the turbidity maximum gave spectral transmission curves indicating that Rayleigh's limiting law was applicable. In contrast to these solutions, other colloidal systems containing larger particles can show very complex scattering phenomena, as found by Barnes and LaMer (1) in the case of sulfur sols.

Let I_t be the amount of light transmitted by the turbid medium. Then, neglecting the light scattered in the forward direction,

$$I_t = I - I_a - I_s$$

where I = amount of incident light, I_a = amount of light absorbed and I_s = amount of light scattered by the solution. In colorless solutions I_a will be zero or very small and I_t will primarily depend on the scattering properties of the solution.

Rayleigh's formula gives the intensity of scattered light (I_s) as a function of wave length

$$I_s = k\, I_0 \frac{V^2}{R^2} \frac{1}{\lambda^4}$$

where I_0 is the intensity of the incident light, V = volume of the scattering particles, R = mean distance: point of observation to scattering particles, λ = wave length of the light and k = constant. For a given geometric set-up and a given intensity of the incident light, Rayleigh's law can be written with good approximation as

$$I_s = \frac{k'}{\lambda^4}$$

where k' is a new constant.

According to this relation the amount of scattered light will decrease greatly with an increase in wave length. Consequently, the amount of light transmitted by a turbid solution can be varied over a wide range by using appropriate filters. In practice, it was found that a blue filter gave very good sensitivity at low turbidity levels, and a red filter facilitated the

measurements at high turbidity levels by reducing the apparent density of the solution. A more extensive study of the light scattering characteristics of solutions obtained during turbidity titrations might furnish indirectly some information regarding the micellar structure of colloidal electrolytes.

For the experimental work described below three different photometers were used, all indicating the relative light transmission of solutions on a density scale. If

$$T = \frac{I_t}{I_0},$$

where T = apparent transmission, I_t = the amount of light transmitted by the solution, and I_0 = the amount of light transmitted by water, then the apparent density (D) is defined as

$$D = \log\frac{1}{T}.$$

The advantage of the density scale can be seen by considering solutions of widely different light transmission, say 50%, 10%, 1%, and 0.1%; the corresponding density values are 0.3, 1.0, 2.0, and 3.0.

Description of Photometers

Not all the instruments described in the following covered an especially wide density range. Nevertheless, each photometer could be used for turbidity titrations if the concentrations of the solutions and the light filters were properly selected.

a. The Ansco Sweet Densitometer (10) was provided with a special adapter holding the stabilized light source, the light filter, and a 2 × 4 × 8 cm. rectangular solution cell. The length of the light path in the solution was 2 cm. This instrument covered a very wide density range, *i.e.*, up to $D = 3$. One of the special features of this electronic photometer is a direct reading linear density scale (reading in 0.05 density units) which was particularly suitable for measurements at high turbidity levels. For good overall sensitivity a blue-green filter (Corning No. 4303) was used.

b. The Klett-Summerson Photoelectric Colorimeter (Model 900–3) was used with blue filter KS-42 or red filter KS-66 for low and high turbidity levels, respectively. The same rectangular solution cells were used as described under (*a*). Fig. 2 shows the instrument and the assembly of equipment for turbidity titration. It seemed unnecessary to cover the cell compartment during measurements if the instrument was used in subdued light. This colorimeter has a fairly long non-linear density scale up to $D = 2$, with good sensitivity up to a density of about 1.5. The scale is

calibrated in 500 × density units; the lower range up to $D = 1$ affords excellent sensitivity and permits one to read $D = 0.002$ per division.

c. The AC-Model Fisher Electrophotometer was used with special absorption cells similar to the Fisher tubes No. 7-102, but 1 in. longer.

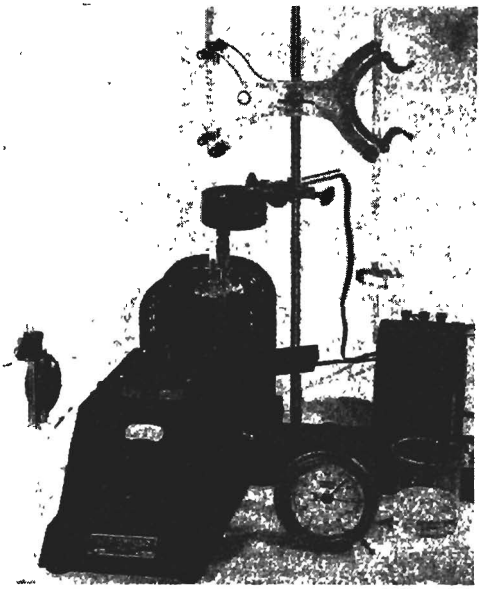

FIG. 2. Assembly of equipment for turbidity titration.

The cover of the cell compartment was replaced with one having a circular opening of 1 in. diameter, thus providing access to the solution cell. With this instrument care had to be taken that the stirring rod would not protrude in the light path of the photometer. The instrument was used on range C with blue filter No. 425-B for high sensitivity and on range B with red filter No. 650-A for measurements at high turbidity levels. The non-linear photometric scale "A" of this colorimeter is comparatively short, reading only up to $D = 1$; it is calibrated in 100 × density units.

Reagents Used and Materials Titrated

A cationic and an anionic surface-active agent of relatively high purity was selected to serve as reagent. Cetyl pyridinium chloride (Tech.) obtained from Edwal Laboratories, Inc., was used as the cationic agent; Igepon TD [2] manufactured by General Aniline & Film Corp. as the anionic agent.

[2] This product is Igepon TD in the highest commercial concentration and is also designated Igepon TFS Conc.

Both products were analyzed by conventional chemical methods to determine the content of active material. The cetyl pyridinium chloride sample was found to contain N, 4.36%; Cl, 10.19%. Calculated: N, 4.12%; Cl, 10.43%. In view of this result the product was assumed to be 97% pure. The Igepon TD sample (active principle: sodium N-acyl-N-methyl-taurate) was found to have a total content of anionic material close to 76%.

Using the above materials, stock solutions were prepared in distilled water containing approximately 0.01 *N* cationic and anionic agent, respectively. These solutions, usually in 1:1 dilution with distilled water, served as the reagents for the turbidity titrations. Cetyl pyridinium chloride (also designated CPC in the following) was employed for the anionic active materials and Igepon TD for the cationic active materials.

The commercial surface-active agents which were titrated are described in the following: The *anionic detergents* were sodium salts of oleic acid (sodium oleate, Baker Chemical Co.), fatty alcohol sulfates (Dreft, Procter & Gamble; Gardinol WA, E. I. duPont de Nemours Co.), high molecular weight methyl taurides (Cyclopon A and Igepon TD, General Aniline & Film Corp.), and alkyl aryl sulfonates (Nacconol NR, National Aniline & Chemical Co.). The *anionic wetting agents* were sodium salts of organic sulfonates (Aerosol OT, American Cyanamide & Chem. Co.; Nekal BX and Nekal NS, General Aniline & Film Corp.). The *cationic agents* were cetyl pyridinium chloride (Edwal Laboratories, Inc.), dimethyl-2-hydroxyethyloctadecyl ammonium chloride[3] (General Aniline & Film Corp.), benzyldimethyloctyl-phenoxyethoxyethyl ammonium chloride (Hyamine 1622, Rohm & Haas Co.), and a mixture of alkyl benzyl-dimethyl ammonium chlorides (Zephiran Chloride, Winthrop Chem. Co.).

Typical Turbidity Titrations

Fig. 3 shows the titration curve which was obtained by titrating 40 ml. of Igepon TD (0.001 *N*, based on active material) with CPC. Photometer (*b*) with the blue filter was used giving a very sharp end-point indicated by a maximum turbidity reading of 85 (in $500 \times D$ units). The procedure for this and for most of the other titrations was as follows. The individual additions of reagent varied during the titration depending on the proximity to the end-point. In the beginning the reagent was added in 0.25 ml. steps while stirring, and the turbidity determined after each addition. Further additions followed immediately until an appreciable increase in turbidity was indicated by the photometer. Then the reagent was added in 0.05 ml. steps and the turbidity reading was taken after

[3] This product was prepared experimentally by Dr. R. T. Olsen of the Central Research Laboratory.

stirring for an additional ten seconds. Before adding more reagent, successive readings were taken after further stirring for 10 or 30 seconds, in order to assure that the precipitation reaction was completed; this was indicated by essentially constant turbidity readings (usually within about 0.01 density units).

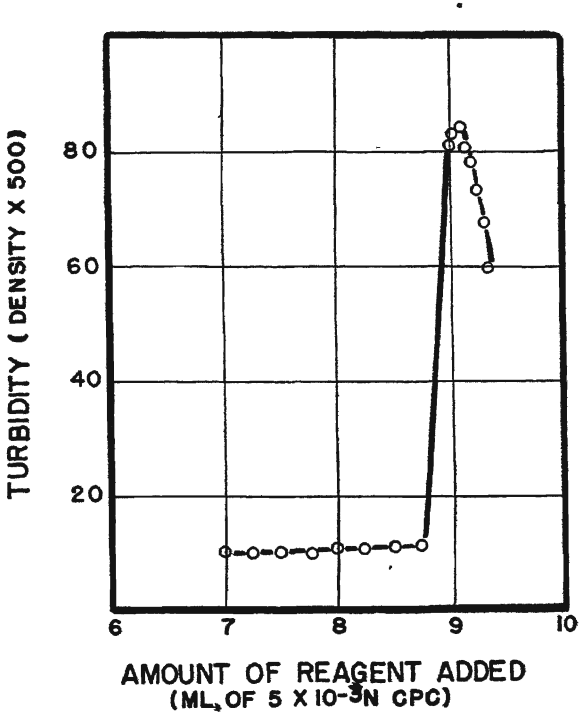

FIG. 3. Typical turbidity titration curve: Igepon TD titrated with cetyl pyridinum chloride (CPC).

The active materials reacting in this particular titration are Igepon T and CPC with the following structural formulae:

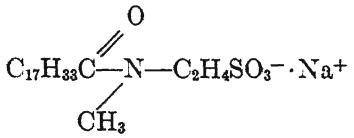

Igepon T

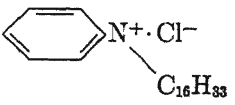

Cetyl pyridinium chloride

In general the precipitation reaction between two colloidal electrolytes forming an insoluble complex can be written

$$A^-c^+ + C^+a^- \rightarrow AC + a^-c^+$$

where A^- and C^+ represent surface-active anions and cations respectively, a^- and c^+ the simple ions of inorganic salts, and AC the precipitate. This presentation is a simplification, since the surface-active agents are used at concentrations sufficiently high for micelle formation, which is typical for all colloidal electrolytes according to McBain and collaborators (8). The precipitation presumably occurs between ionic micelles rather than between individual surface-active ions. Since the titrations are carried out fairly rapidly, this reaction does not always lead to quantitative precipitation. Near the equivalence-point, however, the colloidal system has no charge and will be in a state comparable to the isoelectric point at which other colloids, such as proteins, are known to exhibit minimum solubility. It might be this relatively low solubility which is indicated by the maximum turbidity registered in the photometer.

The reagent used in the titration is a colloidal electrolyte and usually has sufficient solubilizing power for the precipitate beyond the end-point when an excess of reagent is present. Nevertheless, it was found that some

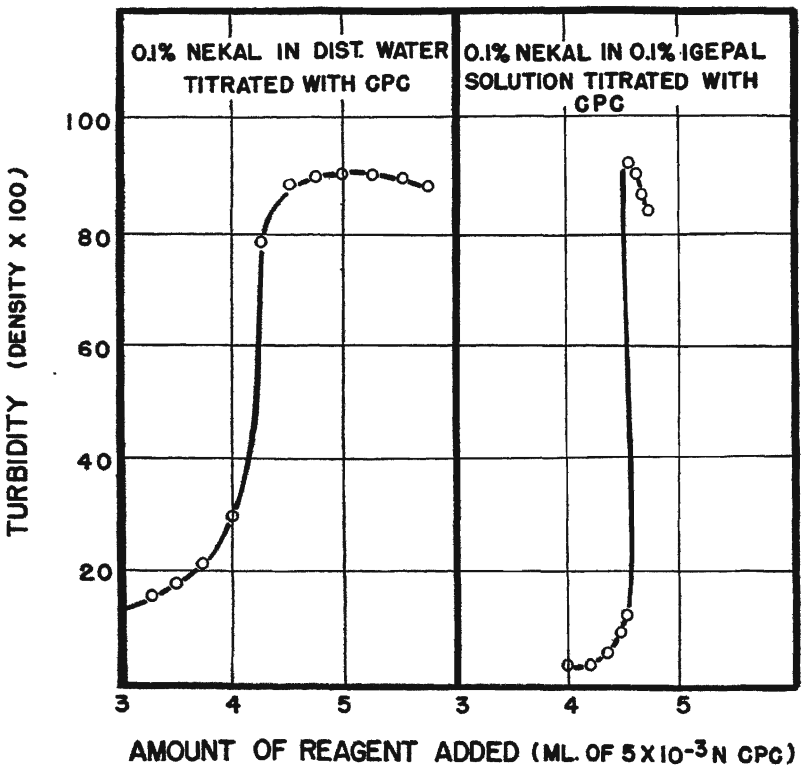

FIG. 4. Effect of Igepal CA on sharpness of end-point obtained in turbidity titration of Nekal NS.

materials cannot be accurately titrated because of the formation of an excessively stable precipitate. A typical example is given in Fig. 4 showing the titration curve on the left which was obtained by titrating 50 ml. of 0.1% Nekal NS in distilled water with CPC using photometer (*b*) with blue filter. The very broad end-point which was obtained made the method appear unsatisfactory in this case. A similar effect was observed in titrations of Aerosol OT with CPC and of Hyamine 1622 with Igepon TD. It was found, however, that by addition of a certain amount of a non-ionic surface-active agent (*e.g.*, a condensation product of a substituted phenol with ethylene oxide) to the solution to be titrated, sharp end-points could be obtained also with these agents. This effect is illustrated by the titration curve on the right in Fig. 4, showing that a satisfactory end-point was obtained by titrating 50 ml. of 0.1% Nekal NS to which a small amount of Igepal CA Ex.[4] had been added.

In one instance, *viz.*, titrating Nacconol NR with CPC, sharp end-points were obtained although no solubilization of the colloidal precipitate occurred beyond the equivalence-point. It was noticed in this case that the finely divided precipitate, which had formed, coagulated with a small excess of reagent. Since light was then transmitted by the almost clear solution surrounding the flocculate, the density reading decreased and a sharp end-point resulted.

Titrations of Known Solutions

Before applying the turbidity titration method to routine analyses of experimental solutions a series of tests were made which served as calibrations for each individual surface-active agent. Figs. 5–7 give some of the results obtained with one wetting agent and two detergents. In each graph the amount of reagent used to attain the end-point was plotted against the known concentration of the particular agent in solution. All points on the respective graphs fell on straight lines within the experimental error, indicating proportionality throughout the concentration ranges tested.

Fig. 5 shows the end-points obtained by titrating Aerosol OT solutions within the concentration range from 0.075 to 0.75 g./l. with 0.005 *N* CPC. Photometer (*b*) with blue or red filter (*cf.* Table I) was used and Igepal CA Ex. was added to the solutions before titration.

The end-points obtained by titrating Igepon TD with CPC, and *vice versa*, are shown in Fig. 6. The concentrations ranged from about 0.3 to 1.4 g./l. Photometer (*c*) with blue filter was used. The influence of higher pH and bivalent ions was determined by titrating a number of Igepon TD solutions to which had been added NaOH and $CaCl_2$ respectively. As

[4] A non-ionic agent manufactured by General Aniline & Film Corp.

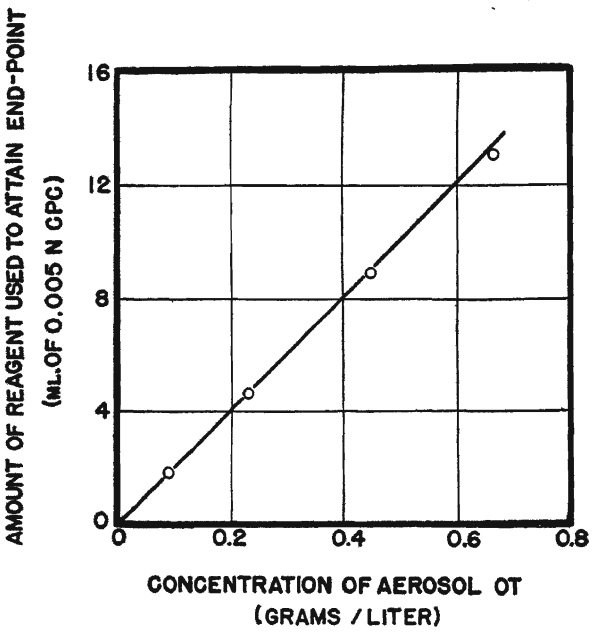

FIG. 5. Titrations of Aerosol OT with CPC. (Amount titrated: 40 ml.)

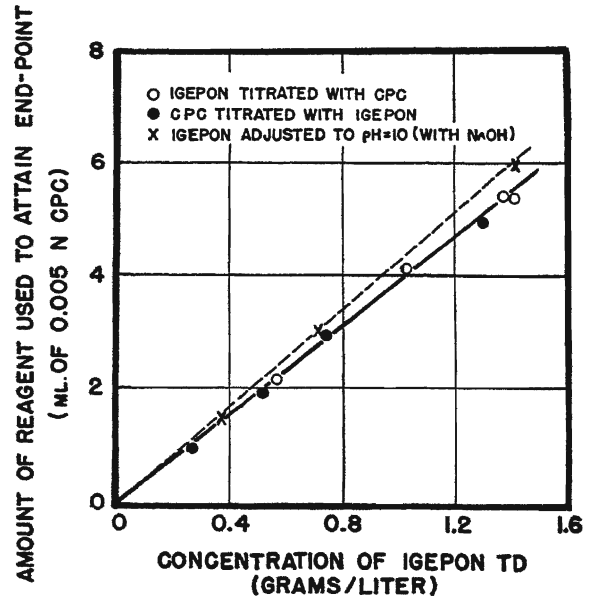

FIG. 6. Titrations of Igepon TD with CPC and *vice versa*. (Amount titrated: 20 ml.)

can be seen in Fig. 6 there was somewhat more reagent required to attain the end-points when Igepon was titrated in an alkaline medium. The maximum turbidities at the end-points increased appreciably (*cf.* Table I). Two titrations of 2.2 g. of Igepon/l., one in distilled water, the other in water containing 0.2% $CaCl_2 \cdot 2H_2O$, gave exactly the same end-points. The turbidity maxima as measured on photometer (*c*) with blue filter were $D = 0.32$ for the distilled water titration and $D = 0.9$ for the titration in presence of Ca ions.

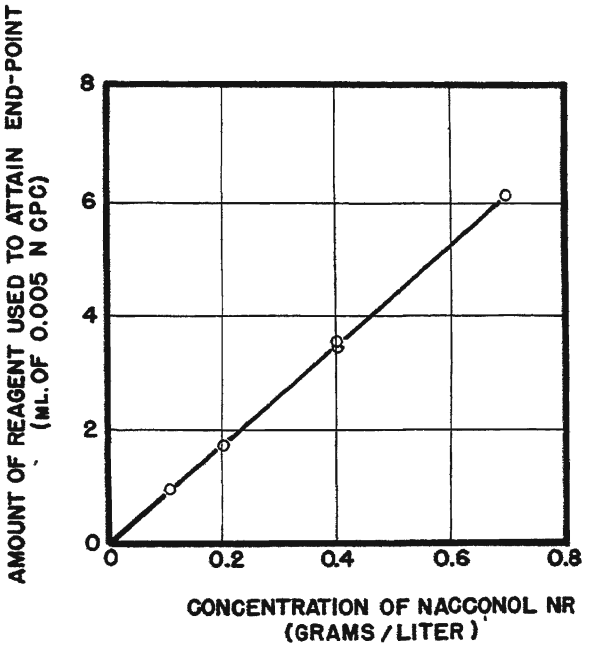

FIG. 7. Titration of Nacconol NR with CPC. (Amount titrated: 50 ml.)

Fig. 7 shows the end-points obtained by titrating Nacconol NR over the concentration range indicated in the graph. Photometer (*b*) with blue filter was used and distilled water was the titration medium for the titrations.

SUMMARY AND RESULTS

Table I summarized some of the successful titrations made on 12 different surface-active agents, including the ones discussed previously. The approximate concentration range of the commercial products in distilled water at which the titrations were made, the additions (if any), and other experimental details are shown in successive columns.

TABLE I

Summary of Turbidity Titrations

Material titrated	Approx. concentration range	Titration medium	Photometer	Filter	Apparent density range at max. turbidity	Estimated correction factor for titration error
	g./l.					*f*
Anionic Detergents Titrated with Cetyl Pyridinium Chloride						
Cyclopon A Extra	2.5	Water	*c*	Blue	0.55	1.11
Dreft; Gardinol WA	0.7	Water	*c*	Blue	0.40–0.70	1.12
Igepon TD	0.1–0.5	Water	*b*	Blue	0.04–0.30	0.94
Igepon TD	1.2–3.0	Water	*c*	Blue	0.34–0.56	0.94
Igepon TD	0.4–1.0	Water+NaOH	*c*	Blue	0.20–0.94	0.86
Nacconol NR	0.1–0.8	Water	*b*	Blue	0.16–0.64	0.98
Sodium Oleate	0.3	Water	*b*	Blue	0.43	1.07
Sodium Oleate	0.1–0.3	Water+NH_4OH	*b*	Blue	0.25	1.02
Anionic Wetting Agents Titrated with Cetyl Pyridinium Chloride						
Aerosol OT	0.1–0.8	0.01% Igepal	*a*	Blue	1.23–1.31	1.06
Aerosol OT	0.1	0.01% Igepal	*b*	Blue	0.56–0.94	1.03
Aerosol OT	0.1–0.3	0.01% Igepal	*b*	Red	0.08–1.16	1.05
Nekal BX	0.1–0.4	Water	*b*	Blue	0.30–0.98	1.04
Nekal NS	0.1–1.6	0.01% Igepal	*b*	Blue	0.45–1.20	1.05
Cationic Agents Titrated with Igepon TD						
Hyamine 1622	0.45	0.01% Igepal	*b*	Blue	0.64	1.10
Octadecyldimethyl-2-hydroxyethyl ammonium chloride	0.38	Water	*b*	Blue	0.34	1.04
Cetyl pyridinium chloride	0.2–0.8	Water	*c*	Blue	0.07–0.28	1.06
Zephiran Chloride	0.5–10.0	Water	*c*	Blue	0.12–1.00	*

* Indeterminate value.

Cyclopon, Dreft, and Gardinol are detergents which exhibited relatively low solubility and had to be titrated rapidly to prevent permanent precipitation. In these titrations the reagent was added while stirring, the photometer read, and further additions of reagent made immediately without waiting for the completion of the precipitation reaction. This procedure furnished reproducible results also with these materials, but might have caused the somewhat higher titration errors to be discussed below.

Sodium oleate is shown as a typical soap-like detergent. When titrated in distilled water the soap solutions had a tendency to give rather broad end-points at high turbidity levels. Titrations in alkalized solutions, adjusted with a few drops of 28% ammonium hydroxide, thus repressing hydrolysis, gave very satisfactory end-points at lower turbidity levels.

Nekal NS and Hyamine 1622 could be titrated satisfactorily when a small amount of Igepal was added to the solutions before titration, so that the Igepal concentration in the solutions was 0.01%.

Titration Errors

No attempt was made to determine independently the *titration errors* and the *experimental errors* of the turbidity titrations. The reproducibility of 10 titrations, made over a period of 6 months, with Igepon TD at various concentrations (0.1–0.5 g./l.) indicates the overall precision which was achieved. A standard deviation of 2.3% from the mean was obtained for this series of determinations.

The *titration errors*, on the other hand, are defined as the errors which occur because the end-points obtained by titration do not exactly coincide with the equivalence points (5). Adsorption and coprecipitation phenomena, which occur frequently in colloidal systems, are recognized as some of the causes for these errors (6). An estimate as to their magnitude in turbidity titrations was made by taking the chemically analyzed CPC sample as a primary standard and using the reported activities of the commercial materials for the calculations below.

The relation

$$ac_x = bc_r$$

where a = amount (ml.) of solution titrated, c_x = concentration (eq./l.) of this solution, b = amount (ml.) of reagent used and c_r = concentration (eq./l.) of reagent, does not hold if the end-point differs from the equivalence-point. To obtain a measure for this titration error, a correction factor (f) was defined so that

$$b_{eq.} = fb_{end}$$

where $b_{eq.}$ = amount of reagent needed to attain the equivalence-point

and b_{end} = amount of reagent used to attain the end-point. When the correction factor (f) is once established for a particular system, the concentration of an unknown solution is given by

$$c_x = \frac{f b_{end} c_r}{a}.$$

By combining the above expression with the formula

$$c_x = \frac{cA}{100\ M},$$

which relates the concentration of a surface-active agent in eq./l. (c_x) to its concentration in g./l. (c), where A = activity of product (per cent active material) and M = molecular weight of active principle, it was possible to compute the correction factors (f) shown in Table I. As can be seen the titration errors (which include also some experimental errors) were in most cases below 10%. The cause of the larger deviations found with Cyclopon, Dreft and Gardinol was discussed previously.

In the case of Zephiran Chloride which has a wide molecular weight distribution (alkyl radicals vary from C_8H_{17} to $C_{18}H_{37}$) no correction factor could be determined. There are indications that, in the titration with Igepon TD, only the colloidal, higher molecular weight species is contributing to the formation of the precipitate. This fact permits one to estimate the content of colloidal electrolyte in such samples, if the result of the turbidity titration is compared with the results of chemical analyses. An estimate made for the Zephiran Chloride sample gave a colloidal electrolyte content of about 80% based on the amount of active material.

Acknowledgment

The author is grateful to Dr. A. L. Fox, director of the laboratory, for the permission to publish this paper. He is indebted to Dr. W. F. Busse and Prof. G. J. Kirkwood for their encouragement and many helpful suggestions; also to Miss B. J. Hill and Mrs. L. Ackerman for their help in obtaining the data.

Summary

The concentration of most surface-active agents falling into the class of colloidal electrolytes can be determined in dilute solutions by a new titrimetric method. It consists of titrating an anionic agent with a cationic agent (or *vice versa*) under such conditions that a colloidal precipitate is produced near the equivalence-point and solubilized or coagulated by a small excess of reagent. The end-point of the titration is indicated by the maximum turbidity of the solution, which is easily detected with a conventional colorimeter.

The test measures the total amount of ionic surface-active materials in solution, and is therefore not specific for a particular surface-active agent. The method has many applications, however, such as the determination of the relative activity of different production batches of a given product; it also works for the quantitative analysis of dilute solutions often encountered in surface physics, adsorption studies, *etc.*

Equipment and methods are described, with which a variety of synthetic detergents and wetting agents were rapidly analyzed with an accuracy of about $\pm 5\%$ of the amount present. The solutions tested were in the concentration range from 0.05 to 2.0 g./l. active material. In some cases where the method failed at first, the titration was made possible by the addition of a non-ionic surface-active agent to the unknown solution.

References

1. Barnes, M. D., and LaMer, V. K., *J. Colloid Sci.* **1**, 79 (1946); **2**, 361 (1947).
2. DuBois, A. S., *Soap Sanit. Chemicals* **22**, 125 (Nov., 1946).
3. Hartley, G. S., and Runnicles, D. F., *Proc. Roy. Soc.* (*London*) **168A**, 420 (1938)
4. Hoffpauir, C. L., and Kettering, J. H., *Am. Dyestuff Reptr.* **35**, 265 (1946).
5. Kolthoff, I. M., and Stenger, V. A., Volumetric Analysis, Vol. I, Chap. VI. Interscience, New York, 1942.
6. *Ibid.*, Chap. VIII.
7. Marron, T. U., and Schifferli, J., *Ind. Eng. Chem., Anal. Ed.* **18**, 49 (1946).
8. McBain, J. W., and Salmon, C. S., *J. Am. Chem. Soc.* **42**, 426 (1920), and earlier papers.
9. Preston, J. M., *J. Soc. Dyers Colourists* **61**, 165 (1945).
10. Sweet, M. H., *J. Soc. Motion Picture Engrs.* **38**, 148 (1942).

MEMBRANE POTENTIALS FOR KERATIN

S. Baxter

Wool Industries Research Association, Leeds, England

Received July 30, 1947

Introduction

Little work has been done on the interesting study of amphoteric membrane potentials. Satisfactory keratin membranes can be made and their selectivity characteristics can be altered at will by soaking in suitable buffer solutions, which result in an excess of immobile positive or negative ions within the membrane. Membranes after such treatment show a remarkable stability in neutral salt solutions over a period of days.

A theory of membrane behavior has been put forward by Toerell; the results presented here were designed, in the first place, to test the validity of this theory for keratin membranes. The success of this theory enables the excess of immobile positive or negative ions to be determined for any pH value, the method being most sensitive over the pH range from 4 to 8. These results, which should compare with the corresponding titration curve for keratin, are thus most accurate in the region where chemical titration is difficult.

It seemed also that the condition of zero selectivity might be expected to correspond to the isoelectric point as measured by electrophoresis. This was found not to be the case, and a qualitative explanation of the discrepancy has been put forward. Finally, membrane potential measurements with pure hydrochloric acid solutions were made to test Gilbert and Rideal's theory of the combination of fibrous proteins with acid.

Theoretical

The theory of membrane behavior put forward by Toerell (1) in 1935 can be checked in a satisfactory manner by the use of keratin membranes, whose characteristics can be easily altered. As Toerell's theory is used extensively in this investigation, it will be briefly restated. Assume the membrane, which is represented as a phase containing a number of immobile negative ions of concentration X,[1] which remains constant across the membrane, to separate two potassium chloride solutions of concentra-

[1] In a keratin membrane there are immobile positive and negative ions but only their difference, X, is taken into account in Toerell's theory, and this appears to fit the present experimental data.

tion C_1 and C_2, Fig. 1. Toerell assumed that the total membrane potential, *i.e.*, the potential between solutions 1 and 2 was made up of three parts: two boundary potentials at the membrane surfaces and a diffusion potential within the membrane. Further, by assuming thermodynamic equilib-

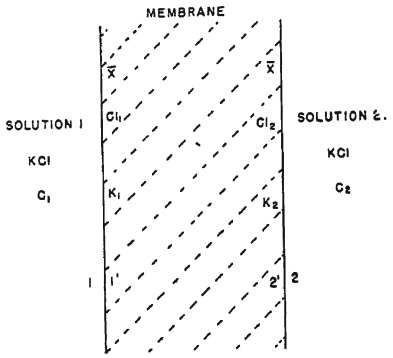

FIG. 1. Membrane separating two solutions.

rium across the boundaries 1–1′ and 2–2′ the boundary potentials become Donnan potentials, and the diffusion potential can be expressed by means of the Henderson formula (2). At room temperatures the membrane potential in millivolts is given by:

$$E = 58\left[\log\frac{C_1\cdot K_2}{C_2\cdot K_1} + \frac{u-v}{u+v}\cdot\log\cdot\frac{K_1(u+v)-Xv}{K_2(u+v)-Xv}\right], \qquad (1)$$

where u and v are the mobilities of the cation and anion respectively, and K_1 and K_2 are the concentrations of the potassium ions just inside the two surfaces of the membrane. The first term in the bracket represents the sum of the two boundary potentials and the second term the diffusion potential within the membrane. To express eq. (1) in terms of values measured in a typical experiment, we must express K_1 and K_2 in terms of C_1, C_2 and X. This is done by use of the equations for the equilibrium across the faces 1–1′ and 2–2′, remembering that electrical neutrality must be maintained. Thus we have

$$C_1^2 = K_1\cdot Cl_1 = K_1(K_1 - X) \qquad (2)$$

and

$$C_2^2 = K_2\cdot Cl_2 = K_2(K_2 - X) \qquad (3)$$

where Cl_1 and Cl_2 are the concentrations of the chlorine ions just inside the two surfaces of the membrane.

Eqs. (2) and (3) give K_1 and K_2 in terms of C_1, C_2 and X, and on substituting these values in Eq. (1) we get

$$E = 58\left[\frac{1}{2}\log\frac{(Y_1/X-1)(Y_2/X+1)}{(Y_2/X-1)(Y_1/X+1)} + C\log\frac{(Y_1/X+C)}{(Y_2/X+C)}\right] \qquad (4)$$

where $Y_1 = \sqrt{4C_1^2 + X^2}$; $Y_2 = \sqrt{4C_2^2 + X^2}$ and $C = \frac{u - v}{u + v}$. If the membrane is composed of immobile positive ions, the membrane potential is given by the equation obtained by changing the sign of X in Eq. (4). If we make $C_1 = 2C_2$, then, in Eq. (4), E is a function of u/v and X/C_2. We can then plot a series of curves of E against log X/C_2, each curve corresponding to a given value of u/v. This has been done and the curves are shown in Figs. 2 and 3. Fig. 2 is for a membrane composed of fixed positive ions and Fig. 3 is for a membrane of fixed negative ions. The sign of E for each set of curves is the sign of the weaker solution. When X/C_2 is large, the diffusion potential term in Eq. (4) approaches zero and the first term, *i.e.*, the boundary potential term, takes up a limiting value of 17.5 mV. When X/C_2 becomes very small, the boundary potential term approaches zero and we are left with the diffusion potential term which approaches a limiting value given by

$$E = 58 \frac{u - v}{u + v} \log 2,$$

i.e.,

$$E = 17.5 \frac{u - v}{u + v}. \tag{5}$$

If, using a given membrane, a series of measurements of E are made, keeping the ratio of the concentrations equal to 1:2, and E is plotted against log $1/C_2$ we obtain a curve from which we can estimate the values of u/v and X by comparison with the curves of either Fig. 2 or Fig. 3,

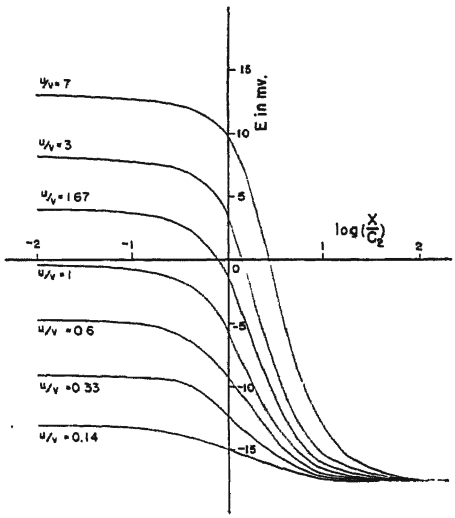

FIG. 2. Theoretical curves for X positive.

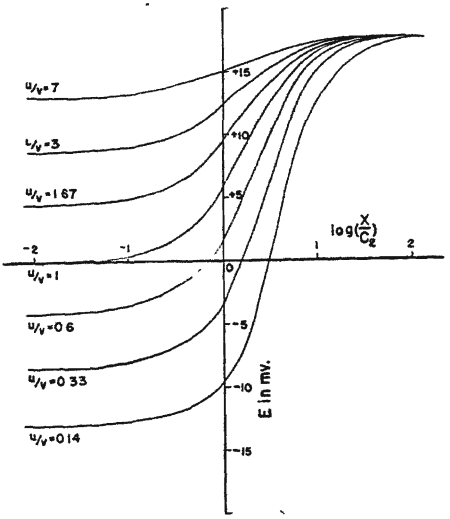

FIG. 3. Theoretical curves for X negative.

whichever is appropriate. This is done as follows (3): the experimental curve (plotted on the same scale as the theoretical curves) is displaced parallel to the abscissae until it fits a theoretical curve. The curve it fits gives the value of u/v and the amount of the displacement will give the value of X.

EXPERIMENTAL METHOD

The keratin membranes were made from cow's horn by cutting a section of horn approximately 4.5 cm. square and pressing it between parallel plates under boiling water. On allowing to cool while still under pressure, the sample remained flat when released from the clamps. It was then fixed to a flat brass plate with Chatterton's compound,[2] and the top of the sample milled flat. It was then turned over, the milled side being fixed to the plate, and milled down to the required thickness. The membranes used had a thickness of approximately 0.01 cm.

The apparatus used for measuring the potentials is shown diagrammatically in Fig. 4. The solutions to be used were contained in the cylinders A and B, the flow of solution being controlled by the taps, T. The solutions on the two sides of the membrane were connected to saturated calomel electrodes by means of cotton wicks, enclosed in narrow glass tubes, which dipped into the tubes E and F. The wicks were allowed to dip into the tubes for a time sufficiently long to enable the potential reading to be taken. The solution exit tubes were shaped so as

[2] Known also as marine glue: a mixture of shellac and caoutchouc.

to prevent any potassium chloride, which diffused out of the wicks into tubes E or F, from reaching the membrane. The E.M.F. developed was measured with a Cambridge potentiometer, the average accuracy being to 0.2 mV depending, of course, on the resistance of the circuit.

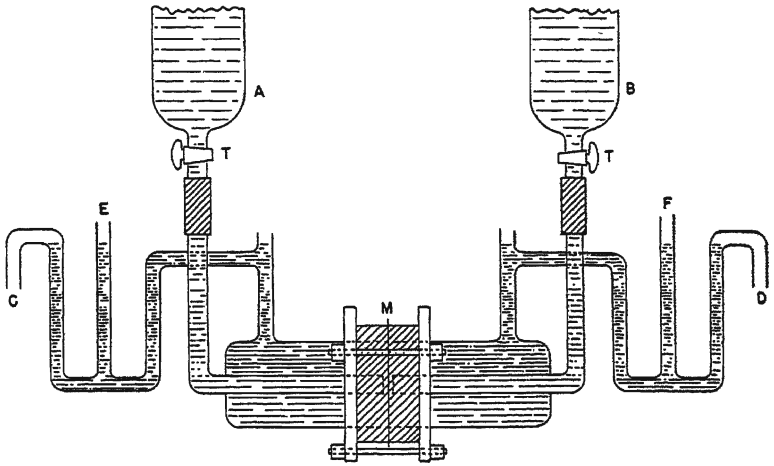

FIG. 4. Apparatus for measuring membrane potentials.

The procedure was as follows: the membrane was placed in a buffer solution of known pH for at least 24 hrs.; it was then taken out, rinsed in distilled water, dried between filter papers and fixed in the apparatus. The taps T were opened and both sides of the apparatus filled with the required solutions. Contact with the calomel cells was periodically made by dipping the wicks into the tubes E and F, to measure the E.M.F. developed. The wicks were then withdrawn. Readings of the E.M.F. were taken from time to time until a steady value was obtained. The solutions were periodically changed by opening the taps, T. All the E.M.F.'s quoted refer to steady values. The time taken for a steady E.M.F. to be attained was somewhat variable, ranging from 2 to 10 hrs.

RESULTS

In Fig. 5 are given a typical set of experimental curves obtained with potassium chloride solution always in the concentration ratio 1:2, and with membranes after soaking in buffer solutions of various pHs. In obtaining the points for a given curve the membrane was returned to the buffer solution, usually for an overnight period, between the E.M.F. determination for each point. The buffer solutions used are given in Table I. Curves A and B are the curves of log X/C_2 against E for $u/v = 1$ taken from Figs. 2 and 3, respectively. The graphs for $u/v = 1$ fit the

experimental curves best, the slopes being similar, and also with both theoretical and experimental curves the E.M.F. approaches zero for high concentrations. The displacement of the experimental curve in the abscissae direction from the position of the curves A and B gives an

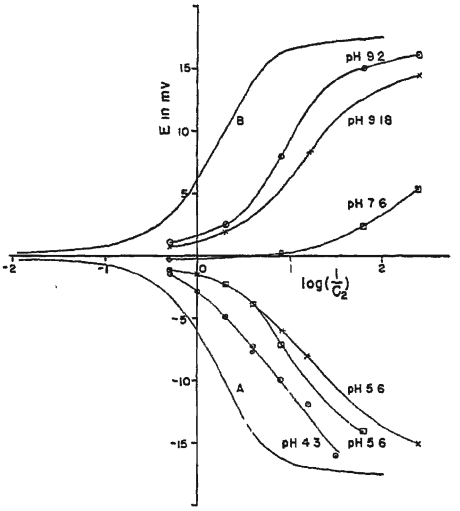

FIG. 5. Experimental curves using KCl.

TABLE I

Buffer Solutions used for Curves of Fig. 5

Solution	pH[a]
Mixtures of 0.1 *M* acetic acid and 0.1 *M* sodium acetate	4.3 5.6
94 parts 0.2 *M* Boric acid 6 parts 0.05 *M* Borax	7.6
83 parts 0.1 *M* KH_2PO_4 17 parts 0.05 *M* Borax	9.18
0.05 *M* Borax	9.2

[a] pH values as measured by Cambridge pH meter.

estimate of the value of X. As was to be expected, the membranes buffered in alkaline solutions produced negative membranes (*i.e.*, E. positive), while those buffered in acid solutions gave positive membranes (*i.e.*, E. negative). It was not possible to measure the pH [3] which produced a zero value of X using the buffer solutions tabulated in Table I, as they did

[3] The pH value producing zero value of X will not be unique but will depend also on the binding energy of the anion with the protein. In the present case, however, this effect will be small.

not cover the gap in Fig. 5 between pH 5.6 and pH 7.6. This was done in a separate experiment in which KCl solutions of fixed strengths were used to determine the E.M.F. of membranes soaked in buffer solutions whose range covered the transition from X positive to X negative. The buffer solutions used in this experiment and the values obtained are given in Table II and Fig. 6, respectively. The point of intersection of the

TABLE II

Buffer Solutions used for Curves of Fig. 6

Solution		pH[a]
Cc. of 0.2 M Na_2HPO_4 + cc. of 0.1 M citric acid		
49.4	150	3.26
71.0	129	3.65
88.2	112	4.10
103	97	4.68
116	84	5.36
132	67.8	6.22
154	45.5	6.86
182	18.3	7.40
195	5.5	7.87

[a] pH values as measured by Cambridge pH meter.

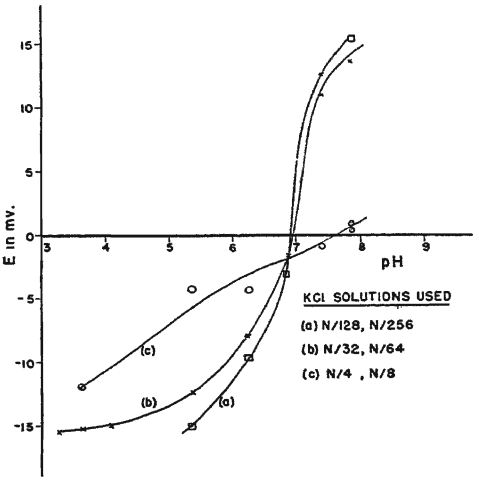

FIG. 6. Change of membrane potential with pH at different concentrations.

curves gives the pH of the buffer solution which gives zero value of X and the value of E at the point of intersection gives, by use of Eq. (5), an estimate of u/v. The value of u/v obtained by this method was 0.9, which is in good agreement with the value estimated from the slope of the curves in Fig. 5. If we take u/v equal to 0.9 for potassium and chlorine ions in the membrane, as seems justified by the evidence of Fig. 6, then

the curves of Fig. 6 can be converted to give the variation of X, the quantity of immobile ions in the membrane, with the pH of the solution in which it was soaked. The result of this conversion, for curve (b) of Fig. 6, which was carried out by the method described earlier, is shown in Fig. 7, The results for the other two curves (a) and (c) do not coincide with the graph of Fig. 7, but this could easily be due to the errors involved in the estimation of X by this method. Thus, for the diffusion of potassium chloride through a keratin membrane the value of u/v is approximately the same as for diffusion in water. This result could not, of course, have been anticipated, and to check the effect of the membrane on other ions a set of results were obtained with NaCl in place of KCl. A series of

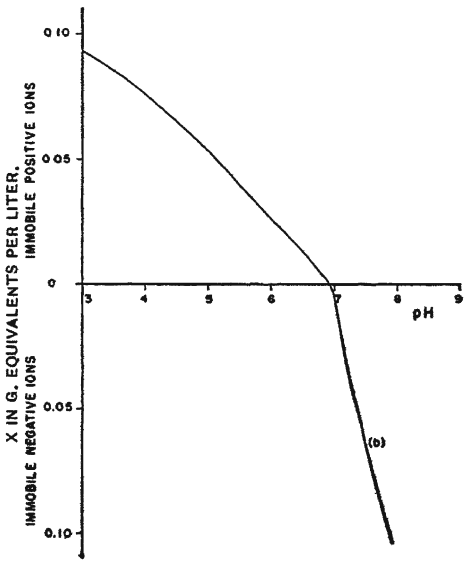

FIG. 7. Variation of X with pH.

selection curves are shown in Fig. 8, the buffer solutions used being similar to those detailed in Table II. The curves again show the general shape of those in Figs. 2 and 3, but the fit with the theoretical curves is not so good as with the KCl. The value of u/v can best be deduced from the limiting value of E as $1/C_2$ becomes small. This suggests a value of u/v approximately 1.2 which is very different from the value in water, which is 0.66. This must mean that in the membrane $\frac{u_K}{u_{Na}} = \frac{0.9}{1.2} = 0.75$, whereas in water $\frac{u_K}{u_{Na}} = 1.5$.

It is not possible to give a selectivity curve for HCl of the type given above for KCl and NaCl, as changes in concentration give rise to pH variations causing changes in the value of X. The acid strengths used

were within the range $N/10$ (pH 1.0) and $N/320$ (pH 2.5). At such low pH values X would be large, giving rise to a large value of X/C_2 which, for a membrane where there is an excess of immobile positive ions (Fig. 2), on Toerell's theory should give rise to strongly negative membrane potentials, This was, in fact, found to be the case. The values obtained

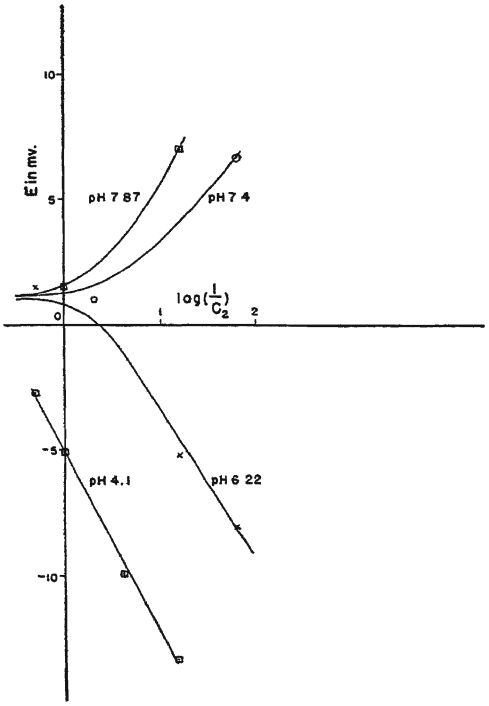

FIG. 8. Experimental curves using NaCl.

are given in Table III; the concentration ratio used was 1:2, as in the previous cases.

TABLE III

Membrane Potentials using HCl

Strength of weaker solutions	E.M.F. mV.
$N/20$	−13.6
$N/160$	−15.0
$N/320$	−15.5

DISCUSSION

The shape of the curves of Figs. 5 and 8 conform very well to the shape of the curves of Figs. 2 and 3 indicating that the theory of membrane potentials, as developed by Toerell, explains the experimental results adequately and suggests that the assumptions made by him are

valid. It is interesting to note that, when in a solution of pH 7, the membrane has an equal number of immobile positive and negative ions, *i.e.*, X is zero, and the membrane potential in such a case will be independent of the concentration of salt used (assuming always that a given concentration ratio is used) and its magnitude should be given by Eq. 5. The variation of X with pH, as shown in Fig. 7, should correspond to a titration curve for keratin. Comparison cannot, however, be made as the titration curves for keratin do not accurately cover this range. It is rather unfortunate that the value of X cannot be determined from membrane potential measurements over a wide range of pH values owing to the membrane potential rapidly approaching a limiting value for the range of permissible electrolyte concentrations as X becomes large.

One might expect the isoelectric point of keratin to occur in a buffer solution giving rise to zero value of X, and hence to zero boundary potential. This is by no means the case, as it is well known that for wool keratin the isoelectric point is in the region, pH 3–4.5, depending on the type and strength of the buffer solutions used (4). Measurements of the isoelectric point of horn ground in a ball mill, using the Abramson cell method (5) and the buffer solutions of Table II, confirm that the isoelectric point for horn is far removed from pH 7 on the acid side.

The fact that the isoelectric point of keratin does not occur at pH 7, where the Donnan boundary potential is zero, can be readily explained if we assume that the potential between the two phases is made up of two parts: a double layer potential in the water due primarily to the orientation of water molecules and a potential due to the Donnan distribution of ions across the surface. The view that water molecules are oriented at an interface with their negative ends pointed towards the interface is suggested by the negative potential of particles such as glass, air bubbles, hydrocarbon oils, *etc.*, when in water. This negative electrophoretic potential is shown by almost any phase when in contact with water (6). Adam (7), in fact, suggests that potentials, caused by oriented dipoles, exist at almost every phase boundary. Their actual magnitude cannot be directly measured although changes can be observed when a surface picks up neutral oriented molecules.

The variation of potential with distance across a water-air interface due to oriented water molecules would be as shown in Fig. 9 (a). The presence of electrolytes tends, in general, to lower this potential and the presence of multivalent cations may even cause a reversal of sign. This ion effect must be due to a preferential absorption of the cations at the water surface giving rise to a double layer in opposition to that due to the oriented water molecules. If now we have keratin, which has previously been buffered, *i.e.*, the sign and value of X are fixed, in contact with, say, a KCl solution of concentration C_1, the boundary potential due to the Donnan distribution of the mobile ions gives rise to a potential between

the two phases given by

$$E_B = 58 \log \left\{ \frac{2C_1/X}{1 + \sqrt{1 + 4C_1^2/X^2}} \right\}, \qquad (6)$$

i.e., E_B is a function of X/C_1. The Donnan potential will spread on both sides of the phase boundary similar to the curve shown in Fig. 9 (b), the thickness of the double layer decreasing with increasing concentration of the solution. Debye-Hückel effects have not been considered in this qualitative treatment. These two effects must be added together to give the resultant potential distance curve between the two phases. For a positive Donnan potential we might, on the basis of this argument, expect a curve of the type shown in Fig. 10. If we assume a stationary boundary layer, then the value of the potential at this layer gives the ζ potential. The variation of the ζ potential or electrophoretic mobility with pH can be qualitatively followed by the use of Fig. 10. Since the maximum values of X are fixed (being characteristics of the keratin), then for a given value of C_1, E_B has fixed limits which become closer as C_1 is increased.

If the keratin is first buffered in a strongly acid solution, we would expect X to have its maximum positive value and hence E_B its maximum positive value. On decreasing the acid strength of the buffer used, X would remain constant at first and then begin to decrease as the buffering pH was increased, *i.e.*, E_B would at first remain constant and then begin to decrease as the buffering pH increased. By considering Fig. 10 it is seen that ζ would first remain constant with pH and then commence to fall as the buffering pH was increased and would become zero at an acid pH. This phenomenon is due primarily to the surface characteristics of the solution. As the value of E_B passes through zero it becomes very insensitive to changes in X (*i.e.*, to changes in pH of the buffer solution) and so we would expect the mobility-pH curve to flatten out, and then as E_B reached larger negative values, the mobility would increase rapidly with increasing pH and ultimately flatten out as X reached its final negative value. Thus, the general shape of the mobility or ζ $-$pH curve would be expected, on this argument, to have the shape indicated in Fig. 11. This general shape is well borne out in practice. The effect of increasing the strength of the solution, *i.e.*, decreasing X/C_1, will cause a general flattening of the curve but whether the isoelectric point is altered or not depends on two opposing effects; the narrowing of the Donnan double layer and the reduction in the value of E_l. Thus it would be fortuitous if the isoelectric point remained unchanged with concentration. Smith (8) has shown that the isoelectric point of egg albumin adsorbed on collodion particles varies with the ionic strength of the solution. Divalent and trivalent cations caused the isoelectric point to increase with increasing ionic strength while univalent cations caused a decrease. These results would be expected on the above argument as multivalent cations cause a marked lowering of E_l which indicates a higher pH for the isoelectric point.

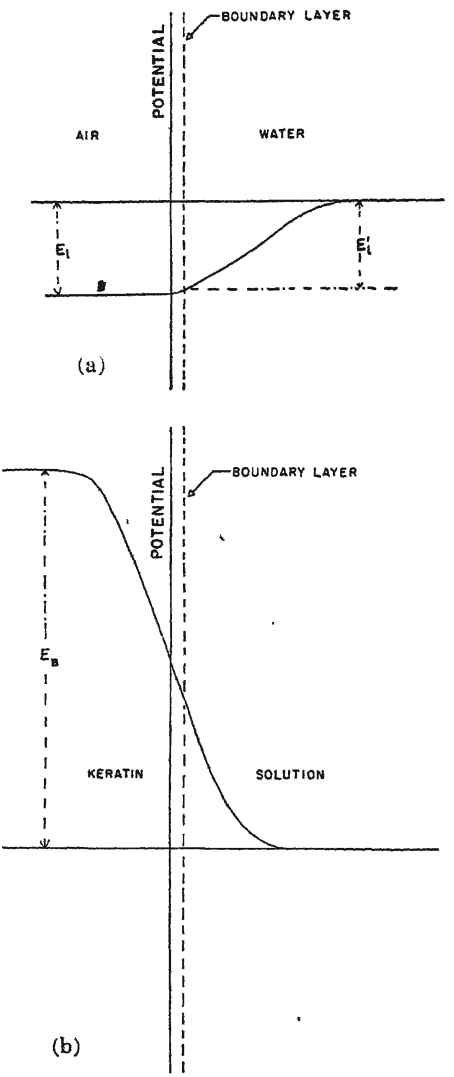

FIG. 9. Suggested potential-distance curve at surface of water due to oriented water molecules (a). Potential-distance curve caused by Donnan distribution of ions (b).

The depth of the potential fall between the liquid and the stationary layer, E'_l, could be estimated by streaming potential measurements of the type recently described by Neale and Peters (9). From Fig. 10 it is seen that only a fraction of the Donnan boundary potential, E_B, is balanced against the potential due to the liquid phase, E'_l. This explains why large changes in E_B caused by changing the solution concentration give rise to much smaller changes in ζ.

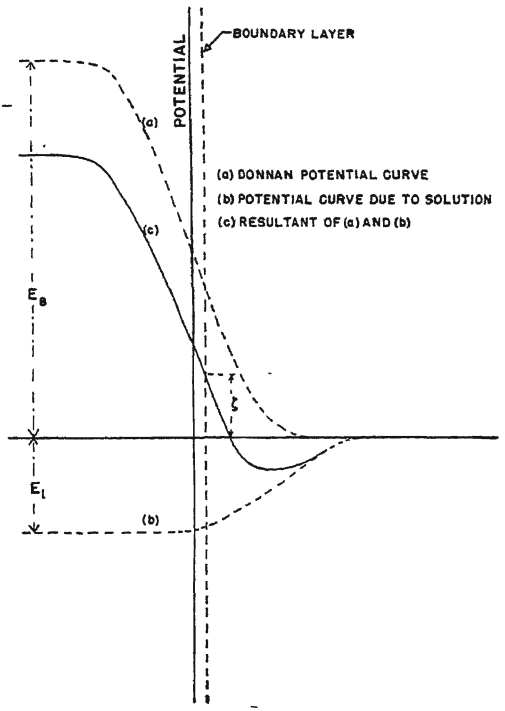

FIG. 10. Suggested potential-distance curve for keratin—water interface, E_B positive.

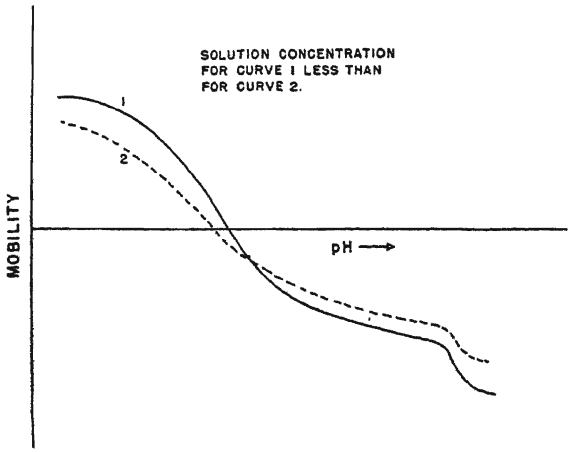

FIG. 11. Shape of mobility-pH curve to be expected.

The potential difference between the two phases which is effective in membrane potential measurements is not the Donnan potential, E_B, but $E_B - E_l$. We can, however, only measure the potential between the solutions on the two sides of the membrane and, as the theory of Toerell fits the experimental results, the values of E_l on the two sides of the membrane must be approximately equal in the experiments described.

Gilbert and Rideal (10), from their recent theory on the combination of fibrous proteins with acids, state that when wool is in pure hydrochloric acid the fiber potential should be independent of the concentration of acid. The prediction has been tested by measuring the membrane potential of keratin with hydrochloric acid of different strengths on the two sides. The results, which were given earlier in Table III, are inconsistent with Gilbert and Rideal's view, which would mean that the boundary potential terms of Eq. (1) would disappear leaving only the diffusion potential term (*cf.* Eq. 5). Thus the membrane potential would have been expected to be between 0 and +17.5 mV, if u was greater than v, as is most likely, whereas the value found was strongly negative.

Acknowledgments

The author's thanks are due to Mr. B. H. Wilsdon and Dr. A. B. D. Cassie for useful discussions.

The electrophoretic measurements were made by Mr. J. M. Valentine.

Summary

Measurements of the membrane potentials of keratin membranes have been made using KCl and NaCl and the results show how the selectivity of the membranes can be altered by soaking in suitable buffer solutions. The results support Toerell's theory of membrane behavior in neutral salts, and some membrane potential measurements using HCl solutions are compared with Gilbert and Rideal's predictions.

A qualitative theory is suggested for the mobility-pH curves obtained by electrophoresis. It also explains why the isoelectric point of keratin is not at pH 7, the point of zero membrane selectivity.

References

1. Toerell, *Proc. Soc. Exptl. Biol. Med.* **33**, 282 (1935).
2. Henderson, *Z. physik. Chem.* **59**, 118 (1907).
3. Meyer and Bernfeld, *J. Gen. Phys.* **29**, 353 (1946).
4. Sookne and Harris, *J. Research Natl. Bur. Standards*, **23**, 471 (1939).
5. Abramson, Moyer and Gorin, Electrophoresis of Proteins, p. 44. Reinhold, 1942.
6. Freundlich, Colloid and Capilliary Chemistry, p. 278. Methuen, 1926.
7. Adam, Physics and Chemistry of Surfaces, 3rd Ed., p. 302. Oxford.
8. Smith, *J. Biol. Chem.* **113**, 473 (1936).
9. Neale and Peters, *Trans. Faraday Soc.* **42**, 478 (1946).
10. Gilbert and Rideal, *Proc. Roy. Soc.* (*London*), **182A**, 335 (1944).

THE SORPTION OF OXALATE BY HYDROUS ALUMINA

Ronald P. Graham and Donald J. Crawford

From the Department of Chemistry, McMaster University, Hamilton, Ontario

Received August 11, 1947

Introduction

In the literature may be found the records of a number of investigations in which the interaction of anions with hydrous alumina has been studied. Alumina in the form of a hydrosol, of a dispersed hydrous gel, and as hydrous oxide powder has been employed, but in none of the papers with which the writers are familiar has an appreciable amount of attention been given to the rate at which sorption has occurred. The present paper contains the results of an investigation in which the extent of anion (particularly oxalate) sorption has been studied as a function of time of interaction of hydrous alumina powder with an aqueous solution of the acid and as a function of the temperature of preparation of the hydrous oxide. The data obtained are interpreted utilizing the concept that hydrous alumina powder may be regarded as a coordinated structure in which both olated and oxolated linkages are involved (3,6).

Studies of the interaction of hydrous alumina with acids have recently been discussed by Graham and Thomas (6), and work published prior to 1935 on the sorption of anions by colloidal alumina has been reviewed by Weiser (18). The well known aging properties of systems involving hydrous alumina have been observed in sorption studies, *e.g.*, the aging of an alumina sol for some months results in a decreased sorption affinity for chloride ion (14) and the sorption of arsenious acid [1] by alumina precipitated by aqueous ammonia from an aluminum salt solution is decreased by heating the suspension of the hydrous alumina gel (10, 12, 21). Valence considerations have long been considered to be the most important factor controlling the sorption of anions by hydrous oxide systems, but it has been pointed out (*e.g.*, (20)) that the order of anion sorption on aluminum "hydroxide" depends also on specific chemical factors such as the formation of insoluble or complex salts. Baker (1), in a study of the sorption of anions by hydrous alumina powder from salt solutions, found that the monovalent fluoride ion was sorbed to a much greater extent than

[1] Properly speaking, the sorption of trivalent arsenic because analyses were performed by titration with standard iodine solution. The distinction is a very real one, as will be made evident in the present paper.

were oxalate or sulfate ions, that sorption increased with decreasing pH, and that oxides prepared by the action of cold water upon amalgamated aluminum were less reactive than those prepared in hot water. Baker explained his results on the basis of a coordination mechanism of sorption. Graham and Horning (5) explained the pH raising effect they observed upon adding hydrous alumina powder to neutral salt solutions by assuming that displacement of hydroxo groups from the surface of the alumina occurred as a result of anion sorption by means of coordinative binding to the aluminum. Baker (1) gave the same interpretation to the results of the similar experiments he carried out with hydrous alumina powder.

Materials and Methods

Preparation of Hydrous Alumina

The samples of hydrous alumina were prepared by the interaction of distilled water and amalgamated aluminum. Cleaned ingots of aluminum [2] were amalgamated by immersion in a 5% aqueous solution of mercuric chloride for 3–4 minutes, were washed in distilled water, and then were used to prepare hydrous alumina as noted below. The composition of the samples, expressed as $Al_2O_3 \cdot xH_2O$, was determined gravimetrically, in triplicate, by ignition in a platinum crucible using a Fisher blast burner. Previous experience with this method of preparing hydrous alumina has shown that the samples contain not more than 0.03%, if any, mercury (as a result of the amalgamation procedure).

Sample "30"

Several batches of alumina were prepared at 30° ± 1°C. by allowing amalgamated aluminum (80 g.) to react with 1500 ml. of distilled water for one week, during which time the suspension was stirred intermittently. The ingot was then removed, and the suspension stirred at room temperature for a further period of 15 hours before it was filtered. The alumina was spread on a glass plate and allowed to dry at room temperature. During the drying period the mixed lots were pulverized from time to time. Before bottling, the material was ground in a Mullite mortar and fractionated, using Tyler Standard sieves, into the mesh sizes −60/+115, −115/+250, and −250. The analysis of the −60/+115 fraction can be expressed as equivalent to $Al_2O_3 \cdot 2.91\ H_2O$.

Sample "60"

A number of batches of alumina were prepared at 60° ± 3°C. in a manner otherwise similar to the above except that the reaction time was

[2] The aluminum was obtained from the Aluminum Company of America and had a specified purity of 99.85%.

10 hours. After removal of the aluminum, stirring was continued for 15 hours while the temperature was allowed to fall to that of the room. The batches, after filtering, were mixed, dried, ground and fractionated as above. The −60/+115 and −250 fractions analyzed to compositions equivalent to $Al_2O_3 \cdot 2.74\ H_2O$, and $Al_2O_3 \cdot 2.86\ H_2O$, respectively.

Sample "95"

This sample was prepared and the experiments using it were performed some years ago. The preparation of the sample, which took place at 95° ± 2°C. using the principle of the method described above for the other samples, is given under this same heading in a paper by Graham and Thomas (6). The analysis of the −325 mesh fraction, which was used in the experiments reported in the present paper, was $Al_2O_3 \cdot 2.65\ H_2O$.

Sample "1310"

This sample was prepared from the −115/+250 fraction of alumina "30" by ignition for 3 hours in a platinum dish in a furnace maintained at 1310° ± 10°C. After ignition, the sample was stored in a desiccator over phosphorus pentoxide until use. The composition may be assumed to be Al_2O_3.

Acid Solutions

The oxalic and hydrochloric acids used were analyzed grades meeting A.C.S. specifications. The solutions of specified molarity were prepared by quantitative dilution of ones that had been appropriately standardized.

Measurement of Extent of Sorption

A weighed sample of hydrous alumina was placed in a 250 ml. glass-stoppered Pyrex bottle and there were added to it, by the use of a pipet, 100.0 ml. of 0.0500 *M* oxalic acid solution. By means of paraffin the stopper was sealed in the bottle, and the latter was rotated at 15 r.p.m. in a water bath maintained at 25.0° ± 0.1°C. for an appropriate length of time. Upon removal from the water bath, the contents of the bottle were rapidly divided between two 50 ml. tubes and the latter centrifuged (*ca.* 2000 r.p.m.) for 4 minutes in an International clinical centrifuge (Model 416). Using a pipet, a 25.00 ml. aliquot sample of the clear supernatant liquid [3] was removed from each tube very carefully (to prevent the withdrawal of particles of solid hydrous alumina) and transferred to a flask. There were

[3] Oxalic acid is a very inefficient acid for the preparation of colloidal dispersions of hydrous alumina from the solid oxide (15), although it is an efficient acid for the dissolution (*i.e.*, to the aqueous crystalloidal condition) of hydrous alumina powder (3).

added 10 ml. of an 18 *M* solution of sulfuric acid, the contents of the flask were heated to 90°C., and the solution was titrated with 0.02 *M* potassium permanganate solution. By comparison with the cross-ratio (determined daily) of the potassium permanganate solution and the oxalic acid solution before contact of the latter with alumina, the extent of oxalate sorption was readily calculated.[4]

Chloride analyses were carried out by the volumetric procedure recommended by Roberts (8) employing a 0.04 *M* solution of mercuric nitrate (analyzed grade reagent) with diphenylcarbazide as the indicator. Control tests showed that aluminum ion did not interfere with this determination.

Neutralization of Oxonium Ion by Alumina

The decrease in the normality, as an acid, of oxalic acid as a result of its contact with hydrous alumina sample "95" was measured by methods described elsewhere (4, 6).

Experimental Results

In Table I there are given the results of sorption experiments involving the interaction of various quantities of hydrous alumina sample "60" (of mesh size −60/+115) with 100.0 ml. of 0.0500 *M* oxalic acid solution at 25.0°C.

The sorption values of 658 mg. of sample "60" of −250 mesh (equivalent to 650 mg. of −60/+115 material) were found to be 0.6–0.7% lower than those for the −60/+115 fraction.

Similar experiments were carried out with hydrous alumina samples "30" and "1310." The data, given in Table II, refer as before to sorption experiments at 25.0°C. in which 100.0 ml. of 0.0500 *M* oxalic acid solution were used.

In Tables I and II the precision of the sorption values is given as ±0.2%. This is a calculated precision, taking account of the uncertainty

[4] Sorption of oxalate by hydrous alumina samples "30," "60," and "1310" was determined using this permanganate method. In the experiments using sample "95," the oxalate sorption was determined using a similar procedure, but employing ceric sulfate. A 0.1 *M* solution of the latter, using the ceric ammonium salt, was prepared according to the method recommended by Smith (13), and standardized against sodium oxalate (from the Bureau of Standards) using the room temperature procedure of Walden, Hammett and Chapman (17) employing ferrous ammonium sulfate for the titration of the excess ceric ion, with orthophenanthroline ferrous ion as indicator. The determination of oxalate in the unknown samples was carried out in a manner similar to the standardization, with the titer ratio of the ferrous and ceric solutions freshly determined for each analysis. The validity of the method in the presence of aluminum ions was proved by means of suitable control experiments.

TABLE I

Sorption of Oxalate Ion by Hydrous Alumina "60"

Mass of alumina	Time of contact with oxalic acid *hrs.*	Percentage sorption of oxalate ion (±0.2%)
650 mg. (equivalent to 437 mg. of Al_2O_3)	0.05	6.3
	1.00	6.6
	2.00	6.9
	4.00	6.9
	5.00	6.8
	6.00	6.7
	7.50	6.7
	10.0	6.6
	17.5	6.2
1300 mg. (equivalent to 874 mg. of Al_2O_3)	0.05	11.6
	1.00	13.1
	2.00	13.2
	3.00	13.2
	4.00	13.3
	15.0	11.8
1949 mg. (equivalent to 1310 mg. of Al_2O_3)	0.05	16.6
	0.40	18.3
	1.00	19.9
	2.00	19.8
	3.00	19.9
	4.00	19.5
	16.0	18.2
	35.0	16.4
	392	16.6

TABLE II

Sorption of Oxalate Ion by Hydrous Aluminas "30" and "1310"

Mass of alumina	Time of contact with oxalic acid *hrs.*	Percentage sorption of oxalate ion (±0.2%)
1990 mg. of Alumina "30" (equivalent to 1310 mg. of Al_2O_3)	0.05	2.7
	1.00	2.5
	3.00	1.8
	22.5	1.4
1310 mg. of Alumina "1310" (equivalent to 1310 mg. of Al_2O_3)	0.05	0.3
	1.00	0.3
	3.00	0.3
	4.00	0.4

in the buret readings; the titration values of the duplicate aliquot samples withdrawn for analysis in every case led to sorption percentages within ±0.1% of one another. The data given in Tables I and II are presented graphically in Fig. 1.

Some experiments were carried out with alumina "95" in which not only was the sorption of oxalate followed over many days but also, for a 24-hour period, the decrease in the oxonium ion concentration of the

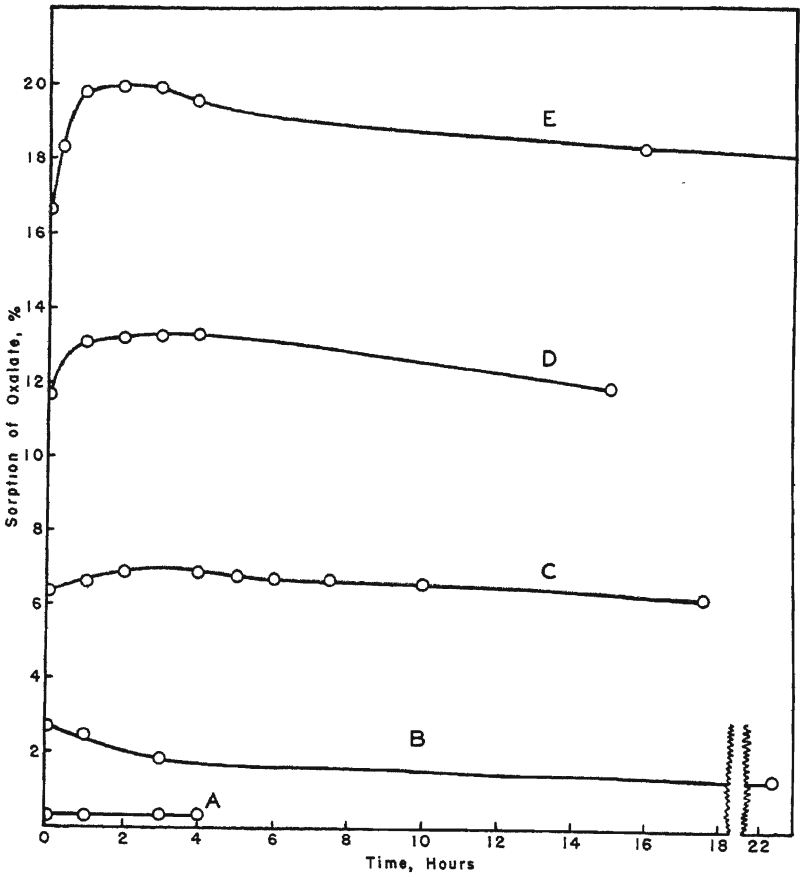

FIG. 1. Sorption of Oxalate Ion at 25°C. by Various Alumina Samples from 100.0 ml. of 0.0500 *M* Oxalic Acid Solution. A: 1310 mg. of alumina "1310" (ignited alumina). B: 1990 mg. of −60/+115 alumina "30." C: 650 mg. of −60/+116 alumina "60." D: 1300 mg. of −60/+115 alumina "60," E: 1949 mg. of −60/+115 alumina "60." In the case of curves A, B, and E the mass of alumina used was equivalent to 1310 mg. of aluminum oxide.

solution. The data from these experiments, in which 249 mg. of the −325 mesh fraction of alumina "95" (equivalent to 170 mg. of aluminum oxide) were allowed to react, at 25.0°C., with 100.0 ml. of 0.0500 *M* oxalic acid solution, are recorded in Table III.

TABLE III

Sorption of Oxalate Ion and Neutralization of Oxonium Ion by Alumina "95"

Time of contact with oxalic acid	Normality of oxalic acid solution	Percentage of oxonium ion neutralized	Percentage of oxalate ion sorbed
hrs.			
0.07	—	—	1.6
1.00	—	—	2.2
1.53	0.0913	8.7	—
2.82	—	—	2.4
3.05	0.0890	11.0	—
4.43	—	—	2.5
5.97	0.0856	14.4	—
6.02	—	—	2.4
12.35	0.0808	19.2	—
13.83	—	—	2.4
21.77	—	—	2.1
24.05	0.0742	25.8	—
36.32	0.0687	31.3	—
47.15	—	—	2.0
47.90	0.0642	35.8	—
72.20	—	—	1.7
118.7	—	—	1.4
186.7	—	—	1.0
309.3	—	—	0.6

The data given in Table III are plotted in Fig. 2.

Experiments with hydrochloric and oxalic acids comparing the sorption of chloride and oxalate under similar conditions showed that the removal of chloride ion from solution was approximately 10% of the oxalate sorption.

Discussion

It is evident from the data of Table III and from Fig. 2 that the assumption, made in some previous investigations of the reaction of acids with hydrous oxides (11, 19), that the anion sorption and the removal of oxonium ion from solution occur in equivalent quantities is an unwarranted one. The percentage of the oxonium ion neutralized continuously increases with time (6), whereas the concentration of oxalate in solution, subsequent to reaching a minimum value within a few hours, increases continuously approaching the initial oxalate concentration of the solution. Our interpretation of this observation is that, in the first stages of the reaction of oxalic acid with hydrous alumina, the rate of binding of oxalate to the solid oxide is greater than the rate of return of oxalate to the solution caused by the dissolution of the alumina after deolation (3). Within a few hours, however, the latter effect predominates, and thus the

curve for the sorption of oxalate exhibits a reversal of slope. Provided that the number of equivalents of oxonium ion contained in the oxalic acid originally added to the alumina is equal to or greater than the number

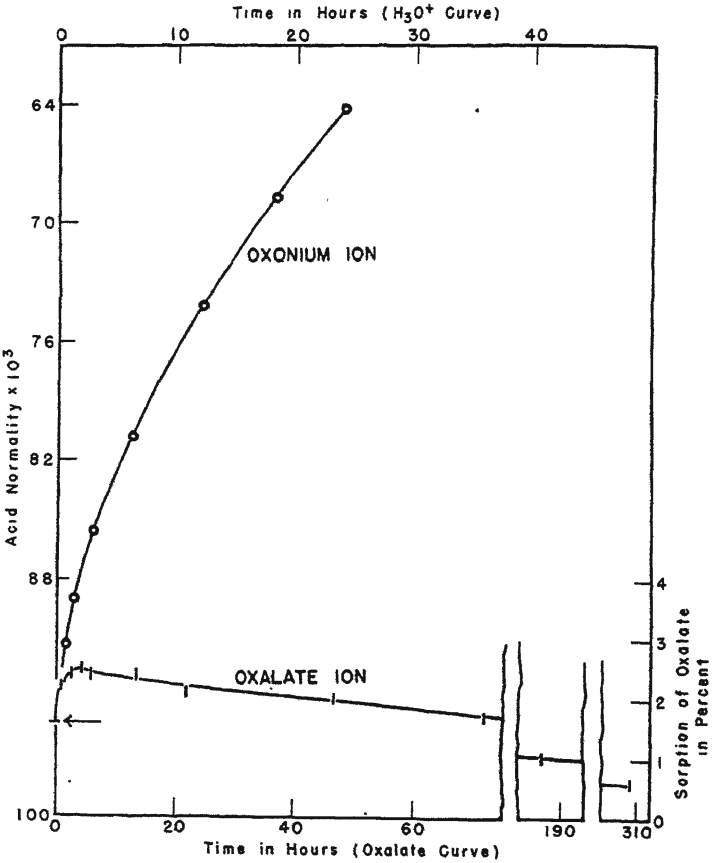

FIG. 2. Sorption of Oxalate Ion and Neutralization of Oxonium Ion by Alumina "95" at 25°C. A mass of 249 mg. (equivalent to 170 mg. of aluminum oxide) of the −325 mesh fraction of the alumina was allowed to interact with 100.0 ml. of 0.0500 *M* oxalic acid solution.

of equivalents of aluminum,[5] then, at equilibrium, the oxalate concentration of the solution should be the initial concentration (there being no hydrous alumina remaining, and hence no surface for sorption). It is evident from Figs. 1 and 2 that a large proportion of the maximal removal

[5] In the experiments with alumina "95," the ratio of equivalents of oxonium ion to aluminum was 1.00; it was less than 1.00 (ranging from 0.13 to 0.39) in the experiments with aluminas "30," "60," and "1310."

of oxalate from solution occurs within the time (0.05–0.07 hr.) of the earliest measurement (this value is marked by an arrow in Fig. 2). In view of the rapid conversion of the surface hydroxo groups of hydrous alumina to aquo groups in the presence of oxonium ion (6), and the fact that oxalic acid produces comparatively little colloidal alumina (15), such rapid sorption of oxalate ions is to be expected. Particles of alumina will become positively charged colloidal micelles only if a sufficiently high ratio of charge to mass is built up; this is less likely to occur when both oxonium and oxalate ions are reacting with the surface to an appreciable extent than when anion sorption is very slight. It was found in this work that, under similar conditions of sorption from acid solutions, chloride ions are sorbed to a much lesser extent by hydrous alumina than are oxalate ions; Mehrotra and Dhar obtained similar results when studying the sorption of anions by freshly-precipitated aluminum "hydroxide" (7) (*cf.* however, (2)). This fact should favor the production of colloidal alumina, and it is well known that hydrochloric acid is a very efficient acid for the peptization of alumina. That the sorption of oxalate ion by hydrous alumina from either an acid solution or a neutral salt solution (1) is greater than that of chloride is explained by the fact that oxalate ion possesses a relatively much greater tendency to be bound coordinatively to aluminum than does chloride ion. Oxalato complexes of aluminum are well known, but chlorido complexes of aluminum are not stable in aqueous solution (16).

From Tables I and II or Fig. 2, it is immediately evident that the activity of the samples of hydrous alumina, as regards the sorption of oxalate ion, depends on their temperature of preparation. For a mass of alumina equivalent to 1310 mg. of aluminum oxide, the "instantaneous" (0.05 hr. value) sorption of oxalate ion was 16.6% for alumina "60," 2.7% for alumina "30," and 0.3% for alumina "1310." The data of Table I permit the conclusion that, at least within the range of the experiments, the extent of sorption is a linear function of the mass of alumina used. It is reasonable to suppose that this relationship is at least approximately true for alumina "95," and if this is so, a simple calculation involving the data of Table III shows that, under similar conditions, alumina "95" would sorb almost the same (slightly less) amount of oxalate ion[6] as did alumina "60," and very considerably more than alumina "30." The sorption of oxalate may be interpreted as being due, in large measure, to an exchange reaction involving the displacement, from the surface of the

[6] The calculation also assumes that the activity of an alumina sample with respect to oxalate sorption is not a function of the mesh size. Experiments noted in this paper showed that alumina "60" of −250 mesh size sorbed about 90% of the oxalate that the −60/+115 fraction of the same alumina sorbed. Earlier work (6) has shown that the reactivity of hydrous alumina toward acid is not significantly dependent upon mesh size.

hydrous alumina, of aquo groups. These aquo groups may have been (and some almost certainly were) present on the surface of the alumina before the addition of the solution of oxalic acid, but most of them arose by the conversion of surface hydroxo groups to aquo groups by the instantaneous action of oxonium ion. It is our view that the extent of surface hydroxo groups depends on the temperature of preparation of the hydrous oxide, and we assume that alumina samples "60" and "95" possess more surface hydroxo groups than does alumina "30," and that alumina "1310" (being an ignited sample) is essentially free of hydroxo and aquo groups. This view that ignited alumina possesses a completely oxolated structure explains its lack of reactivity toward either the oxonium ion (6) or the oxalate ion of a solution of oxalic acid.[7] These same assumptions have proved valuable in interpreting the very rapid partial neutralization of oxalic acid solutions by hydrous alumina (6) and the raising of the pH of a neutral solution of potassium oxalate (5) (with respect to which properties, it was also found that aluminas prepared at 60°C. and 95°C. possessed almost the same activity, and one significantly greater than that of an alumina prepared at 26°C.), and other experiments involving the interaction of samples of hydrous alumina with acid and neutral salt solutions (1, 3).

It has been shown (6) that, insofar as breakdown of the alumina structure by acid is concerned, the reactivity of hydrous alumina samples decreases with increasing temperature of preparation, *i.e.*, the higher the temperature of preparation the greater the degree of oxolation. The relatively greater ease with which alumina "30" is deolated would explain the absence of a peak (Fig. 1) in the curve for the sorption of oxalate by this sample.

Acknowledgment

It is to Professor Arthur W. Thomas that thanks are due, and gratefully given, for arousing the interest of one of us (R.P.G.) in the chemistry of the hydrous oxides.

Summary

The sorption of oxalate from an acid solution by hydrous alumina powder has been studied as a function of time and of the temperature of preparation of the alumina.

It has been shown that, with increasing time, the sorption of oxalate reaches a maximum and then decreases steadily. The sorption of chloride ion is much less than that of oxalate.

[7] The relative inertness of ignited alumina toward acids was a phenomenon familiar to the chemist Heinrich Rose well over a century ago: "ignition renders it [alumina] difficultly soluble, and in many acids nearly insoluble" (9).

The extent of the sorption of oxalate depends on the temperature of preparation of the hydrous alumina.

The phenomena observed have been explained on the assumption that hydrous alumina is an olated and partially oxolated structure and that surface hydroxo groups play an important part in sorption phenomena.

References

1. Baker, P. D., Thesis, Columbia University, New York, 1940.
2. Chakravarti, D. N., and Dhar, N. R., *J. Indian Chem. Soc.* **5**, 539 (1928).
3. Clay, J. P., and Thomas, A. W., *J. Am. Chem. Soc.* **60**, 2384 (1938).
4. Graham, R. P., *Ind. Eng. Chem., Anal. Ed.* **18**, 472 (1946).
5. Graham, R. P., and Horning, A. E., *J. Am. Chem. Soc.* **69**, 1214 (1947).
6. Graham, R. P., and Thomas, A. W., *ibid.* **69**, 816 (1947).
7. Mehrotra, M. R., and Dhar, N. R., *J. Phys. Chem.* **30**, 1185 (1926).
8. Roberts, I., *Ind. Eng. Chem., Anal. Ed.* **8**, 365 (1936).
9. Rose, H., A Manual of Analytical Chemistry, translated from the German by J. Griffin, p. 74. T. Tegg, London, 1831.
10. Sen, K. C., *J. Phys. Chem.* **31**, 686 (1927).
11. Sen, K. C., *Z. anorg. allgem. Chem.* **182**, 118 (1929).
12. Sen, K. C., *ibid.* **182**, 129 (1929).
13. Smith, G. F., Ceric Sulfate, p. 52. The G. Frederick Smith Chem. Co., Columbus, Ohio, 1935.
14. Tartar, H. V., and Damerell, V. R., *J. Phys. Chem.* **36**, 1419 (1932).
15. Thomas, A. W., and Vartanian, R. D., *J. Am. Chem. Soc.* **57**, 4 (1935).
16. Thorne, P. C. L., and Ward, A. M., Ephraim's Inorganic Chemistry, pp. 300–301. Gurney and Jackson, London, 1939.
17. Walden, G. H., Hammett, L. P., and Chapman, R. P., *J. Am. Chem. Soc.* **55**, 2649 (1933).
18. Weiser, H. B., Inorganic Colloid Chemistry, Vol. II, pp. 112–119. Wiley, New York, 1935.
19. Weiser, H. B., and Middleton, E. B., *J. Phys. Chem.* **24**, 30 (1920).
20. Yajnik, N. A., Kapur, P. L., and Malhotra, R. L., *Kolloid-Z.* **80**, 152 (1937). Through *Chem. Abstracts* **31**, 7720 (1937).
21. Yoe, J. H., *J. Am. Chem. Soc.* **46**, 2390 (1924).

ASSOCIATION PHENOMENA. I. THE GROWTH OF PARTICLES OF SILVER CHLORIDE AND THE HIGHER-ORDER TYNDALL EFFECT [1]

Robert Ginell,[2] A. Margot Ginell and Paul E. Spoerri

From the Chemistry Departments, Polytechnic Institute of Brooklyn and Brooklyn College

Received August 22, 1947

Introduction

The formation of precipitates by the reaction of two ionic species is generally so rapid that it is often described as happening instantaneously. However, it is definitely a process, or series of processes, that are time-dependent although the rate at which they occur may be very great. A typical case of this sort is the formation of silver chloride from silver ion and chloride ion. When a solution containing silver ions is added to one containing chloride ions, the first step is probably the combination of the silver ions and the chloride ions to form silver chloride units (which will here be called monomer units).

$$Ag^+ + Cl^- \rightarrow AgCl$$

This process is not, however, as simple as this equation would imply, since the ions, while in solution, are surrounded by an atmosphere of solvent molecules which must in some way be modified to enable this process to go forward. While this simple process, the formation of monomers, is probably very rapid, little is known of its rate since the subsequent events complicate the picture.

The next process that occurs is the aggregation of these minute monomer units to form larger polymer units which, when grown sufficiently, interfere with the propagation of light through the medium and give rise ultimately to a visible precipitate.

$$n\ Ag^+Cl^- \rightarrow (Ag^+Cl^-)_n$$

The rate of this process of aggregation or association is probably much slower than the rate of the first process, the formation of the monomer units. The formation of the polymer from monomers may follow two

[1] Abstracted in part from the dissertation submitted to the Graduate Faculty of the Polytechnic Institute of Brooklyn by Robert Ginell in partial fulfillment of the requirements for the degree of Doctor of Philosophy, June, 1943.

[2] Present address: Department of Chemistry, Brooklyn College.

mechanisms. In the first mechanism the monomers grow through the successive addition of monomer units; that is:

$$\begin{aligned} Ag^+Cl^- + Ag^+Cl^- &\rightleftarrows (Ag^+Cl^-)_2 \\ (Ag^+Cl^-)_2 + Ag^+Cl^- &\rightleftarrows (Ag^+Cl^-)_3 \\ (Ag^+Cl^-)_3 + Ag^+Cl^- &\rightleftarrows (Ag^+Cl^-)_4 \\ \textit{etc.} & \end{aligned}$$

This is a kind of molecular mechanism and is most likely what occurs during the formation of sulfur sols (1). The other mechanism, which is only possible when the monomer is composed of ions, essentially consists of half steps and gives alternate paths for each step: *i.e.*

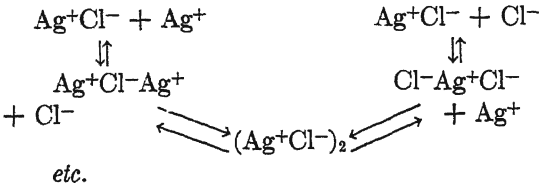

That is, to go from the monomer to the dimer, we may first add a chloride ion and then a silver ion or *vice versa*. A mechanism of this sort is very probable in the case of ionic substances. Other more complicated mechanisms which involve the addition of more than monomers or half-monomers may also be postulated and may be important in the formation of precipitates, but they would essentially be combinations or extensions of these basic mechanisms.

Experimental

To be able to follow the rate of association it was necessary to retard the rate of precipitation of the silver chloride. This was accomplished by the use of 95% ethanol as a solvent. Some experiments were also run with more dilute alcoholic solutions.

Reagents: Commercial 95% Ethanol. (No apparent advantages resulted from special distillation of the alcohol.) Distilled water. The silver nitrate and ammonium chloride used were ordinary C.P. materials.

Apparatus: White light was used in all experiments. The measurements were made with a linear photoelectric setup constructed according to Shepard (2). The beam of white light was passed through an optical cell which was kept in a constant temperature bath. For the Tyndall light scattering measurements a Zeiss Spectrometer whose prism had been removed was used. The container for the solution was a pyrex glass cylinder which was made from 50 mm. tubing.

Method: The order of addition of the reagents was first the ammonium chloride solution and then the silver nitrate solution. In various experi-

ments an excess of either chloride ion or silver ion was used. The exact concentrations are noted in Table I. For the turbidity experiments a large excess of silver ion was used.

TABLE I

Molarity		Initial appearance	First color noticed	Colored beam disappeared after	Colors at maximum[a]
Ag^+	Cl^-				
0.002795	0.000584	Turbid: blue beam	Yellow after 5 minutes	4 hours	2 orders yellow[b] 1 order blue 1 order red
0.000584	0.000584	Somewhat turbid: blue beam	2 yellow beams after 10 minutes	about 18 days	2 orders yellow[b] 1 order blue 2 orders red
0.0001839	0.000584	Clear: blue beam visible	Yellow after 30 minutes	about 30 days	2 orders yellow[b, c] 1 order blue 2 orders red
0.0000922	0.000584	Clear: blue beam visible	Yellow about 8 hours	colors still visible after 4 months	1 order yellow[b, c] 1 order blue 2 orders red

[a] In the instrument used, scattered light less than 27° from the incident beam was not observable.

[b] The yellow and blue bands seemed to interfere, giving also intermediate greens.

[c] Fine blue and red, and also yellow and red, and green and red bands were noticed in addition to the broad beams.

In Fig. 1 are shown the results of a typical experiment with the turbidimeter. The curve is a plot of I/I_0 *vs.* time. As can be seen from the magnified curve, with these concentrations there is no apparent induction period. The decrease in turbidity in the latter part of the curve is due to the formation of large particles which settled out of the path of the light beam. At the beginning of the process (immediately after mixing) only a very faint turbidity existed which gave a blue Tyndall light. As the particles increased in size the Tyndall light changed in color progressively to green, yellow, orange and red. This is the effect first reported by Ray (3) to occur with sulfur sols and which has since been described in detail by LaMer and coworkers (1, 4, 5, 6).

In Table I are shown the results of the experiments with the higher

order Tyndall effect. Experiments were made using an excess of either chloride or silver ions. The stability of the color effects was much more pronounced with an excess of chloride ion and with more dilute solutions.

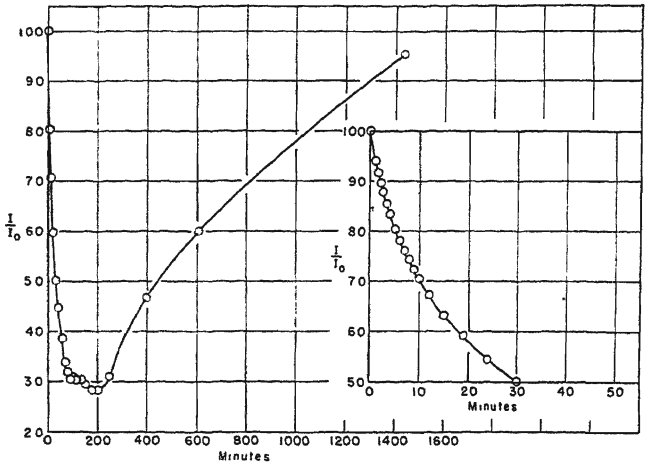

FIG. 1.

DISCUSSION OF RESULTS

The time of appearance of the higher order Tyndall effect was roughly inversely proportional to the concentration. Some preliminary experiments were also performed with lower concentrations of alcohol. The same effects were observed except that they appeared more rapidly and were not as distinct.

In some of these experiments it was noted that large particles formed and settled out while the color bands were still distinct. This indicates that while the size of the particles is fairly homogeneous in the region of size of the order of the wavelength of light, some particles grow to larger sizes. It is as if there were a large reservoir of uniform size particles of a size comparable to the wavelength of light from which large particles are being manufactured. In ordinary colloidal preparations the particles in this reservoir appear to be polydispersed (white Tyndall light) or else are very small (blue Tyndall light).

Some of these sols are quite stable, and continue to show these color effects for weeks and months. The stability is increased by increasing the dilution. Sols having an excess of chloride ion appear to be more stable than those having an excess of silver ion.

SUMMARY

1. Monodispersed silver chloride sols were prepared which were stable for various periods of time depending on the initial concentrations.

2. The higher order Tyndall light given off by such silver chloride sols was investigated.

3. The transmittance of silver chloride sols was studied as a function of time.

References

1. LaMer, V. K., and Barnes, M. D., *J. Colloid Sci.* **1**, 71 (1946).
2. Shepard, F. H., Jr., *Proc. Radio Club of America*, June, 1935.
3. Ray, B., *Proc. Indian Assoc. Cultivation Sci.* **7**, 1 (1921).
4. Barnes, M. D., and LaMer, V. K., *J. Colloid Sci.* **1**, 79 (1946).
5. LaMer, V. K., and Kenyon, A. S., *ibid.* **2**, 257 (1947).
6. Johnson, I., and LaMer, V. K., *J. Am. Chem. Soc.* **67**, 2055 (1945); **69**, 1184 (1947).

STATISTICAL THEORY OF RUBBER-LIKE SUBSTANCES

Ryogo Kubo

From the Department of Physics, Faculty of Science, Tokyo Imperial University, Tokyo

Received August 22, 1947

Introduction

In recent years remarkable progress has been made in the physics of high molecular substances. Considerable theoretical work has appeared in our country, but most of this has not yet been published owing to the war. This year for the first time I could obtain some information on the recent work by Americans (1, 2). It seems that their results differ from ours in some fundamental points. Therefore, it will be worth while to describe briefly our theories which have been developed since 1943. Detailed statements will appear in *J. Phys. Soc. (Japan)*.

First a summary will be given of the theoretical results on the intramolecular statistics of long chain polymers, which must be the basis of statistical theories on systems composed of macromolecules. Then, on the idea of network structure, theories will be developed for rubber-like substances. It will be seen how elastic modulus and double refraction depend upon the characteristic properties of polymers and network structures.

1. Intramolecular Statistics

We investigate the partition function as a function of parameters specifying the form of a single macromolecule, in other words, the relative probabilities of the forms it can assume. Among various conceivable parameters we choose the length, r, of the distance between the ends of the macromolecule, for it is most fundamental as a parameter.

Changes in the form of the macromolecule are caused mainly by internal rotation, which is naturally hindered at ordinary temperatures. The macromolecule jumps spontaneously from one stable configuration of its constituent units to another by thermal motion. Other modes of motion can presumably be separated from the partition function as vibrations independent of the form. On these assumptions, we can remove all kinetic terms from our partition function and construct it in configurational space rather than in phase space.

Then the free energy of a single molecule $F(r)$ can be shown to take

the form

$$F = kT(sr - n\mu), \tag{1}$$

$$n\frac{d\mu}{ds} = r, \quad \mu = \log \lambda, \tag{2}$$

where the number of the constituent units n is assumed to be large, and μ and λ are even functions of s, their functional form being determined by the nature of internal rotation. In Eq. (1), the parameter s is regarded as a function of r given by the inversion of Eq. (2). For the tensional force X to be applied at the ends to maintain the length r, we have

$$X = \frac{\partial F}{\partial r} = kTs. \tag{3}$$

Thus we can see at once that $-\mu(X/kT)$ is nothing but the Gibbs free energy per unit divided by kT. The proof of (1) and (2) is as follows. We choose several units as a new element so that we need consider only the interaction energy between two neighboring elements. The configuration of an element is specified by a set of variables q. Then we consider the modified partition function $Z_n(r, q)$ which is defined as the relative probability density that the length vector and the configuration of the end element are r and q, respectively. Its Laplace transformation $Q_n(s, q)$ or the grand partition function as a function of $s = X/kT$ is shown to satisfy a simple recurrence equation, which can be solved by means of an eigen value problem. The function Q_n has the asymptotic form

$$Q_n(s, q) \sim \lambda^n(s)\psi(s, q). \tag{4}$$

Then, evaluating the inverse transformation of Q_n, we get the asymptotic theorem (1) and (2). The free energy F is naturally defined by

$$F = -kT \log Z_n(r), \quad Z_n(r) = \int Z_n(r, q)dq. \tag{5}$$

The merit of this method is that it simultaneously gives the orientation probability of the elements when the length is specified as r. It is given by

$$f(r, q) = e^{sa(q)}\psi(s, q)^2 / \int e^{sa}\psi^2 dq, \tag{6}$$

$$\mu'(s) = r/n,$$

where $a(q)$ is the skeletal length vector of the element.

When we neglect correlation between elements we at once obtain

$$\mu = \log \frac{\sinh as}{as}, \tag{7}$$

$$r = na\left(\coth as - \frac{1}{as}\right), \quad s = X/kT.$$

In a general case we can get λ and ψ in power series in s. We define the index curling of the chain by

$$\rho = r/na, \tag{8}$$

where na is the maximum length of the chain. Then by Eq. (1) and (2) the free energy F can be written as

$$F = nkT(as\rho - \mu(\rho)) = nkTg(\rho) = nkT\sum_{t=1}^{\infty} g_{2t}\rho^{2t}, \tag{9}$$

where the expansion coefficients can be calculated considering the nature of the molecule. We remark here only that the first important coefficient g_2 is related to the so-called mean square length of the free long chain molecule by

$$g_2 = \tfrac{3}{2}\frac{\langle r^2\rangle}{na^2}. \tag{10}$$

2. The Elastic Property

It seems that the idea of the network structure of rubber-like substances is now widely accepted, so we need no detailed explanations. In vulcanized rubber the junctures are mainly sulfur bridges, all of which, in ideal cases, can be assumed to be so tight that they suffer no change by reversible elastic deformations. When weak junctures caused by secondary bonds are present, relaxation phenomena are naturally expected if the rate of deformation is so slow as to permit any change in their state of binding. In this paper we treat only of the case of ideal rubber in which the junctures are tight. By a chain we mean the part of a macromolecule connecting two neighboring junctures. They are assumed to be in fairly vigorous thermal motion.

The free energy for a whole block of rubber consists of those of the chains given in Sec. *1* and the cohesive energy of constituent units. Free energy due to thermal vibration is assumed to be independent of the deformation. The cohesive energy also should be independent of the deformation except for the case of hydrostatic compression, because the Poisson ratio is almost $\frac{1}{2}$, which is naturally to be expected considering that elastic forces for elongation are much smaller than those of ordinary solids, while the compressibility is of the same order of magnitude. Thus, in discussion of the characteristic rubber elasticity we can always make the volume change equal to zero.

Even in the unstrained state of the block, the chains must be in strained states because of the repulsive and attractive forces between the units, which hold the volume at constant value as stated above. This strained state of a chain in the initial state may be specified by the initial value ρ_0 of the index of curling. In the strained state of the whole

block, the chain will have the index of curling ρ. Then we must seek for the relation between ρ_0 and ρ.

We define a deformation by the linear transformation

$$x' = Ax, \quad y' = By, \quad z' = Cz.$$

In this case the most plausible assumption will be that ρ of the chain with initial values of direction cosines (ξ, η, ζ) is given by

$$\rho = \rho_0(A^2\xi^2 + B^2\eta^2 + C^2\zeta^2)^{\frac{1}{2}} \tag{11}$$

and that its directional cosines are proportional to $(A\xi, B\eta, C\zeta)$. In the undeformed state all orientations of chains are equally probable. Thus we obtain the free energy of deformed rubber

$$F = \frac{dRT}{m}\left(\frac{g^2}{3}\langle\rho_0^2\rangle(A^2 + B^2 + C^2) + \frac{g^4}{5}\langle\rho_0^4\rangle\{A^4 + B^4 + C^4 + \tfrac{2}{3}(B^2C^2 + C^2A^2 + A^2B^2)\} + \cdots\right), \tag{12}$$

which is derived by the average of free energies of the chains over all possible orientations. The average $\langle\rho_0\rangle$ must be taken over the possible distribution of ρ_0. In Eq. (12), d = the density, m = the molecular weight of the unit. The stress X_0 referred to the initial cross section in the case of uniaxial tension is given by

$$X_0 = \frac{dRT}{m}\left[\tfrac{2}{3}g_2\langle\rho_0^2\rangle\left(A - \frac{1}{A^2}\right) + \pi g^4\langle\rho_0^4\rangle\left(A^3 + \tfrac{1}{3} - \frac{4}{3A^3}\right) + \cdots\right] \tag{13}$$

and the initial Young's modulus ϵ_0 by

$$\epsilon_0 = \frac{dRT}{m}2g_2\langle\rho_0^2\rangle, \tag{14}$$

when ρ_0 is small.

At this stage we must clarify the meaning of ρ_0. In my opinion it is determined by the structure of the net and the cohesive forces between the units, rather than by the behavior of chains in their free states. As the volume is constant by the nature of cohesive forces and is proportional to the product of the number of junctures and the third power of the chain length, that is $(na\rho_0)^3$, we get the relation

$$\langle\rho_0^2\rangle = c(b/N)^{\frac{2}{3}}, \tag{15}$$

where c is a constant of the order of 1, and b/N is the concentration of junctures.

The behavior of X_0 given by Eq. (13) fits the experimental curves

very well, at least up to 300 or 400% elongation, for suitably vulcanized rubber. This form of equation of state seems to be generally accepted now. It has been derived by several workers. The essential point is the interpretation of the coefficient. It involves the molecular weight of the unit molecule of the chain and does not involve that of the whole chain. The index of curling ρ_0 must be of the order of the ratio of natural length to maximum possible elongation of the rubber, namely near $\frac{1}{8}$ or $\frac{1}{10}$ in the ordinary conditions.

As Sakai pointed out in his criticism of Kuhn's theory, the equation of state must not involve the molecular weight of the large molecule because its thermal motion as a whole is inhibited in the rubber state (3). For the same reason the molecular weight of the chain must not appear in it.

Fig. 1 gives the theoretical stress-strain curve for the case of chains without correlation. Fig. 2 shows the initial values of rigidity G_0 and the

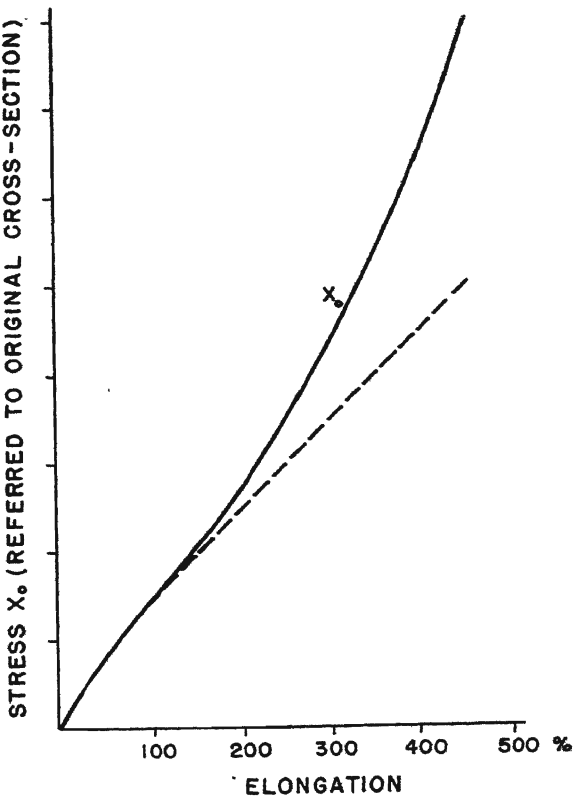

FIG. 1. Theoretical stress-strain curve for vulcanized rubber. —— calculated by Eq. (13), – – – calculated by the first term in the bracket of Eq. (13).

number of units contained in a chain (between two neighboring junctures) as functions of ρ_0 where the coefficient c in Eq. (15) is assumed equal to 1.

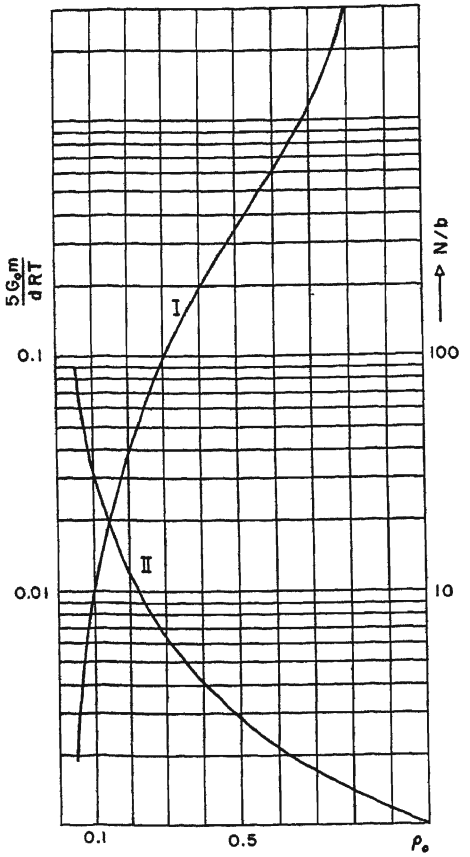

FIG. 2. Initial rigidity and the number of elements per juncture as functions of ρ_0. Curve I for $5G_0m/dRT$, curve II for N/b.

3. Double Refraction

The unit molecules belonging to a chain are oriented in some degree to the direction of its length, the distribution function of which is given by Eq. (6). In the unstrained state the directions of chains are at random, hence the units show no orientation as a whole. When deformed, the orientation of chains occurs as explained in Sec. *2*, and the units must have orientation. Thus, optical anisotropy appears. Practically, the crystallization accompanying the elongation causes additional anisotropy. As the experiment by Thiessen and Wittstadt shows, the crystallization

effect is negligible up to 300 or 400% elongation at ordinary temperatures, and increases slowly with time and shows hysteresis loops in some cases. Thus, the two effects due to orientation and crystallization can be separated experimentally. Our theory deals only with the former.

A theory of the double refraction was presented by Horst-Müller in 1941 (4). In my opinion, however, his basic assumption can by no means be justified. Hence, we wish to develop a theory based upon the intramolecular statistics given in Sec. *1*.

As details of the calculations will be published in *J. Phys. Soc.* (*Japan*), only a brief description will be given here. The orientation distribution of chains w in deformed state will be given by the assumption stated in connection with Eq. (11). As the orientation probability (6) refers to the axis of the chain, we transform it into a function referred to the axes of deformation. Then multiplying by w and averaging over all directions of the chains we obtain the required orientation function of unit molecules in the deformed state. It can be obtained in an expanded form in spherical harmonics, in which we need only the terms for second order harmonics, as we are dealing only with the average values of a tensor of the second order.

Taking averages of the polarizability tensor of the unit with the distribution function obtained, and making use of the Lorentz-Lorenz equation, we arrive at the tensor of refractivity as a function of deformation. For small ρ_0, in other words, for small density of junctures, this simplifies to

$$n_x - n_0 = \frac{4\pi}{405} D_2 \frac{dN_L \rho_0^2}{m} \frac{(n_0^2+2)^2}{n_0} \Delta\alpha \left(A^2 - \frac{B^2+C^2}{2} \right), \quad (16)$$

where n_0 = refractivity in unstrained state, N_L = Loschmidt's number and $\Delta\alpha = \alpha_{11} - \frac{\alpha_{22}+\alpha_{33}}{2}$ = polarizability in the skeletal direction—the average of those in transverse directions. Similar expressions can be obtained for the other principal axes of deformation. For uniaxial elongation the double refraction reduces to

$$\Delta n = n_{\parallel} - n_{\perp} = \frac{2\pi}{135} D_2 \frac{dN_L \rho_0^2}{m} \frac{(n_0^2+2)^2}{n_0} \Delta\alpha \left(A^2 - \frac{1}{A} \right). \quad (17)$$

The coefficient D_2 can be calculated from the nature of internal rotation of the chain molecule.

Eq. (17) shows that the double refraction is proportional to the stress referred to the actual cross section in a wider region than the range where Hooke's law is valid. The functional form given by (1) represents well the experimental curve of Thiessen and Wittstadt (5) (Fig. 3). Horst-Müller has assumed from the beginning that both the double refraction

and stress are proportional to the elongation. Moreover, his assumption has no sound basis regarding the coefficient in the expansion of the distribution function. We obtain from Eqs. (13) and (17) the relation

$$\frac{\Delta n}{X} = \Gamma \frac{(n_0^2 + 2)^2}{n_0 kT} \Delta\alpha \tag{18}$$

for not too great an elongation. The values of the coefficient Γ calculated for various types of chain molecules are given in the table (Column 2), where the numerical values of $\Delta\alpha$ (lines 3, 4, and 5) calculated by Eq. (18) from experimental data and those obtained from the Kerr effect for liquids of monomers (line 1). Considering that the electronic states are different in the polymerized state, they need not necessarily coincide with each other. Nevertheless, I believe the discrepancies

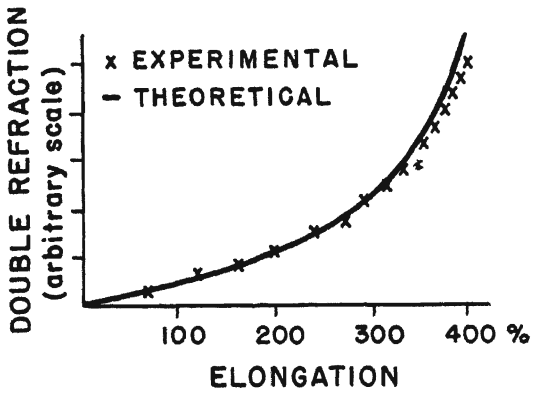

FIG. 3. Double refraction of rubber as a function of elongation. x:experimental, —— theoretical curve.

found by use of Horst-Müller's equation (line 2) are too large, and our equation (18) is much more reasonable than his. In the table we give the values of coefficient $\exp U/kT$ for the hindrance of rotation calculated by the assumption that the anisotropy of polarizabilities $\Delta\alpha$ of unit molecules are equal to those of monomers in liquid states. Of course the long paraffin-like chain model assumed in the calculation is not adequate for the substances listed in the table. But the values obtained can be regarded as reasonable in order of magnitude.

The unit of anisotropy of polarizability tensor is 10^{-25}. In lines 5 and 6, U denotes the energy difference between the planar and twisted forms of paraffin chains.

CONCLUSION

We have given a theory of elasticity and double refraction of network structures formed by linear polymers. Though several difficult problems

TABLE I

	Γ	Polystyrene	Polyvinylchloride	Polyisoprene
Optical anisotropy of monomers in liquid states		− 50	1∼5	20
Horst-Müller	$\frac{16\pi}{9}$	3.5∼ −2.5	0.45	0.87
Chains without correlation	$\frac{2\pi}{45}$	−140∼ −100	18	35
Free rotation with bond angle of 109°	$\frac{\pi}{18}$	−110∼ −80	14	28
Long paraffin-like chain ($kT \gg U$)	$\frac{526\pi}{9009}$	−105∼ −75	12	26
Long paraffin-like chain ($kT < U$)	$\frac{17\pi}{405} e^{U/kT}$	3.2∼2.3	20∼4.1	2.0

still remain unsolved on the statistics of chain molecules, the main features of the theory will probably be right. If the junctures composed of weak secondary bonds are important, as in the case of raw rubber, some characteristic features can be expected in the rate process as well as in the equilibrium theory. Discussions on raw rubber will be given elsewhere.

References

1. Guth, E., and James, H. M., *J. Chem. Phys.* **11**, 455 (1943).
2. Green, M. S., and Tobolsky, A. V., *ibid.* **94**, 80 (1946).
3. Sakai, T., *Proc. Phys.-Math. Soc. Japan* **17**, 226 (1943).
4. Horst-Müller, *Kolloid-Z.* **75**, 138 (1941).
5. Thiessen and Wittstadt, *Z. physik. Chem.* **47B.**, 33 (1938).

BOOK REVIEWS

Advances in Protein Chemistry, Vol. III, M. L. ANSON AND JOHN T. EDSALL (Eds.). Academic Press, New York, 1947. Pp. xii + 524. Price $7.50.

The new volume of this important series devoted to contemporary work in protein chemistry deserves renewed praise for the authors and editors who are making available timely, authoritative articles in this active field. General readers will find the texts highly readable and informative; those with a deeper interest in the subjects will welcome the fact that the discussions are, for the most part, well documented with data and detailed bibliographies.

A general picture of the scope and significance of the interrelations between the dicarboxylic acid system and various aspects of the metabolism of nitrogenous and non-nitrogenous body constituents is presented by Alexander E. Braunstein. Anthony A. Albanese reviews amino acid requirements in man, and Robert Elman discusses the use of proteins and its hydrolyzates for intravenous feeding.

The interesting chapter on adsorption analysis of amino acid mixtures by Arne Tiselius deals with a field which is so active that more on this rapidly growing subject might well be included in the next volume. The preparation and criteria of purity of amino acids is reviewed by Max S. Dunn and Louis B. Rockland, while Paul L. Kirk discusses chemical and physical methods for the determination of proteins. Reactions of native proteins with various chemical agents are reviewed by Roger M. Herriott.

The subject of protein monolayers, with the technique for their production and study, is discussed by Henry B. Bull. Alexandre Rothen provides a section on protein films in biological processes. He includes some of his own highly stimulating results which appear to indicate that specific antigen-antibody action and also enzymatic action can take place "at a distance," that is, while a protein film and a reactant are relatively far from contact.

The iron-rich protein, ferritin, and the related iron-free substance, apoferritin, are discussed by Leonor Michaelis.

Finally, John T. Edsall presents an excellent, detailed review of plasma proteins and their fractionation.

It would not be fair to criticize a book such as this one for the omission of certain important work in a field which is growing so rapidly. But the high quality of the material which we have seen makes us look forward with interest to the appearance of subsequent volumes.

THEODORE SHEDLOVSKY, New York, N.Y.

Mechanisms of Reactions at Carbon-Carbon Double Bonds. By CHARLES C. PRICE. Interscience Publishers, Inc., New York, N. Y., 1946. 118 pages. Price $2.50. (Lectures on Progress in Chemistry, Editor: H. Mark, Institute of Polymer Research, Polytechnic Institute of Brooklyn.)

This book consists of a series of lectures delivered at the Polytechnic Institute of Brooklyn in the summer of 1945. Those who attended these lectures clearly had a stimulating experience; the author, well known for his many and fertile ideas and for his lively style as a lecturer, was discussing some of the subjects in which he is most interested. Being now published as a part of the permanent literature, this material cannot be judged by its larger public on the basis of how it sounded from the lecture platform. In the conversion from lecture to print, statements from a limited viewpoint begin to look like misstatements, unsound speculations can no longer be promptly

erased, and the flexibility of the blackboard is replaced by a rigidity of printers' symbols which has seldom been more serious than in the present lack of proper resonance notation where called for in the text. However it may have been in this case, too many lectureships are now accompanied by pressure to publish the material in book form, although the lecturer is often not in a position to give his material the revision called for by such a change.

Chapters 2–7 deal in turn with reactions of the double bond of polar type, of free radical type, free radical polymerization, copolymerization, emulsion and suspension polymerization, and polar polymerization. The treatment of each of these topics is interesting and appropriate for a lecture. The mechanisms are presented in the main from a modern standpoint and would be largely concurred in by active workers in the field. Yet the writing shows evidence of haste and one cannot, in general, rely upon the statements to represent the summation of the pertinent literature. For example, although more than a page is devoted to phenanthrene bromination, it is stated that the addition and substitution reactions proceed by polar mechanisms "through a common intermediate" (p. 36) with no reference to the interesting and important fact, established largely by Dr. Price himself in a series of papers, that the usual preparation of phenanthrene dibromide is a photochemical chain reaction of free radical type, having nothing in common with the polar substitution.

A less happy part of the book is the first chapter, headed "Electronic Structure of Unsaturated Organic Molecules." Overlooking the fact that nearly all present users of the terms "mesomerism" and "resonance," including the original proponents of the earlier term, regard the two as meaning the same thing, Dr. Price has a section entitled "Mesomerism *vs.* Resonance" in which he compares this modern concept (under the name "resonance") unfavorably with a "pulsating resonant mesomerism in the true physical sense," which apparently pictures actual oscillations of the electrons between positions in mesomeric structures. No treatment is given of the physical evidence leading to the present view of the nature of the electron and of chemical bonds, and hence no limitations are felt in the process of setting such evidence aside.

Unimpressed by the success of the modern theory of resonance in accounting for aromatic substitution, the author presents again the numerical calculations of so-called "polarizing force" due to aromatic substituents, originally presented in a review in 1941. A set of numbers is derived for the various substituent groups in the benzene ring which exhibits a parallelism with the experimental fractions of *meta* orientation shown by those substituents. Such numerical parallelisms are important theoretical tools, and may often indicate a direct connection by physical law between different phenomena. In the present case, however, the numbers are arrived at by a kind of non-coulombian electrostatics involving alternate observance and violation of accepted physical principles. These numbers are, therefore, no part of any physical theory, whatever congruence they may show with other series of numbers. Among the features of the calculations open to criticism are the treatment of a dipole as an isolated charge, only the charge at the remote end of the dipole being considered, although the charge at the near end by electrostatic principles is the more potent of the two; and the classification of the electrons in the molecule into two sorts, one of which is impervious to influence by a charge at A and influenced by a charge at B, while the other shows the opposite behavior. Both of these eccentric features are necessary in order to yield the series of numbers referred to above. A young student, reading this material, might be tempted to conclude that the whole theory of aromatic substitution is in its infancy. Actually, it came of age 20 years ago, and adequate accounts of it are to be found in the modern literature (see, for example, Fieser in Gilman, "Organic Chemistry," New York, 1943, pp. 205–213, and Wheland, "The Theory of Resonance," New York, 1944, pp. 256–272).

PAUL D. BARTLETT, Cambridge, Massachusetts.

THE INFLUENCE OF THE PARTICLE SIZE OF HOMOGENEOUS INSECTICIDAL AEROSOLS ON THE MORTALITY OF MOSQUITOES IN CONFINED ATMOSPHERES

Victor K. LaMer, Seymore Hochberg, Kenneth Hodges and Irwin Wilson

The Department of Chemistry, Columbia University

and

John A. Fales and Randall Latta

U. S. Dept. Agr., Agr. Res. Adm., Bureau of Entomology and Plant Quarantine[1]

Received July 2, 1947

In November, 1943, the Bureau of Entomology and Plant Quarantine made some exploratory tests wherein DDT was added to the oil supply in a military screening smoke generator, and the aerosol cloud so created was drifted through woodland areas heavily infested with the salt marsh mosquito, *Aedes taeniorhynchus* (Wied). The results were promising enough to warrant further study. Cooperation was accordingly arranged with Division 10, National Defense Research Committee, which had sponsored the research and development of screening smoke generators of the type used in the exploratory tests, as well as perfecting the methods of producing and measuring the particle size of homogeneous aerosols.

The liquified gas aerosols in common use for mosquito control in enclosed atmospheres were known to be composed of particles covering a wide range of particle sizes up to 20 or 30 μ in diameter, with the average size ranging between 10 and 20 μ.[2] Screening smokes were known from studies made in the Columbia University Laboratories to be composed of much smaller particles, practically all of them ranging below 1 μ in diameter. Laboratory studies were accordingly undertaken to ascertain

[1] A portion of the studies reported here was done under funds allotted to the Central Aerosol Laboratory, Columbia University, New York, N. Y., by the Office of Scientific Research and Development upon recommendation of Division 10 of the National Defense Research Committee under Contract O.E.M.s.r. 148. It is based upon O.S.R.D. Report No. 4447 (December 11, 1944) to which the reader is referred for further details of execution.

[2] L. D. Goodhue and R. L. Riley, "The Particle Size Distribution in Liquified Gas Aerosols." (In press.) See also N.D.R.C. Informal Report 10.2–14 by LaMer, Hochberg, *et al.* (April 24, 1944), entitled "Particle Size Measurements on Certain Aerosol Bombs for the Department of Agriculture."

the minimum particle size that would be efficient as a first step in seeing if screening smoke generators could be used without modification for the generation of insecticidal aerosols.

It was recognized that clear-cut and unambiguous results could be obtained only if aerosols of uniform particle size were employed. In previous studies relative to screening and other types of smokes, the Central Aerosol Laboratory, Columbia University, had developed certain types of equipment for the generation of such homogeneous aerosols and the rapid measurement of their particle size and concentration. This equipment was employed in the laboratory studies on insecticidal aerosols. Details will be reported in *The Journal of Colloid Science.*

Orienting experiments (November, 1943) on the thermal stability of DDT showed that it would be partially decomposed at the high temperatures encountered in screening smoke generators in which the oil is completely vaporized before recondensation to a fine aerosol. The decomposition was also catalyzed by the presence of metal surfaces at these high temperatures, so that it soon became obvious that specially designed generators, operating at lower temperatures, would have to be developed. A fundamental study of the optimum particle size to be sought was, therefore, urgently needed.

It was also found that, although the then commercially available impure DDT decomposed when heated in the molten state to 130°C., a solution of 5% of DDT in lubricating oil did not decompose appreciably until heated above 260°C. yielding HCl. Purified DDT dissolved in oil appeared to be more stable and this finding enabled us to use the homogeneous laboratory aerosol generator developed by LaMer and Sinclair (O.S.R.D. Reports No. 57 and No. 1668). By the use of this all-glass apparatus, and by holding the temperatures below 230°C., repeated chemical analyses of the resulting aerosol showed that no decomposition of DDT occurred in thus preparing the aerosol. DDT (Geigy) furnished by the Department of Agriculture was recrystallized from alcohol, yielding a pure white product melting sharply at 107°C. This recrystallized DDT was used in all of the laboratory toxicity work.

During the month of December, 1943, orienting biological experiments were carried out at the Columbia University Laboratory with uniform particle size aerosols using *Drosophila* spp. as the test insects. These experiments showed that the small particles giving the optimum optical screening smoke efficiency were relatively ineffective as compared to larger droplets. They also clearly indicated that a diameter of 10–20 μ would be necessary for optimum insecticidal effects, and that the screening smoke generators would have to be modified to produce larger particles to become fully effective as insecticidal aerosol generators. A large scale generator employing the principle of thermal generation of

oil-DDT aerosols by the use of steam was developed in the Spring of 1944 by two of the authors (V. K. L. and S. H.) of this paper, and was used overseas by the Navy and Army for control of mosquitoes.

The present tests were performed at the Agricultural Research Center, Beltsville, Maryland, during the month of January, 1944, where laboratory-reared mosquitoes were available.[3] Adult *Aedes aegypti* in cages were exposed in a small chamber to a known concentration of aerosol of known particle size for varying lengths of time, and the resulting mortality recorded. Aerosols of very uniform particle size were prepared in the LaMer-Sinclair homogeneous laboratory aerosol generator. In this generator, DDT dissolved in an oil fraction prepared by vacuum distillation of a lubricating oil having a narrow boiling point range and a vapor pressure equivalent to that of DDT, was vaporized in glass vessels, mixed with known amounts of air, mixed with a controllable number of nuclei, and the diluted vapor allowed to cool and condense upon these nuclei under carefully regulated conditions. The particle size was controlled by regulating the vapor pressure by adjusting the temperature and the number of nuclei. The nuclei were produced by heating NaCl deposited upon an electrically heated nichrome wire.

The size and homogeneity of the particles were checked frequently by microscopic examination of aerosol samples collected by settling on glass slides coated with an oleophobic substance. Particular care was taken when working in the smaller particle range that a few larger particles were not present among the small ones as accidental contaminants.

Measurements of particle size were also made using a falling drop apparatus and, in addition, with an optical instrument developed in the Columbia Laboratories which measured the degree of polarization of a beam of light passed through the aerosol. This optical method [4] was rapid and accurate when the aerosol was homogeneous. The clarity of the spectral orders—a phenomenon which is exhibited in the scattered light of the Tyndall beam in certain ranges of sizes in very homogeneous aerosols—furnished an additional check upon the uniformity of the particle diameters.

The aerosol concentrations were determined by two methods; depending upon the particle size. For particles up to 1.2 μ diameter, the attenuation of a light beam in passing through the aerosol-filled chamber was measured with a photronic cell equipped with a green filter. This permitted estimates of the change of concentration due to settling in the range of larger particles and enabled the operator to estimate the maxi-

[3] The mosquitoes were supplied by Abby Casanges and her associates.

[4] V. K. LaMer and D. Sinclair, O.S.R.D. Reports No. 1668 and 1857 (1943). See also LaMer and Barnes, *J. Colloid Sci.* 1, 71, 79 (1946); I. Johnson and V. K. LaMer, *J. Am. Chem. Soc.* 69, 1184 (1947).

mum exposure time permissible for a given concentration. The concentration was calculated from optical data previously developed.[4]

For larger particles an oleophobic slide was laid in the bottom of the chamber when the mosquitoes were introduced and allowed to remain until all of the aerosol had settled. From the surface concentration of particles on the slide and the height of the chamber, the concentration could be calculated. Also, since the rate of production of the aerosol was known, by measuring the increase in weight of a glass wool filter, the quantity of aerosol introduced into the chamber during a known period could be determined.

The techniques and equipment described above were developed in previous studies on smokes by the Central Aerosol Laboratory, and will be described elsewhere.

The DDT concentration in the oil of the aerosol was determined by collecting the aerosol upon a weighed glass wool filter and washing out with xylene, followed by dehydrohalogenation and potentiometric determination of the chloride.

Exposure of Insects

Adult mosquitoes were placed in small cylindrical cages 8 inches long by 3 inches in diameter. For each test, one cage was exposed to an aerosol of known concentration and particle size in a glass and wood chamber 18″ × 17 3/16″ × 16 7/8″ having a volume of 85.5 liters. Exposure periods ranged from 0.5–30 minutes. γ = micrograms.

The chamber was filled with the aerosol to the desired concentration before the cage of insects was introduced. A small slowly revolving fan was operated for a short time to insure good distribution before the insect exposure began. When the proper conditions in relation to the aerosol were obtained, the cage of insects was quickly lowered into the chamber and suspended there during the exposure period.

Following exposure the mosquitoes were removed to clean cages for observation. A mortality count was made the following day. Males and females were segregated in counting, and only data of female mortality is presented here.

It was recognized that the screen wire of the insect cage would remove a portion of the aerosol. However, this error would be fairly constant for all tests so it has been disregarded for the purpose of comparison of results.

Results

The mortality of female *Aedes aegypti* resulting from exposure to the homogeneous aerosols is given in Table I. It can be seen that with small particles in concentrations of aerosol around 100γ/l., exposures on the

order of 10–30 minutes or more were necessary to produce a high mortality. With the larger particles, aerosol concentrations around 25 γ/l. gave good mortalities at exposures from 0.5–2 minutes.

Analysis and Conclusions

Experimenters studying chemical warfare agents and fumigants often use the product of the concentration of the fumigant by the time of exposure as a value in determining lethal dosage schedules. By this method a decrease in concentration can be compensated for by an increase in exposure time. In analyzing the results of these tests, use has been made of this method as a means of comparing the tests where different concentrations of aerosol were recorded. When these products, represented by the symbol *Ct*, were taken from the data in Table I, and plotted against the per cent mortality, the values of *Ct* which produced 50% mortality were

TABLE I

Mortality of Female Aedes aegypti Resulting from Various Exposures to Homogeneous Aerosols in Confined Atmospheres

Particle diameter	Aerosol concentration	Exposure	DDT	Female mosquitoes		
				Total	Dead	Mortality
μ	*γ/l.*	*mins.*	*per cent*	*number*	*number*	*per cent*
0.33	36	9	8.2	20	0	0
	25	20	8.2	25	0	0
	30	31	8.2	22	1	4.5
0.46	80	½	7.2	77	0	0
	102	2	7.2	68	0	0
	92	10	7.2	51	22	43
	80	30	7.2	55	55	100
0.66	73.1	10	8.2	14	1	7.1
	58	19	8.2	17	1	5.8
	63.5	30	8.2	8	7	87.5
	63.5	30	8.2	15	12	80
0.68	132	2	7.9	69	2	2.9
	104	10	7.9	58	19	32.7
	94	20	7.9	22	21	65.6
	105	30	7.9	60	60	100
0.88	138	½	7.2	87	2	2.3
	244	½	7.2	70	1	1.4
	131	10	7.2	47	27	57.4
	244	30	7.2	60	60	100

TABLE I.—*Continued*

Particle diameter	Aerosol concentration	Exposure	DDT	Female mosquitoes		
				Total	Dead	Mortality
μ	*γ/l.*	*mins.*	*per cent*	*number*	*number*	*per cent*
1.16	103	2	7.9	49	0	0
	119	10	7.9	36	31	86.1
	101	20	7.9	41	41	100
	108	30	7.9	55	55	100
1.7	146–290[a]	½	8.1	12	7	58.3
	138–270	2	8.1	20	20	100
	142–270	5	8.1	25	25	100
2	350–210	2	8.1	41	39	95.1
	350–210	5	8.1	53	53	100
	350–210	10	8.1	64	64	100
	350–210	20	8.1	37	37	100
5	29	½	8	60	0	0
	29	1	8	44	5	11.3
	29	2	8	45	10	22.2
8.6	23	½	8	8	5	62.5
	23	1.3	8	9	9	100
11	14	¼	8	9	4	44.4
	14	½	8	10	7	70
16	20	½	5.9	32	8	25
	30	½	5.9	32	10	31.2

[a] Higher figure is from filter weight, lower one from light intensity.

determined by graphical interpolation to be as follows:

Diameter	*Ct* value producing 50% mortality
0.33	1700
0.46	975
0.66	1500
0.68	1420
0.88	1125
1.16	750
1.7	130
2	160
5	140
8.6	9
11	4.2
16	18

When these Ct values which produced 50% mortality were plotted against the particle diameter of the various homogeneous aerosols tested, which for the purposes of this evaluation are all considered to have essentially the same content of DDT namely, 8%, a curve as shown in Fig. 1 is produced. The toxicity, as measured by time of exposure-con-

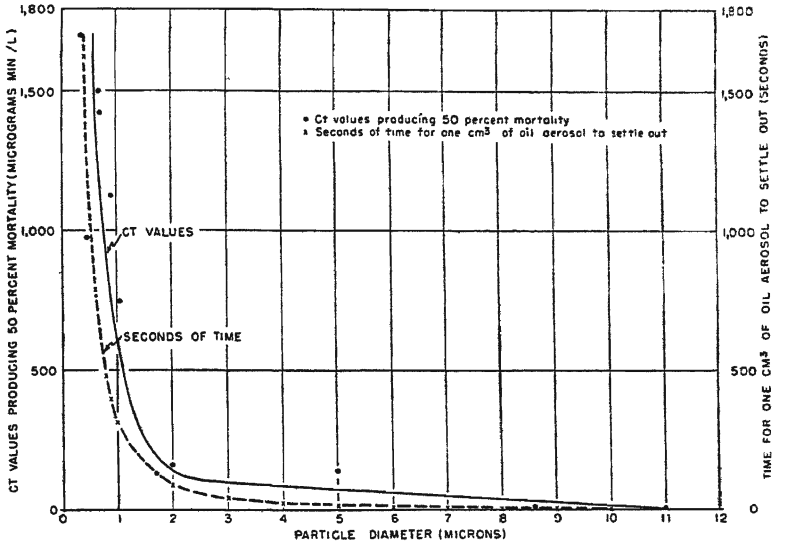

FIG. 1. The toxicity of aerosols to mosquitoes in confined atmospheres in relation to particle size, and a graphical presentation of the rate of settling of the same sized particles.

centration product, is increased 250 or more times by increasing the diameter of the particle from 0.33 to 11 μ.

In a confined atmosphere, it can be assumed that the deposition of aerosol particles on an insect is principally by settling, although this is also accomplished by impingement due to the influence of convection currents, and to the flight of the insects. In these tests, the convection currents were apparently minor, and the insects exhibited very little movement due to their confinement in small cages. Since it is also logical to assume that the amount of insecticide needed to produce mortality is the same, regardless of particle size, the mortalities given in Table I should be in the same order as the deposition per unit area for each sized particle as could be calculated by Stokes' Law.[5]

The settling rates of oil particles (sp. gr. 0.9) in air are given in Table II, as calculated by Stokes' Law for particles 0.2 μ and larger in diameter,

[5] C. D. Hodgman, 1944, Handbook of Chemistry and Physics, 28th ed., p. 2265. Chemical Rubber Pub. Co., Cleveland, Ohio.

TABLE II

Settling Rates of Oil Particles (sp. gr. 9) in Air According to Stokes' Law for Particles 0.2 μ and More in Size and Cunningham's Correction for Particles 1 μ and Less

Particle diameter	Ft./min.	Cm./min.	Time to settle 1 cm.
μ			*Seconds*
20	2.12	64.6	0.93
19	1.92	58.6	1.02
18	1.72	52.4	1.14
17	1.53	46.7	1.28
16	1.35	41.2	1.45
15	1.19	36.3	1.65
14	1.03	31.4	1.91
13	0.89	27.1	2.2
12	0.76	23.2	2.6
11	0.64	19.5	3.1
10	0.53	16.2	3.7
9	0.43	13.1	4.6
8	0.34	10.4	5.7
7	0.26	7.9	7.6
6	0.19	6.1	9.8
5	0.13	4.0	15.0
4	0.08	2.4	25
3	0.047	1.45	41
2	0.021	0.64	94
1	0.0062	0.19	315
.9	0.0051	0.15	400
.8	0.0041	0.125	480
.6	0.0025	0.076	789
.4	0.00121	0.037	1626
.2	0.00039	0.012	5000

and by Cunningham's correction to Stokes' Law[6] for particles of 1 μ or less.

The time necessary for all particles to settle out of 1 cc. is also plotted against particle size in Fig. 1. The values of Ct which produced 50% mortality, while showing some deviation from the curve, are of the same order.

According to Stokes' Law the time required for an aerosol droplet to fall 1 cm. is inversely proportional to D^2, the square of the diameter of the droplet. Since we have postulated that the toxicity as measured by Ct for 50% mortality is governed by the mass of the droplets that descend upon a resting insect in a given time, then

$$Ct = k \frac{1}{D^2}$$

[6] Lionel S. Marks, 1941, Mechanical and Engineering Handbook, 4th ed., pp. 835, 836. McGraw-Hill Book Co., New York.

or

$$\log (Ct) = -2 \log D + \log k,$$

where D is the diameter of the droplet and k is a proportionality constant depending upon the viscosity of the air and the density of the droplet. This means that if both Ct and D are plotted on a logarithmic scale, then, for the region for which this law applies, the data should fall on a straight

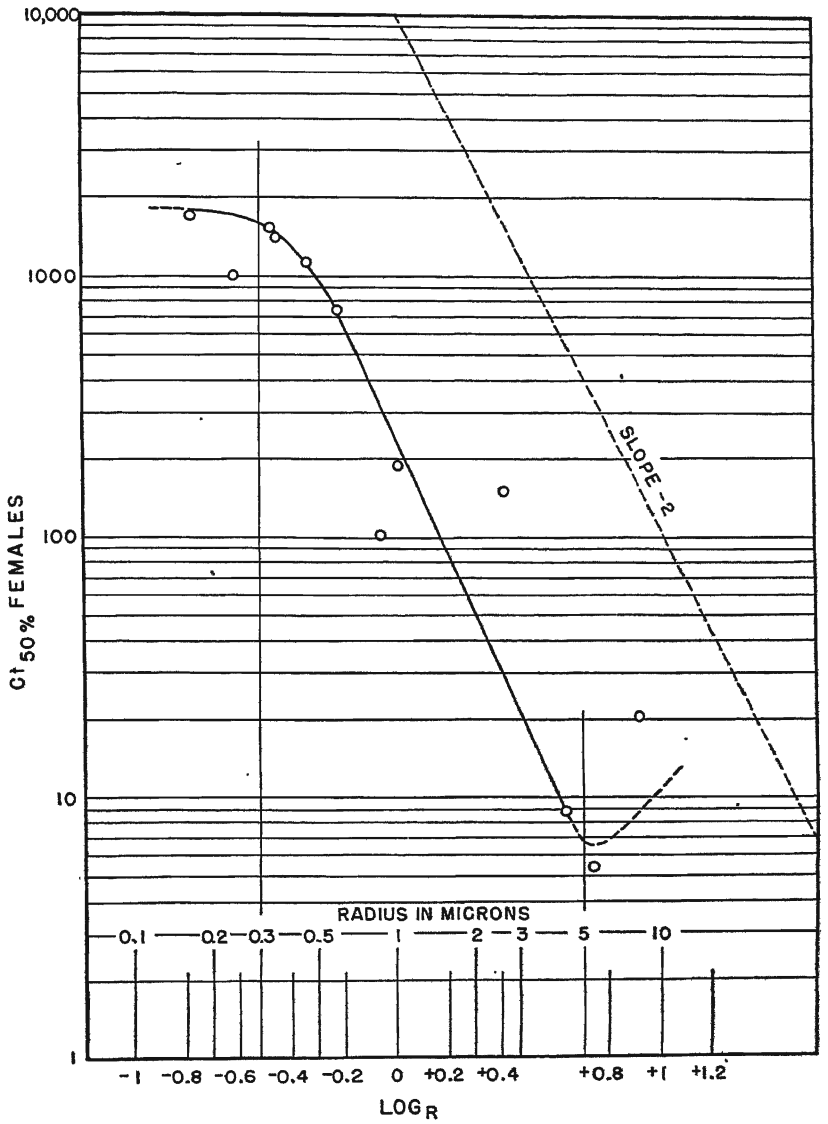

FIG. 2.

line with a slope of -2. This method of plotting, as shown in Fig. 2, exaggerates the experimental error as compared to Fig. 1, but, nevertheless, it is clearly evident for this more discriminating representation of the data that for values of the radii of the droplets between 0.3–5 μ (0.6–10 μ diameter) the Ct values decrease as predicted.

For radii less than 0.3 μ (0.6 μ diameter) the rate of fall is so slow (789 seconds or 13 minutes are required to fall 1 cm.) that the occasional movements of the insects become a more important factor than settling. Hence, the law cannot be expected to hold for very fine aerosols.

On the other hand, as the droplets become progressively larger, the statistical probability that a given droplet will encounter a mosquito decreases. If a large drop, containing twice the minimum lethal dose, falls on a mosquito, the effect will be recorded as only one death, whereas, if the droplet had been subdivided into 2 droplets, it could have killed 2 mosquitoes.

It is clearly evident, therefore, that Ct must finally increase for large droplets and that the curve in Fig. 2 must eventually pass through a minimum value for increasing droplet size. The increased value of Ct for the 16 μ diameter point is consistent with this prediction but is not offered as establishing the position of the minimum.

One year later (January to May, 1945), the problem was reinvestigated using improved methods for preparing the larger aerosols (up to 20 μ diameter). In this study insects were exposed in cages in a wind tunnel with wind velocities at 2, 4, 8 and 16 miles per hour (MPH). In this more extensive study[7], it was shown conclusively that the toxicity is again dependent upon the square of the diameter D of the droplet and also upon the first power of V, the wind velocity, provided the product (D^2V) is below a value of about 300.

For larger values of D^2V, corresponding to larger values of either diameter or wind velocity, the linear dependence of Ct upon (D^2V) no longer holds. A saturation effect becomes important and the curve flattens out, *i.e.*, Ct becomes independent of both wind velocity and particle size. This transition point corresponds to 10 μ diameter at 3 MPH.

Summary

Cooperative tests were made between the Bureau of Entomology and Plant Quarantine, and the Central Aerosol Laboratory, Columbia Uni-

[7] O.S.R.D. Rept. No. 5566. N.R.C. Insect Control No. 119. Effect of particle size and speed of motion of DDT aerosols of uniform particle size in a wind tunnel on the mortality of mosquitoes by Randall Latta *et al.* and V. K. LaMer, S. Hochberg *et al.* To be republished in J. Washington D. C. Acad. of Sciences. A detailed field report (O.S.R.D. No. 5731) in which these principles were applied to the control of Salt Marsh and Anopheline Mosquitoes by the ground dispersal of DDT aerosols has been published. Frank Brescia *et al.*, *J. Economic Entomol.* 39, 698 (1946).

versity, to compare the mortalities produced in confined atmospheres by aerosols of different sized particles. Apparatus for the generation of homogeneous aerosols, and instruments and methods of measuring the particle size and concentration, which had been developed by the Central Aerosol Laboratory in previous studies related to screening and other smokes, were utilized. Exposures of 10–30 minutes in aerosol concentrations of around 100 γ/l. were necessary to produce high mortalities when particles of 1 μ or less in diameter were used. Exposure of 0.5–2 minutes in aerosol concentrations of around 25 γ/l. produced high mortality when particles were 5–16 μ in diameter. When Ct (concentration of oil in γ containing 8% DDT multiplied by time of exposure in minutes) values which produced 50% mortality of females (calculated by graphical interpolation) were plotted against particle size, the toxicity was shown to be increased by 250 or more times by increasing the diameter of the particle from 0.33 to 11 μ. This curve corresponds to a curve in which the time necessary for an aerosol to settle out of 1 cc. is plotted against particle size, as calculated according to Stokes' Law and Cunningham's correction. It also shows that the toxicity is proportional to the rate of deposition which, in turn, is proportional to the square of the radius (or diameter) of the aerosol particle for the sizes discussed.

THE EFFECT OF STRONGLY HYDROGEN BONDING AGENTS ON SOME POLAR POLYMERS

G. King

From The Wool Industries Research Association, Torridon, Headingley, Leeds 6, England

Received July 16, 1947

Introduction

Two properties common to polar polymers are that they show pronounced swelling accompanied by a reduction in elastic moduli on sorbing polar vapors. These phenomena are, in general, accompanied by an abnormally large increase in the dielectric constant and electric power loss. X-ray studies of such systems show that polymers which are initially partially crystalline may become amorphous in the swollen state, and, indeed, some approach the state of rubberlike elasticity and indicate appreciable entropy changes on stretching.

Previous work in these laboratories (1) has covered the sorption of water and methyl alcohol by keratin, from which it was concluded that the increased dielectric constant of such systems could not be attributed to the absorbate alone. A connection was drawn between the increased molecular rotation and the decrease in elastic moduli. On the assumption that it was the bound fraction of the absorbate which breaks hydrogen bonds between adjacent polypeptide chains to increase the freedom of rotation of the NHCO groups, a semiqualitative description of these phenomena was developed.

The relative contributions of absorbate and absorbent to the increased dielectric constant of such systems was further examined by a study of keratin swollen with formic acid vapor. The preliminary results (2) reported, showed that the increase in dielectric constant was not dependent on the dipole moment of the absorbate, but was correlated to the decrease in elastic moduli.

In the present paper the investigations have been extended to cover the sorption of water and formic acid by nylon, thus generalizing the earlier results.

Experimental

1. *Dielectric Constant Measurements*

A condenser of the parallel plate type was used. The dielectric was in the form of two films each about 2.5 cm.^{2} in area and 5×10^{-3} cm. thick,

separating one inner and two outer electrodes, the latter grounded to serve as a screen. The electrodes were of lead foil, and, to ensure good electrical contact, each film was coated on either side with colloidal graphite over the area of contact. The assembled condenser was then clamped between two rigid brass plates at a pressure such that any further increase had no effect on the capacity when dry. No correction was made for any increase in pressure due to swelling.

The condenser (A), Fig. 1, was placed in a vacuum system which, in turn, was housed in an air thermostat at 25°C. Vapor was introduced

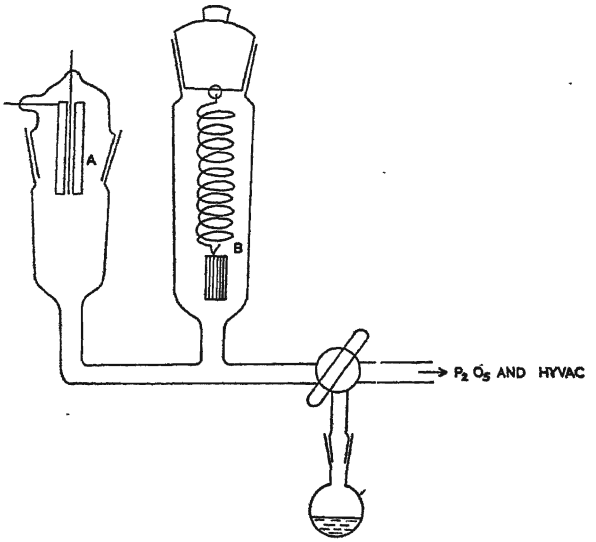

FIG. 1. Sorption system.

from the reservoir R, and after about 24 hours for the attainment of equilibrium conditions, as indicated by a constant capacity value, the amount of vapor absorbed was measured directly using a second sample of film suspended from a spring.

The capacities of the condensers used were measured at 1.1×10^4 cps. using the well known resonance method employing an oscillator and valve detector. The audio frequency oscillator was calibrated with a phonic wheel and a cathode ray oscillograph. Condensers were made from unoriented nylon film and horn films cut parallel to the fiber axis. Preliminary examination showed that after 24 hours no appreciable capacity change occurred for a period up to three days.

Accurate estimation of the dielectric constant depends largely on accurate measurement of the mean thickness of the films, error in which introduces a constant error of 3–4% in the results, so that the close agree-

ment with Errera and Sack's results (3) for dry keratin and nylon is fortuitous. Increased accuracy could no doubt be achieved in this respect by the use of thicker samples, but this would slow down the rate of sorption and make it impossible to ascertain when equilibrium had been reached. The results are shown in Fig. 2.

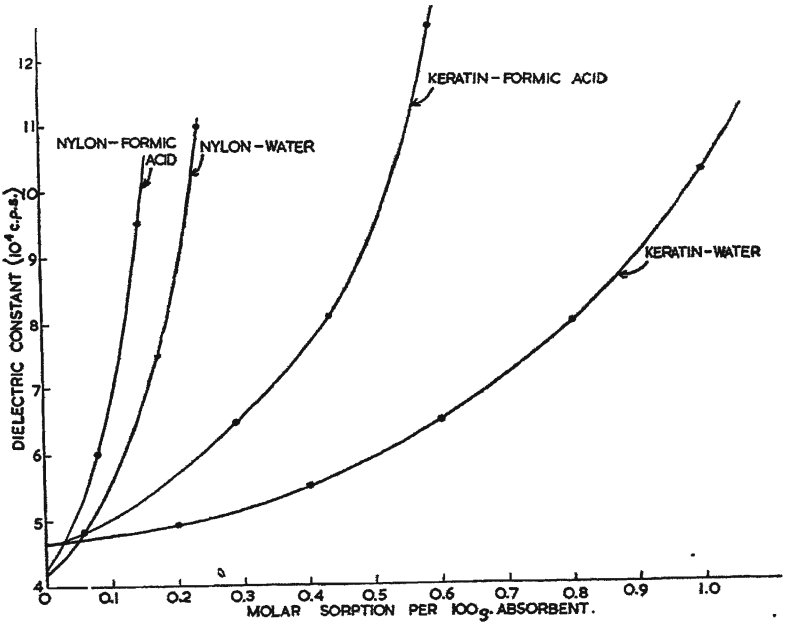

FIG. 2. Dielectric sorption relations.

2. *Rigidity Modulus Determinations*

The reduction in the rigidity modulus of wool and nylon fibers due to the sorption of water and formic acid, respectively, was measured, Fig. 3, using essentially the method of Speakman (4, 7). The apparatus in Fig. 1 was employed, replacing the condenser system by one enclosing a fiber capable of undergoing torsional oscillation. The results were corrected for the swelling of the fibers using known swelling relations in the case of water. In the case of formic acid, it was assumed that the swelling for a given amount absorbed was less than water, in proportion to their respective densities. This empirical relation has been found to be true for the adsorption of aliphatic alcohols by keratin (5); in the case of formic acid the assumption was verified experimentally, Fig. 5.

3. *Rigidity Temperature Effect*

The effect of temperature on the rigidity of dry nylon was also determined, Fig. 4. This was done by surrounding that part of the apparatus

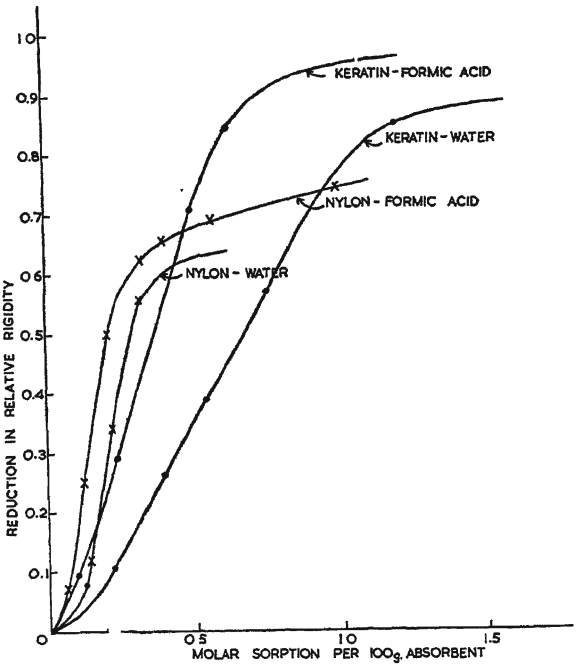

FIG. 3. Rigidity sorption relations.

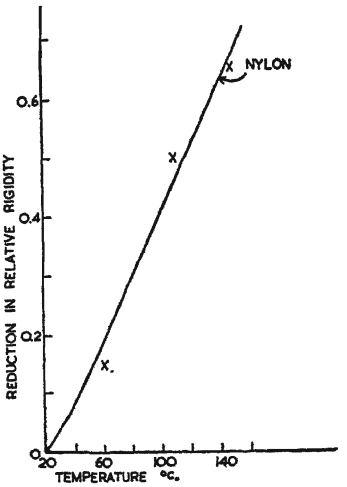

FIG. 4. Temperature rigidity relation for nylon.

containing the oscillating fiber system by an oil bath which could be controlled electrically at temperatures up to 140°C.

4. Formic Acid Swelling Relation

The oscillating fiber system was replaced by a strip of film about 3 cm. by 0.5 cm. by 5 × 10^{-3} cm. This was suspended from a small paper clip, a second clip at the lower end serving to keep the film taut without being heavy enough to cause any stretching of the film in the swollen state. The length of the film between the edges of the two clips was measured using a travelling microscope. In the case of nylon, the film was the same as

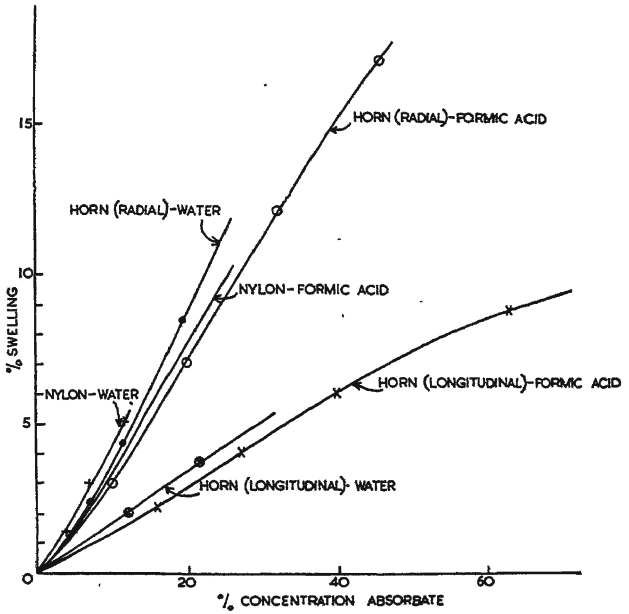

FIG. 5. Swelling of keratin and nylon in water and formic acid.

that used for the dielectric measurements, while two sections of horn film were cut, one parallel and one perpendicular to the fiber axis. The results are shown in Fig. 5.

5. Heats of Wetting and Absorption

Heats of wetting were determined by a method very similar to that used by Hedges (6) for wool-water systems. Samples of the absorbent were enclosed in thin-walled glass bulbs and evacuated for 24 hours prior to use; the bulbs were then broken in the appropriate liquid as required. With formic acid as adsorbate, the heats of wetting of keratin and nylon were measured for increasing initial amounts adsorbed, Fig. 6. The heat of wetting of nylon in the dry state only, was determined using water as adsorbent, the corresponding heats of adsorption having already been determined (7). The results are shown in Table I.

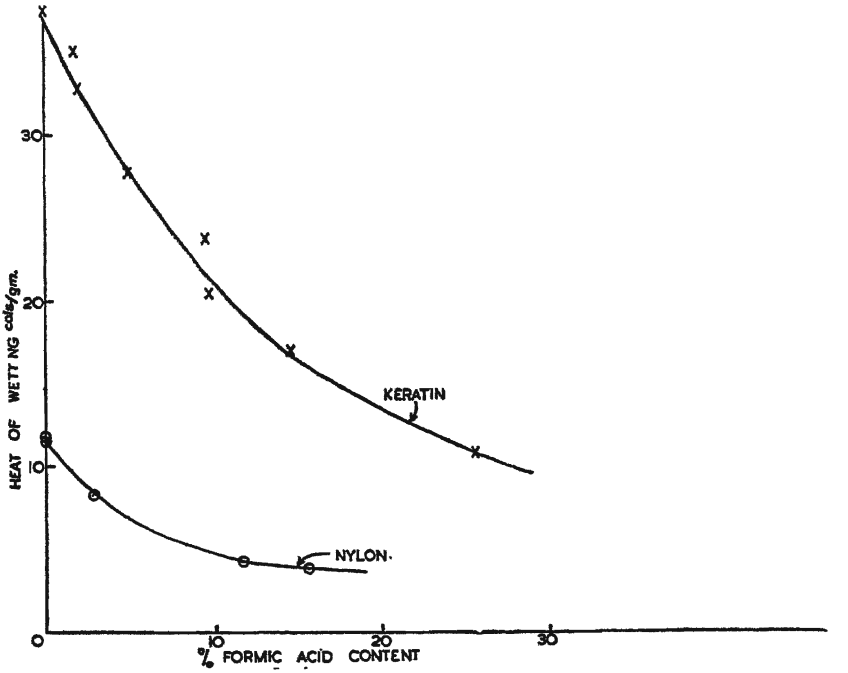

FIG. 6. Heats of wetting of keratin and nylon in water and formic acid.

6. *Formic Acid Adsorption Isotherms*

To demonstrate that the sorption of formic acid vapor by keratin and nylon is essentially the same process as for water, isotherms were determined in each case, using methods previously described; the results are shown in Fig. 7. Most of the formic acid may be pumped out of the samples directly, but, as in the case of alcohol-keratin systems, a small fraction remains which may be removed by "washing out" with water vapor. This is no doubt due to the fact that, although formic acid is adsorbed up to 20 times as fast as water vapor, at low concentrations its diffusion coefficient falls to values lower than those for water.

TABLE I

Adsorbate	Adsorbent	Heat of wetting	Heat of adsorption "zero" concentration
		cal./g.	*kcal./mol*
Formic acid	Keratin	36.0	6.7
	Nylon	11.6	6.5
Water	Nylon	6.7	4.0

Discussion and Results

1. Dielectric Effects

The nylon-water relation agrees reasonably well with the rather meager values of Yager and Baker (8) for this system. It is seen that both absorbates have an enhanced effect on the dielectric constant of nylon as compared with keratin for an equal molar concentration of absorbate. This is accompanied by a correspondingly large power loss effect, so that,

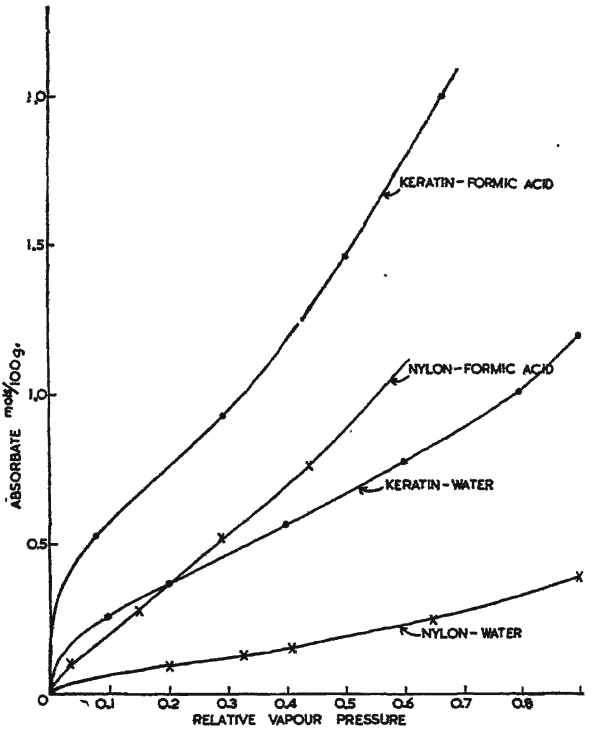

Fig. 7. Sorption isotherms.

although nylon adsorbs relatively little water as compared with keratin for a given relative humidity, its electrical properties are no better.

As in the case of keratin, formic acid has a greater effect, per mol adsorbed, on the dielectric constant of nylon than has water in spite of the smaller dipole moment of the former, thus confirming the view, previously suggested, that the increase is not due entirely to rotation of the adsorbed polar molecules (1, 2).

It would seem that there are sufficient polar groups in nylon to contribute to this large increase in dielectric constant. According to Baker and Yager (8) a dielectric constant of about 20 is attainable by raising

the temperature of polyhexamethylene sebacamide to about 140°C., well below its melting point, for a frequency of 10^4 cps., the frequency used in these investigations. This polyamide has fewer polar groups per unit mass than nylon, assuming the latter to be the corresponding adipamide. By comparison, dry keratin shows a very small increase in dielectric constant with increased temperature.

2. Rigidity Modulus

It is noticeable from Fig. 3 that the rigidity-sorption relations for keratin and nylon follow the dielectric relations very closely, giving support to the theory that the fundamental mechanism in both cases is rotation of polar groups in the polymer chains facilitated by the breaking of interchain hydrogen bonds by the absorbate.

The reduction in rigidity of nylon due to the presence of a solvent is very closely paralleled by the change in Young's modulus of polydecamethylene sebacamide by the substitution of increased porportions of methyl groups for the hydrogen atoms in the diamine group. Baker and Yager (9) show that, for about 50% methylation, the modulus may be reduced to as low as one-fifth of its original value, and they attribute this to the greatly reduced hydrogen bonding between NHCO groups.

The effect of temperature on the rigidity of these dry polymers also follows the corresponding dielectric constant relations. A small temperature coefficient is obtained for keratin causing a slight reduction in rigidity. Nylon, however, shows a correspondingly large reduction in relative rigidity, Fig. 4 (*i.e.*, of the same order as that obtained using a solvent at constant temperature), for a temperature range identical with that used in the dielectric measurements. Bunn and Garner (10) suggest that a most prominent thermal oscillation of nylon molecules will be a rotational tendency about the chain axis, *i.e.*, rotation of the polar groups, which would naturally cause an increase in dielectric constant.

An interesting feature of the results obtained with formic acid, is that on first passing the fiber through a sorption-desorption cycle, the rigidity did not return to its initial value, and an appreciable stiffening of the fiber was observed, both for keratin and nylon. A possible explanation may be that, due to the intense swelling, a "solvent-annealing" process has taken place with a corresponding increase in crystallinity, in keeping with the results of Mathieu (11) and Spence (12) for nitrocellulose and cellulose triacetate.

3. Reduction in Rigidity and the Low Energy Adsorption Sites

According to Fig. 3, the reduction in the relative rigidity of nylon becomes less rapid well before saturation is reached, the water and formic acid relations following one another very closely in this respect. In the

case of the cotton-water system, Pierce (13) explains this feature of the rigidity relation by associating the rigidity reduction with the bound fraction of the adsorbed water, so that the rate decreases as the adsorption sites become filled. The effect is not so marked for keratin systems because the saturation effect occurs at low rigidity values. Nevertheless, a change in slope occurs at about 25% water content, at which point, according to Cassie (14), most of the available low energy sites are filled.

All the systems may be tested for this condition by obtaining an estimate of the number of available low energy sites, using a relation developed by Cassie (14) for a wool-water system. This states

$$100W = \omega B + \int_0^{\Delta V} \Delta P.\, d(\Delta V), \tag{1}$$

where W is the heat of wetting/g. of dry absorbent;
ΔP is the increase in hydrostatic pressure for an increase in volume ΔV due to swelling;
ω is the molar heat of sorption from the liquid state on to the low energy sites; and
B is the number of mols of low energy sites/100 g. of absorbent.

For water-nylon systems the required elastic and swelling relations are available (7) for the estimation of the swelling energy. In the case of formic acid the required elastic modulus—sorption relation was deduced from the corresponding water value by reducing it in the ratio of the known relative rigidities. Values of the swelling energies obtained in this way are shown in Table II.

TABLE II

Absorbate	Swelling energy cal./g. Keratin	Nylon
Water	9.0	1.0
Formic Acid	10.0	9.0

The following values for B were then obtained:

	Keratin	Nylon
Water	1.1 mols (14)	0.2 mols
Formic Acid	0.7 mols	0.3 mols

It is now possible to estimate the relative fractions of free and bound water present for a water concentration corresponding to the turning point of the rigidity relation using Cassie's (14) expression

$$(A - X)(B - X) = \beta X^2, \tag{2}$$

where A is the total number of mols of water adsorbed/100 g. of adsorbent;
X is the number of mols of bound water/100 g. of adsorbent;

and $\beta = \alpha \cdot e^{-\omega/RT}$,

where R is the gas constant/mol;

T is the absolute temperature;

α is the ratio of the partition functions for water in the bound and liquid states (14).

The following values for A and X are obtained:

	A	X
Keratin	1.4 mols	0.94 mols
Nylon	0.35 mols	0.2 mols

These results show that the adsorption sites as determined by the energy relations are nearly full when the initial rapid reduction in rigidity begins to fall away. One would expect a similar condition to hold for the sorption of formic acid for the corresponding turning points for keratin and nylon occur at values of A equal to 0.8 and 0.4 mols, respectively, only a little greater than the corresponding values for B.

4. Inaccessibility of Adsorption Sites

It is possible to make a direct estimate of the number of polar groups in nylon assuming the chemical formula to correspond with polyhexamethylene adipamide. For this compound there are 0.88 mols of NHCO groups/100 g., so it would seem that only a small fraction of these groups is available as low energy adsorption sites.

In this respect it is interesting to compare silk with nylon. Fig. 8

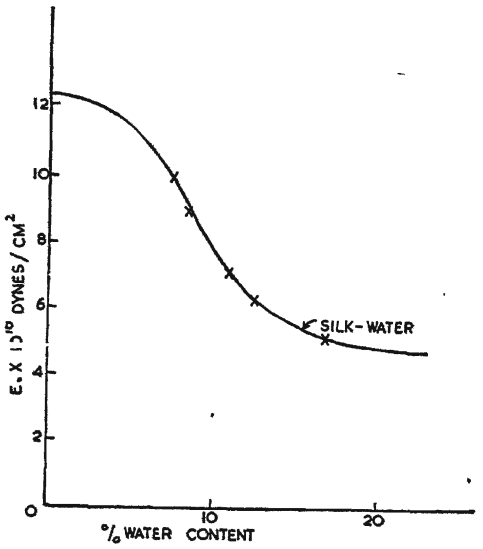

FIG. 8. Young's modulus for silk-water system.

shows the reduction in Young's modulus for silk due to the adsorption of water, as given by Denham and Lonsdale (15). It is very similar to the corresponding rigidity relation for the nylon-water system, as a saturation effect is obtained for a reduction in modulus of about 50% well before saturation is reached. Using these results, together with the corresponding swelling relations (16), and Hedges (6) data on the heats of wetting of silk, it is possible to estimate the number of available low energy sites as above, using relations (1) and (2). One then finds that, for a heat of total wetting of 1.6 Kcal./100 g., a swelling energy of 2.5 Kcal./100 g., and a molar heat of sorption on to the low energy sites of 3.6 Kcal./mol, there must be 1.1 mols of low energy sites/100 g., while at the turning point (Fig. 8), at about 18% water content, there are approximately 0.80 mols of bound water present/100 g. The number of available low energy sites per average amino acid residue turns out to be less than the number of available NHCO groups, *i.e.*, 0.77 mols assuming an average residue weight of 70 (17).

One explanation of this apparent anomaly is that the water cannot penetrate the crystalline phase of such polar polymers, and both silk and nylon can assume highly orientated forms. Rather unexpectedly it would seem that a similar theory also holds for the sorption of formic acid, in which case penetration of the crystalline fraction can only take place to any extent in the later stages of sorption (indicated by the X-ray picture of swollen silk, and the solution of nylon) and without a net evolution of heat which would otherwise become apparent during wetting.

The small number of available adsorption sites in nylon both for formic acid and water is indicated by the shape of the isotherms (Fig. 7). These are of the extreme sigmoid form showing a rapid increase in sorption as saturation vapor pressure is approached. It would seem that in both cases the greater part of the sorption is due to the existence of a mixing process, this is especially evident in the case of formic acid, where it leads to complete solution.

Acknowledgments

I am grateful to Mr. B. H. Wilsdon, Director of Research, for his continued interest in the work, to Dr. A. B. D. Cassie for discussion, and to the Council of the Wool Industries Research Association for permission to publish the results.

Summary

The effect of polar absorbates such as water and formic acid on the dielectric and elastic properties of keratin and nylon has been investigated. The results show that these are closely interlinked and depend on the ease of the rotation of polar groups in the polymer chains.

The rigidity-sorption, and heat of sorption relations support the view

that the bound fraction of the absorbate is associated with the initial reduction in elastic moduli, and that all the polar groups in these polymers are not available as low energy sorption sites.

REFERENCES

1. KING, *Trans. Faraday Soc.* **43**, 601 (1947).
2. KING, *Nature* **158**, 134 (1946).
3. ERRERA AND SACK, *Ind. Eng. Chem.* **35**, 712 (1943).
4. SPEAKMAN, *Trans. Faraday Soc.* **25**, 92 (1929).
5. KING, *ibid.* **43**, 552 (1947).
6. HEDGES, *ibid.* **22**, 178 (1926).
7. SPEAKMAN, *J. Textile Inst.* **37**, P271 (1946).
8. BAKER AND YAGER, *J. Am. Chem. Soc.* **64**, 2176 (1942).
9. BAKER AND YAGER, *ibid.* **65**, 1120 (1943).
10. BUNN AND GARNER, *Proc. Roy. Soc.* (*London*) **189A**, 39 (1947).
11. MATHIEU, *Trans. Faraday Soc.* **29**, 122 (1933).
12. SPENCE, *J. Phys. Chem.* **45**, 401 (1941).
13. PIERCE, *J. Textile Inst.* **20**, T133 (1929).
14. CASSIE, *Trans. Faraday Soc.* **41**, 450 (1945).
15. DENHAM AND LONSDALE, *ibid.* **29**, 305 (1933).
16. DENHAM AND DICKINSON, *ibid.* **29**, 300 (1933).
17. HOWITT, Bibliography of Silk, p. 43. Hutchinson's Sci. and Tech. Pub., 1947.

OLEOPHOBIC MONOLAYERS. II. TEMPERATURE EFFECTS AND ENERGY OF ADSORPTION [1]

W. C. Bigelow,[2] E. Glass and W. A. Zisman

From the Naval Research Laboratory, Anacostia Station, Washington, D. C.

Received July 30, 1947

A. Effect of Temperature on Films from Dilute Solutions

It was found, in the course of our earlier experiments (1), that increasing the temperature of solutions of long-chain polar compounds in non-polar solvents caused a decrease in the ability of the polar compounds to adsorb on solid surfaces as oleophobic monolayers. The effect of temperature changes on oleophobic properties was conveniently studied by using a simple apparatus named a "dip cell" (Fig. 1). Satisfactory cells were made from pyrex in sizes of 5, 10 and 25 ml. total capacity, the smallest size being used for the study of rare chemicals. The temperature of the liquid was measured with a thermometer inserted into the cell through a ground glass joint so arranged that the bulb was entirely immersed in the liquid which half filled the well of the cell. A rectangular dipper of platinum foil was spot welded to the end of a long, rigid platinum wire which projected beyond the ground glass joint, thus permitting the dipper to be lowered in and out of the solution by the manipulation of the free end of the wire. The cell was heated inside an electrically controlled oven which was equipped with a window and an internal light source to facilitate observation of the condition of the dipper and with an opening in the top of the oven through which the free end of the platinum wire and the thermometer stem projected. At intervals, while the temperature of the solution was being slowly increased, the dipper was raised out of the solution to observe whether the dipper surface was repellant to the liquid. If the liquid rolled off, leaving a dry surface, it indicated that the foil was covered with an adsorbed film which was oleophobic to the solution at the temperature of observation. The dipper was lowered back into the solution and the temperature was further increased until time for the next observation. This was repeated until a critical temperature (T_W) was reached at which the dipper remained completely wetted by the solution when withdrawn from the solution.

[1] The opinions or assertions contained in this paper are the authors' and are not to be onstrued as official or reflecting the views of the Navy Department.

[2] Present address: Department of Chemistry, University of Michigan, Ann Arbor, Michigan.

Interesting results were obtained from solutions of polar materials dissolved in hexadecane and in dicyclohexyl. The solutes were the pure preparations already discussed in Part I. The hexadecane was prepared from a commercial product by stirring it for some time in contact with concentrated sulphuric acid, separating the acid and washing the oil with an aqueous solution of sodium hydroxide. The fluid was then dried and freed from adsorbable impurities by repeated percolation through adsorption columns packed with layers of alumina and silica gel. The resulting material was divided into two batches called cetane A and cetane B; these hydrocarbon fluids consisted primarily of *n*-hexadecane and melted at 17.3°C. and 17.6°C., respectively. The dicyclohexyl was an

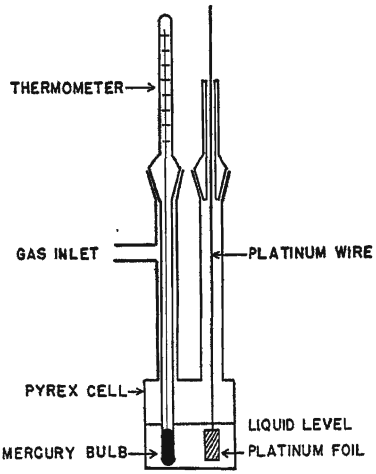

FIG. 1. "Dip cell" for observing effect of temperature on oleophobic films.

Eastman product having a melting point of 3.6°C. A drop of each liquid did not spread on the clean surface of water maintained either at pH 3 or at pH 11, indicating high purity as far as hydrophilic adsorbable impurities were concerned.

At or above a critical temperature T_W the oleophobic property of each solution always disappeared; *i.e.*, the platinum dipper was wetted permanently by the solution. It was found that T_W varied with the nature and concentration of the solute and also with the nature of the solvent. It could be reproduced with an uncertainty of less than ± 1°C. and was reversible with temperature unless decomposition, oxidation, or other chemical changes occurred in the solute or solvent, or unless precipitation of the solute upon the dipper occurred during the preparation or cooling of the system. Increasing the weight percent concentration (W) of the solute always caused T_W to increase, and the initial value of

$\partial T_W/\partial W$ was the larger for the compounds which in (1) were shown by dilution experiments to be the more adsorbable on platinum. These compounds also had the longer average lifetimes of adsorption at the oil-water interface (2). The results obtained with some pure alcohols, acids, amines and amides dissolved in cetane and dicyclohexyl are summarized in Tables I and II, respectively.

A comparison of the effect on T_W of changing W for a series of straight-chain polar compounds derived from n-octadecane is given in Fig. 2 for

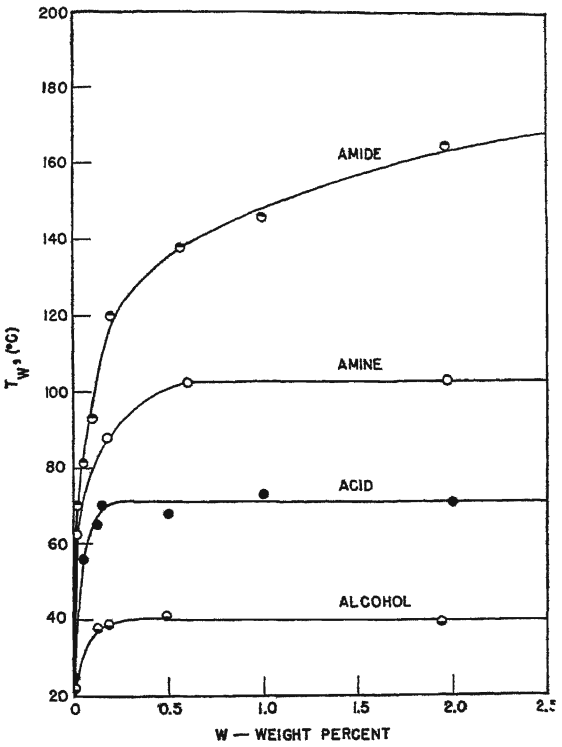

FIG. 2. Effect of concentration and polar group on 18-carbon compounds dissolved in cetane-A.

solutions in cetane A. The existence of a saturation effect is evidenced by the nearly horizontal asymptotic maximum of each of these curves. The asymptotic value of T_W is smallest for the least adsorbable compounds and greatest for the most adsorbable. This agrees with the conclusions already reached from a comparison of the relative values of the initial slopes of the T_W *vs.* W curves. It will be noted that the highly adsorbable amide still shows curvature at the relatively high concentration of 2.0%. In Fig. 3 will be found data on the effect of varying the chain length of

alcohols or acids dissolved in cetane A, while in Fig. 4 is the effect for homologous primary amines in dicyclohexyl. Evidently, the longer the chain length (or the smaller the solubility in the solvent) the greater is the initial value of $\partial T_W/\partial W$ and the higher the horizontal asymptotic value of T_W. In Fig. 5 are the results for octadecyl alcohol and stearic acid dissolved in dicyclohexyl and in cetane A. Evidently the observed differences arise from the fact that these compounds are less soluble in the dicyclohexyl than in the cetane A and hence adsorb from the former more

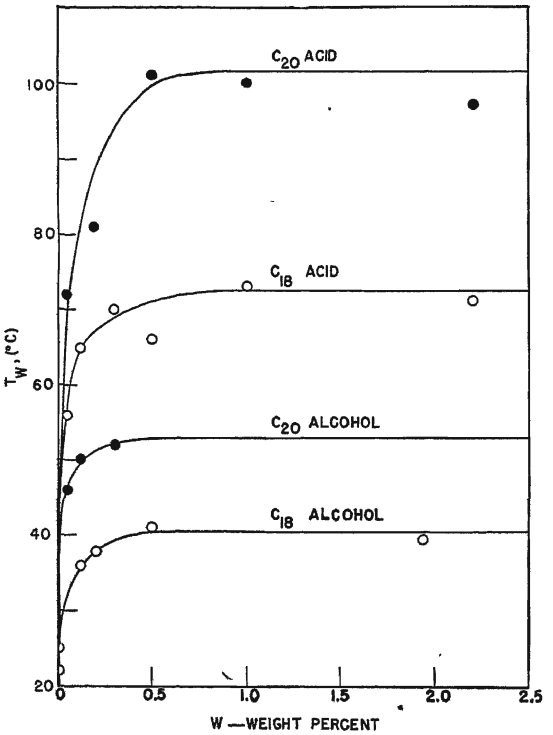

FIG. 3. Effect of chain length of acids and alcohols dissolved in cetane-A.

readily. This is seen on comparing the results for octadecyl alcohol. The alcohol adsorbs more readily from the dicyclohexyl since the initial rapid increase of T_W with W is greater in that solvent and the curve attains its maximum value at a temperature 60°C. higher. The same qualitative results and the same 60° difference in the maxima are found on comparing the results for the C_{18} acid in the same two solvents. Similarly, the horizontal asymptote for C_{18} amine in cetane A occurs at a temperature of 103°C. while in dicyclohexyl it occurs at 160° (compare item 9 of Table I with item 7 of Table II).

B. Theoretical Development

An evident interpretation of the wetting of the oleophobic film at the temperature T_W is that it is caused by the desorption of some of the polar molecules and the resulting formation of holes in the film. The increased thermal agitation of the hydrocarbon chains of the adsorbed molecules with rise in temperature will act to nullify the cohesive forces between the adjacent molecules, while the polar groups adhering to the surface of the metal will also vibrate and try to leave the surface. Both thermal phenom-

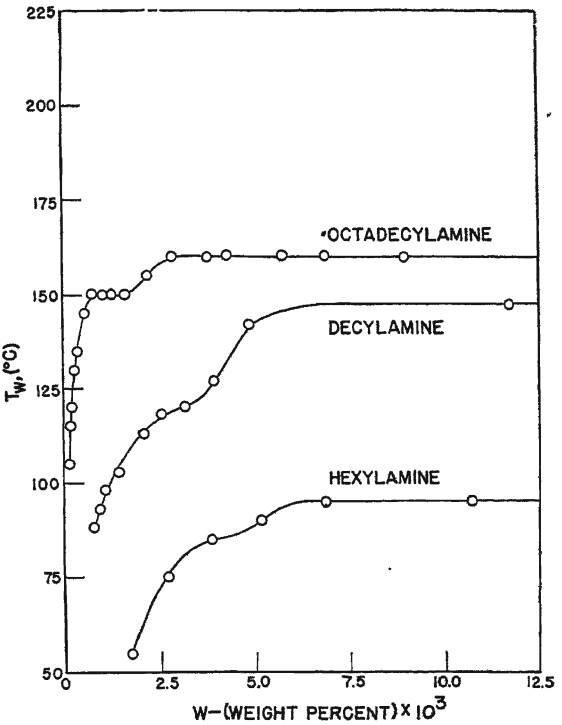

Fig. 4. Effect of chain length of amines dissolved in dicyclohexyl.

ena will act together to cause an increase in the rate of desorption of the molecules. When the factors causing desorption become dominant, the adsorbed film at dynamic equilibrium will not be packed closely enough to prevent the liquid from penetrating the film and wetting will result.

Increasing the concentration of the polar molecules increases the probability of adsorption from solution and makes the equilibrium monolayer more closely packed, Hence, wetting will not occur unless the temperature (T) is increased sufficiently to overcome the effect of the increase in molal concentration (C).

It is possible to express these ideas in a quantitative form by using the generalized Boltzmann relation of classical statistical mechanics. If the concentrations at thermal equilibrium of the molecules in two regions or states A and S having *a priori* probabilities P_A and P_S are n_A and n_S, and if the change in the potential energy per mole in going from state A to state S is U, then

$$n_A/n_S = P_A/P_S \exp(U/RT), \qquad \text{(i)}$$

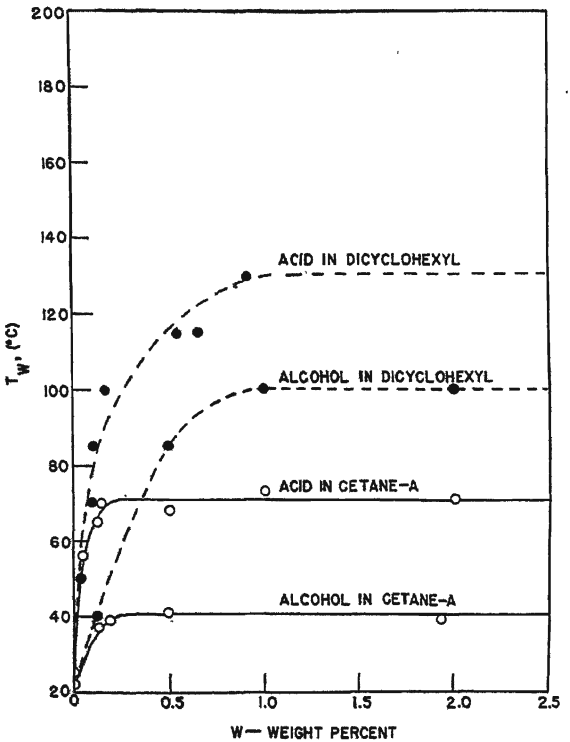

FIG. 5. Comparison of 18-carbon acid and alcohol dissolved in two solvents.

where R is the gas constant/gram mole or 1.986 cal./°C./mole. State A is selected to be that of adsorption of the solute molecules as a monolayer on the surface of the platinum foil, while state S is that of uniform distribution of the adsorbable molecues in the solution in adsorption equilibrium with the surface. The number of moles of adsorbed solute molecules per unit area (n_A) can be written $n_A = r\nu$ where r approaches unity, as the adsorbed monolayer approaches the condition of closest packing, ν obviously representing the number of adsorbed molecules in a closest packed film, and evidently $n_S = C$. Now P_A and P_S are the probabilities that the polar molecules are adsorbed or in solution, respectively, a ı

U is evidently the energy required to remove a mole of the adsorbed film to a condition of uniform distribution in the solution. Relation (i) can now be written

$$r\nu = C\left(\frac{P_A}{P_S}\right)\exp.\ (U/RT). \tag{ii}$$

This is true whatever the precise mechanism involved in the adsorption and desorption equilibrium. Now P_A and P_S concern the probability of being adsorbed or in solution, respectively, due to all mechanisms other than those involving the thermal movement of the molecules over the potential barrier U. It should be a reasonably good first approximation to assume that

$$P_A = \alpha p\ (1 - r), \tag{iii}$$

where p is the osmotic pressure of the solute and α is a constant of the materials of the system. If there are strong mutual forces between adsorbed molecules this may not be correct, especially when r approaches unity. If the solution is dilute

$$p = CRT. \tag{iv}$$

It is also assumed that the desorption of molecules merely involves the development by a sufficient number of molecules of kinetic energy in excess of the barrier value (*i.e.*, solvent reactions with the adsorbed molecules are neglected). Hence,

$$P_S = K\,C, \tag{v}$$

where K is assumed independent of the temperature. Applying relations (iii), (iv) and (v) to (ii) there results:

$$(r/1 - r)\,\nu = \frac{\alpha CRT}{K}\exp.\ (U/RT). \tag{vi}$$

At constant temperature relation (vi) becomes the familiar adsorption isotherm.

The experimental results in Part I indicate that films are oleophobic only when r is equal to or greater than some constant f which is itself not much less than unity; that is, wetting occurs only when r is less than f.

In order to keep the film oleophobic as the temperature is raised, it is necessary to increase the probability of adsorption from solution by increasing C so that the following relation holds:

$$C = (f/1 - f)K/\alpha R\cdot\exp.\ (-U/RT). \tag{vii}$$

Assuming f like α and K is constant (or is nearly so), relation (vii) is to a good approximation equivalent to

$$C = A\ \exp.\ (-U/RT). \tag{viii}$$

TABLE I

Effect of Concentration of Cetane Solution on Temperature of Wetting

Solute	M.Pt.	Cetane type	Conc. W	Temperature of wetting T_W		$\frac{1}{°K} \times 10^3$	Heat of adsorption	Figure
	°C.		*Per cent by wt.*	°C.	°K,		*cal./g. mole*	
1.								
n-Hexacosanol	79–80	A	0.093	50	323	3.10	*	
			0.506	52	325	3.08		
			1.08	56	329	3.04		
			1.90	56	329	3.04		
			2.31	51	324	3.09		
2.								
n-Eicosanol	64–5	A	0.044	25	298	3.35	*	3
			0.054	46	319	3.13		
			0.125	50	323	3.10		
			0.300	52	325	3.08		
			0.728	60	333	3.00		
			1.32	67	340	2.94		
3.								
n-Octadecanol	55.5	A	0.129	37	310	3.23	*	2, 3 & 5
			0.188	39	312	3.21		
			0.485	41	314	3.18		
			1.94	39.5	312.5	3.20		
			30.8	78	351	2.85		
4.								
n-Octadecanol (purified)	58.0	A	0.132	46	319	3.14	10,700	9
			0.247	48	321	3.12	to	
			0.271	57	330	3.03	11,200	
			0.387	57	330	3.03		
			0.585	64	337	2.96		
			0.813	83	356	2.81		
			0.990	68	341	2.93		
			1.24	80	353	2.83		
5.								
n-Hexacosanoic acid		A	0.050	63	336	2.98	*	
			0.100	71	344	2.91		
			0.498	78	351	2.85		
			1.00	75	348	2.87		
			2.00	75	348	2.87		
			3.01	83	356	2.81		
6.								
n-Eicosanoic acid	74.35	A	0.049	72	345	2.90	*	3
			0.100	81	354	2.82		
			0.50	101	374	2.67		
			1.00	100	373	2.68		
			2.00	97	370	2.70		
			3.10	104	377	2.65		

* Early runs. Too much scatter for good determination of U.

TABLE I (*Continued*)

Solute	M.Pt.	Cetane type	Conc. W	Temperature of wetting T_W		$\frac{1}{°K} \times 10^3$	Heat of adsorption	Figure
	°C.		*Per cent by wt.*	°C.	°K.		*cal./g. mole*	
7.								
n-Eicosanoic acid	74.35	A	0.0016	29	302	3.13	10,100	
			0.00194	32	305	3.28		
			0.00375	45	318	3.18		
			0.00599	60	333	3.00		
			0.00756	64	337	2.97		
			0.0102	68	341	2.94		
			0.0124	74	347	2.88		
			0.0253	73	346	2.89		
8.								
n-Octadecanoic acid	69.8	A	0.0001	25	298	3.35	*	2, 3 & 5
			0.05	56	329	3.04		
			0.126	65	338	2.96		
			0.299	70	343	2.92		
			0.500	68	341	2.93		
			1.00	73	346	2.89		
			2.01	71	344	2.91		
			3.00	73	346	2.89		
9.								
n-Octadecylamine bicarbonate	80	A	0.00005	25	298	3.35	12,400	2
			0.020	62.5	315.5	3.17		
			0.1836	88	361	2.77		
			0.497	103	376	2.66		
			1.97	103	376	2.66		
			2.07	104	377	2.65		
10.								
n-Octadecylamine bicarbonate	80	B	0.00082	65	338	2.96	14,200	6 C
			0.0024	80	353	2.83		
			0.0039	90	363	2.76		
			0.0055	97	370	2.70		
			0.0117	113	386	2.59		
			0.0234	111	384	2.60		
			0.0504	111	384	2.60		
			0.0775	112	385	2.59		
			0.130	113	386	2.59		
			0.252	110	383	2.61		
			1.3	115	388	2.58		
			6.2	130	403	2.48		
11.								
n-Octadecylamide	108–109	A	0.020	70	343	2.92	14,300	2 & 8
			0.050	81	354	2.82		
			0.100	93	366	2.73		
			0.200	120	393	2.54		
			0.463	138	411	2.43		
			0.987	146	419	2.39		
			1.97	165	438	2.28		
			3.08	171	444	2.25		

Several other derivations of (vii) can be made and each leads to the same exponential function of temperature multiplied by a weaker function of T such as T, $T^{\frac{1}{2}}$ or $1/T$. As in the classic studies of Richardson, Dushman and Langmuir on the effect of temperature on thermionic emission and on the evaporation rates of liquids, all these relations will lead to identical values of U over a considerable range of temperatures. From this theoretical argument it is evident that C should be an exponential function of T at low concentrations.

C. Energy of Adsorption

From (viii) the more convenient relation (ix) is derived:

$$2.30 \log_{10} C = \text{Const.} - 1/T\ (U/R). \qquad \text{(ix)}$$

Thus a plot of log C against $1/T$ should result in a straight line whose slope, multiplied by 4.57, equals the energy of adsorption U in calories/gram mole. The same value of U results if log W is used instead of log C. In the 4th column of Tables I and II are given the temperatures of wetting in degrees Kelvin, while in the 5th column are the reciprocals of those values. The data of the second and fifth columns were graphed on semilogarithmic paper, and a straight line relation was found. Generally, only small deviations from the straight line resulted. From the slope of this line and relation (ix) the value of U given in the 6th column was calculated.

Fig. 6 gives the results for octadecylamine in dicyclohexyl and in cetane B. Equally good linear graphs having practically the same slopes but different limiting or asymptotic temperatures were obtained using these solvents. Nearly as good straight lines were also obtained with the acids (see Fig. 7) and with the amide (see Fig. 8). The results with the alcohols (see Fig. 9) were more erratic due to the much lower temperature at which the T_W *vs.* W curve attains its asymptotic maximum value. The same difficulty became increasingly evident in going to all lower molecular weight solutes. Thus, the curve for decylamine (Fig. 4) approached a maximum T_W value nearly 25°C. less than that of octadecylamine, while the maximum for hexylamine was 50°C. lower. In agreement with the theory advanced in section B the lower concentration region of the T_W *vs.* W curve was exponential. At the higher concentrations, T_W increased much more rapidly with W, so that even in a logarithmic plot the higher concentration region of each curve was practically a vertical line (see Figs. 6, 7, 9). The observed temperatures of wetting and the calculated energies of adsorption were the more reproducible the greater the care exercised in handling the platinum foil dippers. It was found advisable not to flame the foil oftener, longer or hotter than necessary because a physical change in the surface structure of the platinum foil

TABLE II

Effect of Concentration of Dicyclohexyl Solution on Temperature of Wetting

Solute	M.Pt.	Special atmosphere	Conc. W	Temperature of wetting T_W		$\frac{1}{T_K} \times 10^3$	Heat of adsorption	Figure
	°C.		*Per cent by wt.*	°C.	°K.		*cal./g.-mole*	
1.								
n-Octadecanol	55.5		0.115	40	313	3.19	8,600	5 & 9
			0.500	85	358	2.79		
			1.00	100	373	2.68		
			2.00	100	373	2.68		
			2.99	100	373	2.68		
			4.02	105	382	2.62		
2.								
n-Octadecanol	58.0		0.112	34	307	3.26	10,000	9
			0.157	33	306	3.27		
			0.360	55	328	3.05		
			0.383	56	329	3.04		
			0.602	72	345	2.90		
			0.895	77	350	2.86		
			3.14	110	383	2.61		
3.								
n-Eicosanoic acid	74.35		0.010	67	340	2.94	12,700	7
			0.020	75	348	2.87		
			0.040	89	362	2.76		
			0.080	118	391	2.56		
			0.16	119	392	2.55		
			0.49	118	391	2.56		
			1.0	117	390	2.57		
			1.9	118	391	2.56		
			2.0	134	407	2.46		
4.								
n-Octadecanoic acid			0.0413	50	323	3.10	10,000	5 & 7
			0.15	80	353	2.83		
			0.176	100	373	2.68		
			0.553	115	388	2.58		
			0.915	130	403	2.48		
5.								
n-Dodecanoic acid	43.8		0.0416	26	299	3.34	2,800	7
			0.102	99	372	2.69		
			0.114	110–115	383–388	2.67–2.58		
			0.559	120	393	2.54		
			1.47	127	400	2.50		
			2.61	127	400	2.50		
6.								
pri-*n*-Octadecylamine	51.5–52.5	Helium & CO_2-free air	0.000380	135	408	2.45	14,800	6 B
			0.000622	145	418	2.39		
			0.000860	150	423	2.36		

TABLE II (*Continued*)

Solute	M.Pt.	Special atmosphere	Conc. W	Temperature of wetting T_W		$\frac{1}{°K} \times 10^3$	Heat of adsorption	Figure
	°C.		*Per cent by wt.*	°C.	°K.		*cal./g.-mole*	
			0.00132	150	423	2.36		
			0.00191	150	423	2.36		
			0.00291	150	423	2.36		
			0.00389	150	423	2.36		
			0.00553	150	423	2.36		
			0.00833	150	423	2.36		
7. *n*-Octadecylamine bicarbonate	80		0.0000372	90	363	2.75	14,800	4,6 A
			0.0000656	100	373	2.68		
			0.000101	105	378	2.65		
			0.000131	115	388	2.58		
			0.000177	120	393	2.54		
			0.000280	130	403	2.48		
			0.000350	135	408	2.45		
			0.000358	135	408	2.45		
			0.000550	145	418	2.39		
			0.000750	150	423	2.36		
			0.00102	150	423	2.36		
			0.00126	150	423	2.36		
			0.00162	150	423	2.36		
			0.00218	155	428	2.34		
			0.00281	160	433	2.31		
			0.00374	160	433	2.31		
			0.00427	160	433	2.31		
			0.00572	160	433	2.31		
			0.00685	160	433	2.31		
			0.00898	160	433	2.31		
8. *n*-Decylamine bicarbonate			0.000770	88	361	2.77	11,500	4
			0.000965	93	366	2.73		
			0.00108	98	371	2.69		
			0.00144	103	376	2.66		
			0.00208	113	386	2.59		
			0.00252	118	391	2.56		
			0.00316	120	393	2.54		
			0.00391	127	400	2.50		
			0.00485	142	415	2.41		
			0.117	147	420	2.38		
9. *n*-Hexylamine bicarbonate			0.00172	55	328	3.05	6,400	4
			0.00269	75	348	2.88		
			0.00341	90	363	2.75		
			0.00382	85	358	2.79		
			0.00511	90	363	2.75		
			0.00689	95	368	2.71		
			0.0107	95	368	2.71		

TABLE II (*Continued*)

Solute	M.Pt.	Special atmosphere	Conc. W	Temperature of wetting T_W		$\frac{1}{°K} \times 10^3$	Heat of adsorption	Figure
	°C.		*Per cent by wt.*	°C.	°K.		*cal./g.-mole*	
10. *n*-Octadecylamide			0.000480	100	373	2.68	13,100	
			0.000995	110	383	2.61		
			0.00172	120	393	2.54		
			0.00199	125	398	2.51		
			0.00236	130	403	2.48		
			0.00251	130	403	2.48		
			0.00355	135	408	2.45		
			0.00364	135	408	2.45		
			0.00381	135	408	2.45		
			0.00442	135	408	2.45		
			0.00580	135	408	2.45		

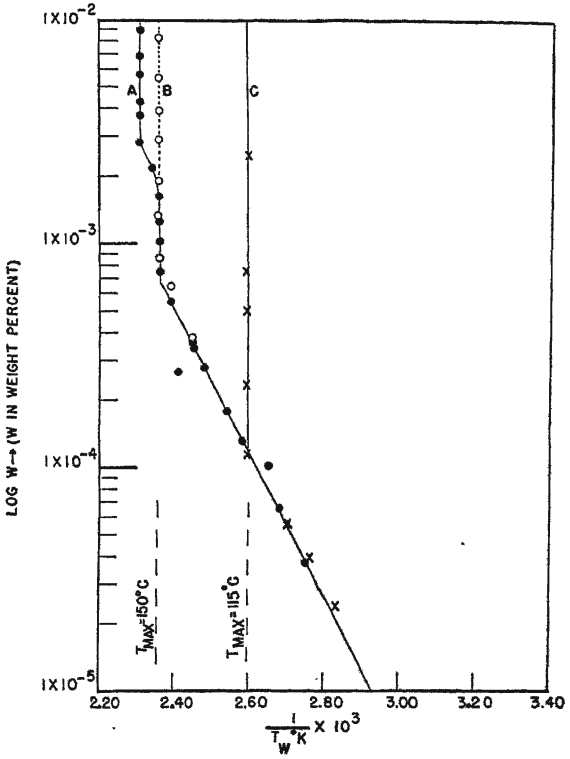

FIG. 6. Adsorption of octadecylamine from solutions in dicyclohexyl: ● Curve A, bicarbonate in atmosphere; ○ Curve B, amine in CO_2-free air; × Curve C, bicarbonate in atmosphere using cetane B.

developed gradually as the result of such treatment. This was evidenced by the appearance of a dull gray color in the foil which microscopic examination showed was associated with the formation of a network of fine cracks. The occurrence of this greying was unpredictable, the results varying with the sample of foil, the source, and the heat treatment. Variations in U and T_W were found to occur as this physical change de-

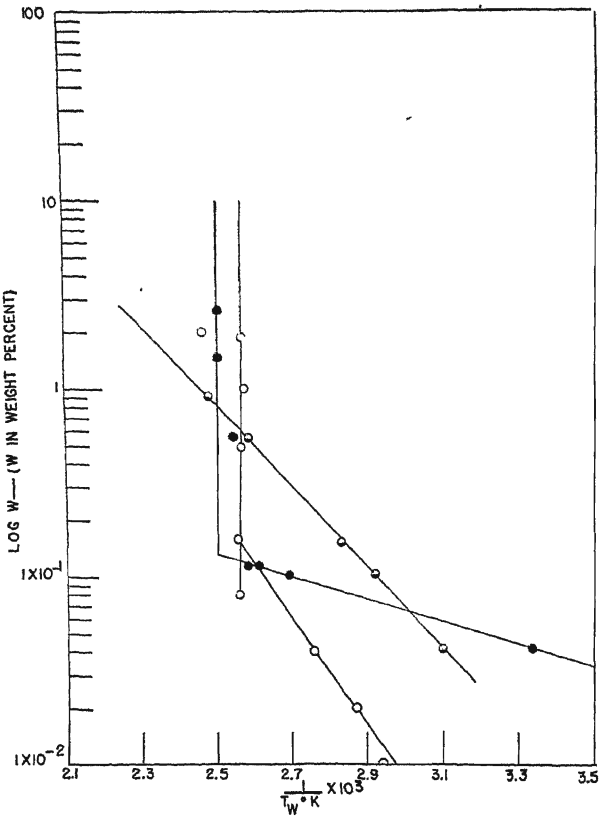

FIG. 7. Effect of chain length of acids dissolved in dicyclohexyl. ● Lauric Acid (C_{12}); ◒ Stearic Acid (C_{18}); ○ Arachidic Acid (C_{20}).

veloped. This difficulty was avoided by using new pieces of foil from the same production batch and by avoiding the use of any single piece of foil to obtain too many measurements of T_W. However, these variations are peculiarities of commercial platinum foil and of the changes in surface structure with use.

In experimenting with the amines it was noted that the vertical rise of the log W *vs.* $1/T$ curve contained an abrupt but reproducible bend or

displacement of 10°C. (see curve A of Fig. 6). It was finally discovered that an impurity in the octadecylamine was the cause. The melting point of the amine used was around 80°C. and the reported value in Beilstein is 53°C. As the formation of an amine bicarbonate by reaction of the amine with CO_2 in the moist air was likely, some of the compound was heated for 30 minutes in a vacuum just above its melting point and, after the evolved CO_2 had been pumped off, the sample was cooled in CO_2-free air. The melting point was then 51.5–52.5°C. indicating good purity. While

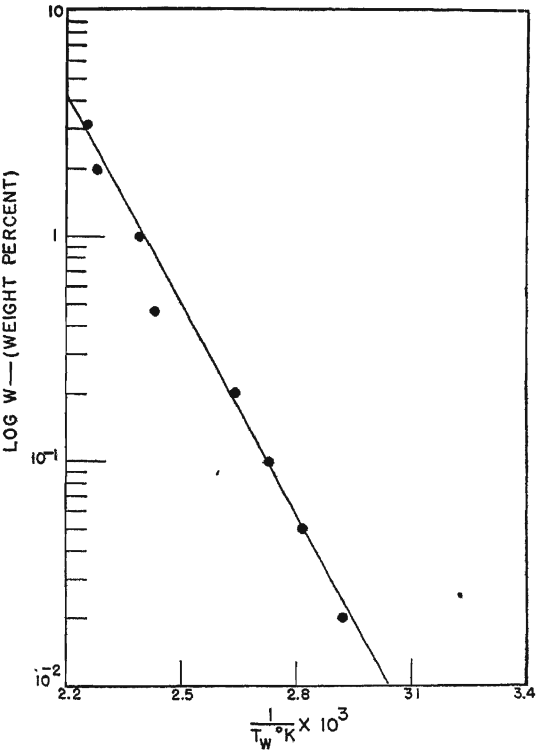

FIG. 8. Adsorption of octadecylamide dissolved in cetane A.

in CO_2-free air this amine was transferred to the dicyclohexyl and measurements of T_W were made. The resulting curve (see Curve B of Fig. 6) was identical with that obtained before the heat treatment and degassing except that the abrupt bend was absent. Hence U was the same for the amine and the amine bicarbonate and the presence of bicarbonate merely increased by 10°C. the maximum value of T_W attainable. A similar displacement of 25°C. was encountered in the experiments with decylamine in dicyclohexyl, and even the less detailed hexylamine curve showed evidence for a 10°C. displacement (see Fig. 4).

A comparison has been made in Table III of the values of U taken from Tables I and II. It will be noted that the value of U for films on platinum is, to a first approximation, independent of the solvent. Thus, the best value for octadecylamine in cetane is 14,200 cal./mole while in dicyclohexyl it is 14,800. Similarly, the adsorption energy of octadecyl amide is 14,300 in the former solvent and 13,100 in the latter. There is

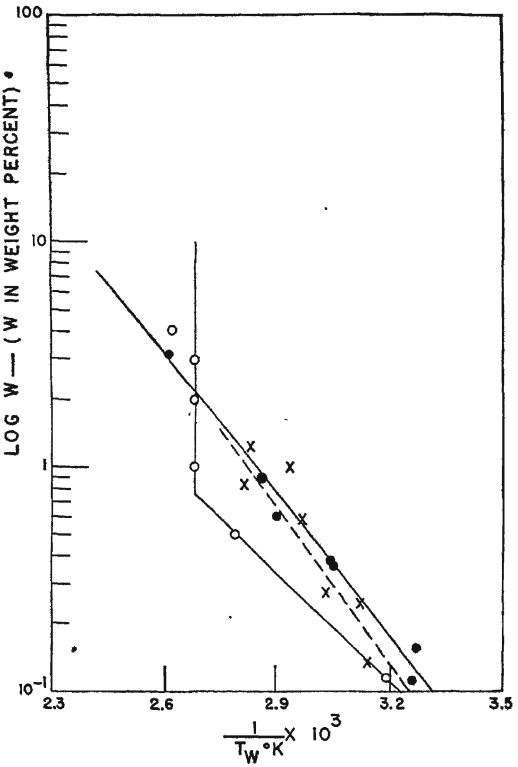

FIG. 9. Adsorption of octadecyl alcohol from solutions in dicyclohexyl;—○— alcohol m. pt. 55.5°C.; —●— alcohol purified 58.0°C.; - - x- - alcohol purified 58.0°C. and in cetane.

evidently some decrease in U with the number of carbon atoms per molecule, since with dicyclohexyl the values of U obtained are 14,800 cal./mole for the octadecylamine, 11,500 for the decylamine, and around 6,400 for the hexylamine. This indicates a rate of decrease for long-chain compounds of approximately 400 cal./mole per carbon atom. From the values of 12,700 obtained for eicosanoic acid, 10,000 for stearic acid, and 2,800 for lauric acid in dicyclohexyl, there appears to be a linear decrease in energy per carbon atom of approximately 1,200 cal./mole (see Fig. 11).

On comparing the results for the group of C_{18} compounds in the same solvent, dicyclohexyl, the values of U are 14,800 cal./mole for the amine, 13,100 for the amide, 10,000 for the acid and between 8,600 and 10,000 for the alcohol.

The work of Smyth and Rogers on the dimerization of carboxylic acids in nonpolar solvents is well known (4) and it might be inferred that it is the dimer molecule which adsorbs on the platinum foil in these experi-

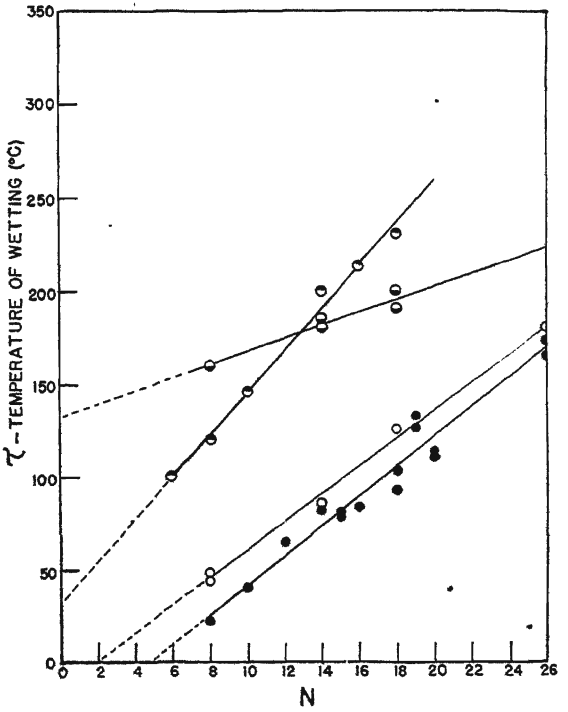

FIG. 10. Temperature of wetting τ of oleophobic films from molten pure compounds.

● Acids ⊖ Amines
○ Alcohols ⊖ Amides

ments; in fact, Frewing (5) concluded from his study of the stick-slip phenomena for oil solutions of the fatty acids that the acids adsorbed on steel as dimers. But in our earlier work on oleophobic films (1) it was concluded that the adsorbed molecules were vertically oriented monomers which were nearly close packed. The later electron diffraction studies by Brockway and Karle (3) have demonstrated the essential correctness of those conclusions. If only dimer molecules were adsorbed, it is difficult to understand how the observed orientation of monomers could have occurred. It is much more likely that in the dilute solutions used in these

experiments the acid molecules were present as both monomers and dimers and the adsorption equilibrium observed was between the monomers in solution and those attached to the adsorbing surface. Hence, U is believed to be the energy of adsorption of the monomeric acid. For the same reason it is believed that the value of U obtained for each of the other polar solutes discussed here is the adsorption energy of the unassociated molecule.

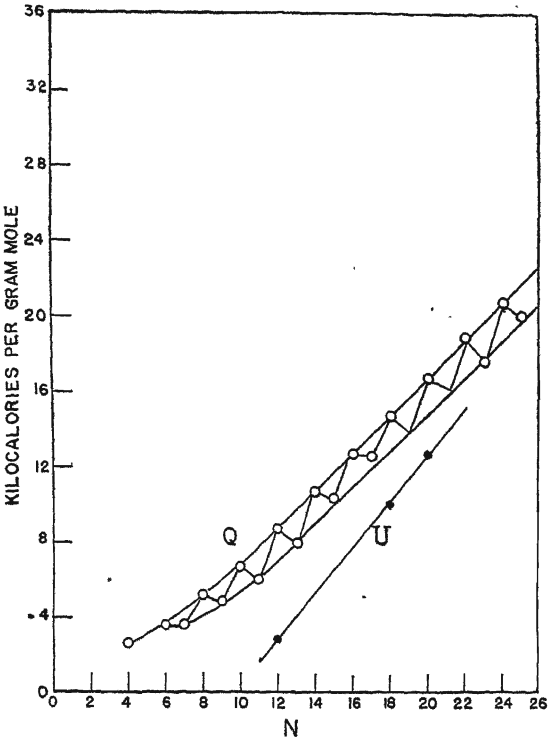

FIG. 11. Energy of adsorption and heat of crystallization of acids. Note: Q from data of Garner, King *et al.*; U from solutions in dicyclohexyl.

The more recent dielectric constant studies of Le Fevre and Vine (6) and of Pohl, Hobbs and Gross (7) on solutions of carboxylic acids in nonpolar solvents have shown that equilibrium mixtures of monomers and dimers must exist, the proportion of monomers increasing with the dilution. The results of the latter showed that at a molal concentration of 10^{-3} almost half of the solute molecules were monomers. It is to be expected that the proportion of monomers to dimers will also increase with the temperature, and a statistical treatment having that result has been given by Rushbrooke (8). These dielectric studies lend support to

TABLE III

Comparison of Melting Points, T_{max}, U and τ for Solutes Studied

Compound	M.Pt.	Approximate T_{max}[a]		U in cal./g.-mole		τ Pure, molten
		in cetane	in dicyclohexyl	in cetane	in dicyclohexyl	
	°C.	°C.	°C.			°C.
C_{26} Alcohol	79–80	56				180
C_{20} Alcohol	64–65	67				
C_{18} Alcohol	55.5	41	105		8,600	125
	58.0	80	110	10,700–11,200	10,000	
C_{26} Acid		80				165,175
C_{20} Acid	74.4	101	120		12,700	110,113
		75		10,100		
C_{18} Acid	69.8	73	130		10,000	92,103
C_{12} Acid	43.8		127		2,800	65
C_{18} Amine	51.5–52.5		150		14,800	
C_{18} Amine·HCO_3	80	105,115	165	12,400–14,200	14,800	230
C_{10} Amine·HCO_3			147		11,500	145
C_6 Amine·HCO_3			95		6,400	100
C_{18} Amide	108–109	>170	135	14,300	13,100	190,200

[a] T_{max} = Approximate asymptotic value of T_W *vs.* W curve from measurements on dilute solutions.

our conclusion that under the conditions of our adsorption experiments enough monomers were present to have been responsible for the adsorbed films observed.

D. Apparent Saturation Effects in Dilute Solutions

As an aid to interpreting the phenomenon at high concentrations (as in Fig. 3), the asymptotic maximum values of the T_W *vs.* W curves (denoted here as T_{max}) have been compared with the melting points of the solutes. For a given solute T_{max} bears an inverse relationship to the solubility. Although T_{max} may be smaller, equal to, or larger than the melting point of the solute when dissolved in cetane, it is always larger than the melting point when dissolved in dicyclohexyl. For a series of polar compounds of the same chain length, the values of T_{max} in a given solvent increase with the energy of adsorption U.

Several possible explanations for this asymptotic behavior can be suggested: (1) The adsorbed monolayer may become liquid due to increased thermal agitation at the temperature T_{max}; (2) Although the solubility of the solute rises with temperature, it is not a significant factor

until micelle formation begins at temperature T_{max}. Thereafter, increasing the concentration cannot increase the probability of adsorption and there results a constant value of T_W; (3) Although the solubility increases with temperature, it does not increase rapidly enough, and the observed T_W *vs.* W curve is merely the effect of increased thermal agitation causing desorption. However, at a high enough temperature, T_{max}, solubility effects become so important that the increased probability of adsorption due to a rise in concentration is compensated by the increased rate of desorption due to the effect of temperature on the solubility.

Theory (1) is not acceptable since it does not provide an explanation for the observed large differences in T_{max} with solvent nor does it account for the persistence of oleophobic behavior at and above the same T_{max} when the concentration of the solution is greatly increased. Explanations (2) and (3) are both consistent with the theoretical treatment advanced in section B in which it was postulated that solvent effects were unimportant in the low concentration region. They are also consistent with the observed marked increase of T_{max} in going to a poorer solvent. The nearly vertical rise in the log W *vs.* $1/T_W$ graphs of Figs. 6, 7 and 9 is also understandable if a rapid increase in the solvent action occurs at the temperature T_{max}.

E. Adsorbed Films from Molten Polar Compounds

A small pyrex dip cell permitting manipulation with from 1 to 2 ml. of solution was used to study the formation of oleophobic films on platinum from a melt of each of the pure polar solutes described in sections A through D. The temperature at which the film commenced to be wetted by the molten liquid is denoted as τ. In such experiments it was found absolutely essential to use polar compounds of high purity. In many instances a small percentage impurity which had caused a melting point change of a few degrees caused changes in τ of 10°–60°C. The values of τ obtained are given in Table IV and are graphed in Fig. 10 as a function of the number (N) of carbon atoms per molecule. The result is a series of straight lines which (except for the amides) tend to converge close to O°K. Where compounds gave graphic points which deviated greatly from the straight line, they were found to be less pure and subsequent careful purification always resulted in a good fit leaving no doubt of the essential correctness of the linear relationship between τ and N. It is noteworthy that the graph for the alcohols lies between that for the acids and that for the amines.

Oleophobic films on platinum could always be prepared from those melted polar compounds which had been found to adsorb as oleophobic films from solutions in nonpolar solvents. But these films could not be prepared from such pure liquid compounds as oleic acid, oleyl alcohol,

stearolic acid and linoleic acid. After oleophobic films have been formed from the melted polar compounds, the contact angles with drops of hexadecane and water were observed at 25°C. Typical results were as follows:

	Against cetane	Against water
Octadecyl Acid.....	27°	80°
Octadecyl Alcohol..... ..	30°	84°
Octadecyl Amide..... ..	27–30°	88°
Octadecyl Amine.....	31–35°	88°
Decyl Amine.....	30°	high, but drops rapidly

These angles are of the same magnitude as those reported in Part I, Sections (d) and (g), for oleophobic films formed from dilute solutions. The results of Table IV qualify the earlier statement in Section (d) of Part I that

TABLE IV

Effect of Chain Length on Temperature of Wetting τ (°C.) of Films Adsorbed from Molten Pure Normal Aliphatic Compounds

Number of carbon atoms	Acids	Alcohols	Amines	Amides
4				
6			100	
8	22	44,48	120	160
10	40		145	
12	65			
14	82	85	200	180,185
15	78,80			
16	83		215	
18	92,103	125	230	190,200
19	123,125			
20	110,113			
26	165,175	180		

oleophobic films on platinum could not be prepared from solutions of amines, acids and alcohols having values of N less than 8 for the first two series and less than 10 for the third. If the pure melted solute is used, the lowest homologues giving oleophobic films are hexylamine, octanoic acid and octyl alcohol. It was not possible to prepare films from pure butylamine, even at low temperatures.

To facilitate comparison, the pertinent values of τ from Fig. 10 have been inserted in the last column of Table III. It will be seen that τ is sometimes approximately equal to the largest value of T_{max} found from the studies of dilute solutions, but more often it is larger; for the long-chain compounds τ is much greater than T_{max}. It appears that only when a poor solvent is used does T_{max} approach the value of τ. The larger values

of τ are understandable, for the liquid polar compound is then in equilibrium with the adsorbed monolayers. Whenever an adsorbed molecule is released by the surface it is replaced rapidly by a like molecule. Here it is difficult to understand how wetting can occur unless: (a) a temperature is reached at which the liquid compound begins to wet the close-packed adsorbed film of like molecules; (b) a temperature is reached at which the probability of desorption or "evaporation" from the surface becomes so great that an oriented film becomes very improbable. The most plausible interpretation is that given in (b).

The preceding conclusion leads to an interesting calculation based on the hypothesis that condition (b) occurs when the probability of desorption due to thermal effects becomes sufficiently large. The probability of desorption is assumed as in Section B to be proportional to Exp $(-U/RT)$; this is equivalent to the requirement that U/RT shall be small. Hence, at temperature τ it is assumed that

$$\frac{U}{R\tau} \leqq b^2, \tag{x}$$

where b^2 is not large. Since our earlier experimental results (1) and later electron diffraction measurements (3) have shown these adsorbed films are monomolecular and closely packed, it is reasonable to assume that the molar energy of adsorption U should consist of a term U_o due to attraction of the polar group for the adsorbing surface and a term U_c due to the cohesive forces between adjacent methylene groups of the hydrocarbon chains. If the number of carbon atoms (N) per molecule is large enough, and if the polar groups aren't so large as to prevent close enough approach of the methylene group, then $U_c = Nu$, where u is the energy of cohesion per methylene group. Hence,

$$U = U_o + Nu. \tag{xi}$$

The condition (x) for wetting of the film from the melted oleophobic polar compound can now be written

$$\frac{U_o + Nu}{R\tau} \leqq b^2 \tag{xii}$$

or

$$\tau \geqq \frac{U_o}{b^2R} + N\frac{u}{b^2R}. \tag{xiii}$$

Relation (xiii) predicts a straight line relation between τ and N with a positive slope just as was found in Fig. 10. Evidently from (xiii) the constant u can be computed from

$$u = b^2R\frac{\partial\tau}{\partial N}. \tag{xiv}$$

The observed values of $\frac{\partial \tau}{\partial N}$ from Fig. 10 were inserted in (xiv) and values were found for u/b^2. The best values of U given in Table III for the C_{18} compounds were inserted in relation (x) as were the corresponding values of τ of Table IV. The resulting calculated values for b^2 were then applied to the above values of u/b^2 to calculate u. When these values of U, u and N were inserted in relation (xii) U_o could be computed. In Table V are listed U, τ, b^2, u and U_o for the four types of compounds

TABLE V

Summary of Calculated Data on Cohesional and Polar Energies of Adsorption

Type compound	U	τ	b^2 from x	u from xiv	U_o from xi	u from xvii
	cal./mole	°K.		*cal./mole*	*cal./mole*	*cal./mole*
C_{18} Alcohol	10,000	393	12.8	188	6,600	
C_{18} Acid	10,000	378	13.3	212	6,200	1,200
C_{18} Amine	14,500	508	14.4	336	8,400	400
C_{18} Amide	13,700	468	14.7	103	11,900	

studied. It is noteworthy that the four calculated values of b^2 vary less than 15%.

F. Relation of U to Heat of Crystallization

From Table III the energy of adsorption (U) increases with the number of carbon atoms (N). A linear relation of U and N could be expected for large values of N from relation (xi) provided the polar group is not too large. In Fig. 11 the results for acids have been graphed and do lie on a straight line. Turning to the condition of aliphatic acids when in the 3-dimensional crystal state, it is known that the molecules cohere in plane layers due to the weak forces between adjacent aliphatic chains and the layers adhere in pairs by hydrogen bonding between the carboxyl groups. If Q_p is the molal energy of the crystal due to the hydrogen bonding (or to dimerization), Q_c the molal energy of the cohesional forces between the adjacent chains in the same layer, and Q_{me} the molal energy due to end-to-end cohesion occurring in alternate layers between the methyl terminal groups of the acid molecules, then the total molal energy of crystallization Q is

$$Q = Q_p + Q_{me} + Q_c. \qquad \text{(xv)}$$

If N is large and the polar group does not prevent close packing, then it is reasonable to assume that $Q_c = Nq$, where q is the cohesional energy per methylene group. Hence,

$$Q = (Q_p + Q_{me}) + Nq. \qquad \text{(xvi)}$$

On recalling the earlier similar relation (xi) between U and Nu, an evident and reasonable approximation is that $q = u$. This need not be exactly true, since the unit of the crystal of acid is the dimer and when it melts little dissociation occurs, while the unit of the adsorbed film is the monomer. Hence conditions of packing are not identical. The error in the energy by making the approximation $q = u$ becomes smaller as N increases. Differentiation of (xi) and (xvi) then gives the result that if N is large:

$$\left(\frac{\partial U}{\partial N}\right)_{N \text{ large}} = \left(\frac{\partial Q}{\partial N}\right)_{N \text{ large}}. \qquad \text{(xvii)}$$

Garner and his coworkers have published accurate data on the molal heats of crystallization of the fatty acids (15, 16, 17, 18); their results have been plotted in Fig. 11 also. It will be noted that U is always less than Q but at large values of N both graphs have become straight lines which should meet at values of N of approximately 30. This is a check on relations (xvi) and (xvii). From Fig. 11 it is found that $q = 1000$ cal./mole of methylene groups for the series of even numbered acids, while U is 1200 cal./mole of methylene groups. These values have been inserted in Table V for comparison with those computed from relation (xiv). The value of $\frac{\partial U}{\partial N}$ for amines for large N computed from the data of Table III is 400 cal./mole of methylene groups, and this value has been added to the last column of Table V. The agreement of the two values of u is good in this case.

G. Discussion

From the theoretical interpretation given the T_W *vs.* W curve, the values of $T_{\max}$, τ, U and U_o would be expected to vary with the nature of the adsorbing surface, τ and U being higher when the polar group is able to react with the atoms of the adsorbing surface. An interesting calculation can be made using the values of U_o listed in Table V in conjunction with dipole moment data to obtain approximate values for the distance between the center of the dipole and the surface of the metal on which the polar material is adsorbed. A simple treatment for the interaction of a rigid dipole with a conducting and polarizable surface can be made by assuming that the only forces involved are those of attraction between the dipole and its mirror image, as was done by Lorenz and Landé (19, 20) using the formula

$$U_o = \frac{\mu^2}{4r^3}(6.06 \times 10^{23}),$$

where μ, r and 6.06×10^{23} are the dipole moment, the distance of the midpoint of the dipole to the surface and Avogadro's number, respect-

ively. Maximum possible distances of 1.2 A for the alcohols and 0.9 A for the amines were obtained where the dipoles were assumed to be normal to the surface. A more plausible approach in the case of the alcohols oriented with their long hydrocarbon axes normal to the surface is made by assuming that the dipole is not codirectional with the molecular axis. A deviation of up to 65° from normal can be calculated using the tetrahedral carbon angle and 105° for the C—O—H angle together with the moments associated with the O—C and O—H bonds. The resulting smaller normal component of the moment leads to the shorter calculated distance of 0.7 A for the alcohols. Measurements on ball models showed that the midpoint of the dipole lies between 1.1 and 1.9 A for the alcohol and 1.1 and 1.6 A for the amines. The agreement is as good as can be expected from the simple assumptions made.

The results of similar experiments with adsorbing materials other than platinum will be presented in Part III. These methods and results appear to be of value in the study of adsorption from solution and of adsorbed monolayers. Some of the conclusions obtained here are also closely related to basic phenomena involved in the wear-preventive action of mild boundary lubricants as well as to the rust-inhibitive property imparted to oils by aliphatic polar additives. A theoretical discussion and the results of experiments on the latter will soon be presented elsewhere. The connection with the early studies of wear-prevention is obvious, for many of the polar compounds described here were among those most carefully investigated by Sir William Hardy in his classic experiments on the static coefficient of friction of lubricated surfaces (9). An authoritative review of the subject of boundary lubrication has recently been given by Bowden and Tabor (10).

We have demonstrated the existence of an adsorption equilibrium between the polar molecules adsorbed by the metal and dissolved in the oil, and of the rapid decrease at higher temperatures in the number of adsorbed molecules per unit area. Although the temperature of wetting, (T_W) increases considerably with the concentration of additive used, in present day practice polar additives are rarely used in excess of a few per cent by weight. Therefore, the temperature of wetting to be expected from such a range of concentrations of additives in hexadecane will be around the apparent asymptotic values (T_{max}) indicated earlier. These values are from 40°–100°C. for the alcohols, 70°–130°C. for the acids, 100°–150°C. for the amines, and 140°–170°C. or more for the amides. Of course, these temperature ranges will vary if solvents other than cetane or dicyclohexyl are used; they may also vary considerably where a chemical reaction with the adsorbing metal takes place. However, the relative order of these values is, in all likelihood, the relative order of the chemical activity of these compounds when adsorbed from any of the petroleum oils used in

practice. The aliphatic amines are not particularly stable in contact with iron or steel above 60°C., and the metals used in practice would eventually react at temperatures above 100°C. with the additives discussed here with the exception of the alcohols. Hence, it appears unlikely that additives will be found which will remain adsorbed from oil solutions at high temperatures but which will not react chemically with the usual bearing metals. When boundary lubricants are employed it is desired that the load-carrying capacity be improved over the entire range of operating temperatures. Temperatures of from 50° to 100°C. in bearings and up to 150–200°C in internal combustion engine cylinders can be expected. The preceding conclusions make it evident that improvements in boundary lubrication manifested in tests with lubricants and bearings or engines at ordinary temperatures can be expected to be lost at the higher operating temperatures unless it is permissible to use wear-preventive additives capable of chemically reacting to some extent with the metals in contact with the oil. It would also appear that the more unreactive the bearing metal used, the lower the load-carrying capacity which can be imparted to it by an oil containing a boundary lubricant. This suggests that bearings made of unreactive metals like gold and platinum will be unsatisfactory for reasons other than the high cost of the metal.

In the past seven years Tabor (11), Hughes and Whittingham (12), Frewing (13) and Bowden, Gregory and Tabor (14) have used the Bowden "stick-slip" apparatus for numerous boundary friction and lubrication studies of the effect of temperature on pure compounds such as aliphatic hydrocarbons, acids, alcohols, esters and soaps. A transition from smooth sliding to "stick-slip" occurred at or above a temperature (T_S) which was characteristic of the metals, the polar compound, and the concentration. They concluded that the transition effect was due to the disorientation or desorption of the polar molecules above a critical value which depended upon the nature of the metal surface, the chain length, and the active end group of the polar compound.

Frewing (5) studied the value of T_S for mild steel on steel with solutions in white mineral oil and found that the concentration of solute was an exponential function of the temperature for each solute studied. By assuming that (1) desorption occurred at higher temperatures, (2) "stick-slip" occurred when the film density dropped below a critical value, and (3) the Van't Hoff isochore could be applied to the adsorption equilibrium constant, he derived a relation equivalent to our relation (viii). This was applied to a large number of careful measurements of T_S as a function of W, and from these he was able to calculate U for a series of aliphatic compounds. At present, a good comparison of our results with Frewing's (5) is difficult since our observations relate to platinum surfaces with dicyclohexyl or cetane as the solvent while his

concerned mild steel and solutions in a white mineral oil. The effects of temperature on solubility are involved in our observation of T_W, but in observations of T_S the shearing stress caused by the motion of the slides may be important in determining the temperature of the film transition observed.

Despite these differences, Frewing's work and ours agree in that the concentration and reciprocal of the absolute temperature involved in the transition have an accurate linear relation; however, the almost vertical rise in log W at temperature T_{max} was not encountered by Frewing. Another interesting difference is the much larger solute concentrations needed by Frewing to observe the change in T_S with concentration: for example, his data on stearic acid involved concentrations in white oil varying from 0.1% to almost 3% while ours involved concentrations in cetane or in dicyclohexyl of from 0.01% to 0.5%. These differences may be partly due to a greater solubility of the acid in the white mineral oil and to the need in Frewing's work for closer packing of the adsorbed molecules in order to prevent metal-to-metal contact and subsequent stick-slip. Frewing's values of U for capric, myristic, and stearic acids were 12.5, 13.0 and 13.0 Kcal./mole while for α-bromostearic, α-iodostearic, and α-hydroxystearic acid they were 10.0, 10.0 and 13.5 Kcal./mole. Our values for stearic and arachidic acids of 10.0 and 12.7 are in as good agreement as could be expected, considering these differences in metals and methods.

It is not theoretically necessary that our temperature of wetting (T_W) and the stick-slip transition temperature (T_S) should be equal even when identical concentration of solute and the same metals are used. It appears from a comparison of our work with that of Bowden, Gregory and Tabor (15) that it is essential to have closer packing in an adsorbed monolayer to prevent stick-slip than to prevent wetting. Therefore, with a given concentration (W) of solute, a film which will just give an oleophobic effect will already be giving stick-slip. Hence, the stick-slip effect will have occurred at a lower temperature, *i.e.*, $T_S < T_W$. Since a shearing stress on the adsorbed films causes the stick-slip transition, it is possible for the film to collapse under the action of the slider when it would still be oleophobic. It may not always be necessary to desorb molecules of the film to get stick-slip. All that is needed is sufficient loss in shear strength through softening or reorientation of the film; hence, it is again evident that $T_S < T_W$.

As a practical matter, it is very unlikely that films of these compounds adsorbed from solution in oils will be any more closely packed than those discussed here. Films on metals made by melting the pure polar compound or by using concentrations in oils of from 5 to 50% of solute will be the exception rather than the rule. Hence, the adsorption effects reported

here should be typical of those to be encountered in working with the usual ranges of solutions in oils of these classes of polar additives. It is evidently essential to obtain more information on how the adsorptivity of oleophobic films varies with the nature of the adsorbing material.

Since the molal energy of adsorption (U) for long chain compounds has been shown here to contain an appreciable contribution from the energy of cohesion between hydrocarbon chains ($U_c = Nu$), it is evident that any branched chain molecules having the same polar groups will have lower values of U and will be even less adsorptive. Therefore, their ability to resist the desorptive effect of increased temperature and, hence, their usefulness as wear-preventives will be even more limited.

Acknowledgments

The authors wish to acknowledge their obligation to Mr. D. L. Pickett for assistance in the early measurements of T_W wetting temperatures and to Mr. N. L. Smith of this laboratory for purifying a number of the acids and alcohols used.

Summary

Experimental methods are described for observing the effect of temperature on oleophobic films adsorbed from solution. It was found that a critical temperature (T_W) existed above which the oleophobic property disappeared. The concentration of the solute (W) was found to be proportional to e^{-U/RT_W} where T_W is in degrees Kelvin. The temperature effects are reported for a number of homologous acids, amines, amides and alcohols dissolved in either cetane or dicyclohexyl.

A quantitative kinetic treatment of the observed effects in terms of adsorption-desorption equilibria is given, and this is shown to lead to the observed relation of T_W, W and U where U is the energy of adsorption. The relation of U to the nature of the polar group, the aliphatic chain length (N) and the solvent are discussed. The observed values of U are shown to be in good agreement with those reported for acids from data on the effect of temperature on the stick-slip boundary friction transition.

In the pure molten state these aliphatic compounds (from values of $N = 6$–8 to $N = 26$) were found to deposit monolayers on platinum which were also oleophobic. This happened at all temperatures above the melting point until a critical temperature τ was reached. An accurately linear relation between τ and N was found for each homologous series provided very pure compounds were used.

The relation of U to the heat of crystallization (Q) and to the chain length (N) are discussed, and it is concluded that U, like Q, may consist largely of the energy of cohesion due to van der Waals' forces between adjacent methylene groups of the hydrocarbon chains. Estimates are given of the adhesional energy between polar groups and the platinum foil. Calculations based on dipole moment data show that the adhesional

energy consists largely of the electrical interaction between the polar group and the metal surface.

The relation of these observations and conclusions to fundamental aspects of adsorption from solution, corrosion-inhibition and wear-prevention are discussed.

References

1. Bigelow, W. C., Pickett, D. L., and Zisman, W. A., *J. Colloid Sci.* **1**, 513 (1946).
2. Zisman, W. A., *J. Chem. Phys.* **9**, 534, 729, 789 (1941).
3. Brockway, L. O., and Karle, J., *J. Colloid Sci.* **2**, 277 (1947).
4. Smyth, C. P., and Rogers, H. E., *J. Am. Chem. Soc.* **52**, 1824 (1930).
5. Frewing, J. J., *Proc. Roy. Soc.* (*London*) **183A**, 270 (1944).
6. Le Fevre, R. J. W., and Vine, H., *J. Chem. Soc.* **1938**, 1795.
7. Pohl, H. A., Hobbs, M. E., and Gross, P. M., *Ann. N. Y. Acad. Sci.* **40**, No. 5, 389 (1940).
8. Rushbrooke, G. S., *Proc. Cambridge Phil. Soc.* **39**, 202 (1943).
9. Hardy, Sir Wm. B., Collected Papers. Cambridge Univ. Press, 1936.
10. Bowden, F. P., and Tabor, D., *Ann. Repts. Progress Chem.* (*Chem. Soc. London*) **42**, 20 (1945).
11. Tabor, D., *Nature* **147**, 609 (1941).
12. Hughes, T. P., and Whittingham, G., *Trans. Faraday Soc.* **38**, 9 (1942).
13. Frewing, J. J., *Proc. Roy. Soc.* (*London*) **181A**, 23 (1942).
14. Bowden, F. P., Gregory, J. N., and Tabor, D., *Nature* **156**, 97 (1945).
15. Garner, W. E., Madden, F. C., and Rushbrooke, J. E., *J. Chem. Soc.* **1926**, 2491.
16. Garner, W. E., and Rushbrooke, J. E., *ibid.* **1927**, 1351.
17. Garner, W. E., and King, A. M., *ibid.* **1929**, 1849.
18. Garner, W. E., and King, A. M., *ibid.* **1931**, 578.
19. Loren., R., and Landé, A., *Z. anorg. Chem.* **125**, 47 (1922).
20. Brunauer, S., Adsorption of Gases and Vapors, I. Princeton Univ. Press, 1943.

A NEW SUGGESTION FOR A MODEL REPRESENTING THE STRUCTURE OF CARBON BLACK

Hideo Akamatu and Kazuo Nagamatsu

From the Chemical Institute, Faculty of Science, Imperial University of Tokyo
Received May 14, 1947

Introduction

Since the first X-ray diffraction pattern from carbon was obtained by Debye and Scherrer (1), it has been believed that "amorphous" carbon is also made up of minute crystals of graphite. Some investigators, however, have reported that it is not sufficient to consider carbon merely as made up of minute crystals of graphite differing only in size from macrocrystalline graphite. To account for the relatively few lines which appear in powder photographs of "amorphous" carbons (2), it has been inferred that, when the crystallites are very small, their hexagonal layer planes are parallel to each other, but are not otherwise arranged in any definite manner with respect to each other. Considering intensity distribution of interference, U. Hofmann (3) has shown that the pattern may be ascribed to the diffraction by cross-gratings of the hexagonal plane itself. Germer and White (4) have also arrived at the same conclusion from their results on the cathode-ray analyses made on their specimens, prepared by the pyrolysis of methane.

Conclusions from these investigations are as follows. In graphite, and also "amorphous" carbon, the "molecule" is the hexagonal plane itself. In graphite, the giant molecule, *i.e.*, the hexagonal planes, are arranged so that they are parallel to each other along every crystal axis, thus producing the three-dimensional atomic lattice. In "amorphous" carbon, however, molecules are arranged in such a way that although the hexagonal planes are also paralled to each other, still along the *a*- or *b*-axis, they are not arranged in any definite manner. Consequently, the perfect three-dimensional atomic lattice is not produced.

This state of aggregation may be considered as a pseudo-crystal, or better, as a kind of macromolecular lattice such as is well known in the case of mixed polymers consisting of linear molecules (paraffin or some artificial resins). This analogy will be useful in understanding the structure of carbon black. A verification for this analogy will be described in this paper.

If we consider a hexagonal plane as a "molecule" of carbon, then we

can find some analogous substances among the well known organic compounds, and may also expect some common characteristics for the state of aggregation between them.

We have chosen violanthrone, isoviolanthrone and pyranthrone, and considered them as a kind of model for the elementary carbon. There are, of course, some discrepancies between these compounds and carbon. The chemical composition is, in the case of violanthrone for example, C:89.5%, H:3.5%, O:7.0%. Nevertheless, an amount of hydrogen or oxygen of this order can also be found in some types of charcoals. The hexagonal planes of these molecules may be too small to compare to those of carbon, but in many cases, the mean linear dimensions of the crystals of carbons are of the order of 20 Å or less. Hence, it is not absurd to consider these compounds as a kind of model for the molecule of carbon black.

The specimens which we could obtain were the commercial dyestuffs, *i.e.*, "Indanthrene Dark Blue B.O." as violanthrone, "Indanthrene Violet R. extra" as isoviolanthrone and "Indanthrene Gold Orange G." as pyranthrone.

We have obtained X-ray diffraction patterns from these dyestuffs, which had first been washed with dilute HCl for purification. They consist of 2 or 3 diffuse rings (*cf.* Fig. 1, Plate 5), of which spacings have been estimated from photometer curves as 3.46 Å and 2.17 Å for Indanthrene Dark Blue and 3.48 Å, 2.14 Å and 1.8 Å for Indanthrene Violet. In the X-ray powder photograph of carbon, as is well known, the pattern consists of 3 or 4 diffuse rings, the spacings of which are those shown in the last column of Table II, and they correspond to the lattice planes of graphite as (002), (100), (004) and (110), respectively. The values for spacings are not definite in carbons, but fluctuate according to variations of the specimens. It can be said that the patterns of these dyestuffs closely resemble that of carbon. The pattern obtained from Indanthrene Gold Orange differs, consisting of several sharp lines.

It has become clear, however, that the specimens used for this experiment still contain many impurities. Pure specimens were prepared from the dyestuffs by the following methods. The dyestuff was dissolved in concentrated sulfuric acid, and then, after filtration, the filtrate was poured into a large amount of water. The precipitate obtained was again dissolved in a basic sodium hydrosulfite solution. After filtration, the specimen was reprecipitated by driving air into the filtrate. The precipitate was washed with hot caustic soda solution, glacial acetic acid and chlorobenzene successively. Finally, by sublimation under reduced pressure at about 400°C., the pure specimens were obtained as needles. It is difficult, however, to obtain large crystals which can be used for determination of crystal structure. As a consequence, we have not yet been

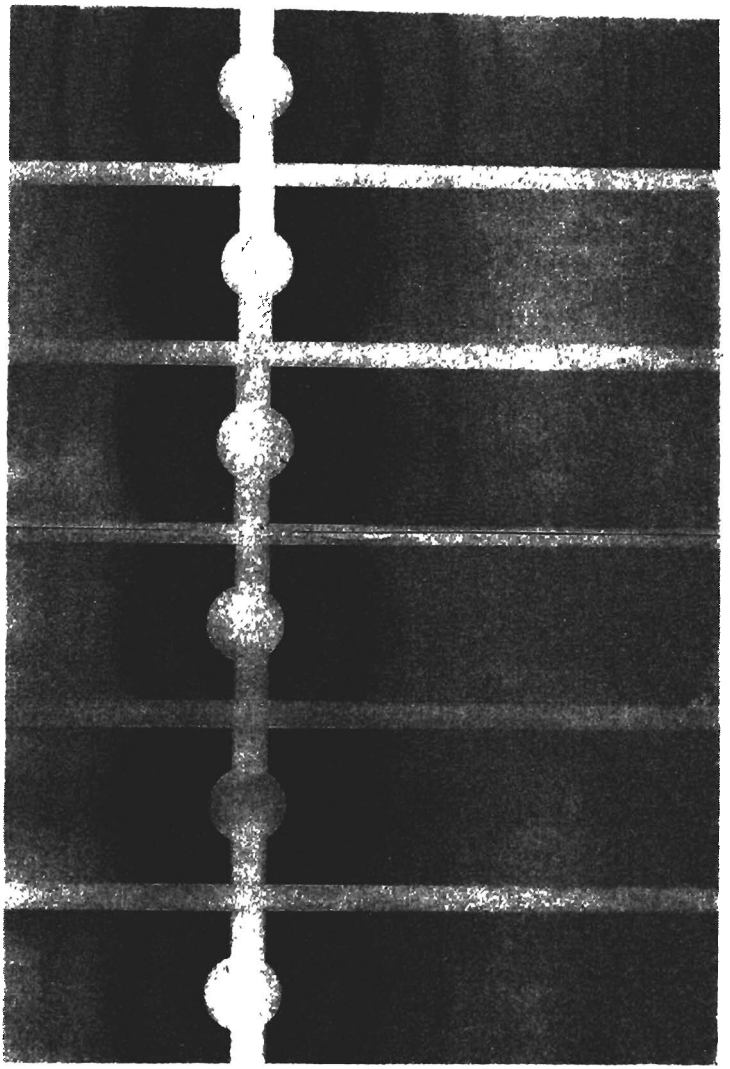

FIG. 1

able to determine the crystal structure, but the patterns of powder photographs are those given in Table I. (*Cf.* Fig. 1, Plate 6.)

The patterns of violanthrone and isoviolanthrone almost coincide with each other, while that for pyranthrone is different. They are, of course, different from the patterns for carbon or graphite.

The question then arises as to why the diffraction patterns obtained for impure specimens resemble that of carbon. To resolve this question is,

TABLE I

X-ray Data for Violanthrone, Isoviolanthrone and Pyranthrone. Values of Spacings
(X-ray: Cu Kα Ni-filtered)

Violanthrone		Isoviolanthrone		Pyranthrone	
7.55 Å	ff	7.58 Å	ff	7.07 Å	mf
6.23	p	5.87	p	4.90	f
5.14	f	4.78	f	4.35	pp
4.23	mf	4.15	mf	3.87	p
3.73	mf	3.76	mf	3.52	ff
3.40	mf	3.42	mf	2.73	mp
3.05	f	3.05	f	2.21	mp
2.72	p	2.82	p	1.97	p
2.53	mp	2.54	mp	1.80	p
2.33	mp	2.31	mp	1.67	p
2.10	f	2.10	f	1.50	p
1.97	p				
1.88	p	1.88	p		
1.79	p	1.78	p		
1.69	pp	1.69	pp		
1.60	pp	1.60	pp		
1.49	pp				
1.22	pp				
1.19	pp				
1.08	pp				

at the same time, to get some suggestion about the state of aggregation of carbon. This problem has been resolved in the following manner.

We took the same amount of pure violanthrone and isoviolanthrone and dissolved them together in concentrated sulfuric acid. After stirring the solution thoroughly, it was poured into a large amount of water. The specimen was reprecipitated in the same way. In this treatment, no essential change occurs in the molecules of the compounds themselves, the only change to be presumed being that the state of aggregation of the molecules will be disturbed by mixing different kinds of molecules. The diffraction pattern obtained from this "conglomerate," or the mixed aggregate, is somewhat different from the original patterns of the individual components. Some of sharp lines have disappeared and many of them are diffused. From the photometer curve, however, lines can still be distinguished as shown in Table II. It may be seen that there are some disturbances in the molecular lattice, but it does not differ greatly from the pattern of the component, which may be ascribed to the fact that the molecular structures of these two compounds resemble each other so closely.

If, however, we take the same amount of pyranthrone and isoviolanthrone, and make a mixed aggregate by the treatment mentioned above,

the diffraction pattern from this mixed aggregate begins to resemble the carbon pattern.

Finally, the diffraction pattern from the mixed aggregate of the three components, *i.e.*, violanthrone, isoviolanthrone and pyranthrone, which was made in the same manner, resembles that of carbon so closely that we can hardly distinguish it from the carbon pattern. It consists of three diffused rings of which spacings are estimated from the photometer curve as 3.54 Å, 2.13 Å and 1.78 Å, respectively. Their first ring is extremely strong and the other two are weak in intensity. The whole appearance resembles the pattern of carbon very closely (*cf.* Fig. 1, Plate 4). It is worthy of note that this carbon-like pattern has been obtained from substances unrelated to graphite.

TABLE II

X-ray Data for the Mixed Aggregate, Compared with Carbon. Values of Spacings

(X-ray: Cu Kα Ni-filtered)

Violanthrone and isoviolanthrone	Pyranthrone and isoviolanthrone	Violanthrone, isoviolanthrone and Pyranthrone	Carbon
7.55 Å ff	7.66 Å f		
6.12 p dif.	3.46 ff dif.	3.54 Å ff dif.	3.4–3.8 Å ff dif.
3.83 mf dif.	2.09 p dif.	2.13 p dif.	ca. 2.1 f dif.
3.39 ff dif.	1.71 p dif.	1.78 p dif.	ca. 1.8 p dif.
3.07 mf			ca. 1.2 pp dif.
2.59 p			
2.11 f dif.			
1.77 p dif.			

The state of the mixed aggregate obtained here can be compared to an "alloy" consisting of a molecular lattice, or a pseudo-crystal made up of several kinds of paraffin, for instance. When paraffin consists of a single kind of molecule, a true molecular lattice will be produced. If, however, it contains several kinds of molecules, differing in their degree of polymerization, then it will form a pseudo-crystal, or better, a macromolecular lattice rather than a perfect lattice. In this state, paraffin molecules are arranged so that molecular axes are parallel to each other, but are not otherwise arranged in any definite manner with respect to each other. This is the case of a two-dimensional molecule as a hexagonal plane, instead of a linear one, where molecules are supposed to be arranged so that the molecular planes are parallel to each other, but are not otherwise arranged in any definite manner. It can be assumed that the spacing for 3.54 Å corresponds to the distance between molecular planes which are parallel to each other, and the value of 1.78 Å is its second order interference. The value of 2.13 Å can be referred to diffraction by cross-gratings

of hexagonal planes, and from this value the distance between carbon atoms in the hexagonal plane can be calculated as 1.42 Å. The fact that (110) interference does not appear in such patterns may be ascribed to the fact that hexagonal planes are too small to give (11) interference by cross-gratings. In practice, (110) interference also cannot be recognized for some kinds of charcoals.

One must consider here that carbon blacks which are made by the process of carbonization would contain various kinds of hexagonal planes, differing in the degree of polymerization. This analogy between pseudo-crystals of such substances and carbon will be useful in interpreting the structure of carbon, especially when one reflects that the number of measurable parameters in an X-ray photograph of carbon is so limited that, on the basis of such a pattern alone, no deduction as to the structure of carbon can be confidently made.

Summary

We have shown that if we consider a hexagonal plane of carbon atoms as a molecule of black carbon, then we can find analogous molecules among the well-known organic compounds. We have assumed such compounds as violanthrone, isoviolanthrone or pyranthrone, as models for a molecule of elementary carbon. The state of aggregation of these compounds were investigated by the X-ray diffraction method. It has been found that the X-ray diffraction pattern of the mixed aggregate consisting of violanthrone, isoviolanthrone and pyranthrone, resembles the pattern of carbon black very closely. This state of aggregation may be considered as a type of a macromolecular lattice. From this analogy, without reference to graphite, it has been inferred that "amorphous" carbon is also made up of pseudo-crystals, or better, a macromolecular lattice of hexagonal plane molecules.

References

1. Debye, P., and Scherrer, P., *Physik. Z.* **18**, 291 (1917).
2. Berl, E., Andress, K., Reinhardt, L., and Herbert, W., *Z. physik. Chem.* **158A**, 273 (1931).
3. Hofmann, U., and Wilm, D., *Z. Elektrochem.* **42**, 504 (1936).
4. White, A. H., and Germer, H., *J. Chem. Phys.* **9**, 492 (1941).

BOOK REVIEWS

Colloids—Their Properties and Applications. By A. G. WARD, M.A., Formerly Scholar of Trinity College, Cambridge. 6 plates, 133 pages. Blackie's "Technique" Series. Interscience Publishers, Inc., New York, 1946. Price $1.75.

"This little book attempts to give a simple account of the physics and chemistry of colloids, with their many applications in physics, engineering, geology and biology in an elementary way." "It is designed to serve as an introduction to the subject for those meeting it for the first time."

Parts I and II deal with the nature of the colloidal state, with clear expositions of the properties of suspensoids, emulsoids, gels, emulsions, foams, dusts, smokes, and fogs as typical systems. Part III deals with industrial and biological applications. Here the topics are rubber, cellulose, proteins, clays, paints, detergency, and living matter.

Although the treatment is completely non-mathematical, the book is compactly and clearly written, and well illustrated. No unwarranted or exaggerated claims are made, the presentation is up-to-date and free from errors. The book can be heartily recommended to the group of readers to which it is addressed, while more advanced readers will find brief remarks about recent discoveries which may have escaped their attention.

VICTOR K. LAMER,
New York, N. Y.

Physical Methods of Organic Chemistry, Vol. I and II. Editor: ARNOLD WEISSBERGER. 1367 pages in two volumes (1945 and 1946). Interscience Publishers, Inc., New York. Price $9.50 each.

Although these two volumes were written primarily for the organic chemist to enable him to use physics advantageously as a tool in solving problems of structure and chemical mechanism, nevertheless, chemists of varied interest and training will find the subject matter interestingly written, authoritative and highly profitable reading. Modern colloid chemists, in particular, will find almost all of the chapters of immediate value.

When the list of authors and the subjects of their respective chapters are inspected, the reader recognizes at once the names of the most active and authoritative workers in the field in America. A study of their contributions indicates that they have produced a work comparable with their well-deserved reputations for accomplishment.

In some chapters, a discussion of theory was unnecessary, in some a relatively brief theoretical treatment sufficed, and in other chapters, a rather complete exposition of the theory appeared necessary. The book abounds in good illustrations of apparatus, expositions of principles and pertinent tables of data. The index occupies 52 pages, and, like the printing and format, is well done. Editor, authors, and publishers have rendered all branches of chemistry a real service in the publication of these two volumes.

Chapters

1. E. L. Skau and H. Wakeham—Determination of Melting and Freezing Temperatures.
2. W. Swietoslawski—Determination of Boiling and Condensation Temperatures.

3. N. Bauer—Determination of Density.
4. R. D. Vold and M. J. Vold—Determination of Solubility.
5. H. Mark—Determination of Vicosity.
6. W. D. Harkins—Determination of Surface and Interfacial Tension.
7. W. D. Harkins—Determination of Properties of Monolayers and Duplex Films.
8. R. H. Wagner—Determination of Osmotic Pressure.
9. A. L. Geddes—Determination of Diffusivity.
10. J. M. Sturtevant—Calorimetry.
11. E. E. Jelley—Microscopy.
12. M. A. Peacock—Determination of Crystal Form.
13. J. D. H. Donnay—Crystallochemical Analysis.
14. I. Fankuchen—X-Ray Diffraction.
15. L. O. Brockway—Electron Diffraction.
16. N. Bauer and K. Fajans—Refractometry.
17. W. West—Spectroscopy and Spectrophotometry.
18. W. West—Colorimetry, Photometric Analysis and Fluorimetry.
19. W. Heller—Polarimetry.
20. C. P. Smyth—Determination of Dipole Moments.
21. T. Shedlovsky—Conductometry.
22. L. Michaelis—Potentiometry.
23. O. H. Muller—Polarography.
24. L. Michaelis—Determination of Magnetic Susceptibility.
25. W. F. Bale and J. F. Bonner, Jr.—Determination of Radioactivity.
26. D. W. Stewart—Mass Spectrometry.

VICTOR K. LAMER,
New York, N. Y.

Advances in Colloid Science. Vol. II. Scientific Progress in the Field of Rubber and Synthetic Elastomers. Edited by H. MARK AND G. S. WHITBY. xl + 453 pp.; 104 Figs. Interscience Publishers, Inc., New York, 1946. Price $7.00.

Like the preceding Volume I of this series, this book is a collection of independent monographs written by authors eminent in their field. In their preface the editors express the hope "that the various chapters will serve as an up-to-date representation of fact and theory and as an inspiration to the further development of the scientific knowledge of elastic polymers." The first of these aims has been achieved in a most clear and comprehensive way and as for the second one the reviewer feels that the thorough discussions of the physical aspects of the rubbery state may also be of interest for the study of the structure of the pure liquid and the pure solid state.

Following a biography on the initiator of the series, the late E. O. Kraemer, and an introduction by G. S. Whitby, there are chapters on "Second-Order Transition Effects in Rubber and Other High Polymers" by R. F. Boyer and R. S. Spencer; "Crystallization Phenomena in Natural and Synthetic Rubbers" by L. A. Wood; "The Study of Rubberlike Substances by X-Ray Diffraction Methods" by C. W. Bunn; "The Thermodynamic Study of Rubber Solutions and Gels" by G. Gee; "Significance of Viscosity Measurements on Dilute Solutions of High Polymers" by R. H. Ewart; "The Kinetic Theory of Rubber Elasticity" by E. Guth, H. M. James and H. Mark; "Vulcanization" by E. H. Farmer; "Rubber Photogels and Photovulcanizates" by H. P. Stevens; and "Reinforcing and Other Properties of Compounding Ingredients" by D. Parkinson.

From a chemical point of view the chapter by Farmer on the mechanism of vulcanization is of particular interest. As to the structure of polysulfides it may be emphasized that the existence of branched sulfur chains (with "coordinated" sulfur) is doubtful, to

say the least. Thus the pentathionate ion and other polythionic compounds of the pentathionic type contain unbranched sulfur chains, and so do the hydrogen polysulfides as recently demonstrated by Fehér.

The book can be heartily recommended not only to the rubber and colloid chemist, but also to the physical chemist in general.

OLAV FOSS, New York, N. Y.

Physical Biochemistry. By HENRY B. BULL, Associate Professor of Physiological Chemistry, Medical School of Northwestern University. 347 pp. John Wiley and Sons, Inc., New York. Price $3.75.

This volume is an outgrowth of a series of about 36 lectures given by the author in alternate years to graduate students in biochemistry, physiology, bacteriology, and neurology, and attended also by medical students.

The author has succeeded in making an appropriate selection of topics from the broad field of physical chemistry and has presented the material in the following chapters in a scientific and up-to-date manner:

I. Atoms and Molecules
II. Energetics
III. Reaction Kinetics
IV. Electrostatics and Dielectrics
V. Ions in Solution
VI. Electromotive Force Cells
VII. Acids and Bases
VIII. Oxidation-Reduction
IX. Electrical Conductance
X. Electrokinetics
XI. Surface Activity
XII. Colloidal Solutions
XIII. Viscosity and the Flow of Liquids
XIV. Diffusion
XV. The Ultracentrifuge
XVI. Osmotic Pressure
XVII. Membranes and Cell Penetration
XVIII. Colloidal Structures

Colloid scientists will be interested in the material in Chapters IX through XVIII.

VICTOR K. LAMER,
New York, N. Y.

BOOKS RECEIVED

Colloid Chemistry—Theoretical and Applied. Volume VI. By JEROME ALEXANDER, Editor. Reinhold Publishing Corporation, 330 West Forty-second St., New York, N. Y., 1946. 1182 pp. $20.00.

Introduction to Emulsions. By GEORGE M. SUTHEIM. Chemical Publishing Company, Inc., 26 Court St., Brooklyn 2, N. Y., 1946. 243 pp. $4.75.

Encyclopedia of Hydrocarbon Compounds. Volume I. By JOSEPH E. FARADAY. Chemical Publishing Company, Inc., 26 Court St., Brooklyn 2, N. Y., 1946. $15.00.

Emulsion Technology, Theoretical and Applied. A Symposium. Second edition. Chemical Publishing Company, Inc., 26 Court St., Brooklyn 2, N. Y., 1946. 360 pp. $6.50.

Modern Organic Finishes. Their Application to Industrial Products. By ROLLIN H. WAMPLER. Chemical Publishing Company, Inc., 26 Court St., Brooklyn 2, N. Y., 1946. 452 pp. $8.50.

Industrial Experimentation. By V. A. BROWNLEE. Ministry of Supply, Directorate of Royal Ordnance Factories, His Majesty's Stationery Office, London, England.

Organic Chemistry. By PAUL KARRER. Second English edition. Translated by A. J. MEE. Elsevier Publishing Company, Inc., 215 Fourth Avenue, New York 3, N. Y., 1946. 953 pp. $7.50.

Advances in Carbohydrate Chemistry. Volume II. By W. W. PIGMAN AND M. L. WOLFROM, Editors. Academic Press, Inc., 125 East Twenty-third St., New York 10, N. Y., 1946. 323 pp. $6.60.

Concise Chemical and Technical Dictionary. By. H. BENNETT, Editor. Chemical Publishing Company, Inc., 26 Court St., Brooklyn 2, N. Y., 1947. 1055 pp. $10.00.

Technological and Physical Investigations on Natural and Synthetic Rubbers. By A. J. WILDSCHUT. One of a series of monographs on the progress of research in Holland during the war. Elsevier Publishing Company, Inc., 215 Fourth Avenue, New York 3, N. Y., 1946. 173 pp. $3.00.

AUTHOR INDEX

A

AKAMATU, H., AND NAGAMATSU, K. A new suggestion for a model representing the structure of carbon black, 593

ALFREY, T. The influence of solvent composition on the specific viscosities of polymer solutions, 99

B

BAKER, W. O. Rheological properties of polymers and plastics, 115

BARNES, M. D., KENYON, A. S., ZAISER, E. M., AND LAMER, V. K. Monodispersed sulfur sols. IV. Comparison of the particle radius determined by transmittance and by the angular position of higher order tyndall spectra from the Mie theory, 349

BAXTER, S. Membrane potentials for keratin, 495

BIGELOW, W. C., GLASS, G., AND ZISMAN, W. A. Oleophobic monolayers. II. Temperature effects and energy of adsorption, 563

BIKERMAN, J. J. The fundamentals of tackiness and adhesion, 163

BLAIR, G. W. S. The role of psychophysics in rheology, 21

BRIDGMAN, P. W. The rheological properties of matter under high pressure, 7

BROCKWAY, L. O., AND KARLE, J. Electron diffraction study of oleophobic films on copper, iron and aluminum, 277

C

CRAWFORD, D. J. See Graham, R. P., 509

D

DEAN, R. B., AND McBAIN, J. W. The sorption of organic vapors by monolayers of soap, 383

DIENES, G. J. Viscoelastic properties of thermoplastics at elevated temperatures, 131

DOLIAN, F. E. See Hormats, S., 307

DOW, R. B. The rheology of lubricants, 81

DRAKE, L. C. See Plank, C. J., 399

E

EYRING, H., AND HALSEY, G. Some recent advances in non-Newtonian viscosity, 17

F

FALES, J. S. See La Mer, V. K., 539

FRANCE, W. G. See Lang, E. R., 315

FULWEILER, W. H. E. C. Bingham and the ASTM—an appreciation, 5

G

GINELL, A. M. See Ginell, R., 521

GINELL, R., GINELL, A. M., AND SPOERRI, P. E. Association phenomena. I. The growth of particles of silver chloride and the higher order Tyndall effect, 521

GLASS, G. See Bigelow, W. C., 563

GRAHAM, R. P., AND CRAWFORD, D. J. The sorption of oxalate by hydrous alumina, 509

GREEN, H. Rheological properties of paints, varnishes, lacquers, and printing inks, 93

H

HALSEY, G. See Eyring, H., 17

HATTIANGDI, G. S. See Prasad, M., 467

HERMANS, J. J. Diffusion with discontinuous boundary, 387

HOCHBERG, S. See LaMer, V. K., 539

HODGES, K. See LaMer, V. K., 539

HORMATS, S., ZEFFERT, B. M., AND DOLIAN, F. E. Heat of wetting of charcoal and its retentivity for ethyl chloride, 307

K

KARLE, J. See Brockway, L. O., 277

KATSURAI, T., AND NAKAHIRA, M. Note on a new mode of sol-gel transformation, 289

KENYON, A. S. See Barnes, M. D., 349

See La Mer, V. K., 257

KING, G. Effect of strongly hydrogen-bonded agents on some polar polymers, 551
KLEVENS, H. B. Effect of temperature on micelle formation as determined by refraction, 301
Latex particle sizes as determined by soap titration and light scattering, 365
KUBO, R. Statistical theory of rubber-like substances, 527

L

LAMBERT, J. M. Volumetric analysis of colloidal electrolytes by turbidity titration, 479
LAMER, V. K., AND BARNES, M. D. A note on the symbols and definitions involved in light scattering equations, 361
See Barnes, M. D., 349
LAMER, V. K., HOCHBERG, S., HODGES, K., WILSON, E., FALES, J. A., AND LATTA, R. Influence of particle size of homogeneous insecticidal aerosols on the mortality of mosquitos in confined atmospheres, 539
LAMER, V. K., AND KENYON, A. S. Kinetics of the formation of monodispersed sulfur sols from thiosulfate and acid, 257
See Barnes, M. D., 349
LANG, E. R., VANWINKLE, Q., AND FRANCE, W. G. Electrophoresis in an ultracentrifugal field, 315
LANNI, F. Higher order Tyndall spectra with mixtures of antigen and antiserum, 463
LATTA, R. See LaMer, V. K. 539
LOOS, R. See Ruyssen, R., 429

M

MCBAIN, J. W. See Dean, R. B., 383
MARSDEN, S. S., JR., MYSELS, K. J., AND SMITH, G. H. Gels and jellies of aluminum dilaurate in cyclohexane and benzene, examined by X-ray diffraction, 265
MIKLOWITZ, J. The initiation and propagation of the plastic zone along a tension specimen of nylon, 193
The stress-strain relationship of nylon under biaxial stress conditions, 217
MOONEY, M. The rheology of processing quality of raw rubbers, 69
MUKHERJEE, J. N., CHATTERJEE, B., AND BANERJEE, B. M. Liberation of H^+, Al^{+++} and Fe^{+++} ions from hydrogen clays by neutral salts, 247
MYSELS, K. J. Study of aluminum soap-hydrocarbon systems: "Calotropy" and true stability of the jelly phase, 375
See Marsden, S. S., Jr., 265

N

NADAI, A. Eugene Cook Bingham, 1
NAGAMATSU, K. See Akamatu, H., 593
NAKAHIRA, M. See Katsurai, T., 289

O

OSTER, G. Light scattering from polymerizing and coagulating systems, 291

P

PAULI, WO. The structure and properties of colloidal sulfur, 333
PLANK, C. J. Differences between silica and silica-alumina gels. II. A proposed mechanism for the gelation and syneresis of these gels, 413
PLANK, C. J., AND DRAKE, L. C. Differences between silica and silica-alumina gels. I. Factors affecting the porous structure of these gels, 399
PRASAD, M., HATTIANGDI, G. S., AND WAGLE, B. K. Behavior of some alkali soap in organic solvents, 467

R

ROMBERG, J. W., AND TRAXLER, R. N. Rheology of asphalt, 33
RUYSSEN, R., AND LOOS, R. Properties of saponins. Surface activity and degree of dispersion, 429

S

SIMHA, R. See Weissberg, S. G., 305
SMITH, G. H. See Marsden, S. S., Jr., 265
SPENCER, R. S., AND WILLIAMS, J. L. Concentrated solution viscosity of polystyrene, 117
SPOERRI, P. E. See Ginell, R., 521
SWINDELLS, J. F. The Bingham viscometer and viscosity standards, 177

T

TAYLOR, N. W. Mechanism of brittle fracture, 185
THRODAHL, M. C. Statistical analysis of plasticity measurements of natural and synthetic rubber, 187
TRAXLER, R. N. A review of the rheology of bituminous materials, 49
See Romberg, J. W., 33
TREITEL, O. The submicroscopic structure of plant cell walls, 237
The thermoelastic behavior of cylindrical plant tissues, 453

V

VAN WAZER, J. R. Some rheological measurements on the surface of saponin in water, 223
VANWINKLE, Q. See Lang, E. R., 315

W

WAGLE, B. K. See Prasad, M., 467
WEISSBERG, S. G., AND SIMHA, R. Viscosities of solutions of cellulose acetate in solvent-precipitant mixtures, 305
WILLIAMS, J. L. See Spencer, R. S., 117
WILSON, E. See LaMer, V. K., 539
WILSON, I. B. The deposition of charged particles in tubes, with reference to the retention of therapeutic aerosols in the human lung, 271

Z

ZAISER, E. M. See Barnes, M. A., 349
ZEFFERT, B. M. See Hormats, S., 307
ZISMAN, W. A. See Bigelow, W. C., 563

SUBJECT INDEX

Activities, E. C. Bingham and the ASTM, FULWILER 5

Activity, surface, properties of saponins. —and degree of dispersion, RUYSSEN AND LOOS, 429

Adhesion, Fundamentals of tackiness and —, BIKERMAN, 163

Adsorption, energy of, Oleophobic monolayers. Temperature effects and —, BIGELOW, GLASS AND ZISMAN, 563

Aerosols, Deposition of charged particles in tubes, with reference to the retention of therapeutic — in the human lung, WILSON, 271

Aerosols, homogeneous insecticidal, Effect of — on the mortality of mosquitos in confined atmospheres, LAMER, HOCHBERG, HODGES, WILSON, FALES AND LATTA, 539

Agents, hydrogen-bonded, Effect of strongly — on some polar polymers, KING, 551

Alumina, hydrous, Sorption of oxalate by —, GRAHAM AND CRAWFORD, 509

Aluminum dilaurate, Gels and jellies of — in cyclohexane and benzene examined by X-ray diffraction, MARSDEN, MYSELS AND SMITH, 265

Aluminum, Electron diffraction study of oleophobic films on copper, iron and —, BROCKWAY AND KARLE, 277

Aluminum soap-hydrocarbon systems: calotropy and true stability of the jelly phase, MYSELS, 375

Analysis, statistical, Of plasticity measurements of natural and synthetic rubber, THRODAHL, 187

Analysis, volumetric, Of colloidal electrolytes by turbidity titration, LAMBERT, 479

Asphalt, Rheology of —, ROMBERG AND TRAXLER, 33

Association phenomena. Growth of particles of silver chloride and the higher-order Tyndall effect, GINELL, GINELL AND SPOERRI, 521

Atmospheres, confined, Effect of homogeneous insectidical aerosols and the mortality of mosquitos in —, LAMER, HOCHBERG, HODGES, WILSON, FALES AND LATTA, 539

Benzene, Gels and jellies of aluminum dilaurate in cyclohexane and — examined by X-ray diffraction, MARSDEN, MYSELS AND SMITH, 265

Biography, Eugene Cook Bingham, NADAI, 1

Bituminous materials, Review of the rheology of —, TRAXLER, 49

Boundary, discontinuous, Diffusion with —, HERMANS, 387

Calotropy, Aluminum soap-hydrocarbon systems: — and true stability of the jelly phase, MYSELS, 375

Carbon black, structure of, A new suggestion for a model representing the —, AKAMATU AND NAGAMATSU, 593

Cellulose acetate, Viscosities of solutions of — in solvent-precipitant mixtures, WEISSBERG AND SIMHA, 305

Charcoal, Heat of wetting of — and its retentivity for ethyl chloride, HORMATS, ZEFFERT AND DOLIAN, 307

Charged particles, Deposition of — in tubes, with reference to the retention of therapeutic aerosols in the human lung, WILSON, 271

Clays, hydrogen, liberation of H^+, Al^{+++} and Fe^{+++} ions from — by neutral salts, MUKHERJEE, CHATTERJEE AND BANERJEE, 247

Colloidal sulfur, Structure and properties of —, PAULI, 333

Copper, Electron diffraction study of oleophobic films on —, iron and aluminum, BROCKWAY AND KARLE, 277

Cyclohexane, Gels and jellies of aluminum dilaurate in — and benzene examined by X-ray diffraction, MARSDEN, MYSELS AND SMITH, 265

Definitions, A note on the symbols and — involved in light scattering equations, LaMer and Barnes, 349
Diffraction, electron, Study of oleophobic films on copper, iron and aluminum, Brockway and Karle, 277
Diffraction, X-ray, Gels and jellies of aluminum dilaurate in cyclohexane and benzene examined by —, Marsden, Mysels and Smith, 265
Diffusion with discontinuous boundary, Hermans, 387
Dispersion, degree of, Properties of saponins. Surface activity and —, Ruyssen and Loos, 429

Effects, temperature, Oleophobic monolayers. — and energy of adsorption, Bigelow, Glass and Zisman, 563
Electrolytes, colloidal, Volumetric analysis of — by turbidity titration, Lambert, 479
Electrophoresis in an ultracentrifugal field, Lang, VanWinkle and France, 315
Equations, light scattering, A note on the symbols and definitions involved in —, LaMer and Barnes, 349
Ethyl chloride, Heat of wetting of charcoal and its retentivity for —, Hormats, Zeffert and Dolian, 307

Field, ultracentrifugal, Electrophoresis in an —, Lang, VanWinkle and France, 315
Films, oleophobic, Electron diffraction study of — on copper, iron and aluminum, Brockway and Karle, 277
Fracture, Mechanism of — of brittle solids, Taylor, 185

Gelation, Differences between silica and silica-alumina gels. Proposed mechanism for — and syneresis of these gels, Plank, 413
Gels, and jellies of aluminum dilaurate in cyclohexane and benzene examined by X-ray diffraction, Marsden, Mysels and Smith, 265
Gels, silica, Differences between — and silica-alumina —. Factors affecting the porous structure of these gels, Plank and Drake. 399
Gels, silica, Differences between — and silica-alumina —. Proposed mechanism for gelation and syneresis of these gels, Plank, 413
Gels, silica-alumina, Differences between silica and —. Factors affecting the porous structure of these gels, Plank and Drake, 399
Gels, silica-alumina, Differences between silica and —. Proposed mechanism for gelation and syneresis of these gels, Plank, 413

Heat of wetting of charcoal and its retentivity for ethyl chloride, Hormats, Zeffert and Dolian, 307

Inks, printing, Rheological properties of paints, varnishes, lacquers, and —, Green, 93
Ions, Liberation of H^+, Al^{+++} and Fe^{+++} — from hydrogen clays by neutral salts, Mukherjee, Chatterjee and Banerjee, 247
Iron, Electron diffraction study of oleophobic films on copper, — and aluminum, Brockway and Karle, 277

Jellies, Gels and — of aluminum dialurate in cyclohexane and benzene examined by X-ray diffraction, Marsden, Mysels and Smith, 265

Keratin, Membrane potentials for —, Baxter, 495
Kinetics, Of formation of monodispersed sulfur sols from thiosulfate and acid, LaMer and Kenyon, 257

Lacquers, Rheological properties of paints, varnishes —, and printing inks, Green, 93
Light scattering, From polymerizing and coagulating systems, Oster, 291
Light scattering, Latex particle sizes as determined by soap titration and —, Klevens, 365
Lubricants, Rheology of —, Dow, 81
Lung, human, Deposition of charged particles in tubes, with reference to the retention of therapeutic aerosols in the —, Wilson, 271

Matter, Rheological properties of —, under high pressure, BRIDGMAN, 7
Measurements, plasticity, Statistical analysis of — of natural and synthetic rubber, THRODAHL, 187
Measurements, rheological, Some — on the surface of saponin in water, VAN WAZER, 223
Micelle formation, Effect of temperature on — as determined by refraction, KLEVENS, 301
Mixtures, antigen and antiserum, Higher order Tyndall spectra with —, LANNI, 463
Mixtures, solvent-precipitant, Viscosities of solutions of cellulose acetate in —, WEISSBERG AND SIMHA, 305
Monolayers, oleophobic. Temperature effects and energy of adsorption, BIGELOW, GLASS AND ZISMAN, 563
Monolayers, soap, Sorption of organic vapors by —, DEAN AND MCBAIN, 383
Mosquitos, mortality of, Effect of homogeneous insecticidal aerosols on the — in confined atmospheres, LAMER, HOCHBERG, HODGES, WILSON, FALES AND LATTA, 539

Nylon, Initiation and propagation of the plastic zone along a tension specimen of —, MIKLOWITZ, 193
Nylon, Stress-strain relationship of — under biaxial stress conditions, MIKLOWITZ, 217

Oleophobic films, Electron diffraction study of — on copper, iron and aluminum, BROCKWAY AND KARLE, 277
Oleophobic monolayers. Temperature effects and energy of adsorption, BIGELOW, GLASS AND ZISMAN, 563
Oxalate, Sorption of — by hydrous alumina, GRAHAM AND CRAWFORD, 509

Paints, Rheological properties of — varnishes, lacquers, and printing inks, GREEN, 93
Particles, growth of, Silver chloride and the higher-order Tyndall effect, GINELL, GINELL AND SPOERRI, 521
Particle size, Effect of — of homogeneous insecticidal aerosols on the mortality of mosquitos in confined atmospheres, LAMER, HOCHBERG, HODGES, WILSON, FALES AND LATTA, 539
Particle sizes, Latex — as determined by soap titration and light scattering, KLEVENS, 365
Plant cell walls, Submicroscopic structure of —, TREITEL, 237
Plant tissues, cylindrical, Thermolelastic behavior of —, TREITEL, 453
Plastics, Rheological properties of polymers and —, BAKER, 115
Plastics, thermo, Viscoelastic properties of — at elevated temperatures, DIENES, 131
Plastic zone, Initiation and propagation of the — along a tension specimen of nylon, MIKLOWITZ, 193
Polymers, polar, Effect of strongly hydrogen-bonded agents on some —, KING, 551
Polymers, Rheological properties of — and plastics, BAKER, 115
Polystyrene, Concentrated solution viscosity of —, SPENCER AND WILLIAMS, 117
Potentials, membrane, For keratin, BAXTER, 495
Pressure, high, Rheological properties of matter under —, BRIDGMAN, 7
Processing quality, Rheology of — of raw rubbers, MOONEY, 69
Properties, Rheological — of matter under high pressure, BRIDGMAN, 7
Properties, Rheological — of paints, varnishes, lacquers, and printing inks, GREEN, 93
Properties, Rheological — of polymers and plastics, BAKER, 115
Properties, Structure and — of colloidal sulfur, PAULI, 333
Properties, Viscoelastic — of thermoplastics at elevated temperatures, DIENES, 131
Psychophysics, Role of — in rheology, SCOTT BLAIR, 21

Refraction, Effect of temperature on micelle formation by —, KLEVENS, 301

Review, Of the rheology of bituminous, materials, TRAXLER, 49
Rheology, of asphalt, ROMBERG AND TRAXLER, 33
Rheology, Of lubricants, Dow, 81
Rheology, Of processing quality of new rubbers, MOONEY, 69
Rheology, Review of the — of bituminous materials, TRAXLER, 49
Rheology, Role of psychophysics in, SCOTT BLAIR, 21
Rubber-like substances, Statistical theory of —, KUBO, 527
Rubber, natural, Statistical analysis of plasticity measurements of — and synthetic, THRODAHL, 187
Rubbers, raw, Rheology of processing quality of —, MOONEY, 69
Rubber, synthetic, Statistical analysis of plasticity measurements of natural and —, THRODAHL, 187

Salts, neutral, liberation of H^+, Al^{+++} and Fe^{+++} ions from hydrogen clays by —, MUKHERJEE, CHATTERJEE AND BANERJEE, 247
Saponins, Properties of —. Surface activity and degree of dispersion, RUYSSEN AND LOOS, 429
Saponins, Some rheological measurements on the surface of — in water, VAN WAZER, 223
Silver chloride, Growth of particles of — and the higher-order Tyndall effect, GINELL, GINELL AND SPOERRI, 521
Soap, alkali, Behavior of some — systems in organic solvents, PRASAD, HATTIANGDI AND WAGLE, 467
Soap, Sorption of organic vapors by monolayers of —, DEAN AND MCBAIN, 383
Soap titration, Latex particle sizes as determined by — and light scattering, KLEVENS, 365
Sol-gel transformation, Note on a new mode of —, KATSURAI AND NAKAHIRA, 289
Solids, brittle, Mechanism of fracture of —, TAYLOR, 185
Sols, monodispersed sulfur. Comparison of the particle radius determined by transmittance and by the angular position of higher order Tyndall spectra from the Mie theory, BARNES, KENYON, ZAISER AND LAMER, 349
Sols, monodispersed sulfur, Kinetics of the formation of — from thiosulfate and acid, LAMER AND KENYON, 257
Solution, Concentrated — viscosity of polystyrene, SPENCER AND WILLIAMS, 117
Solutions, polymer, Influence of solvent composition on the specific viscosities —, ALFREY, 99
Solutions, Viscosities of — of cellulose acetate in solvent-precipitant mixtures, WEISSBERG AND SIMHA, 305
Solvent composition, Influence of — on the specific viscosities of polymer solutions, ALFREY, 99
Solvents, organic, Behavior of some alkali soap systems in —, PRASAD, HATTIANGDI AND WAGLE, 467
Sorption of organic vapors by monolayers of soap, DEAN AND MCBAIN, 383
Sorption of oxalate by hydrous alumina, GRAHAM AND CRAWFORD, 509
Specimen, tension, Initiation and propagation of the plastic zone along a — of nylon, MIKLOWITZ, 193
Spectra, higher order Tyndall, with mixtures of antigen and antiserum, LANNI, 463
Standards, viscosity, Bingham viscometer and —, SWINDELLS, 177
Statistical Analysis, Of plasticity measurements of natural and synthetic rubber, THRODAHL, 187
Structure and properties of colloidal sulfur, PAULI, 333
Structure, A new suggestion for a model representing the — of carbon black, AKAMATU AND NAGAMATSU, 593
Structure, porous, Differences between silica and silica-alumina gels. Factors affecting the — of these gels, PLANK AND DRAKE, 399
Structure, submicroscopic, Of plant cell walls, TREITEL 237
Stress, biaxial, Stress-strain relationship of nylon under — conditions, MIKLOWITZ, 217

Stress-strain, Relationship of nylon under biaxial stress conditions, MIKLOWITZ, 217
Substances, rubber-like, Statistical theory of —, KUBO, 527
Sulfur, colloidal, Structure and properties of —, PAULI, 333
Sulfur sols, monodispersed. Comparison of the particle radius determined by transmittance and by the angular position of higher order Tyndall spectra from the Mie theory, BARNES, KENYON, ZAISER AND LAMER, 349
Sulfur sols, monodispersed, Kinetics of the formation of — from thiosulfate and acid, LAMER AND KENYON, 257
Surface, Some rheological measurements on the — of saponin in water, VAN WAZER, 223
Symbols, A note on the — and definitions involved in light scattering equations, LAMER AND BARNES, 349
Syneresis, Differences between silica and silica-alumina gels. Proposed mechanism for gelation and — of these gels, PLANK, 413
Systems, alkali soap, Behavior of some — in organic solvents, PRASAD, HATTIANGDI AND WAGLE, 467
Systems, Aluminum soap-hydrocarbon: "Calotropy" and true stability of the jelly phase, MYSELS, 375
Systems, coagulating, Light scattering from polymerizing and —, OSTER, 291
Systems, polymerizing, Light scattering from — and coagulating, OSTER, 291

Tackiness, Fundamentals of — and adhesion, BIKERMAN, 163
Temperature, Effect of — on micelle formation as determined by refraction, KLEVENS, 301
Temperature effects. Oleophobic monolayers, — and energy of adsorption, BIGELOW, GLASS AND ZISMAN, 563
Temperature, elevated, Viscoelastic properties of thermoplastics at —, DIENES, 131
Theory, statistical, Of rubber-like substances, KUBO, 527
Thermoplastics, Viscoelastic properties of — at elevated temperatures, DIENES, 131
Titration, soap, Latex particle sizes as determined by — and light scattering, KLEVENS, 365
Titration, turbidity, Volumetric analysis of colloidal electrolytes by —, LAMBERT, 479
Transformation, sol-gel, Note on a new mode of —, KATSURAI AND NAKAHIRA, 289
Tubes, Deposition of charged particles in —, with reference to the retention of therapeutic aerosols in the human lung, WILSON, 271
Tyndall effect, higher order, Growth of particles of silver chloride and the —, GINELL, GINELL AND SPOERRI, 521
Tyndall spectra, higher order, With mixtures of antigen and antiserum, LANNI, 463

Ultracentrifugal field, Electrophoresis in an —, LANG, VAN WINKLE AND FRANCE, 315

Vapors, organic, Sorption of — by monolayers of soap, DEAN AND MCBAIN, 383
Varnishes, Rheological properties of paints, —, lacquers, and printing inks, GREEN, 93
Viscometer, The Bingham — and viscosity standards, SWINDELLS, 177
Viscosities of solutions of cellulose acetate in solvent-precipitant mixtures, WEISSBERG AND SIMHA, 305
Viscosity, Concentrated solution — of polystyrene, SPENCER AND WILLIAMS, 117
Viscosity, specific, Influence of solvent composition on — of polymer solutions, ALFREY, 99
Viscosity standards, Bingham viscometer and —, SWINDELLS, 177

Walls, plant cell, Submicroscopic structure of —, TREITEL, 237
Water, Some rheological measurements on the surface of saponin in —, VAN WAZER, 223

Wetting, heat of, Of charcoal and its retentivity for ethyl chloride, HORMATS, ZÉFFERT AND DOLIAN, 307

X-ray diffraction, Gels and jellies of aluminum dilaurate in cyclohexane and benzene examined by —, MARSDEN, MYSELS AND SMITH, 265

Zone, plastic, Initiation and propagation of the — along a tension specimen of nylon, MIKLOWITZ, 193

INDEX OF BOOK REVIEWS

ANSON, M. L., AND EDSALL, J. T. (editors), Advances in Protein Chemistry, Vol. III(*T. Shedlovsky*), 537

BULL, H. B. Physical Biochemistry (*V. K. LaMer*), 601

MARK, H., AND WHITBY, G. S. (editors), Advances in Colloid Science. Volume II. Scientific Progress in the Field of Rubber and Synthetic Elastomers (*O. Foss*), 600

PRICE, C. C. Mechanisms of Reactions at Carbon-Carbon Bonds (*P. D. Bartlett*), 537

WARD, A. G. Colloids—Their Properties and Applications (*V. K. LaMer*), 599

WEISSBERGER, A. (editor), Physical Methods of Organic Chemistry, Vols. I and II (*V. K. LaMer*), 599

I. A. R. I. 75.

INDIAN AGRICULTURAL RESEARCH
INSTITUTE LIBRARY,
NEW DELHI.

Date of issue.	Date of issue.	Date of issue.
6-8-55.		
23-8-60		
18.9.61		
2-8-62		

MGIPC—S5—38 AR/54—7-7-54—7,000.